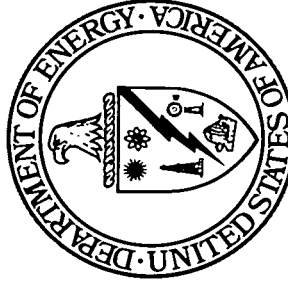


ChemRisk Document No. 1211

ChemRisk1211

A Facsimile Report



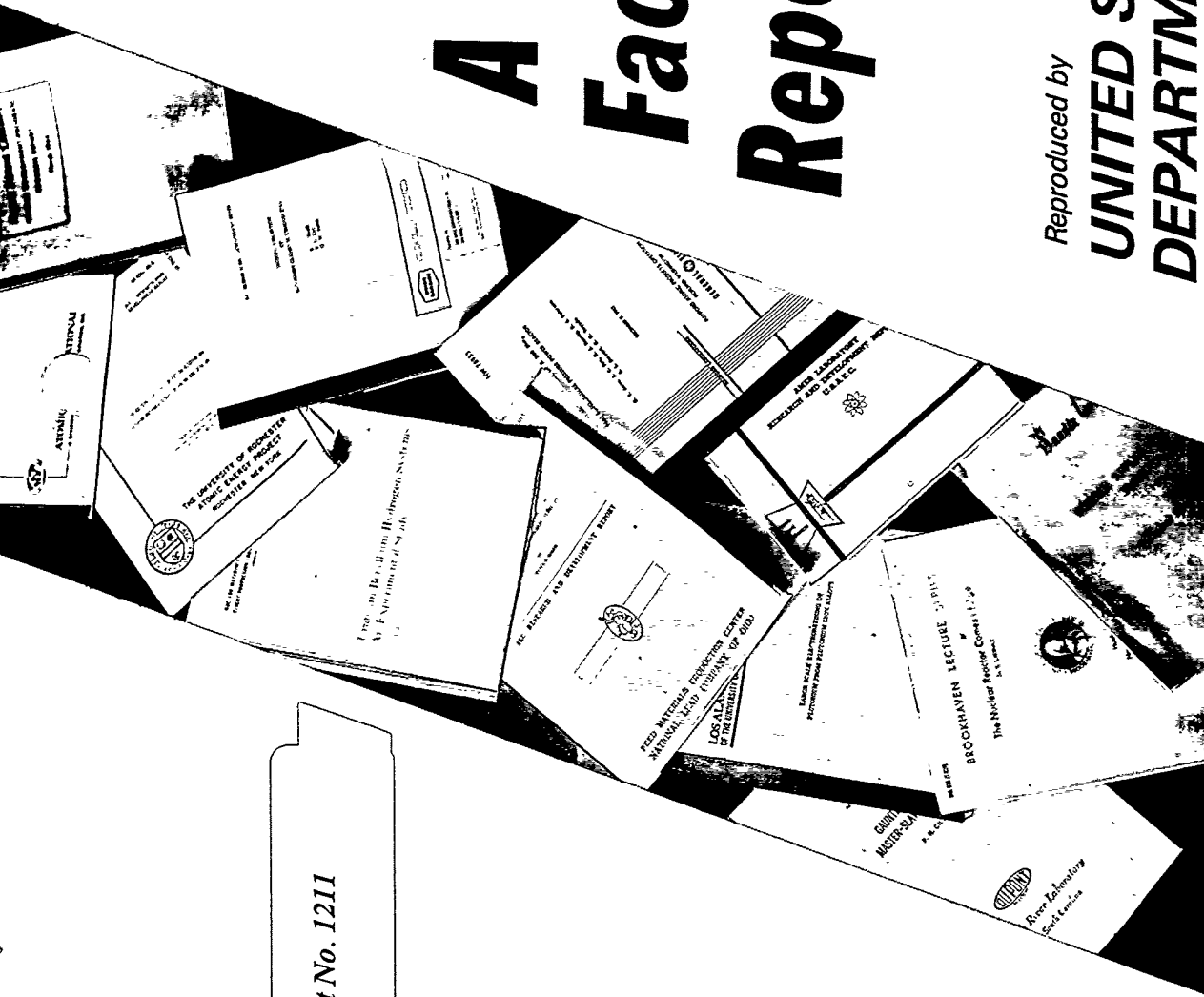
Reproduced by
**UNITED STATES
DEPARTMENT OF ENERGY**

Office of Scientific and Technical Information

Post Office Box 62 Oak Ridge, Tennessee 37831

This document has been approved for release to the public by:

David R. Hamlin 9/5/95
Technical Information Officer
ORNL Site



A METEOROLOGICAL SURVEY OF THE OAK RIDGE AREA

U. S. Weather Bureau
Oak Ridge, Tennessee

ABSTRACT

ORO-99

This is a comprehensive final report on the observations and analysis conducted during 1948-1952 by the Weather Bureau Office, Oak Ridge, Tennessee for the Atomic Energy Commission.

Part I (Background) presents the purposes of the meteorological survey program, the geographical factors of importance, an enumeration of the available climatological records in the vicinity, and a brief review of the history of the project.

Part II (Observational Equipment and Procedures) describes the instrumentation and techniques employed. Only those which were novel or unique are discussed and illustrated in detail. Each source of data is evaluated with respect to accuracy and representativeness. Procedures of reduction and processing of the observational data are also reviewed briefly.

Part III (Climatology) summarizes the findings of the survey with respect to purely meteorological phenomena. The climate of this small, hilly reservation is studied in relation to that of the Southern Appalachian area as a whole in an attempt to deduce long-term normal patterns from a short record of local observations. The elements are discussed in order of increasing dependence and complexity, starting with those having the largest-scale influence (barometric pressure, precipitation, cloudiness and sunshine) and proceeding to those requiring the most minute detail

in time and space (temperature, humidity, temperature-gradient, wind flow and turbulence). The relation of the wind flow and turbulence to the independent variables governing them is developed while, at the same time, each element is summarized in sufficient detail for direct practical application.

Part IV (Atmospheric Diffusion) summarizes attempts at the application of generalized theory combined with local climatological parameters to the problem of the dispersion of pollutants in the lower atmosphere. The variations in the behavior of radioactive argon emitted by the Oak Ridge National Laboratory Graphite Pile under the normal range of meteorological conditions are described qualitatively and quantitatively. The quantitative analysis is necessarily crude, since the concentrations and radiation dosage-rates are, for the most part, small in comparison with a variable natural background and, at distances greater than one mile, are detected with difficulty by means of the most sensitive instruments.

A METEOROLOGICAL SURVEY OF THE OAK RIDGE AREA

U. S. Weather Bureau
Oak Ridge, Tennessee

PREFACE

This report is intended to serve simultaneously three different purposes:

1. To record work performed by the Weather Bureau Office, Oak Ridge, Tennessee, during the past five years, under a cooperative agreement between the Weather Bureau and the U. S. Atomic Energy Commission, and financially supported by the latter.
2. To serve as a sourcebook of meteorological and climatological information for this area, applicable by meteorologists, health physicists, engineers, scientists and administrators to problems of design and construction, operations and research, health and safety and, especially, estimation of atmospheric contamination risks.
3. To add to the available fund of knowledge with respect to observational techniques, microclimatology of the Southern Appalachian Valley, and relationships between stability, wind flow, turbulence and diffusion in rugged terrain, for the benefit of other workers in these fields.

The roster of Weather Bureau personnel who contributed directly to the contents of this report has been lengthened by several replacements since the inception of the meteorological survey program in 1948. Throughout the program, the Meteorologist in Charge has been assisted by R. F. Myers in planning, administration, supervision, and meteorological analysis.

Mr. Myers has taken the major responsibility for procurement, installation, maintenance and evaluation of meteorological instruments and is the author of most of Part II of this report. He was assisted in the instrument work by E. M. Crume in 1949-50 and by R. D. Ogden in 1951-52. The observations and much of the data reduction were carried out by J. C. Holland (supervising observer), E. M. Crume, H. M. Day, B. H. Goad, P. J. Rhodes, R. W. Sanders and J. W. Tondee. In addition Mr. Goad and Mr. Rhodes contributed greatly to the preliminary analysis and preparation of graphs and charts. Final analysis of the neutral balloon observations was accomplished by Frank Gifford, Jr. Drafting of the many illustrations was done by P. J. Rhodes, R. D. Ogden and R. F. Myers. The tedious work of reading the instrument charts and manually computing and tabulating data was largely done with remarkable care, by Mrs. G. L. Addison, Mrs. E. P. Bellows, Mrs. D. W. Brown, Mr. J. E. Day, Mrs. V. K. Howerton, and B. L. McArthur. Typing of the large amount of correspondence connected with this project and of the preliminary drafts of this report has been done by Miss Earlene Chandler and that of the final draft largely by Mrs. M. Anderson, both of the AEC.

In the Weather Bureau outside of Oak Ridge, Dr. F. W. Reichelderfer, Chief of Bureau, has materially furthered this program by his constant personal interest and encouragement. Dr. Harry Wexler, Chief, Scientific Services Division and F. D. White of this Division are to be thanked for their technical and administrative guidance, for helping in many details and, with R. C. Wanta, for laying much of the groundwork for this project. The Weather Bureau Office, Knoxville, and the Weather Records Processing

Center, Chattanooga, have always responded willingly when information and assistance were needed.

To Dr. A. H. Holland, Jr., formerly Director of Research and Medicine, AEC, Oak Ridge, the credit is due for conceiving and initiating the meteorological survey. To his successors, Dr. J. H. Roberson, Dr. N. H. Woodruff and Mr. K. Kasschau, and to their staffs, particularly the Administrative Officer, Mrs. Alice M. Corley, and the Biology Division Chiefs, Dr. H. G. Stoeckle, Dr. E. McGrady and Dr. C. S. Shoup, thanks are due for their patience, understanding and active support in many large and small matters. The Photographic Unit, Purchasing Section, Technical Information Service and many other groups and individuals in the AEC at Oak Ridge have also frequently gone out of their way to render indispensable services.

In the Carbide and Carbon Chemicals Company organization, special thanks are due to Dr. K. Z. Morgan, Dr. F. J. Davis, P. W. Reinhardt, E. B. Wagner and Mrs. M. L. McKee of the ORNL Health Physics Division, for their interest and efforts in obtaining necessary radiological and meteorological observations; to W. H. Brand, P. E. Brown, C. A. Mossman and J. Lundholm of the ORNL Instrument Department for making possible some of the unique meteorological measurements; to F. C. Uffelman, Mrs. H. C. Leicht, Miss P. C. Johnson and Miss R. Buttles of the Y-12 IBM unit for their unselfish assistance without which the exhaustive analysis of the large mass of observational data could not have been done; and to J. Moshman of the ORNL Mathematics Panel for many helpful suggestions for

the improvement and streamlining of the statistical analysis.

The librarians of the Oak Ridge Institute of Nuclear Studies and of the Weather Bureau Library, Washington, D. C., deserve our thanks for their helpfulness and indulgence in supplying reference material. Many valuable observational data were also obtained through the cooperation of the Hydraulic Data Branch and the Division of Health and Safety of the Tennessee Valley Authority. Finally, Dr. H. E. Landsberg, Director, Geophysics Research Division, Air Force Cambridge Research Center, Cambridge, Massachusetts and O. G. Sutton, Bashforth Professor of Mathematical Physics, The Military College of Science, Shrivenham, England deserve our gratitude for the many approaches suggested by them not only in their writings and lectures, but also in stimulating personal consultations.

J. Z. Holland
Meteorologist in Charge
Weather Bureau Office
Oak Ridge, Tennessee
May 15, 1953

A METEOROLOGICAL SURVEY OF THE OAK RIDGE AREA

U. S. Weather Bureau
Oak Ridge, Tennessee

CONTENTS

	<u>Page Number</u>
<u>Part I - Background</u>	33
<u>Purpose of the Meteorological Survey</u>	33
1. Activities subject to effects of weather and climate	33
2. Objectives of the survey	35
3. Scope of this report	38
<u>Description of the Area</u>	38
4. Topography	38
5. Commission facilities	40
6. Nearby towns and industries	42
<u>History of Meteorological Observations</u>	43
7. Nearby weather stations	43
8. Oak Ridge observations prior to the survey program	45
<u>Program of the Meteorological Survey</u>	48
9. Scope of the survey	48
10. Chronological resume	48
<u>Part II - Observational Equipment and Procedures</u>	57
<u>Observational Requirements and Limitations</u>	57
1. Observational requirements for diffusion studies	57
2. Observational requirements for climatology and general service	63
3. Limitations of the observational program	64
<u>Station 001 Instrumentation</u>	66
4. The site and "hutment"	66
5. Contacting wind equipment	67
6. Wind profiles and gustiness: anemograph	73
7. Wind profiles and gustiness: airmeter	76
8. Wind profiles and gustiness: comparison and evaluation	81
9. Pilot balloon equipment	84
10. Temperature and humidity: hygrothermographs and max-min thermometers	86
11. Temperature and humidity: thermocouples	89
12. Vertical temperature gradient thermopile, T ₅₄ - T ₄ .	92
13. Captive balloon temperature sounding system	94
14. Station 001 rain gage	94
15. Pyrheliometer	95
16. Barometric pressure instruments	95
17. Smoke photograph equipment	96

	<u>Page Number</u>
<u>Manual Operation Procedures</u>	97
18. Surface weather observations	97
19. Winds aloft observation procedure	98
20. Neutral balloon observations	103
21. Temperature sounding procedure	108
22. Smoke photograph procedure	111
23. Automobile temperature surveys	113
 <u>Micronet of Unmanned Substations</u>	 117
24. Distribution of stations	117
25. Basic micronet instrumentation	120
26. Non-standard micronet instrumentation	123
27. Evaluation of micronet data	127
 <u>Diffusion Measurements</u>	 127
28. Radioactivity	127
29. Beryllium	133
30. Quarry dust	134
 <u>Summary of Data Production and Processing</u>	 134
31. Quantity and quality	134
32. Data processing	140
33. Data from other stations	147
34. Classification code	149
 <u>Part III - Climatology</u>	 184
 <u>The Period of Record</u>	 184
1. Weather during the observation period in relation to climatic normals	184
2. The range of conditions occurring within the observations period	187
 <u>Presentation of data</u>	 189
3. Order of the elements	189
4. Tabulations and graphs	190
 <u>Barometric Pressure</u>	 192
5. Regional pattern of barometric pressure	192
6. Oak Ridge pressure observations	196
 <u>Precipitation</u>	 198
7. Regional pattern of precipitation	198
8. Local variations of precipitation	201
9. Time-variability of precipitation	204
10. Seasonal distribution of precipitation	206
11. Extreme precipitation	211
12. Snowfall	217

	<u>Page Number</u>
<u>Weather and Sky Conditions</u>	218
13. Weather phenomena	218
14. Cloudiness	223
15. Solar radiation	227
16. Ceiling and cloud height	234
17. Obstructions to vision	238
18. State of the ground	241
<u>Surface Temperature and Humidity</u>	242
19. Regional temperature pattern	242
20. Seasonal temperature and humidity variation	246
21. Diurnal temperature and humidity variation	251
22. Local temperature and humidity variations	259
<u>Vertical Temperature Gradient</u>	272
23. Diurnal cycle of vertical temperature distribution	272
24. Seasonal temperature-gradient variation	278
25. The three-dimensional temperature structure	282
<u>Wind Flow</u>	286
26. Regional pattern of wind direction and speed	286
27. Local variation of wind direction and speed	301
28. Diurnal wind variations	313
29. Wind-flow patterns determined by large-scale aperiodic variables	335
30. The three-dimensional wind pattern	347
31. Turbulence	355
32. Summary of the climatology of the Oak Ridge area	370
 <u>Part IV - Atmospheric Diffusion</u>	 518
<u>Descriptive Observations of Diffusion</u>	518
1. Smoke trails	518
2. Radioactivity traces	522
3. Effects of buildings, forest, ridges and gaps	531
<u>Diffusion Formulas and Parameters</u>	533
4. General point source formulas	533
5. Formulas for special cases	537
6. Special formulas for radioactive contaminants	543
7. Determination of Sutton's concentration-distance index n	544
8. Appropriate values of Sutton's diffusion coefficients C_x , C_y and C_z .	549
9. Studies of plume rise	554
<u>Quantitative Diffusion Observations</u>	560
10. Radioargon concentrations	560
11. Radioargon gamma dose-rate	565

List of Illustrations

Part I - Background

Fig. No.		Page
1.	Map of the Southern Appalachian Area. 1000 ft. contours	54
2.	Map of Oak Ridge reservation showing micronet stations. 100 ft. contours	55
3.	Map of Whiteoak Creek drainage area (Bethel and Melton Valleys and adjoining ridges). 20 ft. contours.	56
<u>Part II - Observational Equipment and Procedures</u>		
4.	X-10 Hutment, Station 001, seen from the northwest. Left to right: double hutment building, theodolite platform, thermometer shelter, 5/4 t. wind and temperature profile pole. Haw Ridge in the background.	155
5.	Contacting wind and rain recorder: internal wiring of recorder and interconnection of units.	156
6.	Examples of contacting wind records with activation of the direction pens by the 1-mile speed contact.	157
7.	Biased and corrected wind direction frequency roses for 4 test stations, June 1949.	158
8.	Design of safety platform for anemometer poles.	159
9.	Resonant period of oscillation of the "Anemograph" spread-tail wind direction vane as a function of wind speed.	160
10.	Wiring diagram of the "Anemograph" wind system.	161
11.	Example of "Anemograph" wind direction and speed record.	162
12.	Circuit of "Airmeter" heated-thermopile anemometer.	163
13.	Uncompensated non-directional "Airmeter" probes. Left: cap closed as for zeroing. Right: thermopile exposed as for wind measurement.	163
14.	Directional response of horizontally non-directional "Airmeter" probe.	164
15.	Calibration curve for horizontally non-directional probes for "Precision Airmeter", Model B-5, Meter No. 633.	165
16.	Circuit diagram of Model B-5 "Precision Airmeter" and linearized recorder.	166

Part II - Observational Equipment and Procedures

Fig. No.	Page
17. Sample records of 6 ft., 18 ft. and 54 ft. wind direction, cup-generator wind speed, heated-thermopile wind speed and 50 ft. vertical temperature gradient records at Station 001 for 1 hr., illustrating methods of reading charts.	167
18. Recorders in Station 001 hutment. Upper row, left to right: T_{54} , - T_{18} , thermopile recorder, 54 ft. generator-selsyn (anemograph) wind recorder, linearized heated-thermopile (airmeter) wind recorder, 18 ft. contacting wind and rain recorder. Lower row: air-grass-wet-bulb thermocouple recorder, 18 ft. anemograph recorder, pyrliometer recorder. The 6 ft. anemograph recorder is just off the lower edge of the picture.	168
19. Intercalibrations of cup-generator (anemograph), contacting-cup, uncompensated thermopile (airmeter) and compensated (for short-period temperature fluctuations) thermopile anemometers in the natural wind. Vertical bars show $\pm \sigma$.	169
20. Thermocouple psychrometer aspirator unit.	170
21. Grass temperature thermocouple.	171
22. Wiring diagram of temperature-difference thermopile recorder.	172
23. Examples of T_{54} , - T_{18} record showing typical change from afternoon lapse to evening inversion.	173
24. Photograph of captive balloon temperature sounding system in operation. The thermistor, in its small rectangular plastic support, is hanging at about 4 ft. above ground.	174
25. Smoke hood for X-10 Pile stack.	175
26. Summary of double-theodolite height measurements on standard 30-gram pilot balloon ascents.	176
27. Error in double-theodolite distance measurement with a 782 ft. baseline, assuming a tracking error of 0.02° at one station or additive 0.01° errors at both stations. Each curve shows the distance at which the error reaches a given magnitude, as a function of balloon bearing with respect to baseline azimuth.	177
28. Captive balloon temperature sounding data sheet.	178
29. Circuit diagram of automobile thermistor temperature indicator.	179
30. Photographs of automobile temperature survey equipment. a. Panel showing temperature indicator and altimeter. b. Front view of thermistor shield. c. Side view of thermistor shield.	180
31. Wiring diagram of micronet contacting wind system with timing relay.	181

Part II - Observational Equipment and Procedures

Fig. No.	Page
32. Examples of contacting wind records with direction pens controlled by timing relay.	182
33. Plywood housing for micronet wind recorder.	183

Part III - Climatology

34. Daily weather graph, 1949.	375
35. Daily weather graph, 1950.	376
36. Normal sea level pressure distribution over North America and the North Atlantic Ocean: Annual, February, July, and October.	377
37. Average monthly barometric pressure, Oak Ridge and Knoxville (1949-1951).	378
38. Frequency distribution of station pressure difference (Oak Ridge minus Knoxville).	379
39. Map of average annual precipitation, 1948-1951, Southern Appalachian Area.	380
40. Map of departure of 1948-1951 average precipitation from normal, based on stations in the Southern Appalachian Area having 20 yrs. record or more.	381
41. Annual total precipitation for each year of record: Clinton and Knoxville compared with Oak Ridge (X-10)	382
42. Average annual precipitation for Clinton, Knoxville and Oak Ridge (X-10) as a function of length of record used.	383
43. Frequency distributions of: (a) Knoxville annual precipitation, (b) Knoxville monthly precipitation, and (c) the ratio of Oak Ridge (X-10) to Knoxville monthly precipitation.	384
44. Probability graph of Knoxville monthly precipitation (1871-1949) expressed as a percentage of the monthly average of record.	385
45. Probability graph of the ratio of Oak Ridge (X-10) to Knoxville monthly precipitation, 1944-1951.	386
46. Monthly average and extreme precipitation, Oak Ridge (X-10), 1944-1951.	387
47. Average monthly frequency of precipitation equal to or exceeding 0.01, 0.10 and 0.25 in., Townsite (011) and X-10 (012) stations.	388
48. Frequency distribution of number of consecutive days without measurable precipitation, seasonal and annual, Townsite (011) and X-10 (012) stations.	389

Part III - Climatology

Fig No.	Page
49. Probability graph of logarithm of 24 hr. precipitation, with frequency expressed as a percentage of precipitation days (days with 0.01 in. or more), Oak Ridge and neighboring stations.	390
50. Schematic maps of the Southern Appalachian Area divided into broad zones, showing the annual frequencies of various weather phenomena in each zone.	391
51. Annual variation of average and extreme daily total solar radiation: (a) in units of cal/cm ² , (b) expressed as a percentage of theoretical extraterrestrial solar radiation.	392-393
52. Monthly average solar radiation (Oak Ridge) vs. sunshine duration (Knoxville).	394
53. Examples of diurnal variation of solar radiation: (a) hourly total, and (b) accumulated total.	395
54. Combined annual and diurnal pattern of solar radiation: (a) hourly average, and (b) average total accumulated since sunrise each day.	396
55. Series of photographs showing dissipation of morning ground fog simultaneously in two valleys.	397
56. Map of mean annual temperature, 1948-1951, Southern Appalachian Area.	398
57. Map of departure of 1948-1951 mean temperature from average of record based on stations in the Southern Appalachian Area having 20 yrs. record or more.	399
58. Average daily maximum, minimum, and mean temperature vs. altitude, Southern Appalachian Area, Jan. 1950.	400
59. Average daily maximum, minimum and mean temperature vs. altitude, Southern Appalachian Area, July 1950.	401
60. Monthly average and extreme temperatures, Oak Ridge (X-10) 1945-1952.	402
61. Probability graphs of daily mean temperature, Oak Ridge (X-10); (a) annual, stations 001 (1949-1950, based on hourly temperatures) and 012 (1945-1951, based on average of daily maximum and minimum), and (b) seasonal, station 012, 1945-1951.	403-404
62. Probability graphs of daily maximum temperature, Oak Ridge (X-10, Station 012, 1947-1951): (a) annual, and (b) seasonal	405-406
63. Probability graphs of daily minimum temperature, Oak Ridge (X-10, Station 012, 1947-1951): (a) annual, and (b) seasonal	407-408
64. Normal degree days, Knoxville, Oak Ridge Townsite (011) and X-10 (012) adjusted to the 30 yr. period 1921-1950: (a) monthly total, and (b) accumulated seasonal total.	409-410

Part III - Climatology

Fig. No.	Page
65. Probability graph of daily temperature range, Station 012, annual, 1949-1950.	411
66. Monthly averages of the daily temperature range at Knoxville and Oak Ridge, percent of possible sunshine and number of clear days at Knoxville.	412
67. Diurnal curves of temperature, wet bulb temperature, dew point and relative humidity for Station 001 (X-10 hutment) by seasons, Dec. 1949-Feb. 1951.	413
68. Average daily maximum, minimum and mean temperature and average daily temperature range at micronet stations plotted against station elevation, Fall, 1949.	414
69. Diurnal curves of temperature and dew point at micronet stations compared with Station 001, Fall, 1949.	415
70. Probability graphs of temperature difference, Oak Ridge (001) minus Knoxville, June 1949-Oct. 1950: (a) temperature, wet bulb temperature and dew point; (b) 7 a.m. 6-hour minimum and 7 p.m. 6-hour maximum; (c) 7 a.m. 6-hour maximum and 7 p.m. 6-hour minimum.	416-418
71. Difference between stations in monthly frequency of daily temperature extremes.	419
72. Diurnal curves of average temperature difference, by seasons, between hill and valley stations (compared with corresponding free-air vertical temperature differential) and between opposing slope stations.	420
73. Monthly average hill-valley differential of daily maximum and minimum temperature, 1949-1950.	421
74. NW-SE terrain profiles adjoining automobile, micronet and blimp temperature observation points.	422
75. Average hourly temperature differentials with respect to valley bottoms, obtained by various methods during automobile temperature surveys, Sept. 12-Oct. 31, 1950.	423
76. Average hourly horizontal temperature differentials at hilltop and mid-slope levels obtained during automobile temperature surveys, Sept. 12-Oct. 31, 1950.	424
77. Comparison of diurnal curves of $T_{grass} - T_{4'}$ and solar radiation for a summer period and a fall period, separated into two classes of cloudiness.	425
78. Comparison of average diurnal curves of $T_{4'} - T_{grass}$, $T_{54'} - T_{4'}$, $T_{183'} - T_{5'}$, T_{grass} , $T_{4'}$, 4' wet bulb temperature and 4' dew point temperature for a summer period (July 14-Sept. 20, 1950), separated into two classes of cloudiness.	426

Part III - Climatology

Fig. No.	Page
79. Comparison of average diurnal curves of T_{11} , T_{grass} , T_{54} , T_{11} , T_{183} , T_5 , T_{grass} , T_{11} , 4' wet bulb temperature and 4' dew point temperature for a fall period (Sept. 21-Nov. 30, 1950), separated into two classes of cloudiness.	427
80. Hourly and total frequency distribution of $T_{200} - T_{11}$, $T_{500} - T_{11}$, $T_{1000} - T_{11}$ and sounding type, and hourly curves of temperature vs. height based on average lapse rates, obtained from captive balloon temperature soundings, Aug. 28-Nov. 3, 1950.	428
81. Average temperature time cross-section of the lowest 5000 ft., Sept. - Oct. 1950.	429
82. Frequency distribution of $T_{183} - T_5$ and $T_{850\text{ mb}'} - T_5$ by seasons and annually, 1949-1950.	430
83. Diurnal curves of cumulative frequency of $T_{183} - T_5$ by seasons, 1949-1950.	431
84. Diurnal curves of cumulative frequency of $T_{850\text{ mb}'} - T_5$ by seasons, 1949-1950.	432
85. Average monthly frequency of inversion ($T_{183} - T_5 \geq 0$), Station 012, 1944-1951.	433
86. Frequency distribution of $T_{200} - T_{11}$ by time of day and season.	434
87. Frequency distribution of $T_{500} - T_{11}$ by time of day and season.	435
88. Frequency distribution of $T_{1000} - T_{11}$ by time of day and season.	436
89. Frequency distribution of sounding type by time of day and season.	437
90. Average temperature vs. height curves for the lowest 1500 ft. by time of day and season.	438
91. Temperature 80 ft. above Pine Ridge top vs. free-air temperature, and comparison of temperature differentials between this level and valley bottom.	439
92. Annual pilot balloon wind rose map for the 2000 m (6600 ft.) MSL level, Southern Appalachian Area.	440
93. Annual pilot balloon wind rose map for the 1500 m (5000 ft.) MSL level, Southern Appalachian Area.	441
94. Annual pilot balloon wind rose map for the 1000 m (3300 ft.) MSL level, Southern Appalachian Area.	442
95. Annual pilot balloon wind rose map for the 500 m (1700 ft.) MSL level, Southern Appalachian Area.	443

Part III - Climatology

Fig. No.	Page
96. Annual surface wind rose map, Southern Appalachian Area.	444
97. 1500 m wind roses, winter, Southern Appalachian Area.	445
98. 1500 m wind roses, spring, Southern Appalachian Area.	446
99. 1500 m wind roses, summer, Southern Appalachian Area.	447
100. 1500 m wind roses, fall, Southern Appalachian Area.	448
101. Surface wind rose map, winter, Southern Appalachian Area.	449
102. Surface wind rose map, spring, Southern Appalachian Area.	450
103. Surface wind rose map, summer, Southern Appalachian Area.	451
104. Surface wind rose map, fall, Southern Appalachian Area.	452
105. Annual daytime surface wind rose map, Southern Appalachian Area.	453
106. Annual nighttime surface wind rose map, Southern Appalachian Area.	454
107. Annual surface wind rose map for observations with precipitation occurring, Southern Appalachian Area.	455
108. Annual upper air wind roses comparing Knoxville pibals, Nashville pibals, all Nashville rawins and Nashville rawins with precipitation occurring at time of observation.	456
109. Winter upper air wind roses comparing Knoxville pibals, Nashville pibals, all Nashville rawins and Nashville rawins with precipitation occurring at time of observation.	457
110. Spring upper air wind roses comparing Knoxville pibals, Nashville pibals, all Nashville rawins and Nashville rawins with precipitation occurring at time of observation.	458
111. Summer upper air wind roses comparing Knoxville pibals, Nashville pibals, all Nashville rawins and Nashville rawins with precipitation occurring at time of observation.	459
112. Fall upper air wind roses comparing Knoxville pibals, Nashville pibals, all Nashville rawins and Nashville rawins with precipitation occurring at time of observation.	460
113. 36-point Oak Ridge and Knoxville upper air wind direction frequency and mean wind speed from each direction, by seasons and annual, 1949-1950.	461
114. Daily peak gust velocity frequency distribution by seasons and annual, X-10 (012), Sept. 1949-Nov. 1951.	462

Part III - Climatology

Fig. No.	Page
115. Average daily peak gust as a function of average wind speed for hour containing peak gust, seasonal and annual, X-10 (012), Sept. 1949 - Nov. 1951.	463
116. Daily peak gust frequency by direction and speed, seasonal and annual, X-10 (012), Sept. 1949-Nov. 1951.	464
117. Annual wind rose map, Bethel Valley - Melton Valley area.	465
118. Spring wind rose map, 1949, Bethel Valley - Melton Valley area.	466
119. Summer wind rose map, 1949, Bethel Valley - Melton Valley area.	467
120. Fall wind rose map, 1949, Bethel Valley - Melton Valley area.	468
121. Winter wind rose map, 1949-1950, Bethel Valley - Melton Valley area.	469
122. Spring wind rose map, 1950, Bethel Valley - Melton Valley area.	470
123. Summer wind rose map, 1950, Bethel Valley - Melton Valley area.	471
124. Fall wind rose map, 1950, Bethel Valley - Melton Valley area.	472
125. Average wind speed at micronet stations plotted against anemometer height above sea level and above ground, Fall 1949 and Fall 1950.	473
126. Annual wind roses for Oak Ridge plant and town sites.	474
127. X-10 (012) wind roses for stable ($T_{183} - T_5 \geq 0$) and unstable ($T_{183} - T_5 < 0$) conditions, observations with precipitation, and total by seasons and annual, 1950 - 1952.	475
128. Annual curves of monthly mean and extreme wind speed, Townsite (011) and X-10 (012).	476
129. Probability graphs of wind speed by altitude and season.	477
130. Probability graphs of wind speed at variously exposed micronet stations, annual.	478
131. Diurnal curves of average upper-air wind speed by altitude and season.	479
132. Diurnal curves of average mid-valley anemometer wind speeds by altitude and season.	480
133. Diurnal graphs of wind direction frequency and average speed by seasons, comparing hilltop (007) and valley (003) stations.	481
134. Diurnal graphs of wind direction frequency and average speed by seasons, comparing a ridge top (006) and mid-valley near ridge-top level (012).	482

Part III - Climatology

Fig. No.	Page
135. Diurnal graphs of wind direction frequency and average speed by seasons, comparing southwestward-draining (004) and a northeastward-draining (001) valley stations.	483
136. Diurnal graphs of wind direction frequency and average speed by seasons, comparing different altitudes and exposures at and above ridge top level, Fall 1949.	484
137. Diurnal graphs of wind direction frequency and average speed by seasons, comparing parallel-draining stations in different valleys.	485
138. Diurnal graphs of wind direction frequency and average speed by seasons, comparing opposite slope exposures and different altitudes near valley bottom.	486
139. Photograph of smoke from HC pot, near Station 001, June 2, 1949, 6:45 a.m. looking SE, and showing SW wind in lowest 50 ft., NE wind above.	487
140. Resultant surface wind maps for Bethel-Melton Valley area, by time of day, Summer 1949.	488
141. Resultant surface wind maps for Bethel-Melton Valley area, by time of day, Summer 1950.	489
142. Diurnal resultant wind hodographs for Oak Ridge micronet stations by seasons.	490
143. Diurnal resultant wind hodographs for Southern Appalachian Area stations by seasons.	491
144. Local wind flow pattern as a function of large-scale variables: maps 1-4 showing effects of time of day and season.	492
145. Local wind flow pattern as a function of large-scale variables: maps 5-8 showing effects of large-scale wind direction in midday Conditions	493
146. Local wind flow pattern as a function of large-scale variables: maps 9-12 showing effects of large-scale wind direction in nighttime conditions.	494
147. Local wind flow pattern as a function of large-scale variables: maps 13-16 showing effects of large-scale wind speed.	495
148. Local wind flow pattern as a function of large-scale variables: maps 17-20 showing effects of stability variations.	496
149. Vertical profiles of mean wind speed in the lowest 5300 ft., Oak Ridge and Knoxville, by seasons.	497
150. Vertical profiles of mean wind speed in the lowest 850 ft., at Oak Ridge, day, night, and average, by seasons.	498

Part III - Climatology

Fig. No.	Page
151. Vertical profiles and diurnal curves of annual mean wind speed: (a) profiles up to 5300 ft.; (b) diurnal curves up to 5300 ft. (Pibal); (c) more detailed profiles up to 850 ft.; and (d) diurnal curves up to 140 ft. (anemometers).	499-502
152. Average wind speed time cross-section, Sept.-Oct. 1950	503
153. Schematic X-Z plots of the four types of neutral balloon trajectories.	504
154. Scatter-diagram of neutral balloon trajectory type as a function of 5000 ft. wind speed and 180 ft. stability.	505
155. Average vertical velocity of neutral balloons in two narrow azimuth sectors, as a function of distance and height, by turbulence type.	506
156. Frequency distributions of vertical velocity of neutral balloons, azimuth 230° - 249° , by turbulence type and aspect of underlying terrain.	507
157. Diurnal curves of average 15-min. wind direction range, 154 ft. (Station 012), by wind speed and season.	508
158. Diurnal curves of average 15-min. wind speed range, 154 ft. (Station 012), by wind speed and season.	509
159. Ratio of 15-min. wind speed range to hourly mean speed as a function of hourly mean speed, 154 ft. (Station 012), by stability and season.	510
160. 15-min. wind direction range as a function of hourly mean wind speed, 154 ft. (Station 012), by stability and season.	511
161. Annual graphs of 15-min. wind direction and speed ranges as functions of time of day, wind speed and stability, 154 ft. (Station 012), 1950.	512
162. Definitions and approximations used in turbulence analysis.	513
163. Tests of turbulence approximations and determination of the ratio of 15-min. range to standard deviation, based on fast runs.	514
164. Longitudinal and transverse components of absolute (σ_u, σ_v) and relative (T_x, T_y) intensity of turbulence as functions of hourly mean wind speed, sorted by stability, 54 ft. (Station 001), July 19- Oct. 3, 1950.	515
165. Absolute intensity of turbulence as a function of hourly mean wind speed, in neutral stability, comparing different methods of measurement at the same height (54 ft.) and the same method of measurement at different heights.	516
166. Isotropy parameter K, mechanical coefficient $2\sigma/2\bar{v}$ and thermal component $\sigma(0)$ of the turbulence as functions of wind speed, height and stability.	517

Part IV - Atmospheric Diffusion

Fig. No.		<u>Page</u>
167.	Selected photographs of surface smoke trails, station 001, looking SE from "A ₂ " theodolite position, with ENE or NE winds, arranged by stability (T ₁₈₃ - T ₅ , station 012) and wind speed (18 ft. contacting anemometer, station 001).	570
168.	Ratio of vertical half-width (z) of surface and stack smoke plumes to length (x) at approximately 400 ft. along the plume, obtained from photographs and averaged by wind speed and stability groups, compared with similarly averaged observations of vertical gustiness (σ_w/\bar{u} obtained from "airmeter") and lateral gustiness ($\tan \sigma_d$ from wind vane).	571
169.	Typical 3-day sequence of half-hourly radioactivity and meteorological observations. Top to bottom: 154 ft. wind direction, 154 ft. wind speed, T ₁₈₃ - T ₅ , 4 ft. relative humidity, radon (alpha) concentration (unit 10 ⁻¹⁰ curie/m. ³), beta-gamma particulate concentration at 0.4 mi. SW and 1 mi. NE of Pile stack (unit 10 ⁻¹⁰ curie/m. ³), incident gamma radiation above background at 1 mi. SW, 1 mi. NE and 3 mi. NE of Pile stack (unit 10 ⁻⁶ roentgen/hr.).	572
170.	Beta and gamma count-rate-meter traces at 1, 3 and 5 $\frac{1}{2}$ mi. NE of the X-10 Pile stack (arbitrary units not uniform), April 29, 1951, 1 a.m. to 1 p.m., with prevailing SW winds. Graph of 4-min. average departure of wind direction from detectors added for comparison.	573
171.	Gamma traces at 1 mi. and 5 $\frac{1}{2}$ mi., T ₁₈₃ - T ₅ and wind direction and speed at stations 012 and 019, May 4, 1951, 2-8 a.m.	574
172.	Gamma traces at 1- and 3-min. wind speed and wind direction at station 012, T ₅₄ - T ₄ (station 001), and T ₁₈₃ - T ₅ (station 012), Aug. 2, 1950, 5-10 a.m.	575
173.	Gamma trace at 1 mi., wind direction and speed at stations 012 (154 ft.) and 004 (1 mi. NE of stack, 18 ft. above ground), T ₅₄ - T ₄ (station 001) and T ₁₈₃ - T ₅ (station 012), Aug. 8, 1950, 3-8:30 p.m.	576
174.	Sutton's parameter n vs. stability by wind speed, altitude and instrument type.	577
175.	Observed C _x , C _y and C _z vs. wind speed and stability.	578
176.	Variation of C _y with height.	579
177.	Observed vs. calculated smoke plume width.	580
178.	Observed and calculated plume heights.	581
179.	Thermal component of plume rise.	582

Part IV - Atmospheric Diffusion (Cont'd)

Fig. No.		<u>Page</u>
180.	Concentration of A^{41} in units of 10^{-9} curie/m. ³ at 1.0, 3.1 and 5.4 mi. NE of X-10 Pile, under neutral ($T_{183} - T_5 = 0$ or -1° F.), moderately stable ($T_{183} - T_5 = -1$ to -5° F.) and very stable ($T_{183} - T_5 = -6^\circ$ F. or more) conditions, plotted vs. station 012 wind speed and compared with theoretical downwind concentration \bar{X} and average concentration \bar{X} . Average and highest 15-min. observed concentration are shown; the vertical segments from the "high-background" value to the "low-background" value and indicate the degree of uncertainty due to choice of beta background level. The number of 15-min. observations is shown above each symbol.	583
181.	A^{41} gamma dose-rate, units of 10^{-6} roentgen/hr. at 1.0, 3.1 and 5.4 mi. NE and 1.4 mi. SW of the Pile stack, vs. wind speed, compared with theoretical radiation from a line source of strength Q/u at plume height at a horizontal angle $\theta = 0^\circ, 7\frac{1}{2}^\circ$ and 15° with the line of detectors.	584

List of Tables

Part I - Background

<u>Table No.</u>	<u>Page</u>
1. Towns of 1000 or over.	43
2. Types and numbers of observations.	51
3. Number of employees	53
<u>Part II - Observational Equipment and Procedures</u>	
4. Double theodolite baseline data	86
5. Winds-aloft observation levels	100
6. Cable length at standard levels	109
7. Micronet stations	118
8. Scheduled observations	135
9. Number of routine observations	136
10. Comparison of instrumental observations	138-139
11. Weekly instrument chart readings	141
12. Routine punched card tabulations	143-145
13. Classification code	153
<u>Part III - Climatology</u>	
14. Knoxville barometric pressure	194
15. Average number of days with high or low pressure centers between 30°-40° N, 80° - 90° W (1899-1938)	195
16. Local variations of precipitation	203
17. Knoxville-Oak Ridge joint frequency	204
18. Seasonal precipitation in the Southern Appalachian area	208
19. 30-yr. normal monthly precipitation, in.	209

Part III - Climatology (Cont'd)

<u>No.</u>	<u>Page</u>
20. Normal daily precipitation frequency, Knoxville and Oak Ridge	210
21. Maximum observed precipitation	212-213
22. Record September 24-hr. precipitation set on September 29, 1944	215
23. Normal recurrence intervals for excessive 24 hr. point precipitation	216
24. Probable maximum precipitation, in.	216-217
25. Seasonal distribution of weather and sky conditions, Knoxville	221
26. Comparative frequency (%) of weather, sky and ground conditions, Oak Ridge vs. Knoxville, June, 1949 - November, 1950	225
27. Seasonal and diurnal cloudiness comparison (% frequency), Oak Ridge vs. Knoxville	226
28. Daily total solar radiation	232
29. Oak Ridge cloud height frequency (%), June, 1949 - November, 1950	233
30. Oak Ridge visibility frequency (%)	236
31. State of ground frequency (%), Oak Ridge, October, 1949 - September, 1952	241
32. Oak Ridge area temperatures (°F.)	248
33. Frequencies of temperature extremes	249
34. Heating degree days	252
35. Average relative humidity (%), and wet bulb temperature (°F.)	253
36. Annual frequency distribution of hourly wet and dry bulb temperature (%)	254
37. Temperature and moisture difference, Oak Ridge minus Knoxville (°F.)	263
38. Difference in extreme temperature frequencies between pairs of stations	265
39. Frequency (%) of westerly winds (SSW-NNW)	290
40. Regional average wind speeds (mph)	296

Part III - Climatology (Cont'd)

<u>Table No.</u>		<u>Page</u>
41.	Regional fastest mile of wind on record (mph)	299
42.	Oak Ridge extreme observed wind speeds	300
43.	Wind rose types	303
44.	Percent of time wind directions at two stations agree within one point	307
45.	Joint direction frequency (%), stations 012 and 005, by quadrants	309

Part IV - Atmospheric Diffusion

46.	Radioactive exposure, concentration and cloud radius, April 29, 1951	527
47.	Radioactive decay of A^{131} : fraction remaining at each distance as a function of wind speed	528
48.	n from average wind speed profiles	546
49.	n from decrease of atmospheric gamma radiation between 1 and $5\frac{1}{2}$ mi., downwind of the pile stack, April 27-29, 1951	548
50.	Observed values of C_x , C_y and C_z for typical conditions.	550
51.	Calculated and observed smoke plume widths at 400 ft.	552
52.	Stack and effluent parameters	555
53.	Product of plume height (ft.) and wind speed (mph)	557
54.	Parameters for concentration and exposure calculations	563
55.	Beta/gamma ratios and cloud radius	565
56.	Number of gamma observations, September 1 - November 3, 1950	567

REFERENCES

- (1) Weather Bureau Office, Oak Ridge, Tenn., Weather Conditions, section in Construction Contract Specifications (1952) - U. S. Atomic Energy Commission, Oak Ridge, Tenn. (mimeographed)
- (2) J. Z. Holland, Estimates of Ground Concentrations from Chemical Stacks (1950) - unpublished
- (3) Weather Bureau Office, Oak Ridge, Tenn., Winds in the Vicinity of X-10 Correlated with Thermal Stability and Precipitation - Weather Bureau Office, Oak Ridge, Tenn. (mimeographed)
- (4) J. Z. Holland and R. F. Myers, miscellaneous unpublished reports on stack height calculations and reactor disaster calculations (1948-53)
- (5) U. S. Atomic Energy Commission, Oak Ridge, Tenn., Office of Public Information, AEC Handbook on Oak Ridge (1951) - U. S. Atomic Energy Commission, Oak Ridge, Tenn. (mimeographed)
- (6) P. B. Stockdale, Geologic Conditions at the Oak Ridge National Laboratory (X-10) Area Relevant to the Disposal of Radioactive Waste (1951), ORO-58 (Restricted) - U. S. Atomic Energy Commission, Technical Information Service, Oak Ridge, Tenn.
- (7) Rand-McNally Commercial Atlas and Marketing Guide (1952) - Rand-McNally
- (8) J. Z. Holland, Program for a Meteorological Investigation of the Oak Ridge Reservation and Neighborhood (1948) - unpublished
- (9) J. Z. Holland, Formulae for Estimating Concentrations and Exposures from Radioactive Stack Gases (1951) - Weather Bureau Office, Oak Ridge, Tenn. (mimeographed)
- (10) R. F. Myers, The Development of a Digital Telemeter System (1952) - Weather Bureau Office, Oak Ridge, Tenn. (mimeographed)
- (11) National Defense Research Committee, Division 10, Handbook on Aerosols (1950) - U. S. Government Printing Office, Washington
- (12) L. E. Wood, The Development of a New Wind-Measuring System (1945) - Bull. Am. Meteor. Soc., Vol. 26, No. 9
- (13) B. Ratner, A Method for Eliminating Directional Bias in Wind Roses (1950) - Monthly Weather Review, Vol. 78, No. 10
- (14) L. V. King, The Convection of Heat from Small Cylinders in a Stream Fluid (1914) - Phil. Trans. Roy Soc. Lond., Series A, Vol. 214

- (15) C. W. Thornthwaite and M. H. Holstead, Micrometeorology of the Surface Layer of the Atmosphere; Interim Report No. 3 (1948) - Johns Hopkins University, Laboratory of Climatology, Seabrook, N. J.
- (16) W. E. K. Middleton, Meteorological Instruments (1941) - The University of Toronto Press, Toronto
- (17) C. A. Mossman, J. Lundholm and P. E. Brown, A Thermistor Temperature Recorder for Meteorological Survey (1950) - ORNL 556 (unclassified), Oak Ridge National Laboratory, Oak Ridge, Tenn.
- (18) R. F. Myers, A Low-Level Temperature Sounding System for Routine Use (1952) - Bull. Am. Meteor. Soc., Vol. 33, No. 1
- (19) U. S. Weather Bureau, Manual of Solar Radiation Observations (1952) - Chapter A 16, Circular N, U. S. Department of Commerce, Weather Bureau, Washington
- (20) U. S. Weather Bureau, Barometers and the Measurement of Atmospheric Pressure (1941), Circular F - U. S. Government Printing Office, Washington
- (21) U. S. Weather Bureau, Manual of Surface Observations (1951), Circular N - U. S. Government Printing Office, Washington
- (22) U. S. Weather Bureau, Instructions for Making Pilot Balloon Observations (1942), Circular O - U. S. Government Printing Office, Washington
- (23) M. C. Leverett, A. F. Rupp, S. E. Beall, L. P. Bornwasser, Behavior of Stack Gases in Still Air (1950), AECD-2909 (unclassified) - U. S. Atomic Energy Commission, Technical Information Service, Oak Ridge
- (24) A. F. Rupp, S. E. Beall, L. P. Bornwasser and D. H. Johnson, Dilution of Stack Gases in Cross Winds (1948) - AECD-1811 - U. S. AEC, Tech. Information Service, Oak Ridge
- (25) H. M. Parker, Review of Air Monitoring Procedures at Clinton Laboratories (1946), MDDC-471 (unclassified) and unpublished report by J. S. Cheka - U.S.A.E.C. Tech. Information Service, Oak Ridge
- (26) T. H. J. Burnett, A Preliminary Correlation of Airborne Activity, Temperature Inversions, and Wind Conditions (1947) - unpublished
- (27) J. S. Cheka and H. J. McAlduff, Unpublished reports dealing with particulate air contamination at Oak Ridge National Laboratory (1949)
- (28) U. S. Weather Bureau, Normal Weather Maps (1946) - U. S. Department of Commerce, Weather Bureau, Washington

- (29) W. H. Klein, A Hemispheric Study of Daily Pressure Variability at Sea Level and Aloft - J. Met., 5.6, No. 5, Oct., 1951, pp. 332-346
- (30) J. L. H. Paulhus and H. A. Kohler, Interpolation of Missing Precipitation Records (1952) - Monthly Weather Review, Vol. 80, No. 8
- (31) U. S. Weather Bureau, Climatic Summary of the United States, Section 77: Eastern Tennessee (1931), Bulletin W - U. S. Government Printing Office, Washington
- (32) A. L. Shands and D. Ammerman, Maximum Recorded United States Point Rainfall, Technical Paper No. 2 (1947) - U. S. Department of Commerce, Weather Bureau, Washington
- (33) A. H. Jennings, Maximum 24-Hour Precipitation in the United States, Weather Bureau Technical Paper No. 16 (1952) - U. S. Government Printing Office, Washington
- (34) U. S. Weather Bureau, Climatological Data, monthly and annual, by states - U. S. Department of Commerce, Weather Bureau, Chattanooga, Tenn.
- (35) U. S. Weather Bureau, Local Climatological Summary, monthly and annual, by stations - U. S. Department of Commerce, Weather Bureau, Chattanooga, Tenn.
- (36) Tennessee Valley Authority, Precipitation in Tennessee River Basin, monthly and annual - U. S. T.V.A., Hydraulic Data Branch, Knoxville
- (37) W. C. Ackerman, Possible Floods on White Oak Creek - Oak Ridge Project (1949) - unpublished
- (38) U. S. Weather Bureau, Generalized Estimates of Maximum Possible Precipitation over the United States East of the 105th Meridian, Hydrometeorological Report No. 23 (1947) - U. S. Department of Commerce, Weather Bureau, Washington
- (39) L. R. Setter and O. W. Kochtizky, Studies of the White Oak Creek Drainage System I: Drainage Area of the Creek and Capacity of White Oak Lake, ORNL 562 (1950) - Oak Ridge National Laboratory, Oak Ridge (Restricted)
- (40) L. R. Setter and O. W. Kochtizky, Studies of White Oak Creek Drainage System II: Determination of Discharge at White Oak Dam, ORNL-582 (1950) - Oak Ridge National Laboratory, Oak Ridge (Restricted)
- (41) U. S. Weather Bureau, Airway Meteorological Atlas for the United States (1941) - New Orleans, La.
- (42) A. L. Shands, Thunderstorm Probabilities in the United States (1948), Bull. Am. Meteor. Soc., Vol. 29, No. 5

- (43) U. S. Weather Bureau, Climatological Services Division, Tornado Occurrences in the United States (1952) - U. S. Government Printing Office, Washington
- (44) R. J. List, Smithsonian Meteorological Tables (1951) - Smithsonian Institution, Washington
- (45) P. E. Church, C. A. Gosline, O. H. Newton, J. F. Mattingly and L. F. Markus, Unpublished reports from Hanford Meteorology Section, Jan., 1943 - July, 1944.
- (46) R. E. Shanks, Climates of the Great Smoky Mountains (1952) - To be published in Ecology
- (47) J. Z. Holland, Time-Sections of the Lowest 5000 Ft. (1952) - Bull. Am. Meteor. Soc., Vol. 33, No. 1
- (48) V. Conrad, Fundamentals of Physical Climatology (1942) - Howard University Press, Cambridge, Mass.
- (49) R. Peattie, Mountain Geography (1936) - Howard University Press, Cambridge, Mass.
- (50) A. Court, Temperature Frequencies in the United States (1951) - J. Meteor., Vol. 8, No. 6
- (51) L. A. Ramdas, Micro-Climatological Investigations in India - Arch. Met. Geoph. Biokl., B., Vol. III
- (52) R. Geiger, The Climate Near the Ground, Trans. M. N. Stewart (1950) - Harvard University Press, Cambridge, Mass.
- (53) H. E. Landsberg, Comfortable Living Depends on Microclimate (1950) - Weatherwise, Vol. 3, No. 1
- (54) C. G. Rossby, On the Vertical and Horizontal Concentration of Momentum in Air and Ocean Currents (1951) - Tellus, Vol. 3, No. 1
- (55) L. Prandtl and O. G. Tietjens, Applied Hydro- and Aeromechanics (1934) - McGraw-Hill, New York
- (56) D. Brunt, Physical and Dynamical Meteorology (1944) - Cambridge University Press, Cambridge, England
- (57) B. Haurvitz, Dynamic Meteorology (1941) - McGraw-Hill, New York
- (58) U. S. Army Service Forces, Local Winds (1945) - Army Service Forces, Signal Corps Ground Signal Agency, Eatontown Signal Laboratory Group, Dugway Proving Ground, Tooele, Utah
- (59) F. Defant, Zur Theorie der Hangwinde, nebst Bemerkungen Zur Theorie der Berg - und Talwinde (1949) - Arch. Met., Geoph., Biokl., A, Vol. I, No. 3-4.

- (60) R. G. Fleagle, A Theory of Air Drainage (1950) - J. Meteor. Vol. 7, No. 3
- (61) E. W. Hewson and G. C. Gill, Meteorological Investigations in Columbia River Valley Near Trail (1944), Part II of U. S. Dept. Interior, Bureau of Mines, Bull. 453, "Report Submitted to Trail Smelter Arbitral Tribunals" - U. S. Government Printing Office, Washington
- (62) C. M. Cross, Slope and Valley Winds in the Columbia River Valley (1950) - Bull. Am. Meteor. Soc., Vol. 31, No. 3
- (63) T. A. Gleason, On the Theory of Cross-Valley Winds Arising from Differential Heating of the Slopes (1951) - J. Meteor. Vol. 8, No. 6
- (64) W. R. Morgans, A Memorandum Giving a Summary of Present Knowledge on the Relation between Ground Contours, Atmospheric Turbulence, Wind Speed and Direction (1931) - G. B. Met. Office, Reports and Memoranda No. 1456
- (65) D. Colson, Air Flow over a Mountain Barrier (1949) - Trans. Am. Geophys. Union, Vol. 30
- (66) D. Colson, Effect of a Mountain Range on Quasi-Stationary Waves (1950) - J. Meteor. Vol. 7, No. 4
- (67) D. Colson, Results of Double-Theodolite Observations at Bishop, Cal. in Connection with the "Bishop-Wave" Phenomena (1952) - Bull. Am. Meteor. Soc., Vol. 33, No. 3
- (68) P. Fueney, The Problem of Air Flow over Mountains (1948) - Bull. Am. Meteor. Soc. Vol. 29
- (69) A. Wagner, Über die Tageswinde in der Freien Atmosphäre (1938) - Beitr. Z. Physik der Atm., Vol. 25, p. 145
- (70) E. Kleinschmidt, Sr., Über der Tagesgang des Windes, (1948-49) - Annalen der Meteorologie, Part I: March, 1948; Part 2: Dec., 1948; Part 3: No. 7-9, 1951
- (71) G. S. P. Heywood, Katabatic Winds in a Valley (1933) - Q. J. Roy. Soc., Vol. 59, p. 47
- (72) O. G. Sutton, Atmospheric Turbulence (1949) - Methuen, London
- (73) J. Z. Holland, The Diffusion Problem in Hilly Terrain (1952) - Chapter 96 of "Air Pollution", McGraw-Hill, New York
- (74) K. L. Calder, The Diffusive Properties of the Lower Atmosphere (1948) - G. B. Ministry of Supply

- (75) H. F. Poppendiek, Investigation of Velocity and Temperature Profiles in Air Layers within and above Trees and Brush (1949) - Univ. of Calif., Dept. of Engineering, Los Angeles
- (76) F. Gifford, Jr., Analysis of Low-Level Trajectories at Oak Ridge (1952) - unpublished
- (77) M. E. Smith, The Forecasting of Micrometeorological Variables (1951) - Am. Meteor. Soc., Meteorological Monographs, Vol. 1, No. 4
- (78) M. A. Giblett et al., The Structure of Wind Over Level Country (1932) - G. B. Met. Office, Geophysical Memoirs, No. 54
- (79) P. H. Lowry, Microclimate Factors in Smoke Pollution from Tall Stacks (1951) - Am. Met. Soc., Met. Monog. Vol. 1, No. 4
- (80) J. Z. Holland and R. F. Myers, A Contribution to the Climatology of Turbulence (1952) - Abstract in Bull. Am. Meteor. Soc., Vol. 33, No. 2, p. 78.
- (81) F. N. Frenkiel, Frequency Distributions of Velocities in Turbulent Flow (1951) - J. Meteor., Vol. 8, No. 5
- (82) P. E. Church, Dilution of Waste Stack Gases in the Atmosphere (1949) - Ind. Eng. Chem. Vol. 41, No. 12
- (83) N. R. Beers, Stack Meteorology and Atmospheric Disposal of Radioactive Waste (1949) - Nucleonics, Vol. 4, No. 4
- (84) F. J. Davis (Oak Ridge National Laboratory) - unpublished work
- (85) E. W. Hewson, Atmospheric Pollution by Heavy Industry (1944) - Ind. Eng. Chem., Vol. 36, p. 195
- (86) O. G. Sutton, A Theory of Eddy Diffusion in the Atmosphere (1932) - Proc. Roy. Soc., Lond., A, Vol. 135
- (87) O. G. Sutton, Micrometeorology (1953) - McGraw-Hill, New York
- (88) T. K. Sherwood, The Geometry of Smoke Screens (1949) - J. Meteor. Vol. 6, No. 6
- (89) O. G. Sutton, The Theoretical Distribution of Airborne Pollution from Factory Chimneys (1947) - Q. J. Roy. Met. Soc., Vol. 73
- (90) M. D. Thomas, G. R. Hill and J. N. Abersold, Dispersion of Gases from Tall Stacks (1949) - Ind. Eng. Chem., Vol. 41, No. 11
- (91) M. Eisenbud and W. B. Harris, Meteorological Technics in Air Pollution Surveys (1951) - A.M.A. Archives Ind. Hyg. Occup. Med., Vol. 3

- (92) C. A. Gosline, Dispersion from Short Stacks (1950) - Delivered Am. Inst. Chem. Eng., Annual Meeting, Columbus, Ohio, Dec. 3-6, 1950
- (93) U. S. Geological Survey, Water-Loss Investigations: Volume I - Lake Hefner Studies Technical Report (1952), Geological Survey Circular 229 - U. S. Dept. of the Interior, Geological Survey, Washington
- (94) O. G. Sutton, The Problem of Diffusion in the Lower Atmosphere (1947) - Q. J. Roy. Met. Soc., Vol. 73
- (95) O. G. Sutton, The Atom Bomb Trial as an Experiment in Convection (1947) - Weather, Vol. 2, No. 4
- (96) M. L. Barad and G. R. Hilst, A Recomputation and Extension of Parameters Involved in Sutton's Diffusion Hypothesis (1951), HW-21415 - General Electric Co., Hanford Works, Richland, Wash.
- (97) R. H. Sherlock and E. A. Stalker, A Study of Flow Phenomena in the Wake of Smokestacks (1941), Engineering Research Bull. No. 29 - Univ. of Mich., Dept. of Eng. Res., Ann Arbor
- (98) R. F. von Hobenleiten and E. F. Wolf, Wind-Tunnel Tests to Establish Stack Height for Riverside Generating Station (1942) - Trans. A.S.M.E., Vol. 64, p. 671
- (99) T. Baron, E. R. Gerhard and H. F. Johnstone, Dissemination of Aerosol Particles Dispersed from Stacks (1949) - Ind. Eng. Chem., Vol. 41, No. 11
- (100) P. H. Lowry, The Theoretical Ground-Level Dose-Rate from the Radio-argon Emitted by the Brookhaven Reactor Stack (1950), BNL-81(T-19) - Brookhaven National Laboratory, Upton, N. Y.
- (101) D. E. Jenne and G. R. Hilst, Meteorological and Climatological Investigations of the Hanford Works Area (1950), HW-19723 - General Electric Co., Hanford Works, Richland, Wash.
- (102) M. L. Barad, Diffusion of Stack Gases in Very Stable Atmospheres (1951) - Am. Met. Soc., Met. Monog., Vol. 1, No. 4
- (103) C. H. Bosanquet, W. F. Carey and E. M. Halton, Dust Deposition from Chimney Stacks (1949) - Institution of Mech. Eng., London
- (104) W. F. Davidson, The Dispersion and Spreading of Gases and Dusts from Chimneys (1949) - Ind. Hyg. Found., Mellon Inst., Pittsburgh, Trans. Bull. No. 13

- (105) F. W. Thomas (T.V.A., Wilson Dam, Ala.), Plume Observations - Watts Bar Steam Plant (1952) - Unpublished manuscript
- (106) O. F. T. Roberts, The Theoretical Scattering of Smoke in a Turbulent Atmosphere (1923) - Proc. Roy. Soc. Lond., A, Vol. 104, p. 640
- (107) W. Schmidt, Zur Berechnung der Raumlischen Verteilung von Rauch und Abgasen in der Freien Luft (1926) - Gesundheits - Ingenieur, Vol. 49, No. 28

A METEOROLOGICAL SURVEY OF THE OAK RIDGE AREA

U. S. Weather Bureau

Oak Ridge, Tennessee

Part I. Background

Purpose of the Meteorological Survey

1. Activities Subject to Effects of Weather and Climate

At Oak Ridge, Tennessee, the U. S. Atomic Energy Commission is engaged in a costly and highly complex program of production and research. Several large industrial plants and research laboratories, as well as a large government-owned town and an experimental farm are spread over an area of nearly 100 square miles. The effects of weather and climate are felt in many ways, but three broad categories may be said to be of greatest importance to the Commission. These are:

- (a) the effects on atmospheric transport and dilution of contaminants,
- (b) the effects on design and construction of facilities, and (c)

the effects on day-to-day operations.

Atmospheric transport and dilution, subject as they are to variations due to meteorological conditions, are of importance largely because of the peculiarities of the atomic energy industry. It is known that human beings and other organisms can be harmed by excessive exposure to nuclear radiation, either from external sources or from radioactive substances taken into the body. For this reason, disposal to the atmosphere of volatile or particulate radioactive wastes must be done

with some knowledge of the concentrations likely to reach populated areas. Such radioactive wastes are produced in the Oak Ridge area by fission or neutron absorption in nuclear reactors, their reflectors, shields, coolants and associated apparatus, by chemical separation processes applied to radioactive mixtures, and by experimental uses of radioactive elements. In addition, huge amounts of radioactive materials are constantly in storage or process. These must be handled with a minimum of risk to surrounding populations from possible discharge to the atmosphere, due either to accidental equipment failure or to willful sabotage. Potential hazards of dispersion in the atmosphere must also be considered in the case of several highly toxic non-radioactive chemicals used and stored in large quantities, or discharged as wastes from industrial processes in the Oak Ridge plants.

The effects of climatological factors on design and construction of facilities are more familiar. As long as the physical facilities at Oak Ridge are subject to modification and expansion to keep pace with the developing atomic energy program, design and construction work are a major preoccupation. Knowledge of the averages, frequencies, and local variations of climatological factors such as temperature, wind, and rainfall can be of considerable practical value in locating and designing such facilities, estimating heating, air cooling or water cooling capacities, planning drainage and waste disposal systems,

scheduling various phases of construction such as earth work, road work, concrete laying and plastering, and estimating costs. Many items of technical equipment, too, must be designed with allowance for the range of temperature, pressure or humidity to which they will be exposed.

In short-range and long-range planning of day-to-day operations and in evaluating their progress, climatological factors are often important. Past records as well as forecasts are useful in estimating fuel needs, planning outdoor maintenance work and scheduling certain types of experiments and tests. Current weather records are of assistance in analyzing progress of construction, performance of equipment, and variations in biological or agricultural experimental results.

The foregoing enumeration of activities subject to effects of weather and climate, while not exhaustive, is sufficient to give an indication of the Commission's reasons for undertaking in 1948 a detailed meteorological survey of the Oak Ridge area. The scope of the survey program was largely determined by the nature of these activities, their relative importance, and their susceptibility to meteorological effects not deducible from the standard climatological records.

2. Objectives of the Survey

The meteorological survey program has had three basic objectives:

- (a) to supply detailed climatological information for the Oak Ridge Area;

(b) to apply meteorological theory and observations to the operational problems of the AEC at Oak Ridge, and,

(c) to make recommendations as to a continuing meteorological service program which would suit the needs of the AEC.

Under the heading of climatology, the main emphasis has been placed on those elements most directly involved in the transport and dilution of contaminants, namely, wind speed and direction, turbulence, and vertical temperature gradient in the lower atmosphere. In hilly country such as that at Oak Ridge, the horizontal and vertical variations of these elements in relation to the topography and prevailing weather conditions had to be investigated. At the same time an effort was made to secure sufficiently complete data on standard climatological elements such as temperature, precipitation, humidity, barometric pressure and general weather conditions to satisfy the needs of the AEC and its contractors. The results of these climatological studies are summarized in Part III of the present report.

The application of meteorology to operational problems can be subdivided into two phases. The first phase consisted of the development of techniques. It was not known to what extent existing atmospheric diffusion formulas would be applicable in terrain of this type. The objective was to arrive at a set of combined theoretical-empirical techniques and formulas suitable for solving the range of atmospheric contamination hazard problems likely to be encountered in this area. The results of this phase are contained in Part IV of the present report.

The second phase of the application to operational problems consisted of consultation with the AEC and its contractors on specific problems as they arose. Many of the problems were unrelated to atmospheric diffusion. The objective has been to provide the best estimates of probable risks in each case, utilizing the means at hand. This phase has been essentially a service program, not an integral part of the meteorological survey, and the results are summarized elsewhere (Ref. 1 - 4).

The question of suitable permanent meteorological facilities and the requirements for continuing meteorological service have been kept in mind throughout the survey program. Specific efforts have been made to obtain climatological data, instrument evaluation data and experience with the meteorological needs of the AEC and its contractors on the basis of which recommendations could be made as to the types and numbers of observations to be made, methods of recording these observations, and permanent arrangements for meteorological consultation. The specific results and recommendations do not come within the scope of the present report but have been presented separately.

The thoroughness with which the above objectives could be pursued was subject, of course, to certain limitations of time, money and manpower. Such a quantity and variety of observational data have been collected, however, that an analysis limited to the practical

objectives of the program cannot have extracted more than a fraction of their meteorological value. It is hoped that some of their interesting implications can be looked into more deeply in the future.

3. Scope of This Report

This report is intended to present the background, history, methods and results of the meteorological survey of the Oak Ridge area, carried out by the Weather Bureau for the Atomic Energy Commission. In the description of equipment and techniques, the emphasis will be on such departures from standard methods as were necessitated by the peculiarities of the problem. It is intended that the meteorological summaries be presented in sufficiently complete and useful form to be directly applicable to most of the practical problems of the future, and also to indicate to research workers the content of the detailed records from which they are drawn.

Description of the Area

4. Topography

The Oak Ridge reservation is located west of Knoxville, Tennessee within the large valley which splits the southern Appalachian Range into the Great Smoky Mountains on the southeast and the Cumberland Plateau on the northwest (fig. 1). Oriented ENE-WSW north of Tennessee-Virginia line, where it is narrow and indistinct, the valley

turns southwestward in the Knoxville-Oak Ridge Area, where it is about 40 miles wide and enclosed by relatively steep walls, then south-southwestward to Chattanooga and southward to Rome, Georgia, becoming gradually wider and less clearly defined. The valley floor slopes from over 1500 ft. (Mean Sea Level) at Bristol, Tennessee to below 700 ft. MSL at Chattanooga, and is highly corrugated with broken ridges 300 to 500 ft. high oriented parallel to the main valley. The Great Smoky Mountains and Blue Ridge east and southeast of Knoxville exceed 6500 ft. MSL at several points; this highland, about 70 miles wide, is largely drained by the Tennessee River, and falls off relatively abruptly to the Piedmont of North and South Carolina. The Cumberland Mountains rise to heights above 3500 ft. MSL 10 to 15 miles north and northwest of Oak Ridge; drained by the Cumberland River, the Plateau gives way gradually to the hilly country of middle Tennessee and Kentucky.

The Government reservation at Oak Ridge is bounded on the NE, SE and SW sides by the Clinch River, a tributary of the Tennessee; the NW side is formed by Blackoak Ridge, one of the corrugations of the large valley (Fig. 2). The over-all length of the reservation in a SW-NE direction is about 17 mi., the over-all width about 9 mi. and the actual area about 92 sq. mi. (Ref. 5). Six parallel ridges, cut by many ravines and occasional gaps run lengthwise through the reservation spaced, on the average, about one mile apart. Their tops vary from below 1000 to above 1200 ft. MSL. The valleys fall from above 900 ft. MSL.

in the north-central part of the reservation to below 800 ft. MSL near the river. The ridges are almost completely wooded, while the valleys are mainly overgrown farm land. A thorough study of the geology of the area has been made by Prof. Paris B. Stockdale (Ref. 6)..

5. Commission Facilities

The Atomic Energy Commission facilities virtually cover the entire area if storages, waste disposal, communications, water supply and recreational facilities are included. Major concentrations, however, are (a) the Oak Ridge townsite, (b) the K-25 area, (c) the Y-12 area, (d) the X-10 area and associated drainage area, and (e) the University of Tennessee-AEC Agricultural Research farm.

The town of Oak Ridge occupies the northern corner of the reservation (Fig. 2), including the eastern half of Blackoak Ridge and East Fork Valley as well as the adjoining portions of Emory Valley, Gamble Valley and the northern slopes of East Fork Ridge and Pine Ridge. It is drained by the East Fork of Poplar Creek, which flows southwestward to join the main Creek at the western end of the reservation. The town contains all the residential and commercial property on the area, as well as the AEC administrative headquarters and the educational and research facilities of the Oak Ridge Institute of Nuclear Studies. It covers an area of about 10 sq. mi., a range of altitudes from about 800 to 1200 ft. MSL, and a great variety of terrain.

The K-25 Area, in the western corner of the reservation, lies on both sides of Poplar Creek between the point of entry of East Fork and the Clinch River. The land is mostly below 800 ft. MSL. This area is devoted to the huge Gaseous Diffusion Plant for the separation of U-235 from natural uranium. Almost entirely a closed process, this operation does not give rise to atmospheric diffusion problems in the ordinary course of events. However, evaporative cooling towers are employed on a large scale, and numerous other engineering problems involve climatic factors. This plant as well as the Y-12 and X-10 plants are operated for the AEC by the Carbide and Carbon Chemicals Company.

Y-12 is the designation of a large plant occupying the upper end of Bear Creek Valley, between Pine Ridge and Chestnut Ridge. Actually drained by the East Fork of Poplar Creek which runs northeastward to Midway Gap, this is the highest valley on the area, bracketing the 1000 ft. contour. At this site are located the Electromagnetic Separation Plant, the Biology Division of the Oak Ridge National Laboratory, and a variety of other production and research installations.

The Oak Ridge National Laboratory proper occupies the area known as X-10, in the portion of Bethel Valley drained by Whiteoak Creek. Here, and in the adjacent Melton Valley, are located several nuclear reactors of widely different types, a variety of radiochemical pilot plants, the AEC's primary radioisotope production plant, and extensive research

laboratories. Numerous sources of radioactive waste gases and aerosols exist in this area, including notably the air-cooled graphite pile and the production-scale chemical separations plants. Liquid wastes are decontaminated to a certain point, then discharged into Whiteoak Creek; after passing through the gap in Haw Ridge, this stream is impounded behind an earth-fill dam to allow the radioactivity to settle and decay before release at a controlled rate into the Clinch River. The entire Whiteoak Creek drainage area, covering about 6 sq. mi. between Chestnut Ridge and Melton Hill (Fig. 3), has been subjected to particularly intensive study during the present meteorological survey program.

About 1,000 acres of farm land in the southeastern portion of the area are being used for the maintenance of large animals used in radiation exposure studies, and for agricultural experiments utilizing radioisotopes. This research farm and its laboratories are operated for the AEC by the University of Tennessee.

6. Nearby Towns and Industries

There are over 60 towns within about 25 miles of the Oak Ridge area, with a combined population of about 200,000 (Ref. 7). More than 60% of this population is concentrated in Knoxville, and more than 95% in the twelve towns of 1000 or over, listed in Table 1.

Table 1 Towns of 1000 or Over

<u>Town</u>	<u>Population, 1950</u>	<u>Distance from X-10 (Miles)</u>	<u>Direction</u>
Knoxville	124,769	19 to 25	E
Oak Ridge	30,229	8	NNE
Harriman	6,389	16	W
Lenoir City	5,159	9	S
Rockwood	4,272	21	WSW
Clinton	3,712	16	NE
Loudon	3,567	13	S
South Harriman	2,761	17	W
Lake City	1,827	21	NNE
Kingston	1,627	12	WSW
Norris	1,134	22	NE
Oliver Springs	1,089	9	N

A diversity of small industries is located in Knoxville and outlying areas.

The largest single plant in the vicinity is the ~~Aluminum Company of America~~, Alcoa Plant, 22 mi. SE of the X-10 site. The nearest Tennessee Valley Authority dams are the Fort Loudon dam, 10 mi. S, Norris Dam, 25 mi. NNE, and Watts Bar Dam, 35 mi. SW. A large steam power plant is under construction by the TVA near Kingston, about 11 mi. W of this site.

History of Meteorological Observations

7. Nearby Weather Stations

Three different types of standard weather records have been utilized as background material for the present survey: (a) complete surface weather observations at first-order Weather Bureau stations; (b) climatological substation records of temperature and precipitation; and (c) upper-air observations.

Complete surface weather observations include hourly temperature, relative

humidity, wind direction, wind speed, and precipitation, 6-hourly to hourly visual observations of sky conditions, weather phenomena, and barometric pressure, and daily maximum and minimum temperature, total precipitation, prevailing wind direction, and fraction of possible sunshine. Such observations have been recorded at Knoxville continuously since 1871, first by the Signal Corps, and, since its establishment in 1891, by the U. S. Weather Bureau. After having been located at various buildings in Knoxville, the Weather Bureau office was installed in its present location at McGhee-Tyson Airport, about 15 mi. SSW of the city and 21 mi. ESE of the Oak Ridge National Laboratory, on March 1, 1942. Other stations in the southern Appalachian area having long records of complete surface observations are Chattanooga, Tennessee, 75 mi. SW, Bristol, Tenn., 120 mi. ENE, Smithville, Tenn., 75 mi. W, Asheville, N. C., 100 mi. ESE, and Rome Ga., 120 mi. SSW.

At climatological substations, often manned by unpaid cooperative observers, records are kept of daily total precipitation and, in most cases, daily maximum and minimum temperature. Such stations have been in operation for over 60 years at many places in the United States. Because of the interest of the TVA in accurate precipitation data, and because of the large local variations in precipitation associated with the irregularity of the terrain, many more precipitation stations are maintained in this region than temperature stations. There are 25 rain-gage stations within 20 miles of the Oak Ridge area, of which only four also have temperature records at present. These four

are Knoxville (82 years), Knoxville Airport (14 years), Loudon (58 years), and Norris (16 years).

Upper-air wind observations are normally obtained by tracking a free balloon in one of two ways; visually, or by radio direction finding. The visual type of observation employing an optical theodolite, is called a pilot balloon observation, abbreviated "pibal", and is limited to the levels below cloud layers. Pibals have been taken four times a day at Knoxville for nearly 25 years, and long records are also available at Chattanooga, Nashville, Atlanta, Ga., and Spartanburg, S. C. Radio wind observations, abbreviated "rawin", which are independent of intervening clouds, have been made twice a day at Nashville since January 1947. There were no other winds-aloft stations within 200 mi. of Oak Ridge during the period of the survey.

Observations of upper-air temperature, humidity and pressure have been made twice a day since 1939 at a number of weather stations in the United States by means of free balloons carrying radio-telemetering transmitters called radiosondes. The abbreviated name for this type of observation is "raob". The nearest raob stations are Nashville, 130 mi. W, Atlanta, 140 mi. S, and Greensboro, N. C., 250 mi. E.

8. Oak Ridge Observations Prior to the Survey Program

No known meteorological observation stations were in existence within the present Government reservation prior to the advent of the Manhattan

Engineer District (wartime atomic energy project). With the initiation of scientific and industrial activities, however, meteorological records of one kind or another were kept by various groups on the area.

Simultaneously with the startup of the "Clinton pile" (X-10 graphite reactor) in November 1943, instruments were installed on a 120 ft. water tank with an added 60 ft. mast to record continuously the temperatures at six levels from 4 ft. to 183 ft., the wind direction and speed at about 130 ft., and the wet-bulb temperature at 4 ft. Hourly, daily and monthly records obtained from the instrument charts were kept by the Health Physics Division of the Clinton Laboratories (now Oak Ridge National Laboratory). In addition to these items daily rainfall, barometric pressure, and cloudiness were also recorded. This station became an official Weather Bureau cooperative station in 1947. With minor modification, the X-10 Health Physics Division records have been continued up to the present (referred to as station 012 in following sections of this report). During this same period hourly readings of the barometric pressure, temperature and wet-bulb temperature at the air intake of the X-10 pile building have been recorded by the Pile Operations Department.

Since the K-25 Gaseous Diffusion Plant began operation early in 1945, hourly records of temperature and wet-bulb temperature have been maintained by the Process Utilities Department at two cooling tower installations (one of these is station 013 in the present report).

Partial records of barometric pressure have been kept by scientists of the K-25 Research and Development Laboratory during this period. Starting in May 1948, this laboratory has maintained a recording anemometer and wind vane, installed about 4 ft. above the roof (station 014).

In the town of Oak Ridge, the earliest meteorological records were those of Mr. R. A. Ward, 493 W. Outer Drive, a cooperative observer for the Weather Bureau. His carefully kept records of daily maximum and minimum temperature and daily total precipitation cover the period May 1947 through April 1948. In November 1947, the AEC Department of Public Works installed instruments at Cheyenne Hall (now Management Services, Inc., Bldg. No. 1) to record continuously temperature, relative humidity, wind direction and wind speed. Daily observations of maximum and minimum temperature and precipitation were begun in May 1948 by that department as a Weather Bureau cooperative station, continuing the record begun by Mr. Ward, the purpose being to check the claims of construction contractors for extensions of time. This station (numbered 011) was taken over by the Oak Ridge Weather Bureau Office in December 1948 and has been maintained in operation up to the present time with minor changes.

Informal records of temperature, barometric pressure, rainfall, wind speed and direction, state of ground and weather conditions have been maintained for shorter periods by laboratory scientists, construction and maintenance contractors, sewage plant operators, and others on the

area, but only the more complete records enumerated above have been utilized in the present study.

Program of the Meteorological Survey

9. Scope of the Survey

The following excerpt from the "Proposed Meteorological Program" submitted to the Medical Advisor, Oak Ridge Operations, Atomic Energy Commission by the Scientific Services Division of the Weather Bureau in March 1948, presents the survey program as originally conceived: "the principal effort at Oak Ridge should be concentrated on the acquisition of detailed knowledge of wind and temperature fields in the lower kilometer (the friction layer) over the reservation and its neighborhood, and their correlation with the general fields shown on standard maps and charts for large areas; the existing and newly acquired knowledge of atmospheric diffusion would be applied with those data as parameters."

This was essentially the scope of the survey. No weather forecasting was done by the Oak Ridge office, responsibility for the function remaining with the Weather Bureau Office at Knoxville.

10. Chronological Resume

It is convenient to distinguish three periods in the history of this project: (1) preparation, December 1947 to November 1948; (2) observation, December 1948 to November 1950; (3) analysis, November 1950 to present.

On December 4, 1947, Dr. Albert H. Holland, Jr., then Medical Advisor to the Manager of Oak Ridge Operations, addressed a letter to Dr. F. W. Reichelderfer, Chief, U. S. Weather Bureau, requesting advice with respect to a proposed meteorological survey of the Oak Ridge Area. Subsequently, two visits to Oak Ridge were made by meteorologists R. C. Wanta and F. D. White, representing the Scientific Services Division of the Weather Bureau. Following the detailed recommendations

of Messrs. Wanta and White, a formal request for the Weather Bureau to undertake such a survey was submitted to Dr. Reichelderfer by Dr. Holland in a letter dated May 24, 1948, and agreed to by Dr. Reichelderfer June 4, 1948. A Weather Bureau Office was established at Oak Ridge, to operate under the local administrative control of the Medical Advisor's office, later transferred to the Office of Research and Medicine. The Atomic Energy Commission agreed to transfer to the Weather Bureau sufficient funds to cover the salaries of the Weather Bureau employees and other Weather Bureau expenses necessary to the program, to procure directly all necessary equipment and supplies, and to furnish stenographic service to the Weather Bureau Office. J. Z. Holland, Meteorologist in Charge of the new office, reported at Oak Ridge on July 26, 1948, and the remainder of the initial staff appeared on the scene during the following four months. The preoccupations of this period included procurement of equipment, choice of sites for instrument installations, preliminary collation of existing meteorological records in the area, and numerous conferences with technical personnel in the local plants and offices for the purpose of defining the problems of mutual interest. To culminate this preparatory phase of the program a detailed plan for the main study was drawn up (Ref. 8).

The observational phase of the program was begun with surface and winds aloft observations in November 1948, and with the installation of temperature and humidity recorders, the first instruments to be received. By March 1949 the bulk of the instrumentation for area coverage of wind, temperature and humidity was in operation, and by mid-summer of 1949, the entire observation program was in full swing. In order to obtain representative data for all seasons, and in order to make up for gaps occasioned by turnover of personnel,

the intensive observation schedule and full instrumentation were continued in operation through November 3, 1950. During this observation period of approximately two years, instrument chart reading and routine summarizing of data by means of IBM punched cards were kept on a current basis, several specialized meteorological studies were prepared for local interests, and a cooperative program of atmospheric radioactivity measurements was undertaken with the Health Physics Division, Oak Ridge National Laboratory. Continuous review and preliminary analysis of the observational data were carried on as they accumulated, resulting in occasional changes in observational schedules and techniques.

To indicate briefly the scope of the two-year observational program, the types and numbers of observations are summarized in Table 2. They were of two types with respect to spatial coverage: (1) automatic records at a number of fixed stations (Fig. 2) distributed so as to cover the characteristic terrain features of the area, and (2) automatic or manual observations from a single master observation station of meteorological phenomena and vertical gradients more or less representative of conditions over the area as a whole. The basic elements whose horizontal and vertical distributions were thus recorded consisted of wind direction, wind speed and temperature. Relative humidity and rainfall were also observed at a number of points. Second-order properties of the basic elements such as gradients and short-period fluctuations were measured mainly at the master station. Supplementary observations made at this station included weather, cloudiness, visibility, ceiling height, solar radiation, barometric pressure, smoke behavior, trajectories of zero-lift

balloons and state of the ground. Manual observations were carried on only during the 5-day working week but an attempt was made to approximate 24-hour coverage during this period. The types and numbers of observations are summarized in Table 2.

Table 2 Types and Numbers of Observations

<u>Meteorological</u>	<u>Automatic or Manual</u>	<u>Number of Stations</u>	<u>Height Ft.</u>	<u>Readings per day</u>	<u>Period of Record</u>
Surface Temperature	Aut	6-14	4-5	24	11/48-present
Surface Wind Direction and Speed	Aut	6-14	20-140	24	3/49-present
Relative Humidity	Aut	10-14	4-5	24	11/48-11/50
Rainfall	Man	1	3	4	11/48-11/50
	Aut	3-5	3	24	5/49-present
Solar Radiation	Aut	1	20	24	12/48-present
Barometric Pressure	Man	1	3		11/48-11/50
	Aut	1	3	24	11/50-present
Grass Temperature	Aut	1	0	24	7/50-11/50
50-foot temperature Differential	Aut	1	4-54	24	6/50-12/51
180-foot Temperature Differential	Aut	1	5-183	24	1/44-present
Low-level wind profile	Aut	1	6-54	24	9/49-11/50
Weather, clouds, etc.	Man	1		4-8	11/48-11/50
Upper-air temperature	Man	1	4-1500	4-15	4/49-11/50
Upper-air wind	Man	1	175-9400	4-8	11/48-11/50
Smoke trail	Man	1	0-200	2-3	4/49-2/50
Zero-lift balloon trajectory	Man	1	0-2000	(2-4 series (2-5 runs/series (20-60 readings/run 24/	12/48-11/50 (intermittent)
Radioactivity	Aut	3	3-4	24/	9/50-4/51 (intermittent)

A simplified summary of the operating personnel is shown in Table 3.

While the intensive observation program was in progress, four observers, one of whom was a supervisor, maintained nearly round-the-clock schedules five days a week at the X-10 field station, taking all the manual

observations and doing some checking and chart reading. One observer-technician devoted most of his time to maintaining the recording instruments in operation, changing charts and checking calibrations, the remainder of his time being devoted to assisting in observations and processing. Three statistical clerks were employed in the AEC Administration Building, Oak Ridge, reading charts, doing routine computations and summaries, and assisting in personnel, supply, office administration, and public contacts. Much of the statistical summarizing was done by a well equipped IBM unit at the Y-12 plant. The two meteorologists were almost completely occupied with short and long range planning, checking and evaluation of data, technical consultation on service problems and station administration. The remaining fraction of their time was given to analysis of data, preparation of technical papers, study of the literature in this rapidly developing field, and, not the least important, familiarizing many local groups of scientists and engineers with the fundamentals of meteorology in relation to Oak Ridge activities.

Between November 1950 and the present, the final phase of the survey has been completed, namely, that of digesting the observational material of the previous two years. During November 1950, nearly all manual observations ceased and most of the recording instruments were shut down. The observers were assigned to summarizing, analysis and drafting. The instrument technician was put to work part-time on tests and experiments connected with the development of a suitable permanent instrument network for

the area in addition to maintaining a small number of automatic recording stations in operation. Employees were gradually released, and by the summer of 1951 the two remaining observers were promoted to meteorologist positions and virtually all the effort (over and above that devoted to specialized service problems and maintenance of current records at a minimum level dictated by service requirements) was shifted to analysis and preparation of final charts and tables. By June 1952 the personnel consisted of three meteorologists, one technician and one clerk.

Table 3 Number of employees

Year ending:	6/30/49	6/30/50	6/30/51	6/30/52	6/30/53
Meteorologist	2	2	2	4	3
Observer	4	4	3	0	0
Instrument technician	0	1	1	1	1
Statistical Clerk	2	3	3	2	1
Total	8	10	9	7	5

Several technical papers have been published or prepared for restricted use during the course of the investigation (Ref. 1 - 4, 9, 10, 12, 15, 46, 73, 76, 80). The results contained in these papers will be utilized in the present report wherever they apply.

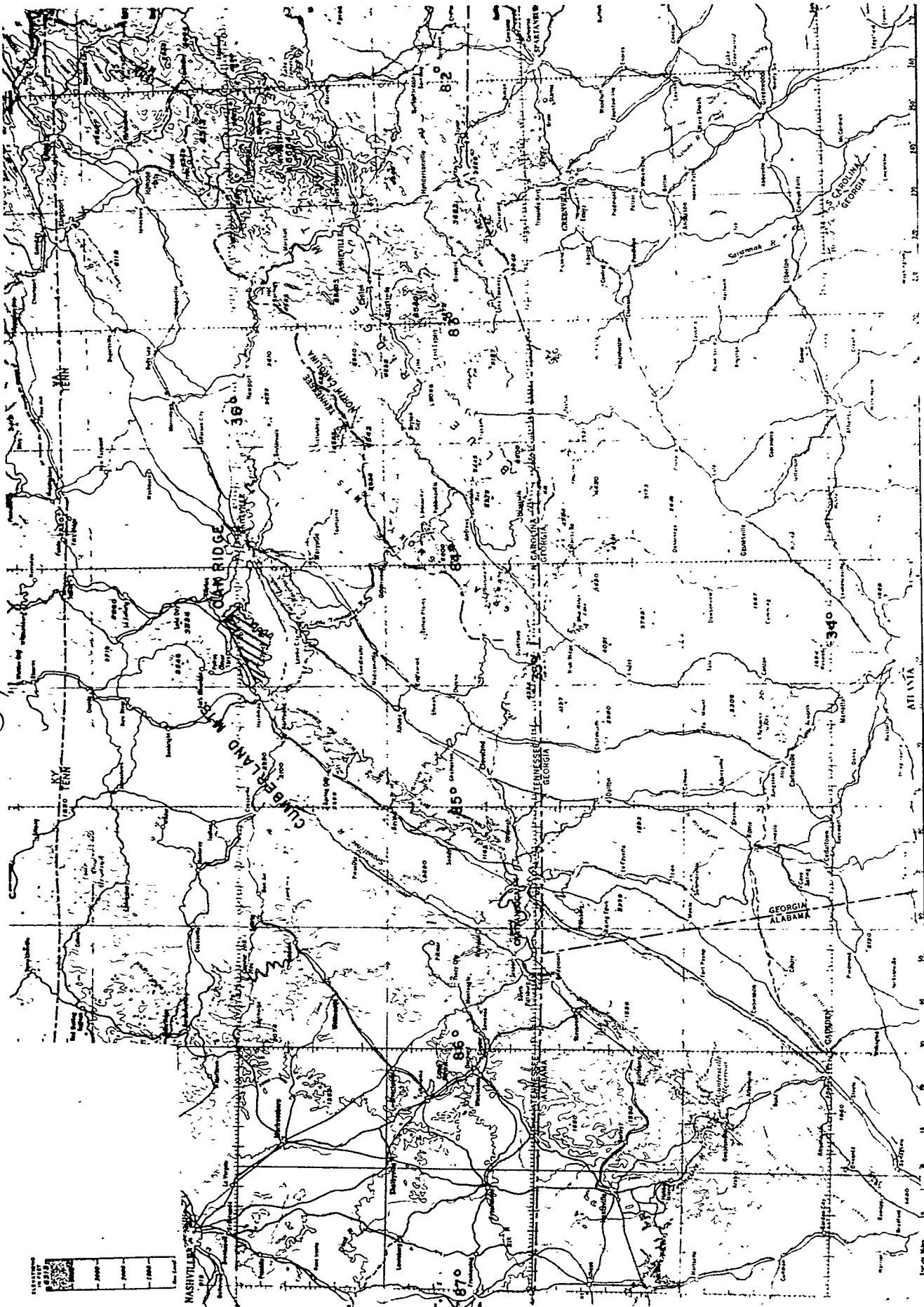


Fig. 1 Map of the Southern Appalachian Area. 1000-ft. contours.

55

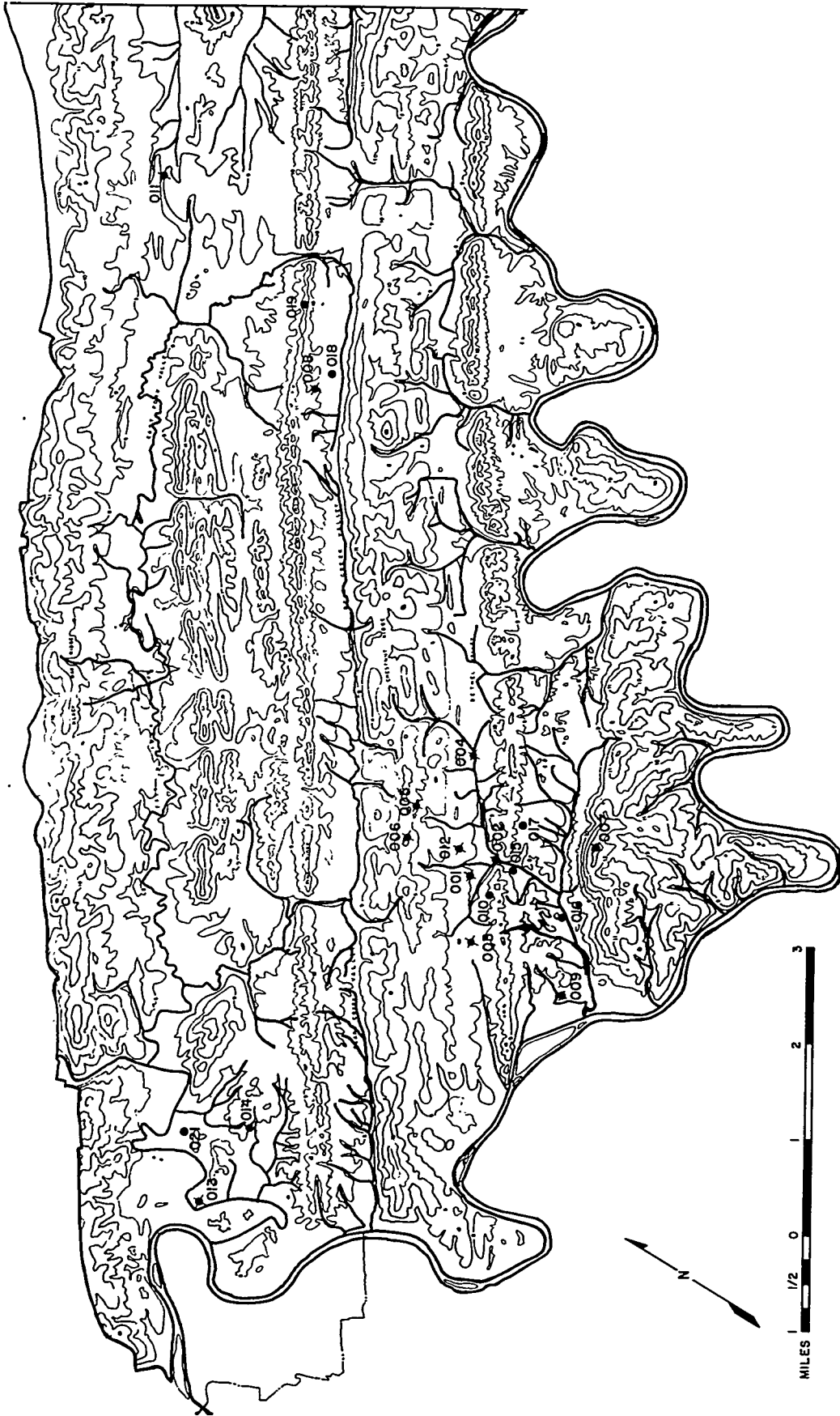


Fig. 2 Map of Oak Ridge reservation showing micronet stations. 100-ft. contours.

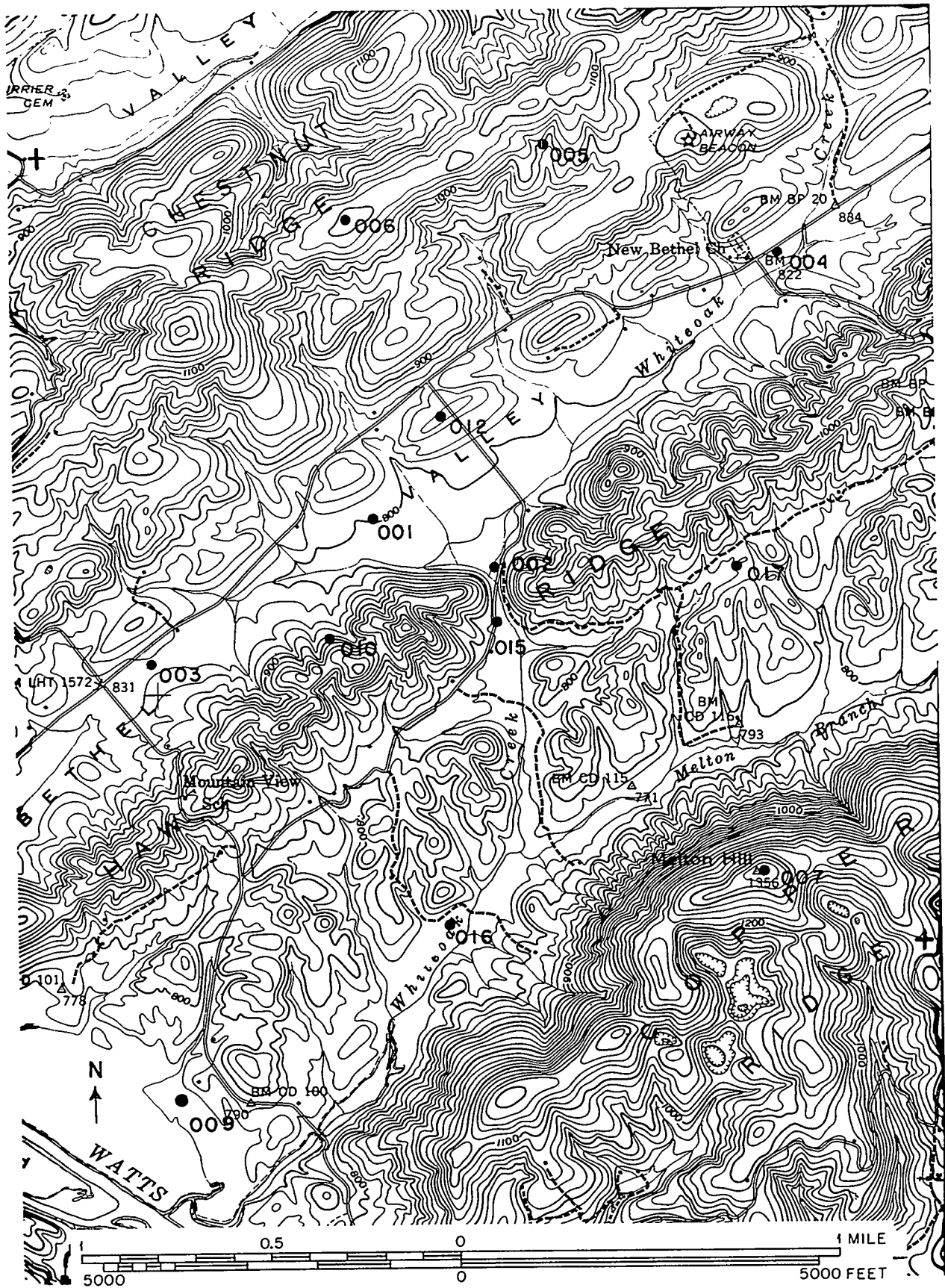


Fig. 3 Map of Whiteoak Creek drainage area (Bethel and Melton Valleys and adjoining ridges). 20-ft. contours.

A METEOROLOGICAL SURVEY OF THE OAK RIDGE AREA

U. S. Weather Bureau

Oak Ridge, Tennessee

Part II. Observational Equipment and Procedures

Observational Requirements and Limitations

1. Observational Requirements for Diffusion Studies

It has been recognized for some time that turbulent eddies are responsible for the observed diffusion of suspended matter in the atmosphere (Ref. 11). The intensity of turbulent mixing is known to be dependent primarily upon the wind shear, the roughness of the underlying surface, and the vertical gradient of temperature in the atmosphere. In order to obtain a coherent picture of the diffusion phenomena at a given site, then, it is evident that one must have observations of the following kinds:

- (a) Wind direction and speed; their horizontal, vertical, diurnal and seasonal distribution and interrelations with the other elements, both as an indication of the direction and speed of travel of contaminants and as a measure of the diffusion potential.
- (b) Temperature distribution; horizontal, vertical, diurnal and seasonal, primarily as a causal factor in the development or suppression of convection currents.
- (c) Turbulence: the intensity of the eddies themselves, insofar as they can be directly observed by measuring the fluctuations of speed and direction at a point or, better, along the path of a freely drifting particle in the atmosphere.

(d) Indicators of diffusion: these may be natural properties such as water vapor content, radioactive emanations, or mean horizontal momentum, whose observed distribution is the result of turbulent exchange between the earth's surface and the free atmosphere, or they may be artificially introduced substances such as smoke or radioactive gases, the rate and character of whose dispersion from a known source can be observed under a variety of meteorological conditions.

It would appear that (a) and (b) are the independent variables in the problem, (d) the dependent variable whose functional form is desired, and (c) the physical mechanism relating the variables and that, if satisfactory observations of these variables could be obtained, a complete solution should be possible. However, the interrelations and uncontrollable variations are so complex as to have defied analysis thus far by the leading researchers even for level grassland. In such irregular terrain as that of the Oak Ridge area any hope of success in a fundamental scientific attack on the problem within a few years' time was precluded. Thus, as recommended in the 1948 proposal, the approach taken has been essentially a descriptive one, with the object of determining the range and distribution of the variables, relating the observed diffusion behavior semi-quantitatively (by broad categories) to the presumed independent variables, and adapting the existing diffusion equations for use as extrapolation formulas incorporating locally observed parameters. Accordingly, the observational

equipment and techniques were not required to meet the exacting standards of a fundamental diffusion investigation. Maximum use was made of commercially available instruments and well-established methods. The accuracy specifications which were decided upon were such as to permit a definite resolution of the major meteorological patterns while still being attainable within the budget and time scale of the survey.

For the horizontal pattern of wind flow, it was decided that observations of wind speed accurate to about 1 mph and wind direction to 16 points of the compass should be obtained at one suitable height at each of about 10 sites selected so as to sample a typical ridge-slope-valley-gap configuration plus a few comparison points in other sections of the area. Since the Whiteoak Creek drainage area surrounding the X-10 site contains a suitable variety of terrain as well as being of greatest interest from the standpoint of atmospheric contamination, it was chosen as the area of concentrated sampling.

For the vertical distribution of wind speed and direction similar absolute accuracy was considered adequate. Relative accuracy at adjacent levels, however, had to be approximately $\frac{1}{2}$ mph and 10° of the compass or better, with observations spaced in proportion to the height above ground up to 5000-10,000 ft., where regional flow patterns shown by the existing pibal stations would be expected to prevail. It was realized that the vertical distribution at a single representative point within the area of concentration combined with a horizontal

distribution at a single height might not give a complete picture of the three-dimensional wind structure. However, such a compromise was considered acceptable since the cost of more elaborate instrumentation would be far out of proportion to the value of the additional information obtained. The vertical structure could be observed with relative ease at a conveniently located valley station: to instrument in addition for vertical sampling above slopes and hilltops would have been prohibitive.

Horizontal variations of temperature were to be measured over a range of altitudes and terrain forms similar to that selected for wind. It was expected that in hills 300 to 600 ft high, an accuracy of $\pm 1^{\circ}\text{F}$ would be sufficient to reveal significant differentials such as might produce convective circulations; the extreme inhomogeneity of the land and vegetation cover precluded finer temperature comparisons between different locations. For the vertical temperature distribution, it was considered necessary to have a relative accuracy of the order of 0.1°F between levels since small variations in the temperature gradient over relatively small height intervals can have quite pronounced effects on the eddy diffusion. In order to follow the heating and cooling processes, initiated at the earth's surface, which produce the variations in vertical temperature gradient, temperature measurements at the ground surface, standard 4-ft. height and approximately each hundred feet up to several thousand feet above ground at time intervals of 1 hour or less near the ground and 6 hours or

less at the higher levels were required. It was hoped that local observations up to about 1500 ft. could be combined with broader regional patterns derived from the nearest radiosonde stations (about 200 miles) to arrive at a coherent structure.

Detailed requirements for turbulence observations could not be set up at the start. So little was known about the existing frequency spectrum of turbulent eddies in relation to terrain, weather and altitude, or about the important portions of the spectrum for diffusion, and it was so doubtful that any instruments available commercially would be suitable for these measurements, that a certain amount of trial and error was anticipated. However, it was apparent that the gustiness as shown by continuous records from conventional anemometers and wind vanes would be useful as a starting point, and that the most serious deficiencies of such data requiring supplementary instrumentation would be their insensitivity to short periods (less than about 10 sec.) and low speeds (less than about 2 mph), their failure to show the history of any particular air parcel and their restriction to motions in the horizontal plane. Since the diffusion theory utilizes the "Lagrangian" (coordinate system moving with the fluid) turbulence parameters, which cannot ordinarily be directly deduced from the "Eulerian" (fixed coordinate system) parameters, it was desirable to have some measurement of the path of a particle carried by the wind. Similarly, while the mean air motion must be very nearly parallel to the earth's surface, there are vertical components

of the short-period eddies which are of primary importance in stack-gas diffusion. Thus the requirements for turbulence data were difficult both to define and to fulfill.

Ideal requirements for observations of the effects of diffusion such as the steady-state distribution of a tracer from a steady source could be set up without difficulty. One would desire a complete specification of the spatial distribution of concentration, at least to the distance of the major population centers, from a point source of known, constant emission rate at a height above ground which could be varied from zero to a few hundred feet above the highest stacks. However, in view of the virtual impossibility of obtaining such data at a reasonable cost by any known methods, some compromises had to be accepted. The aims which were adopted were to obtain qualitative information on cloud behavior by visual observation of smoke, and quantitative measurements of the concentration of a suitable tracer (preferably one of the actual radioactive contaminants from the plant) at a few selected points in space. Natural properties of the atmosphere such as temperature, humidity, momentum, and natural atmospheric radioactivity, whose distribution is partly controlled by eddy diffusion, could be used semiquantitatively for corroboration, although uncontrollable extraneous sources of variation would limit their usefulness.

Along with the direct observation of the variables of primary interest enumerated above, it was necessary that observations of the weather,

cloudiness, precipitation and state of the ground at intervals of at most six hours be available for use in interpreting the data. Furthermore, since the changes in thermal stability are caused primarily by gains and losses from the earth's surface of heat absorbed from the sun, continuous records of the intensity of solar and terrestrial radiation were considered to be highly desirable. In the absence of available instruments for the latter, however, only the incoming solar radiation was actually measured.

2. Observational Requirements for Climatology and General Service

As has been shown above, records of wind, temperature, humidity or precipitation were already being kept at several sites within the Oak Ridge reservation prior to the survey program. It was considered advisable to expand these climatological observations to the extent of having a complete representative station at each plant and the Townsite, in view of the expected value of such records in relation to their small cost. These records would also permit evaluation of the transferability of general patterns observed in the Whiteoak Creek Area to similar terrain features in other parts of the reservation. In addition, the observations of weather, cloudiness, state of ground, etc. required for the diffusion investigation were augmented by ceiling, visibility and barometric pressure to provide as complete a record of the standard climatological elements for general purposes as could be obtained without interfering with the wind flow and diffusion studies.

3. Limitations of the Observational Program

The usefulness of observational data obtained in a short-term survey of this type is subject to certain limitations which had to be borne in mind from the outset.

First, the short-term nature of the program limits the generality of the results. From one or two years' record of any climatological element, (e.g. temperature, wind direction or speed, rainfall) long-term normal values cannot possibly be deduced. It is often possible, from similar records at a nearby station having a long record, to obtain a rough idea of the deviations from normal during the short observation period, but such estimates become less reliable the greater the distance between the stations in question, and the less homogeneous the terrain. In the southern Appalachian area, appreciable variations in the climate occur over relatively short distances, so that the use of the long Knoxville record in attempting to extrapolate climatic normals for Oak Ridge might be of doubtful validity.

Nevertheless, it might be expected that interrelations between the elements could be correctly evaluated from observations extending over a long enough period to sample the predominant types of meteorological situations. For instance, the diurnal variation of vertical temperature gradient on clear and cloudy days, in each season, might be adequately determined in a year or two of observations, although the normal frequency of clear and cloudy days might not be known. Observations of all the elements in the cause-effect chain might thus yield relative

expectancies of the desired elements with respect to related elements. However, studies of objective forecasting methods utilizing past observations have shown that apparent interrelations between meteorological phenomena established on the basis of a few years' observations may fail to hold true in other years.

Secondly, limitations of time and money precluded the extensive, well planned program of instrument development necessary for a quantitative evaluation of existing diffusion theories. The observations had to be planned so as to yield parameters for substitution into the available formulas, and to indicate whether there is sufficient likelihood of adverse diffusion conditions developing within the expected range of meteorological conditions to justify a more refined study.

Similarly, practical limitations of time, money and manpower precluded a completely three-dimensional exploration of the temperature and wind fields, and it has been necessary to accept many gaps in the spatial distributions of these elements.

A final limitation which should be mentioned is the undeveloped state of this branch of meteorology. Lacking experience or guidance in many details of the investigation, it has been necessary to acquire the "feel" of the subject through trial and error. Needless to say, some of the lines of attack which were taken would be avoided or greatly modified if such a project were to be repeated.

Station 001 Instrumentation

4. The Site and "Hutment"

The master station, numbered 001 (Fig. 3) was located at the western edge of the X-10 plant site in the center of Bethel Valley. It was here that all manual observations were taken (except, of course, mobile surveys), and most of the data on vertical gradients and turbulent fluctuations of the elements were obtained. At the same time, the standard instrumentation of the outlying unmanned stations ("micronet") was virtually duplicated here. Thus station 001 provided a necessary link between the areal and vertical observations, and also a point of comparison between the Oak Ridge observations and the standard meteorological observations at nearby Weather Bureau stations.

Chosen for its relative flatness, freedom from obstructions to the wind, nearness to the main sources of atmospheric contamination, and availability of utilities, the site is at 810 ft. MSL and comprises an area about 100' x 300'. The only important obstructions to the horizon are the ridges on either side, the worst being Haw Ridge on the southeast which subtends about 15° in elevation. A two-story building about 100 yards north is in a relative depression of the ground and extends only about 15 ft. above the level of the station site. Fortunately, the directions from which the prevailing winds blow, namely, southwest and northeast, are the least obstructed.

A 16' x 32' double "hutment" type building (Fig. 4) was erected at this site to provide shelter for personnel and instruments, storage space, balloon inflation facilities and shop space for instrument calibration and maintenance. The prefabricated plywood structure required extensive reinforcement, remodelling and insulation before it was adequate for these purposes.

5. Contacting Wind Equipment

A contacting 3-cup anemometer, Instrument Corporation type 428, an Instrument Corporation type 3148 straight tailed 3 foot metal vane and an Instrument Corporation type 1014 8 point bearing were mounted on a standard 18 ft. stepped and guyed steel pipe support (Fig. 4) about 80 feet SW of the hutment. Inside the hutment was located an Esterline-Angus 10 pen operation recorder with a chart speed of $1\frac{1}{2}$ inches per hour. This system, designed for 8 volt D.C. operation, was used with a 9 volt Burgess type 4F6H battery which was later replaced with an 8 volt selenium rectifier. The initial installation at this station was identical with the wind systems initially installed at most of the micronet stations.

The operation recorder was also used to show the hundredths of an inch of precipitation on pen number 9 and the tenths of an inch of precipitation on pen number 10. The wiring of the switching unit for the rainfall record, internal wiring of the recorder, and inter-connection of units are shown in Figure 5.

The anemometer was carefully adjusted to have the minimum reliable contact pressure, the counter was disconnected and the 1/60 mile contact was removed to reduce the load on the cups. After this modification, the cups would begin to move at an air speed of about 30 feet per minute (1/3 mph) as measured by a heated thermopile anemometer. According to Wood (Ref. 12) the calibration error of this model anemometer is substantially constant at 0.5 to 0.75 mph from 3 mph to 40 mph. For the purposes of the survey, no instrumental corrections were applied to the wind speeds as read from the charts.

The wind speed was determined by counting the leading edges of the 1 mi. contacts shown in the direction traces within the hour. All data were recorded as of the end of the hour.

The wind direction was recorded to 16 points with the primary points (N, NE, E, etc.) shown as deflections of a single pen (Fig. 6A). The 8 intermediate points (NNE, ENE, etc.) are shown as simultaneous deflections of two adjacent pens (Fig. 6B). The mile contact of the anemometer was in series with the vane contacts so that a continuous direction record was produced during each speed contact. Consequently, when the wind was light and fluctuating, a number of directions in rapid succession occur during each hour (Fig. 6C).

The direction recorded for the greatest portion of the hour was taken as the prevailing direction. If two directions were recorded for an equal time, the following criteria were used in resolving the tie, applied in the order given:

- (1) The direction with the greatest duration of adjacent directions.
- (2) The direction with the greatest wind speed during the hour.
- (3) If the tied directions were two points apart, the intermediate direction was chosen, and if one point apart, the "even" direction, counting clockwise starting with NNE ("primary" or direction with least letters in abbreviation).
- (4) Direction Indeterminate (DI) was used if the tied directions were more than two points apart and could not be resolved by any of the above criteria.

The application of these rules to a chart such as Fig. 6C was rather difficult since it would be necessary for the chart reader to compare the duration of two simultaneous contacts (the intermediate direction) with the duration of each contact alone (the primary directions). The chart reader in such cases tended to favor the intermediate directions since there would usually be two adjacent direction traces which appeared to be more frequent than the directions on either side such as E and NE in Fig. 6C. Either a single contact would have to appear much more consistently than any other (Fig. 6A) or three adjacent contacts of almost equal frequency (Fig. 6D) in order for the reader to choose a primary direction.

These facts became evident when the first wind roses from the station were prepared. Wind roses for the same period from the other stations in the micronet employing the same wind system showed the same type of bias in favor of the intermediate points. A bias of similar type but favoring the primary directions had also been noticed in the published wind roses of the Knoxville Airport station when comparisons were made between that station and older data from the Oak Ridge area.

Two simple methods of correcting the wind rose data were considered, as well as the method of Ratner (Ref. 13). One would be a smoothing method: substitute for each direction frequency (f_i) the average of that frequency weighted double with the frequencies of the two adjacent directions $\frac{(f_{i-1} + 2f_i + f_{i+1})}{4}$. The second method would be based on the following two assumptions: (a) The bias consists in a constant proportional reduction of each primary and constant proportional exaggeration of each intermediate direction frequency; (b) the correct total frequency of primary directions is equal to the correct total frequency of intermediate directions. The second method, which we call "odd-even" correction, then consists of multiplying each observed primary direction frequency by the ratio of half the total direction frequency (excluding calm) to the total frequency of primary directions, and multiplying each intermediate direction frequency by the ratio of half the total frequency of all directions to the total frequency of intermediate directions.

The reasoning involved in the second method may be expressed as follows: Let a true primary direction frequency be f_i , and the biased frequency f_i' and let f_j and f_j' be the corresponding symbols for an intermediate direction frequency. Assumption (a) becomes:

$$(a) \frac{f_i}{f_i'} = \frac{\sum f_i}{\sum f_i'}, \frac{f_j}{f_j'} = \frac{\sum f_j}{\sum f_j'}$$

$$\text{or (a')} f_i = f_i' \frac{\sum f_i}{\sum f_i'}, f_j = f_j' \frac{\sum f_j}{\sum f_j'}$$

Assumption (b) becomes

$$(b) \sum f_i = \sum f_j = \frac{\sum (f_i + f_j)}{2}$$

Since the total frequency is unaffected by the bias:

$$\sum f_i + \sum f_j = \sum f_i' + \sum f_j'$$

and (b) becomes

$$(b') \sum f_i = \sum f_j = \frac{\sum f_i' + \sum f_j'}{2}$$

It is seen from (a') and (b') that the multiplier for f_i' is

$$\frac{\sum f_i}{\sum f_i'} = \frac{\sum f_i' + \sum f_j'}{2 \sum f_i'}$$

and the multiplier for f_j' is similarly

$$\frac{\sum f_i' + \sum f_j'}{2 \sum f_j'}$$

The two methods of correcting the wind roses were tested on (1) two wind roses from stations showing no apparent terrain channeling (Fig. 7, stations 006 and 009) and (2) two wind roses showing strong terrain

channelling (Fig. 7, stations 002 and 003) since it might be expected that channelling could produce such a preponderance of one or two directions as to upset the balance of primaries and intermediates. Data for the month of June 1949 were used. The correlation of the direction frequencies in each corrected rose with the direction frequencies obtained by carefully rereading the original instrument charts was used as a test of the ability of the corrected rose to represent the true distribution. The correlation of the original biased rose with the reread rose was computed in order to determine the improvement produced by the two correction methods. The original, reread, and corrected wind roses are shown in Fig. 7.

It was concluded that (1) in reading this type of wind chart the intermediate directions tend to be favored over the primary directions, (2) the bias is proportionally the same for all directions to a good degree of approximation, (3) the assumption of equal frequency of primaries and intermediates for 16-point wind roses is a useful approximation even under relatively strong terrain channelling, (4) the odd-even corrected rose gives a satisfactory representation of the true distribution of directions, and (5) simple smoothing is equally satisfactory only for stations without marked terrain channelling, (6) in view of the high correlation coefficients obtained with the odd-even correction method it was not necessary to utilize the more complex method of Ratner.

All wind data used in this survey were checked for bias and corrected by the odd-even method whenever the bias exceeded 10%, that is when the

multiplier for f_i or f_j was not between .90 and 1.10. This rule was applied to upper air data as well as surface data and to off-site data as well as local survey data.

6. Wind Profiles and Gustiness: Anemograph:

The contacting wind equipment, although adequate for measuring mean winds over periods down to a minute's duration (by using 1/60 mile contacts), gave no record of short-period gustiness. In order to obtain such a record at various levels above the ground, continuous-recording anemometers were needed. Of the many types available on the market, no single one combined the short-period response (down to the order of 1 second), accuracy (better than $\pm\frac{1}{2}$ mph from 0 to 30 mph), and freedom from resonance effects, which were desired. A combination of two systems was decided upon. One was the "anemograph" manufactured by the Instruments Corporation, employing a split-tail wind vane with a selsyn direction transmitter, a 3-cup anemometer with a D.C. magneto transmitter, and a combined selsyn-voltmeter recorder which produces two pen traces side by side, one for wind direction and one for speed. The main defect of this system, namely, insensitivity of the anemometer to speeds less than about 2 mph, was overcome by the second system: the "Airmeter" manufactured by Hastings Instrument Company, employing a heated thermopile (to be described in a later section). A vane, generator-cup anemometer and thermopile anemometer were installed at 6, 18, and 54 ft. above ground on a 50 ft. wooden pole with a 4 ft. steel pipe extension (Fig. 4). A higher mast was not considered justified since station O12, operated by the ORNL Health Physics Division in the same valley

only half a mile away, was equipped with an anemometer mounted on a water tower 140 ft. above ground on a small knoll, or 216 ft. above the station 001 ground level. The spacing of the levels at constant intervals of the logarithm of height was intended, as is commonly done, to facilitate calculation of the parameters in the two forms of wind profile formulas appearing in the literature: if a logarithmic profile applied, constant velocity differences would be observed between adjacent levels, or if a power law were correct, constant ratios would be found. A 4' x 4' platform of welded steel with a steel grating floor and 3' welded railing was installed at the top of the profile pole to provide a safe working space (Fig. 8).

The anemograph wind system employs an aluminum alloy spread tail vane coupled to a size 1, 60-cycle, 110 volt AC selsyn motor as a direction sensing element. The weight of the combined vane and hub is 1-1/4 pounds. The vane swings in permanently lubricated ball bearings and has required no attention or lubrication during the survey program. The resonant period of this vane has been determined by displacing the vane and measuring the period of the swing in wind speeds of 2 to 13 mph. (Fig. 9). The swings are heavily damped by the spread tail so that at 2 mph, an error of less than 5° was observed after two swings of the vane (12 seconds). The tests were made under neutral or slightly stable temperature gradient to allow as little interference from natural gustiness as possible.

The velocity sensing element is a D.C. generator driven by conical, beaded cups of monel metal. The total weight of the rotor is 10.6 oz. This velocity unit has not required any attention to either the sealed bearings or the brushes and commutator. The silver-graphite brushes operating on a silver-palladium commutator have been extremely satisfactory. The cup speed is linear with wind speed, turning 1000 rpm at 100 mph. The output of the generator is 1.5 volts per 100 rpm (1175 ohm load) above 3 mph. The starting speed of the cups has been measured at 90 to 130 feet per minute (about 1 to 1.5 mph). The system includes magnetic damping of the recorder so that as the cups were released from rest at various wind speeds, the time required for a steady velocity to be indicated was found to be 4 seconds. A wiring diagram of the anemograph system is shown in Figure 10. Five anemometers were each driven at 300 rpm with a synchronous motor and the three with most closely matched output were chosen for use on the profile pole. The variation between these three was less than 0.5 mph.

The recorder for this system used a 9" chart to record separate direction and velocity channels. The chart is driven by a single sprocket in the center, reducing the error caused by chart expansion to 50% of that found in the usual system where one edge of the chart is fixed and all expansion must result in moving the chart in one direction. A two pen mechanism produces a direction record on a single 0-360° scale by employing one pen at a time to follow the wind fluctuation and another which is latched at the opposite side of the chart. If

a wind shift occurs which rotates the vane past 360° , the first pen is released from the selsyn control and returned to its side of the chart with the second pen now unlatched and connected to the selsyn (see Figure 11). Thus if the wind direction fluctuates about north, both pens are used and no skipping across the chart is necessary.

In order to increase the reading accuracy of the wind speed chart, the recorders were all operated on a 0-37.5 mph full scale range and all velocities were recorded in half miles per hour. The prevailing wind direction and average velocity were recorded for the hour on which the 60 minute reading period ended. Two measures of the gustiness, the 15 minute ranges of direction and speed, were also recorded for the third quarter of each hour. The significance of these quantities will be discussed later.

7. Wind Profiles and Gustiness: Airmeter

The Hastings "Airmeter" was chosen as the low speed anemometer to complement the anemograph gustiness and wind profile measurements obtained at the 6, 18, and 54 foot levels at station 001. This instrument consists of a series of noble metal thermocouples arranged so that they are heated by a constant voltage AC source with a DC output measured between the center tap of the heating supply and the center tap of the couple. The circuit reduced to its simplest form is shown in Fig. 12. Alternate junctions of the heated couples are cooled by mounting in high thermal

conductivity studs. A temperature difference between successive junctions results which generates a DC voltage having a relationship to the air velocity past the unsupported junctions in accordance with the equations developed by King (Ref. 14). The junctions are butt-welded from .003" wire under controlled conditions. The diameter of the weld, the spacing of the junctions and the heating current may all be varied to obtain a wide range of sensitivities. In addition, the aerodynamics of the head in which the couples are mounted can be used to control the directional characteristics and the high speed sensitivity of the unit. The basic simplicity of the circuit makes it possible to utilize this instrument for routine operation under field conditions. Most of the previously available hot wire anemometers were not reliable or rugged enough for the routine operation desired in the accumulation of statistics on gustiness in the natural atmosphere.

The effect of humidity and temperature on the Airmeter probe has been determined by the Hastings Instrument Company not to exceed 2.6% with temperature variations between 70 and 115°F and humidity variations between 40 and 95%. The effect can be compensated by resetting the zero of the instrument since the shape of the calibration curve is not changed.

The calibration methods of the instrument manufacturer were analyzed and found to be as accurate as the present state of the art permits. A number of different techniques were employed to give a master calibration curve which was then standardized and matched by comparison in a tunnel.

A large number of values were obtained in wind tunnels equipped with an orifice and manometer, with pitot tubes, on whirling arms with a swirl correction, by traverse of measured distances in still air at night and by the use of the probe as a circular pendulum in a closed room. After comparison of the readings from these sources on a standard probe with a wind tunnel calibration from the National Bureau of Standards, the tunnel manometers were calibrated to read directly in velocity and the probes adjusted to match a standard curve in the tunnel.

The 3 original 8-junction probes (Fig. 13) supplied with the Precision Airmeter had calibration curves which matched exactly over the range 0-5 mph (low range). Probes B and C matched over the range 2-30 mph (high range) but Probe A departed considerably above 7 mph. A 2 second Brown Electronik recorder was used to record the output of the horizontally non-directional probes mounted at the three levels on the pole. A 2-junction probe mounted in the center of a $1\frac{1}{2}$ inch length of $\frac{1}{2}$ " tubing was also mounted at 18' above the ground to measure the magnitude of the vertical velocity although no differentiation was possible between the up and down motion. The calibration curves of the three probes and the directional characteristics of the ten-junction probes are shown in Figs. 14 and 15.

The Precision Airmeter unit included a timing switch which connected each of the four probes to the recorder in turn for a 3 minute period followed

by a 1 min. full scale deflection to permit positive identification of the switching points.

In order to obtain an average velocity for hourly periods by visual integration of the time cycled record, it was necessary to have a linear scale. It was also apparent that the time required to read off 5-min. velocities from the chart with a transparent overlay was much greater than that available in the small computing group.

Linearization of the output of the Precision Airmeter was accomplished through the cooperation of C. A. Mossman and P. E. Brown of the Application Section, Instrument Department, ORNL. The development of a non-linear analogue circuit was precluded by the short time available; instead, the following curve matching technique, suggested by W. G. James of the Circuit Development Group at ORNL, was adopted. The slide wire of a Brown Electronik recorder was divided into 5 sections and an appropriate shunting resistance for four of the sections was calculated from the Airmeter calibration so that the length-resistance relationship was the inverse of the voltage-velocity relationship. Since it was desired to use the data for average wind speeds up to 5 mph, the low range of the Airmeter was used, and the calibration curve was extended up to 15 mph by means of an empirical formula in order to allow for gustiness measurements.

The circuit shown in Fig. 16 was finally developed in which the recorder span was 10.08 mv to match the nominal 10 mv output of the

Airmeter. A 100 ohm 3 turn helipot was shunted by a 1 ohm resistor and inserted in the calibration network to give an adjustment which would allow correction for any creep in calibration as the resistors aged. An input filter of 10 henries and 500 mfd. was added to the input circuit to eliminate the AC pickup in the 250' unshielded leads from the profile pole. Two resistors of 27 and 0.3 ohms respectively, were added to shunt the input circuit to decrease the sensitivity of the recorder at the low end of the scale. This was necessary since the upper 37% of the velocity scale (slide wire length) is equivalent to only 3.3% of the total slide wire resistance while the lower 36% of the velocity scale is equivalent to 81% of the total slide wire resistance. In order to prevent the balance motor from driving the slide wire contact to the stops, making considerable noise, whenever the wind speed reached or exceeded 15 mph, a desensitizing circuit was added. This consisted of a limit switch which inserted an additional 1000 ohms in the cathode of the output tubes whenever the slide wire contact reached about 98% of full scale. When the gust velocities dropped below 15 mph, the slide wire moved comparatively slowly downscale until the limit switch was de-energized and full sensitivity was returned. The recorder could then be permitted to run without damage or inconvenience even though the wind velocity might exceed the full scale range of the unit for considerable periods. The linearization of the 2-junction vertical velocity probe is considered to be approximate since the curvature of the calibration curve is not identical with that of the 8-junction probes.

The record was in units of $\frac{1}{2}$ mph and the average hourly velocity was obtained by integrating the trace for each 3 min. sample at each level visually, connecting the 4 samples in each hour by lines as shown in Fig. 17, and visually estimating the hourly mean of the resulting curve for each of the three horizontal probes (6, 18, and 54 ft.). The portions of the trace corresponding to the vertical velocity could always be easily identified because the output of the vertical probe was only about $\frac{1}{4}$ the output of each of the horizontal probes, and this provided a convenient reference point in the time cycle. The mean vertical velocity was not recorded, but was assumed to be approximately zero on an hourly time scale.

Horizontal gustiness values were read by recording the average range of the three minute samples obtained from each level during the hour. The vertical gustiness was approximated by adding the highest two peaks of each recording period and converting to half miles per hour. The contacting, generator-selsyn and heated-thermopile recorders are shown in Fig. 18.

8. Wind Profiles and Gustiness - Comparison and Evaluation

A comparison of 960 hourly average wind speed readings taken from three separate Anemograph (cup-generator type) anemometers and three horizontally non-directional airmeter (heated-thermopile) probes located at the 6, 18 and 54 foot levels on the profile pole showed that the agreement was excellent between 3 mph. and the top limit of 5 mph. for which airmeter data were ordinarily read. A plot of thermopile velocity against cup velocity is shown in Figure 19. Above 3 mph the cup driven generator is linear, according to wind tunnel tests made by the Bureau of Standards for the Instrument Corporation. The agreement with the

modes of the thermopile data shows that the calibration curve of the airmeter has been linearized. Below three miles per hour, the thermopile may still be presumed to be linear, but the cup generator output decreases due to the frictional drag and low speed non-linearity of the generator. The large scatter of the original thermopile anemometer at moderate wind speeds was investigated and an individual case study indicated that there were times when the average values over several hours time would be in good agreement but the speeds shown for periods of a few minutes were considerably different. In many cases this seemed to be at a time when cold air was moving into the area with strong heating from below. A sharp gust of cold air moving into the warmer air near the ground would cause the thermopile to be cooled more rapidly than it should by reason of the movement of air past the warm junction because the temperature of the .003 wire would follow the ambient temperature more closely than that of the cold junction studs. Warm gusts also gave the same effect in the opposite sense. This effect added the micro temperature fluctuations to the velocity fluctuations and cause the velocities to be too high or too low according to the temperature of the gusts of air. This effect had also been noted by Thornthwaite and Halstead (Ref. 15).

Hastings Instrument Company was asked to redesign the probe to eliminate the thermal lag in the temperature compensation. This was accomplished by adding unheated couples of the same diameter wire to buck out the ambient temperature fluctuations with the same response time in the compensation couple as in the heated couples. The probes were to have the

same calibration as the original probes within 2%. Comparisons between the compensated probes and the same generator anemometer and in the same season of the following year showed by the reduction in scatter that the temperature compensation was much better, but it is evident from Figure 19 that the calibration curve was not exactly the same as the original probes and hence the linearization was not as good as that obtained when the recorder was used with the original probes. The error is small, however, below the reading limit of 5 mph. The gust peaks recorded by the airmeter-recorder combination would be incorrect but it seemed that the recorded values might be affected as much by the response time of the element and the recorder servo system as by the inaccuracy of linearization.

At the same time that the comparison of the compensated cups and the generator cup anemometer were made, a contacting cup anemometer arranged to record miles and tenths was mounted at each level on the profile pole so that simultaneous comparisons could be made of the standard contacting cup anemometer with the other two instruments. The results of these inter-comparisons are shown in the lower two graphs in Figure 19.

Above 10 mph, the contacting and generator anemometers are in good agreement with a very small standard deviation. The compensated thermopile is within about $\frac{1}{2}$ mph of the contacting anemometer over the range of velocities tested.

On the basis of these tests, the use of $\frac{1}{2}$ mph as the coding unit appears to have been appropriate. The relative accuracy as well as the scatter in each set of comparison measurements was of the order of 0.5 mph and,

in general, only data obtained by means of the same type of instrument have been combined in the profile studies. The gustiness data derived from the generator anemometers above 3 mph and the airmeter below 3 mph fit into the same pattern when plotted against mean speed, stability or heights, using fairly large numbers of observations.

9. Pilot Balloon Equipment

Pilot balloon techniques were used for two purposes: to obtain the vertical distribution of wind speed and direction above the anemometer levels, and to observe the trajectories of particles drifting with the wind. For winds-aloft observations, the single theodolite method was used. This consists of visually tracking a free balloon having a standard buoyancy, recording at fixed time intervals its elevation and azimuth angles, obtaining its height and distance from tables based on the average ascent rate for such balloons, and graphically calculating its horizontal direction and speed of movement by means of a plotting board and suitable scales. For the low-level trajectory observations, balloons with zero net buoyancy (neutral) were observed through theodolites simultaneously by two observers at the ends of a measured baseline. From carefully synchronized angle measurements, successive coordinates of the balloons could be calculated by trigonometry, and from these the three-dimensional velocity components.

The inflation equipment used for the pilot balloon and neutral balloon observations consisted of the standard Weather Bureau inflation balance with the regulation weight (154 gms.) for inflating 30 gram balloons with helium to give an ascent rate of 180 m./min. The 10 gm. neutral

balloons were filled on this balance to a slight positive lift and then adjusted outdoors after a few minutes ageing to allow the temperature of the gas in the balloon to become equalized to the ambient.

The theodolites used were David White model 6061 with a trough compass and finder telescope. These instruments were mounted on wooden tripods, and were oriented on a fixed reference point before each winds aloft observation, and on each other for each series of neutral balloon observations.

The timing signals were generated at 30 second intervals with a 5 second warning by a 2 rpm Bodine synchronous motor which drove a cam actuating 2 pole microswitches. Auxiliary switches provided a means for the observer nearest the hutment station to signal his partner when to begin and end observation of the neutral balloons. The switches keyed simultaneously a buzzer and the carrier of a small 1-watt radio transmitter (4397.5Kc). The hutment station received the timing signal on a buzzer while the remote end of the 782 foot baseline received a signal on a portable battery operated radio. This equipment operated satisfactorily for about a year until increasing use of the shared frequency channel by other stations caused too much interference. At this time (the fall of 1949) a complete wired buzzer system was installed and the radio channel was discontinued for the remainder of the program.

The baseline was oriented across the valley to permit the maximum accuracy in tracking the neutral balloons which would usually float up or

down the valley rather than across the ridges. Some shifts were made in the remote station from time to time. Table 4 gives the length and orientation of the baseline used during the period of the survey.

Table 4. Double theodolite baseline data

<u>Starting Date</u>	<u>Orientation of Baseline (True)</u>	<u>Length of Baseline (feet)</u>
1-6-49	139.6	642
1-19-49	141.2	642
3-7-49	144.2	635
3-30-49	135.6	635
4-6-49	131.2	628
4-6-49	128.7	782
10-25-49	140.4	788

10. Temperature and Humidity: Hygrothermographs and Max-Min Thermometers

Continuous records of temperature and humidity in a standard "cotton region" instrument shelter with the floor 4 ft. above ground were obtained by means of a hygrothermograph in combination with maximum and minimum thermometers at station 001 as well as at the unmanned ("micronet") stations during most of the observation period. The two exceptions were station 001 at which an aspirated wet-and-dry-thermocouple recorder was used from July, 1950 to November, 1950, and station 012, at which the original thermohm (resistance bulb) installation remained in use throughout the survey.

Standard hygrothermographs (Bendix-Friez type 594 and Instrument Corp. type 1690 were used) are capable of an accuracy of better than $\pm 2^{\circ}\text{F}$.

and 15%RH when the calibration is checked regularly. Calibrated maximum and minimum thermometers in a Townsend support were mounted in the shelter for this purpose.

An insulated calibration chamber obtained from the Instrument Division of the Weather Bureau was used for the initial checking adjustment of the hygrothermographs. Temperature was checked in the 40-50°F. range and at a point near 90° F. Humidity was checked by allowing equilibrium to be reached at 100% and near 50%. When the instrument was placed in service a record was kept of its corrections. After about 9 months' service, or if an instrument showed excessive drift or sudden calibration shifts, it was rotated to the shop for cleaning, calibration and repair.

At first, control of the temperature calibration in the field was based on the weekly minimum thermometer reading, in accordance with Middleton's (Ref. 16) recommendation. Although 6-hourly readings of the thermometers were made during most of the week at this station, those at the unmanned stations were only read once a week, and a uniform procedure was desired for all hygrothermograph corrections. After a few months it was found, both by comparison between stations on the area and by comparison with nearby Weather Bureau cooperative climatological stations, that the average temperatures obtained by this method were 1°F. to 3°F. too low. Fortunately, the weekly maximum thermometer readings, although not used, had been recorded. A comparison of the hourly data from two hygrothermographs made by different manufacturers with the hourly readings from a shielded, aspirated thermocouple on a Brown recorder which had a maximum

error of 0.25°F. , showed that the average errors during a typical two day period were $0.4^{\circ} \pm 0.8^{\circ}\text{F.}$ (Instrument Corporation #347) and $0.6^{\circ} \pm 1.5^{\circ}\text{F.}$ (Bendix-Friez #5296), when the minimum temperature correction alone was used. When the hourly hygrothermograph readings were corrected with the average of the weekly maximum and minimum corrections the error was reduced to $0.2^{\circ} \pm 0.7^{\circ}\text{F.}$ and $0.3 \pm 1.0^{\circ}\text{F.}$ respectively.

A test was made using a hygrothermograph (Bendix-Friez #3632) for which daily maximum and minimum thermometer readings were available during the period May, 1948 to January, 1949. It was found that the use of the weekly maximum as a calibration point for the entire week introduced an error of $0.4^{\pm} 1.7^{\circ}\text{F.}$ in the daily maximum temperatures. When the weekly minimum temperature was used as a calibration point for the daily minimum, an error of $0.3^{\pm} 1.2^{\circ}\text{F.}$ was introduced. These weekly calibration points were those actually used for routine daily maximum and minimum temperatures. The temperature correction finally applied to all hourly hygrothermograph data was the average of the weekly maximum correction (maximum thermometer reading minus highest point of the temperature trace) and the weekly minimum correction (minimum thermometer reading minus lowest point of the temperature trace). The humidity calibration was checked weekly against a saturated atmosphere; this was based on the assumption that the flat top of the relative humidity curve observed on most nights represented saturation. This assumption has been verified many times by psychrometer observations.

As a further test, the hourly humidities were calculated from the wet and dry bulb temperatures of the shielded aspirated thermocouple for

the same two day test period used in the temperature comparison. These calculated humidities were compared with the hourly readings from two hygrothermographs, showing an error of $-1.0 \pm 3.2\%$ for Instrument Corporation #347 and $+0.8 \pm 4.5\%$ for Bendix-Friez #5296. The correction of $\pm 1\%$ was applied to both traces to bring the highest portion of the curve to 100% and the errors of the corrected data were then $0.0 \pm 3.2\%$ for Instrument Corporation #347 and $+1.8 \pm 4.5\%$ for the Bendix-Friez #5296 instruments respectively. The relative humidity ranged from 44% to 100% during this test. Thus, while the saturation correction was a part of the chart reading routine, there is some doubt as to whether such a small correction would improve the data materially.

The greatest difficulty associated with the use of these instruments was the change of time rate with temperature and humidity. The design of the clock housing of the Instruments Corporation hygrothermograph allowed the winding spring to drag on the clock gear at low temperature, and the clock would run slow. Gradually most of the clocks were brought to a time accuracy of 1 hr. to $1\frac{1}{2}$ hrs. per week or better and the rest were replaced by the manufacturer with redesigned units.

Hourly readings (on the hour) with temperature, humidity and time corrections applied, were posted on a data sheet for each day (Form OR 408).

11. Temperature and Humidity: Thermocouples

After a comparison period, the hygrothermograph at station 001 was replaced on July 14, 1950 by aspirated thermocouples and a multipoint Brown recorder whose response was 24 seconds full scale. The sensing

elements were single #20 gauge iron-constantan couples for the wet and dry bulb measurements and a single #30 gauge couple for a grass temperature measurement. The couples were twisted and soft soldered, tested for calibration accuracy and homogeneity of the wire, and then sprayed with two coats of plastic for protection against weathering and corrosion. Water was fed to the wet-bulb couple by a wick which extended through a glass tube into a 2 oz. bottle mounted on a stopper in the outer radiation shield.

Figure 20 shows the details of the aspirator construction. The aluminum outer shield was highly polished when installed but had become oxidized by November when the station was closed. A ventilation rate of about 800 ft./min. was maintained over the junctions by the Fasco blower in the plenum chamber of the aspirator unit. Alternate shading and exposure of the aspirator on a clear day did not cause a detectable change in the temperature trace on the recorder. Although the reflection efficiency of the outer shield was considerably reduced by November, the temperatures as recorded, checked within about 0.5°F. with sling psychrometer readings made in the shade a few feet from the aspirator. Wet bulb temperatures were also checked with a sling psychrometer inserted into the airstream and agreed within 0.5° F. Psychrometer checks were made at the 6 hourly observation times for a period of about a month. After this trial period, only a weekly check was made on the recorded wet bulb temperatures which were then used for all the 3 hourly observations. The recorder system was accurate within 0.25°F. for the 0-200°F. range.

A considerable amount of experimentation was done in order to expose a thermocouple so that it would indicate a temperature which would be representative of the earth's thermal radiating surface, or the earth-air interface. The couple was first soldered to a sheet of copper foil placed on the bare soil and sprinkled with pulverized soil. The temperature trace from this installation showed that the surface couple remained considerably warmer than the air in the aspirator (about $4\frac{1}{2}$ ft. above ground) during the night. The day temperatures were higher than the aspirator, as would be expected, but it appeared that contact of the metal with the soil conducted heat to the thermocouple at night at too great a rate to be representative.

The second installation utilized a thermocouple cemented to the back of a sheet of 0 grade sandpaper, in contact with the soil surface. The temperature trace from this mounting showed the same departure from the necessary behavior of the primary heating-cooling surface that the first installation did, except for increased amplitude of temperature variation.

The third installation consisted of a bare #30 gage couple stretched between wooden pegs inserted into the ground so that the couple was just above the bare surface. The temperatures measured by this element were colder than the aspirator temperature at night and warmer than the aspirator temperature during the day. The couple was waterproofed by coating with a thin layer of plastic. Further, consideration of the ground cover in the surrounding area led to the belief that a clover and grass ground cover was a much more representative radiating surface than bare soil. Accordingly a fourth installation was made in which the

#30 gauge iron-constantan couple was located in the free air, between wooden pegs which extended to the height of the grass and clover. A circular area 3 feet in diameter was marked by a set of connected stakes to prevent accidental damage to the thermocouple and the grass and clover were kept trimmed to the height of the thermocouple for the duration of the program Figure 21. Only data from this final exposure have been used in the meteorological analysis (T_{grass}).

12. Vertical Temperature Gradient Thermopile, $T_{54} - T_4$.

Prior to June, 1950 the vertical temperature gradients measured over a 180 ft. interval by the ORNL Health Physics Division at station 012 were used in the interpretation of the 54 ft. wind profile at station 001. Due to the difference in ground elevation and insensitivity of this instrument, an 8 junction iron-constantan thermopile was mounted on the profile pole.

The elements were mounted at 54 and 4 feet above the ground in the same type of aspirated shield that was used for the thermocouple psychrometer. The four #20 gauge junctions in each aspirator tube were sprayed with two coats of plastic to protect them from corrosion. Iron-constantan was chosen for the couple material in preference to copper-constantan because of its linearity over the temperature range expected. The iron-constantan couples have an emf of 28.8 microvolts per degree from 0° to 65° F. rising slowly to 29.3 microvolts per degree at 100°F. as compared with a change from 21 microvolts per degree to 23 microvolts per degree for copper-constantan. Thus a 5°F. differential would be equivalent to an emf of .576 mv at 0°F and .586 mv at 100°F. for an 8 junction thermopile of iron-constantan. If a copper-constantan 8 junction thermopile

were used, the emf would be .420 mv at 0°F and .460 mv at 100°F. The error in measuring a 5°F differential introduced by the non-linearity of the calibration curves under these conditions, assuming each of the thermopiles was used with a scale designed to match at 50°F, would be .08°F for the iron-constantan thermopile and .43°F for the copper-constantan.

The recorder was a Brown "Elektronik" potentiometer whose full scale response was 12 seconds with no cold junction compensation. The span of the recorder was 1.7380 mv from -0.3476 mv to +1.3904 mv. The wiring diagram of the measuring circuit of the recorder, with the required changes, is shown in Figure 22. The only chart available from the manufacturer which had a suitable scale was -3 to +12 (evenly divided) originally designed for feet of water above a spillway. This chart, #5408 was used to represent temperature difference in degrees F. When the couples were made, the iron-constantan wire was tested carefully for homogeneity and matched against the calibration given in the Engineering Specifications, Temperature - EMF equivalent tables for iron-constantan (Brown Instrument Division of Minneapolis - Honeywell Corporation). A supply of wire was found which matched these specifications very closely. The recorder was then adjusted by means of the span adjustment until the scale -3° to +12°F. read correctly when the plastic coated couples were immersed in two baths whose temperatures were measured with a 76 mm mercurial thermometer which had been previously checked against an NBS calibrated platinum-in-quartz resistance thermometer. At no time during these tests, which were conducted by P. E. Brown of ORNL, did the temperature differential as measured by

the thermometer differ from the recorder reading more than 0.06°F. These couples were then mounted on the profile pole in their aspirators and connected so that a positive reading of temperature gradient was obtained when T_{54} was warmer than T_4 . Figure 23 shows samples of the temperature difference record obtained from the aspirated thermopile and Brown recorder.

13. Captive Balloon Temperature Sounding System

To obtain the vertical temperature distribution above the heights of the pole and tower installations, a captive balloon borne thermistor, wired to a recorder at the ground, was used. The complete system, consisting of a 400 cu. ft. helium-filled Seyfang blimp, specially calibrated radiosonde-type thermistor mounted on a Plexiglas protective support, 3-conductor light-weight cable, nylon safety cord, universal cable pulley, electric motor driven winch with foot-counter, and potentiometer recorder (Figure 24) was designed and assembled during the period January to July, 1949, with the cooperation of the Oak Ridge National Laboratory Instrument Department. It has been described quite fully in References 17 and 18.

14. Station 001 Rain Gage

A recording rain gage of the tipping bucket type was installed at station 011 (Oak Ridge Townsite) prior to the commencement of the meteorological survey. In May, 1949 it was replaced at that site by a weighing gage of the type used at two other stations on the area, and the tipping bucket gage was moved to station 001, where it could be checked frequently by stick measurements. This tipping bucket gage recorded

the tenths and hundredths of an inch of precipitation on two pens of the contacting wind recorder described above. Figure 5 shows the wiring diagram of the relay system used with the gage.

15. Pyrheliometer

Total incident short-wave solar and sky radiation was recorded by means of a standard Eppley 10-junction pyrheliometer. This instrument consists of a thermopile which measures the temperature difference between white-coated and black-coated portions of the horizontal surface of a silver disc enclosed in a quartz bulb. A Leeds and Northrup Micromax potentiometer recorder, 0 to 2 cal/cm²/min. (langleys per min) full scale, provided the record in the form of a strip chart, 2 inches per hour. The records were evaluated by a method nearly identical with the standard method employed at U.S. Weather Bureau pyrheliometer stations: visually integrated totals were read off the chart for each 15-min. period and added to give an hourly total in langleys (cal./cm.²) for each hour of the day, True Solar Time (Reference 19).

16. Barometric Pressure Instruments

Readings of a standard Fortin-type mercurial barometer, mounted on an 8" x 8" post set in concrete in a corner of the hutment, were made every 6 hours at the standard synoptic observation times. Corrections for gravity, temperature and instrumental errors were made to obtain the station pressure, accurate to about ±0.002 in. mercury. This was reduced to sea level pressure by the standard method (Reference 20). A continuous record of the station pressure was obtained by means of an open scale aneroid microbarograph (Instrument Corporation) accurate to

±0.005 in. mercury when checked frequently by comparison with the mercurial barometer.

17. Smoke Photograph Equipment

Smoke for qualitative observations of atmospheric diffusion was generated by means of surplus U. S. Army Chemical Warfare Service HC smoke pots, type M1. These expendable smoke pots, each weighing about 8 lbs., produce a dense, hygroscopic zinc chloride smoke for approximately 12 mins. Considerable heat is released in the reaction, so that some elevation of the smoke plume occurs in light winds. At least 90% of the pots functioned properly, which was gratifying in view of the age and history of these World War II munitions. Photographs of the smoke trails were taken with an Argoflex 620 camera, using a Weston Master II exposure meter.

In order to obtain pictures of the ordinarily invisible stack-gas stream from the ORNL graphite pile, HC smoke was introduced on the vacuum side of the stack fans through a hood, especially constructed for this purpose through the cooperation of the ORNL Pile Operations Department. This hood consisted of a steel-plate box 20" x 22" with a 1" expanded mesh grill for a floor and a mesh fly ash filter in a sliding rack near the top. The hood was attached to the suction side of the stack fans by means of a tee, elbow and valve in a 3 inch pipe line (Figure 25). The pots were placed in the box, ignited, and the door closed. As the valve was opened slowly all the smoke was pulled into the stack stream. It was found that, in spite of the mesh filter, fly ash from the burning pots would choke the valve and prevent it being closed so a second

screen was added in the box which effectively stopped the fly ash from entering the stack line. The upper screen would become clogged after about two runs and had to be scraped clean. After several months' use, the stack fans were examined by ORNL personnel and some evidence of slight corrosion by the zinc chloride was found. The use of this smoke was then abandoned to prevent any damage to the stack fans. The smoke pots were ignited by the personnel of the Pile Department of ORNL on a prearranged schedule which allowed both morning and late afternoon pictures to be taken.

C. Manual Observation Procedures

18. Surface Weather Observations

Standard "synoptic" type surface weather observations (Reference 21) were made at station 001 at 3-hourly intervals, from 7:30 a.m. on Monday to 4:30 a.m. on Saturday during the two-year observation period with the following exceptions: the 7:30 p.m. observation was omitted prior to February 1, 1949, only the odd-numbered 6-hourlies were taken between March 6, 1950, and August 26, 1950, and all except the 4:30 a.m. observation were resumed from August 28, 1950 to November 4, 1950. These observations included sky conditions, ceiling height (measured by pilot balloon or estimated), type and amount of all cloud layers, visibility, weather, type of precipitation and obstructions to vision, station pressure (by means of the mercurial barometer), sea level pressure, character and amount of 3-hourly pressure change (by means of the aneroid microbarograph), temperature, wet-bulb temperature, dew point

and relative humidity (by means of a sling psychrometer), wind direction to 16 points (by means of wind vane recorder), and wind speed (by means of generator-type anemometer indicator). The odd numbered 6-hourlies also included 6-hourly maximum and minimum temperature (by means of maximum and minimum thermometers), 6-hourly total precipitation and snowfall (by means of a stick measurement of precipitation collected in the tipping-bucket rain gage reservoir), snow depth and state of the ground. These observations were entered on Forms WB 1130 A and WB 1130 B, and, from June 2, 1949 on were also punched by the observers into the standard WBAN #1 and WBAN #2 cards utilizing an IBM mechanical key punch loaned by the Weather Bureau. The cards have been checked by the Weather Records Processing Center, Weather Bureau Office, Chattanooga, Tennessee for internal inconsistencies which have subsequently been corrected and both the data sheets and the punched cards have been retained on file at Oak Ridge for future reference. These standard observations not only represent a fund of useful climatological information, but also permit direct comparison with observations of identical content made at Knoxville. Furthermore, they are invaluable in analyzing individual cases and relating the observed local micrometrological phenomena to the larger-scale processes such as are shown on ordinary weather maps.

19. Winds Aloft Observation Procedure

Winds aloft observations (pibal) were taken every three hours from 7 a.m. on Mondays through 4 a.m. on Saturdays (with some exceptions during periods of personnel shortage) from the beginning of observations,

November 24, 1948 through March 4, 1950. From March 6 through August 26, 1950, only the odd observations (1 and 7 a.m. and p.m.) were taken, and Knoxville pibals used for the remaining four observation times. From August 28 through November 3, 1950, observations were increased to every two hours on the even hour and occasionally hourly from 6 a.m. through 1 p.m. and 4 p.m. through 1 a.m. Beginning on the hour ± 20 min., the pilot balloon observations followed the standard Weather Bureau 30 gm. balloon procedure (Ref. 22) with minor modifications to obtain greater detail in the lowest 2000 ft. and to simplify the observation as much as possible.

Instead of taking theodolite readings at 1 min. intervals during the ascent, and computing average winds over 2 min. intervals, as is done in standard pibals, $\frac{1}{2}$ min. reading intervals were used during the first $3\frac{1}{2}$ min. of the observation and winds computed over each interval between readings. Tables of horizontal distance as a function of elevation angle for the intermediate half-minutes were prepared and inserted in the standard 30-gram pilot balloon tables to facilitate plotting. The graphs of wind direction and speed vs. altitude ordinarily constructed so as to interpolate winds at standard 1000 ft. intervals above sea level were eliminated. Instead the wind was measured on the plotting board for each reading interval and used directly, assigned to the altitude of the balloon at the midpoint of the interval. Above the first 2000 ft. above ground, only selected levels, falling closest to thousands of feet MSL, were worked up for comparison with other pilot balloon stations. Observations were terminated at 16 min., since the winds

above 10,000 ft. MSL were not of sufficient interest to justify the added expenditure of time in observation and computation. Table 5 shows, for each reading time, the assumed balloon height, wind observation level above the release point (the theodolite platform, 20 ft. above ground) and above mean sea level, and corresponding level of standard pibals for comparison.

Table 5

Winds-Aloft Observation Levels

<u>Time After Release, Min.</u>	<u>Balloon Height, Ft. Above Release</u>	<u>Wind Level, Ft. Above Release</u>	<u>Wind Level, Ft. Above MSL</u>	<u>Standard Level, Ft. Above MSL</u>
0	0	0*	830*	
$\frac{1}{2}$	360	175	1005	1000
1	710	525	1355	
$1\frac{1}{2}$	1040	875	1705	
2	1360	1200	2030	2000
$2\frac{1}{2}$	1690	1525	2355	
3	2010	1850	2680	
$3\frac{1}{2}$	2320	2175	3005	3000
$4\frac{1}{2}$	2950			
$5\frac{1}{2}$	3550	3250	4080	4000
6	3850			
7	4450	4150	4980	5000
8	5000			
9	5600	5300	6130	6000
10	6200			
11	6800			
12	7400	7100	7930	8000
13	8000			
14	8600			
15	9200			
16	9700	9450	10,280	10,000

*Obtained from surface wind instruments.

The accuracy of the single-theodolite method is dependent on the closeness with which the individual balloon ascent rates match the standard

curve. In order to check on any gross distortion introduced by local terrain effects, 20 double theodolite observations on standard pilot balloon ascents were carried out during the summer of 1950. The results of these few tests, summarized in Figure 26, while not definitive by comparison with the much larger and more evenly distributed sample with respect to season and time of day used by the Weather Bureau in developing the standard curve, nevertheless appear to show certain characteristic deviations.

On the average, the measured heights were greater than standard, the excess building up during the first 3 min. (about 2000 ft.), then remaining about 300 to 400 ft. above standard height. The range of measured heights at each reading time is very large, being of the order of half the average. The mid-day pattern (1 p.m.) departs most markedly from the average although fully half the observations were at this time. In mid-day there was a large and progressively increasing range of heights in the first 6 min. during which 8 of the 10 balloons, including those with the largest ascent rates, became lost in clouds; the two remaining balloons were followed the full 16 min. and showed less than standard elevation with good agreement between them. The average height of all the balloons observed at 1 p.m. actually decreased between the sixth minute (last level below clouds) and the seventh minute. It is obvious that afternoon ascents which terminate in cumulus clouds at 3000 to 5000 ft. are subject to large underestimation of height and consequently, horizontal distance by the standard procedure, presumably due to large updrafts. Similarly, the balloons which rise through the clear

spaces between clouds are subject to downdrafts. The remainder of the observation times (7 a.m., 4 p.m., 10 p.m.) show no pronounced abnormality other than a gradually increasing positive departure from standard and gradually increasing range of values with increasing altitude. The large and increasing ranges in the whole body of observations after the sixth minute are due to the large midday negative deviations and large positive deviations at other times, the ranges within each observation time being comparatively small.

Despite the apparently large average values and pronounced diurnal trend of the height deviations, no height corrections have been made in the routine pilot balloon observations in view of the small number of test runs and the large scatter of observed heights. It should be noted that, on the average, there is some compensation for the underestimation of height in the resulting underestimation of the wind speed, since the wind speed normally increases with height. The standard error in the wind vector at any level is estimated to be about 10% which is not excessively large in relation to the range and short-period variability of the wind vector at each level. This error is no more serious than is the selective sampling introduced by the requirement of visual contact with the balloon, which so strikingly influences even the average height curve for the midday runs, and which definitely distorts the upper-air wind roses, as will be shown later by comparison with "rawins" (observed by radio direction finding methods). Furthermore, while inaccurate in itself, the observed upper-air wind profile permits an unbiased comparison with those obtained at other pilot balloon stations.

20. Neutral Balloon Observations

Double-theodolite observations of zero-lift (neutral) 10-gram ceiling balloons were made in two sessions per day, about noon and midnight, from November 24, 1948 through February 28, 1950 when they were discontinued. During this period, the aim was to take synchronized readings at 30-sec. intervals on each balloon as long as both observers could track it, and to make enough consecutive releases to obtain a total of approximately 90 readings (45 minutes of observation) in each session. From August 28 until November 3, 1950, a series of similar observations was conducted using a 2-gram free lift. In this series only two balloon releases were made in each session, 20 readings (10 min.) per balloon, with sessions repeated at two-hour intervals on the odd hour, three days per week (Monday, Wednesday and Friday), alternately 7 a.m. to 1 p.m. one week and 5 p.m. to 11 p.m. the next.

The 10-gram balloons for "neutral" observations were inflated indoors until they had a perceptible lift, then taken outside and ballasted with scotch tape and rubber scraps until the net lift in still air was zero. For night observation, a pibal lighting unit was inserted inside the neck of the balloon with the bulb outside. The observers at the two theodolites, 782 ft. apart, signalled one another by means of the timing buzzer system when ready, and the balloon was released at the station 001 theodolite platform. Each 30-sec. reading was taken by both observers at the start of the main buzzer signal following a 5-sec. warning signal. Azimuth and elevation angles were recorded to the nearest hundredth of a degree. Some practice and plotting of

trajectories by the observers was necessary before sufficient skill and precision was attained to produce accurate tracks. As an aid in checking and improving the quality of the observations it was occasionally found helpful to plot the azimuth vs. time for the two stations on one graph. Unevenness in tracking, lagging and "catching up" on the part of one of the observers and hints for correction of some of the more irregular trajectories were evident from such graphs. An additional check was provided by the recording of four angles, only three being required for the computation. Later the recording of elevation at the north station (E_2) was discontinued to simplify card punching.

The computations of distance and height were at first carried out by statistical clerks, using trigonometric tables and calculating machines. Horizontal trajectories were then plotted by the observers and studied individually; no attempt was made to compute wind directions and speeds regularly. Thus although many man-days per week were spent in computing and plotting, the results needed for a statistical study of the three-dimensional velocity variations were still not obtainable without additional labor.

Starting in June, 1950, with the cooperation of the IBM punched card machine unit at the Y-12 plant, the observations were all punched, one reading per card, and the following calculations were carried out on the IBM type 604 calculating punch: distance in feet, height in feet, azimuth corrected from baseline orientation to true north, wind direction in degrees, wind speed in miles per hour, and vertical velocity

component in miles per hour. The velocity components averaged over a 1-min. interval were calculated by vector subtraction of the position coordinates on the preceding card from those on the following card, and punched into the intermediate card. In addition to the relative speed (100 readings per minute), accuracy, and economy of manpower with which these calculations were carried out, the results were produced in a form specifically adapted for statistical treatment: sorting by meteorological categories or by space coordinates, averaging, frequency distribution analysis, etc. as well as for tabulation, plotting and individual study.

The inherent accuracy of location by the double theodolite method, with theodolites 782 ft. apart and readings taken to the nearest hundredth degree is summarized in Figure 27. Assuming that the two observers make simultaneous errors of $.01^\circ$ (or timing errors of 1 second at an angular velocity of $0.6^\circ/\text{min.}$) in opposite senses on a single reading a position error of 50 ft., corresponding to about $\frac{1}{2}$ mph in the 1-min. average velocity, occurs when the balloon is at a distance of 10,000 ft. or more at right angles to the baseline, and at progressively smaller distances as the baseline orientation is approached. The distance at which the error reaches this magnitude at 10° off the baseline is 4000 ft. and the observation becomes indeterminate when the theodolites are aligned parallel to the baseline. The baseline was set up as nearly as practicable perpendicular to the valley axis, along which the majority of the winds blow, so that, in general, observations were considered usable out to about 10,000 ft. Most baseline

readings occurred during rapid shifts of wind direction encountered by the balloon, and have been corrected by interpolation.

While relatively convenient as a method of measuring particle trajectories in the atmosphere, the neutral balloon technique is fraught with severe limitations and uncertainties. Among these the following must be mentioned:

- a. The balloon's mass (10 gms.) and volume (about a cubic foot) set a rather high lower limit to the space and time scale of eddies which can be observed.
- b. The practicable lower limit of the reading interval with only one observer at each theodolite is of the order of 30 sec. (i.e., the interval actually used) if strong, turbulent or shifting winds must be included. This placed a higher limit on the minimum observable scale of eddies than does (a).
- c. The balloons may have a relative velocity due to buoyancy, which cannot be completely eliminated with certainty. Even if the balloons are perfectly neutral at the moment of release, the unknown effects of helium loss by diffusion, warming by the sun, cooling by radiation, and relative temperature anomaly in upper strata when strong vertical gradients are present make the assumption of continued neutral buoyancy throughout the run somewhat uncertain. It was learned in experimenting with small free lifts prior to the 2 gm. ascents in the fall of 1950 that only very slight buoyancy is required to impart to the balloon vertical velocities much greater than those due to the atmosphere eddies.

Since the slightest negative buoyancy would prevent carrying out the observation, any bias must be positive. Trials with non-extensible plastic balloons failed since no plastic bags were available which could hold sufficient helium to support their own weight.

- d. Termination of observations due to disappearance of balloons behind hills, trees or buildings, or settling to the ground, results in an attrition of low or downward moving balloons at small distances and constitutes a process of natural selection favoring high or upward moving balloons. This necessarily introduces a positive bias in the statistics of height and vertical velocity, increasing with distance and time after release.
- e. Use of a single release point near the ground results in a unique average history and consequently a very limited range of wind directions (roughly from the release point) for all balloons arriving at any particular point in space. Thus the effects of each topographic feature on the air flow are represented only under certain limited conditions, which would not be applicable to the trajectories of particles originating at any other point.

The 2-gm. free lift ascents during the fall of 1950 were made in order to gain better control of the buoyancy and natural selection effects so as to obtain a representative sampling in the vertical direction of horizontal and vertical velocity components. No attempts were made during this period to map out local currents in the horizontal directions, or to obtain particle trajectories for diffusion analysis by the neutral

balloon method. The use of a positive lift in order to avoid loss of balloons to the ground was prompted by a suggestion by Dr. L. J. Savage, consultant in mathematical statistics to the ORNL.

21. Temperature Sounding Procedure

Captive balloon soundings of temperature, utilizing the system described in Reference 18, were scheduled every 6 hours from 8:30 a.m. on Mondays to 2:30 a.m. on Saturdays, during the period July 19, 1949 to August 24, 1950, with the exception a few weeks during August-October, 1949. From August 28, 1950 to November 3, 1950, soundings were taken approximately every hour except 1 to 5 a.m., 2 to 3 p.m. and when neutral balloon observations were scheduled.

Prior to each ascent the blimp, tightly sandbagged down on a canvas ground cloth between observations, was freed except for one anchor line, and the cable, thermistor and safety cord were attached to the ring at the apex of the rigging by means of a length of elastic shock-cord and a snap-hook. The thermistor was swung to and fro for about a minute at 3 to 4 ft. above ground in the shade to obtain a representative surface temperature, the balloon was then allowed to pull the 5 to 10 ft. of loose cable up taut, the cable-length odometer (foot-counter) was checked and adjusted to the correct length (measured from the universal pulley) if necessary, the winch motor was switched on "up", and the ascent was begun. The observer watched the blimp and cable for any signs of trouble such as excessive instability, breakage or fouling of the cable or nylon cord, cable sag, etc. Occasionally he glanced at

the temperature recorder to see that the circuit was free from breaks or excessive resistance (such as was sometimes caused by dirt or corrosion on the winch slip-rings). Since the chart speed was about $1\frac{1}{2}$ in./min. and the balloon ascent rate about 100 ft./min., he would know from the temperature chart when the 100 ft. reading levels were being approached. He then observed the odometer and, at the reading level, opened the circuit momentarily by means of the "line check" switch to mark the chart and simultaneously check the line resistance (a slight adjustment was occasionally necessary). The reading levels were determined from a table of average cable length for each standard height, part of which is shown in Table 6.

Table 6

Cable Length at Standard Levels

<u>Blimp Height, Ft.</u>	<u>Cable Length, Ft.</u>
500	540
1000	1080
1500	1850

The ascent was continued until excessive cable sag indicated that the blimp was no longer rising, then the descent was begun, using the same procedure as on the ascent. Termination of the ascent occurred at a height of about 1500 ft. or more in moderate, steady winds and with the blimp dry and freshly inflated. Helium was added before the next ascent if the blimp failed to reach 1000 ft. under good ascent conditions. With rain or heavy dew and calm or very light winds, as occurred frequently during night and early morning runs, termination occurred at 400 to 600 ft. even with new helium. Normally the blimp was deflated

and refilled once or twice each week and "booster" injections of helium made one to three times a day. No flights were made in showery or threatening weather to avoid dangerous electrical discharges, nor in windy (surface wind over 15 mph), gusty (gusts over 25 mph) or excessively unstable (lapse rate greater than 2.5°F./50 ft.) conditions. Thus the mid-morning and evening soundings were most successful, early morning conditions frequently reducing the altitude reached, and midday conditions requiring occasional cancellation of scheduled observations.

Six blimp escapes due to cable failure occurred during the program, four within the 6-month period (less than 200 flights) preceding the use of a nylon safety cord, and two in the following year (over 800 flights). Five of the escaping blimps were recovered, two having been found and returned by people off the reservation and one by an AEC patrolman on the area, one picked up in a nearby thicket after having been tracked by theodolite, one similarly tracked then located and recovered by means of a helicopter which happened to be available at the time. The sixth was permanently lost in rough, wooded terrain on the area. All the recovered balloons, more or less mutilated, as well as those which became leaky through normal wear, were sent to the factory for repair and reconditioning at a fraction of their initial cost and later returned to service.

Ascent and descent temperatures at each level were averaged, a graph of the average temperature vs. height drawn, and the following summary

data entered on the data sheet (Figure 28):

- a. Sounding type: one of the 10 standard types (temperature vs. height curves) which most closely resembled the observed curve (provided the 1000 ft. level was reached).
- b. Temperature differentials through the lowest 200 and 500 ft.
- c. Height of base, height of top and intensity of the inversion nearest the ground (if any).

The average temperatures and summary data were punched on IBM cards by the Y-12 IBM group.

22. Smoke Photograph Procedure

Photographs of smoke from HC pots ignited at the ground near station 001 were taken about 3 times a day on most days from March 1, 1949 through January 5, 1950. In January and February, 1950, a series of stack smoke photographs were taken, utilizing a steam plant stack and the Graphite Pile stack in the X-10 area. Short periods of intensive smoke observations employing helicopters were conducted in the vicinity of X-10 and Y-12 during April 5-7, 1950, and in the K-25 plant area during June 12-15, 1951. Additional intensive smoke observations were made near the Y-12 plant in Bear Creek Valley and adjoining ridges and gaps during March 5-9, 1951.

The procedure from March 1, 1949 to January 5, 1950, consisted of lighting one or two smoke pots in an open area near the hutment, driving up to the north theodolite station, a distance of about 1000 ft. usually across wind from the smoke pot, and shooting about 6 or 8

pictures. Rapid series of overlapping shots were taken, if necessary, to show the entire smoke trail with repetition at intervals of a few minutes to record changes in the pattern. Smoke runs were made early in the morning (before 7:30 a.m. if light permitted in order not to smoke up roads and parking lots during the 8:00 a.m. traffic rush at the Laboratory) to record well developed nocturnal inversion conditions, about midday to obtain typical lapse pictures, and just before dark to record the formative stage of the inversion.

During the latter portion of this same period an arrangement was in effect whereby the operator of the X-10 steam plant would cause dense smoke to be emitted from the stack for a 3-min. period on request. Usually stack smoke runs were combined with surface smoke runs. From January 12, 1950 to February 22, 1950, the pile stack smoke hood was used with the cooperation of the Pile Department of ORNL. The observer would notify the Pile superintendent (and also the steam plant superintendent) when ready for a smoke run and would then proceed in a car to a position on the south slope of Chestnut Ridge, on a level with the Pile stack top in a cross-valley direction, from which a broad, relatively unobstructed view of the X-10 plant and adjoining valley was obtainable. The Pile personnel would meanwhile light a smoke pot in the hood, and the observer would take a series of pictures of the two smoke trails, which were ordinarily distinguishable for some distance by virtue of the fact that the Pile smoke was white and the steam plant smoke black. No surface smoke runs were made during this period.

Each of the special, intensive smoke studies involved an all-out effort for brief periods, with smoke releases made simultaneously at several locations over an area of about a square mile, at intervals of 1 to 3 hours from dawn until dark, with associated intensive observations of wind and temperature distribution.

All exposed films were processed by the AEC Photographic Unit. Each roll of film was given a number and each exposure was logged by the observer as it was made. The log, containing the roll and exposure number, date, time, location, direction, subject, aperture, speed, filter data and the observer's initials for each shot, was indispensable in identifying and interpreting the prints and in improving quality with time.

23. Automobile Temperature Surveys

At the suggestion of Dr. H. E. Landsberg (then Executive Director of the Committee on Geophysics and Geography, Research and Development Board, Department of Defense) during a visit to Oak Ridge, a program of automobile temperature surveys was undertaken in the summer of 1950. The purpose was to obtain a more nearly continuous temperature profile across ridges and valleys than was obtainable by means of a limited number of fixed stations, and also to check some apparent discrepancies among micronet stations with respect to temperature distribution.

A temperature indicator was constructed which consisted of a pair of standard radiosonde thermistors type ML-405/AM which were linearized by

utilizing a Wheatstone bridge circuit. Approximate matching of the non-linear output of the unbalanced bridge to the non-linear temperature resistance curve of the thermistors was accomplished by a choice of the proper resistor values for the arms of the bridge. The bridge was then adjusted to balance at the lowest temperature desired and the temperature was read on the scale of a 0-50 microampere meter. The accuracy of the linearization was such that the scale read within 0.5°F. of the correct value over the whole range.

The circuit of the indicator is shown in Figure 29 with the resistance values shown for the two ranges of 0-50°F and 50°-100°F. which were used. Figure 30 shows the instrument panel with the 5" altimeter, range selection switch, calibration potentiometer, check switches and 4" Westinghouse meter.

The sensing elements were mounted in a plastic tube painted with aluminum paint on the outside to reflect the sunshine. This unit was mounted well forward on the fender of the carryall assigned to the program. A thin coat of plastic was sprayed over the thermistors and terminal connections for waterproofing.

In operation, the car was driven at a speed of 15 mph to provide adequate ventilation of the thermistors. The proper resistance standard corresponding to 50°F. or 100°F. were switched into the circuit and the calibration potentiometer was adjusted to give the correct full scale indication on the meter. An additional check was made by observing the reading of a shaded mercury thermometer held in the free air while the

car was in motion. If the mercury cell batteries were near exhaustion or the humidity was near saturation, some drifting of the calibration was observed. Abrupt changes in the calibration were always found to be caused by poor connections in the plugs or at the terminals of the thermistor mounting. Driving from shade into sunshine did not cause a noticeable change in the indication as long as the ventilation was maintained at about 12 miles per hour. Starting from rest, about a minute was required for the temperature to fall to a steady value in the day time. Relative temperatures could be determined within about 0.2°F , although the uncorrected absolute readings were sometimes 1° or 2° different from the shaded thermometer. The response time of the unit was of the order of 5 seconds for small temperature changes at the standard ventilation rates which would correspond to a distance of 110 feet traveled by the vehicle.

With the cooperation of the U.S. Air Force field office then associated with the NEPA (Nuclear Energy for Propulsion of Aircraft) project on the area, a sensitive altimeter was obtained on loan in May, 1950, and installed next to the temperature indicator on the dashboard of the vehicle where the glove compartment had been removed.

In operation, a route was selected which covered a suitable terrain profile, and several traverses made both ways with the altimeter adjusted at a point of known elevation. Easily recognizable temperature reading

points were selected so as to give good coverage of the route, altitude readings taken at each of these points on each traverse, and the average altitude thus determined, together with identifiable topographic features, were used to establish the locations of the reading points on a topographic map so that accurate profiles could then be drawn. After this preliminary survey of the route had been made (temperature readings could, of course, be taken simultaneously, although ordinarily a slower speed than adequate for thermistor ventilation would favor accurate altimeter readings), the identical route and reading points were used for a series of runs covering diurnal changes and various meteorological conditions. The driver would watch for the reading points and would signal the observer when to read the time and temperature. Readings taken going both ways on a round trip were averaged to give one profile representative of the time at the turn-around point and with lag effects (which could be quite considerable on steep slopes during strong inversions) largely cancelled out.

The greatest number of automobile temperature surveys was made across Bear Creek Valley from the crest of Pine Ridge through the Y-12 plant to the crest of Chestnut Ridge during August 28 to November 3, 1950. A series of runs was made on two days each week covering, on alternate weeks, the periods 6 a.m. to 1 p.m. and 3 p.m. to midnight. Other series of a few days' duration were made over this same route and also across Chestnut Ridge from Bear Creek Valley to Whiteoak Gap, near the X-10 plant.

D. Micronet of Unmanned Substations

24. Distribution of Stations

To sample the local variations of wind and temperature within the reservation 10 self-powered, automatic-recording stations were added to those already in existence. These stations were concentrated in the Whiteoak Creek drainage area containing the X-10 site. As the collection and interpretation of the data proceeded, it became desirable from time to time to abandon less profitable sites in favor of others critically chosen to supply answers to specific questions raised by previous observations.

The original micronet (Spring 1949 to Spring 1950) included all stations numbered up to 014 (Table 7 and Figure 2). Stations 011-014 were pre-existing stations slightly modified. Stations 001-007 and 009-010 provided coverage of the Whiteoak Creek drainage area and adjacent ridges and valleys. Station 001 was in the eastward draining portion of Bethel Valley, 004 in the southwestward-draining portion, 003 in an adjacent level col, 002 in the entrance to Whiteoak Gap, 009 in the Clinch River Valley just downstream from the mouth of Whiteoak Creek, 005 on the southeast-facing slope of Chestnut Ridge, 010 on the northwest facing slope of Haw Ridge, 006 on a typical ridge top, and 007 on the highest peak in the area. Coverage of the Y-12 plant in Bear Creek Valley by station 008 completed the basic pattern.

In the spring of 1950 two moves were made. Equipment from station 010, poorly exposed due to the unbroken forest cover of Haw Ridge, was moved

TABLE 7

MICRONET STATIONS

Station No.	Station Name	Ground Elevation, Ft. MSL	Anemometer Support	Equipment		
				Wind	Temp.	Precip.
001	X-10 Hutment	810	18'S 6,18,54'P	16,1 G	H C	T-B
002	Whiteoak Creek (N. Gap)	770	35'P	16,1/10	H	
003	W. Bethel Valley	840	36'P	16,1/10	H	
004	Bethel Church	820	18'S	16,1/10	H	
005	Chestnut Ridge Slope	995	35'P	16,1/10	H	
006	Chestnut Ridge Top	1120	52'P	16,1/10	H	
007	Melton Hill	1356	75'P	16,1/10	H	
008	Y-12, Bldg. 9212	1020	35'P	16,1/10	H	
009	Watts Bar (Clinch R. Valley)	760	18'S	16,1/10	H	DT
010	Haw Ridge	900	18'S	16,1/10	H	
011	Public Works Bldg. Townsite	905	40'B	8,1	H	DT
012	X-10 Health Physics	887	140'T 154'T	8,1 G	H R	DT ST
013	K-25, Bldg. K-832	756	45'B	G	H	DT
014	K-25, Bldg. K-1004-D	770	25'B	8,1		
015	S. Whiteoak Gap	768	18'S	16,1/10		
016	Whiteoak Lake	750	18'S	16,1/10	H	DT
017	Melton Valley	859	70'P	16,1/10		
018	Y-12 Health Physics	945	60'P	G	H	
019	Pine Ridge	1150	81'T	G	H	

Abbreviations:

S - Standard support	8 - 8 Point contacting	C - Thermocouples
P - Telephone pole	16 - 16 Point contacting	R - Thermohms
T - Steel tower	1/10 - 1/10 mile contacts	T-B - Tipping bucket
B - Building	1 - 1 mile contacts	DT - Weighing gage, 12" dual traverse
G - Generator-Selsyn	H - Hygrothermograph	ST - Weighing gage, 9" single traverse

to station 015 at the south end of the narrow Whiteoak Gap in order to verify the lack of through-flow of air indicated by the station 002 records.

Remoteness of station 009, and lack of apparent connection between its local wind regime and that in Whiteoak Valley, as well as a new interest in the Whiteoak Lake area associated with the start of an ecological survey of that area by the TVA for the AEC, motivated the removal of station 009 equipment to the station 016 site on the shore of the lake.

In the fall of 1950 station 005 which had been in operation over a year and a half was abandoned and the wind equipment moved to station 017, in a secluded valley across Haw Ridge from X-10, where experimental nuclear reactor installations were planned. The contacting wind equipment from station 001 was moved to station 019, a tall radio tower which became available on Pine Ridge between Y-12 and the Gamble Valley section of Oak Ridge. About this time also a new, more permanent station, 018, was installed at a more central location in the Y-12 area, to replace station 008.

Special care was taken during these station shifts to secure a few months of concurrent records from certain combinations of stations for comparison. Such combinations included stations 006, 007, 012 and 019, all high above the alleys; stations 002 and 015, at opposite ends of Whiteoak Gap; stations 005 and 010, on opposing slopes; stations 016 and 017, representative of lower and higher parts of Melton Valley, and these combined with 001 and 012, the low and high Bethel Valley stations and with 002 and 015, the gap stations; and of course, 008 and 018, the temporary and permanent Y-12 stations.

5. Basic Micronet Instrumentation

With few exceptions, the micronet stations installed during the survey program were equipped with battery-powered contacting wind instruments basically similar to those at station 001, and with hygrothermographs and maximum-minimum thermometers in cotton region shelters. The anemometer supports and heights of exposure varied somewhat. Three of the stations were also provided with 12-inch capacity dual-traverse weighing rain gages.

The difficulty of reading unbiased wind directions from the chart of the contacting wind system recorder previously discussed in connection with station 001, made it desirable to modify the method of recording, so as to produce a series of short direction contacts at uniform intervals of about 1 minute. It was first necessary to separate the anemometer circuit from the vane bearing circuit and to record the wind speed contacts by means of one of the spare pens. At the same time the 1/60 mile contact was modified by reducing the length of all but one of the six teeth on the contacting

cam. The $1/10$ mile contact resulting from this change was connected to the second spare recorder pen, so that hourly average wind speeds could easily be read to the nearest $1/10$ mph when desired.

To key the direction circuit, at first a mechanical contacting arm was placed on a 1 r.p.m. shaft of the chart drive to give a short electrical contact on every revolution. A few weeks testing of the instrument showed that the adjustment of the contacts was delicate and just a slight excess of drag would cause the chart drive to stop in cold weather.

The timing relay which was developed to replace the shaft contact is shown in the wiring diagram in Figure 31. The contacts of relay R1 are normally closed, allowing battery B2 to charge condenser C1 rapidly to about 40-60 volts. This voltage operates the relay, opening both the battery circuit and the direction magnet circuit. The charge on C1 holds the relay in its operate position during the time the voltage across the relay coil drops from approximately 40 volts to 12-15 volts. When the coil voltage has dropped to about 12 volts, the armature of the relay is released, allowing momentary closure of both the battery circuit and the wind direction magnet circuit, and the condenser is recharged allowing the cycle to be repeated. An examination of many months of wind charts such as shown in Figure 32 - made with the aid of this timing relay did not show any cases where 3 direction pens operated during the brief period of the direction contact.

If the timing circuit should fail either through low voltage of B2, or through leakage of C1, a continuous record of direction is made, insuring

against a loss of record. Since the velocity and direction records were not dependent as they were when the wind systems utilized the velocity contacts to sample the direction, the failure of an anemometer contact would not cause a loss of all of the wind records. About 5-6% of the data were missing from the micronet stations from all causes during the early months of the program. Almost all of these data were lost because of chart drive stoppage by spilled ink or humidity effects.

The recorders and timing relays were originally installed in the thermometer shelter to protect them from the weather. When the wind systems were modified, the recorders were moved to plywood boxes which contained bags of silica gel to reduce the effect of humidity on the rolls of chart paper (Figure 33). No data were lost as a result of chart jamming after the recorders were protected from moisture. An added advantage of using a separate recorder housing was sectionalization of the equipment. The leads from the direction bearing and the anemometer were brought to a 12-point AN-type connector which allowed the instruments to be wired prior to their installation. The recorder wiring harness was also made up and the connector inserted in the housing to allow easy removal for maintenance. The timing relay units plugged into the recorder harness and could be removed separately for checking or adjustment of the relays.

The micronet stations were visited on Mondays and Fridays after the first few months when the equipment was being installed and adjusted. Timing of the clocks on all instruments was checked and corrections were made for the benefit of the clerks who worked up the data. The weekly maximum and

minimum thermometer readings were recorded to determine the chart correction to be applied to the hygrothermograph readings. Calibration of the weighing type raingage with standard weights was carried out at intervals of 3-6 months. Every 6 months each wind recorder was replaced with a spare while it was thoroughly cleaned and adjusted. Very little trouble was experienced with the Esterline-Angus recorders after they were moved to the enclosed housing. The 9-volt batteries which operated the recorder magnets were changed when the voltage dropped below 6 volts. This usually occurred after about 700 hours of service.

26. Non-Standard Micronet Instrumentation

Station 011 had been established previous to the Survey Program. Wind records were obtained from a 4-point bearing and a standard 3-cup anemometer since 1947. The H. J. Green two-pen recorder was replaced with a 4-pen Esterline-Angus recorder to obtain a more legible record which could be read by the clerks without change in their routine methods. The direction circuit was closed at 60-second intervals by a synchronous motor, permitting D. C. voltage from a selenium rectifier to operate the proper pen. The tipping bucket raingage was replaced with a 12-inch dual traverse weighing gage. These changes permitted incorporation of the records into the weekly routine which was established for the unmanned stations of the micronet. A considerable saving in manpower was effected by the elimination of the daily change of charts and by the substitution of larger charts for the small H. J. Green charts.

Station 012 had been in operation since 1943 with observations of rainfall,

wind at 140 ft, surface wet and dry bulb temperature and temperatures at several higher levels. Some modifications were found to be required after an analysis of the past data. Much of the wind data recorded on a double register were incorrect either because a direction contact was inoperative or the anemometer was not functioning properly. Often several months would go by before the fault was recognized and repaired. The original installation included a Leeds and Northrup Micromax temperature recorder for nickel thermohms located at 6 levels between 3 ft. and 183 ft. Surface wet bulb temperatures were also obtained from a thermohm and wick. The thermohm elements were unspirated but were exposed in louvered boxes mounted on the water tank tower structure and an extension which reached the elevation of the stack top. A 9-inch single traverse rain-gage was included in the original instrumentation.

In the fall of 1949, the contacting wind instruments at station 012 were replaced with the anemograph wind system previously described. The instruments were raised from 6 feet to 20 feet above the top of the water tank.

The temperature gradient had been obtained by subtracting the surface temperature from the temperature recorded at each level. The points were quite crowded, and the gradients were only obtained to the closest degree F. The adiabatic temperature gradient for the 179' layer is slightly less than 1° F. so the changeover from isothermal to lapse condition was not accurately indicated. A modification of this system was made by the Special Application Section of the ORNL Instrument Department which consisted of recording surface (5') temperature, surface wet bulb depression (the water

container was replaced by a continuous water supply) and the temperature difference between the surface and 133 feet. The wet bulb depression was obtained from a pair of aspirated thermohms located in a cotton region shelter. All the thermohms used for measurements at the 5 ft level were located in the same shelter to give a more uniform exposure. This change resulted in greater ease and accuracy in reading the desired data from the chart since extra points and subtraction of readings were eliminated. Additional modifications have been initiated during 1952 to locate all the thermohms in aspirated radiation shields. The raingage has been calibrated during the Survey Program with standard weights following regular Weather Bureau procedures to insure more accurate precipitation records.

Station 013 was established in May, 1949, with a standard cotton region shelter, hygrothermograph and 12" dual traverse weighing type raingage. An anemograph wind instrument was installed on a 20-foot support on the roof of Building K-832. Some wet and dry bulb data had been previously obtained at this location by the Process Utility Department prior to the Survey Program using an unaspirated thermometer set held in the shade of the building, but these records were found not to be representative for meteorological purposes.

Station 014 originally consisted of a wind vane with an 8-point bearing and contacting anemometer mounted about 4 feet above a low roof. The double register which was in poor condition was replaced by an Esterline-Angus recorder to improve the reliability of the record. Since this recorder did not require daily changing of the chart (as did the double register), data

were obtained on week-ends when the laboratory personnel were not working. The height of the installation was left unchanged with the expectation that it would only be used for comparison in view of the better exposure of wind instruments at station 013 in the same plant area.

In addition to the pre-existing stations which have been described above, several additional stations were installed towards the end of the Survey Program which did not conform to the standard micronet installation.

Wind instruments were installed on a 70-foot pole at station 017 to provide wind data for a particular site in Melton Valley. A standard micronet installation of contacting wind instruments was made which has since been replaced with an Anemograph wind system when 110 volt AC power was made available. A temperature difference obtained from an aspirated, shielded thermocouple has also been installed at the site between 5 ft and 70 ft above the surface.

After a comparison period, station 008 was replaced by station 018 which was located more nearly in the valley bottom. An anemograph wind system was mounted on a 60 ft pole with aspirated, shielded thermopile elements for temperature gradient measurements mounted at the 5 ft and 60 ft levels. A cotton region shelter with a hygrothermograph completed the station instrumentation. Continuous measurements of temperature gradient have been made on several occasions for special studies.

A radio tower on top of Pine Ridge, station 019, has been utilized as a

support for wind and temperature gradient instruments at 80 feet above the ground. Surface temperatures have been obtained from a hygrothermograph located in a standard cotton region shelter near the base of the tower. Temperature gradient measurements have been obtained from this site for special studies.

27. Evaluation of Micronet Data

Charts were collected from all micronet instruments once each week, normally on Monday mornings, at which time any necessary notations were made on them as to calibration or timing errors. Hourly readings of all elements, corrected by the same methods as were used for station 001 data, were posted on "hourly weather data" forms, one data sheet per station per day. Weighing raingage charts were read to the nearest .01 in. allowing for apparent decreases due to evaporation from the bucket. The data sheets, usually completed by the end of the week, were sent to the IBM group at Y-12 for card punching.

E. Diffusion Measurements

28. Radioactivity

A major preoccupation of the atomic energy project from its earliest days has been the measurement and control of radiation exposure. Many studies have been specifically related to atmospheric contamination by stack discharges at Oak Ridge. A few of the more important ones will be mentioned. In 1943 and 1944 wind tunnel measurements of plume rise and dilution from model stacks of various sizes were made by A. F. Rupp, D. H. Johnson, S. E. Beall and L. P. Bornwasser (References 23 and 24). Between November, 1943 and June, 1945, J. S. Cheka conducted a thorough observational study

of atmospheric contamination from the X-10 stacks (Reference 25). His most conclusive results were obtained using integrating thin-walled ionization chambers, although Cheka also exposed film badges, G-M tubes and electroscopes as well as determining specific isotopes in air samples and counting gross activity of collected rain water. These results were all correlated with concurrent meteorological records from the X-10 Health Physics Division installation and with records of the relevant operations. This study can be considered fairly definitive as to long-period (8 hours or more) exposures under average operating conditions, showing that they were generally near the threshold of detection above natural background. However, they gave little information on shorter period variations, such as would be required for comparison with meteorological theory and extrapolation to hypothetical cases. Contributory to Cheka's analysis was a Xe^{135} sampling program carried out by K. J. Sax, D. C. Overholt and T. L. Carson in the X-10 Area during 1944. Between 1945 and 1947, various attempts were made to correlate gross airborne activity detected at various distances from the plant with wind direction and the presence of temperature inversions. An inconclusive series of measurements was made by R. D. Cameron at a distance of 8 mi. NE of X-10 using an exposed G-M tube whose pulses were recorded by "Trafficcounters". Continuous G-M counts of accumulated activity on filter papers through which air was drawn were recorded by Cameron at several locations in the X-10 area and compared by T. H. J. Burnett (Ref. 26), with the concurrent meteorological records with some clear correlations emerging. This filtering technique which has been used for years as the standard health physics air monitoring procedure, has the

disadvantage from the standpoint of meteorological analysis that it specifically excludes gaseous contamination. The question of particulate air contamination at X-10 was thoroughly investigated in 1948 - 1949 by J. S. Cheka and H. J. McAlduff (Ref. 27), with the purpose of determining the seriousness of the situation and recommending corrective measures. Information on source emission rates was largely lacking.

To summarize briefly the previous work on atmospheric dilution of radioactive contaminants at this site, it can be said that the immediate objectives of determining the existing exposure levels and isolating the major offenders were generally attained, but that the lack of sufficiently sensitive detectors at a range of distances from the source, short-period continuous recording, and precise knowledge of source emission rates, all achieved simultaneously, prohibited generalization of the results. A major difficulty in all such investigations is the inference of atmospheric concentration from beta-gamma exposure or sedimentation of particulates.

In order to determine the variations in the pattern of radioactive contamination in relation to the wind and temperature distributions, neutral-balloon trajectories, and smoke plume behavior observed during the Meteorological Survey Program, the cooperation of the ORNL Health Physics Division was enlisted during 1949. Instruments designed and assembled by Dr. Francis J. Davis and Paul W. Reinhardt to measure incident beta and gamma radiation, air conductivity and radon concentration continuously were installed in three trailers and located in Bethel Valley at points chosen so as to facilitate the meteorological analysis. It was hoped that by

continuous, independent measurements of these different components of the radioactivity, the actual concentrations of the A^{41} from the pile could be deduced. The source emission rate is quite well known and nearly constant when the pile is on.

From June, 1950 through November, 1950, the trailers were located 1.4 mi. WSW, 1.0 mi. ENE and 3.1 mi. ENE of the pile stack in order to obtain one upwind observation and two downwind observations when the wind was in the prevailing direction. In December, 1950, the WSW trailer was moved to 5.8 mi. ENE so as to cover an increased distance downwind. Four high-pressure argon ionization chambers were made available by the AEC in the spring of 1950 and were installed at approximately one and three miles ENE and WSW. Several experimental blimp-borne Geiger counters were built for the purpose of obtaining vertical radioactivity soundings through the stack gas stream, but none were successfully operated.

The mobile monitoring instruments which were mounted in the trailers consisted of a standard NRL gamma count rate meter which utilized a bundle of 48^m copper wall G-M tubes with coincidence circuits to reduce the background from cosmic radiation and a beta-gamma count rate meter which was fed by a group of four glass-walled G-M tubes mounted on top of the trailer in a light-tight enclosure to reduce the photosensitivity. In one trailer a moving filter paper collected the radon decay products from a constant air stream. These decay products were measured by recording the alpha count rate. The continuously moving filter tape was counted 4 hours after collection to allow the decay of the various daughters of radon, Po^{218} , Pb^{214}

and Po^{214} to be essentially completed. The longest half-life in the radon decay chain from Po^{218} to Pb^{210} is 26.8 minutes so the 4-hour decay between collection and counting is in excess of 8 half-lives of the longest life intermediate product. All of the thoron daughters will have decayed before the alpha count (on the remaining Pb^{210}) is determined, separating the radon from thoron. The trailers were operated by 1.5 kilowatt, 110V AC Onan generators where commercial power was not available.

The large ionization chambers charged with argon at high pressure which were also located at the sites of the trailers were connected by telephone lines with a modified Speedomax recorder located in the Health Physics building at ORNL. A vibrating reed electrometer measured the current from the ion chamber. The output of the electrometer was telemetered to a converter unit where it was changed to a signal which would operate the Speedomax recorder. Since the steel walls of the high pressure ion chambers were quite thick, only gamma and cosmic radiation would be detected by these units.

The mobile detection units were operated for a period of a few months in an effort to obtain satisfactory measurements of airborne radiation. The generators were not well suited to continuous operation and often stopped, requiring a complete overhaul. The timing of the charts was not very accurate as the generator speeds shifted and changed. The components of the rather complex electronic circuits did not break down very often, but the drift and change in sensitivity were quite severe. Calibration was accomplished by exposing the detector to an appropriate gamma source such as Co^{60} or radium and a beta source such as Pb^{210} at a measured distance.

The calibration formulas used to convert chart divisions to radiation were calculated by F. J. Davis of ORNL Health Physics Division on the assumption of an infinite, uniform cloud above a horizontal plane which contains a point detector.

For a gamma source:

$$S = 4.32 \times 10^{-10} \times \frac{S_0}{R_0} \times R \text{ for } S_0 = 1 \text{ rutherford Co}^{60} \text{ source at 3 feet}$$

$$S = 1.51 \times 10^{-10} \times \frac{S_0}{R_0} \times R \text{ for } S_0 = 1 \text{ rutherford Co}^{60} \text{ source at 5 feet}$$

For a beta source:

$$S = 2.58 \times 10^{-5} \times \frac{S_0}{R_0} \times R \text{ for } S_0 = 2.9 \times 10^{-8} \text{ curie Ra D at 3"}$$

$$S = 1.23 \times 10^{-6} \times \frac{S_0}{R_0} \times R \text{ for } S_0 = 2.9 \times 10^{-8} \text{ curie Ra D at 9"}$$

where S = concentrations in curies/m³ of A⁴¹
 R = chart divisions above background
 R_0 = chart divisions above background for source.

The range of the 1.24 to 2.5 Mev beta radiation from A⁴¹ in air is 200-300 inches. Both the total beta strength and the concentration of any argon cloud which is not in contact with the detector is measured with gross errors by means of a point source calibration such as that used here. Likewise, although the half-thickness of 1.3 Mev gamma radiation in air can be measured in hundreds of feet, the use of this type of calibration may give erroneous values of concentration of argon in the air when it is not known whether the cloud exists as a thin sheet high overhead or whether it is more nearly a cone, cylinder, line, or group of

spherical puffs at one side of the detector or at an unknown height above it. The use of this type of calibration is thus very misleading but it was the only approximation which had been worked out and was utilized during the Survey Program.

Over the period September, 1950 to May, 1951, the sensitivity of a typical NRL gamma count rate meter varied from 0.73×10^{-10} curies/m³/division to 3.89×10^{-10} curies/m³/division, largely due to changes in the number of G-M tubes in operation.

In the fall of 1950 a program of special releases of radioactive A⁴¹ was undertaken jointly by the Pile Department and the Health Physics Division of ORNL. The releases were made by discharging 100-200 curies of A⁴¹ into the pile stack over a period of about 20-30 minutes. This was done at about 3 a.m. and about 2 p.m. daily.

29. Beryllium

Outdoor beryllium dust sampling equipment and meteorological instruments were installed in the vicinity of a beryllium machining shop which began operation during 1950. The shop air, after considerable cleaning, was exhausted through a 50 ft. stack which contained a sampling unit. Except for a few erratic events in the initial stages of operations, when leaks occurred in the filter house near ground level, no significant outdoor concentrations were observed during the two subsequent years. Thus this well equipped installation never provided any useful data for atmospheric diffusion analysis.

30. Quarry Dust

Some weeks of effort were expended by H. J. McAlduff of the ORNL Health Physics Division during 1950 in attempting to obtain downwind concentrations of industrial dust from rock crushers at a quarry and a cement plant on the area. Electrostatic precipitators and widge impingers were used, but lack of source rate data and particle size distribution, as well as difficulties in choosing sampling points in very rough terrain, so obscured the interpretation that the project was abandoned.

Summary of Data Production and Processing

31. Quantity and Quality

During the two-year observational program, roughly 200,000 complete hourly microneet observations (wind, temperature humidity and precipitation), 2500 surface weather observations, 2500 winds aloft observations, 1100 temperature soundings, 800 neutral balloon runs comprising over 20,000 readings, and over 2000 photographs of 300 smoke runs were taken by the Weather Bureau group at Oak Ridge. The manual observation schedules, summarized in Table 8, were carried out by three full time observers and one supervising observer. To illustrate the distribution of observations during the two-year period, Table 9 shows the monthly totals of microneet observations, regularly scheduled winds-aloft observations (approximately equal to the number of surface weather observations) and captive-balloon temperature soundings. It should be noted in comparing the number of microneet hourly cards with the number of stations, that the number of stations shown represents the largest number in simultaneous operation at any time during each month and that cards were not punched for one station (014) which was in

TABLE 8

SCHEDULED OBSERVATIONS

<u>Type</u>	<u>Equipment</u>	<u>Period</u>	<u>Obs. per Day</u>	<u>Days per Week</u>
Weather	Sling psychrometer, max-min	11/10/48-12/4/48	2-6	5
	thermometers, mercurial	12/6/48-3/4/50	8	5
	barometer, aneroid microbar-	3/6/50-8/26/50	4	5
	ograph, can-type rain gage, recording anemometer and wind vane	8/28/50-11/3/50	7	5
Winds aloft	30 gm. pilot balloon, helium inflation equipment, theodo- lite on 16 ft. platform, tim- ing buzzer	11/10/48-12/5/48	2-6	5
		12/6/48-3/4/50	8	5
		3/6/50-8/26/50	4	5
		8/28/50-11/3/50	9-15	5
Neutral balloon	10 gm. ceiling balloon, hel- ium inflation equipment, 2 theodolites, synchronized timing buzzers	11/24/48-2/28/50	{ 2 series	5
		8/28/50-11/3/50	{ 45 min./series 4-5 series	3
Temperature sounding	Thermistor, support, captive blimp, 2000 ft. light-weight cable, motor-driven winch, linearized recorder	4/25/49-8/26/50	4	5
		8/28/50-11/3/50	9-15	5
Smoke photograph	OWS HC-M1 smoke pots, Argo- flex Camera, stack smoke hood	3/17/49-2/22/50	2-3 runs	5
Automobile temperature survey	Shielded thermistor, indicat- ing temperature bridge and altimeter mounted on carryall	8/28/50-11/3/50	8-12	2

TABLE 9

NUMBER OF ROUTINE OBSERVATIONS

	<u>Micronet Stations (Wind)</u>	<u>Hourly Cards (Wind)</u>	<u>Winds Aloft Observations</u>	<u>Temperature Soundings</u>
1949				
Jan.	3	1488	110	0
Feb.	6	1900	102	0
Mar.	12	6194	96	0
Apr.	12	7356	125	4
May	13	7623	163	23
June	13	8044	117	0
July	13	8184	87	8
Aug.	14	8442	76	22
Sept.	14	9118	73	11
Oct.	14	9419	134	13
Nov.	14	9101	144	45
Dec.	14	9321	111	55
1950				
Jan.	14	9235	108	39
Feb.	14	8284	117	33
Mar.	14	8921	79	52
Apr.	14	8877	77	52
May	14	9455	86	55
June	14	8737	77	72
July	15	10033	70	58
Aug.	15	9882	97	70
Sept.	15	9409	170	192
Oct.	16	10364	196	210
Nov.	16	9729	22	17
Dec.	7	4408	0	0
TOTAL	19	193,502	2,437	1,031

operation throughout the period. In addition to those tabulated, several intensive series of special winds-aloft observation and temperature soundings were made during this period.

An attempt has been made in Table 10 to compare the various methods of observing each meteorological element with respect to useful range, accuracy, duration and frequency of samples, and time resolution. Many of these figures are, of course, order-of-magnitude estimates for purposes of comparison only; others are the results of tests described in the preceding paragraphs.

Two distinctions should be borne in mind in interpreting the accuracy of the observations as shown by Table 10: : relative vs. absolute accuracy, and instrument capability vs. system or operational accuracy. The relative accuracy of the generator anemometers on the 54 ft. profile pole, for example, was probably better than $\frac{1}{2}$ mph within the useful range. The figure 1 mph in the table represents absolute accuracy. Similarly, the accuracy of the automobile thermistor was entirely relative, since it had to be calibrated by reference to another thermometer. In general, relative accuracy between instruments of the same type or between readings of the same instrument (precision or reproducibility) is somewhat better than absolute accuracy.

System accuracy, or usable accuracy in actual operation, on the other hand, may be considerably poorer than the accuracy of which the recording instrument is capable. An outstanding example of this is the wind direction as obtained from the contacting wind vane records. It has already been shown that although the recorded directions were accurate to 16 points of the

138

TABLE 10

COMPARISON OF INSTRUMENTAL OBSERVATIONS

<u>Element</u>	<u>Instrument</u>	<u>Height Above Ground</u>	<u>Useful Range</u>	<u>Est. Prob. Error</u>	<u>Sampling Duration</u>	<u>Sampling Interval</u>	<u>Est. 90% Response</u>	<u>Coding Unit</u>	<u>Chart Speed</u>
Wind speed	Contacting anemometer	18-75'	0-45 mph	1 mph	$\sqrt{1}$ mi. wind 0.1 mi.	1 mi. wind	few sec.	1 mph	$1\frac{1}{2}$ " / hr.
	Generator anemometer	6-54' { 60-140'	3-37.5 mph	1 mph	continuous	----	<4 sec.	$\frac{1}{2}$ mph	3" / hr.
			3-75 mph	1 mph	continuous	----	<4 sec.	1 mph	3" / hr.
	Thermopile anemometer	6-54'	0-5 mph (horiz. & vert.)	0.3 mph	continuous	----	<2 sec.	$\frac{1}{2}$ mph	2" / hr.
	Pilot balloon	175-9400'	any speed	10%	$\frac{1}{2}$ - 1 min.	2-6 hrs.	negligible	1 mph	----
	Neutral balloon	0-3000'	any speed (horiz. & vert.)	1 mph	1 min.	{ 15-30 min. 12 hrs.	negligible	0.1 mph	----
Wind direction	Contacting vane	18-75'	0-360°	12°	0.2 sec.	1 min.	1-15 sec.	16 points	$1\frac{1}{2}$ " / hr.
	Selsyn vane	6-140'	0-360°	2°	continuous	----	1-10 sec.	10°	3" / hr.
	Pilot balloon	175-9400'	0-360°	5°	$\frac{1}{2}$ -1 min.	2-6 hrs.	negligible	100	----
	Neutral balloon	0-3000'	0-360°	<5° when speed \geq 5 mph	1 min.	{ 15-30 min. 12 hrs.	negligible	1°	----
Temperature & humidity	Hygrothomograph	4'	-10 to +110° F	1° F, 3% RH	continuous	----	5-15 min.	1° F, $1\frac{1}{2}$ RH	$1\frac{1}{2}$ " / day
	Thermocouple, grass	4'	0 to 200° F	0.2° F	instantaneous	1 min.	<12 sec.	1° F	2" / hr.
	Thermistor (blimp)	4-2000'	10 to 115° F	0.1° F	instantaneous	1-6 hrs.	17 sec.	0.1° F	2" / min.

TABLE 10 - COMPARISON OF INSTRUMENTAL OBSERVATIONS - (Cont'd.)

Element	Instrument	Height Above Ground	Useful Range	Est. Prob. Error	Sampling Duration	Sampling Interval	Est. 90% Response	Coding Unit	Chart Speed
	Thermistor (auto)	3½'	0 to 100°F	0.5°F	instantaneous	20-60 min.	15 sec.	0.1°F	----
	Thermohm	4'	-10 to 110°F	1°F	instantaneous	3 min.	1-3 min.	1°F	2" / hr.
	Max.-Min. Thermometer	5'	-10 to 110°F	0.5°F	6-24 hrs.	6-24 hrs.	1-3 min.	0.1°F	----
	Sling Psychrometer	4'	-10 to 110°F	0.2°F	1 min.	3 hrs.	1-3 min.	0.1°F	----
	Thermopile	4-54'	-3 to 120°F	0.1°F	continuous	----	<12 sec.	0.1°F	2" / hr.
	Thermohm	4-183'	-10 to +20°F	1°F	continuous	----	1-3 min.	1°F	2" / hr.
	Weighing gage	4'	0-12" 0-9"	0.02" 0.03"	continuous	----	negligible	0.01"	1½" / day
	Tipping-bucket gage	3'	0-1"	5%	.01" precip.	.01" precip.	----	0.01"	1½" / hr.
	Can gage	3'	0-10"	0.04"	6-24 hrs.	6-24 hrs.	----	0.01"	----
	Mercurial barometer	5'	<31.5" Hg.	.002" Hg.	instantaneous	6 hrs.	negligible	0.001"	----
	Aneroid microbarograph	5'	27.5-30" Hg.	.005" Hg.	continuous	----	few min.	0.001"	2½" / day
	Pyrheliometer	18'	0-2 ly/min.	0.02 ly/min.	continuous	----	3 min.	0.1 ly/hr.	2" / hr.

compass ($\pm 1\frac{1}{4}^{\circ}$), it was impossible to read the hourly prevailing directions this accurately while maintaining the necessary rapidity of reading. The subjective estimation of prevailing direction was usually biased in favor of either the primary (one-pen) or intermediate (two-pen) directions. Similarly, where the coding units were larger than the probable error of the instrument, the full capabilities were not being utilized. This was true of the thermopile anemometer, selsyn wind vane and thermocouple temperature records. In these cases the full accuracy of the instruments was not necessary for the analysis or was rendered useless by larger errors in associated observation. However, where the quantity being measured fluctuated with an amplitude larger than the probable error of the instrument, and with periods larger than the duration of sampling but smaller than the intervals between samples, the resulting indeterminacy, rather than instrument error, set the limit of usable accuracy. This was true of the winds aloft and also of the grass temperature.

32. Data Processing

Each Monday during the peak of the observation program, the preceding week's charts were collected from 38 recording instruments and brought to the Weather Bureau Office for processing. Table 11 shows that 102 individual readings for each hour of the week were entered in the data sheets, that 18 of these hourly items were computed and that 45 corrections or conversions were required. Seventy-nine daily values were also obtained by manual computation. This chart processing job was normally completed by three clerks in about three working days, with the assistance of the observers on solar

TABLE 11

WEEKLY INSTRUMENT CHART READINGS

<u>Recording Instrument</u>	<u>Number of Charts</u>	<u>Hourly Readings</u>	<u>Daily Readings</u>	<u>Corrections and Conversions</u>
Hygrothermograph	12	temp RH dew pt*	max temp min temp max dew pt min dew pt	temp RH time
Thermohm	1	temp WB dep RH* dew pt* temp grad	max temp min temp max dew pt min dew pt	none
Thermocouple	1	temp WB temp WB dep* RH* dew pt* grass temp	max temp min temp max dew pt min dew pt	none
50' Temp. grad.	1	temp grad	none	none
Contacting wind	11	prev dir avg speed	prev dir	
Gen-selsyn wind	6	prev dir avg speed	prev dir	360° to 16 points (3)
		dir range (4) speed range (4)	none	
Thermopile anem.	1	avg speed (3) speed range (4)	none	vertical; peak to range
Rain gage	4	Total precip.	Total precip.	tipping bucket to stick total
Pyrheliometer	1	Total sol rad*	Total sol rad	solar mean time, ly/min to ly/hr
Total number	38	102 (18*)	79	43

*Computed from raw data.

Number of readings; where different from number of charts, shown in parentheses.

radiation and wind profile charts. In addition, special chart reading projects were almost constantly in progress. For special climatological summaries, research studies or instrument tests, additional records such as barograph charts, original records of temperature soundings, speed runs on the gustiness recorders, simultaneous wind or temperature records at a single station and radioactivity charts were read and the data tabulated in various ways.

When this manual process of collection, conversion to numerical form, correction and reorganization of the weekly load of observational records was completed, the data sheets were logged in duplicate and sent to the Y-12 IBM group, under the direction of Mr. Fred C. Uffelman, for punching and summarizing. Six basic card layouts were developed for key-punching into the 80-column IBM cards from the following six types of data sheets: (1) hourly microneut data, (2) double theodolite (neutral balloon) readings, (3) pilot balloon (winds aloft) observations, (4) low level temperature soundings, (5) wind profile data and (6) classification code. This last item, a 10-digit code representing ten meteorological typing parameters for use in stratifying the observations, will be described more fully in a later paragraph.

The routine monthly and quarterly tabulations which were prepared from these punched cards can be considered a part of the data processing program. These routine summaries are listed in Table 12. Averages, totals, frequency distributions and the complicated neutral balloon position and velocity computations, as well as resultant wind computations, various differences and ratios, conversions of units, etc., were carried out by these versatile

TABLE 12

ROUTINE PUNCHED CARD TABULATIONS

<u>Designation</u>	<u>Description</u>	<u>Unit</u>	<u>Columns</u>	<u>Lines</u>	<u>Period</u>
<u>Form A</u>	<u>Daily and Monthly Micronet Data</u>		<u>Stations</u>	<u>Days & Month</u>	<u>Monthly</u>
A-1	Maximum temperature	1° F.			
A-2	Minimum temperature	1° F.			
A-3	Mean hourly temperature	1° F.			
A-4	Temperature range	1° F.			
A-5	Maximum dew point	1° F.			
A-6	Minimum dew point	1° F.			
A-7	Mean dew point	1° F.			
A-8	Dew point range	1° F.			
A-9	Mean relative humidity	1%			
A-10	Duration rel. hum. 95% or higher	1 hr.			
A-11	Total precipitation	.01 in.			
A-12	Mean wind speed	1 mph			
A-13	Prevailing wind direction	16 points			
A-14	Resultant wind direction	1°			
A-15	Resultant wind speed	0.1 mph			
<u>Form B</u>	<u>Mean Hourly Micronet Data</u>		<u>Stations</u>	<u>Hr. & Total</u>	<u>Monthly & Quarterly</u>
B-1	Temperature	0.1° F.			
B-2	Dew point	0.1° F.			
B-3	Relative humidity	1%			
B-4	Wind speed	0.1 mph			
B-5	Frequency of NNE-E wind	1%			
B-6	Frequency of ESE-S wind	1%			
B-7	Frequency of SSW-W wind	1%			
B-8	Frequency of WW-N wind	1%			
B-9	Frequency of calms	1%			
B-10	Frequency of indeterminate wind direction (DI)	1%			
B-11	Resultant wind direction	1°			
B-12	Resultant wind speed	0.1 mph			
<u>Form C</u>	<u>Micronet Wind Roses</u>		<u>Stations</u>	<u>Directions</u>	<u>Monthly</u>
C-1	Mean wind speed	0.1 mph			
C-2	Frequency	0.1%			
<u>Form D</u>	<u>Hours of Micronet Data</u>	1 hr.	<u>Stations</u>	<u>Elements</u>	<u>Monthly</u>
<u>Form E</u>	<u>Detailed Micronet Wind Rose</u>	0.1%	<u>Speed Classes</u>	<u>Directions</u>	<u>Quarterly</u>
E-1	Station 001				
E-2, etc.	Station 002, etc.				

TABLE 12 - ROUTINE PUNCHED
CARD TABULATIONS (Cont'd)

<u>Designation</u>	<u>Description</u>	<u>Unit</u>	<u>Columns</u>	<u>Lines</u>	<u>Period</u>
<u>Form F</u>	<u>Neutral Balloon Listing</u>	Bearing .01° dist: 1 ft. dir: 1° vel: 0.1 mph	Raw & computed data	Reading number	Continuous
<u>Form G</u>	<u>Detailed Upper Air Wind Rose</u>	0.1%	Speed classes	Direc- tions	Quarterly
G-1	Level 1, station 001 (175 ft.)				
G-2, etc.	Level 2, station 001 (525 ft.), etc.				
<u>Form H</u>	<u>Upper Air Wind Roses</u>		Levels	Direc- tions	Monthly
H-1	Mean wind speed, X-10	0.1 mph			
H-2	Frequency, X-10	0.1%			
H-3	Mean wind speed, Knoxville	0.1 mph			
H-4	Frequency, Knoxville	0.1%			
<u>Form I</u>	<u>Diurnal Variation of Winds Aloft</u>		Levels	Obs. times & total	Monthly & Quarterly
I-1	Number of observations, X-10	1 obs.			
I-2	Number of observations, Knox.	1 obs.			
I-3	Mean wind speed, X-10	1 mph			
I-4	Mean wind speed, Knoxville	1 mph			
I-5	Freq. of dir. 10-90°, X-10	1%			
I-6	Freq. of dir. 100-180°, X-10	1%			
I-7	Freq. of dir. 190-270°, X-10	1%			
I-8	Freq. of dir. 280-360°, X-10	1%			
I-9	Frequency of calms, X-10	1%			
I-10	Resultant direction, X-10	1°			
I-11	Resultant speed, X-10	0.1 mph			
I-12	Resultant direction, Knoxville	1°			
I-13	Resultant speed, Knoxville	0.1 mph			
<u>Form J</u>	<u>Temperature Sounding Data</u>		Levels	Obs. times	Quarterly
J-1	Mean temperature	0.1° F.			
J-2	Number of observations	1 obs.			
J-3	Mean temperature gradient	0.1° F.			
<u>Form K</u>	<u>Sounding Summary Data</u>	1%	Classes	Obs. times	Quarterly
K-1	T ₂₀₀ -T _{surface}				
K-2	T ₅₀₀ -T _{surface}				
K-3	T ₁₀₀₀ -T _{surface}				
K-4	Sounding type				

TABLE 12 - ROUTINE PUNCHED
CARD TABULATIONS (Cont'd)

<u>Designation</u>	<u>Description</u>	<u>Unit</u>	<u>Columns</u>	<u>Lines</u>	<u>Period</u>
<u>Form L</u>	<u>54 ft. Wind Profile Summary</u>				Monthly & Quarterly
L-1	{Speeds, ratios, differences, speed gustiness, direction gustiness, direction difference	Various	17 Vari- ables	Hours	Quarterly
L-2	Direction quadrant frequencies	1%	15 Classes	Hours	
L-3	Wind Roses	$\frac{1}{2}$ mph, 0.1%	{Speeds & Frequencies	{Diréc- tions	
L-4	Resultant winds	1°, 0.1 mph	{Directions & Speeds	Hours	
<u>Form M</u>	<u>Classification Code Frequency Distribution</u>	1 obs.	{Code Column	{Code Number	Monthly
<u>Form N</u>	<u>Neutral Balloon Summary</u>				
	Spatial distribution of balloon frequency and resultant velocity. After one quarter discontinued in favor of combining entire body of data.				

machines. Of course, the more refined results were obtained at considerable cost in man-hours and machine-hours. Later these routine tabulations were supplemented by a variety of special punched-card studies including:

- (1) Daily data inventory, by elements.
- (2) Comparison of wind directions at pairs of stations (joint frequency).
- (3) Test of various classification code variables with respect to differentiation and homogeneity of wind patterns, wind profiles and gustiness sorted by them singly and in combination (ratios between wind speeds at pairs of stations, resultant winds, and standard vector deviations were obtained in the preliminary run).
- (4) Large scale sorting of area wind flow patterns, profiles and gustiness by means of most potent classification parameters.
- (5) Wind roses during stable and unstable thermal stratifications.
- (6) Wind roses during precipitation.
- (7) Frequencies of specific wind flow patterns represented by selected combinations of wind directions at a group of stations.
- (8) Summary of wind speed gustiness and directional gustiness at 6, 18 and 54 ft. anemometers by 54 ft. speed and temperature gradient.
- (9) Sorting and summarizing of neutral balloon observations on the basis of classification criteria and additional independent variables (done by IBM unit in Scientific Services Division, USWB, Washington).
- (10) Seasonal and annual surface and upper air wind roses for all Weather Bureau stations in the southern Appalachian area, for selected conditions (all observations, day only, night only, precipitation only)

utilizing at least 10 years of record at each station; also hourly resultant winds for these stations (done by Weather Bureau - Air Force - Navy Tabulation Unit, New Orleans).

- (11) Internal consistency check of Oak Ridge 3-hourly surface weather observation cards and item-by-item comparison (by difference or joint frequency) with corresponding Knoxville observation cards (done by USWB Weather Records Processing Center, Chattanooga).

The routine tabulations listed in Table 12 (including the neutral balloon computations), and the preliminary test of sorting effectiveness of the classification criteria were the earliest projects to be set up and were by far the most elaborate. As time went on, it became apparent that more efficient use could be made of the machines by accepting less refined results. By obtaining from the machines, as often as possible, raw totals or card counts in various categories, thus relying upon them primarily for the massive sorting and collating operations, and then computing final percentages, ratios, means, etc., by hand, the results were obtained more quickly and inexpensively and were more easily checked.

33. Data from Other Stations

Much use has been made of comparative data from surrounding Weather Bureau stations at every stage of the meteorological survey program. Published climatological summaries (monthly and annual State and National Climatological Data, annual Local Meteorological Summaries, TVA monthly and annual Precipitation Summaries, etc.), satisfied many of the requirements, but

numerous special arrangements were also necessary. In the absence of direct weather teletypewriter service, it was necessary to rely upon the cooperation of the Knoxville Weather Bureau Office (T. W. Kleinsasser, Meteorologist in charge), for complete daily pilot balloon and radiosonde data from the stations mentioned above. The teletypewriter reports were mailed from the Knoxville office daily on completion of their use there. The Atlanta, Greensboro and Nashville raobs were plotted on "pseudo-adiabatic" diagrams and the Knoxville pibals were recorded for the local punched card unit. Many upper-level wind maps for the southeastern United States were also plotted.

The need for documentation of larger-scale processes accompanying the local observations was partially filled by the printed Daily Weather Map mailed from Washington. In order to obtain sufficient information for all our purposes, however, it was arranged that copies of the 6-hourly synoptic weather maps, and 12-hourly 850 mb (5000 ft.) and 700 mb (10,000 ft.) charts would be mailed daily from the Weather Bureau-Air Force-Navy (WBAN) Analysis Center in Washington. Later all but the 850 mb charts (used in classification coding) were discontinued. Additional summaries of wind data from other stations have been mentioned in a previous paragraph in connection with the punched card processing program. Finally, photostats were made of portions of the Station Climatological Records of the Weather Bureau Offices at Knoxville and Chattanooga, which contain many items not included in published summaries.

34. Classification Code

Mentioned briefly in connection with the data processing program, the 10-digit classification code represents a selection of 10 variables which were regarded as independent or controlling with respect to the detailed observations taken during the survey program. The 10 variables were evaluated for each hour of the observation period, coded, and punched into all the observation cards for that hour. It was at first planned to include some variables of a more subjective or synthetic type, such as the location and intensity of high or low pressure centers or fronts, gradient winds computed from isobaric analysis, or estimates of cloudiness. However, the need for a complete classification for each hour of observation virtually dictated that the classifying elements be derived directly from the most frequent and reliable observations with only the most simple and objective conversions. In a consultation on this important phase of the groundwork for the analysis of the observational data in 1949, Dr. Harry Wexler, Chief of the Scientific Services Division, U.S.W.B., cautioned against allowing complicated hypotheses to influence unduly the choice of independent variables and encouraged the direct use of objectively observable variables known to be fundamentally related to flow patterns and turbulence. He suggested the Richardson number evaluated over an appropriate height interval as the only relatively complex derived quantity which had repeatedly shown a significant sorting ability in previous allied researches.

The 10 elements and their respective class intervals finally adopted

following numerous comparative tests on samples of data were as follows:

- (1) 5000 ft. (MSL) wind direction obtained from the 3-hourly Oak Ridge pilot balloon observations coded to 8 points and hourly values obtained by interpolation. Alternate sources: first, Knoxville pibal; second, contours on WBAN Analysis Center 850 mb. chart.
- (2) 5000 ft. (MSL) wind speed, same source as (1). These two digits represent the prevailing large-scale flow in the lower troposphere, and were used as a substitute for the gradient wind determined by the sea-level pressure field.
- (3) Daily temperature range, station 012, (ORNL Health Physics) midnight to midnight. Alternate sources: first, station 003 (West Bethel Valley); second, station 001 (X-10 Hutment). This figure, a constant for each calendar day, is indicative of the degree of radiational heating and cooling at the base of the atmosphere and therefore of the strength of the diurnal thermal stability cycle in the lowest layers. Although direct measurements of stability were available continuously for certain shallow layers, the temperature range, in combination with time of day, would be an attractive parameter if its sorting power were comparable, since it is a readily available datum at any location having a climatological record. Station 012 was chosen for this purpose because it had the longest, most complete record.
- (4) Persistency of stable conditions combined with light winds, obtained by counting the number of consecutive 12-hour periods, preceding the

hour in question with 5000 ft. wind speed less than 20 mph and with 850 mb. temperature minus surface temperature greater than -15° F. Very few hours received any score at all within this arbitrary and seemingly broad definition of stagnant conditions (conducive to building up of pollution concentration).

- (5) 850 mb. (about 5000 ft. MSL) temperature minus surface temperature, a measure of gross stability in the lowest 4000 ft. of the atmosphere. The 850 mb. temperature was obtained by visual averaging of the Atlanta, Greensboro, and Nashville raob temperatures; alternate source: 850 mb. chart; hourly values between the 12-hourly raob times were interpolated. The hourly surface temperature was obtained from station 012; alternate: station 003.
- (6) 180 ft. vertical temperature differential from ORNL Health Physics Division water tower instrument, a measure of the stability within the valley formed by the local ridges. (5) and (6) would be expected to play somewhat different roles in their effects on ridge-valley flow patterns and turbulence in the lower atmosphere. Alternate source: two-thirds of the temperature difference between station 007 (Melton Hill) and station 009 (Watts Bar) or 016 (Whiteoak Lake).
- (7) Direction of wind shear vector, 175 ft. level to 1200 ft. level, from Oak Ridge pibal, with hourly vaues interpolated. To allow for the possibility that the shear, rather than the gradient wind itself, might be the determining vector with respect to flow patterns and turbulence, this quantity, representative of a 1000 ft. layer based just below ridge-top level, was included. Alternate source: direction

of vector difference, Knoxville 2000 ft. (MSL) wind level minus station 012 wind.

- (8) Magnitude of wind shear vector, 175 ft. to 1200 ft. same source as (7).
- (9) Richardson number nominally for the layer 200 to 1200 ft. above the valley. This dimensionless parameter represents the ratio of the potential energy of thermal stability (gravity), tending to damp out turbulence, to the kinetic energy of the shearing motion, tending to generate turbulence. The stability term was obtained from (6), adjusted empirically to the reference layer. The shear term was obtained from (8). Unfortunately the cumulative error of indirect inference of stability, inaccuracy of the vector difference of small winds-aloft vectors, frequent substitutions of data from alternate sources, and interpolation of hourly values was so great as to decrease the reliability of this sorting parameter below those of some of the other classification variables.
- (10) 850 mb. (5000 ft. MSL) dew point, an indicator of the moisture content of the lower troposphere, and consequently of the cloudiness, the air mass source and the transmission of terrestrial radiation, obtained from the plotted raobs; alternate source: 850 mb. chart. This parameter, of secondary importance in itself, was included in order to increase the resolving power of the other parameters if necessary.

The units and class intervals of these 10 variables are shown in Table 13. Two additional classifying variables were present in each card, namely, season and time of day. When these are taken into account, it is obvious that the number of possible categories obtainable by combinations of these

153

TABLE 13

CLASSIFICATION CODE

Digit	1	2	3	4	5	6	7	8	9	10
Variable	5000 ft. wind dir (from)	5000 ft. wind speed	Daily temp range	Persis- tence	T _{850 mb} minus T _{surface}	T _{183 ft} minus T _{surface}	Shear dir (towards)	Shear magni- tude	Richardson number	5000 ft. dew point
Unit	8 points	1 mph	1° F. 12 hrs.	12 hrs.	1° F.	1° F.	8 points	1 mph	pure number	1° C.
Code	0	0	0-4	0	≤-30	≤-7	none	0	<0	≤-20
1	NE	1-4	5-9	1	-29 to -25	-6 to -4	NE	1-4	0-.09	-19 to -15
2	E	5-9	10-14	2	-24 to -20	-3 to -1	E	5-9	.10-.29	-14 to -10
3	SE	10-14	15-19	3	-19 to -15	0 to +2	SE	10-14	.30-.59	-9 to -5
4	S	15-19	20-24	4	-14 to -10	+3 to +5	S	15-19	.60-.99	-4 to -1
5	SW	20-29	25-29	5	-9 to -5	+6 to +8	SW	20-29	1.00-1.49	0 to +4
6	W	30-39	30-34	6	-4 to 0	+9 to +11	W	30-39	1.59-1.99	+ to +9
7	NW	40-49	35-39	7	+1 to +5	+12 to +14	NW	40-49	2.00-2.99	+10 to +14
8	N	50-59	40-44	8	+6 to +10	+15 to +17	N	50-59	3.00-4.99	+15 to +19
9		≥60	≥45	≥9	≥+11	≥+18		≥60	≥5.00	≥+20

ORO-99

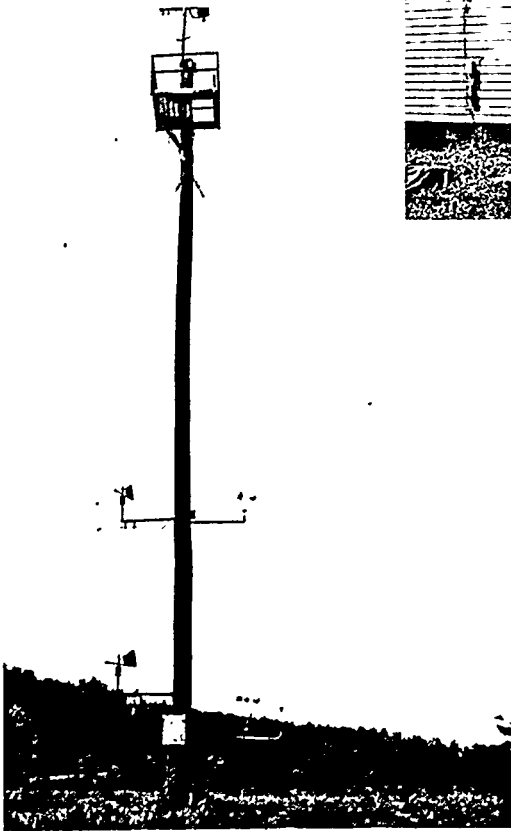
variables is far beyond the usable realm. Not all the variables were, in fact, even tested on the mass of data, and only a small fraction of the possible combinations of the remaining variables were actually required in order to cover both the typical cases and the important extremes.

We have now described the observational requirements of the Oak Ridge meteorological survey, the observational equipment, methods of observation, siting of stations, observation schedules, procedures for processing observational data, machine tabulation of routine summaries, utilization of observational data from other sources, and reduction of a few controlling elements from various sources to a master meteorological sorting code for all observations. This discussion has been intended to provide an adequate basis for evaluation of the meteorological results which follow, and also to set down such of our innovations and experiences as may prove useful to other workers in this field.

(a)



(b)



(c)



Fig. 4 (a) Double hutment and theodolite platform.
 (b) Wind and temperature profile pole.
 (c) X-10 hutment area seen from the Northwest. (Haw Ridge in the background.)

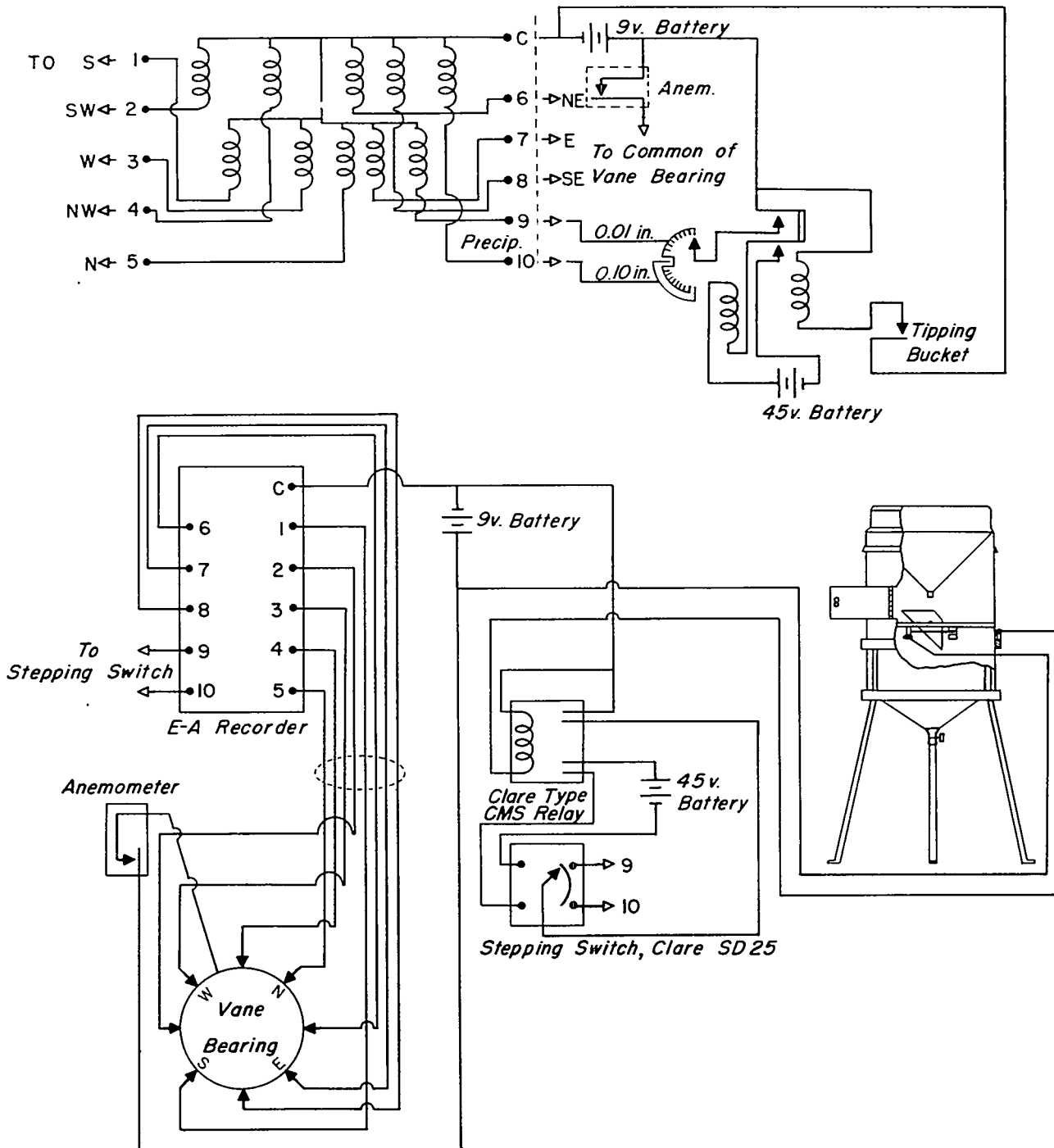


Fig. 5 Contacting rain and wind recorder: internal wiring of recorder and interconnection of units.

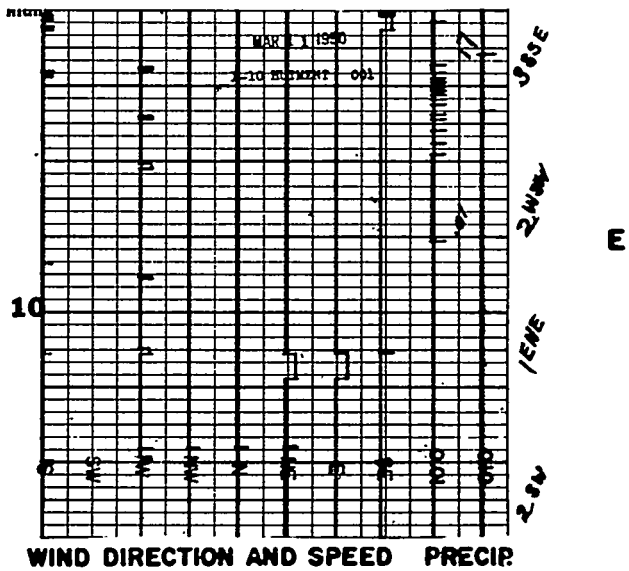
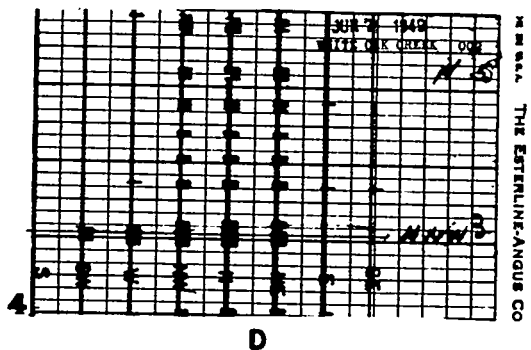
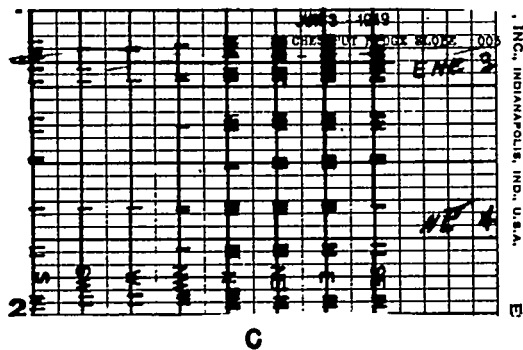
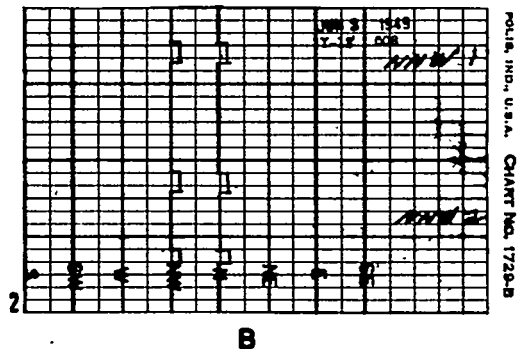
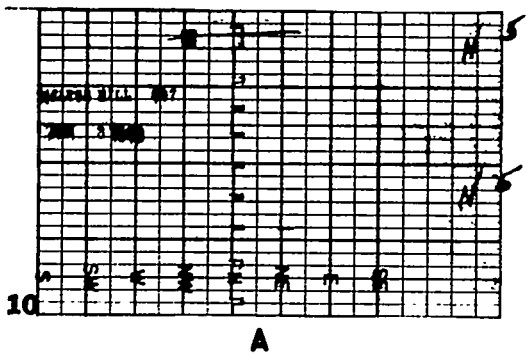


Fig. 6 Examples of contacting wind records with activation of the direction pens by the 1-mile speed contact.

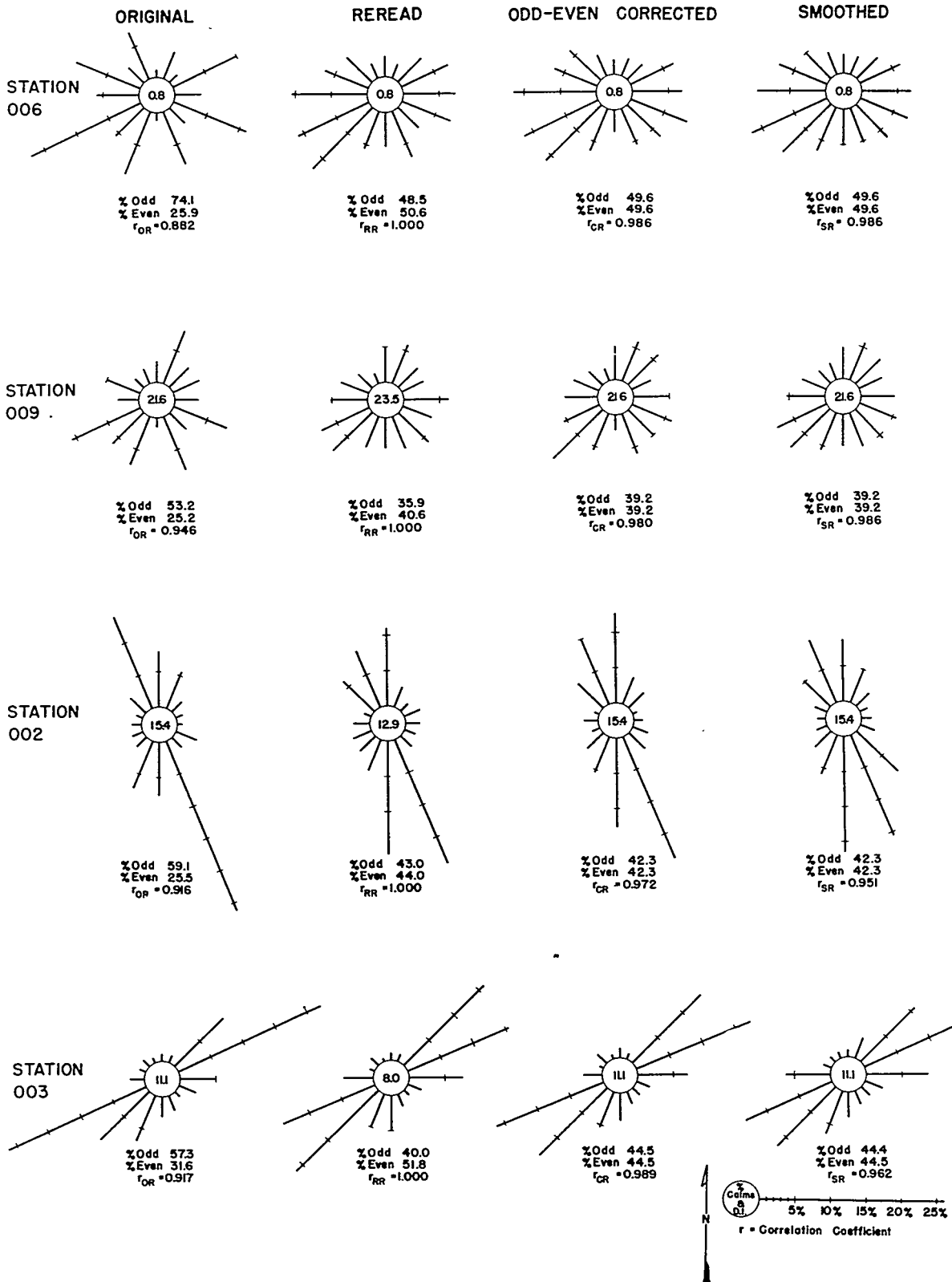


Fig. 7 Biased and corrected wind direction frequency roses for 4 test stations, June, 1949.

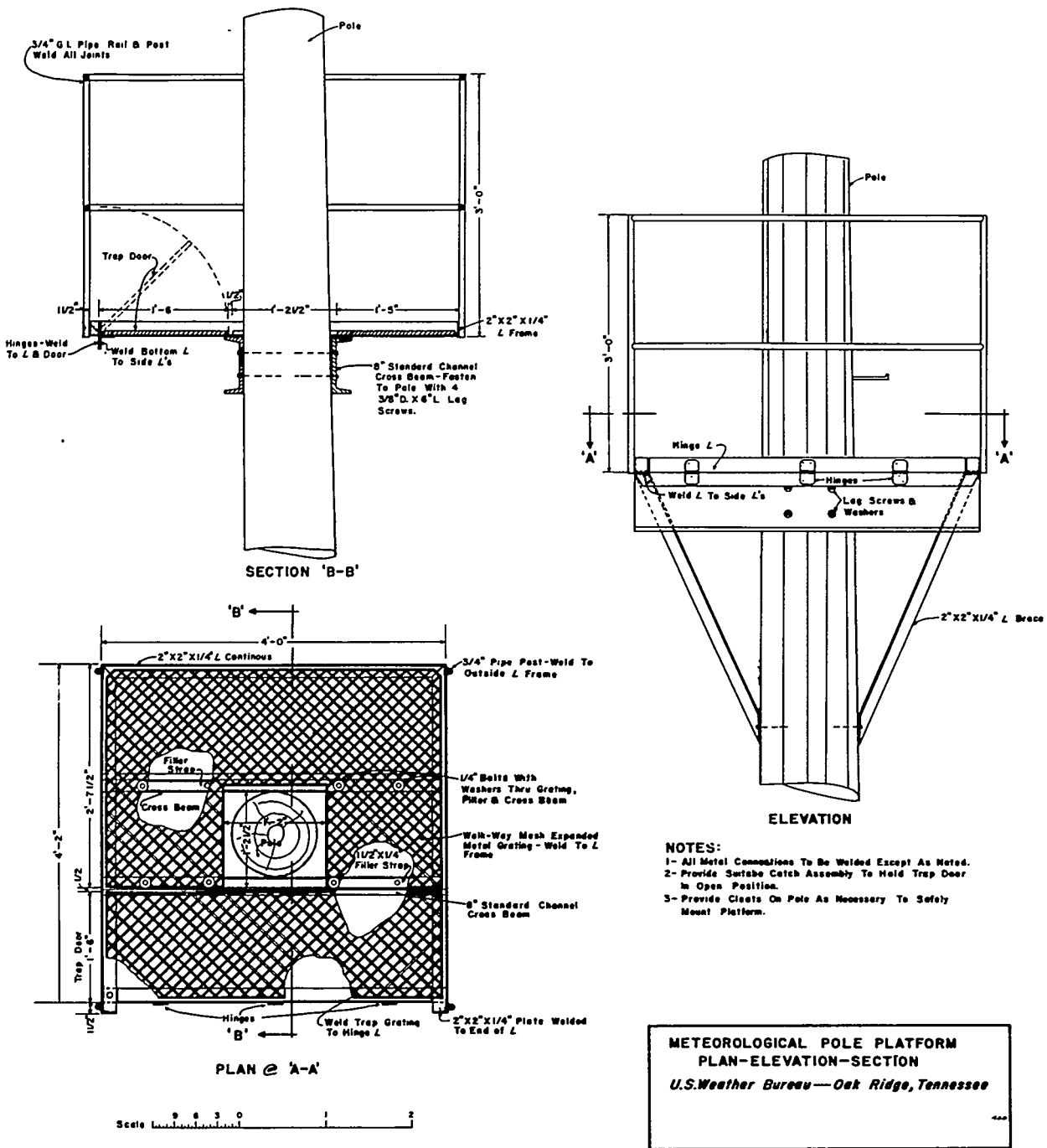


Fig. 8 Design of safety platform for anemometer poles.

RESONANT PERIOD OF INSTRUMENT CORPORATION ANEMOGRAPH VANE

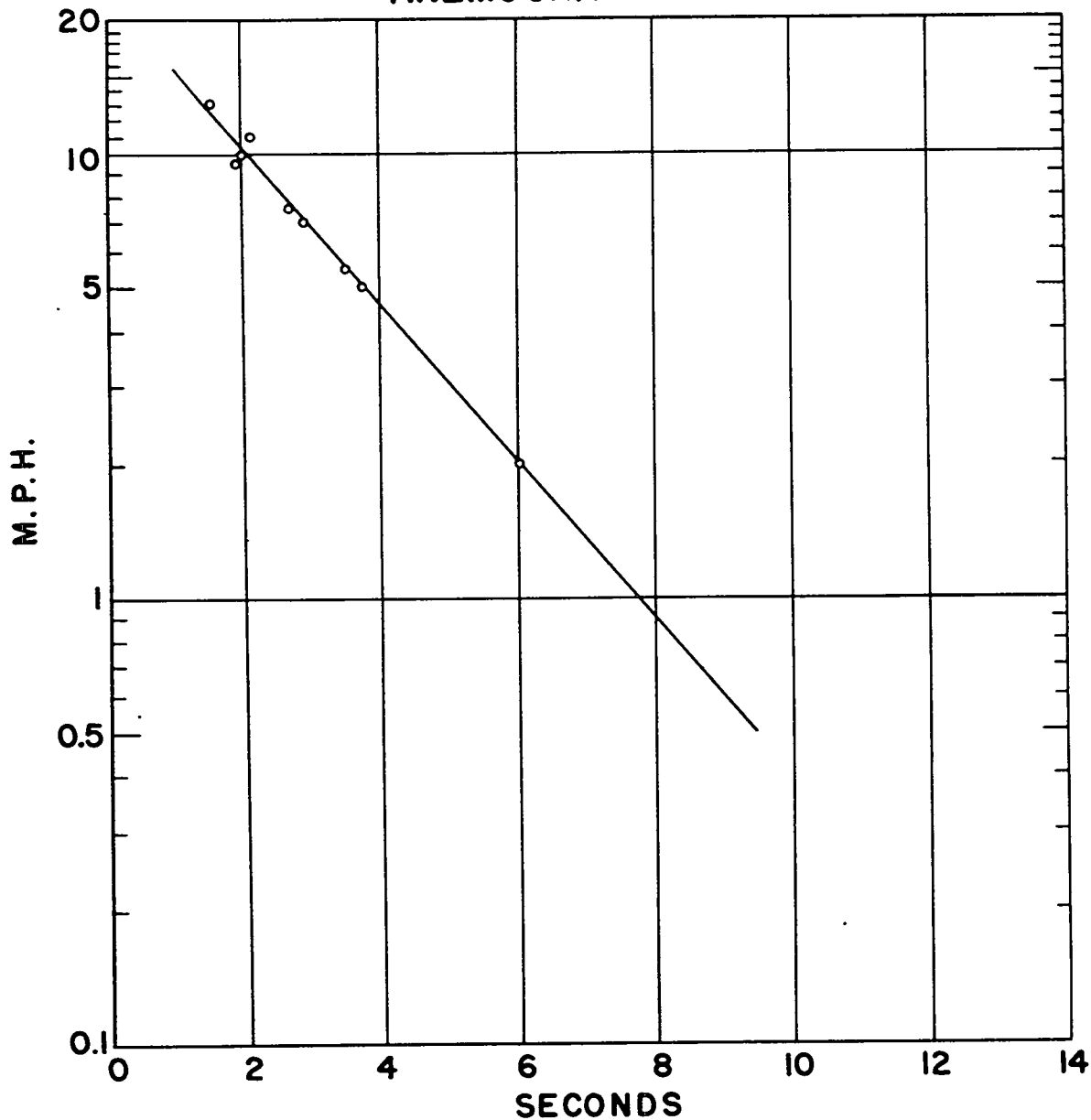


Fig. 9 Resonant period of oscillation of the Instruments Corporation aluminum alloy spread-tail wind direction vane as a function of wind speed.

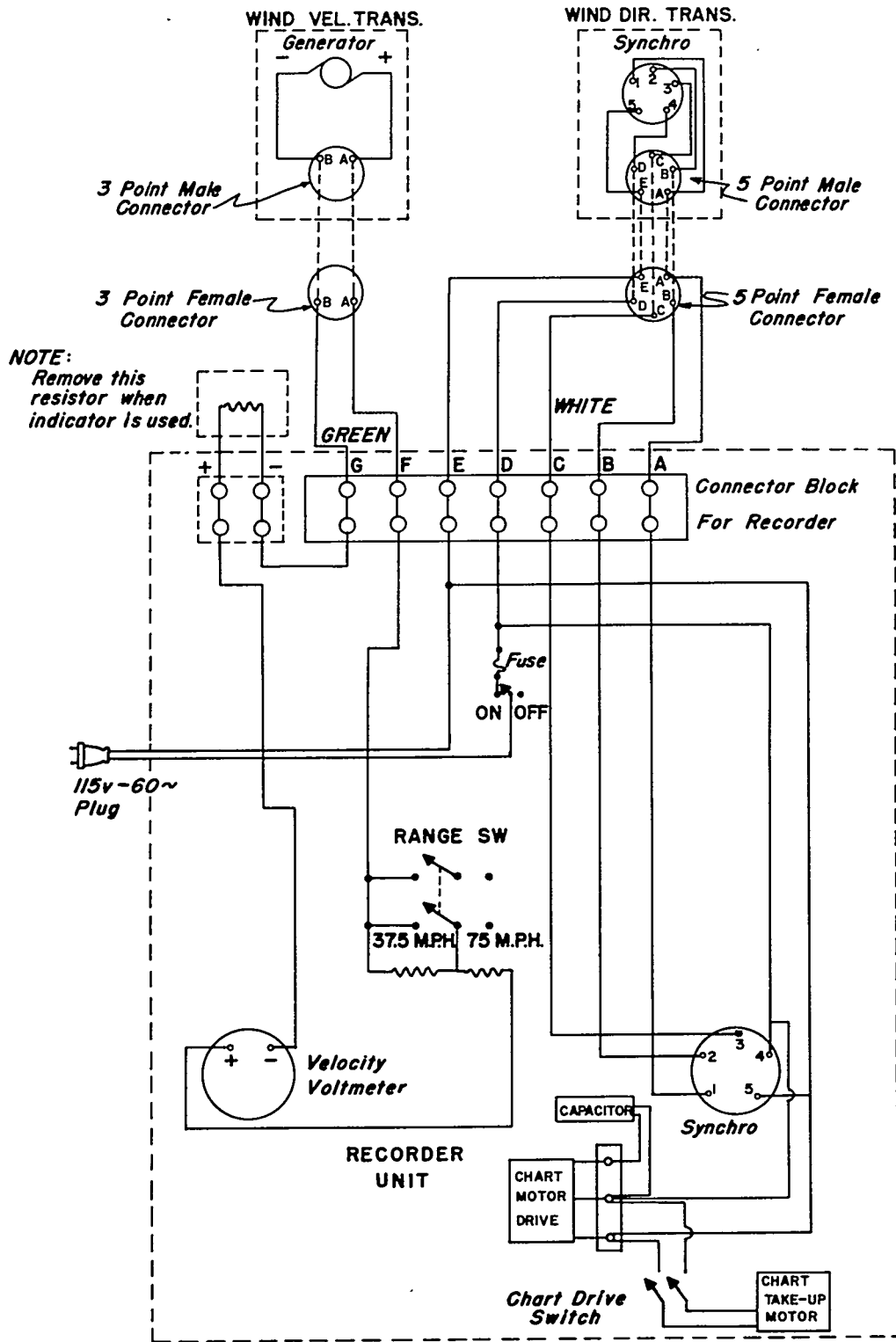
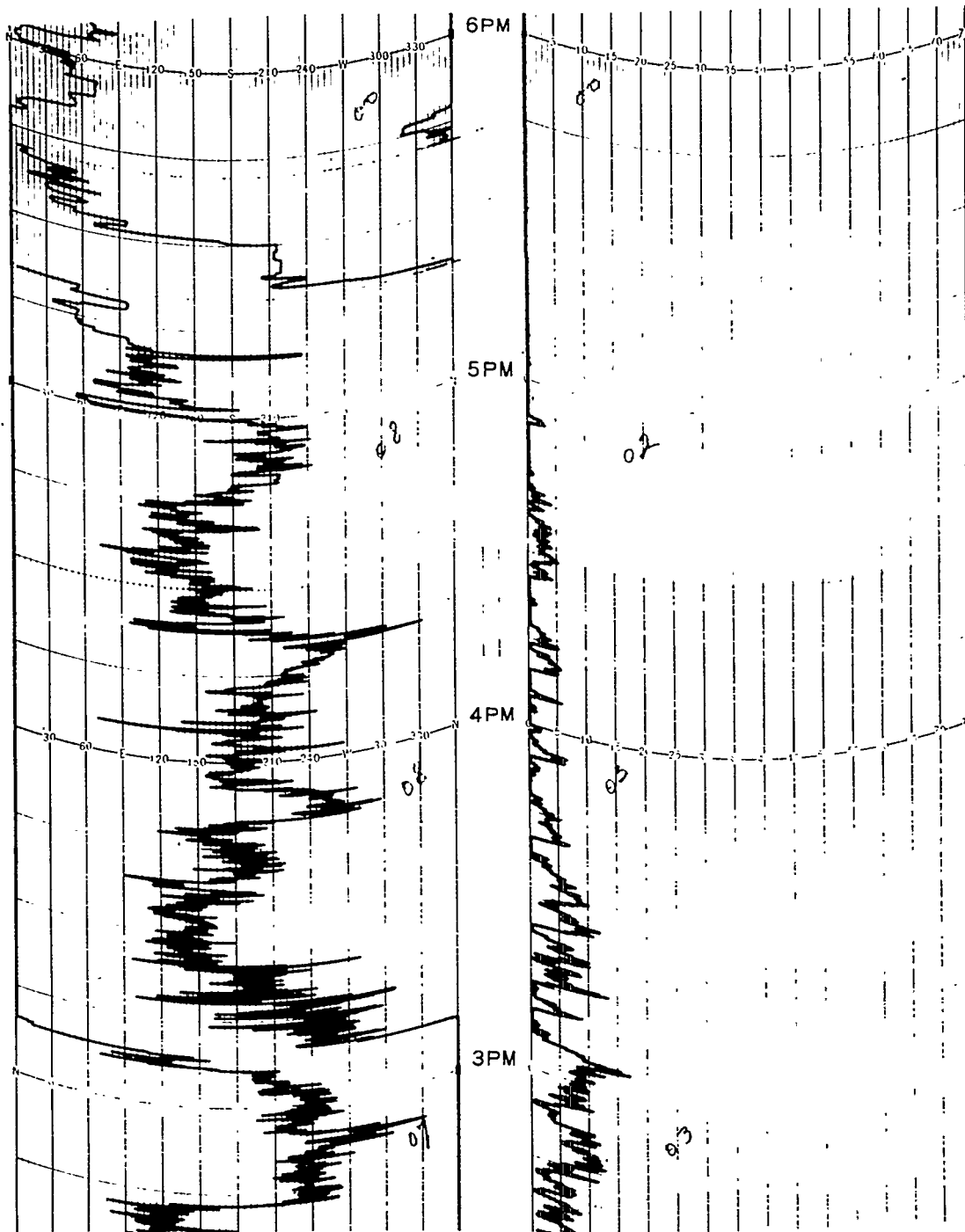


Fig. 10 Wiring diagram of the Instruments Corporation "Anemograph" system.



**ANEMOGRAPH RECORD
STATION 001**

Fig. 11 Example of "Anemograph" wind direction and speed record.

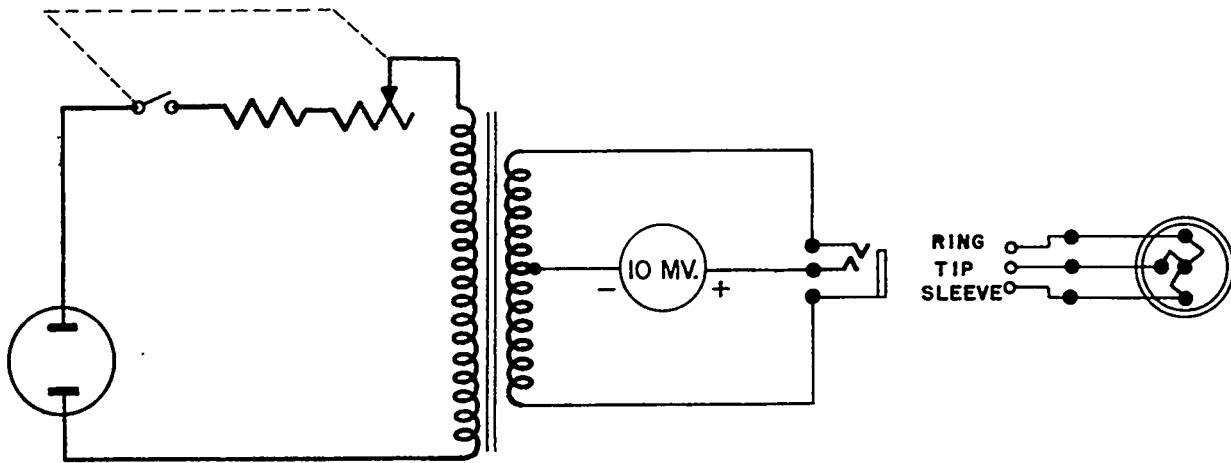


Fig. 12 Circuit of "Airmeter" heated-thermopile anemometer.

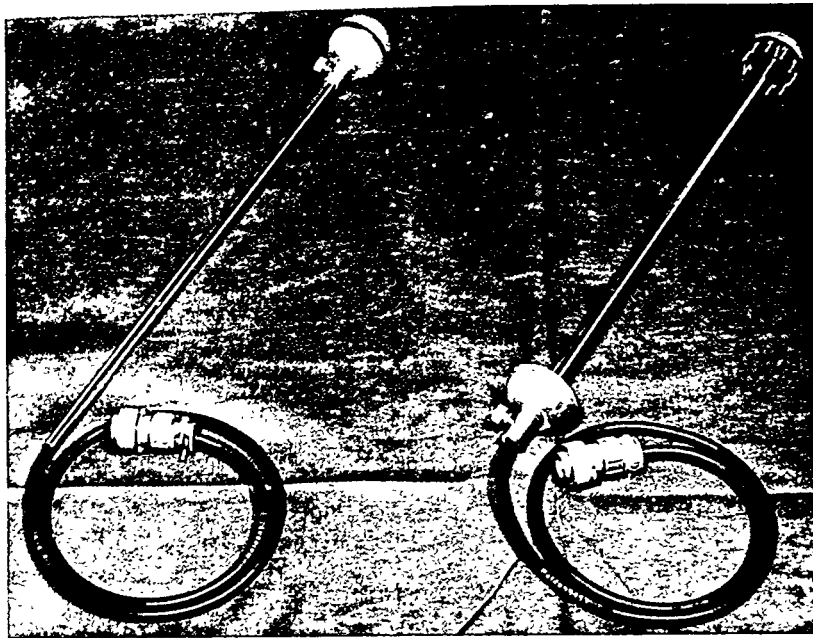


Fig. 13 Uncompensated non-directional "Airmeter" probes. Left: cap closed as for zeroing. Right: thermopile exposed as for wind measurement.

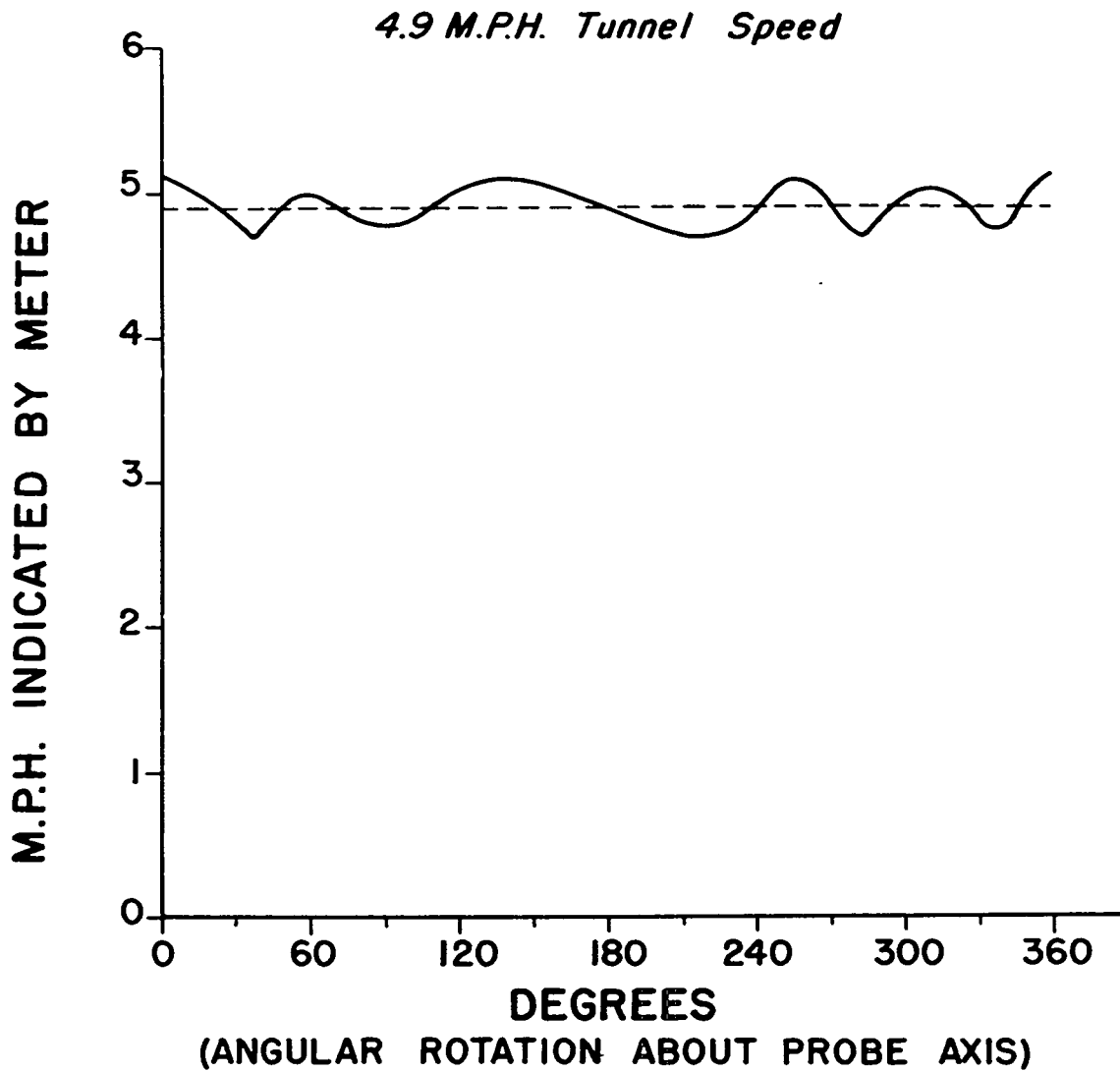


Fig. 14 Directional response of horizontally non-directional "Airmeter" probe.

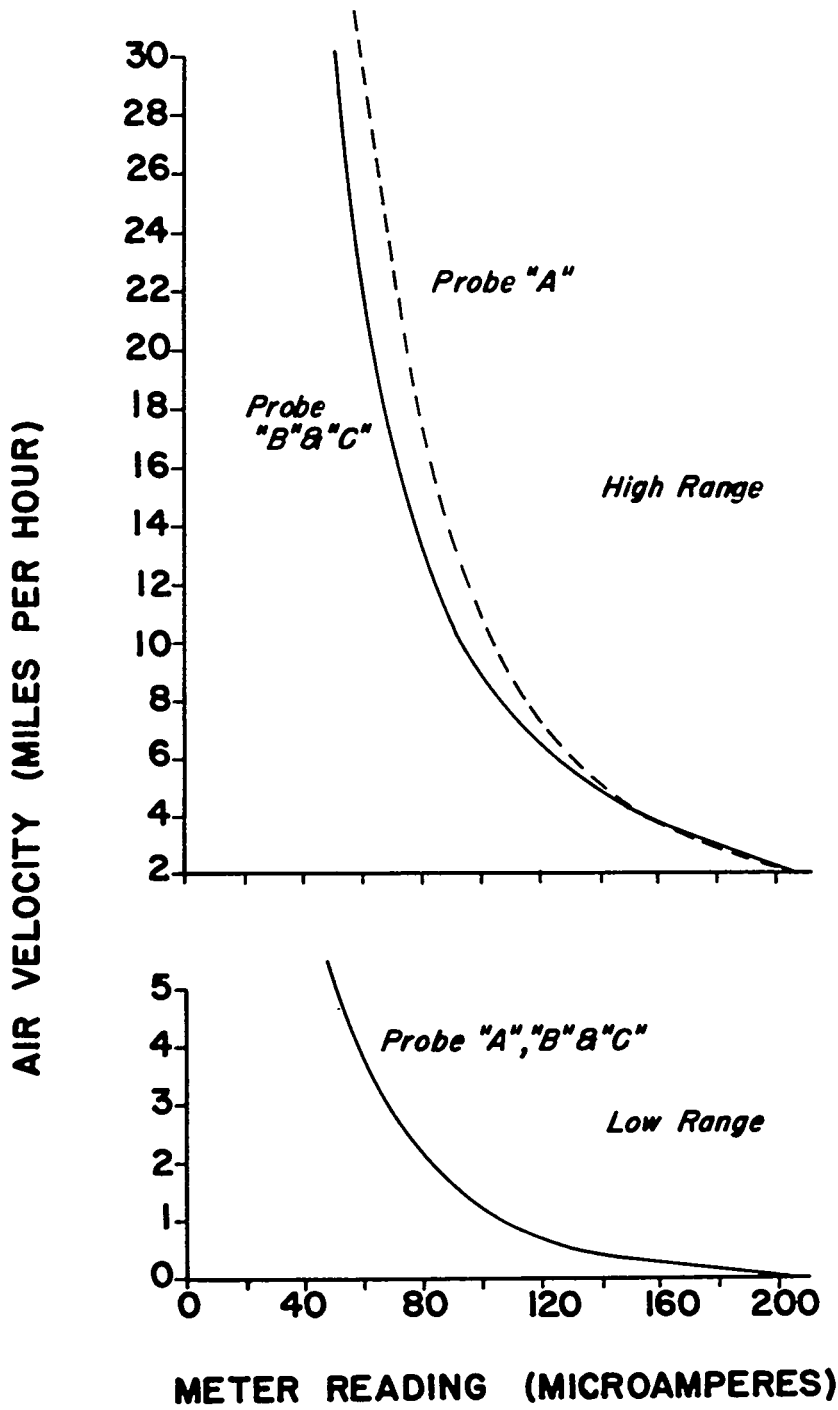
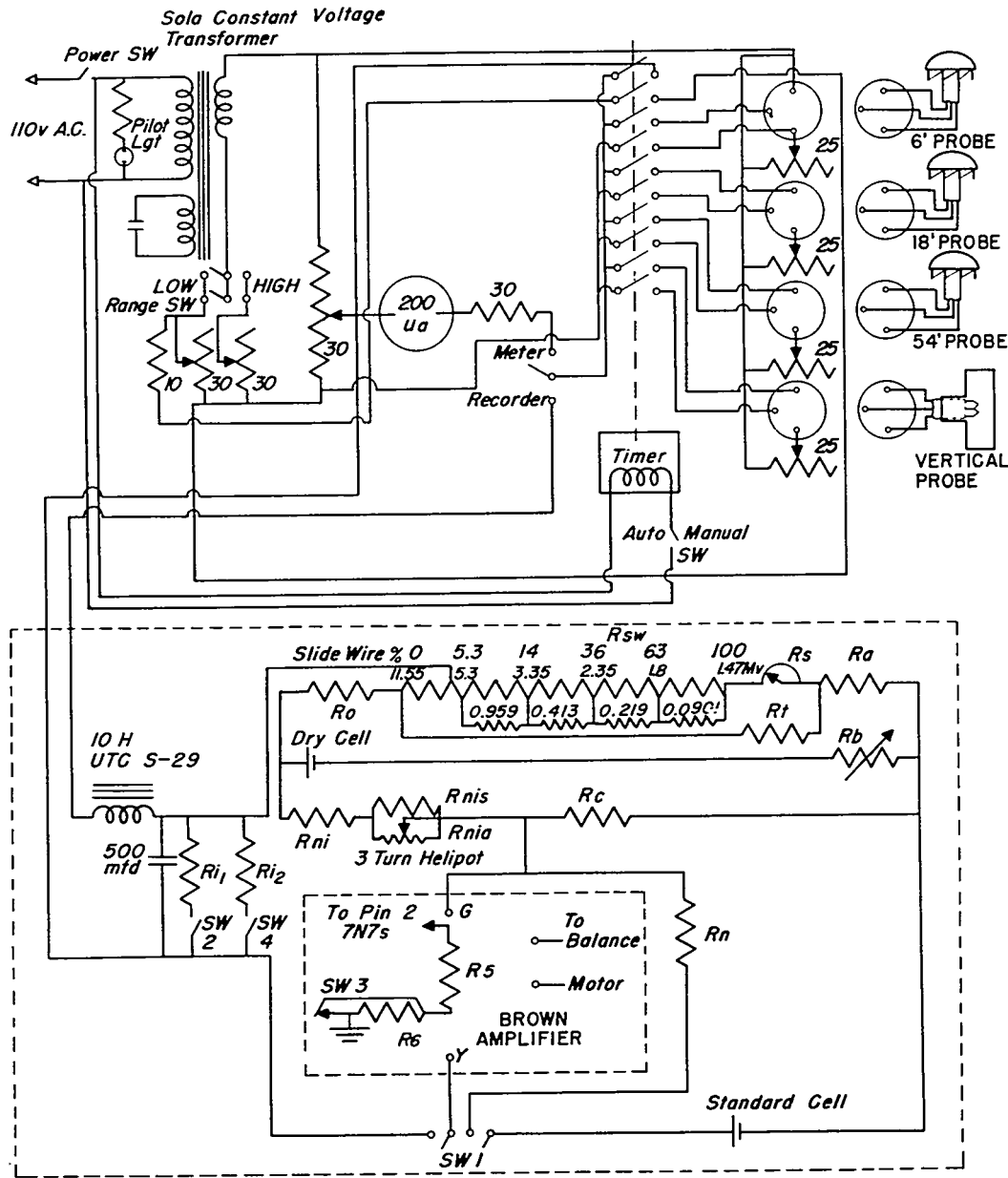


Fig. 15 Calibration curve for horizontally non-directional probes for precision air meter, model B-5, meter no. 633.



- | | |
|---|--|
| R ₀ - Scale Resistor 3.328 ~ | R _n - Calibration Resistor 5.0 ~ |
| R _a - Current Adjustment Resistor 252.1 ~ | R _{nis} - Fine Calibration Shunt 1.0 ~ |
| R _t - Span Resistor 6.314 ~ | R _{nia} - Fine Calibration Control 100 ~ |
| R _s - Span Adjustment | R _{i1} - Input Resistor, High Sensitivity 27 ~ |
| R _c - Standardization Resistor 509.4 ~ | R _{i2} - Input Resistor, Low Sensitivity 0.3 ~ |
| R _b - Battery Rheostat | R ₅ - Normal Amplifier Cathode Resistor 150 ~ |
| R _n - Standardization Input Resistor 3.9 ~ | R ₆ - Desensitizing Cathode Resistor 1000 ~ |
| SW 2,3,4 - Sensitivity Switches | R _{sw} - Slide Wire 20 ~ |

ALL RESISTORS IN OHMS

Fig. 16 Circuit diagram of "Precision Airmeter" (model B-5) and linearized recorder.

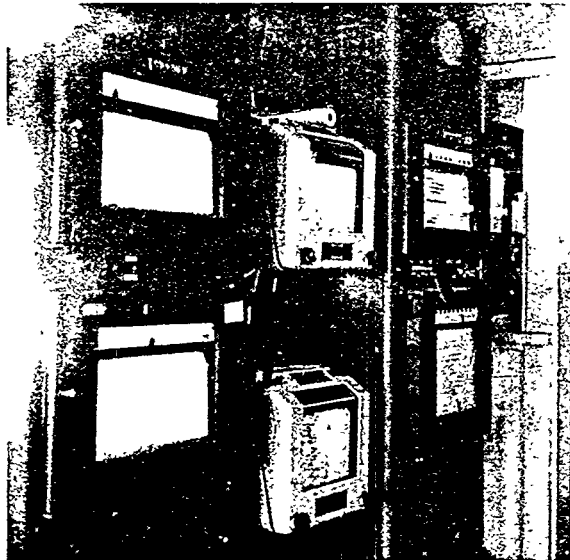


Fig. 18 Recorders in station 001 hutment. Upper row, left to right: T_{54} , - T_{41} thermopile recorder, 54 ft. generator-selsyn (Anemograph) wind recorder, linearized heated-thermopile (Airmeter) wind recorder, 19 ft. contacting wind and rain recorder. Lower row: air-grass-wet-bulb thermocouple temperature recorder, 18 ft. Anemograph recorder, pyrliometer recorder. The 6 ft. Anemograph recorder is just off the lower edge of the picture.

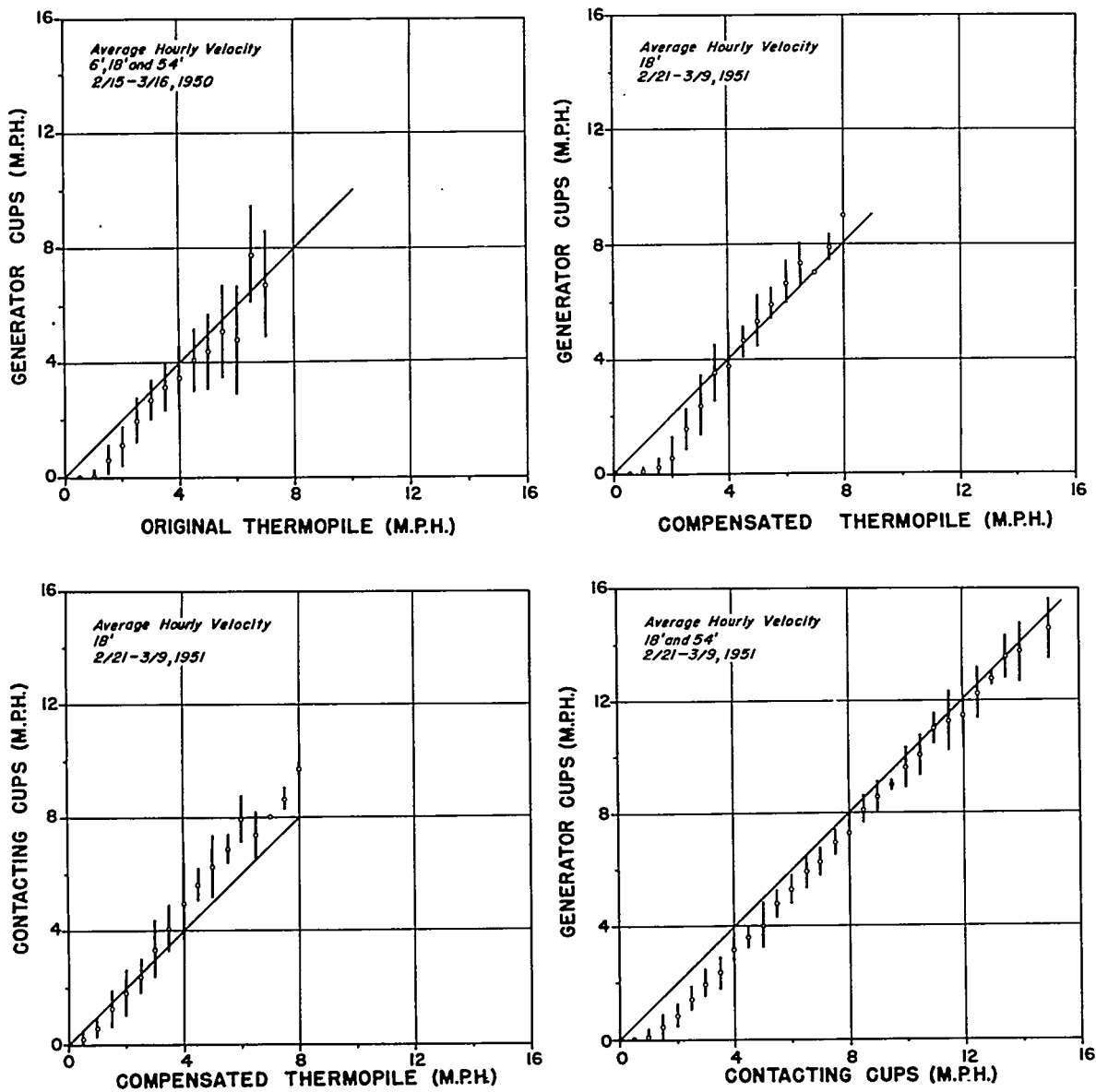


Fig. 19 Intercalibrations of cup-generator (Airmeter), contacting-cup, uncompensated thermopile (Airmeter) and compensated (for short-period temperature fluctuations) thermopile anemometers in the natural wind. Vertical bars show $\pm \sigma$.

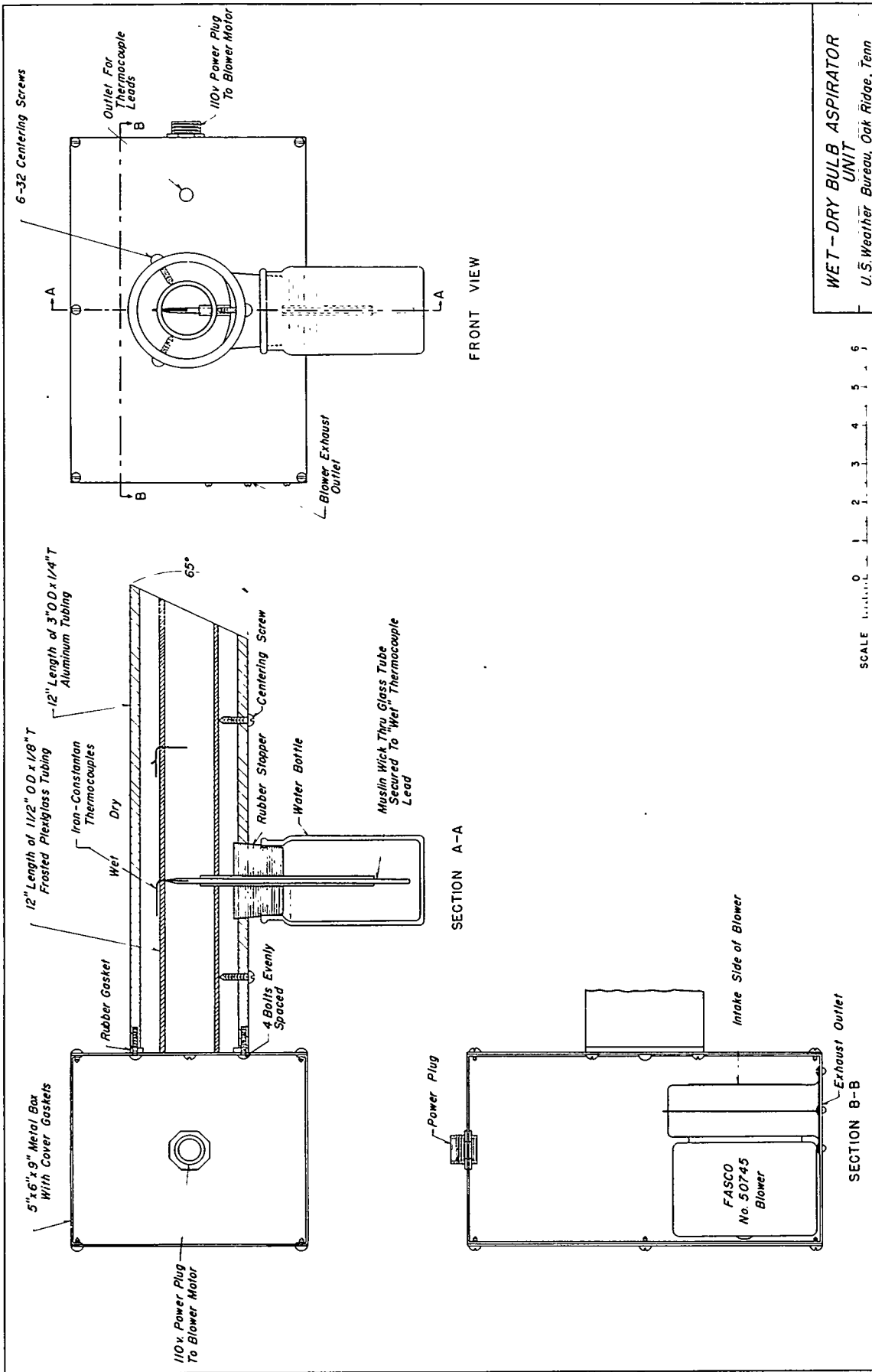


Fig. 20 Thermocouple psychrometer aspirator unit.

171

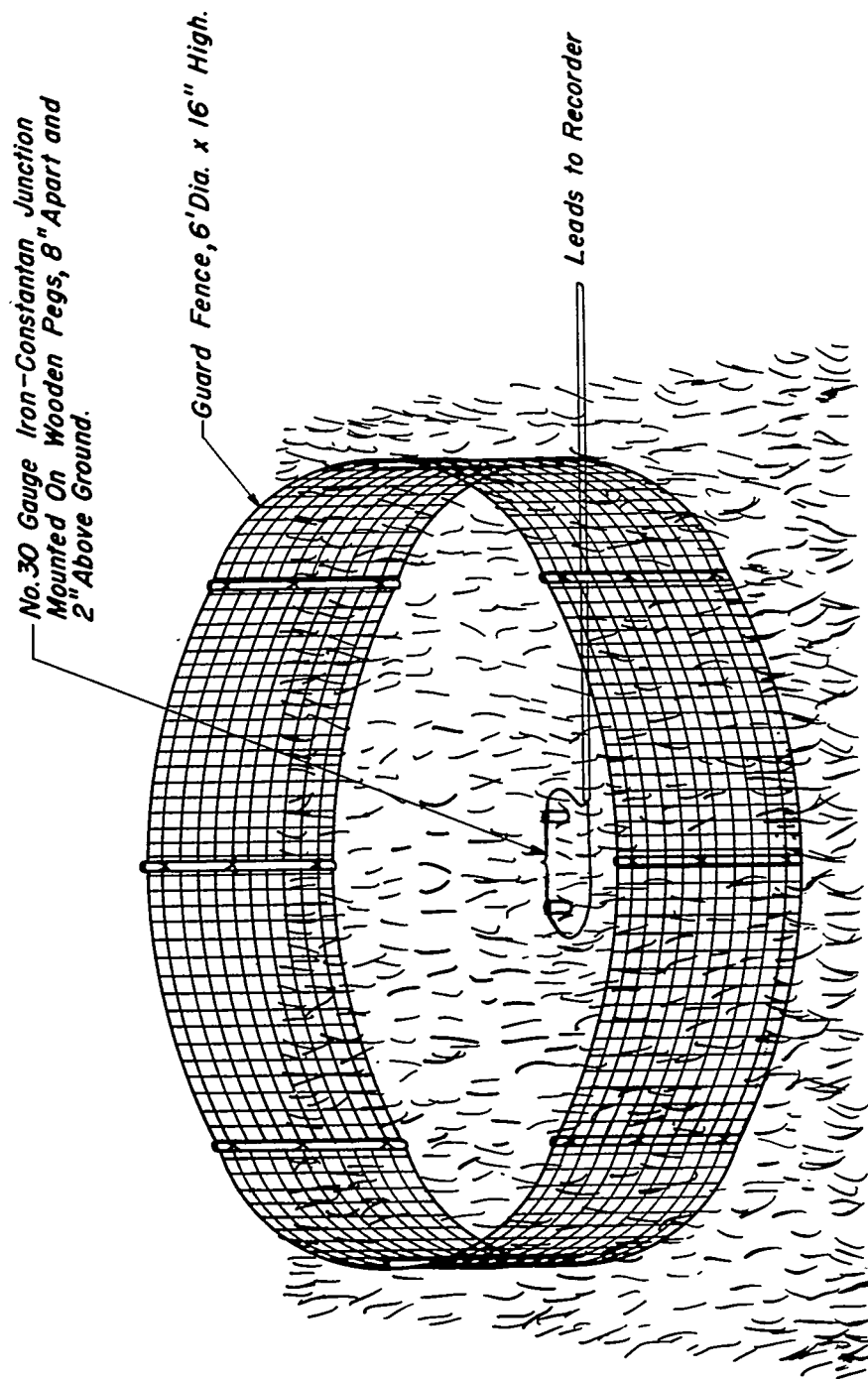
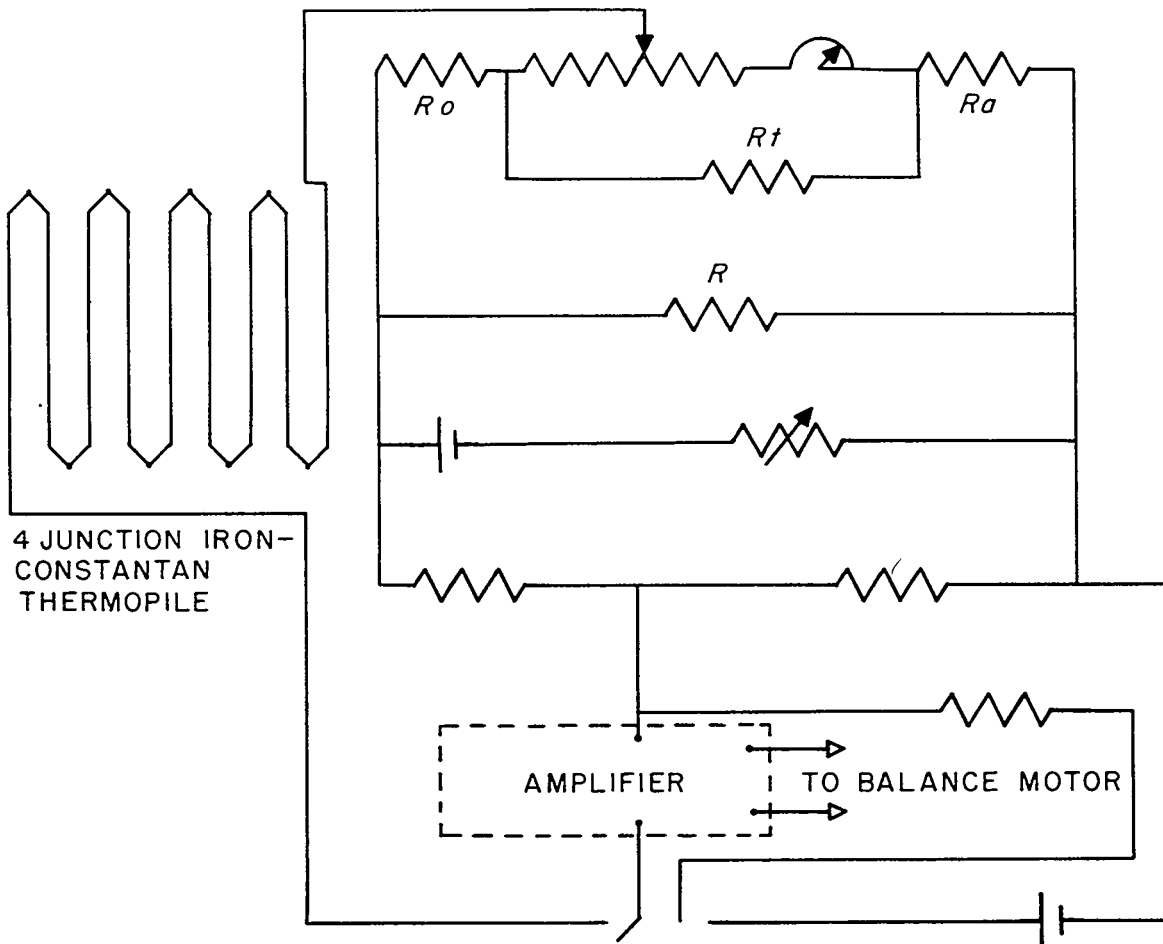


Fig. 21 Grass temperature thermocouple.



R_o - Scale Resistor 9.6846 \sim R_t - Span Resistor 2.031 \sim
 R_a - Current Adjustment Resistor 1017.5 \sim R - Shunt Resistor 343 \sim

ALL OTHER MEASURING CIRCUIT RESISTORS
 ARE STANDARD

BROWN ELECTRONIK 1.7380 MV. RECORDER

Fig. 22 Wiring diagram of temperature-difference thermopile recorder.

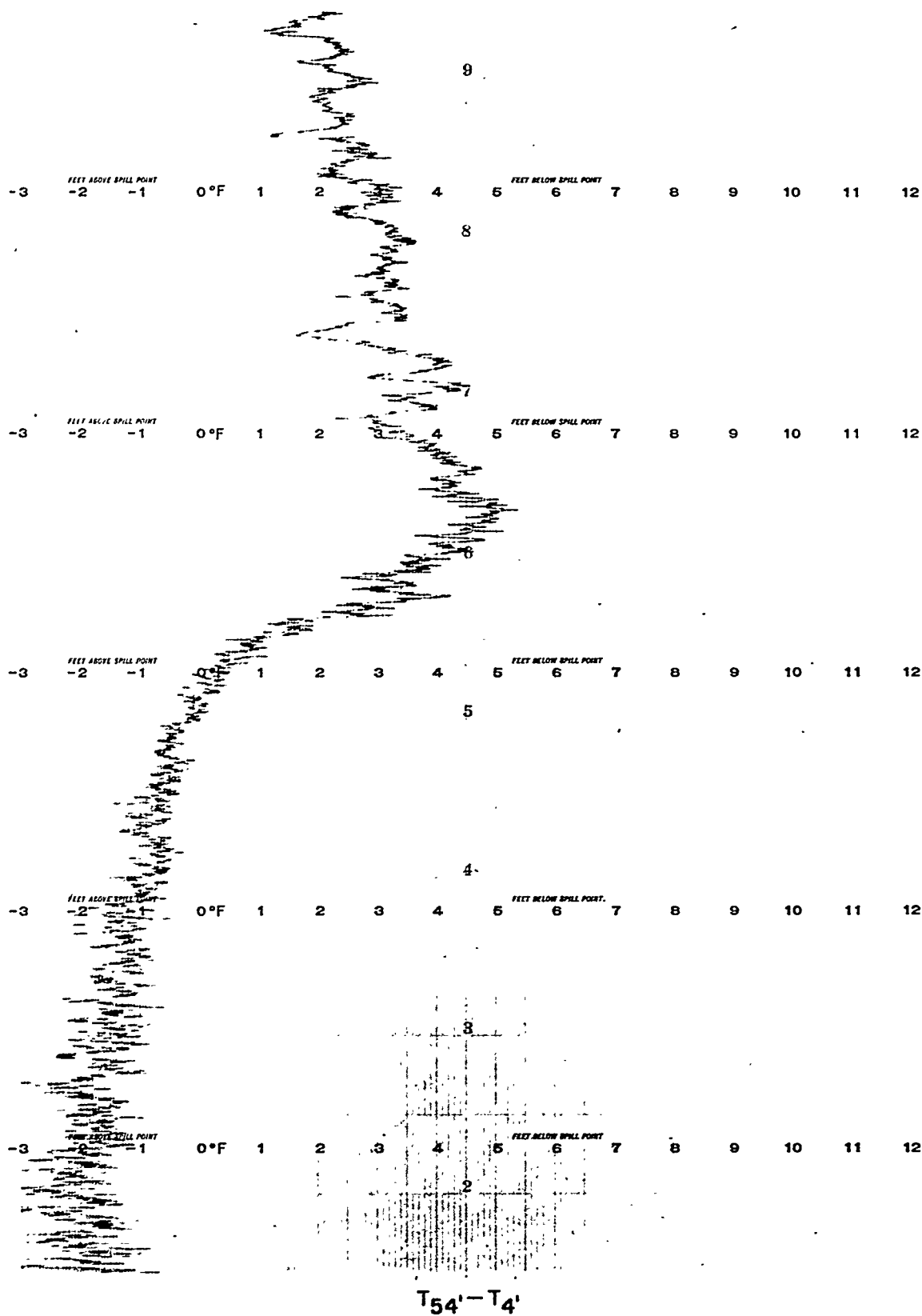


Fig. 23 Example of $T_{54'} - T_{4'}$ record showing typical change from afternoon lapse to evening inversion.

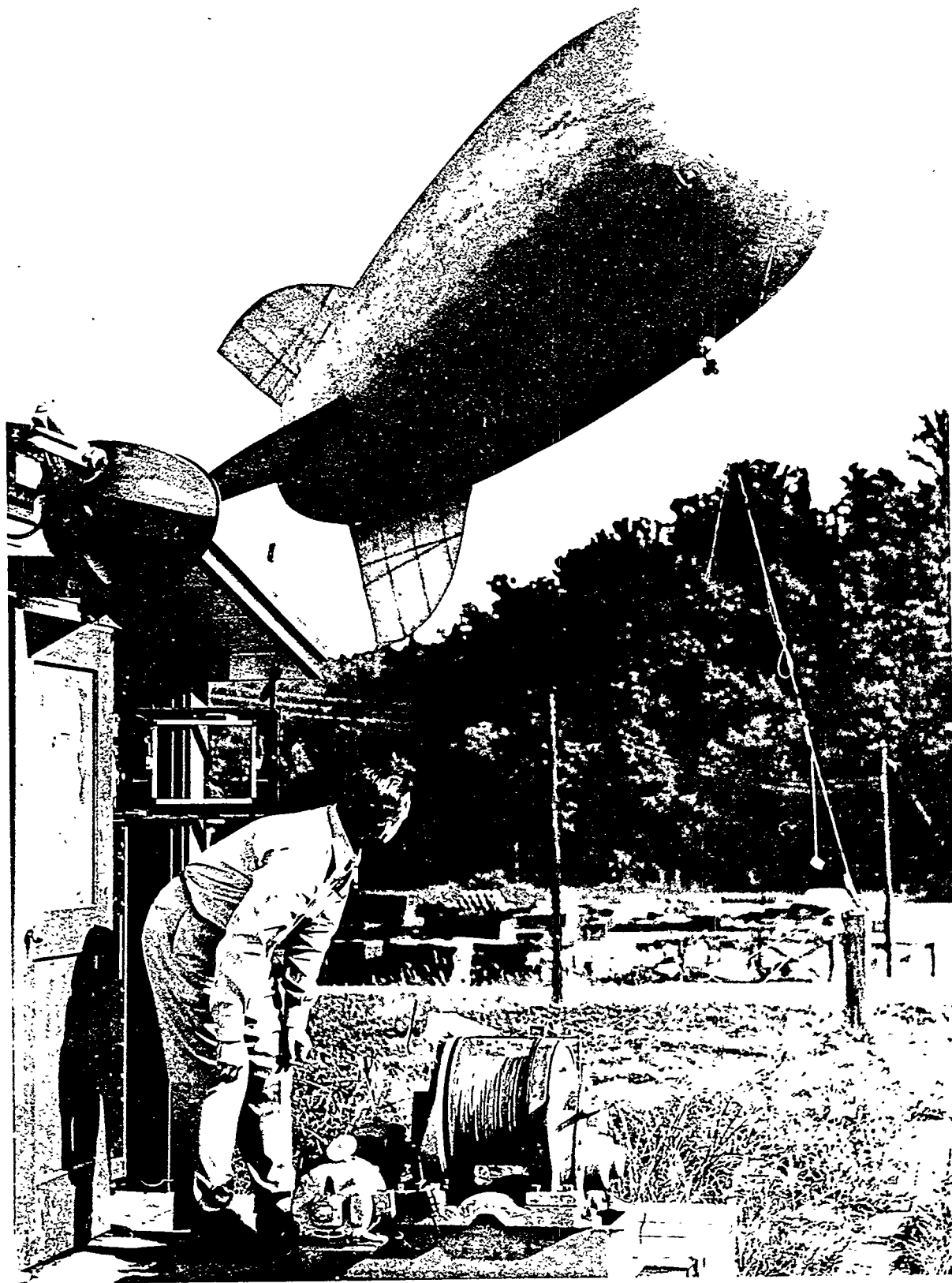
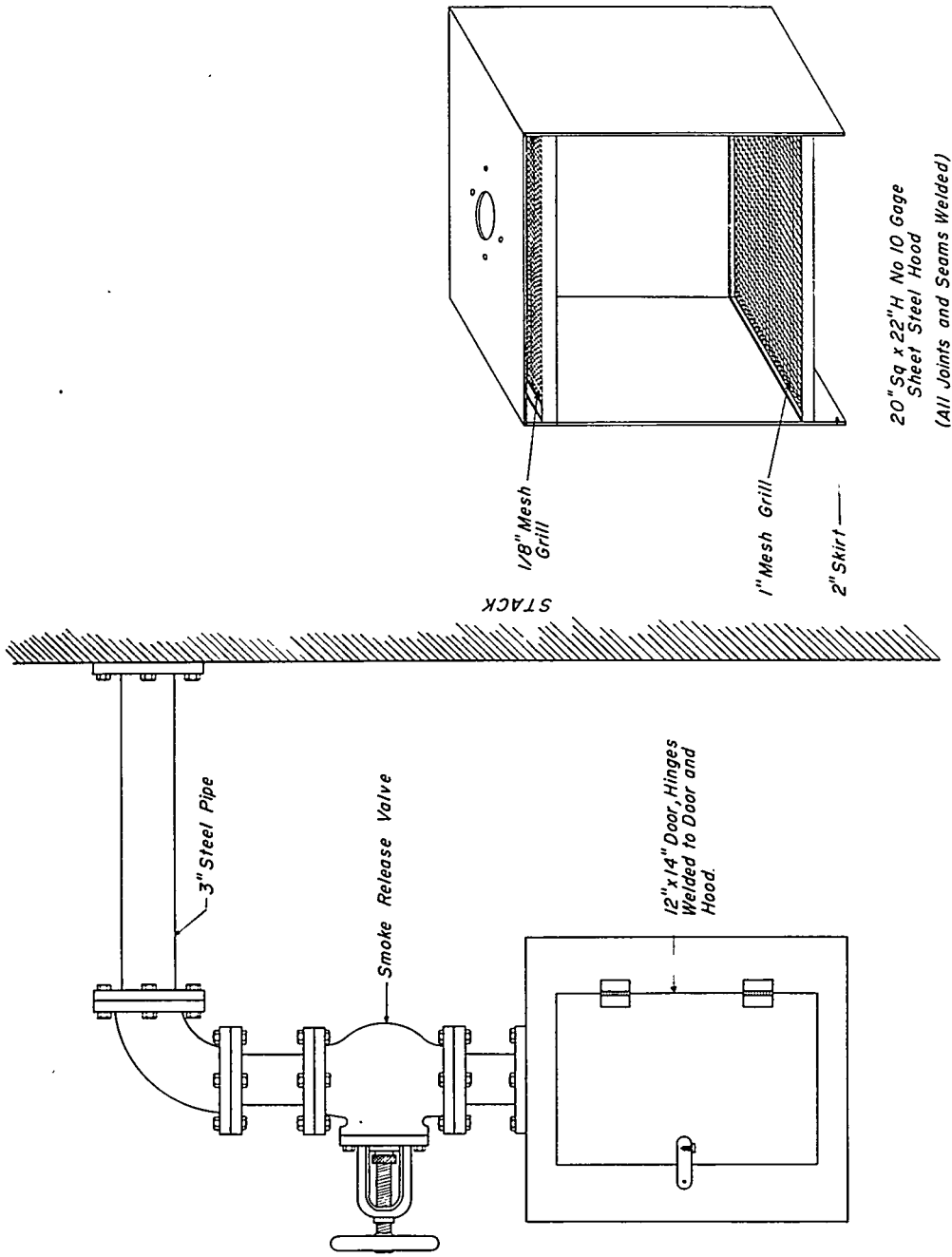


Fig. 24 Photograph of captive balloon temperature sounding system in operation. The thermistor, in its small rectangular plastic support, is hanging about 4 ft. above ground.

175



SCALE 0 1 2 3 4 5 6 7 8 9 10 12
INCHES

Fig. 25 Smoke hood for X-10 pile stack.

DISTANCE ERROR FOR TRACKING ERROR OF 0.02° USING 782 FOOT BASELINE

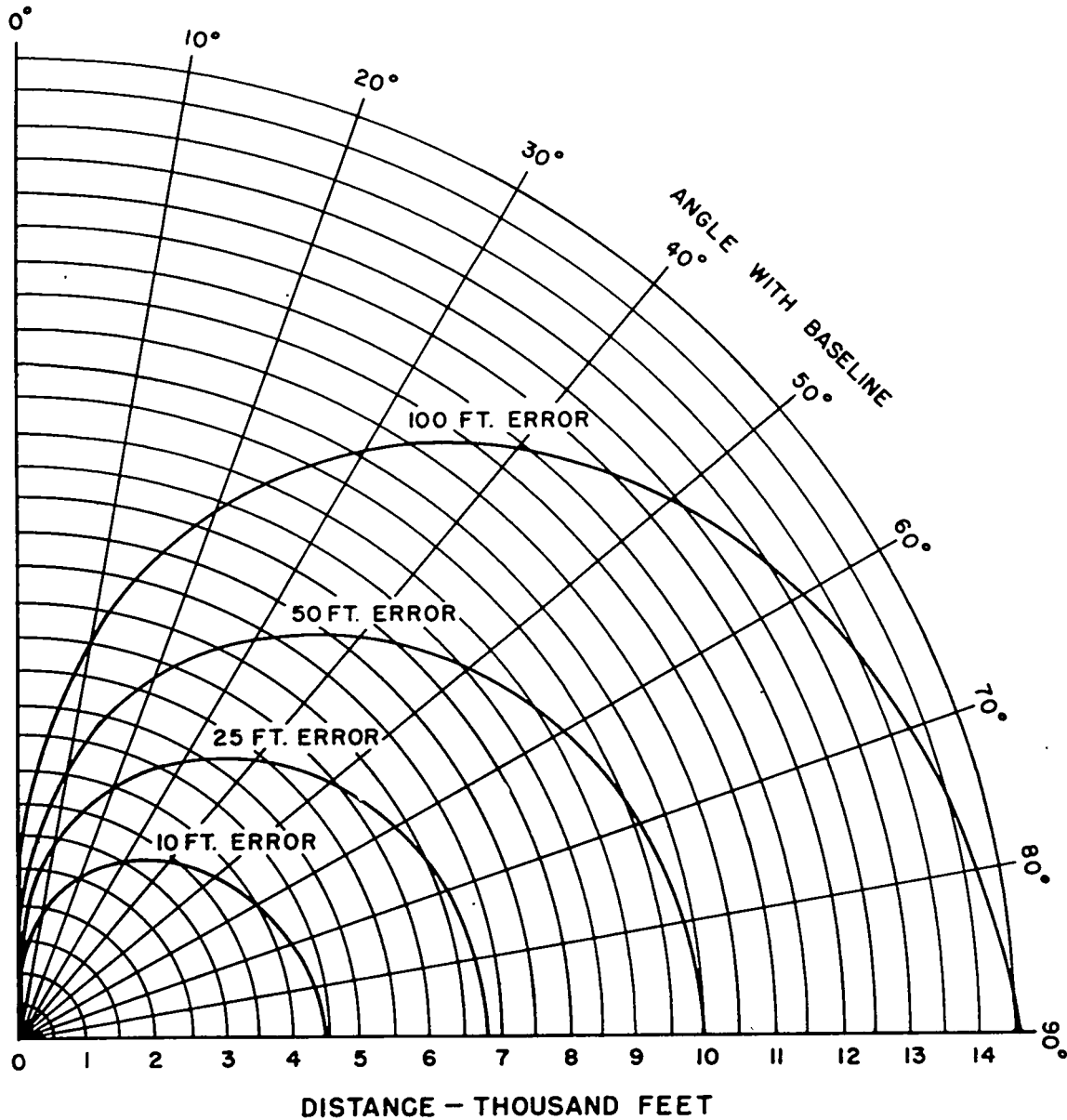
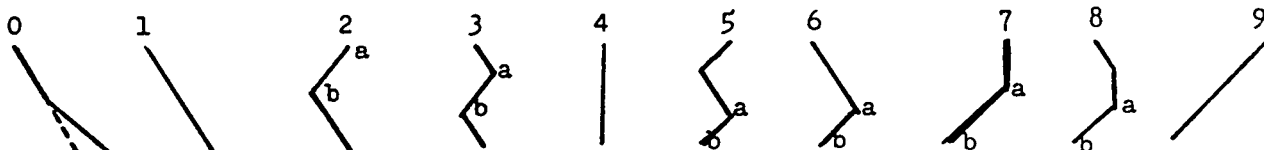


Fig. 27 Error in double-theodolite distance measurement with a 782 ft. baseline, assuming a tracking error of 0.02° at one station or additive 0.01° errors at both stations. Each curve shows the distance at which the error reaches a given magnitude, as a function of balloon bearing with respect to baseline azimuth.

FORM OR-475 (MAY 1949)												
LOW LEVEL SOUNDING DATA											DATE	
STATION			EL.	LAT.	LONG.							
TIME	EST											
HEIGHT	T _{asc} °F	T _{dsc} °F	T _{avg} °F	T _{asc} °F	T _{dsc} °F	T _{avg} °F	T _{asc} °F	T _{dsc} °F	T _{avg} °F	T _{asc} °F	T _{dsc} °F	T _{avg} °F
Sfc												
100												
200												
300												
400												
500												
600												
700												
800												
900												
1000												
1500												
2000												
2500												
T 200 - T 0 (°F)												
T 500 - T 0 (°F)												
Type												
Inver. Intens. (°F)												
Top of Invers. (a)												
Base of Invers. (b)												

TYPE CODE



LAPSE CODE

0	1	2	3	4	5	6	7	8	9
-9	-6	-3	0	3	6	9	12	15	18
-8	-5	-2	1	4	7	10	13	16	19
-7	-4	-1	2	5	8	11	14	17	20

Fig. 28 Captive balloon temperature sounding data sheet.

AUTOMOBILE TEMPERATURE INDICATOR

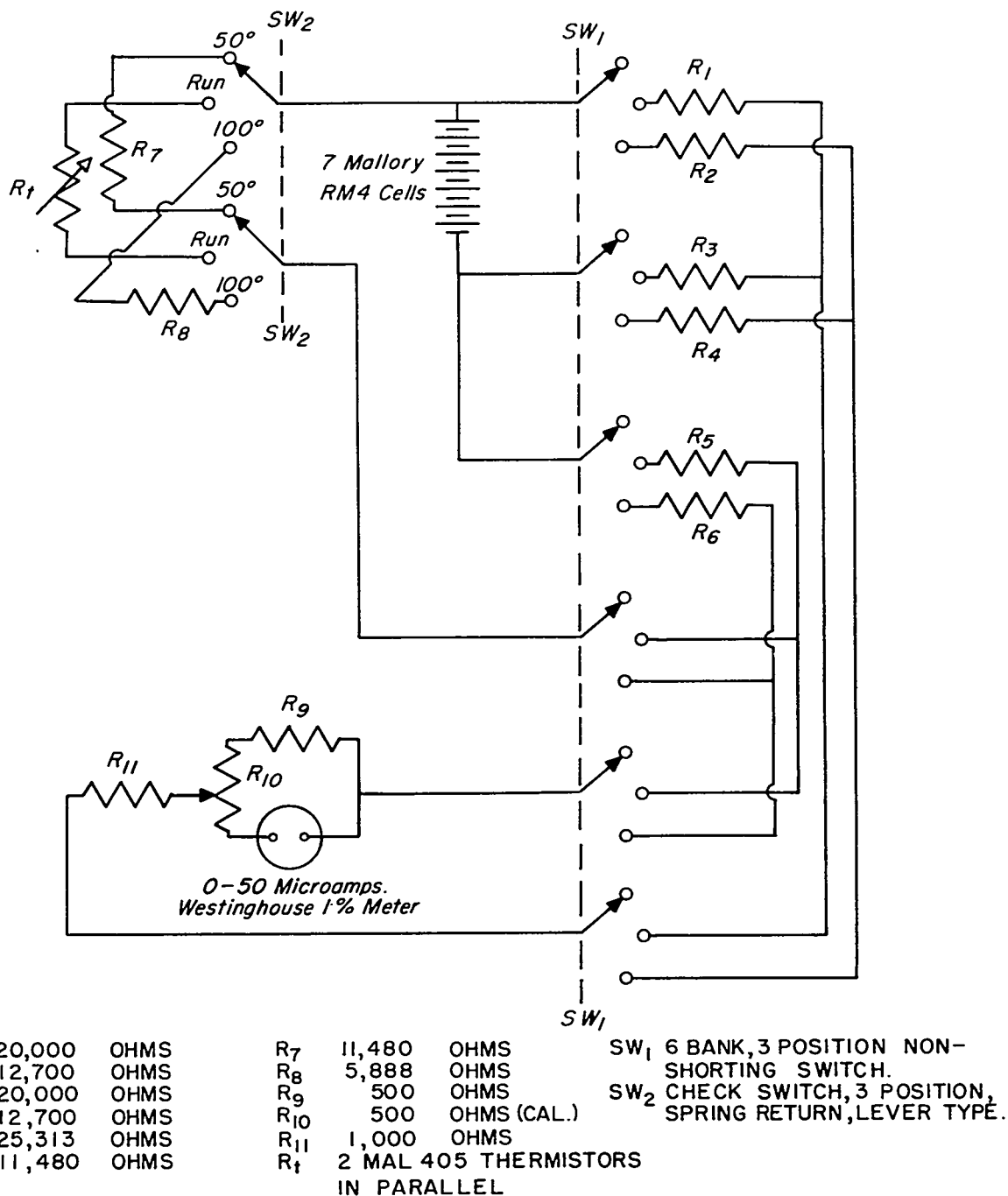


Fig. 29 Circuit diagram of automobile thermistor temperature indicator.

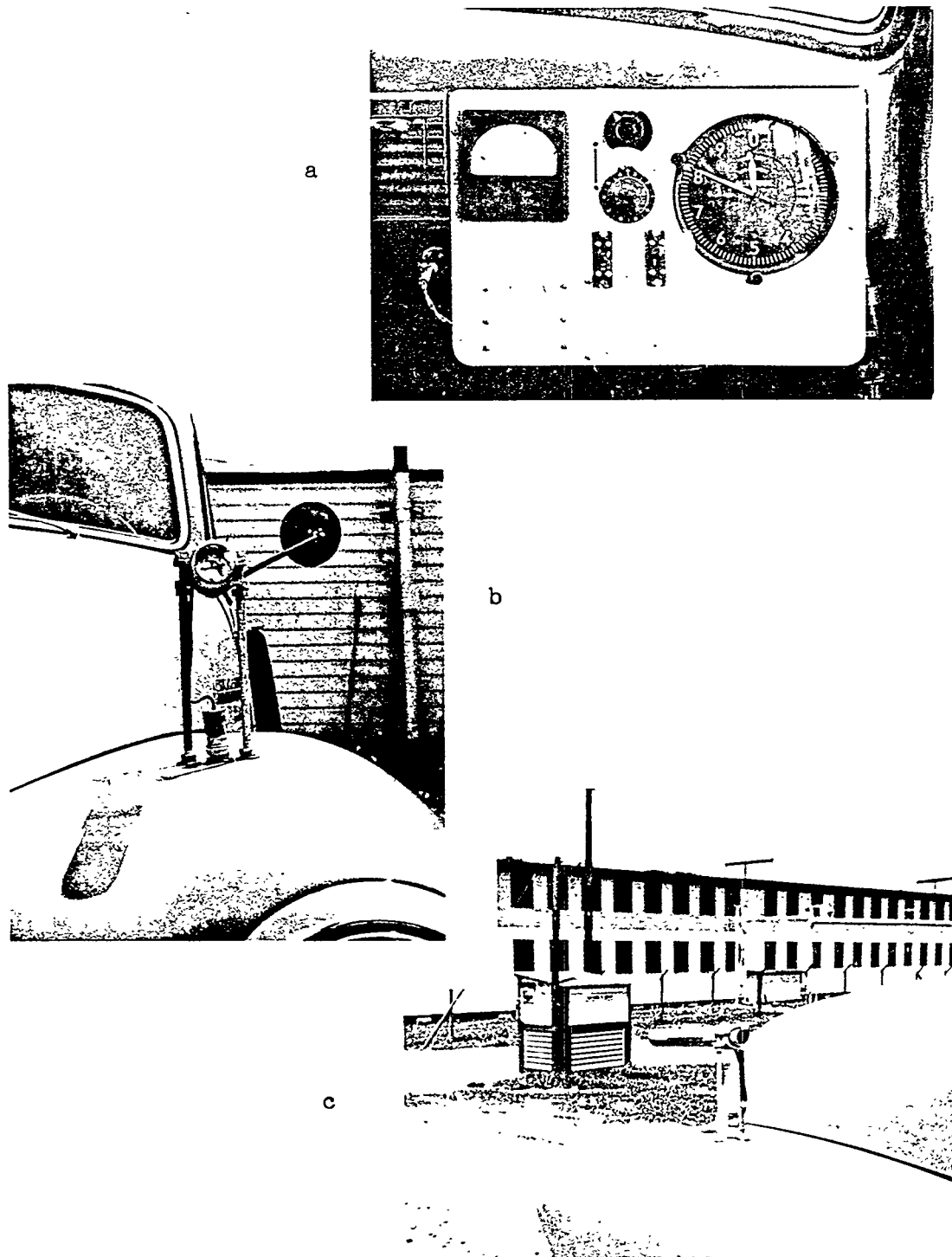
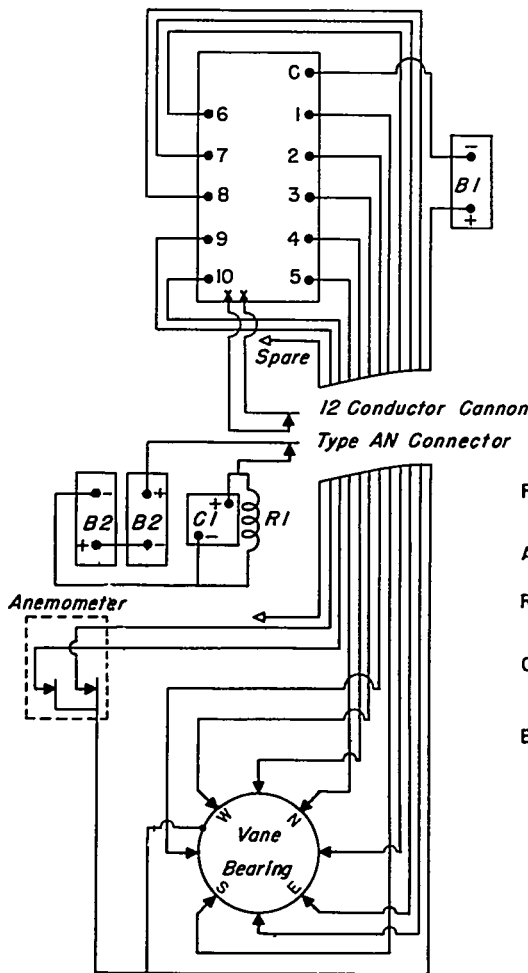
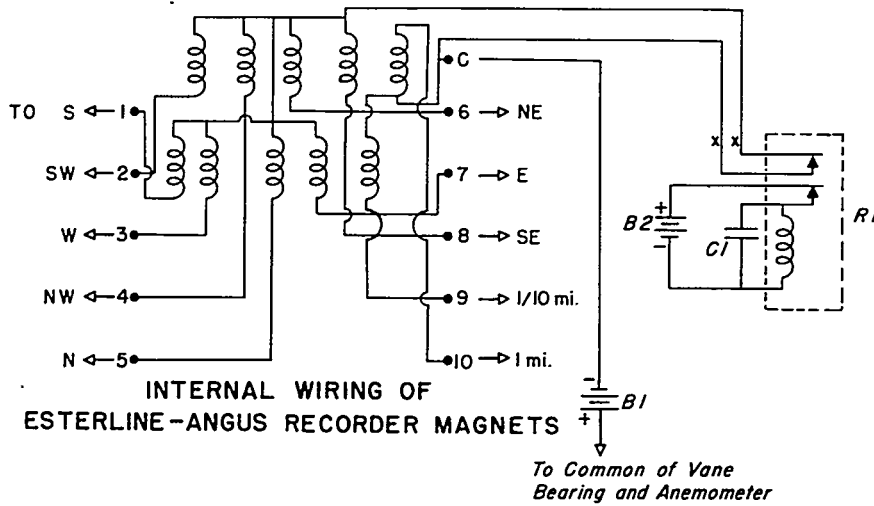


Fig. 30 Photographs of automobile temperature survey equipment.
a. Panel showing temperature indicator and altimeter.
b. Front view of thermistor shield. c. Side view of thermistor shield.



INTERCONNECTION OF UNITS



*Modification of 1/60 mi.
Contactor to 1/10 mi.*

LIST OF MATERIAL

- RECORDER - Esterline-Angus 10 pen operation recorder 8 v.D.C. 68 ohm coils, modified.
- ANEMOMETER - Bendix-Friez type 349 or Instr. Corp. type 428.
- RELAY R1 - Clare type CMS 10,000 ohm coil 55600 T. Contact 1A DPST normally closed.
- CAPACITOR C1 - 3000 mfd. 35 v.v. min. C-D #FV3530/FA3530A, or 2 Mallory type HC5020 (paralleled).
- BATTERIES B1 - Burgess type 4F6H 9v.
B2 - Burgess type 5308 45v.

Fig. 31 Wiring diagram of micronet contacting wind system with timing relay.

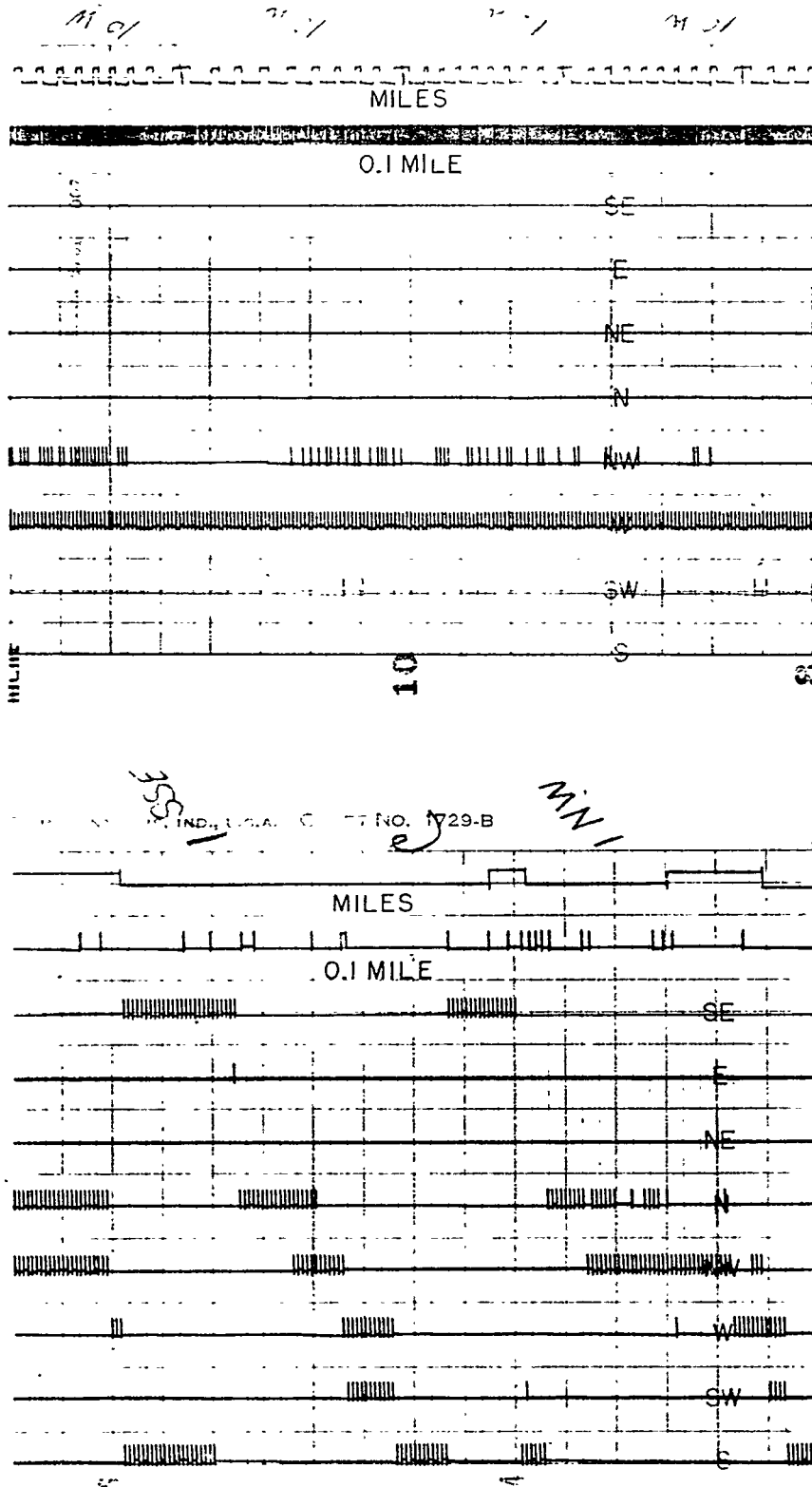


Fig. 32 Examples of contacting wind records with direction pens controlled by timing relay.

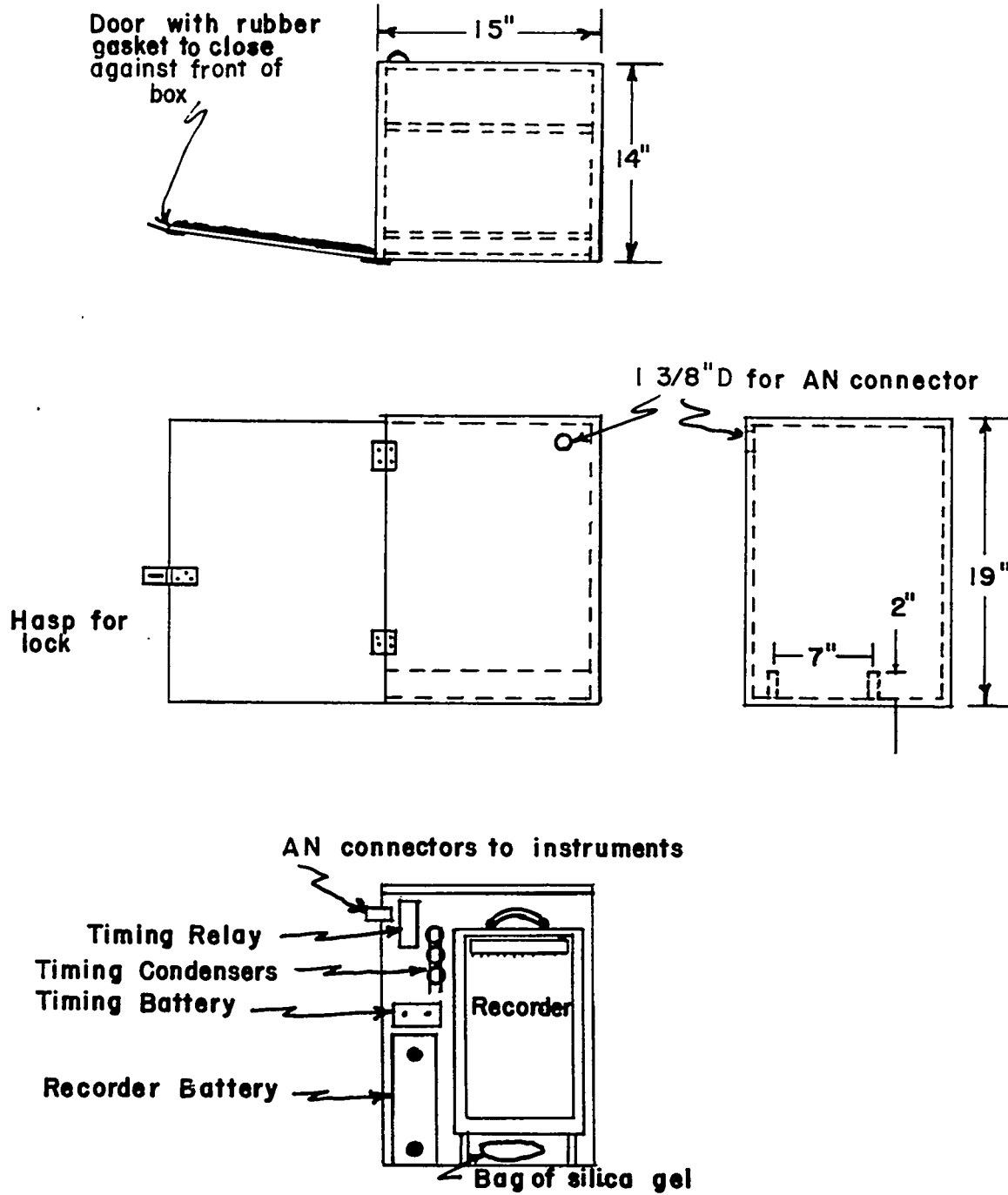


Fig. 33 Plywood housing for micronet wind recorder.

A METEOROLOGICAL SURVEY OF THE OAK RIDGE AREA

U. S. Weather Bureau

Oak Ridge, Tennessee

Part III. Climatology

The Period of Record

1. Weather During the Observation Period in Relation to Climatic Normals

The term "climatology" as used here denotes the study of meteorological variables specifically with respect to their dependence upon geographical location. The variables of particular interest in this study include some which have been commonly studied, such as wind direction and speed, temperature and precipitation, as well as some which are more complex and less well-known, such as gustiness and vertical distributions of temperature and wind. The geographical location in this case is the Oak Ridge area and its surroundings. However, in attempting to associate any properties observed over a finite period of time with specific localities, it is necessary to eliminate those components of the time variation which are not in themselves characteristic of the locality. To illustrate, the mean daily range of temperature may be considered a meteorological property of a locality, resulting from a characteristic cyclical time variation of the temperature. This climatological daily temperature range always appears in combination with another component which results from the particular degree of cloudiness, wind, air mass advection, etc. occurring during the period of observation. The climatological daily temperature range may show a seasonal variation, but should remain the same in all years, were

it not for the fact that the climate itself changes. From the practical standpoint, the climate must be defined in terms of averages taken over some suitably long period of observation, which are considered normals for the locality in question. The greatest difficulty occurs in attempting to establish a suitable averaging period. Average values of meteorological elements for various periods from 5 years to several hundred years have been defined as normals for different purposes.

In spite of this uncertainty as to the definition of "normal", there is little doubt that the period 1948-1951, during which the present survey has been conducted, was characterized by mean temperatures and total precipitation significantly higher than any normals which can reasonably be defined for this part of the world. The opening sentences from the last four annual issues of "Precipitation in Tennessee River Basin", published by the Tennessee Valley Authority, Hydraulic Data Branch, will serve to emphasize this point:

1948: "The greatest average precipitation in the past 16 years occurred in 1948 over the Tennessee River Basin".

1949: "The second wettest year in TVA experience occurred over the Tennessee River Basin in 1949".

1950: "The year 1950 was the wettest since 1932 in the Tennessee Valley and the third wettest in 61 years of record."

1951: "The year 1951 was the fourth consecutive year of above normal precipitation over the Tennessee River Basin and the seventh wettest year in the past 62 years".

This abnormality in the weather of the observation period has unquestionably been reflected to some extent in virtually all aspects of the meteorological observations. The distinction between statistical averages of a particular series of observations on the one hand and climatological normals on the other must therefore be constantly borne in mind. The approach of the present climatological analysis has been twofold:

(1) to study those elements or relationships (between similar elements at different stations, or between different elements at the same station) which are least affected by the abnormality of the weather during the observation period and (2) to utilize these stable relationships together with longer records at nearby localities to estimate climatological normals for the locality under study.

For such an approach to be successful, it is clearly necessary (1) to observe simultaneously a wide variety of elements at one location, (2) to observe some of the same elements at several locations including some having long records and (3) to obtain observations under a sufficient range of meteorological conditions to permit any desired comparisons to be made. The provisions for accomplishing (1) and (2) have been described in Part II of this report. The extent to which (3) has been accomplished is discussed below.

2. The Range of Conditions Occurring Within the Observations Period

Figs. 34 and 35 show the daily sequences of several meteorological elements in this area during the entire period Jan. 1, 1949 to Dec. 31, 1950, which was the period of detailed observational coverage. The data plotted in these figures were obtained from station 012 (ORNL Health Physics Division) with the following exceptions; weekend cloudiness observations and all barometric pressures were obtained from the records of the Knoxville Weather Bureau Office and the 850 mb temperatures used in the stability measurements were based on the Atlanta, Greensboro, and Nashville raobs.

It can be seen at a glance that warm, cool, wet, and dry weather were observed in each season during the observation period. Examples of periods of several days' duration representing various important weather types are:

- (1) Summer, hot, dry: 7/20-7/29/49, 8/9-8/14/49, 6/23-6/24/50.
- (2) Summer, hot, wet: 6/24-6/27/49.
- (3) Summer, cool, dry: 6/27-7/2/50, 8/3-8/9/50.
- (4) Summer, cool, wet: 8/20-8/22/49.
- (5) Winter, warm, dry: 3/4-3/5/49, 1/23-1/25/50.
- (6) Winter, warm, wet: 1/3-1/5/49.
- (7) Winter, cold, dry: 4/13-4/15/50, 11/25-11/30/50.
- (8) Winter, cold, wet: 1/29-1/31/49, 12/18-12/21/50.
- (9) Very hot: 7/27-7/29/49.

- (10) Very cold: 11/25-11/26/50.
- (11) Very clear and dry: 3/1-3/5/49, 7/21-7/29/49, 11/4-11/12/49,
10/11-10/18/50.
- (12) Very cloudy and rainy: 7/2-7/18/49, 1/29-2/2/50.
- (13) Very unstable: 7/8-7/9/49, 8/12-8/15/49, 11/17-11/19/49, 4/19-4/21/50.
- (14) Very stable: 1/2-1/4/49, 1/15-1/21/50, 11/30-12/2/50.
- (15) Very windy: 2/12-2/15/49, 5/21-5/22/49, 9/4-9/9/50.
- (16) Very calm: 5/2-5/7/49, 7/22-7/29/49, 8/1-8/17/49, 11/6-11/11/49.
- (17) Snow: 11/24-11/28/50.

Certain types were definitely better developed than others during 1949 and 1950: in general unusually wet weather was much more common than unusually dry in both summers and winters, and associated with this anomaly was a great excess of unseasonably warm winter weather and a deficiency of both extremely hot (summer) and extremely cold (winter) spells. Nevertheless, there were enough nearly ideal clear, dry spells for some detailed studies of the diurnal cycle to be carried out under these conditions, and the simultaneous occurrence in late November 1950 of the only severe cold wave and the only significant snow cover of the period provided an opportunity to obtain some data on these phenomena.

If one can consider the prevailing weather conditions as constituting a set of independent variables with respect to which the variations of turbulence, local wind flow and diffusion are being studied, it is seen that a fairly adequate range of the independent variables was obtained.

If the nature of the dependence can be determined from these observations, and the normal distribution of the independent variables from other sources, then the normal distribution of the dependent variables can be inferred. This has been the general approach in the analysis, although the actual situation is by no means as simple as may be suggested by the preceding sentences.

Presentation of Data

3. Order of the Elements

It is desirable, in summarizing such a variety of interdependent meteorological variables, to treat one dependent variable at a time. The order in which the dependent variables are taken will be, as far as possible, that of increasing dependence; that is, the elements which are relatively independent within the scope of this study will be taken first.

Thus the barometric pressure, precipitation, weather and sky conditions will be considered first, proceeding in each case from the southern Appalachian regional aspects to the smaller scale variations in the Oak Ridge area. These topics will form the setting for the discussion of the temperature distribution, with its geographical, seasonal and diurnal variations and its dependence upon the other variables (e.g. cloudiness). Finally the distribution of wind and gustiness will be fully discussed. All the variables previously treated plus the "regional" wind flow are considered as independent variables with respect to local wind, wind

gradient and gustiness within the domain of this study. The "regional" wind flow is almost uniquely associated with the horizontal pressure gradient, and will therefore be referred to as the "gradient wind" (it should be noted that this does not conform to strict meteorological usage).

4. Tabulations and Graphs

Numerical tabulation will be reserved for data whose precise values are believed to have direct utility, or whose variables do not lend themselves to graphical presentation. Where patterns rather than individual quantities are of interest, where interpolated values are as useful as observed ones, or where several variables can be effectively represented in combination, graphs and charts will be employed to the fullest possible extent.

In many cases the same observational data will be summarized in several different ways, in order to reveal different relationships. In general, one comprehensive summary of each set of observations will be given, in the form most suitable for extracting data (usually the most nearly standard or familiar form). The additional relationships brought out by other ways of summarizing or graphing these same data will be illustrated by selected examples. Some of the specialized observations were actually not carried on throughout the survey period, and in other cases specialized studies were made which did not utilize all the data. The summaries of these limited series of observations are comparable to the illustrative examples: in order to generalize from them one must take into account the bias of the sample which they represent.

Unless otherwise specified, the following definitions and units will be used throughout:

Seasons:

Winters: Dec.-Jan.-Feb. (12/1 - 2/28)

Spring: Mar.-Apr.-May (3/1 - 5/31)

Summer: June-July-Aug. (6/1 - 8/31)

Fall: Sept.-Oct.-Nov. (9/1 - 11/30)

Time: Eastern Standard

Daytime: 10 a.m. - 5 p.m. (1000-1700 E)

Night-time: 10 p.m. - 5 a.m. (2200 - 0500 E)

Temperature: °F.

Barometric pressure: inches of mercury

Solar radiation: cal./cm²

Precipitation: in.

Altitude: ft.

Wind speed: mph

Wind direction: direction (compass points, or degrees clockwise from north) from which the wind blows.

Cloudiness: tenths of sky cover

Visibility: mi.

Surface level: standard surface observation level, approximately 3 ft. above ground or roof level for precipitation, 4-5 ft. for temperature, 18-40 ft. for wind.

Lapse: decrease of temperature with increasing altitude.

Inversion: increase of temperature with increasing altitude (including 0).

Stability: vertical gradient or differential of temperature, taken positive in the sense of increasing temperature with altitude.

Gradient wind, or gradient (as "southerly gradient"); the wind vector corresponding to the large-scale horizontal distribution of sea-level pressure, blowing parallel to the isobars (perpendicular to the actual pressure-gradient vector) with high pressure on the right; loosely identified with the geostrophic wind or "gradient-level" wind.

Barometric Pressure

5. Regional Pattern of Barometric Pressure

The highest mean annual sea level pressures in the United States are found in the southeastern portion containing Oak Ridge. The long-term (75 years) normal value at Knoxville, 30.06 in. of mercury, or 1018 mb., is among the highest, but is equalled at many stations within 200 to 300 miles. Varying only by one or two hundredths of an inch (less than 1 mb.) from year to year, and virtually independent of the topography, this high mean sea level pressure appears on mean maps (Fig. 36) as a westward extension of the semi-permanent Azores-Bermuda anticyclone, which separates the subtropical easterly (trade) wind belt from the middle-latitude westerlies. The axis of this high pressure belt is, in the mean, slightly south of the latitude of Oak Ridge, and undergoes a seasonal oscillation, being displaced farther south during the winter and spring, and slightly north of this latitude during late summer and fall (Ref. 28). This oscillation is accompanied by a corresponding oscillation of the small resultant surface wind in the Oak Ridge-Knoxville area from westerly to northerly and back. In October a separate cell of high pressure appears centered in West Virginia. This tendency toward anticyclonic circulation is accompanied by fair weather, widespread atmospheric stagnation and smog. It shifts slowly southward during the fall and winter, passing through eastern Tennessee in November, reaching the central Georgia-Alabama area by February, and becoming an indistinguishable part of a continuous high pressure ridge which joins the Azores-Bermuda anticyclone and the polar continental anticyclone

of northwestern Canada. This ridge reflects the paths of cold, shallow, anticyclonically spreading polar air masses migrating southeastward across the continent during the winter. During the spring and summer the mean isobars curve around the western edge of the relatively powerful oceanic anticyclone, accompanied normally by a steady influx of warm, moist tropical air (Fig. 36, July).

Above the lowest 5000 ft. of the troposphere, the mean isobars are oriented west-east in all seasons, with higher pressure on the south and lower on the north. The horizontal pressure-gradients, and hence the resultant westerly winds become quite weak during the summer months, even at high levels. During the winter, however, the mean horizontal pressure gradient is strong, placing this area well within the zone of strong westerly winds aloft.

At Knoxville, 997 ft. MSL, the station pressure is about 1.04 in. Hg. less than the sea level pressure, varying slightly with temperature. At other points in this area, the station pressure decreases about 0.10 in. for each 100 ft. increase in elevation. A pronounced diurnal variation is evident, the normal amplitude in the southern Appalachian region being just under 0.10 in. The maximum occurs between 9 and 11 A. M. EST, the minimum between 3 and 6 P.M., and a weak secondary maximum between 10 P.M. and midnight.

Table 14 gives some useful averages and extremes drawn from the Knoxville records. The lowest graph in Fig. 37 shows the course of mean monthly

station pressure for the period 1931-40: a minimum occurs in April and a maximum in November, the amplitude being almost 0.2 in. Above about 5000 ft. MSL, however, the maximum occurs in August and the minimum in January, the change of phase being accounted for by seasonal changes in the density of the lower troposphere.

Table 14 Knoxville Barometric Pressure

	<u>Station Pressure</u>	<u>Sea Level Pressure</u>
Mean annual, 1871-1945	29.02 in. Hg.	30.06 in. Hg.
Highest, 1871-1945	29.83	30.87
Lowest, 1871-1945	27.91	28.95
Mean annual maximum, 1931-1949	29.63	30.67
Mean annual minimum, 1931-1949	28.34	29.38

Turning to the day-to-day variations of which the climatological means are composed, Figs. 34 and 35 illustrates the sequences which are characteristic of this area and of middle latitude stations in general. During the winter half of the year, the migrating eddies ("Highs" and "Lows") in the broad mid-latitude westerly current, bringing alternately cold and warm air masses, winds of constantly changing direction and speed, fair and stormy weather, and rises and falls of the barometer, pass rapidly and frequently accompanied by changes of as much as 25 mb (0.7 in. Hg) or more from one day to the next. During the summer half, on the other hand, the pace becomes more leisurely, each cycle taking perhaps a week or longer and with the amplitude reduced to the order of 5 or 10 mbs (0.2-0.3 in.). W. H. Klim (Ref. 29) has published maps of the standard deviation of interdiurnal sea-level pressure change from which values of about 7 mb in winter and $2\frac{1}{2}$ mb in summer can be deduced. The majority of

a summer day's pressure change may occur within a few minutes during the passage of a single thunderstorm. All the weather elements reflect this seasonal change of pace.

Since the transient high and low pressure centers are associated with characteristic weather patterns, a tabulation of the frequencies of such centers (defined as a maximum or minimum of sea level pressure with at least one closed 3-mb isobar) within 5° of latitude and longitude of Oak Ridge for the 40-year (1899-1938) period of USWB Northern Hemisphere maps, has been obtained (Table 15). Highs are more common than lows in all months and particularly in the fall season. The November maximum frequency of anticyclones coincides with the maximum mean monthly station pressure (Fig. 37) and the passage through this region of the center of high pressure on the monthly mean maps. (Fig. 36).

Table 15. Average Number of Days with High or Low Pressure Centers Between 30° - 40°N, 80° - 90°W (1899-1938)

	<u>Highs</u>	<u>Lows</u>
January	3.9	2.4
February	3.3	2.4
March	3.4	2.2
April	3.3	2.1
May	3.1	1.7
June	2.9	1.3
July	2.8	1.3
August	2.8	1.3
September	3.3	1.3
October	4.7	1.4
November	5.4	1.5
December	4.4	2.1

6. Oak Ridge Pressure Observations

Little difference is noted between the station pressure variations in the Oak Ridge area and those at Knoxville (Figs. 37 and 38), other than the difference of 0.09 in. Hg due to the lower elevation of the Oak Ridge barometer (815 ft. MSL). During the 1949-1951 period of microbarograph observations (Fig. 203) the monthly extremes, reduced to sea level (Fig. 37A) compared within a few hundredths of an inch. The average annual maximum sea level pressure, (30.63 in. at Oak Ridge, 30.64 in. at Knoxville) occurred at both stations in December and the average minimum (29.49 in. at Oak Ridge and 29.45 at Knoxville) in March. These are comparable to the 19-year averages in Table 14. The average monthly station pressures (Fig. 37C) run parallel at the two stations, and are close to the 10-year mean, (1931-1940) with the exception of November, which had a departure of 0.09 in. Both the average monthly range (Fig. 37A) and the average daily range (Fig. 37B) of station pressure are largest in winter and spring, and least in summer. From 2109 mercurial barometer readings at X-10, compared with simultaneous readings at Knoxville (Fig. 38), it is seen that the mode and median as well as the mean pressure difference is 0.09 in. and the standard deviation of the difference is 0.01 in. The distribution of the difference is normal except for a few erratic readings. Thus the Knoxville barometric pressure statistics, corrected for difference in elevation, can be taken as representative of Oak Ridge with an accuracy of the same order as that of the microbarograph record itself.

Pressure and pressure gradient are important micrometeorological variables, being fundamental both in the process of turbulent flow and in the development of valley and mountain breezes. However, such sensitivity and rapidity of measurement would be required for studies of these relationships, and such difficulties and ambiguities surround their interpretation, that no attempt has been made to go beyond the gross climatology presented above.

Precipitation

7. Regional Pattern of Precipitation

Large and irregular variations in monthly and annual precipitation, unevenly distributed over the southern Appalachian Mountains and adjacent lowlands, occur in association with subtle changes in the relatively regular pattern of barometric pressure. Slight variations in the sources and trajectories of the air masses, and of the degree of convergence and lifting to which they are subjected by the large scale dynamic processes of the atmosphere, as well as the irregular cellular nature of smaller scale convective processes, are sufficient to produce erratic patterns of precipitation even in level country over averaging periods as long as several years. When, in addition, the atmosphere is forced to flow over or around mountainous obstructions of varying slope, height, orientation and extent, the resulting distributions are too complex to be described with the spacing of observation stations ordinarily employed for other elements.

Fortunately for the present survey, the TVA and the Weather Bureau have operated for many years an extraordinarily dense network of rain-gage stations in the area under study. Fig. 39 shows the average annual precipitation for the 4 year period 1948-1951, based on observations at 347 stations, (represented by circles), including the Townsite and X-10 stations at Oak Ridge.

It is apparent from Fig. 39 that variations of tens of inches in the annual total within a few miles are common. Furthermore, while there

is a marked correlation with altitude, the variation between stations at comparable altitudes is sufficient to indicate that other factors are also important. For instance, the highest peak, Mt. Mitchell (6684 ft. MSL), received an average of about 77 in. per year, while several much lower mountains (3600 to 5100 ft. MSL) to the southwest received over 90 in. per year. As to the Southern Appalachian Valley in the vicinity of Oak Ridge and Knoxville (elevation 750 to 1100 MSL), the average annual total during the 4-year period summarized in Fig. 39 varied from less than 45 in. east of Knoxville to over 65 in. a few miles west of the Oak Ridge area. The higher amounts in this valley are part of the precipitation maximum (over 70 in.) on the slope of the high Cumberlands facing the southwesterly winds aloft which predominate during precipitation. The low-rainfall area extends north and northeast of the Great Smoky Mountains and appears to result from a combination of downslope flow and moisture depletion (hence the relatively low figure at Mt. Mitchell). Both these features of the pattern vary in location and intensity from month to month and even from year to year, placing Oak Ridge sometimes within the high-precipitation zone, sometimes well out of it.

That the abnormal amounts of precipitation during this four-year period were accompanied by an anomalous geographical distribution is well illustrated by Fig. 40, a map of the departure from the average of record based on 69 stations (represented by circles) having 20 years of record or more. Departures exceeding 10 in. per year are found just northeast of

the Gumberlands and northwest of the Smokies, some of the larger storms having been accompanied by northerly or northeasterly flow aloft. The "rain-shadow" area was shifted southeastward, as shown by small or negative departures in the Piedmont section. The important consequence of this shift for the Oak Ridge climatology is that the departure from normal apparently varies by at least 2 in. across the reservation itself, and by as much as 5 in. between points within the reservation and the nearest long-period stations. Furthermore, the usefulness of the long-period records at Knoxville or Clinton for normalizing the Oak Ridge observations by standard methods is complicated by the fact that the stations involved were under the influence of different parts of the anomaly pattern, Knoxville showing an average departure of less than 5 in. from the 81 year average, while the Clinton departure from its 62 year record is almost 12 in. Both the relatively greater anomaly during recent years at Clinton than at Knoxville and the association of Oak Ridge (Station 012) sometimes with the high-precipitation zone (1950-51) and sometimes with the low precipitation zone (1946-49) are clearly illustrated in Fig. 41, which shows the total precipitation for each year of record. The normal Oak Ridge rainfall would be determined by the frequencies of these two regimes over a long period of time. Thus the departure of the observed Oak Ridge precipitation from the climatological normal is left in doubt, although the isanomals of Fig. 40 would indicate departures of 5 to 7 in., which lead to normal annual precipitation values of 50 to 53 in.

8. Local Variations of Precipitation

Within the smaller scale of the Oak Ridge reservation, the dramatic geographical variability of precipitation seen in the larger region is not approached on an annual time scale, but is repeated or even exaggerated when shorter intervals are considered, particularly in the summer half of the year. For example, on July 1, 1952, when 2.50 in. of rain were received in the town of Oak Ridge (all within one hour), no rain at all was recorded at K-25, about 11 miles away. Such local showers can affect the monthly totals quite radically, as in June 1951, when 8.45 in. was recorded at K-25, 4.83 in. at Townsite and only 3.87 in. at X-10. The irregularities are still apparent when annual totals are considered. During the very rainy 12 month period October 1949 through September 1950, for example, 69.91 in. was recorded at the Whiteoak Lake station and only 64.61 in. at Townsite, a difference of over 5 in. By the time 4-year averages for the period 1948-1951 are taken, the annual rainfall at X-10, 56.55 in., differs from that at Townsite, 58.13, by less than 2 in., but in view of the shifting order of the inequalities in the examples quoted and many others, it is still questionable whether this difference represents a normal climatological variation between the two locations. In other words, there is no positive evidence of orographic influence on precipitation within the area and scale of relief of the Oak Ridge reservation.

It should be remembered, however, that the rain gages were not located primarily so as to test such influences, but only to provide representative

plant records and therefore were all in valleys.

The question of representativeness, in the absence of orographic variations, resolves itself into that of the allowable distance between rain gage stations. An examination of the data from 5 stations within the reservation shows that the erratic variations of precipitation described in the preceding paragraph only occur between stations several miles apart. In Table 16 are shown the mean monthly precipitation for 6 summer months and 6 winter months at 5 stations (the records for stations 009 and 016 are combined), together with the mean algebraic (systematic) deviations and mean absolute deviation corrected for systematic deviations between pairs of the stations various distances apart. It is evident that the systematic variations are practically negligible in the summer but probably significant in the winter, when the stations nearest the Cumberlands (011 and 013) receive half an inch to an inch more precipitation than those farther away (009 and 012). The non-systematic variations, on the other hand, are far greater in the summer, and increase rapidly with separation of the stations, so that an average absolute error of 1 in. would be made in transposing an observed monthly precipitation total to a point 4 miles away from the point of observation, and 2 in., 8 miles away in a cross-valley direction. The apparent improvement at 10.8 miles separation can be attributed to the fact that stations 011 and 013 are oriented more nearly parallel to the paths of the showers and therefore experience a larger fraction of them in common than do other

pairs of stations at comparable distances. But even in this case an average absolute error of 30 percent with individual monthly totals differing by more than a factor of 2 can hardly be neglected in any practical application.

Table 16. Local Variations of Precipitation

Season	Station A	Station B	Distance mi.	Precip A in.	Precip B in.mi.	Syst.	Non-Syst.
						Deviation A-B in.	Deviation (A-B)-(A-B) in.
Summer (6,7,8/49 and 6,7,8/50)	001	012	0.3	5.55	5.66	-0.11	0.59
	009	012	1.8	5.43	5.66	-0.22	0.81
	013	012	4.6	5.40	5.66	-0.26	0.97
	009	013	4.6	5.43	5.40	+0.03	1.20
	011	012	7.8	5.50	5.66	-0.16	1.51
	001	011	8.1	5.55	5.50	+0.05	2.15
	009	011	10.0	5.43	5.50	-0.07	2.18
	013	011	10.8	5.40	5.50	-0.10	1.55
	Winter (12/49, 1,2,12/50 and 1,2/51)	009	012	1.8	6.38	6.40	-0.03
013		012	4.6	7.19	6.40	+0.79	0.46
009		013	4.6	6.38	7.19	-0.81	0.68
011		012	7.8	6.87	6.40	+0.47	0.62
009		011	10.0	6.38	6.87	-0.49	0.64
013		011	10.8	7.19	6.87	+0.32	0.58

The extent to which the regular Knoxville 6-hourly observations can be taken to represent Oak Ridge is indicated by Table 17, a joint frequency distribution, in 5 broad classes, of 1321 simultaneous pairs of routine observations made during 1949 and 1950. Of the 34% with precipitation at Oak Ridge, 7.6 or almost one fourth, had none recorded at the Knoxville Airport. 10% of the observations with precipitation at either station show discrepancies of 2 or more class intervals between the two.

Table 17. Knoxville-Oak Ridge Joint Precipitation Frequency

	<u>Knoxville: 0</u>	<u>T-0.01</u>	<u>0.02-0.24</u>	<u>0.25-0.99</u>	<u>≥1.00</u>	<u>Total</u>
Oak Ridge						
0	59.7	4.7	0.9	0.5	0	66.0
T-0.01	6.1	7.1	3.0	0.2	0	16.4
0.02-0.24	1.3	3.8	6.1	0.6	0	11.8
0.25-0.99	0.2	1.0	1.1	2.9	0.2	5.4
≥ 1.00	0	0	0.2	0.4	0.1	0.7
Total	67.3	16.8	11.3	4.6	0.3	100.

9. Time-Variability of Precipitation

The preceding discussion of the geographical distribution of precipitation anomaly was based on evidence from all stations having 20 years or more of record, implying that such a period is sufficient to give a relatively steady normal. The great variability from year to year (Fig. 41) suggests that a long period is required: Knoxville has received annual amounts ranging from less than 35 in. to over 73 in. during the 81 years of record, and the Clinton 62 year range is slightly less. Fig. 42 illustrates the effect of increasing length of record on the average annual precipitation for Clinton, Knoxville and two Oak Ridge stations. Apparently an average taken over 20 years will not be changed more than about an inch by adding a comparable number of years to the record, but even 80 years are insufficient to achieve any greater precision, due to long-period climatic fluctuations. There is thus very little justification for specifying the normal annual precipitation more precisely than the nearest whole inch even where long-period records are available, and the uncertainty is greater

when extrapolation is made from records of less than 20 years. The previously given range of 50 to 53 in. per year, then, is probably as precise a statement of the long-term normal precipitation for the Oak Ridge area as can be made at this time.

A better view of the precipitation expectancy is afforded by long-term frequency distributions. Fig. 43 shows the frequency distribution of annual and monthly precipitation at Knoxville expressed as ratios to the mean. In the absence of a long record at Oak Ridge, this can be taken as an approximately correct relative picture for this area. The majority of the yearly totals (60%) are uniformly distributed between 12% below normal and 7% above normal.

Roughly: 1 year out of 5 was more than 10% below normal,
1 year out of 5 was more than 10% above normal,
1 year out of 10 was more than 15% below normal,
1 year out of 10 was more than 15% above normal,
no years were more than 33% below normal,
2 years out of 78 were more than 33% above normal.

The relative scatter of the monthly totals is, of course, much greater (no allowance has been made for seasonal variation, which alone introduces deviations of 25% from the mean). It can be seen from the middle histogram in Fig. 43 and more readily, from the cumulative frequency graph in Fig. 44 that:

1 month in 5 was more than 40% below the mean,
1 month in 5 was more than 40% above the mean,

1 month in 10 was more than 60% below the mean,
1 month in 10 was more than 70% above the mean,
1 month in 20 was more than 70% below the mean,
1 month in 20 was more than 100% above the mean.

The probability that the Knoxville total recorded for a particular month can be considered representative of Oak Ridge is shown by the lower histogram of Fig. 43, which contains the frequency distribution of the ratio of Oak Ridge (station 012) monthly precipitation to that observed at Knoxville. The corresponding probability graph is shown in Fig. 45. Of the 96 months represented, Oak Ridge received:

in 1 out of 20 months over 35% less,
in 1 out of 5 months over 35% more,
in 1 out of 10 months over 55% more,
in 1 out of 20 months over 70% more precipitation than the

Knoxville Airport station.

10. Seasonal Distribution of Precipitation

Seasonally, both the amount and the frequency of precipitation are at a minimum in the fall throughout the southern Appalachian Area. On the whole, the amounts received in the other seasons are nearly equal, with a weak winter or spring maximum in the valley area surrounding Oak Ridge and at most stations to the south and west, and a more pronounced summer maximum through the mountainous area east of Knoxville.

Table 18A shows examples of the seasonal distribution for a few selected stations. The largest part of the variation in annual total precipitation from one station to another is accounted for by variations in the winter and spring. That is to say the summer-maximum stations, Bristol and Asheville, are simply those receiving the least winter and spring rainfall. It should be noted that the upper winds accompanying precipitation are much lighter and more variable in direction in summer than in the other seasons. The summer rainfall consequently shows little directional effect, while the winter precipitation is deposited predominantly in the southwestern portions of the mountainous areas. An indication of this effect has already been seen on a small scale in the discussion of local variations.

That the falling off of winter rainfall towards the northeast is due at least in part to depletion of available moisture rather than to suppression of the rainmaking process (by large-scale descending motion, for instance) is suggested by the relative constancy of daily and hourly frequency (Table 18B and C). In fact, while the total precipitation decreases from Chattanooga to Bristol in winter and spring, the hourly frequency actually increases. The change in character from steady precipitation in winter to showers in summer, already illustrated by the increase in variability over the Oak Ridge area, is further brought out by the striking decrease in hourly frequency while the total amount and daily frequency remain nearly constant or increase.

Table 18. Seasonal Precipitation in the Southern Appalachian Area

Station	A. Seasonal total, in.					Length of Record
	Winter	Spring	Summer	Fall	Annual	
Bristol	10.25	10.07	<u>14.46</u>	7.34	42.12	14 yrs.
Knoxville	<u>13.67</u>	13.18	12.60	8.67	48.12	81 yrs.
Chattanooga	<u>15.35</u>	14.55	12.76	9.64	52.30	73 yrs.
Asheville	8.60	9.71	<u>12.37</u>	7.53	38.16	49 yrs.
	B. Hourly Precipitation Frequency, percent					
Bristol	<u>16.5</u>	11.0	8.4	7.3	10.8	68,557 hrs.
Knoxville	<u>16.2</u>	10.7	7.8	7.5	10.5	78,744 hrs.
Chattanooga	<u>15.1</u>	9.2	6.8	6.7	9.5	101,080 hrs.
Asheville	-	-	-	-	-	-
	C. Number of Days with 0.01 in. or more					
Bristol	36	36	<u>38</u>	24	134	14 yrs.
Knoxville	36	<u>37</u>	36	24	133	81 yrs.
Chattanooga	<u>37</u>	35	<u>37</u>	24	133	73 yrs.
Asheville	32	35	<u>42</u>	24	133	49 yrs.

The pattern of average monthly precipitation for the 8 years of record at station O12 on the Oak Ridge reservation (X-10 Health Physics Division) reflects the characteristic seasonal distribution for this region (Fig. 46), namely, a fall minimum and winter maximum. However, it should be borne in mind in interpreting this graph that January and November have been abnormally wet during the period of observation.

An estimate of the normal monthly precipitation at three stations on the area (Townsite, X-10, K-25) and four nearby stations having long records (Clinton, Kingston, Knoxville, Loudon) is provided by Table 19. The off-area figures are the observed averages for the 30 years 1921-1950, the current Weather Bureau standard normal computation period. The Oak Ridge area figures are adjusted to this same period by the 3-station normal-ratio method recently adopted by the Weather Bureau (Ref. 30) using Clinton, Kingston, and Loudon as reference stations. These normals are useful for computing deviations and for interpolating missing data, but should not be interpreted as physical constants of the precision indicated.

TABLE 19

30-YEAR NORMAL MONTHLY PRECIPITATION, IN.

	<u>Townsite</u>	<u>X-10</u>	<u>K-25</u>	<u>Clinton</u>	<u>Kingston</u>	<u>Knoxville</u>	<u>Loudon</u>
Jan.	5.07	4.94	5.39	5.31	5.03	4.54	5.27
Feb.	5.04	4.91	5.36	5.20	5.05	4.73	5.27
Mar.	5.20	5.07	5.52	5.34	5.19	4.83	5.47
Apr.	4.08	3.97	4.33	4.15	4.14	3.64	4.25
May	4.02	3.92	4.28	4.30	4.07	3.58	4.02
June	4.00	3.90	4.25	4.58	3.95	3.47	3.80
July	4.81	4.69	5.11	5.19	4.54	4.72	5.08
Aug.	3.94	3.83	4.18	3.96	4.27	3.43	3.87
Sept.	3.01	2.93	3.20	3.44	3.01	2.53	2.83
Oct.	2.62	2.55	2.78	2.71	2.65	2.63	2.69
Nov.	3.87	3.77	4.11	4.04	4.03	3.25	3.83
Dec.	4.85	4.72	5.15	5.11	4.86	4.26	4.96
Annual	50.51	49.21	53.66	53.33	50.79	45.51	51.34

Table 20. Normal Daily Precipitation Frequency, Knoxville and Oak Ridge

	Knoxville			Townsite			X-10		
	.01 in.	.10 in.	.25 in. 1.00 in.	.01 in.	.10 in.	.25 in.	.01 in.	.10 in.	.25 in.
Jan.	13	9	6 1	14	10	8	13	9	6
Feb.	11	8	5 1	12	8	5	10	7	5
Mar.	13	9	6 1	13	10	6	13	10	6
Apr.	12	7	5 1	11	6	5	13	8	6
May	12	9	5 1	12	8	5	13	8	5
June	12	8	5 1	11	9	5	14	8	5
July	12	10	5 1	12	10	5	12	10	4
Aug.	12	8	5 1	13	9	6	12	8	6
Sept.	8	4	3 1	7	5	3	8	5	4
Oct.	7	4	3 1	8	4	3	9	4	3
Nov.	9	5	4 1	9	5	4	9	5	4
Dec.	2	8	5 1	13	9	6	13	9	5
Annual	133	89	57 12	135	93	61	139	91	59

The seasonal trend of precipitation frequency at Knoxville, X-10 and Townsite is shown by Fig. 47 and Table 20, which show the monthly frequency of days with precipitation equalling or exceeding 0.01, 0.10, and 0.25 in. The frequencies at the Oak Ridge stations have been normalized with reference to the 81 year Knoxville record by the ratio method (i.e., the Knoxville normal frequency has been multiplied by the ratio of Oak Ridge frequency to Knoxville frequency during the period of observations at Oak Ridge). The frequencies of all amounts are consistently higher at the Oak Ridge stations than at Knoxville or other valley stations listed in Table 18. The differences between the two stations on the Oak Ridge area, 8 miles apart, are erratic and of doubtful significance: an average value of 137 days per year with 0.01 in. or more, 92 days with 0.10 in., and 60 days with 0.25 in. might be considered representative of the area as a whole.

Duration of dry spells is often of interest in connection with construction work. Fig. 48 shows the observed frequency of periods of varying duration free of precipitation (less than .01 in. in one day) seasonally and annually, for station 011 (Townsite) and station 012 (X-10). Dry spells lasting a week or more are most common in the fall, and least common in the winter, and can only be expected about 8 - 10 times per year, on the average.

11. Extreme Precipitation

The extreme monthly and daily precipitation for the 8 years of observations at X-10 are shown in Fig. 46. Their great irregularity is partly due to the short period of record, and a review of the regional data will serve to shed further light on extremes to be expected in various intervals of time.

Table 21 . Maximum Observed Precipitation

Duration	Amount			Location	Date	Ref.
	a*	b*	c*			
5 min.	0.83			Asheville, N. C.	Aug. 18, 1918	32
		0.80		Chattanooga, Tenn.	June 12, 1922	32
10 min.	1.41			Asheville, N. C.	Aug. 18, 1918	32
		1.27		Chattanooga, Tenn.	June 15, 1924	32
15 min.	1.71			Asheville, N. C.	Aug. 18, 1918	32
		1.62		Chattanooga, Tenn.	June 15, 1924	32
30 min.	2.57	2.57		Knoxville, Tenn.	July 8, 1939	32
1 hr.	4.00			Mt. LeConte, Tenn.	Sept. 1, 1951	36
	(7.0)			Winchester Springs, Tenn.	July 8, 1938	37
		3.52		Knoxville, Tenn.	July 8, 1939	32
		2.50	Townsite	July 1, 1952		
2 hrs.	(7.8)	(7.8)		Crossville, Tenn.	May 22, 1938	37
3 hrs.	6.17			Lexington, Ky.	Aug. 2, 1932	32
	(8.9)			Lewisburg, Tenn.	June 18, 1939	37
4 hrs.	(7.2)			Hartselle, Ala.	July 9, 1946	37
		(6.2)		Chattanooga, Tenn.	May 15, 1946	37
6 hrs.	(11.6)			Lebanon, Tenn.	Aug. 3, 1939	37
12 hrs.	(12.6)			Altapass, N. C.	July 15, 1916	37
18 hrs.	(17.0)		3.25	K-25	Feb. 1, 1951	
				Altapass, N. C.	July 15, 1916	37
		(13.1)		Lake City, Tenn.	Sept. 29, 1944	37
24 hrs.	22.22			Altapass, N. C.	July 15, 1916	33
		8.90		Tazewell	Aug. 3, 1916	33
			7.75	X-10	Sept. 29, 1944	
		4.97	K-25	Feb. 1, 1951		

Table 21 (Continued)

Duration	Amount			Location	Date	Ref.
	a*	b*	c*			
1 month (calendar)	23.44			Big E. Fork Pigeon, Tenn.	Nov. 1948	36
		18.04		Clinton, Tenn.	June 1928	31
			13.10	Townsite	Jan. 1950	
31 days			14.60	Townsite	Jan. 10-Feb. 9, 1950	
12 months	145.5			Coweeta #8, N.C.	Nov., '48-Oct. '49	36
		83.37		Petros	Oct., '49-Sept. '50	36
			70.42	K-25	May '50-Apr. '51	

*a - Southern Appalachian Area

b - East Tennessee Valley and Cumberland Plateau near Oak Ridge

c - Oak Ridge reservation

E

Observations of extreme precipitation for various durations in the region under consideration have been obtained from published records of the Weather Bureau and the TVA (Ref. 31-37) and are shown in Table 21. Data for duration less than 1 hr. are based on records for first order Weather Bureau stations only, while those for 1 hr. and longer include hundreds of rain-gage stations. Figures in parentheses are unofficial.

The large relative number of record catches occurring during the past two decades may be due as much to the increase in the density of the rain gage network as to the abnormally heavy precipitation, particularly in the mountainous areas. However, an important point to be noted is that for periods less than 24 hrs., the extreme downpours are not confined to the mountains; nor does the Tennessee Valley-Cumberland Plateau area near Oak Ridge fall far short of those records which have been set at other locations. It should be noted, too, that all these records for shorter durations have been established in the summer half of the year, when the precipitation distribution appears to be most nearly independent of topography.

The maximum 24 hour precipitation observed on the Oak Ridge area during the 8 years of record, 7.75 in. at X-10 on September 29, 1944, is so large as to deserve some discussion. On that date many record breaking 24 hour amounts were recorded at nearby official Weather Bureau climatological stations, a few of which are listed in Table 22 (from Ref. 33).

The Fort Loudon Dam observation was the highest 24 hr amount reported by the Weather Bureau in Tennessee in 1944, and the Clinton monthly total, 16.47 in., was the highest monthly total in the State for that year. The latter figure included 4.33 in. which fell on Sept. 30, to make a 2-day total of 10.08 in. In view of these data and a TVA estimate of 13.1 in. in 18 hrs. near Lake City on September 29 (Ref. 37) the observation of 7.75 in. at X-10 appears to be fairly well substantiated.

Table 22. Record September 24-hr. Precipitation Set on Sept. 29, 1944

<u>Station</u>	<u>Amount, in.</u>	<u>Length of record, yrs.</u>
X-10	7.75	8
Ft. Loudon Dam	6.50	10
Concord	6.10	15
Univ. of Tenn., Knox.	6.09	12
Clinton	5.75	66
UT Farm, near Knox.	5.60	12
Knoxville Airport	4.98	12
Lake City	4.85	10
Kingston	4.84	66
Norris	4.84	15

In attempting to estimate the probable recurrence interval for such extreme 24-hour precipitation, it was found that when the frequencies of 1, 2, 3, 4 and 5 inches or more in 24 hrs at any station, expressed as a percentage of the total number of days with 0.01 in, or more, was plotted on log probability graph paper, a straight line could be fitted to them reasonably well. The following sets of data were treated in this manner:

- (1) X-10 records, Jan. 1944 through July 1951
- (2) Oak Ridge Townsite records, May 1947 through July 1951
- (3) Clinton, Kingston and Loudon records combined, Jan. 1944 through May 1951
- (4) Knoxville records, Jan. 1944 through May 1951
- (5) Knoxville records, 1871 through 1950

The graphs shown in Fig. 49, show surprisingly good agreement between Knoxville long-period statistics and those for the period during which X-10 data were available. The Knoxville line, however, does not fit the Oak Ridge, Clinton, Kingston and Loudon data, which agree well among themselves and show a higher

level of precipitation (or higher probability of any given amount being exceeded). Only the 7.75 in. observation at X-10 is far off the curve, the normal probability of this amount, as extrapolated from the straight line, being 0.01% or once in 10,000 rainy days (.01 in. or more of precipitation). Since the normal frequency of 0.01 in. at X-10 is approximately 139 days per year, the expected recurrence interval for 7.75 in. would be about 70 years. Other normal recurrence intervals extrapolated from this graph are given in Table 23.

Table 23. Normal Recurrence Intervals for Excessive 24 hr. Point Precipitation

<u>24 hr. precipitation, in.</u>	<u>Recurrence Interval, yrs.</u>
3	1 $\frac{1}{4}$
4	3 $\frac{1}{2}$
5	9
6	21
7	40
8	75
9	120
10	200

In an attempt to answer the question as to the maximum possible precipitation, which arises in connection with many problems of hydraulic design, R. A. McCormick and R. W. Schloemer of the Weather Bureau have prepared a set of generalized estimates based on meteorological considerations (Ref. 38). They assume that both the available moisture throughout the troposphere, deduced from surface dew-point observations, and the efficiency of the dynamic precipitation - producing mechanism, deduced from a careful study of all the major storms of record, simultaneously reach their maximum values. By combining these maximized factors they have made estimates of the probable maximum precipitation for various durations and catchment areas. These are presented in Ref. 38 in the form of maps, from which the data in Table 24 have been obtained.

Table 24 Probable Maximum Precipitation, in.

<u>Duration Catchment Area</u>	<u>6 hrs.</u>	<u>12 hrs.</u>	<u>24 hrs.</u>
10 sq. mi.	30	33	35
200 sq. mi.	16	22	26

Table 24 (Continued)

<u>Duration Catchment Area</u>	<u>6 hrs.</u>	<u>12 hrs.</u>	<u>24 hrs.</u>
500 sq. mi.	13	18	22
Max. obs. point precip.	(11.6)	(12.6)	22.22

In view of the fact that even with the present dense network of raingages, the rain entering the 50 sq. in. cross section of the gage must be considered representative of at least 50 sq. mi., the differences between the peak observed amounts (Table 21) and the calculated upper limits (Table 24) are surprisingly small.

The implications of the observed and deduced extreme precipitation data with respect to possible flooding of Whiteoak Creek have been quite thoroughly treated by W. C. Ackerman (Ref. 37), L. R. Setter and O. W. Kochtitzky (Refs. 39, 40).

12. Snowfall

Snowfall is even more variable than rainfall in this region, ranging geographically from an average of less than 5 in. per year in the southern valleys to over 50 in. on the higher mountains. Located close to the average southern limit of snowfall, the Oak Ridge-Knoxville valley area received only traces of snow in some years and over 20 in. in others. A snowfall of 1 in. or more can be expected on an average of one day per month in December, January, and February in the valley and a trace or more on 16 days per year; no measurable amounts have fallen at Knoxville between May and October during 81 years of record. Snow cover rarely persists more than a few days, the maximum consecutive period with 1.0 in. or more on the ground at Knoxville having been 15 days in February 1895.

No snow of any significance occurred during the routine observation period of the meteorological survey, but special observations were

taken when an unusual snowfall and cold wave occurred late in November 1950. There is little evidence that snow cover has any appreciable climatological importance in this area.

Weather and Sky Conditions

13. Weather Phenomena

The Southern Appalachian Valley has a somewhat higher frequency of both fog and thunderstorms than the surrounding lowlands, but a lower frequency of low clouds and strong winds. Schematic maps in Fig. 50 show, for this and neighboring zones, the annual frequency (%) of hourly observations with light and moderate fog, dense fog, ceiling height 600 ft. or less, ceiling height 600-2000 ft., visibility 1 mi. or less, thunderstorms and winds over 15 mphs., and the number of days per year with 0-3 tenths of sky cover (sunrise to sunset), 8-10 tenths, heavy fog and thunderstorms. The hourly data were obtained from Ref. 41 and the daily frequencies from the Local Climatological Summaries published by the Weather Bureau. The stations included are as follows:

- (a) Southern Appalachian Valley: hourly, Chattanooga and Knoxville; daily, Rome, Chattanooga, Knoxville, and Bristol.
- (b) Smoky Mts.-Blue Ridge: hourly, none; daily, Asheville and Roanoke.
- (c) Cumberland-Ohio Valley: hourly, Nashville and Louisville; daily, Nashville, Louisville and Lexington.
- (d) Gulf-Foothills: hourly, Birmingham and Atlanta; daily, Birmingham, Anniston, Ala., and Atlanta.

- (e) Piedmont: hourly, Spartanburg and Greensboro; daily, Athens, Ga., Greenville and Spartanburg, S.C., Charlotte, Winston-Salem and Greensboro, N.C., and Lynchburg, Va.,
- (f) Allegheny Mts.,: Charleston and Elkins, W. Va.

While the hourly percentage charts represent a better measure of the frequency and a more specific choice of conditions, the daily frequencies give somewhat better geographical coverage.

Fog, low clouds, and wind are closely interrelated, the sheltered mountain valleys having frequent fog but infrequent clouds below 600 ft., while the more exposed foothills facing the Gulf receive more frequent low ceilings and fewer ground fogs. In the ceiling range 600-2000 ft. a transition is made from radiation-advection-turbulence stratus to larger-scale cloud systems, and the frequencies are roughly equalized over the various zones; the association of cloudiness in this layer with migrating low-pressure systems is indicated by increasing frequency to the north and a downslope (with respect to the prevailing westerly winds) minimum in the Piedmont Section. The northward increase in frequency of cloudy days seems definitely associated with the latitudinal increase of storminess north of the axis of the Bermuda anticyclone. Still, the Appalachian Valley area has a low frequency of clear days and high frequency of cloudy days for its latitude, perhaps correlated with orographic effects. It can be inferred from the Alleghenies pattern, from the daily frequency of fog

in the Smoky Mts.-Blue Ridge area, and from the frequency of ceilings in the 600-2000 ft. range in adjacent lowlands (which might appear as fogs at higher stations), that sheltered locations on the Cumberland Plateau would also have high frequencies of fogs and low visibilities.

While thunderstorms are observed in the Valley at only 1% of the hourly observations, they occur on 16% of all days, with higher daily frequencies only towards the Gulf of Mexico. In the absence of official data on thunderstorms over the Cumberland Plateau, it should be mentioned that the Crossville-Crab Orchard area is reputed among aviation meteorologists to have more frequent thunderstorms than any other part of the southern highlands. It has already been seen that intense showers of short duration and small horizontal extent account for the major proportion of summer rainfall in this entire area.

The seasonal distribution of these weather types in the Knoxville area is shown in detail in Table 25. Thunderstorms are rare in the winter months but occur on nearly one-third of all summer days. The frequency of hourly observations with thunder is, however, even in the summer, only a little over 1%. A. L. Shands has shown that the probability of a thunderstorm beginning within each quarter-day varies, in summer, from 2% in the period midnight to 6 a.m. to 20% in the period noon to 6 p.m., whereas in winter the probability is less than 1% in all quarter-days (Ref. 42).

Fog is most common in the fall, but low visibilities have a maximum frequency in winter, probably accounted for by greater consumption of smoke-producing fuel and greater stability in the deeper layers of the atmosphere. Over the year as a whole, some atmospheric obstruction to

Table 25. Seasonal distribution of weather and sky conditions, Knoxville

	Winter	Spring	Summer	Fall	Annual	Period of Record
a. Cloudiness						
Avg. sky cover, sunrise-sunset, tenths	6.3	5.7	5.3	4.8	5.5	31 yrs
No. days clear (sunrise-sunset)	24	29	28	39	120	81
No. days partly cloudy "	24	31	40	26	121	81
No. days cloudy "	42	32	24	26	124	81
Avg. percent of possible sunshine	44	59	63	61	57	54
Highest monthly % poss. "	76	85	84	85	64	33
Lowest " " "	22	36	31	27	45	33
b. Ceiling height, hourly % frequency						
0-300 ft.	2.6	0.2	0.4	0.9	1.0	3*
301-600 ft.	2.8	0.7	0.5	1.3	1.4	3*
601-1000 ft.	4.8	1.6	1.4	2.4	2.6	3*
1001-2000 ft.	8.6	4.5	2.5	4.8	5.1	3*
Total 0-2000 ft.	18.8	7.0	4.8	9.4	10.1	3*
c. Fog (visibility ≤ 6 mi)						
Total no. days light fog ($> \frac{1}{4}$ mi)	6	4	6	10	26	10
Total no. days dense fog ($\leq \frac{1}{4}$ mi)	5	2	4	7	18	71
Total no. days with fog	11	6	10	17	44	10
% hrs. light fog ($> \frac{1}{4}$ mi)	19.9	10.1	11.9	13.6	13.9	3*
% hrs. dense fog ($\leq \frac{1}{4}$ mi)	1.4	0.4	0.2	0.9	0.7	3*
Total % hrs. with fog	21.3	10.5	12.1	14.6	14.6	3*
d. Visibility, hourly % frequency						
0- $\frac{1}{2}$ mi.	6.1	2.1	1.0	2.5	2.9	3*
$\frac{5}{8}$ -1 mi	6.6	3.4	1.4	2.4	3.2	3*
$1\frac{1}{4}$ -2 mi	8.2	3.6	2.2	5.2	4.8	3*
$2\frac{1}{2}$ -6 mi	34.2	18.3	15.3	23.5	22.8	3*
e. Thunderstorms						
No. days	1	14	27	6	48	71
% hours	0.0	0.6	1.2	<0.1	0.5	3*
f. Snow, sleet and hail, no. of days						
Snow, trace or more	12	2	0	2	16	10
Sleet	3	0	0	0	3	11
Hail	<1	<1	<1	<1	2	39
Snow, sleet or hail, 1 in. or more	3	0	0	0	3	68

*23,198 hourly observations (Ref. ⁴¹)

vision (visibility ≤ 6 mi) exists about one-third of the time. Fog accounts for over half the obstructions, smoke about one-third, and precipitation for nearly all the remainder. Haze, although very common in the summer, seldom restricts the visibility to 6 mi. or less.

Frozen precipitation has been described in a previous section with respect to amount. As to frequency, on the average, a trace or more of snow can be expected on 16 days per year, sleet on 3 days per year and hail on 2 days per year. No statistics are available on glaze or ice storms (freezing rain), but this part of the country is known to be subject to such storms almost yearly in varying degrees of severity, with an increase in both frequency and severity towards the higher mountainous exposures.

Severe windstorms are not entirely unknown in the Southern Appalachian Valley, but are comparatively rare in comparison with the surrounding area. Winter storms almost invariably lose their force in crossing the Cumberland Plateau, and the local ridges seem further to obstruct the air flow. Tornadoes have an infinitesimal frequency of occurrence per county or per hundred square miles; those few which have been reported within 50 mi. of Oak Ridge during the past half-century were small, had short paths, and caused little damage. This is in contrast with the situation just across the Plateau (Ref. 43), where tornadoes are more common and more destructive. The 5 highest wind speeds recorded during the survey program, ranging from 55 to 70 mph, were of very short duration (one minute or less) and occurred in conjunction with spring or summer thunderstorms. The highest observed sustained wind for 5 min. was 52 mph and for an hour, 32 mph. This is in contrast to an average of 3 days per year with maximum hourly wind speed 40 mph

or more at Knoxville for the period 1892-1930, and 9 days per year with maximum 33 mph or more.

14. Cloudiness

Cloudy days are somewhat more frequent than clear days over the year as a whole in the mountains and valleys surrounding Oak Ridge. It is seen in Table 26 that cloudy days (defined as 8-10 tenths of sky cover, sunrise to sunset) increase in frequency at the expense of clear days (0-3 tenths) as one goes from the foothills facing the Gulf, where clear days predominate, northeastward to the Allegheny Mts. of West Virginia, where about half the days are cloudy, and only one quarter clear. Thus the trend of frequency of cloudy days parallels that of rainy days. The average cloudiness is surprisingly uniform over this region, Knoxville having had an average of 5.5 tenths of sky cover in 31 yrs., Nashville 5.6 in 31 yrs., Asheville 5.4 in 49 years and Chattanooga 5.5 in 52 years.

Seasonally, too, the frequency distribution of cloudiness is closely related to that of precipitation, as can be seen in Table 25. The highest average cloudiness, 6.3 tenths, occurs in winter and the lowest 4.8 in fall. The most common condition is cloudy in winter and spring, clear in fall and partly cloudy in summer. The winter clouds consist mostly of broad, stratified decks generated by large-scale lifting processes usually accompanied by pronounced thermal stability. The summer clouds are largely cumulus types in various stages of development, arising from local convection currents.

A comparison of 2114 simultaneous observations of cloudiness at Oak Ridge and Knoxville, summarized in Table 26a, shows nearly identical gross frequency distributions at the two stations during the 17 month period of these observations. When the observations are classified as clear (0-3 tenths sky cover), partly cloudy (4-7 tenths) and cloudy (8-10 tenths), the frequencies differ by less than 3%, a small deviation in view of the subjective method of observation. However, when the individual observations are compared, as in the third and fourth columns of Table 216a, it is seen that the observers at the two stations disagreed 22% of the time, and differed by 2 classes (opposite categories) 5% of the time. Seasonally (Table 27), the winter of 1949-50 had an abnormally high frequency of overcast skies with the remainder mostly clear, resulting in a minimum of disagreement between the two stations. The greatest percentages of individual discrepancies occurred in the summer, with the majority of partly cloudy periods at Oak Ridge listed as clear or cloudy at Knoxville, and many cloudy periods at Oak Ridge accompanied by clear at Knoxville. The greatest differences in total frequencies also occurred in the summer months, with Knoxville reporting more clear and partly cloudy and fewer cloudy periods than Oak Ridge. The most frequent reports of opposite categories at the two stations occurred in the spring. Diurnally the greatest differences appear at night and in the early morning, again with Oak Ridge showing more cloudiness than Knoxville. It is, of course, well known that cloudiness observations are less certain at night than in the daytime.

Table 26. Comparative frequency (%) of weather, sky and ground conditions, Oak Ridge vs. Knoxville June, 1949-Nov. 1950.

	Oak Ridge	Knoxville	Knoxville different from O.R.	Knoxville differed ≥ 2 classes
a. Cloudiness				
0-3 tenths ("clear")	34.4	34.4	6.4	2.3
4-7 tenths ("partly cloudy")	13.4	16.0	7.3	0.0
8-10 tenths ("cloudy")	52.2	49.6	8.5	2.7
Total (2114 obs.)	100.0	100.0	22.2	5.0
b. Ceiling height				
0-200 ft	2.6	1.2	2.2	1.6
300-900 ft	7.0	4.0	5.1	1.2
1000-4900 ft.	24.7	23.3	10.9	5.8
5000-9500 ft.	9.6	10.7	6.1	0.1
10000 ft or higher	56.2	60.8	6.6	3.8
Total (2114 obs.)	100.0	100.0	30.9	12.5
c. Height of lowest clouds				
0-200 ft.	2.3	1.8	1.7	1.2
300-900 ft.	8.1	6.3	5.3	1.0
1000-4900	40.4	40.9	12.2	2.9
5000-9500 ft.	11.3	15.8	6.8	0.4
10000-ft or higher	37.8	35.3	8.8	5.1
Total (2110 obs.)	100.0	100.0	34.8	10.6
d. Visibility				
0- $\frac{1}{4}$ mi	2.9	1.4	2.1	1.9
$\frac{5}{16}$ - $\frac{3}{4}$ mi	2.8	1.0	2.7	1.8
1-2 $\frac{1}{2}$ mi	5.0	3.5	3.8	1.7
3-6 mi	16.4	14.2	10.7	0.4
7 mi or greater	72.8	79.9	5.3	0.7
Total (2114 obs.)	100.0	100.0	24.6	6.5
e. Weather				
Thunderstorm	2.0	0.9	1.6	0.8*
Rain	15.8	14.3	8.5	3.3*
Snow or sleet	0.5	0.6	0.3	0.3*
Fog	19.0	14.0	11.3	5.1*
Smoke	11.4	7.1	1.0	0.7*
Haze	3.0	0.1	2.9	1.1*
None	58.7	62.9	7.1	7.1*
Total (2533 obs.)	100.0	100.0	32.7	18.4*
f. State of ground				
Dry	53.7	56.6	8.0	1.0
Moist	34.5	27.1	17.4	0.4
Wet (standing puddles)	10.0	14.3	3.3	0.4
Frozen	1.1	1.8	0.3	0.2
Ice, snow, sleet or slush	0.3	0.2	0.3	0.2
Total (1323 obs.)	100.0	100.0	29.3	2.2

*Any weather type occurring at Oak Ridge with none at Knoxville, or vice versa

Table 27. Seasonal and diurnal cloudiness comparison (% frequency), Oak Ridge vs. Knoxville

	Clear	Partly	Cloudy	Differ-	
		Cloudy		ing	Opposite
<u>Winter (12/49, 1/50, 2/50: 507 Obs.)</u>					
Oak Ridge	27.9	7.6	64.8	13.4	2.8
Knoxville	27.9	8.5	63.7		
<u>Spring (3,4,5/50: 274 Obs)</u>					
Oak Ridge	35.4	13.1	51.4	28.0	6.9
Knoxville	32.5	21.2	46.3		
<u>Summer (6,7,8/49 & 6,7,8/50: 622 Obs)</u>					
Oak Ridge	27.8	20.0	52.2	30.0	5.4
Knoxville	30.7	22.2	47.1		
<u>Fall (9,10,11/49 and 9,10/50: 711 obs)</u>					
Oak Ridge	44.7	11.9	43.4	19.7	5.5
Knoxville	43.0	14.1	42.9		
<u>Annual (Avg. of 4 seasons)</u>					
Oak Ridge	33.9	13.1	53.0	22.9	5.2
Knoxville	33.5	16.5	50.0		
<u>1 and 4 A.M. (480 obs.)</u>					
Oak Ridge	42.9	8.7	48.3	24.3	7.5
Knoxville	42.5	13.1	44.4		
<u>7 and 10 AM (549 obs.)</u>					
Oak Ridge	30.0	10.7	59.3	22.1	6.2
Knoxville	33.7	12.8	53.6		
<u>1 and 4 PM (550 obs.)</u>					
Oak Ridge	27.3	19.3	53.4	22.2	1.8
Knoxville	26.7	21.1	52.2		
<u>7 and 10 PM (535 obs.)</u>					
Oak Ridge	38.8	14.2	46.9	21.6	4.8
Knoxville	35.7	16.8	47.5		

15. Solar Radiation

Both astronomical and meteorological factors determine the rate at which solar energy is received at any given location on the earth's surface. The angular elevation and distance of the sun with respect to the earth constitute the astronomical factors; absorption, scattering and reflection by the gases, suspended particles and clouds in the atmosphere are the meteorological ones. The total amount of energy received in any specified period of hours or days depends primarily upon the amount of cloudiness and the thickness of the clouds. When the seasonal variations of solar elevation and length of the day are eliminated, a close relation is found to exist between the daily total solar radiation received on a unit horizontal area and the duration of sunshine. The latter quantity has been recorded for many years at Weather Bureau stations, and, although it is a less fundamental variable in most physical problems, it is useful as an aid in extrapolating from short-period direct measurements of solar radiation to longer-period normals.

Nearly four year of solar radiation records have been obtained at Oak Ridge. The observed annual variation of daily total direct and scattered solar radiation received by a unit horizontal area is summarized in Fig. 51a. The uppermost curve represents the theoretical extraterrestrial radiation (at the top of the atmosphere) obtained from Ref. 44 and shown for comparison. The average observed daily totals are shown by horizontal bars whose lengths span the standard monthly periods, each consisting of a whole multiple of 7 days, which are used by the Weather Bureau for summarizing solar radiation. The average monthly maximum is plotted at the average date of occurrence, and the

minimum of record for each standard month plotted against its date.

The unit is one cal/cm², or one langley.

It is worthy of mention that due to the phase shift between the earth's axial orientation (solstices) and its orbit (perihelion-aphelion), the extraterrestrial radiation is greater in the spring than at corresponding dates in the fall. The aphelion, coming a few days later than the summer solstice, does not materially affect the time of the maximum, the rate of change of earth-sun distance being near zero at that time. The greatest effect is observed in the vicinity of the equinoxes, when both the angular elevation of the sun and its distance from the earth are changing rapidly. The asymmetry of the observed average radiation, however, is much greater than can be explained on astronomical grounds and is, in fact, in the opposite sense. The minimum occurs not in December, but in January, which is the cloudiest month (see Table 25a), and the fall values are higher than those for corresponding periods in the spring, which again parallels the frequency of clear skies. The highest observed values, on the other hand, appear to have a nearly constant relation to the extraterrestrial radiation, as might be expected, since they probably represent almost perfectly cloudless days in each month. These highest values show the astronomical asymmetry. The lowest values, presumably obtained on the most cloudy days, appear to be disproportionately high in the summer, particularly in view of the greater water content of the summer clouds. Several possible explanations suggest themselves: the greater ice content of winter clouds, an inverse relation between reflection and solar altitude, a greater homogeneity and persistency of thick clouds in winter than in summer.

variables is striking, the slightly greater range of the average duration being at least in part due to the fact that daily values range from 0 to 100%, while the solar radiation values, as we have seen, cannot exceed 84%, and apparently also have a lower limit, which varies from one season to another. However, the duration and integrated intensity are not equivalent, even when the intensity is expressed as the percent of that observed with cloudless skies. Ref. 44 gives an empirical relation $I/I_{\max} = 0.61S + 0.35$, due to S. Fritz and T. H. MacDonald, and based on observations at 11 stations having 10 years or more of record. S is here the percent of possible sunshine duration, I is the observed average monthly solar radiation intensity, and I_{\max} is the average for perfectly cloudless days. Fig. 52 shows the Fritz-MacDonald regression line plotted on a scatter diagram of the individual monthly values of average solar radiation at Oak Ridge as a percent of the average monthly maximum (ratios to extraterrestrial were used in order to eliminate effects due to the seasonal rate of change) vs. the percent of possible sunshine at Knoxville for the same months.

Although a better fitting line could obviously be drawn, it is doubtful whether the improvement would be significant, especially in view of the small Oak Ridge sample and the large scatter of the data in comparison with those used in obtaining the Fritz-MacDonald formula. Since adjustment to normal solar radiation will, in fact, involve increases in every month of the year, the values will be shifted from the abnormally low portion of the range, where the greatest average deviations from the formula are observed, towards the higher portion, where the fit is best and where the Fritz-MacDonald data have the greatest advantage of completeness in

with the Oak Ridge data. Table 28 gives the observed data and the extrapolated normals.

Diurnal curves of observed average, observed maximum, and computed extraterrestrial radiation vs solar time for the solstitial months are shown in Fig. 53A. It should be pointed out that although the maximum extraterrestrial radiation on a horizontal surface occurs precisely at solar noon, the diurnal variation of sky conditions produces irregularities in the observed average curves. In particular, midday cumulus clouds in the summer months cause both a drop in the average and an increase in the maximum, due to reflection, over what would be obtained under uniform sky conditions. In the winter, when extensive high cloud decks are frequently present but midday cumulus development largely lacking, reflected radiation makes its most significant contribution in the vicinity of sunrise and sunset, so that values exceeding the extraterrestrial radiation can be observed when the latter are near zero.

The average observed accumulated energy received vs standard time is illustrated in Fig. 53B for June, September, and December. While at any particular standard hour more energy has been accumulated in June than other months, the greatest hourly rates within a few hours after sunrise occur near the equinoxes. For instance, of the three months illustrated, September shows the highest accumulated radiation in the first 6 hours after sunrise. This phenomenon has been pointed out by Markus (Ref. 45) in a similar analysis for the Hanford works.

232

TABLE 28. Daily Total Solar Radiation

Month	I _{avg} 2 cal/cm ² 1949-52	I _o * cal/cm ²	I _{avg} of I _o % of I _o 1949-52	I _{max} 2 cal/cm ² 1949-52	I _{max} % of I _o % of I _o 1949-52	I _{avg} of I _{max} % of I _{max} 1949-52	% poss. sunshine Knoxville 1949-52	% poss. sunshine Knoxville 54 yrs.	I _{normal} 2 cal/cm ²	
Jan. (1/1-1/28)	144.3	422	34.2	321.9	75	46	33	42	61	190
Feb. (1/29-2/25)	231.3	529	43.7	450.2	77	54	47	49	65	270
Mar. (2/26-4/1)	335.0	690	48.6	605.0	79	62	49	54	68	370
Apr. (4/2-4/29)	438.5	843	52.1	686.9	79	66	51	59	71	470
MAY (4/30-6/3)	544.0	945	57.6	742.8	76	75	63	65	74	530
June (6/4-7/1)	558.9	985	56.7	740.4	75	75	63	65	74	550
July (7/2-7/29)	552.3	965	57.2	754.0	77	74	62	64	74	550
Aug. (7/30-9/2)	461.8	885	52.2	667.2	75	71	53	59	71	470
Sept. (9/3-9/30)	428.4	750	57.1	615.7	77	75	58	64	74	430
Oct. (10/1-10/28)	336.8	604	55.8	496.3	75	75	59	64	74	340
Nov. (10/29-12/2)	214.3	462	46.4	379.5	76	61	47	54	68	240
Dec. (12/3-12/31)	165.4	384	43.1	707.7	76	56	38	42	61	180

*I_o - Average monthly extraterrestrial radiation.

233

TABLE 29 - Oak Ridge Cloud Height Frequency, (%) 6/49-11/50

a. Seasonal

	Ceiling Height				Height of Lowest Clouds			
	Winter	Spring	Summer	Fall	Winter	Spring	Summer	Fall
0 - 200 ft.	2.6	0.0	3.2	3.0	2.6	0.0	2.7	2.8
300 - 900 ft.	16.2	3.7	4.3	4.1	16.7	5.1	5.5	5.5
1,000 - 4,900 ft.	32.1	24.5	24.9	19.0	39.2	39.1	51.9	31.6
5,000 - 9,500 ft.	8.1	9.5	10.5	10.0	7.8	13.1	13.3	11.4
10,000 - ft. or higher	41.1	62.4	57.1	64.0	33.8	42.7	26.5	48.7

b. Diurnal

	1 & 4 am			7 & 10 am			1 & 4 pm			7 & 10 pm		
	1 & 4 am	7 & 10 am	1 & 4 pm	7 & 10 am	1 & 4 pm	7 & 10 pm	1 & 4 am	7 & 10 am	1 & 4 pm	7 & 10 pm	1 & 4 am	7 & 10 pm
0 - 200 ft.	4.1	5.0	0.5	4.0	4.7	0.7	4.0	4.7	0.7	0.7	4.0	0.7
300 - 900 ft.	5.5	11.2	6.8	6.5	13.7	7.1	6.5	13.7	7.1	5.2	6.5	5.2
1,000 - 4,900 ft.	24.4	27.4	28.3	30.8	40.1	56.4	30.8	40.1	56.4	33.1	30.8	33.1
5,000 - 9,500 ft.	8.7	9.0	8.6	11.7	9.7	9.7	11.7	9.7	9.7	13.3	11.7	13.3
10,000 - ft. or higher	57.2	47.7	55.8	47.1	31.8	26.1	47.1	31.8	26.1	47.6	47.1	47.6

A condensed picture of the diurnal and annual variations of the average hourly and cumulative solar radiation is given by Fig. 54, which shows isopleths of energy per unit horizontal area plotted against standard time and months of the year. The asymmetry of the true solar time (apparent local solar time) with respect to eastern standard time is apparent in the sunrise, sunset and solar noon curves. Also the spring and fall maxima of accumulated energy 3 and 6 hours after sunrise can readily be seen. The effects of the solar radiation variations on temperature, stability and turbulence will be described in the sections on these meteorological variables.

16. Ceiling and Cloud Height

Standard observations made at Weather Bureau stations include the heights of all visible cloud layers, as well as the ceiling height, defined as the lowest height at which half or more of the sky is obscured. Ceiling and cloud height, while of great practical importance to aviation are not in themselves very useful variables in meteorological problems, due to the complexity of their dependence upon other variables. Given some additional information regarding cloud types and thickness, however, they can be interpreted in terms of the height of elevated inversion bases and the depth of convection, and are therefore of interest in connection with some problems involving dispersion of stack wastes in the atmosphere.

Seasonal frequency distributions of ceiling height up to 2000 ft. above ground at Knoxville, obtained from Ref. 41, are presented in Table 25b.

Low ceilings in all four categories are most frequent by far in the winter, as is true of cloudiness in general. The season of least frequent low ceilings, on the other hand, is not fall, as with cloudiness, but summer, the majority of summer cumulus clouds being above 2000 ft. Spring, too, has less frequent low ceilings than fall, virtually all the difference being accounted for by those below 1000 ft., which are disproportionately infrequent in the spring. From winter to spring, the frequency of ceilings below 300 ft. decreases by a factor of 13.

In the 17 month period of comparison between Oak Ridge (X-10 Area) and Knoxville observations (Table 26b) Oak Ridge had nearly twice as many ceilings below 1000 ft. (9.6%) as Knoxville (5.2%), while discrepancies of a factor of about 5 in ceiling height between the two stations occurred over 12% of the time.

When the heights of the lowest clouds, regardless of amount, are considered (Table 26c), the frequencies of low heights increase slightly, (note: zero ceilings due to fog are not included in height of lowest clouds), and the Knoxville and Oak Ridge frequencies become more nearly equal. The most striking addition occurs in the 1000 to 10,000 ft. range, where, apparently, the majority of "scattered" (covering less than half the sky) clouds occur. This category ^{includes} nearly all the clouds primarily generated by surface heating and turbulent eddies. The 1000-4900 ft. interval alone accounts for 40% of all observations. As might be expected, segregating the observations by seasons and times of day greatly accentuates this feature of the frequency distributions. It is seen in Table 29 that in summer over half the observations show low clouds in the range 1000-4900 ft.,

Table 30. Oak Ridge Visibility frequency (%).a. Seasonal

	<u>Winter</u>	<u>Spring</u>	<u>Summer</u>	<u>Fall</u>
0 - 1/4 mi.	3.4	0.8	2.3	3.9
5/16-3/4 mi.	4.0	1.9	3.1	2.4
1-2 1/2 mi.	11.4	0.0	3.8	3.7
3-6 mi.	20.3	16.4	10.9	18.4
7 mi. or more	60.9	81.0	79.9	71.6

b. Diurnal

	<u>1 and 4 AM</u>	<u>7 and 10 AM</u>	<u>1 and 4 PM</u>	<u>7 and 10 PM</u>
0 - 1/4 mi	4.2	6.0	0.2	1.3
5/16-3/4 mi	4.8	3.8	1.8	1.3
1-2 1/2 mi	6.0	5.8	4.2	4.5
3-6 mi.	17.0	23.9	10.5	13.3
7 mi. or more	67.1	60.5	83.3	79.6

and of these only half were accompanied by ceilings. The other seasons have comparable frequencies of ceilings in this range, but few scattered clouds. It is again shown that more ceilings below 1000 ft. occur in winter than in all other seasons combined, that ceilings below 300 ft. are virtually non-existent in the spring, and that the frequency of any clouds below 10,000 ft. is least in fall. Ceilings in the range 1000-4900 ft. have a slight diurnal maximum (28%) in the afternoon, but when scattered clouds are included more than half the afternoon observations show clouds in this height interval.

The cloud height observations can now be briefly summarized. Clouds below 1000 ft. occur about 10% of the time over the year as a whole, being most common in winter (about 20%) and quite infrequent in spring (about 5%) reaching a diurnal maximum frequency in the morning (about 18%) and a minimum in the evening (about 6%). These include ground fogs and stratus decks below ridge height (300 ft.), which occur only during the night and early morning and hardly ever in the spring. Associated with low-level inversions, their tops are not expected to exceed 1000-1500 ft. so that contamination entering the atmosphere within this layer would be mixed through it but restrained from spreading further vertically. Cumulus and stratocumulus decks in the range 1000-5000 ft. occur at more than half the summer observations, and about one-third of the time in the other seasons, covering half or more of the sky about one-quarter of the time, somewhat more often in winter and less often in fall. Clouds in this height interval are almost twice as frequent during the afternoon as during the night,

but ceilings show considerably less diurnal variation. Absence of clouds below 10,000 ft., including clear skies, occurs about 40% of the time, and absence of ceilings below 10,000 ft. about 60%, the seasonal maximum frequency of this condition occurring in the fall and the diurnal maximum in the evening.

Interpreted in terms of the depth of vertical mixing, both clear nights and those with fog or low stratus would indicate a restriction to the lowest 1000 ft. or so more than half the time during the evening, night and early morning, while the presence of ceilings between 1000 and 10,000 ft. would indicate greater depths about one-third of the time. Daytime convection apparently extends above 1000 ft. at over 90% of the daytime observations and above 5000 ft. at least 10% of the time.

17. Obstructions to Vision

It would seem at first glance that observations of visibility would be an index of the degree of pollution of the atmosphere, and, consequently, of the diffusing properties of the lower atmosphere. Due to the variety of causes of restricted visibility, however, no such simple interpretation can be made. Restriction by fog is related to the temperature and moisture content of the air as much as to the turbulence or the concentration of impurities. Haze and smoke are often brought from distant sources and distributed through a great depth of the atmosphere, so that restriction of visibility due to these phenomena is also not a reliable indicator of local diffusion conditions. Nevertheless, local effects can be discerned by means of comparative studies between neighboring stations, and studies of diurnal patterns.

In 23,198 hourly observations at Knoxville, reported in Ref. 41, the visibility was 6 mi. or less (requiring the observer to report a specific obstruction) 34% of the time, and 2 mi. or less 11% of the time (Table 25d). A pronounced seasonal maximum frequency of low visibility occurs in winter (21% of the time ≤ 2 mi.) and a minimum in summer (5% ≤ 2 mi.).

In 17 months of simultaneous 3-hourly observations at Oak Ridge (X-10 area) and Knoxville, visibilities below 3 mi. were almost twice as frequent at Oak Ridge as at Knoxville, a variation in the same sense as that of low ceilings. Discrepancies between the two stations are somewhat less frequent than in the case of ceiling height, variations of two categories, or roughly a factor of 4 to 8, in the visibility occurring 6.5% of the time. The main differences between Oak Ridge and Knoxville with respect to the factors affecting visibility consist of a greater amount of smoke pollution at Knoxville on the one hand, and, on the other hand, lower wind speed, higher relative humidity and greater night-time stability of the lower atmosphere at the Oak Ridge observation point, probably resulting from the sheltering and drag effect of the ridges and nearby Cumberland Mountains with respect to the winter westerly winds. Evidently the meteorological augmentation at Oak Ridge predominates over the greater availability of pollution at Knoxville in producing low visibilities.

During the comparison period, the seasonal minimum frequency of low visibilities occurred in spring rather than in summer (Table 30a),

the latter being the season of minimum in the longer Knoxville record.

Diurnally (Table 30b), the frequency of visibilities less than 3 mi. reaches a maximum (16% of the Oak Ridge 3-hourly observations, June 1949-Nov. 1950) in the early morning and a minimum (6%) in the afternoon, showing the effects of stability, fog formation, and fuel consumption. Some obstruction to vision (visibility 6 mi. or less) existed 40% of the time at 7 and 10 A.M. and 33% at 1 and 4 A.M. but only 17% at 1 and 4 P.M.

The usefulness of a hypothetical landing strip in one of the Oak Ridge valleys as an alternate for Knoxville airport in bad weather can be estimated from the following data. Out of a total of 2.2% of the 3-hourly observations at which the visibility at Knoxville was less than 1 mi. that at Oak Ridge was 1 mi. or greater only 0.9%. Of the 5.7% at which the Oak Ridge visibility was less than 1 mi., that at Knoxville was 1 mi. or greater 4.4% of the time. Since the frequency of low visibilities is considerably greater than that of equally severe ceiling restriction, it appears that the chances of finding Oak Ridge open when Knoxville is closed are less than 50%, whereas the chances of finding Knoxville open when Oak Ridge is closed are better than 75%.

A very typical diurnal sequence of visibility changes is illustrated by Fig. 55. When the first photograph was taken, the Cumberland Mountain peaks were dimly visible above the Oak Ridge smoke (estimated to be about 300-500 ft. deep) and ground fog (50-100 ft. deep), looking west from Pine Ridge. First the fog broke up into curving wisps and dissolved, then the smoke layer gradually deepened and thinned out, revealing Blackoak Ridge (2 mi.), Walden Ridge (5 mi.) and the mountains (8-15mi.) in turn. On the southeast a pool of fog, thicker in Bethel Valley than in the higher Bear Creek Valley, was dissipated almost simultaneously.

18. State of the Ground

Table 31 gives the average monthly frequencies of dry, moist, wet, frozen and snow-covered ground based on three years of such observations at Oak Ridge. Dependent largely on precipitation, temperature and wind speed, the frequencies show a pronounced seasonal variation, with dry ground occurring about half the time over the year as a whole. In the cold, rainy months January-March, the ground is dry only one-fourth or less of the time, but the frequency rises sharply to over two-thirds in the spring, summer and early fall under the influence of rising temperature and strong winds. Moist or wet ground is the rule from mid-November through March, with frozen ground occurring 7 to 10% of the time during this same period and snow, sleet slush or ice about 3 to 5%. Wet ground (standing puddles) was observed 10% of the time annually, varying from 2% in June to 26% in January.

Table 31

State of Ground, Frequency, (%) Oak Ridge, 10/49-9/52

	<u>Dry</u>	<u>Moist</u>	<u>Wet</u>	<u>Frozen</u>	<u>Snow, Slush or Ice</u>
Jan.	5	58	26	7	4
Feb.	29	41	17	9	3
Mar.	23	44	19	10	3
Apr.	63	29	6	2	0
May	69	27	4	0	0
June	77	21	2	0	0
July	60	35	5	0	0
Aug.	61	34	4	0	0
Sept.	69	28	4	0	0
Oct.	64	29	6	0	0
Nov.	36	42	8	6	9
Dec.	37	38	14	9	2
	—	—	—	—	—
Annual	49	36	10	4	2

Surface Temperature and Humidity19. Regional Temperature Pattern

Over an averaging period of several years, the primary factor influencing the distribution of surface air temperature over the Southern Appalachian area is altitude and the second factor of importance, latitude. Fig. 56 shows the pattern of the 4-year mean annual temperature, (1948-1951) based on data from 65 Weather Bureau climatological stations (shown by small circles) and from the 5 special stations of the Smoky Mountain Snowfall study, operated jointly by the National Park Service, TVA and Weather Bureau from 1946 to 1951 at altitudes ranging from 1400 ft. to 6300 ft. Taking advantage of the close correspondence between mean temperature and altitude, the isotherms have been drawn to fit the observed temperatures and interpolated in accordance with the larger topographical features.

Over the 3° of latitude from Atlanta, Georgia to southern Kentucky, there is a drop in mean annual temperature from about 62° F. to about 57° F. The altitudinal temperature range is much greater, from 43° F. at Mt. Mitchell (6684 ft. MSL) and 47° at Clingmans Dome (6643 ft. MSL) to over 60° F. at several valley stations below 2000 ft. MSL at the same latitude. With respect to mean annual temperature, the mountain tops are comparable with low-altitude stations in Wisconsin or Maine at latitudes 43-45° N. R. E. Shanks (Reference 46) has found that the closest low-level bioclimatic analogue to the spruce-fir rain-forest of the higher Great Smoky Mountains is to be found in northeastern Maine and adjacent New Brunswick. Observations are lacking in the Cumberland Plateau area, but mean annual temperatures in the vicinity of 50° F. would be expected at the higher

levels (about 3500 ft. MSL), comparable to Massachusetts or northern Ohio.

Within the great valley of eastern Tennessee, at elevations of 800 to 1500 ft. MSL, the mean temperatures during this 4-year period varied across the valley from about 57-58° F. on the western side to over 60° F. on the eastern side, with very little variation along the valley axis from southwest to northeast. This uniformity of temperature over a $1\frac{1}{2}^{\circ}$ latitude range is not normal. It can be seen in Figure 57, a map of the departure of 1948-1951 mean temperature from normal based on 45 stations having 20 years of record or more (shown by circles), that the upper end of the valley was about two degrees warmer than the region below the Oak Ridge-Knoxville area, relative to the normal. The temperature anomaly pattern cannot be defined in detail on the basis of so few stations, but, broadly, it appears that the valley areas were abnormally warm by 1 to 3° F. during the observation period, while the mountainous areas were near or slightly below normal. The Oak Ridge area lies between the 0 and +1° F. isanomals of temperature, so that with observed averages of 58.2° F. at Townsite and 57.7° F. at X-10, the normal mean annual temperature would be expected to lie between 57 and 58° F. for elevations of 800-900 ft. over the area as a whole. This is about 1-2° F. colder than at Knoxville, where the 81 year mean temperature is 58.9° F.

We have seen from Figure 57 that the pattern of temperature departures from normal has been such as to increase the differential between mountain and valley. Figure 58 is a plot of the mean temperature and mean daily temperature range for January, 1950, at a selection of stations

covering a range of altitudes from 500 to 6680 ft. MSL, within a narrow latitude range. This shows that the mountain temperatures were, on the average, 3-5° F. below the free-air temperatures as represented by the average 10 p.m. raob temperatures from Nashville and Greensboro, which are located at the western and eastern ends of the sector and agree closely with each other. From a study of the 10 a.m. raobs and interpolated Oak Ridge data analyzed by means of time cross-sections (Reference 47) it appears that the diurnal variation of the free-air temperature is slight at 5000 ft. MSL and higher, and that the average 10 p.m. temperature is probably within a degree or two of the mean. Thus the average mountain temperatures during this abnormally warm and rainy month were considerably lower than the free-air temperatures, and their contribution to the prevailing positive temperature anomaly was relatively small. This relative coolness of the air in the mountainous regions may be due to an abnormal amount of forced lifting, associated with the large excess of precipitation in the stable (winter) months.

During July, 1950, the vertical temperature distribution in the free air was approximately moist-adiabatic, and it is seen from Figure 59 that the average mountain temperatures were almost identical with the free-air temperatures at corresponding levels. The tendency of the mountain temperatures to follow the free-air temperatures closely in the summer and to be somewhat lower in the winter has been verified by comparisons of several additional months. Taking the year as a whole, then, there is evidence that the mountain lapse rate has been abnormally large, and

slightly larger than the free-air lapse rate.

Shanks (Reference 46) has analyzed the temperature data obtained during the period 1946-1950 by the Smoky Mountain Snowfall Study and has found the average lapse rate to be 2.23° F./1000 ft. This is quite a small rate of decrease compared to average figures of about 3 to $3\frac{1}{3}^{\circ}$ F./1000 ft. given by Conrad (Reference 48) and Peattie (Reference 49) for other extratropical mountain ranges. From the considerations presented above, it can be concluded that the unusually small lapse rate observed during the period of observations is, if anything, greater than both the long-period normal and the accompanying free-air lapse rate. This anomaly may be directly associated with the pronounced stabilizing influence of the great Bermuda anticyclone (high-pressure area) already shown to be the dominating feature of the normal pressure distribution in this area.

Average daily temperature ranges are also shown in Figures 58 and 59, as well as the average mid-afternoon and early-morning free-air lapse rate curves for the lowest 1500 ft. obtained at Oak Ridge by captive balloon soundings. The surface temperature range decreases slowly with altitude, from $20-25^{\circ}$ F. in the valley to $10-15^{\circ}$ F. above 5000 ft. while both the captive balloon observations and the raobs indicate a much more rapid decrease in the free-air, dropping to less than 12° F. in summer and 6° F. in winter at 1500 ft. above ground, and practically vanishing above 5000 ft. Thus the air at shelter level on the mountains is some $2-7^{\circ}$ warmer than the free air during the day, and $7-10^{\circ}$ F. cooler during the night, the greatest positive departures occurring in the summer and the greatest negative departures in winter. These heated and cooled air

layers next to the mountain surfaces give rise to the pronounced daytime up-valley and night-time down-valley winds observed throughout the valley.

20. Seasonal Temperature and Humidity Variation

Monthly averages based on eight years of temperature records at X-10 are shown in Figure 60. The normal mean temperatures adjusted to the 30-year period 1921-50 by reference to the Knoxville data, are included for comparison. January has been, on the average, about 2° F. warmer than normal during the period of observations, while the departures in the other months have been, on the whole, much smaller. As a result, December has appeared to be the coldest month of the year, whereas normally it is January which is coldest. July is the warmest month. Similar data are presented in Table 32 for Townsite and K-25 as well as X-10.

The observed average annual range of monthly mean temperature has been about 34-36° F.: in a normal period it would be about 37-40° F., from a mean temperature of 37-39° F. in January to about 77° F. in July. The overall average annual range of temperature has been 90° F., from an average low of 7° F. to an average high of 97° F. The extreme range observed at a representative valley station has been 105° F. at the Townsite station: from 0° F. on November 25, 1950 to 105° F. on July 28, 1952. In the cold wave of November 25, 1950, -3° F. was recorded at the Pine Ridge station (019) and -2° F. at Melton Hill (007). The low of 5° F. at Knoxville during this cold wave set a new record for the month of November, but did not approach the record lows for December (-5° F., December 1880), January (-16° F., January 1884) or February (-10° F., February, 1905). Thus much lower temperatures would ordinarily be expected to

occur in this area, over a period of 50 yrs. or so, than any observed during the period of Oak Ridge observations. The 105°F high at Townsite was equalled on the same date at K-25, and exceeded the 82-yr. Knoxville record of 104°F set in July, 1930, while the maximum at Knoxville during this period was only 103°F. The extreme maxima observed in Oak Ridge during 1952 probably correspond to recurrence intervals of the order of many decades.

The seasonal variation in the frequency of occurrence of various temperature extremes is shown by Table 33. By comparison with the long record at Knoxville, it appears that the total number of days with minimum temperature 32°F or less (days with freezing or "frost days") has been slightly above normal: the excessively frosty Novembers, Decembers and Marches have more than offset the mild Januaries. While variations of 20% apparently exist between different plant stations on the area, some 17-20 days with freezing can normally be expected in each of the winter months, dropping to 2-5 in April, none from May through September and 1 or 2 in October. On only 3 or 4 days per year does the temperature remain below freezing all day (maximum temperature 32°F or less: "ice days"), and these are confined to the period from late November through early March. Daily minimum temperatures of 24°F or less, which are quite restrictive with respect to various construction activities such as earth work and concrete laying, occurred some 4 to 7 times per month between November and March during the observation period, with the exception of December, which had an average of 15 such days at K-25, 11 at Townsite and 10 at X-10, numbers which are probably abnormally high. On the average the temperature can be expected to fall this low on about 30 days per year. As to hot days the frequency of daily maximum temperatures

248

TABLE 32

OAK RIDGES AREA TEMPERATURES, (OF.)

	Jan.	Feb.	Mar.	Apr.	May	June	July	Aug.	Sept.	Oct.	Nov.	Dec.	Annual
X-10 (012): Period of Record June, July, 1944 and January, 1945 - December, 1952													
Average temp.	41.1	41.7	49.2	58.2	65.7	74.5	78.5	75.1	69.3	59.4	46.6	39.4	58.1
Departure*	+2.3	+1.0	+1.6	+0.5	-0.1	+0.4	0.0	-0.2	-1.0	+0.8	-0.4	-0.3	+0.5
Adjusted normal	38.8	40.7	47.6	57.7	65.8	74.1	76.5	75.3	70.3	58.6	47.0	39.7	57.6
Avg. daily max.	49.9	52.4	61.0	70.8	78.5	86.5	88.4	86.7	81.5	72.4	57.3	49.1	69.5
Avg. daily min.	32.2	31.0	37.3	45.5	52.8	62.5	64.7	63.5	57.1	46.3	35.8	29.7	46.5
Avg. daily range	17.7	21.4	23.7	25.3	25.7	24.0	23.7	23.2	24.2	26.1	21.5	19.4	23.0
Highest/yr.	77/52	77/48	87/46	89/47*	92/47	102/44	103/52	98/48	100/51	90/51	82/50	76/51	103/52
Lowest/yr.	1/48	3/51	15/49	25/49	35/47	41/46	50/52	44/46	33/49	21/52	4/50	5/51	1/48

Townsite (011): Period of Record July, 1947 - December, 1952

Average temp.	42.5	43.8	48.5	57.5	66.9	75.3	77.0	75.8	69.5	60.4	45.4	39.9	58.5
Departure*	+3.7	+3.0	+0.5	-0.6	+1.0	+1.1	0.0	+0.2	-1.5	+1.4	-1.8	0.0	+0.6
Adjusted normal	38.8	40.8	48.0	57.9	65.9	74.2	77.0	75.6	71.0	59.0	47.2	39.9	57.9
Average daily max	51.4	54.7	60.2	69.1	80.0	86.8	88.2	86.9	81.3	72.9	56.2	49.6	69.8
Average daily min	33.5	32.9	36.8	45.4	53.8	63.7	65.8	64.8	57.6	47.8	34.4	30.1	47.2
Avg. daily range	17.9	21.8	23.4	23.7	26.2	23.1	22.4	22.1	23.7	25.1	21.8	19.5	22.6
Highest/yr.	75/52	74/48*	83/48	87/48	92/52	100/52	105/52	99/48	99/51	90/51	82/48	74/51	105/52
Lowest/yr.	4/48	4/51	18/49*	24/50	39/51*	46/50	51/50*	53/48*	37/49	21/52	0/50	7/51	0/50

K-25 (013): Period of Record June, 1949 - December, 1952

Average temp.	43.1	42.3	46.2	54.3	65.9	75.6	77.5	75.4	67.7	59.9	42.5	38.3	57.4
Departure*	+6.3	+2.6	-0.7	-1.7	+1.3	+1.3	+0.7	-0.2	-2.3	+1.4	-3.5	-0.3	+0.5
Adjusted normal	36.8	39.7	46.9	56.0	64.6	74.3	76.8	75.6	70.0	58.5	46.0	38.6	56.9
Avg. daily max.	52.7	54.0	57.7	66.8	78.2	87.1	89.2	86.3	79.9	72.8	54.7	49.2	69.1
Avg. daily min.	33.5	30.5	34.5	41.8	53.5	64.1	65.7	64.4	55.5	47.1	30.3	27.4	45.7
Avg. daily range	19.2	23.5	23.2	25.0	24.7	23.0	23.5	21.9	24.4	25.7	24.4	21.8	23.4
Highest/yr.	76/52	76/51	78/52	85/51*	91/52	100/49*	105/52	97/51	98/51	90/51	82/50	75/51	105/52
Lowest/yr.	11/52	1/51	15/50	22/50	29/51	45/50	48/50	53/52	37/49	23/52	0/50	5/51	0/50

*Knoxville departure from 30-yr. average (1921-1950) for period of observations at Oak Ridge station.

TABLE 33

FREQUENCIES OF TEMPERATURE EXTREMES

	Jan.	Feb.	Mar.	Apr.	May	June	July	Aug.	Sept.	Oct.	Nov.	Dec.	Annual
X-10 (012): Period of Record January, 1945 - December, 1952													
Min \leq 32	14	16	13	3	0	0	0	0	0	2	13	20	81
Normal*	18	16	9	3	0	0	0	0	0	1	10	18	75
Max \leq 32	1	1	#	0	0	0	0	0	0	0	#	1	4
Min \leq 24	5	5	3	#	0	0	0	0	0	1	4	9	26
Max \geq 90	0	0	0	0	1	11	13	11	4	#	0	0	40
Townsite (011): Period of Record July, 1947 - December, 1952													
Min \leq 32	15	13	12	3	0	0	0	0	0	2	15	20	80
Normal*	19	15	9	2	0	0	0	0	0	2	10	18	75
Max \leq 32	1	#	#	0	0	0	0	0	0	0	#	1	3
Min \leq 24	4	5	4	#	0	0	0	0	0	1	4	10	29
Max \geq 90	0	0	0	0	1	11	13	11	5	#	0	0	42
K-25 (013): Period of Record June, 1949 - December, 1952													
Min \leq 32	15	17	14	6	0	0	0	0	0	2	19	22	95
Normal*	21	20	11	3	0	0	0	0	0	1	10	20	86
Max \leq 32	1	1	#	0	0	0	0	0	0	0	1	1	3
Min \leq 24	6	7	4	1	0	0	0	0	0	#	7	13	38
Max \geq 90	0	0	0	0	1	12	16	11	2	#	0	0	43

*Adjusted to 30-yr. period 1921-1950 using Knoxville as reference station.
 #Less than $\frac{1}{2}$ day.

of 90°F or above is about 40 per year, nearly all of which are about equally divided among June, July and August.

Frequencies of other extremes of daily mean, maximum or minimum temperature, on either an annual or a seasonal basis, can be interpolated from the cumulative probability graphs ("ogives") in Figures 61-63. It is seen that the distribution is approximately normal in winter (December, January and February) and summer (June, July and August), but tends to be bimodal in fall (September, October, and November) and spring (March, April and May) as well as in the annual curves, these latter being apparently mixtures of the cold and warm seasonal types. The winter distribution is much broader than the summer one, with standard deviations of about 9 to 10°F in the daily mean, maximum and minimum in winter as compared with only 3 to 5°F in summer. The fall, spring and annual distributions are, of course, much broader, with standard deviations of the order of $\pm 15^\circ\text{F}$. A. Court (Ref. 50) has found that the frequency distributions of hourly temperatures too, are essentially normal in this region in January and July, with standard deviations about $12\frac{1}{2}^\circ\text{F}$ in January and 8°F in July.

"Heating degree days" (usually simply called "degree days") provide a useful integration of the severity of the winter season for estimation of heating loads and fuel consumption. Each day's contribution is obtained by subtracting the daily mean temperature from the base temperature of 65°F. Only days with mean temperature less than 65°F are counted. Thus, for example, a day with a mean temperature of 53°F has 12 degree days. The observed and normalized monthly total degree days and normal cumulative total for the heating season (the heating season runs from July 1 to June 30) are given in Table 34 for X-10 and Townsite. Graphs of the adjusted normals are shown in Figure 64 together with the corre-

sponding Knoxville values. As one might expect from the fact that the mean temperature is lower at the Oak Ridge stations than at Knoxville, the total number of degree days is larger. Significant contributions are only accrued during the period October-May, the annual total being approximately 3900 degree days. The abnormality of the winter weather during the period of this survey program is emphasized by the fact that the 4 seasons 1948-49 through 1951-52 had an average deficiency of about 200 degree days with respect to normal.

The relative humidity does not show a pronounced seasonal variation. Table 35 shows averages for 1 and 7 a.m. and p.m. at X-10, Townsite and K-25 over a 2-year period. Generally rising to over 90% during the night hours, it falls to a midday value in the range 40-70% on the average, depending greatly on local air drainage conditions. The wet bulb temperature therefore has a seasonal variation paralleling closely the mean temperature variation: in fact, the monthly average 1 p.m. wet bulb temperature at K-25 is nearly numerically equally to the mean temperature, while the nighttime values are nearly equal to the average daily minimum temperature. Table 36 contains a joint frequency distribution of dry-bulb and wet-bulb temperature, obtained from 3-hourly sling psychrometer observations at the X-10 Field Station (001) from June, 1949 through October, 1950, and adjusted to the full 2-yr. temperature distribution for station 001, January 1949-December, 1950. This can be used to obtain approximate durations of various critical conditions for air conditioning or evaporative cooling-tower design.

21. Diurnal Temperature and Humidity Variation

The diurnal cycle of temperature at the earth's surface is largely determined by the balance between incoming solar energy and outgoing terrestrial

252

TABLE 34

HEATING DEGREE DAYS

Stations	Jan.	Feb.	Mar.	Apr.	May	June	July	Aug.	Sept.	Oct.	Nov.	Dec.	Annual
<u>X-10 (012) Jan. 1945 - Nov. 1952</u>													
Average monthly	657	647	502	232	70	5	0	2	31	198	550	793	3687
Normal*	787	666	535	240	72	3	0	1	30	213	536	768	3851
Seasonal Cum.	2335	3001	3536	3776	3848	3851	0	1	31	244	780	1548	3851
<u>Townsite (011) July 1947 - November 1952</u>													ORO-99
Average monthly	698	598	521	264	46	2	0	0	36	177	595	782	3719
Normal*	823	681	539	249	90	4	0	0	37	204	550	770	3947
Seasonal Cum.	2384	3065	3604	3853	3943	3947	0	0	37	241	791	1561	3947

*Adjusted to 30-yr. period 1921-1950, using Knoxville as reference station.

Table 35

AVERAGE RELATIVE HUMIDITY (%), AND WET BULB TEMPERATURE (°F)

	Jan. 1949 - Dec. 1950	Jan.	Feb.	Mar.	Apr.	May	Jun.	July	Aug.	Sept.	Oct.	Nov.	Dec.	Annual
<u>X-10 (012) Jan. 1949 - Dec. 1950</u>														
1 AM RH	90	94	90	86	91	96	95	98	96	94	92	94	93	93
7 AM RH	88	95	91	89	92	94	93	97	97	96	95	95	94	94
1 PM RH	78	78	77	64	62	70	69	72	71	68	68	79	71	71
7 PM RH	88	88	80	69	73	81	82	88	90	85	85	90	83	83
<u>Average Monthly Maximum Wet Bulb Temperature, Jan. 1949 - Nov. 1952</u>														
	66	64	67	71	76	79	82	81	80	75	66	63	83	83
<u>Townsite (011) Jan. 1949 - May 1951</u>														
1 AM RH	85	79	81	76	88	91	92	94	92	92	81	80	86	86
7 AM RH	87	84	84	83	87	88	90	91	88	90	84	85	87	87
1 PM RH	71	55	57	48	48	56	60	58	54	52	47	56	55	55
7 PM RH	78	59	59	53	57	64	71	77	76	77	63	66	67	67
<u>K-25 (013) March 1949 - Feb. 1951</u>														
1 AM RH	89	84	78	82	90	94	92	94	90	93	86	86	88	88
7 AM RH	86	86	80	81	84	86	89	93	91	92	89	89	87	87
1 PM RH	67	53	42	37	52	58	60	61	58	55	47	54	54	54
7 PM RH	80	67	48	47	65	65	71	80	80	84	76	75	70	70
1 AM WB	29	30	35	44	52	61	65	64	58	47	36	30	46	46
7 AM WB	29	31	36	44	52	61	64	64	58	47	37	30	46	46
1 PM WB	42	45	50	58	66	72	75	74	69	59	50	44	59	59
7 PM WB	35	37	43	49	58	66	69	68	63	53	43	36	52	52

TABLE 36. ANNUAL FREQUENCY DISTRIBUTION OF HOURLY WET AND DRY BULB TEMPERATURE (PER CENT)

(1949-1950)
STATION 001 (X-10 AREA)

DRY BULB TEMPERATURE °F

WET BULB °F	DRY BULB TEMPERATURE °F																	TOTAL % WET BULB			
	0-4	5-9	10-14	15-19	20-24	25-29	30-34	35-39	40-44	45-49	50-54	55-59	60-64	65-69	70-74	75-79	80-84		85-89	90-94	95-99
79																.04	.04	.11	.05	.02	.03
78																.15	.15	.17	.11		.26
77																.17	.45	.55	.11		.43
76																.56	.45	.29	.09		1.28
75																					1.39
74															.31	.99	.79	.29	.09		2.47
73															.44	.73	.38	.11	.02		1.68
72															.88	.86	.41	.11			2.26
71															1.08	.34	.15	.11			1.68
70															2.75	.65	.45	.09			3.94
69														1.16	.95	.39	.15	.11			2.76
68														1.51	.58	.26	.38				2.73
67														.82	.31	.34	.19				1.66
66														1.72	.24	.30	.23	.03			2.52
65														1.38	.41	.43	.07				2.29
64													.43	1.85	.27	.26	.07				2.81
63													1.16	.77	.27	.26	.04				2.46
62													1.64	.77	.17	.09	.04				2.67
61													1.35	.26	.27	.13					2.01
60													2.37	.13	.31	.04					2.85
59												.52	.68	.30	.14	.04					1.68
58												1.24	.97	.26	.10	.13					2.70
57												1.61	.53	.30	.10						2.54
56												1.61	.24	.13	.14						2.12
55												1.52	.10	.13	.07	.04					1.86
54										.99	.57	.19	.13	.03							1.91
53										.94	.28	.24	.13								1.59
52										1.40	.24	.14	.13	.03							1.94
51										.83	.24	.19	.09								1.35
50										2.03	.33	.05	.13								2.54
49									.35	.21	.19	.10									.85
48									1.22	.62	.05										1.89
47									1.12	.26	.24	.05									1.67
46									1.53	.36	.28	.05									2.22
45									1.33	.15	.14	.05									1.67
44									.42	.81	.26	.09									1.58
43									.85	.15	.15	.19									1.34
42									1.06	.30	.31	.09									1.76
41									.48	.35	.21										1.04
40									1.06	.46	.21										1.73
39								.33	.42	.05											.80
38								.56	.64	.30	.05										1.55
37								.56	.69	.35											1.60
36								1.00	.53	.05											1.58
35								.78	.85												1.63
34							.39	.73	.37												1.49
33							.63	.91	.16												1.70
32							.90	.67	.16												1.73
31							.71	.45	.05												1.21
30							1.22	.22													1.44
29					.33	.39	.06														.78
28					.46	.52	.06														1.04
27					.99	.39															1.38
26					.52	.26															.78
25					1.12																1.12
24					.29	.52															.81
23					.52	.20															.72
22					.70	.07															.77
21					.29																.29
20					.17																.17
19				.25	.06																.31
18				.17																	.17
17				.17																	.17
16																					.00
15				.08																	.08
Less than 15																					.51
TOTAL % DRY BULB	.01	.06	.22	.67	2.03	4.21	5.41	6.33	7.74	8.37	8.98	9.43	10.53	12.10	9.85	7.05	4.51	2.00	.47	.02	99.9

radiation, with secondary effects due to variations in atmospheric back-radiation, convective mixing, and advection. The surface temperature oscillation, in turn, is propagated upward through the atmosphere with changing phase and diminishing amplitude, resulting in characteristic diurnal cycles of stability and, in turn, turbulence. This results in a diurnal variation in the rate of vertical exchange of heat, moisture and momentum, modifying the surface air temperature variation slightly, and producing a very marked and important diurnal variation of wind speed throughout the lowest few thousands of feet of the atmosphere. Being horizontally non-uniform in non-homogeneous terrain, the heating-cooling cycle sets up diurnally-varying horizontal gradients of temperature and pressure, giving rise to the characteristic local night and day breezes. It can be said without exaggeration that the major part of the observed variation of wind speed, turbulence, and lapse rate, and an important part of the variation of wind direction can be accounted for in terms of the diurnal temperature cycle.

The altitudinal decrease in daily temperature range (maximum minus minimum) from 20-25° F. in the valleys to 10-15° F. in the upper levels of the Great Smoky Mountains has already been seen in Figures 58 and 59. From Table 32 it can be seen that the average at representative valley stations in the Oak Ridge area is about 22° F. Figure 65 shows the frequency distribution of the daily range at station 012 (X-10 Health Physics) during the period January 1949- October, 1950. The median value and the mean for this period are both about 21.8°, and the distribution is approximately normal down to 5°, with a standard deviation of 4.8°. The average ranges

over a 5-year period, July, 1947-June, 1952, have been evaluated for X-10, Townsite, Knoxville Airport and the Knoxville city station (University of Tennessee) for comparison and estimation of the departure from normal. They were 22.4°, 22.4°, 20.9° and 20.3° respectively, as compared with an average of 19.7° for the 81-year period 1871-1951. Since the official Knoxville observations were taken in the city during most of the 81-year period (until 1942), it is not surprising that the city 5-year average is closest to the long period mean, showing a departure of only +0.60°. However, even this small positive departure must be looked on with suspicion, in view of the pronounced negative departure of both percent of possible sunshine and number of clear days during this period, as well as the fact that during about 55 years of the Knoxville temperature record, the instruments were located on the roofs of various buildings at elevations ranging from 66 to 102 ft. above ground. The average daily range increases in going from the city to the airport, but the airport range is still 1.5° smaller than those observed in the Oak Ridge area. This may not be a real climatological difference, since the airport instruments are still located on the roof of a building about 30 ft. above the ground. It is therefore quite possible that the normal daily temperature range at the Oak Ridge plant stations is actually somewhat larger than the values obtained during the observation period. If the full 8 years of record at X-10 are used, for instance, the average range is 23.0° (Table 32).

There is a pronounced seasonal variation in the daily temperature range. The pattern is similar to those of the number of clear days and the percentage of possible sunshine, namely, maxima in the spring and fall, a deep

winter minimum and a weak summer minimum. Figure 66 shows the monthly averages for the 5-year period July, 1947-June, 1952 at X-10, Townsite and Knoxville Airport, together with the Knoxville average number of clear days, average percentage of possible sunshine, and long-period averages of these elements. The monthly averages for the 8-year period of record at X-10 range from 17.7° in January to 26.1° in October. The lowest average for an individual month was 13.8° in December, 1945 and the highest 29.8° in October, 1952. Daily ranges less than 5° occur only in the winter half of the year, and then only once or twice per season. Ranges exceeding 40° usually occur several times each spring and fall. Forty-six degrees is the largest value observed during 1949-1952, having occurred twice: on April 8, 1950 (stations 002 and 003) and October 19, 1952 (University of Tennessee-AEC Research Farm), while 45° has been recorded four times at one or more stations on the Reservation: April 8, 1950 (stations 004 and 009), April 27, 1950 (station 002), October 25, 1952 (station 011) and October 28, 1952 (UT Farm).

Diurnal curves of seasonal averages of the hourly temperature, wet bulb temperature, dew point and relative humidity at station 001 (X-10 Field Station) for the two winters, 1949-1950 and 1950-1951, and for the other seasons of 1950 (which differed very slightly from the corresponding seasons of 1949), are shown in Figure 67. The lowest hourly average temperature occurs at about sunrise in each season, while the hour of highest average is nearly always 3 p.m. EST. The temperature is thus rising for only 7-9 hours and falling for the remaining 15-17 hours per day. The rise is very rapid averaging 3 to 5°F per hour in the morning hours following sunrise. The rate of temperature fall is of the same magnitude for only a short period

about sunset; during most of the night the average rate of decrease is about $\frac{1}{2}^{\circ}$ per hour.

The dew point depends only on the water vapor pressure and is unaffected by temperature changes unless condensation occurs; therefore the diurnal variations of the dew point reflect only processes which add or remove moisture. Typically the temperature approaches the dew point in the evening, either at the instrument level or closer to the ground raising the relative humidity to near 100%. With a further decrease of temperature, condensation occurs in the form of fog or, more commonly, dew, the relative humidity remains near 100%, and the dew point decreases during the night. Ramda (Ref. 51) has pointed out an additional process removing moisture, namely, hygroscopic absorption by the soil. With the morning temperature rise the air becomes unsaturated, the relative humidity falls, and evaporation of dew, fog, and soil moisture raise the dew point to its daytime value, which is limited by convective exchange with drier air aloft. This is reflected in a slight decrease in the dew point following the morning rise. When convective moisture loss to the upper air decreases with the stabilization of the temperature stratification in late afternoon, the relative humidity rises rapidly and the dew point ordinarily reaches its maximum value of the day just before the condensation point is reached. Even through the averages for a particular season may show nocturnal relative humidities below 90%, the character of the diurnal curve of dew point will usually reflect the frequent occurrence of this cycle including a drop after sunset due, presumably to condensation. If, however, the air masses laying over the station are so dry that depletion by vertical mixing overshadows depletion by nocturnal condensation, as in the

winter of 1950-51 (Figure 67), the minimum dew point occurs during the day. Conversely, in very sheltered locations, or during periods of high air-mass humidity or minimum convection, the midday dew point minimum may be absent. The latter type of diurnal variation is also characteristic of the west few inches of air (Ref. 52).

The dew point has a small diurnal range and is one of the most sensitive indicators of the air mass origin, its variation from one season to another emphasizing very strikingly the changes in atmospheric circulation which occur. The wet bulb temperature varies with both temperature and moisture content of the air, and lies between the temperature and the dew point. Its diurnal minimum is ordinarily close to the minimum temperature and occurs at the same time, while its maximum occurs near or shortly after the time of maximum temperature, and varies considerably according to the character of the air mass.

The diurnal range of temperature and, consequently, of the other meteorological elements, is greatest on clear, dry days and least on cloudy days. This variation will be brought out more fully in the discussion of vertical variations.

22. Local Temperature and Humidity Variations

Altitude and exposure both affect the average and extreme temperatures recorded at the various micronet stations. Figure 68 shows the effect of absolute station elevation on the average daily maximum, minimum, and mean temperature and average daily range, using data from the fall (Sept.-Oct.-Nov.) of 1949 for illustrative purposes. There are definite altitudinal trends in each of these scatter diagrams, of which the dashed lines represent subjective estimates. In the 600 ft. altitude range covered by the stations, the average daily maximum temperature decreases a little over 3°F and the daily minimum increases roughly 6°F, with the

result that the daily mean increases about 2°F and the range decreases about 10°F , from about 26°F to about 16°F . It has already been observed that 26°F is a normal autumn diurnal range at Oak Ridge valley stations; however, the rapid decrease with height seems out of proportion with what has been noted over the larger altitude range of the Great Smoky Mountains where comparable decreases occur only over height intervals of several thousands of feet (Figs. 58 and 59). A possible explanation is that the Chestnut Ridge and Melton Hill temperatures follow the free-air temperatures more closely than do those on the much larger mountains due to the smaller elevated surface areas of the former. This result can be changed considerably by varying the thermometer exposure, however; observations for a short period on Pine Ridge, at an elevation of nearly 1200 ft. MSL, show temperature ranges several degrees larger than would be estimated from the data of Figure 68, but still small by Smoky Mountain standards. The rapid decrease of the range with height is also borne out by automobile temperature surveys, which will be discussed later.

The scatter of the mean values at a given elevation, introduced by exposure, is greatest for the daily minimum temperature. The Bethel Valley stations, 002, 003, and 004 have lower minima than do the stations in the more openly exposed Clinch River Valley stations 009 and 013. Even stations 001 and 012, located on slight rises above the valley bottom, are apparently somewhat less subject to the drainage-stagnation effects which produce the lowest nocturnal temperatures. It is of interest that station 002, in the entrance to Whiteoak Gap in Haw Ridge, had consistently lower minimum temperatures than station 016, lower down along Whiteoak Lake (not illustrated in Figure 68 since it was not yet installed in the fall of 1949), which,

taken together with evidence from the wind observations to be presented later, negates the presumption of downslope drainage flow of air from Bethel Valley to Melton Valley. The daily temperature ranges also show considerable variation at any given altitude. About the only clear pattern that emerges is that those stations which are surrounded by trees (010) or large buildings (008, 011 and 013) have reduced diurnal temperature ranges, equivalent to a rise of 100 ft. or so in elevation.

Diurnal temperature and dew point curves for all the micronet stations for the fall quarter of 1949, compared with those at station 001, are shown in Figure 69. Along with the decrease in amplitude of the temperature cycle already noted, the dew point becomes increasingly steady with increasing elevation. Nocturnal saturation becomes less frequent and of shorter duration. The daytime dew point also shows a general decrease with height, from 52-55° at most of the valley stations to about 50° at the higher stations, but this is almost completely masked by large horizontal variations not all of which are readily explainable. The low values (42-46°) at Townsite and K-25 (stations 011 and 013) seem to indicate the presence of a drier air stream (possibly the result of a downslope current) near the Cumberland Plateau than towards the center of the large valley, but the low daytime dew point (48°) on the well forested slope of Haw Ridge (010) appears anomalous. The wet bulb temperature runs somewhat below midway between the temperature and dew point, and consequently decreases with altitude in the daytime. The night time dew point and wet-bulb temperatures show the same general increase with elevation and variation with station exposure that have been noted in connection with the

daily minimum temperatures.

The differences in 3-month average values of temperature, dew point, etc. from one station to another may be regarded as systematic differences. The non-systematic differences between Oak Ridge and Knoxville have been studied by means of simultaneous 3-hourly observations of current temperature and 6-hourly observations of maximum and minimum temperature during the period June, 1949 to October, 1950, at X-10 and Knoxville airport, which were punched on IBM cards and compared at the Weather Records Processing Center, Chattanooga. Figure 70 shows the cumulative frequency curves of various temperature differences. In Figure 70a, the distribution of differences of 3-hourly temperature, wet-bulb temperature and dew point are shown, in Figure 70b similar curves for 6-hour minimum temperatures at 7 a.m. and 6-hour maximum at 7 p.m., which are usually representative of the day as a whole, and in Figure 70c, the 7 p.m. 6-hour minimum and 7 a.m. 6-hour maximum temperatures, which ordinarily occur at a time of rapid change at the beginning or end of the interval and are thus relatively sensitive to slight differences of rate or phase between the stations. The median differences and standard deviations of the differences obtained from these frequency curves are summarized in Table 37.

The medians, representing systematic variations, show the atmosphere at Oak Ridge (station 001, X-10) to be generally cooler and more humid than at Knoxville airport. The least systematic difference between the two appears in the wet-bulb temperature and in the daily maximum temperature (as approximated by the 7 p.m. maximum) and the greatest difference in the 7 p.m. minimum, from which it must be concluded that the Oak Ridge temperature

TABLE 37

TEMPERATURE AND MOISTURE DIFFERENCE, OAK RIDGE MINUS KNOXVILLE, °F.

	<u>Median</u>	<u>Standard Deviation</u>
3-hourly current temperature	-2.5	±3.8
3-hourly wet-bulb temperature	-0.7	±3.0
3-hourly dew point	+1.1	±3.3
7 a.m. 6-hr. minimum temperature	-3.8	±3.7
7 a.m. 6-hr. maximum temperature	-2.7	±4.4
7 a.m. 6-hr. minimum temperature	-4.7	±3.9
7 p.m. 6-hr. maximum temperature	-0.8	±2.5

drops much more rapidly in the late afternoon than does that at the airport. The microclimatic variation of the evening temperature fall has been studied by Landsberg (Reference 53) and, following his suggestion was found to be quite pronounced among the Oak Ridge stations. It will be noticed in looking back at Figure 69, for example, that whereas the maximum hourly average temperatures at all the valley stations (001, 002, 003, 004, 008, 009, 011, 012 and 013) during the fall of 1949 varied only from 65 to 67° F., the average temperatures at 7 p.m. varied from 53 at Whiteoak Creek (002) to 59 at Y-12 (008), with all the "rural" exposures (001, 002, 003, 004, 009) in the range 53-55° F. and all the "urban" exposures (008, 011, 012, 013) in the range 57-59° F. In the summer of 1949 the corresponding temperatures (7 p.m.) were 73-76° F. for the "rural" exposures and 77-80° F. for the "urban" exposures, an important difference from the standpoint of evening comfort, although the daily maximum temperatures at these same stations cover a range of only 3° (83-86° F.).

The standard deviations given in Table 37 represent the non-systematic component of the differences and are about two-thirds the probable error

involved in using Knoxville observations, with a mean correction applied, to represent conditions at Oak Ridge. Again the daily maximum temperature is the most nearly homogeneous, the scatter being only 2.5° ; the current wet-bulb temperature can be estimated within about 3° , while any current temperature or 6-hour minimum would probably be off by 4° or more if estimated from Knoxville data.

While differences of comparable magnitude exist between pairs of stations within the Oak Ridge area, no tabulation has been made of them as such. However, a more sensitive and useful comparison has been made, namely, of the monthly frequencies of daily minimum temperatures 32° F. or below in winter (November through March), and of daily maximum temperatures 85° F. and above in summer (June, July and August). These are given in Table 38. The algebraic mean (systematic) differences between the pairs of stations are plotted against altitude difference, and the mean absolute non-systematic differences are plotted against both altitude difference and distance between stations in Figure 71. Station 001 (X-10 Field Station) has been paired, as the subtrahend, with all the micronet stations, and in addition the K-25 (013) and Townsite (011) stations have been compared with station 012 (X-10 Health Physics), and all four of these key stations with Knoxville airport. It is seen that both the systematic and non-systematic variations in the frequencies of both "hot" and "cold" days are better correlated with station elevation than with distance between stations. Furthermore, while the mean differences are surprisingly large (12 days with freezing in a typical winter month on Melton Hill, station 007, as compared with 18 in

265

TABLE 38

DIFFERENCE IN EXTREME TEMPERATURE FREQUENCIES BETWEEN PAIRS OF STATIONS

Station A	Station B	No. Mos. Compared	Dist. Mi.	Height Diff. ft.	Avg. Number Days/Month		Avg. Diff. Days/Month		Non-syst. Diff.		Avg. Days/Month		Non-Syst. Diff.	
					Max. ≥ 85	Min. ≤ 85	Max. ≥ 85	Min. ≤ 85	Max. ≥ 85	Min. ≤ 85	Max. ≥ 85	Min. ≤ 85	Max. ≥ 85	Min. ≤ 85
001	Knoxville	6	19.8	-139	16.5	20.0	-3.5	1.8	17.6	12.6	+5.0	2.2	2.2	
011	Knoxville	12	20.7	-44	19.2	22.3	-3.1	2.4	14.9	12.4	+2.5	1.7	1.7	
002	Knoxville	12	19.7	-59	19.6	22.3	-2.7	2.7	15.3	13.1	+2.2	2.2	2.2	
013	Knoxville	12	24.4	-199	20.9	22.3	-1.4	2.1	17.8	13.2	+4.6	2.2	2.2	
002	001	6	0.4	-40	19.0	16.5	+2.5	3.2	17.8	16.3	+1.5	1.4	1.4	
003	001	6	0.7	+30	15.0	16.5	-1.5	1.7	18.4	15.9	+2.5	1.0	1.0	
004	001	6	1.2	+10	15.7	16.5	-0.8	2.2	16.5	15.9	+0.6	1.0	1.0	
005	001	5	0.9	+185	16.8	18.2	-1.4	2.1	13.6	15.9	-2.3	1.6	1.6	
006	001	6	0.8	+310	12.0	16.5	-4.5	3.7	14.4	16.3	-1.9	2.1	2.1	
007	001	6	1.3	+546	6.3	16.5	-10.2	2.9	12.4	17.6	-5.2	3.6	3.6	
008	001	6	5.7	+210	13.2	16.5	-3.3	2.1	14.0	17.6	-3.6	2.0	2.0	
009	001	3	1.6	-50	19.7	22.0	-2.3	1.8	17.6	16.1	+1.5	1.4	1.4	
010	001	3	0.4	+90	16.7	22.0	-5.3	0.4	15.0	17.2	-2.2	1.8	1.8	
011	001	6	8.1	+95	16.5	16.5	-2.0	2.0	15.3	17.6	-2.3	1.1	1.1	
012	001	6	0.3	+80	15.2	16.5	-1.3	3.6	16.6	18.4	-1.8	1.8	1.8	
013	001	6	4.6	-60	17.5	16.5	+1.0	2.3	18.6	18.9	-0.3	1.0	1.0	
013	012	12	4.6	-140	20.0	19.6	+1.3	2.8	17.9	15.6	+2.3	1.1	1.1	
011	012	12	7.8	+15	19.2	19.6	-0.4	2.5	15.5	15.7	-0.2	1.7	1.7	

$$*(A-B) = \frac{\sum (A_i - B_i)}{N}$$

$$**|A' - B'| = \frac{\sum |A_i - B_i - (A-B)|}{N}$$

the valley; only 6 days per summer month with temperature reaching 85° F. as compared with over 16 in the valley) the non-systematic variations between hill and valley stations are also of practical importance. Records at valley stations would be in error, on the average, by 2 to 3 days per month if they were used, with an average correction applied, to estimate the number of days with freezing on the upper parts of the ridges, and by 3 to 4 days for the number of days with temperature reaching 85° F., a point of interest in air conditioning work.

From the difference in the slopes of the daily maximum and daily minimum temperatures against height, Figure 68, it can be concluded that the altitudinal change of surface temperature will have a pronounced diurnal variation. This is well illustrated by Figure 72, which contains seasonal graphs of the hourly average temperature difference between Melton Hill (007) and X-10 (001) for each quarter year of record. The temperature increases with height at night and decreases with height in the daytime. The amplitude of this cycle is somewhat smaller than that of the free-air temperature over a comparable altitude interval above the valley (shown by small circles), but the patterns are so similar in character that the discussion of vertical free-air temperature gradients which follows can be applied qualitatively to the altitudinal pattern of surface temperature in small hills. As we have seen, however, the daily temperature range is not damped out so rapidly with height along the slopes of the more massive mountains, so that the diurnal variation of altitudinal surface temperature gradient in the mountains departs grossly from that of the free-air gradient.

A seasonal variation in the altitudinal temperature differential is visible in Figure 72. This is further brought out, although somewhat irregularly due to the shortness of the record, in Figure 73, which shows the monthly sequence of differences in average daily maximum and minimum temperatures between stations 007 and 001. The difference in the maxima, reflecting the daytime temperature lapse, is greatest in the summer and least in the winter. The difference in the minima, on the other hand, appears to follow a pattern similar to those of the daily temperature range, number of clear days, and sunshine already discussed, having maxima (of absolute value) in the spring and fall, and minima in the winter and summer. It will be seen that this seasonal pattern is also characteristic of the frequency and intensity of temperature inversions in the lowest few hundreds of feet of the atmosphere.

Differential solar heating of variously oriented slopes is an additional mechanism producing systematic local temperature variations which, in turn, give rise to local wind currents. The bottom graph of Fig. 72 shows the hourly average difference in surface air temperature between the southeast-facing slope of Chestnut Ridge (station 005) and the northwest-facing slope of Haw Ridge (station 010) for the summer and fall quarters of 1949 and the winter of 1949-50. The basic pattern is the same in each season: differing by a negligible amount during the night, the temperatures on the opposite slopes diverge after sunrise to a maximum difference in mid-morning (8-11 a.m.), when the direction of the sun is nearly perpendicular to the strike of the ridges. The southeast-facing slope is then 1 to 3° F. warmer than the northwest-facing slope, the greatest difference occurring in summer and the least in winter. The difference decreases during midday,

crossing zero in the autumn at about 3 p.m. when the azimuth of the sun is nearly parallel to the ridges. The reversal takes place earlier in winter and seems not to occur in summer, although the minimum differential of $+0.2^{\circ}$ F. at 5 p.m. cannot be considered unquestionably positive since the observations were made with hygrothermographs. After a brief late-afternoon period during which the northwest-facing slope, now exposed to the late western sun, is slightly (perhaps half a degree) warmer than the opposite slope, now in shadow, the two again become equal under the non-directional effect of outgoing terrestrial radiation.

Both the altitudinal pattern and the cycle of differential slope heating indicated by the hygrothermograph stations in and adjoining Bethel Valley were satisfactorily verified by means of automobile temperature surveys in neighboring Bear Creek Valley and its adjoining ridges. After elimination of incomplete observations and those with doubtful instrument calibration, automobile data are available for 4 mornings (6 a.m. to 2 p.m.) and 6 evenings (3 p.m. to 10 p.m.) in the fall of 1950. For each reading station daily temperature time curves have been drawn from which hourly values were interpolated for averaging and comparison with hygrothermograph readings and captive balloon soundings. All the reading points as well as the relevant microneet stations and blimp levels are shown in a composite terrain cross section in Fig. 74. In Fig. 75 these hourly average temperatures are compared by means of hourly differential temperature curves with the valley base temperature for each type of observation as subtrahend in each case. The reference values for microneet temperatures are the station 001 hygrothermograph readings, for balloon sounding temperatures the surface

reading of the blimp thermistor, and for automobile temperatures the data obtained at reading point #7.

Group A represents differences between temperatures at ridge-top level and the corresponding valley temperatures. Curve 1 is the free-air difference $T_{300} - T_{sfc}$ from the blimp soundings, which resembles closely the fall 1950 quarterly average $T_{500} - T_{sfc}$ in Fig. 72 with slightly reduced amplitude. Curve 2 is the corresponding ridge-valley micronet temperature difference, $T_{006} - T_{001}$. Aside from an apparent negative error in the station 006 data due to an undetermined cause, the pattern is similar to that of the free-air temperature difference, again with reduced amplitude and showing a trend towards large negative values in the afternoon similar to that shown by Melton Hill (Fig. 72). Curves 3 and 4 are automobile temperature differences $T_{\#12} - T_{\#7}$ between Chestnut Ridge top and Bear Creek Valley and $T_{\#4} - T_{\#7}$ between Pine Ridge top and the same valley. The curves for the two ridge-tops agree well with each other and, in basic pattern, with curve 2, although not in absolute value. The ridge-valley temperature difference is certainly positive at night and negative during the day, but less so than that over the same height interval in the free atmosphere, particularly in the case of daytime lapse.

In considering the mid-slope zone, group B in Fig. 75, it should be mentioned that micronet stations 005 and 010 used in constructing the lowest graph of Fig. 72, had unfortunately been removed by the time these automobile surveys were made. Here curve 5, $T_{100} - T_{sfc}$, represents the free-air temperature differential over a comparable layer in Bethel Valley, curve 6, $T_{\#1} - T_{\#7}$,

represents the temperature change along the southeast-facing slope of Pine Ridge and curve 7, $T_{\#9} - T_{\#7}$, along the northwest-facing slope of Chestnut Ridge, both to about 1000 ft. MSL. The free-air difference shows an expected further decrease in amplitude from the previous graphs as the layer is reduced in depth, and the northwest-facing slope follows almost the identical curve; the southeast-facing slope has an even smaller altitudinal temperature lapse, the slope-valley difference during the day being almost zero, while at night this slope, too, closely follows the free-air temperature.

The curves of group C serve as an indication of the degree of comparability between the two valleys, which is of particular interest in view of the elevation difference of 100 ft. between the reference points, station 001 and reading point #7. Curve 8 shows the difference in hourly average temperatures during this series of observations between station 001, the micronet and free air reference point, and reading #7, the automobile reference point: they differ, for the most part, by less than 1° F. Curves 9 and 10 show differences between points within the Y-12 plant, at elevations of about 960-1000 ft. on the one hand, and valley bottom stations, curve 9 comparing hygrothermograph data at Y-12 and station 001 (different valleys), and curve 10 comparing automobile data within the same valley. Both show a higher temperature in the Y-12 plant than in the valley bottoms at night, but the Y-12 (008) hygrothermograph temperatures become several degrees colder than those in the valley at X-10 (001) in late afternoon, an effect not appearing in the automobile curve. A demonstration, by contrast, of the relative

similarity of the two valley base stations is afforded by curve 11, $T_{002} - T_{001}$, showing the effect of the stagnation of a pool of cold air at night in the hollow formed by the Bethel Valley entrance to Whiteoak Creek Gap in Haw Ridge (station 002). The difference in elevation is only about 40 ft. and the distance less than 2000 ft. between the two stations 002 and 001, yet the difference in temperature, particularly in the evening, is greater than that between two similarly exposed mid-valley stations differing by 100 ft. in elevation and some 5 mi. apart.

The final comparison of the local temperature observations made during the automobile surveys is presented in Fig. 76. Graphs A, B and C show directly the differences between hill, ridge and slope temperatures on the one hand and the free-air temperatures at corresponding altitudes on the other obtained by subtracting the appropriate curves of Fig. 75. All (with the exception of the questionable station 006 data) show positive departures from the free air through most of the morning and mid-day period, reaching a maximum before or near noon, and decreasing slowly during the afternoon. This afternoon heat loss from the hills is somewhat unexpected in view of the combined effects of lag due to heat capacity of the hill surface and upward flux of heat from the warmer valley during the period of maximum valley temperature, and it shows the relative unimportance of these two factors in relation to direct radiation exchange and vigorous ventilation. An early daily maximum temperature (noon to 2 p.m.) is also characteristic of the Smoky Mountain stations. The large negative departures in the late evening are apparently similar in origin to the strong

surface inversion which, as will be shown in the next section, is formed in the valley at the same time.

In graph C of Fig. 76 the opposite slope temperature departures from free air are compared, and the greater positive daytime departure on the southeast-facing slope ($T_{\#1} - T_{200}$) already shown in the micronet comparison is seen to be superimposed on a basically very similar pattern on the two slopes. When the two slope locations are compared directly, as in graph D, the slope differential curve shown for stations 005 and 010 in Fig. 72. particularly that for Fall, 1949, is repeated almost identically, although the observations on which this curve is based were made in a different year, in a different valley, and with an entirely different instrument. The maximum positive difference, about 2-3° F., occurs at 10 a.m., the evening reversal 3-5 p.m., and the maximum negative difference, about 1° F., at 2-6 p.m., followed within an hour or two by equalization which persists until sunrise.

Vertical Temperature Gradient

23. Diurnal Cycle of Vertical Temperature Distribution

The processes of daytime solar heating and nighttime radiative heat loss, as they affect the lowest layers of the atmosphere, from the ground up, are illustrated by Figs. 77-79 (see Ref. 11 for an excellent general review of this subject). Grass temperature, shelter air temperature, wet bulb temperature and temperature gradient, 4 to 54 ft., were measured simultaneously by means of thermocouples at station 001, temperature gradient, 4 ft. to 183 ft. was measured by means of thermohms at station 012 and solar radiation was measured by means of the station 001

Eppley pyrliometer. The curves represent averages for "clear" days (0-2 tenths cloudiness as observed visually or estimated by means of the pyrliometer traces) and "cloudy" days (3-10 tenths cloudiness). Only days with complete data were used in the averages, with the exception that grass temperature data were missing during part of the summer period: the hourly average air-grass temperature differentials for the complete days were used in reconstructing the grass temperature curve for this period.

The close correlation between the excess of grass surface temperature over shelter air temperature (about 4 ft.) and the solar radiation during the day can be seen at once from Fig. 77. Here the temperature curves were all drawn to the same scale, while the solar radiation scale was expanded from summer to fall to fit the larger range of temperature difference.

Of course, the energy gain from insolation is constantly opposed by radiative loss, which varies as the fourth power of the temperature and, as a result of the lag of the temperature cycle with respect to the sun, is greater in the afternoon than at corresponding times in the morning. Consequently the grass temperature excess is somewhat asymmetrical, being relatively greater in the morning (when the temperature, and consequently the radiative heat loss, is less) than in the evening, and is negative during the night, the greatest deficiency occurring in the early evening. The amplitude is greatest on clear days, almost exactly in proportion to that of solar radiation. The increase in amplitude for a given amount of insolation in fall over that in summer is associated with the greater dryness of the atmosphere, which permits a much greater proportion of the heat radiated by the earth's surface to escape.

Upward gradients of temperature or differentials over convenient height

intervals taken in the same sense, are used as a measure of stability with respect to vertical air motions. In the upper graphs of Figs. 78 and 79, the $T_{\frac{1}{4}} - T_{\text{grass}}$ curves are simply the curves of Fig. 77 inverted. They are now shown in comparison with the differentials over other height intervals: it is seen that by far the greatest vertical gradients occur in the few feet closest to the surface. The layer $\frac{1}{4}$ ft. to $5\frac{1}{4}$ ft. follows the lowest $\frac{1}{4}$ ft. closely with respect to phase, although greatly reduced in amplitude, while the layer $\frac{1}{4}$ ft. to 183 ft. lags behind as much as several hours during the morning and evening periods of rapid change. The decrease ("lapse") of temperature with height, characteristic of the daytime hours, has its maximum near noon, several times the adiabatic lapse rate in the lowest $\frac{1}{4}$ ft., and approaching the adiabatic lapse rate, $0.55^{\circ}\text{F./100 ft.}$ with increasing height. In late afternoon the grass becomes warmer than the air; and the intensity of the resulting temperature increase with height ("inversion") rises to a pronounced maximum in the lowest few feet at sunset, the rise becoming more gradual and the maximum intensity coming later with increasing height. The falling off of low-level inversion intensity with time during the night is too great to be explained by decreasing temperature of the radiating surface: the combined effects of cool-air drainage from the slopes, deepening the cold layer, and of the release of latent heat of condensation at the ground reinforced by back radiation from accumulated smoke and, later in the night, fog, retarding the rate of temperature fall at the surface, appear to be equally significant.

How dependent the temperature and moisture of the relatively transparent air are on the temperature of the radiating surface can be seen from the lower graphs of Figs. 78 and 79. The familiar daily temperature curve ($\frac{1}{4}$ ft. dry bulb), with its minimum near sunrise, begins to rise rapidly as soon as the ground becomes warmer than the air. Following the flat

maximum in the hourly average air temperature at about 3 p.m. there is little change until the ground becomes colder than the air, then the most rapid fall of the day occurs immediately. The afternoon wet bulb curve, too, remains relatively steady until intersected by the grass temperature curve, then, with condensation (dew formation) presumably occurring on the ground, the wet bulb temperature (affected both by the temperature fall and the downward flux of moisture) takes its greatest drop. The dew point, a measure of the moisture content independent of the temperature, actually rises in most cases during the period when the ground has become cooler than the air but is still warmer than the dew point, indicating that evaporation from the surface is continuing while loss by upward diffusion is greatly reduced. Immediately after the ground cools below the dew point, however, the latter drops abruptly, even though saturation has not been reached at the level of moisture measurement, indicating a downward flux with a sink at the ground, namely condensation as dew (or possibly hygroscopic absorption by the soil).

Typical diurnal changes in the entire lowest 1500 ft. of the atmosphere can be reconstructed from the detailed captive balloon soundings taken during the fall of 1950. Fig. 80. shows frequency histograms of temperature differences in three layers at each observation time and of sounding type, as well as average temperature-height curves for each time constructed from average temperature gradients in each 100 ft. layer. Dashed lines in each graph represent the dry-adiabatic lapse rate, $5.5^{\circ} \text{ F./1000 ft.}$

Sunrise occurred between 6 and 7 a.m. EST during the period covered by the 439 soundings incorporated in Fig. 80 . Little change in the vertical

temperature distribution occurred during this hour: an inversion was almost always present, averaging about 5° F. in the lowest 800 ft., and the prevalent sounding types were those showing a ground-based inversion. Beginning at 8 a.m., the hour in which, on the average, the grass first became warmer than the air (cf. Fig. 79), a large frequency of lapse appeared in the lowest 200 ft., and the predominant sounding types were those with ground-based lapse surmounted by the remains of the nocturnal inversion aloft. The average surface temperature had risen about 3° F., but above the shallow lapse layer, the average temperature distribution remained essentially unchanged.

As the surface temperature rose during the morning, a superadiabatic lapse was set up in the lowest 100-300 ft. and the near-adiabatic layer increased in depth, the upper layers warming appreciably only after the lapse layer had reached them, so that during the period 11 a.m. to 4 p.m. there were hardly any occurrences of types other than pure adiabatic or superadiabatic ones throughout the lowest thousand feet. After 4 p.m., when the ground had become cooler than the air (cf Fig. 79), the surface layer became stable (less than adiabatic lapse), so that by 6 p.m. there was about an equal incidence of lapse types and shallow inversion typed. The rapid surface cooling during the early evening hours was accompanied by the formation of a very intense, shallow inversion, averaging about 8° F. in the lowest 500 ft. by 8-10 p.m. with individual values over 15° F. having been recorded. The nocturnal inversion increased slowly in depth but did not usually intensify after about 10 p.m. In particular, the lowest 200 ft. showed a

decreasing frequency of intense inversions and a decreasing average temperature gradient. This trend continued through the remainder of the cycle resulting in the 6 a.m. picture already discussed. The nocturnal sounding types were almost exclusively ground-based inversion types, the homogeneity being helped very much by the lack of cloudy, windy and rainy weather during the period of observations. The exceptions were cases with early morning fog, in which a surface temperature lapse was established before sunrise. These highly important cases from the standpoint of air pollution appear as a small frequency of lapse in the 0600E $T_{200} - T_4$ histogram, and also as a definite reduction in the average temperature gradient in the lowest 100 ft. by the time the first morning soundings were taken.

The diurnal cycle of the vertical temperature distribution is perhaps best illustrated by the average "time cross-section" in Fig. 81. Here isotherms for the fall of 1950 are drawn on a time-height coordinate system, based on the average observed temperatures (reconstructed from average surface temperature and average temperature gradient) for each sounding time. Average temperatures derived from the 10 a.m. and 10 p.m. raobs are shown above 1500 ft.: for the remainder of the 24 hours, aside from not allowing the lapse rate to exceed adiabatic the isotherms in this upper layer are largely based on imagination. However, it is felt that the main features are beyond doubt: for example, the restriction of diurnal temperature variations to about the lowest 5000 ft. on the average, the rapid vertical propagation of the morning heating wave, the slow upward growth of the nocturnal inversion, and the marked cooling throughout the

night even above the inversion. Application of time-section analysis to meteorological case studies for the Oak Ridge area has been discussed in Ref. 47.

24. Seasonal Temperature-Gradient Variation

It has been noted that the low level temperature gradient has a larger diurnal amplitude on clear days than on cloudy ones (Figs. 78 and 79), as does the temperature itself, and that the frequency of clear days has maxima in spring and fall, (Fig. 66). It might be expected, therefore, that the low-level stability has a wider range in spring and fall than in summer and winter, as is in fact shown to be the case by Figs. 82-84. Intense inversions depend upon unobstructed radiative heat loss: their development is inhibited by short nights and high atmospheric moisture content in summer, and by frequent heavy cloudiness in winter. Large lapses in the lowest 200 ft. are most frequent in the summer under the influence of intense solar radiation, but only slightly less so in the clearer weather of spring and fall. The greatest superadiabatic lapse rates apparently occur in spring, and the greatest inversions in winter, but the greatest frequency of inversions of more than 8°F in 180 ft. occurs in fall. The abnormally cloudy winters during the observation period render the large winter maximum of near-neutral temperature gradients somewhat doubtful as a climatological average.

In the deeper layer extending up to 5000 ft. MSL (850 mb. pressure), the seasonal pattern is shifted slightly, the winter showing the largest frequency of very stable lapse rates, and the lowest frequency of instability, the summer showing the reverse. Broad distributions in spring and fall

reflect a mixture of the summer and winter types, with the spring distribution shifted slightly towards the unstable (summer) side and that of fall towards the stable (winter) side. The diurnal frequency distributions given in Figs. 83 and 84 permit an estimate of the probability of any given stability being exceeded at any particular time of day. Inversions in the valley layer ($T_{183} - T_5 > -0.5^\circ$, that is, $\geq 0^\circ$ within the accuracy of measurement), for instance, occur more than 70% of the time at night and less than 30% during midday in all seasons. The time at which the probability of lapse conditions ($T_{183} - T_5 < -0.5^\circ$) rises to 50% is about 2 hours after sunrise and 90 percent about 4-5 hours after sunrise. The daytime lapse appears to be set up in the shortest time after sunrise in winter (1 hr. 45 min.) and the longest in fall (2 hr. 50 min.). Since we have already seen that the solar energy received in the first few hours after sunrise is greatest in spring and fall, the seasonal variation in "breaking time" must be due to the variation in inversion frequency and intensity preceding sunrise. The nocturnal inversion frequency varies from about 70% in winter to about 95% in fall. Thus while instability does not appear most quickly following sunrise in the spring and fall, the rate of decrease of stability is greatest in these seasons, as can be seen from the spacing of stability lines in the vicinity of sunrise in both Figs. 83 and 84.

These diurnal variations result in the seasonal curve of inversion frequency shown in Fig. 85, ($T_{183} - T_5 \geq 0$, station 012): the frequencies are greater than 50% in all months except June and have spring and late fall maxima. Since these averages are based on the full 8 years of record at station 012, they may be considered fairly reliable, although there appears to be a spurious increase during 1951, apparently due to improper ventilation of the upper temperature sensing element.

Figs. 86-90 contain frequency histograms of the captive balloon temperature difference observations for each observation time in each season. The 200 ft. differentials (Fig. 86), are comparable to the 183 ft. tower observations discussed so far: they show a somewhat larger frequency of adiabatic and superadiabatic lapse than do the tower data, which may be ascribable to better ventilation of the balloon thermistor, especially since the gusty winds accompanying such conditions reduced the number of soundings. In the 500 ft. and 1000 ft. layers (Figs. 87 and 88), the seasonal pattern remains the same, with fall and winter showing the largest frequencies of large inversions (cf. the Oct-Dec maximum in Fig. 85), while spring and summer show the largest frequencies of strong lapse. The frequency of superadiabatic lapse rates decreases gradually with increasing depth of the layer. The frequency of large inversions on the other hand increases from 200 to 500 ft. but decreases slightly from 500 ft. to 1000 ft., especially in the summer. It appears to be true that regardless of decreases in the low-level inversion intensity during the night (after the early evening maximum), the depth of the inversion increases more or less steadily, roughly in proportion to the square root of the time. The summer nights, being shortest, seldom permit growth of the nocturnal inversion as high as 1000 ft. while the longer winter nights allow such developments more frequently and for longer duration. By 9 a.m. (soundings were actually taken at various times during the hour ending at the nominal observation time), for instance, while the 200 ft. stability frequencies have begun to shift toward the midday pattern in all seasons, the shift is much more nearly complete in spring and summer than in fall or winter. In the 1000 ft. layer there is but little decrease in the frequency of large inversions by 9 a.m. in fall

and winter while in spring and summer by this hour they have been largely eliminated.

The frequency distribution of the various characteristic shapes of the temperature-height curve at any given time of day also shows a seasonal variation (Fig. 89). The 3 a.m. sounding may be taken as representative of night-time conditions in all seasons. This curve usually shows a ground-based inversion surmounted by a lapse or isothermal layer within the lowest 1000 ft. It is more common for the upper part to be isothermal or even inversion in winter than in summer. At the 9 a.m. observation in all seasons except winter there are few ground-based inversions left, the predominant types being superadiabatic in summer, neutral in spring, a transitional lapse-inversion-lapse type in fall, and almost the whole spectrum of types excluding superadiabatic in winter. The afternoon (3 p.m.) types lean more toward the superadiabatic in spring and summer and toward neutral (adiabatic) in fall and winter. The predominant type by 9 p.m. in all seasons is the shallow ground inversion surmounted by lapse.

Average temperature soundings by observation time and season are shown in Fig. 90, illustrating in a concise way the variations already discussed. Of particular interest is the variation in the 9 a.m. sounding. Resembling the typical nocturnal form in winter, the 9 a.m. soundings show the effect of prolonged cooling in the upper part and the beginning of warming below. In spring and summer average lapse rates at 9 a.m. are typical of midday although the temperatures have not yet risen much aloft. In fall the partial breaking of the nocturnal inversion shows up clearly in the 9 a.m.

averages. The 3 p.m. average curves are similar in all seasons. The 9 p.m. soundings are also similar throughout the year, and it is of interest that in spite of its extreme nocturnal form, the highest temperatures of the day aloft are observed at this hour during the winter, the spring and the year as a whole. The seasonal average soundings show a net low-level stability, greatest in the winter and least in the summer. In spring and summer, in fact, one would expect a net upward heat flux and consequently an average lapse of temperature, and it is likely that a considerable bias has been introduced in these seasons by the lack of midday soundings during gusty winds.

25. The Three-Dimensional Temperature Structure

It has been shown that the surface air temperatures (about 4-5 ft. above ground) vary with altitude, slope orientation and nature of the ground cover (vegetation, buildings, etc.), and that the effects of these variables are subject to diurnal, seasonal and apparently non-systematic variations associated with the cyclical variation of solar radiation and both the cyclical and aperiodic variations of atmospheric moisture and cloudiness. It has been further shown that the vertical differential temperature distribution in the free air over the valley is subject primarily to diurnal variations, responding directly to radiative heat gains and losses at the ground, and modified mainly by seasonal and aperiodic variations in cloudiness and atmospheric moisture. The three-dimensional temperature structure can now be briefly and qualitatively summarized.

The most nearly homogeneous temperature (more accurately, potential temperature) distribution is observed in midday. Normally at this time the effects of topography and exposure are minimized by intense convective mixing in both the horizontal and vertical directions, giving rise to large short-period fluctuations, but relatively uniform hourly mean temperatures. In the vertical, large temperature gradients are confined at this time to the lowest few feet, where lapse rates many times adiabatic normally exist, while the lapse rates from the lowest 50-100 ft. up to a height of several thousands of feet do not deviate much from adiabatic (uniform potential temperature). In the midday period the ridge tops are somewhat warmer than the free air; that is to say, the lapse rate of temperature along the slopes is less than that in the free air, particularly on the southeast facing slopes, where it is about nil, the temperature being a degree or so higher than on the northwest facing slopes. The depth of the relatively warm air columns above the ridges and heated slopes has not been determined, but the nearly random motions of free balanced balloons as well as the apparently random distribution of cumulus clouds suggest that the small temperature excess (1-2° F.) is damped out relatively soon, probably well within the lowest few hundreds of feet. Temperature measurements on Pine Ridge radio tower at a height of 80 ft. above the ridge top for a short period, summarized in Fig. 91, indicate that the anomaly is already very slight at this level. It follows that the lapse rate above the ridges is greater than that in the free air at the same height, although not necessarily greater than that in the valley bottom.

In late afternoon and early evening large inhomogeneities begin to appear: the ground, both in the valleys and on the hills, radiating heat at a maximum rate while the incoming solar energy is being cut off, becomes much cooler than

the air, giving rise to drainage flow of a shallow layer of cooled air down the slopes, collection of pools of cold air in hollows, and an intense surface-layer temperature inversion. Above the level of maximum temperature, some 200-500 ft. above the ground shortly after sunset, a lapse approaching adiabatic continues to exist, and this entire lapse layer begins to cool, apparently by downward eddy transfer of heat at almost the same rate as through the surface layer (the eddy diffusivity must be much greater while the potential temperature gradient is much smaller), becoming gradually more stable as the night progresses. At the same time the air over built up sites has cooled somewhat less than that in the "rural" areas and is 3-7°F warmer. It follows that the stability above the warmer built-up areas must be less than over natural terrain, i.e., the inversion strength (temperature difference) in the lowest 100-200 ft. must be several degrees less. Similarly the hill tops, which are 4-6°F cooler than the free air, must be surmounted by an intense inversion. The Pine Ridge observations summarized in Fig. 91 indicate that the excessive temperature gradient is largely confined to the lowest eighty feet above the ridge. The contrast between opposite slopes reverses briefly in late afternoon as the sun comes around to the west and then disappears for the night.

During the night the valleys fill up with cool air draining off the slopes, resulting in decreasing inversion intensity in the lowest 100-200 ft. with slightly greater intensity above this layer, and decreasing contrast between the slopes and the free air. Cool air also flows in from the slopes of the large mountains several miles away. The surface temperature continues to fall, but the temperature aloft (500-1500 ft.) falls even more, so that the over-all stability of the lowest 500 ft. is decreased while that of the lowest 4000 ft. increases steadily until sunrise. The temperatures in the built-up areas, although still 1-2°F higher than

these in the open exposures, gradually approach the latter, and, in general, the isothermal surfaces become more nearly horizontal.

By sunrise, accumulations of smoke and, occasionally, fog, have further reduced the inversion intensity in the lowest few hundred feet. In the case of fog, a shallow lapse layer surmounted by an intense inversion is ordinarily produced by overbalancing of the outgoing radiation from the ground by that from the suspended fog particles. Within 2 hrs. after sunrise the inversion has been "broken" in the lowest 50-200 ft., the slopes and hills have become warmer than the free air, and a definite cross-valley temperature differential has developed, amounting to about 2° F. As the morning progresses, the heating extends to greater heights, progressively destroying the inversion, and the relative homogeneity of potential temperature (adiabatic conditions except for a shallow, strongly superadiabatic layer next to the surface), with vigorous convective mixing, characteristic of midday, are again established.

The cycle depicted above is most fully developed in clear, dry periods with relatively light gradient winds and less so in proportion to the prevalence of cloudiness, wind, aperiodic weather changes, etc. The most typical sequences occur in spring and fall, with the nocturnal phase somewhat inhibited in summer and a large variability introduced in winter. The degree to which the details of the typical cycle are followed is thus closely correlated with the daily temperature range, the frequency of clear days, and the percentage of possible solar radiation or sunshine duration.

Wind Flow26. Regional Pattern of Wind Direction and Speed

Above the highest elevations of the Appalachian Mountains, the winds are predominantly westerly throughout the year, with little evidence of orographic deformation. Summaries of pilot balloon observations at 2000 m (6600 ft.) MSL over periods of 10 yrs. or more at Nashville, Knoxville, Chattanooga and Spartanburg (Fig. 92) show essentially similar direction distributions: 71-75% of the observed winds are from westerly directions (SSW through NNW) with no one direction strongly favored. Progressively downward through 1500 m (5000 ft.; Fig. 93), 1000 m (3300 ft.; Fig. 94) and 500 m (1700 ft. MSL, or about 1000 ft. above the lowest valleys; Fig. 95) the symmetrical distribution of westerlies gives way to local patterns which can be directly associated with the orientations of nearby mountain ranges. At Knoxville the southwesterly winds increase in frequency with lowering elevation, at the expense of northwest, while at Chattanooga, where the valley orientation is more nearly N-S, southerly directions become predominant. Below 1000 m northeasterly winds also become important at Knoxville and NNE at Chattanooga giving a bimodal up-down valley wind regime. This is a departure from the regional pressure pattern, discussed in an earlier section, since the latter would indicate predominantly southerly gradient winds, with more or less symmetrical seasonal variations about this prevailing direction, as at Nashville. At Spartanburg, too, below 1000 m, increased frequencies of NE and SW are found, at the expense of the westerly quadrant.

Wind speed frequency distributions reflect the obstructing effect of the

mountains, being almost the same at all four stations at the 2000 m and 1500 m levels but showing a definite relative reduction of frequency of the higher speeds at 1000 m and below, particularly in the cross-ridge direction. Knoxville and Chattanooga, for instance, have only about half the frequency of wind speeds greater than 33 mph shown by Nashville, while Spartanburg has even fewer. The remaining moderately high speeds are virtually restricted to the up-valley winds, southwesterly at Knoxville and southerly at Chattanooga. The relative reduction in speed within the valley with respect to more open country is even more marked at the 500 m level, only some 4% of the wind speeds at Knoxville and Chattanooga being over 22 mph annually compared with more than 20% at Nashville and about 18% at Spartanburg. The frequencies of high wind speeds at the latter two stations, still in the zone dominated by the Bermuda anticyclone, are, in turn, substantially less than at stations farther north. In fact, the slight predominance of westerly wind, taken together with the low prevailing wind speeds place this entire region near the southernmost edge of the westerly belt at 500 m.

At the anemometer level (40-70 ft. above ground, Fig. 96) both the orographic channelling of the wind flow and the relative stagnation of the air in the Southern Appalachian Valley are strikingly revealed by the annual wind roses for Bristol, Knoxville, Chattanooga and Rome, Georgia, in the valley, as compared with Smithville, Tennessee just across the Cumberland Plateau to the west. Following the turning of the valley axis, maxima of wind direction frequency occur from the WSW and NE at Bristol (with a secondary WNW mode in addition) and Knoxville, S and NNE at Chattanooga,

and SE and N at Rome. Smithville, on the other hand, has a simple broad mode from the south characteristic of all of western Tennessee and Kentucky. The valley stations have both a low frequency of strong winds (Fig. 50) and a large frequency of calms (a figure which is partly determined by the anemometer characteristics) in relation to the more open surrounding country.

With the seasonal oscillation of both the strength of the westerly current aloft and its latitude of maximum development, the wind roses at the 1500 m level (chosen as a convenient reference level for much of the later analysis) go through the expected cycle of change, as shown in Figs. 97-100. In winter the speeds are higher than the annual average, with winds stronger than 45 mph occurring about 6% of the time at Knoxville during this season compared with 1% annually, and the westerly directions account for about 80% of all observations. From winter to spring the winds remain relatively strong, the frequency of speeds greater than 33 mph dropping from 17% to 12% at Knoxville and comparably at the other stations. A shift to more southwesterly directions also takes place at all stations. In summer, winds at 1500 m greater than 33 mph become virtually non-existent and the proportion of westerly winds falls to less than 70% (Fig. 99). By fall, when a sea-level anticyclonic cell is present to the north on the mean sea-level pressure map (Fig. 36) the frequency of westerlies has its minimum, observations with directions SSW through NNW falling to 62% (Fig. 100). Wind speeds at this level in the fall are still somewhat lighter than the annual average.

The seasonal variations of the regional wind direction and speed distribution at the surface level (Figs. 101-104) consist mainly in changes in

proportional frequency and intensity of the up- and down- valley directions. The winter wind roses resemble the annual ones quite closely, with a slight increase in the frequency of westerly and northwesterly directions at the expense of calms. Above-average wind speeds are evident from all directions. The shift in the predominant gradient flow from westerly in winter to southwesterly in spring is accompanied, in the Chattanooga-Knoxville sector of the valley bottom, by slight increases in the up-valley mode at the expense of the down-valley one. Thus at Knoxville SW increases a few percent at the expense of NE, and at Chattanooga S at the expense of NNE. At Smithville, outside the valley, the shift reflects simply that of the upper current, namely, an increase in SSW at the expense of WNW and NW. The decrease in intensity of the upper winds in summer is mirrored at the surface (Fig. 103) both in the general decrease in wind speed and in the increase of local control. Cross-valley winds are less frequent and calms more frequent in summer than in winter or spring, and even more so in fall (Fig. 104), when down-valley winds predominate over up-valley ones. Table 39 summarizes the regional vertical and seasonal variation in the frequency of westerly wind. The regional uniformity of the westerly frequency at 2000 m (71-75%) can be seen to be diminished considerably at 500 m (42-56%, the minimum, at Chattanooga, being associated with a nearly N-S orientation of the Cumberland Mountain range. The seasonal variation at Knoxville changes from a quantitative one at 2000 m, with a winter maximum (90%) and fall minimum (67%) of predominantly westerly flow to an oscillation between prevailing northeasterlies in the fall and prevailing southwesterlies in the other seasons at 500 m and below. The fall reversal is characteristic of the region as a whole, and not simply a result of enhanced down-valley drainage. The southern limit of the westerlies

TABLE 39

FREQUENCY (%) OF WESTERLY WINDS (SSW-NW)

	Knoxville				Knoxville	Nashville	Chattanooga	Spartanburg
	Winter	Spring	Summer	Fall	Annual	Annual	Annual	Annual
Surface	48	50	48	37	46	--	33	--
500 m	58	61	60	48	56	53	42	55
1000 m	69	67	63	55	63	63	53	62
1500 m	80	76	67	62	71	60	64	70
2000 m	90	80	69	67	75	74	71	75

in the lowest 1000 ft. of the atmosphere is actually displaced northward during the fall, as shown by the patterns of both wind and pressure. That nocturnal cold air drainage does contribute materially to the down-valley (northerly-northeasterly) modes can be clearly seen by comparing the daytime wind roses (10 a.m. - 5 p.m. EST; Fig. 105) with those for nighttime (10 p.m. - 5 EST; Fig. 106). Up-valley (southerly-southwesterly) directions and cross-valley (westerly-northwesterly) directions are above the average frequency during the day, and below average during the night. Up-valley winds are generated by rising currents along the slopes and ridges, warmed by the sun relative to the free air at the same level, and cross-valley winds by convective mixing from the westerly streams aloft associated with the daytime vertical temperature lapse throughout the valley. The nocturnal temperature inversion, by suppressing vertical mixing, isolates the valley flow from the upper cross-valley currents, while the relatively cold air layers formed along the slopes and ridges gravitate towards the valley bottom and feed the down-valley stream. The large frequencies of calms and low speeds at night are associated with both the low velocity of the drainage current in comparison with the more energetic daytime convective flow

and the enhanced frictional reduction of wind speed next to the ground accompanying reduced downward flux of momentum from the upper strata. The frequency of calms is undoubtedly greatly exaggerated by the drag and inertia of mechanical anemometers. At Chattanooga, for example, NNE winds are more frequent in the 500 m pibal observations than in the surface anemometer observations, indicating a probable underestimate of the frequency of light, shallow drainage winds in the surface wind roses. However, the vertical depth of the drainage current is apparently considerably greater at the lower end of the valley, represented by Chattanooga and Rome, than at the upper end, and it is not unlikely that its maximum frequency and speed are to be found above the surface layer, which may be relatively stagnant. The increase in frequency of nocturnal northerly winds from Chattanooga to Rome at the expense of calms is probably largely an instrumental distortion: earlier records (1923-1930) obtained at Chattanooga by means of a contact-type anemometer with a lower starting speed show only 3-4% calms during the fall (Sept.-Nov.), compared with 27% in the more recent generator-anemometer records. The same early records show over 50% of the winds from the NNE quadrant as compared with only 27% in the later records. Similar distortions also occur at the other anemometer stations, but apparently not to as great an extent. If allowance is made for the probability that many of the recorded calms actually represent light drainage winds (1 mph or less) it must be concluded that the down-valley directions are considerably more prevalent during the autumn, and probably also during the summer, than the wind roses indicate. It is of interest that Smithville, on the NW slope of the Cumberland Plateau, has an entirely different diurnal variation of

direction from those within the valley: while the basic regional pattern of prevailing southerly winds characterizes both the day and night wind roses, northwesterly up-slope winds are favored during the day and southeasterly drainage winds at night. The resulting divergence between the surface currents on opposite sides of the plateau further emphasizes the nocturnal isolation of the Southern Appalachian Valley air from that of the surrounding plain.

Surface wind directions accompanying precipitation (Fig. 107) are distributed very similarly to those of all observations combined, departing somewhat towards the daytime pattern: a slight excess of higher speeds, a deficiency of calms, an excess of up-valley and cross-valley winds, most of which can be attributed as readily to the increased cloudiness and vertical mixing characterizing these occasions as to a shift in the general flow pattern. One feature, at least, however, is apparently due to the latter factor: the frequency of southeasterly winds at Rome is greater than is obtained on any other basis of selection used.

A more unique association of wind direction with precipitation is apparent in the data obtained above the surface layers by means of rawins (radio direction finding winds aloft observations), which reveal a significant bias in the visual pibal statistics. Figs. 108-112 present annual and seasonal wind roses at 5 levels from 500 m (1700 ft. MSL) to 10,000 m. (33,000 ft. MSL) based on $23\frac{1}{2}$ yrs. of pibals at Knoxville, $13\frac{1}{2}$ yrs. of pibals at Nashville and 4 years of rawins at Nashville, as well as wind roses for only those rawins with precipitation recorded at observation

time. Several important relationships stand out among these different sets of observations:

- a. Southwesterly winds are strongly favored at the expense of northwesterly above 500 m. over the year as a whole when precipitation is occurring. At 500 m the favored direction is more southerly.
- b. Almost exclusively southwesterly winds aloft accompany precipitation in fall and winter, whereas the favored direction in spring is WSW and, in summer, W, the normal prevailing direction.
- c. Precipitation is usually accompanied by stronger than average winds aloft in all seasons.
- d. The rawin observations at Nashville contain a relatively larger frequency of southwesterly directions, fewer northwesterly, and higher wind speeds aloft than do the pibals. These deviations are entirely consistent with the omission of rainy and cloudy weather from the pibal observations, and the departure of the wind directions and speeds from normal under these conditions. These departures are present at all levels up to 10 km., and in all seasons except summer, in which only the speeds are affected, but not the directions.
- e. More observations have been obtained at 10 km. in 4 years of twice daily rawins than in 13 yrs. of pibals 4 times per day, so that the rawin roses at the highest levels have smoother distributions which are probably more nearly normal than those of the longer record of pibals.
- f. From 1500 m on up, the Nashville and Knoxville pibal wind roses resemble each other very closely in all seasons, except at the 10

km. level. It can be concluded from this and from argument (e) that the Nashville Rawins, both with and without precipitation, probably give quite a satisfactory representation of the wind flow over Knoxville above the level of the Appalachian Mountain crests, at least in so far as the statistical distributions are concerned.

- g. At the 500 m level and lower, the Knoxville wind roses are dominated by the orientation of the nearby mountain ranges, and differ greatly from those obtained at Nashville. At these low levels, however, the precipitation wind roses differ in relatively minor ways from the over-all wind roses, and also from the surface wind roses. Furthermore, far fewer visual observations are missed through cloudiness than at the higher levels. It is, therefore, not necessary either to take account of the bias of pibal statistics at this low level or to consider the precipitation wind direction probabilities significantly different from normal.

To fit the Oak Ridge winds aloft into the regional pattern, the seasonal and annual pibal wind roses for Oak Ridge and Knoxville for the two years Nov. 1948-Oct. 1950 are presented together in Fig. 113. In these wind roses, total frequency from each direction, to 36 points, is represented by a bar and average speed by a curve. At 2000 ft. MSL the winds at the two stations have slightly different distributions, with Oak Ridge showing a deviation from direct opposition between the up-valley and down-valley directions reflecting the valley curvature (as do the surface and 500 m wind roses at Chattanooga and the surface wind roses at Rome) not appearing at Knoxville. Also distinctive in the 2000 ft. roses at Oak Ridge is an

additional mode from the northwest in all seasons but particularly in the fall and winter. This is most likely an effect due to closeness to the Cumberland Mountains, and is quite reminiscent of a similar effect at Spartanburg in the lee of the Great Smoky Mts. It will be seen later that a similar effect is noticeable in the local hilltop anemometer records, and seems to be almost exclusively associated with westerly or northwesterly winds over 15 mph at the 5000 ft. level and a relatively unstable temperature stratification within the valley. Presumably this "spilled-over" northwesterly current has been deflected to a southwesterly or northeasterly direction by the time it reaches Knoxville.

A weak remnant of this anomalous frequency of northwesterly winds, not duplicated at Knoxville, is visible at the 5000 ft. level, particularly in winter, but in all other respects the wind direction distributions at the two stations are virtually identical from this level upward. An increase in the speed of NW winds at Oak Ridge over that measured at Knoxville, however, is noticeable up to 10,000 ft. This persistence of anomalous northwesterlies to high levels is also repeated at Spartanburg and, in somewhat weaker form, up to at least 2000 m at all pibal stations east of the Appalachians as far south as Atlanta, where channelling has ceased to play a role of any importance (Ref. 41). However, in view of the relatively small frequencies of these northwest winds at 5000 ft. and above, the Knoxville wind observations can be considered representative of Oak Ridge at these levels for practical purposes.

Average wind speeds, as shown in Table 40, are relatively uniform at Weather Bureau stations throughout the Southern Appalachian Valley, where

TABLE 40

REGIONAL AVERAGE WIND SPEEDS (MPH)

<u>Station</u>	<u>Years of Record</u>	<u>Winter</u>	<u>Spring</u>	<u>Summer</u>	<u>Fall</u>	<u>Annual</u>	<u>Anemometer, Height, ft.</u>
<u>S. Appalachian Valley</u>							
Bristol	9	6.5	6.9	4.4	5.0	5.7	68
Knoxville	80	7.1	7.5	5.9	5.9	6.7	45-111
Oak Ridge	7	6.8	7.0	4.4	5.2	5.8	140
Chattanooga	73	7.7	7.7	5.6	6.0	6.7	54-214
Rome	3	7.5	7.7	5.7	6.3	6.9	51
<u>North</u>							
Lexington	47	13.3	12.6	8.9	10.8	11.4	61-230
Elkins	53	6.2	6.1	3.8	4.5	5.1	31-78
<u>East</u>							
Greensboro	23	8.2	8.8	6.7	7.4	7.8	56
Asheville	49	9.6	9.1	6.3	7.6	8.2	75-100
<u>South</u>							
Atlanta	71	11.6	10.6	7.8	9.5	9.9	53-216
Birmingham	48	8.2	7.8	5.4	6.5	7.0	48-144
<u>West</u>							
Nashville	43	9.7	9.9	7.3	8.1	8.7	38-193
Smithville	9	9.4	9.2	6.4	7.4	8.1	
<u>500 m. (1700 ft.) MSL</u>							
Knoxville	23	12.8	13.0	9.6	10.3	11.2	
Oak Ridge	2	13.6	12.3	9.7	11.8	11.9	
Chattanooga	10	13.4	13.6	9.9	11.8	12.3	
Nashville*	14(4)	18.1(18.8)	17.7(16.8)	13.0(11.9)	15.9(16.1)	16.1(15.7)	
Spartanburg	19	16.1	15.1	12.1	13.9	14.3	
<u>1000 m. (3300 ft.) MSL</u>							
Knoxville	23	18.8	17.7	12.3	14.3	15.7	
Chattanooga	10	20.1	18.8	13.2	16.8	17.0	
Nashville*	14(4)	22.8(24.4)	20.8(21.5)	13.9(14.3)	18.1(19.7)	18.6(19.9)	
Spartanburg	19	18.6	17.9	12.8	15.0	15.8	
<u>1500 m. (5000 ft.) MSL</u>							
Knoxville	23	23.7	20.3	12.8	16.1	17.9	
Oak Ridge	2	22.9	16.9	12.4	16.5	16.4	
Chattanooga	10	24.6	20.4	13.0	17.4	18.3	
Nashville*	14(4)	24.6(26.8)	21.2(23.5)	13.4(14.8)	17.9(19.9)	18.8(21.2)	
Spartanburg	19	21.2	18.1	12.1	14.8	16.3	
<u>3000 m. (10,000 ft.) MSL</u>							
Knoxville	23	36.0	26.2	14.8	20.6	22.8	
Oak Ridge	2	34.6	24.3	11.0	19.8	20.4	
Chattanooga	10	34.6	24.8	13.9	21.0	22.1	
Nashville*	14(4)	34.2(39.1)	26.0(31.1)	15.2(16.8)	20.8(26.0)	22.4(28.0)	
Spartanburg	19	33.5	24.4	14.1	19.7	21.9	

*Numbers in parentheses refer to RAWIN data.

the anemometers have been generally well exposed, at least 30 ft. above the prevailing ground or roof levels. There is a gradual decrease northward in the annual average from 6.9 mph at Rome to 5.7 mph at Bristol and further to 5.1 at Elkins in the Allegheny Mts. These average speeds are substantially lower than those outside the valley, and the northward decrease can be directly associated with increasing height and extent of the obstructing mountain ranges on the west, since the average speeds outside the valley increase steadily northward from 7.0 mph at Birmingham to 8.7 mph at Nashville and 11.4 mph at Lexington. East and south of the Appalachians, too, the average speeds are in the range 7-10 mph. At 1700 ft. (500 m) above sea level the wind speed deficit still exists, but has decreased, the speeds within the valley averaging 11-12 mph annually, compared with 16 mph to the west and 14 mph to the east. At 5000 ft. the pibals show still less variation (16-19 mph) and by 10,000 ft. none of significance (all about 22 mph). The higher average speeds aloft shown by the Nashville rawins (2.3 mph higher than the average pibal speed at 5000 ft., 5.6 mph higher at 10,000 ft.) suggest that all the pibal statistics have a negative bias at these levels.

At all stations and all levels the average speeds are larger in winter and spring than the annual average and lower in summer and fall, the minimum always occurring in summer, and the maximum varying between winter and spring at the lowest levels but always occurring in winter aloft. The seasonal variation becomes increasingly pronounced with increasing altitude, from a range of 2-3 mph (or 30%) between winter and summer at the surface

to a range of 20 mph (60%) at 10,000 ft. The rate of vertical increase of wind speed is determined almost entirely by the large-scale horizontal temperature gradient, and the seasonal variation of the former reflects the relative horizontal homogeneity of the air masses overlying the continent in summer in comparison with the strong north-south temperature contrasts in winter. Below 1000 m (3,300 ft.) the effect of the vertical temperature stratification in suppressing or facilitating vertical exchange of momentum is a factor of equal or greater importance operating seasonally in the same sense.

The Oak Ridge average wind speeds, although measured relatively high above the local ground and roof levels by comparison with the other stations, are considerably lower than would be expected in this portion of the valley. This low average speed, of considerable importance in connection with transport and diffusion of contaminants, is apparently caused by the unusual roughness of the terrain.

Extreme wind speeds of record (fastest mile) at the Weather Bureau stations in the region are given in Table 41 and examples of local extreme wind speeds for various time intervals in Table 42. Since the regional extreme fastest miles are in the vicinity of 60 mph or greater in all seasons, their duration is of the order of 1 min. It is seen that these short-lived gusts can reach 70 mph or more and are virtually confined to the spring and summer (generally accompanying thunderstorms), the maximum speed decreasing rapidly as the duration of the sample is increased. Hourly average speeds, on the other hand, reach their highest values, slightly over 30 mph, in the cold half of the year. Hourly average winds over 30 mph are much more common at Knoxville than at any of the Oak Ridge stations, having been observed on an average of 15 days per year during the decade 1921-1930 (the majority in Feb., March, and April).

TABLE 41

REGIONAL FASTEST MILE OF WIND ON RECORD (MPH)

	<u>Bristol</u>	<u>Knoxville</u>	<u>Chattanooga</u>	<u>Nashville</u>	<u>Asheville</u>	<u>Highest</u>	<u>Station</u>	<u>Year</u>
Jan.		49	46	56	52	56	Nash	1949*
Feb.		54	44	57	39	57	Nash	1917
Mar.		61	82	65	44	82	Chat	1947
Apr.		71	43	60	40	71	Knex	1944
May		57	63	57	49	63	Chat	1951
June		65	62	66	49	66	Nash	1941
July		57	39	59	40	59	Nash	1938
Aug.		49	62	49	34	62	Chat	1946
Sept.		56	46	47	43	56	Knox	1943
Oct.		42	35	51	44	51	Nash	1952
Nov.		41	43	58	40	58	Nash	1938
Dec.		52	46	47	40	52	Knex	1951
Ann.		71	82	66	52	82	Chat	3/47
Yrs. record		40	73	40	40			

TABLE 42

OAK RIDGE EXTREME OBSERVED WIND SPEEDS, MPH

<u>Peak Gust</u>	<u>Station</u>	<u>Date</u>
70	012	9/1/51
67	019	6/22/51
57	019	4/13/52
56	012	5/4/51
55	012	7/20/50
Fastest Mile		
60	007	7/20/50
44	019	1/3/51
41	007	11/20/50
41	007	3/8/50
38	007	2/14/50
Highest 5 min.		
52	007	7/20/50
45	012	9/1/51
44	019	6/22/51
39	019	3/23/51
39	019	4/13/52
Highest Hour		
32	007	11/20/50
30	012	2/14/50
30	012	3/23/51
29	019	1/3/51
28	007	3/8/50
29	019	3/23/51
29	012	11/20/50

Figs. 114-116 contain statistics of daily peak gust velocity for station 012 (ORNL Health Physics Division, X-10 Area, 140 ft. above ground), for a period of slightly over 2 yrs. Gusts of 20-40 mph are most common in the spring (Fig. 114), but gusts over 50 mph are equally common in summer. The relation of peak gust velocity to the average wind speed for the hour in which it occurred (Fig. 115) is approximately a linear one on the average, and nearly identical in all seasons. The departures from this average relation, however, are much greater in the summer than in the other seasons, and least in winter. The majority of daily peak gusts blow from southwesterly and westerly directions (Fig. 116), although the very strongest (≥ 50 mph) seem to favor cross-valley directions (NW and SE), and the percentage of daily peak gusts from northwesterly directions is greater in all seasons than the average frequency of winds from these directions.

27. Local Variation of Wind Direction and Speed

The diversity of local wind direction frequency distributions shown, on the larger scale, by the wind roses for Bristol, Knoxville, Chattanooga and Rome is fully equalled by that on the smaller scale of Bethel and Melton Valleys and their adjoining ridges in the vicinity of the X-10 area. These four Weather Bureau stations in the Southern Appalachian Valley are all situated at relatively level airports, more or less in the central portion of the large valley, so that their wind records are representative of the broad valley currents. When, on the other hand, wind observation points are deliberately located on slopes of small ridges, in narrow gaps, and on isolated hills, the resulting local wind roses depart from those of the

broad valley as much as the latter depart from the regional flow aloft. Fig. 117 presents the annual wind direction and speed frequency roses for all the stations in the Bethel Valley-Melton-Valley area for which records were obtained through a major part of each of the four seasons. As in the case of the large-valley stations, all the distributions are at least bimodal, with the exception of station 010 (Haw Ridge slope) at which the down-slope winds were apparently reduced by the forest cover to speeds lower than the threshold of the anemometer. The main differences are in the directions, breadths, and relative magnitudes of the primary, secondary and, in some cases tertiary modes, and in the overall speed distributions.

These wind roses can be sorted into four types, which can be identified with fairly distinct categories of surrounding topography. Since this identification seems to apply to both the large-scale (Southern Appalachian Valley) and small-scale (Bethel Valley, etc.) patterns, it is helpful in revealing the relative importance of each scale of topography at each station. This classification is given in Table 43. The seasonal and annual surface wind roses for the large valley shown in Figs. 96 and 101-104, annual 500 m. wind roses shown in Fig. 95 and seasonal 500 m. wind roses, not illustrated, as well as the annual micronet wind roses shown in Fig. 117 and seasonal micronet wind roses shown in Figs. 118-124 have been used in the classification. The primary, secondary and tertiary modes are not necessarily arranged in the order of decreasing frequency, but always represent the up-valley (spring, day), down-valley (fall, night), and cross-valley (winter and spring, day) modes respectively. Usually, if the frequencies of several adjacent directions are combined, the frequencies fall in this same order.

TABLE 43

WIND ROSE TYPES

<u>Topographical Type</u>	<u>Character of Wind Roses</u>	<u>Stations</u>	<u>Modal Directions</u>			<u>Large or Small Scale</u>
			<u>Prim.</u>	<u>Sec.</u>	<u>Tert.</u>	
Mid-Valley, unobstructed	2 narrow modes; primary up-valley mode broader and with higher speeds; secondary down-valley mode narrower and with lower speeds; very few cross-valley.	Knoxville	SW-WSW	NE		Large
		001	SW-WSW	ENE		Small
		002	NW-N	SSE-S		Small
		003	SW-WSW	NE-ENE		Small
		004	SW	NNE-NE		Small
			SE-SSE	NW		Small
			SW	NE-ENE		Small
	SW-WSW	NE-ENE		Small		
Mid-valley, obstructed	Same as unobstructed but with very broad (>90°) primary mode in all seasons.	Bristol	SW-NW	NE-ENE		Large
		Rome	SE-SW	N-NW		Large
		006	SW-NW	ENE	NW (weak)	Large
		009	ESE-WNW	NNE-NE		Large
Lee-of-Mts.	Same as unobstructed but with additional cold-season W-NW mode, absent in summer.	Spartanburg	SW-WSW	NE-ENE	NW-NW	Large
		Chattanooga	S	NNE	NW (weak)	Large
		007	S-SSW	NNE	W-WNW	Large
		012	SW	NE	WNW (weak)	Large
		OR 2000 ft.	SSW-WSW	NE-ENE	WNW	Large
Slope	2 very broad modes: higher-speed upslope-up-valley; lower-speed downslope-down-valley.	005	SSE-SW	W-NE		Small
		010	WSW-WNW	degenerate		Small

A few points regarding the interpretation of Table 43 should be mentioned:

- a.. The northwesterly primary, or daytime mode at station 002 (Whiteoak Creek) and southeasterly at station 015 (South Whiteoak Gap) will be substantiated by the diurnal variations to be considered later.
- b. Since station 006 (Chestnut Ridge Top) has appreciable frequencies of northwesterly winds throughout the year (the winter maximum is used here as a criterion of large-scale control) only slightly reduced in summer, it is classed as an "obstructed mid-valley" instead of a "lee-of-mountains" station. Actually it is in a transition zone between the small-scale and large-scale wind regimes.
- c. Obstruction of the prevailing winds by terrain irregularities upwind apparently broadens only the daytime mode; a single large obstruction can also split this mode, as at Bristol and, to a lesser extent, at Rome and station 009 (Clinch River flats). The local NW-SE orientation of the river valley in the vicinity of the latter station appears to be ineffective in actually channelling the wind flow.
- d. The most important point brought out by this classification is that while there is a detectable difference between the Oak Ridge area, near the Cumberland Plateau, and Knoxville, near the center of the large valley, with respect to large-scale influences on the wind direction distribution, the effect of the small ridges in filtering out crosswinds is sufficient to cause the wind direction distributions at the Oak Ridge valley-bottom stations to resemble that at Knoxville more closely than they do those above ridge level in their immediate vicinity. The effect of these additional barriers on the wind speeds, on

the other hand, is to lower them much below those observed at Knoxville and other points exposed to the large-valley influence, and also to lower those within a few hundred feet above the level of the small ridge-tops. There is evidence, however, that above the lowest 500-800 ft. a compensation occurs, the wind speeds, particularly from the NW quadrant, being substantially greater at Oak Ridge than at Knoxville (see Fig. 113 and Table 40), thus tending to equalize the volume-transport across the two parts of the valley. The mechanism appears to be of the type described by Rossby (Ref. 54) although weakly developed.

The local variability of the wind speed is illustrated by Fig. 125, in which the average microneb wind speeds for the two fall quarters of 1949 and 1950 are plotted against both the elevation of the anemometer above sea level and its height above ground. The average pibal profile is shown as a dashed curve in each group. The upper graphs show that there is a definite rising trend of wind speed with sea level elevation in the Oak Ridge area, somewhat less on the hills than in the free air, but that variations of exposure introduce quite large deviations from the mean. It is evident that closeness to the earth is an important factor producing deviations, as in the case of stations 005 (Chestnut Ridge Slope) and 012 (X-10 Health Physics Division water tank in mid-valley), which are at the same absolute elevation, and similarly stations 010 (Haw Ridge slope) and 017 (Melton Valley). This factor is isolated in the lower graph, where again a rising trend of wind speed with increasing height above ground is noticeable, the greatest departures in this case being due to absolute elevation, as in the case of stations 007 (Melton Hill) and 017 (Melton Valley), which are on poles of nearly identical height. Some stations have anomalous average speeds even

when both these factors are taken into account: station 010, in particular suffers from severe obstruction of the wind by surrounding vegetation.

When daytime and night-time observations are averaged separately, the daytime points show less scatter when plotted against height above ground than against absolute height, while the reverse is true of the night observations. This suggests that the terrain irregularities have less effect in obstructing the wind during the day than during the night.

As a further measure of the local variability of the wind, 2-station joint frequency distributions of direction were obtained for selected pairs of stations by means of punched cards, sorted into four categories: (1) daytime (10 a.m. - 5 p.m.) with light winds (less than 5 mph at a specified station of the pair), (2) nighttime (10 p.m. - 5 a.m.) with light winds, (3) daytime with strong winds (5 mph or greater) and (4) nighttime with strong winds. The percentages of simultaneous wind direction observations at the two stations differing by 1 point ($22\frac{1}{2}$) or less on a 16-point scale, computed for each category and combinations of categories are shown in Table 44. The best agreement between stations exists during stronger winds. Station 012 agrees best with the low stations (001, 002, 003, 004, 008, 009, 010, 016, 017, 018, 011, and 013) during the day, and with the higher stations (006, 007 and 019) at night. The agreement between directions observed on two 18-ft. masts 1 mi. apart (001/004) is almost perfect on windy nights and almost nil on still nights, even less than between either and a nearby 40 ft. pole (003). The greatest overall frequency of agreement is 70%, between stations 012 and 017 (Melten Valley) in adjoining valleys separated by Haw Ridge. Several

TABLE 44

PER CENT OF TIME WIND DIRECTIONS AGREE WITHIN ONE POINT

<u>Stations</u>	<u>Lt. Wnd. Day</u>	<u>Lt. Wnd. Night</u>	<u>Lt. Wnd. Avg.</u>	<u>Str. Wnd. Day</u>	<u>Str. Wnd. Night</u>	<u>Str. Wnd. Avg.</u>	<u>All Obs.</u>	<u>Period of Sample</u>
012/001	53.3	36.5	44.9	89.3	71.3	80.3	63.5	1/50 - 10/50
012/002	21.2	19.5	20.4	29.9	19.7	24.8	23.0	1/50 - 11/50
012/003	56.9	44.2	50.6	83.3	80.3	81.8	66.1	1/50 - 11/50
012/004	54.2	38.5	46.4	85.2	71.3	78.3	63.0	1/50 - 11/50
012/005	38.8	44.3	41.6	78.5	86.5	82.5	64.3	1/50 - 8/50
012/006	39.7	38.0	38.9	74.8	76.9	75.9	57.4	1/50 - 11/50
012/007	45.1	42.1	43.6	76.4	84.4	80.4	61.8	1/50 - 11/50
012/008	48.6	46.6	47.6	83.2	81.5	82.4	65.4	1/50 - 11/50
012/009	34.1	26.3	30.2	84.9	70.3	77.6	63.4	1/50 - 4/50
012/010	22.7	19.5	21.1	56.1	50.4	53.3	43.4	1/50 - 3/50
012/016	48.1	33.6	40.9	78.1	65.5	71.8	54.9	5/50 - 3/51
012/017	58.4	56.6	57.5	87.8	83.7	85.8	70.4	10/50 - 9/51
012/018	41.9	42.9	42.4	54.5	50.8	52.7	47.1	10/50 - 9/51
012/019	47.7	46.3	46.5	81.8	87.4	84.6	63.2	10/50 - 9/51
012/011	39.8	33.4	36.6	61.2	52.6	56.9	46.3	1/50 - 12/51
012/013	28.0	35.7	31.9	47.9	46.9	47.4	39.8	1/50 - 10/51
012/021	58.8	48.9	53.9	81.6	86.4	84.0	65.0	7/51 - 12/51
001/003	54.8	40.7	47.8	87.1	90.6	88.9	58.3	9 & 12/49, 3 & 6/50
001/004	51.5	28.1	39.8	93.8	96.5	95.2	54.2	"
003/004	55.1	47.6	51.4	83.8	86.9	85.4	61.4	"
001/Knex.	--	--	--	--	--	--	57.0	6/49 - 11/50

other stations agree with station 012 more than 60% of the time, including 019 (Pine Ridge) over 5 miles away. The poorest overall agreement, 23%, is between two stations less than 1 mi. apart, 012 and 002 (Whiteoak Creek) whose prevailing directions are perpendicular to one another. The night-time frequencies of agreement between these two stations, less than 20%, are approximately the same as would be obtained with completely random directions at either station. The percentage of agreement between the X-10 Field Station (001) and Knoxville airport (57%) is about equal to the average for pairs of valley stations within the Oak Ridge area.

In those cases where the percentage of agreement is less than 50%, which occurs most commonly with light winds, it is natural to wonder what the prevailing local wind patterns actually are. As an illustration, the joint direction frequency distributions, combined into quadrants (the original data are to 16 points) for stations 012 and 005 are given in Table 45. It can be seen that the most frequent discrepancies consist of the combination in the daytime of SE winds at station 005 (Chestnut Ridge slope, facing SE) with various other directions at station 012 (X-10 Health Physics Division water tower, about the same elevation), particularly SW, and the combination at night of NW winds at station 005 with calm or other directions, particularly NE, at station 012. These patterns simply reflect the up-slope day wind and down-slope night wind at station 005. If the wind at station 012 is either NW or SE, that at 005 is usually in the same direction regardless of the time of day.

Similarly, characteristic combinations of directions can be found at other

TABLE 45

JOINT DIRECTION FREQUENCY (%), STATIONS 012 AND 005, BY QUADRANTS

A. Light (<5 mph), day (10 a.m. - 5 p.m.)

Station 005	Calm	Station 012		SW	NW	Total
		NE	SE			
Calm	1.3	1.9	0.4	1.4	0.1	5.2
NE	0.7	13.0	0.7	1.7	0.4	16.5
SE	1.9	13.5	11.6	16.0	1.6	44.5
SW	0.5	0.7	0.8	7.0	0.4	9.4
NW	3.7	7.0	1.3	5.8	6.6	24.5
Total	8.2	36.1	14.7	31.9	9.0	100.0

B. Light (<5 mph), night (10 p.m. - 5 a.m.)

Calm	8.8	7.2	0.7	5.8	0.5	23.0
NE	1.8	14.2	0.9	0.7	0.4	18.0
SE	1.7	4.0	3.3	3.1	1.0	13.2
SW	1.3	0.5	0.6	14.1	0.2	16.7
NW	8.1	8.6	0.4	6.2	5.9	29.2
Total	21.7	34.4	6.0	29.9	8.0	100.0

pairs of stations. A few of the more frequent and interesting ones are:

- (a) SE at station 015 (S. Whiteoak Gap) with N at station 002 (N. Whiteoak Gap) during the day: convergence into the gap.
- (b) S at station 002 with any direction at station 012 at night, with low speeds (<5 mph at 012): outflow from the gap, opposite to Whiteoak Creek drainage.
- (c) N at station 002 with NE at station 012, and S at 002 with SW at 012 during the day, or when the speed at 012 is 5 mph or more: frictional through-flow from high towards low barometric pressure.

- (d) W at station 010 (Haw Ridge Slope, NW-facing) with S at 012 in the daytime or with strong winds, and SE at 010 with light W at 012 during the night: diurnal up-slope and down-slope winds, weakly developed.
- (e) SW at station 008 (Y-12: a valley which slopes downward towards the NE with calm at 012, day or night: reflecting the large-valley day wind and small-valley night wind.
- (f) NE at station 016 (Whiteoak Lake in Melton Valley, a relatively long slope downward towards the SW) with light SW or calm at 012; calm at 016 with stronger SW at 012 at night: down-valley wind overcoming or just balancing an opposing general flow.
- (g) SW at station 001 (X-10 Field Station: a slight E-slope) with light NE at 004 (Bethel Church: a slight SW-slope) at night; also calm at 001 with light NE at 004, and calm at 004 with light SW at 001: converging drainage flow from both ends of the Whiteoak Creek drainage basin in Bethel Valley.

These characteristic local wind flow patterns are closely associated with the diurnal temperature cycle. With the exception of the highly channelled gap winds, they are in general not highly frequent in terms of total percentage, occurring on the order of 5-15% of the duration of the appropriate category, or 1-4% of the total time. They are overshadowed by stronger, larger-scale currents the remainder of the time, which, while obviously not producing identical directions at all stations, do keep them more or less

within the same quadrant. The diurnal wind direction patterns will be discussed more fully in the next section.

Wind roses for the plant and town sites (outside the area covered by Figs. 117 - 124) are shown in Fig. 126. Annual wind roses for 1949-1950 are given for stations 008 (Y-12), 011 (Townsite: 8-point direction record), 012 (X-10 Health Physics Division) and 013 (K-25). For comparison, the wind rose for station 012 for the period of record (1944-1951) is also given, and those for the available period of record at the new stations in the K-25 (021) and Y-12 (018) areas and on Pine Ridge (019). It is seen that the short- and long-period wind roses at X-10 do not differ in any important respect. The higher percentage of calms shown in the short-period rose is due to the replacement of the older contacting anemometer in 1949 by a generator type having a higher starting speed. The transfer of the Y-12 instruments from station 008, which was close to the NW edge of the valley (Bear Creek Valley), to station 018, lower and nearer the valley axis, resulted in elimination of the NNE-SSW slope components while the change from a contacting to a generator type anemometer raised the percentage of calms considerably. Both Y-12 stations show more westerly-southwesterly wind in proportion to the northeasterly than do the stations in level or SW-draining valleys. In this respect they are comparable to station 001 (see Fig. 117). Station 013 at K-25, exposed rather low and on a slight slope, shows an anomalous frequency of northwesterly wind which may be a very local effect or one connected with the relative closeness of the Cumberland Mountains and the Clinch River. Station 009 (farther up the Clinch Valley) shows this to a much lesser extent (Fig. 117), while station

021, the new K-25 plant station, high (40 ft.) above the highest building, has a wind rose resembling those at other Oak Ridge valley stations such as 012 (X-10). Station 011 (Oak Ridge Townsite), with an 8-point vane bearing, appears to have a fairly typical mid-valley wind direction distribution. Station 019, high above Pine Ridge, has large frequencies of SSW and NNE with a tertiary mode from W reminiscent of Melton Hill (see Fig. 117 and Table 43). Wind roses for station 012 under average, day, night, stable, unstable and precipitation conditions are shown in Fig. 127. The up-valley (SW) mode is dominant in day and unstable (lapse) conditions, the down-valley (NE) mode in night and inversion conditions, and the precipitation wind rose is quite similar to the average daytime one.

The local variation of average wind speed has been mentioned: the annual course of monthly mean speed at station 011 (Oak Ridge Townsite) and 012 (X-10 Health Physics Division) is shown in Fig. 128. The highest average wind speed occurs in March and the lowest in August at both stations, with station 012 (140 ft. above ground) consistently about 50% higher than 011 (about 10 ft. above a 30 ft. roof). The individual monthly average speeds deviate within narrow limits from the average of record, and there is no evidence to indicate that the annual mean at either station departs from normal by more than a few tenths mph. In view of the complex local effects, recent changes of instruments at many Weather Bureau stations, and the apparent stability of the seasonal averages for the period of record at Oak Ridge, there appears to be no advantage to be gained in deriving adjusted normals of wind speed or direction by reference to longer records

at nearby stations.

With the apparent relative stability of the mean speeds in mind, the short records of this survey can be used to obtain an order of magnitude estimate of the probability of any particular wind speed being exceeded, at a wide selection of altitudes and exposures. Figs. 129 - 130 contain graphs of the observed cumulative frequencies of wind speed, Fig. 129 presenting data from a range of altitudes arranged for easy interpolation of seasonal probabilities, and Fig. 130 comparing various exposures on an annual basis.

28. Diurnal Wind Variations

Local wind patterns are mainly of two types: diurnally varying convective circulations induced by horizontal atmospheric density gradients, and dynamic patterns induced by the large-scale flow in passing across the hills and ridges. The diurnal variation is of sufficient interest and importance to warrant rather detailed examination, which is the subject of this section. The local wind variations associated with larger-scale flow patterns will be considered later.

A preliminary view of the day and night wind regimes in both the larger and smaller valleys has already been presented in the preceding sections. Generally speaking, the air near the ground tends to move upslope during the daytime under the influence of density gradients between the free air over the valleys and the heated layer next to the hill and mountain surfaces, and downslope during the night as it is cooled by contact with the radiating slopes. The day breezes are more vigorous and involve a greater depth of atmosphere, at the same time being more subject to modification

by mixing with upper streams than the night breezes, which are very light, relatively shallow and steady in direction, and insulated by thermal stability from the effects of the upper flow.

This oscillation is repeated in varying degrees on the large scale of the Southern Appalachian Valley (of the order of 50 mi. wide and several thousand feet deep), the smaller scales such as that of Bethel Valley (less than 1 mi. wide) and its adjoining ridges (about 300 ft. high) and the still smaller scales of the local drainage basins within Bethel Valley, such as that of Whiteoak Creek (about a mile in diameter and 50 ft. in depth).

Entirely dependent upon the maintenance of local temperature differentials, its degree of development varies with the cloudiness and daily temperature range as well as with the degree of mixing due to thermal convection or mechanical turbulence. The two-station wind direction comparisons previously discussed show that local patterns are best developed (parallel flow at pairs of stations is least frequent) with low wind speeds at night.

Most of the examples to be discussed are derived from the fall season, since it is in this period that the combination of low wind speeds, clear skies and long nights occurs most frequently, and the diurnal patterns (particularly the nocturnal ones) are brought out to best advantage.

Effects due mainly to daytime heating, however, are best displayed in the summer.

To begin with, the diurnal cycle of wind speed alone, disregarding direction variations, will be considered, as shown by pilot balloon observations (Nov. 1948-Nov. 1950; Fig. 131) and anemometers (Fig. 132). The corresponding annual graphs are shown in Fig. 151 together with average vertical

profiles of wind speed. The most striking features of the cycle in all seasons are the increase in wind speed from night to day at low levels and the reversal aloft. Turbulence tends to mix and equalize the momentum of the various layers: it constitutes an enhanced viscosity. Since daytime surface heating produces instability, convection and, in turn, downward flux of momentum, the speeds of the upper and lower layers are more nearly equal during the day than during the night, when vertical exchange is suppressed. The shearing stress at the earth's surface increases with increasing wind speed in the surface layer, hence the loss of momentum to the ground is greater during the day than during the night, when the surface layer is slowed to a near calm while the winds a few hundred feet above the surface suffer relatively little loss of momentum by downward eddy flux. The resulting daytime thickening of the frictionally retarded layer and concentration of shear in a narrow boundary layer accompanying turbulent flow is well known in laboratory hydrodynamics (Ref. 55).

The level of reversal of the diurnal wind speed curves from the day-maximum to night-maximum type is apparently about 500 ft. above the valley bottom in summer, and somewhat lower in the other seasons. The level at which the diurnal amplitude reaches its maximum is about 3000 ft. in spring, 1200 ft. in fall, and 2000 ft. in winter and summer, and thus apparently varies with both the average wind speed and the instability, both of which would facilitate daytime frictional depletion of momentum from the upper layers. By 5000 ft. above ground, the diurnal variation has become relatively insignificant in all seasons. The daytime up-valley breeze, propagated at

low levels, inverts the normal increase of speed with height in spring and summer between 525 and 875 ft. There is no sign of the nocturnal down-valley breeze in the curves of Figs. 131 and 132. The dependence of the wind speed at the lowest levels upon convective transfer from above is emphasized by the resemblance of the 6 ft. and 18 ft. curves (Fig. 132) to the diurnal curves of temperature lapse rate in comparable layers (Figs. 77 - 79) and, in turn, to those of solar radiation, with a lag of one or two hours.

Both the direction and speed variations will now be considered by means of graphs of hourly wind direction frequency by quadrants and hourly average speed for pairs of stations (Figs. 133 - 138). Fig. 133 compares the highest hill top, Melton Hill (007) with the most representative low mid-valley station, West Bethel Valley (003) during each of the four seasons, Summer 1949 through Spring 1950. Melton Hill, 600 ft. above the valley, is in the layer of day minimum wind speed in all seasons, while station 003 has the typical low-level day maximum. Thus the reversal of phase of the diurnal cycle of wind speed shown by the pilot balloon observations is supported by the anemometer observations, as it is also by the reports of many previous investigators (Ref. 56). The Melton Hill speeds are, however, somewhat lower than those in the free air at a comparable height above the valley (Fig. 136); in fact, in midday they approach closely the values recorded at heights above the valley floor comparable to the height of the Melton Hill anemometer above the treetops (about 30-40 ft.). Thus, as was indicated previously in connection with mean wind speeds, the elevation of the hills has little effect

in the daytime, but is very important at night.

As to the diurnal direction variation, it is clear that the valley winds (003) are not only subject to greater channelling by the ridges (i.e. fewer cross-valley winds) but also to greater diurnal control. Since station 003 is at a location where the local slope is negligible, the proportion of northeasterly and southeasterly winds can be considered representative of the large-valley currents, with the exception that large-scale NW or SE winds appear only as contributions to the frequencies of NE, SW or calm at station 003. It is of particular interest that SW predominates at Melton Hill during most of the night and is in fact more frequent at night than in the daytime, so that while the northeasterlies are more common even at this level at night than in the daytime, they usually do not extend this high, and are even replaced by a counter-current. As a further indication of the low level of maximum development of the NE current it can be seen that the daily peak frequency of NE at Melton Hill occurs at about the time of first coupling between the hill top and valley layers by the onset of turbulent mixing in the morning, as shown by the close approach of the hill and valley speed curves. After that time, deeper mixing, combined with the reversal of the thermal driving force, dissipates the drainage current entirely.

At the slightly lower levels of Chestnut Ridge top (006) and the top of the X-10 water tank (012), about 100-300 ft. above the valley floor (Fig. 134), the day maximum predominates, very weakly on the ridge top, but rather

strongly in the free air. Aside from the difference in elevation between the two stations, there appears to be an additional effect due to frictional retardation by the ridge, since the ridge top speeds, although nearly identical with those in mid-valley at night, are much lighter in the daytime, again resembling those recorded 20-40 ft. above the valley bottom. This daytime retardation results in a nearly constant average speed throughout the day and night, while the free air level of reversal is probably somewhat higher. Similar seasonal changes in amplitude of the speed curves occur at both stations, winter showing the least amplitude and spring the greatest, although the mean speeds are nearly identical.

Again the wind directions at the mid-valley station (012) reflect greater channelling than those at the ridge-top (006), but since the difference in elevation is so small the greater scatter of directions at the ridge top would seem to be at least partly attributable to interference by the ridge. There is a weak diurnal oscillation of the cross-valley frequencies at both stations but particularly at 006, suggestive of a possible effect due to Cumberland Mountain slope winds: maxima of SE in midday and NW in the early evening; also the frequency of nocturnal SW winds increases over that observed in the lowest layers of the valley (e.g. station 003, Fig. 133) at the expense of NE even at this level.

Two valley-floor stations (18 ft. above ground) are next compared (Fig. 135): station 001, (X-10 Field Station) in the eastward-draining portion of Whiteoak Creek basin of Bethel Valley, and station 004 (Bethel Church), in the SW-draining portion. They are at about the same elevation and are 1 mile apart. Their diurnal speed curves are nearly identical, showing

a pronounced day maximum and low average speeds in all seasons. Both show marked channelling, with very few cross-valley winds; the daytime distributions of direction frequency between the NE and SW quadrants agree within a few percent. The main difference is in the nocturnal direction distributions: station 001 shows a predominance of SW, particularly in the early evening, while station 004 generally shows an excess of NE throughout the night. This convergence has already been commented on in the discussion of joint direction frequency distributions at pairs of stations in the preceding section. It is of particular interest that the increase of mean speed in the morning, brought about by the beginning of vertical mixing, is accompanied in all seasons by a transitory increase in the frequency of NE at station 001. This short period after sunrise, in which NE winds are brought down from above the layer of dissipating local SW drainage wind, is the only one in which station 001 has a prevailing NE wind. It is evident that the local slopes of these sub-valley configurations have no significant effect on the daytime wind direction pattern but do affect the nocturnal air drainage in a shallow layer; thus a valley station in a region of local northeastward surface drainage has prevailing SW winds both day and night with the exception of the morning inversion breakup period.

From ridge-top level up to 2200 ft. above the valley (3000 ft. MSL) the diurnal variation of direction weakens rapidly, although the speed variation increases steadily, as illustrated by the observations of Fall, 1949 (upper left hand graph, Fig. 136). The degree of channelling decreases to insignificance. At 525 ft. above the valley, a direction pattern similar to that at Melton Hill is observed (upper right hand graph, Fig. 136), with SW prevailing throughout the day and night except for a brief

period of prevailing NE just after sunrise. A slight increase of NE frequency at the 7 a.m. observation is still noticeable at 1200 ft. but has vanished at 2200 ft.

The Pine Ridge station (019) somewhat higher and better exposed than that on Chestnut Ridge (006), shows a very similar diurnal wind pattern (lower left hand graph, Fig. 136). Some 400 ft. above the valley, it shows a weak day minimum but a very small diurnal amplitude of speed. Its wind directions are more channelled than those at 006 indicating again the probability of disturbance by the surrounding terrain at the latter station. Practically no diurnal wind direction pattern is observed at station 019, SW being the prevailing direction at all hours. This appears to be an anomaly, but is based on a relatively short period of observations. That anemometer and wind vane records give essentially the same results as pibals under comparable conditions is borne out by the comparison of station 012 with the 175 ft. pibal level (lower right hand graph, Fig. 136).

Stations located in parallel valleys are compared in Fig. 173: suitably chosen analogues with respect to local slope apparently have similar diurnal wind direction distributions, while the wind speeds are dependent mainly upon altitude above the surrounding vegetation and buildings. Station 001 is a good analogue for station 008, the two being situated in adjacent valleys (Bethel Valley and Bear Creek Valley) with local east-northeastward surface drainage. Station 004 and 016 both have southeastward local drainage, and stations 003 and 011 are at neutral points between diverging surface drainage slopes. Stations 009 and 013 are both in the Clinch River

valley, which is oriented roughly NW-SE: both exhibit the NE-SW pattern characteristic of the other valley stations, but more weakly developed, particularly at station 013. Both have more wind from the NW and SE quadrants than do the others, station 013 showing the largest proportion of NW, with a weak diurnal oscillation between NW at night and SE in the daytime.

The opposing slope winds of Chestnut Ridge (005) and Haw Ridge (010) in the summer of 1949 are illustrated by the upper left hand graph of Fig. 138. The few winds other than calm observed at station 010 were daytime upslope winds (NW). Station 005 shows both a well developed daytime upslope wind (SE) and a well developed nocturnal downslope wind (NW), the period of maximum SE coinciding with the period of maximum temperature differential between the slope and the free air, in fact the diurnal curves of frequency of NW and SE wind have very similar shapes to the temperature differential curves of Figs. 72 and 76.

Daytime convergence into Whiteoak Creek Gap in Haw Ridge is strikingly illustrated in the upper right hand graph of Fig. 138; night-time outflow on the north side is shown by the station 002 data, while the night winds on the south side are completely obscured by calms owing to the instruments' location among thick brush. The evidence seems to indicate that diurnal through-flow in the usual up-slope or down-slope direction does not occur to any appreciable extent. Instead the air behaves as though the gap were effectively a narrow portion of Haw Ridge, the inflow and outflow simply being up-slope and down-slope

winds with respect to the ridge. The nocturnal convergence of the winds into the lowest part of Bethel Valley shown by stations 001, 002, 004, and 005 would necessitate a continuous upward movement of air in this area. Very little air is actually involved, however. An idea of the depth of the local drainage currents can be obtained from the lower graphs of Fig. 138, diurnal graphs derived from observations at three levels (6 ft., 18 ft. and 54 ft.) on the station 001 "profile pole." There is little change between 6 and 18 ft. In the early evening, the frequency of the SW drainage wind drops by about half between 18 ft. and 54 ft. and probably does not extend far above the latter level. Fig. 139 shows the cloud from a smoke pot ignited under inversion conditions just after sunrise at station 001 and seen from the northwest. The drift to the left (SW drainage) is some 20-50 ft. deep, with reverse flow above (NE drainage). One important aspect of the diurnal direction variations so far presented is that the frequencies of the local prevailing wind, by 90° sectors, seldom exceed 60% in any hour, and are most commonly between 30 and 50%. The remaining observations are from other quadrants or calm, and in the case of the typical valley stations, mostly from the direction opposite the prevailing one. In addition, the cross-valley and along-valley direction frequencies usually vary simultaneously, and, finally, the different directions may be associated with different wind speeds. Thus, while the diurnal trends of average speed and prevailing direction have been indicated, the components of the wind vectors specifically induced by the diurnal temperature cycle have not been isolated by the preceding analysis. In order to find these vectors, quarterly resultant winds at each station have been calculated for each hour of the day. The aperiodic wind variations during each season have thus been eliminated and the residue, although not necessarily itself a commonly observable wind, is the sum of the components contributed by the mean seasonal flow and the diurnal density currents. By

reducing the wind observations at each station to one mean vector, the hourly resultant winds provide a unique representation of the wind flow at each time, such as is shown in Figs. 140 and 141. These two figures contain three-hourly micronet maps of the resultant wind, represented by arrow-shafts with feathers on the end from which the resultant wind blows, the number of feathers (or half-feathers) being equal to the magnitude of the resultant vector in mph. The resultant wind speed increases with both the mean wind speed and the directional steadiness of the wind, since opposing components cancel.

In both the summer of 1949 (Fig. 140) and the summer of 1950 (Fig. 141), the hourly resultant winds at the typical valley stations (003, 004, 012, 016) swung between more northeasterly directions at night and more southwesterly during the day, but superimposed upon this diurnal oscillation there was obviously a westerly or northwesterly mean wind in the summer of 1949 and a more southwesterly or southerly mean wind in the summer of 1950. The result was that the nocturnal northeasterly winds were turned to northerly in 1949 and easterly in 1950, and similarly the daytime southwesterlies were turned to westerly in 1949. Local northerly winds such as the nocturnal downslope wind at station 005 were favored by the 1949 pattern. However, the convergence of nocturnal drainage into the Whiteoak Creek basin of Bethel Valley is evident in both summers. Diurnal transitions such as the cross-valley winds arising from differential slope heating vary between the two summers: in 1949 the midmorning SE valley wind components were largely lacking, while the late afternoon NW winds appeared to advantage, almost the exact reverse being true in 1950.

A more refined approach is necessary in order to separate the climatological diurnal variation of the wind from the accidental mean wind of the particular season. The diurnal curve (hodograph) made by the heads of the hourly resultant wind vectors from a given station when plotted in polar coordinates and connected in sequence is a useful tool for this purpose. Such diurnal resultant hodographs, for a selection of microneet stations and seasons are shown in Fig. 142. They have a number of interesting characteristics.

Before attempting to explain the observed diurnal resultant wind hodographs, it is worthwhile to consider briefly the more important component diurnal cycles contributing to the resultant cycle of the wind under various conditions of exposure. These may be listed as follows:

- (a) Reduction and turning of the gradient wind by friction. It has long been known to meteorologists that the surface wind is less than that (geostrophic wind) necessary to account for a balance between the pressure-gradient force and the Coriolis force due to the earth's rotation. It has also been well known that the direction of the surface wind is neither directly along the isobars (as required by geostrophic balance), nor directly across them from high to low pressure (as in the case of a simple balance between surface frictional force and the pressure-gradient force) but is somewhere in between. Standard textbooks in dynamic meteorology (Refs. 56 and 57, for example) contain summaries of the distinguished researches which led to the derivation and verification of the "Ekman spiral" for the

atmosphere and the relation of both the speed ratio and the direction angle between the surface and gradient winds to the eddy viscosity, thermal stability and surface roughness. Suffice it here to say that in general, disregarding the deformation of the wind flow by topography, the wind vector in the surface layers (lowest 100 ft. or so) approaches the gradient wind most closely, with respect to both direction and speed, during the day or under unstable conditions, and departs most widely from it at night or under inversion conditions. The surface wind is always "backed" (rotated counterclockwise) from the gradient wind, that is, the geostrophic component has high pressure on the right (in the Northern Hemisphere) and the frictional component is directed from high to low pressure. The two components are not in phase, the frictional (cross-isobar) component leading the gradient component by a few hours in the diurnal cycle. The result is an elongated, approximately elliptical, clockwise diurnal hodograph, with the maximum speed near noon and the minimum near sunrise.

- (b) Up- and downslope components. Resulting from the temperature excess of the air next to elevated terrain over the free air during the day, and the reverse during the night, these breezes include an inertial effect and therefore lag slightly behind the temperature difference cycle. In small hills, however, the lag is negligible, the momentum being dissipated almost as soon as it is generated. The effects of inertia and the Coriolis force would be to produce a clockwise elliptical hodograph, but in small ridges this can be approximated by a

direct upslope-downslope oscillation. The literature regarding such winds is reviewed in simple terms in Ref. 58, and recent contributions to the subject have been made by Defant (Ref. 59) and Fleagle (Ref. 60). The latter shows that the nocturnal drainage wind on an infinite slope begins with a damped oscillation with a period of the order of 20 min. Such pulsations are of course obscured by taking hourly resultants, but the original records, under certain conditions, seem to indicate that they do occur.

- (c) Up- and down-valley components. The diverging winds on the opposite sides of a valley are fed partly by recirculation in a plane perpendicular to the valley axis, and partly by a low-level air current into the valley from the adjacent plain, and along the valley axis from lower towards higher elevations. Similarly, the nocturnal drainage winds collect in the valley floor and form a down-valley current. These currents, involving larger volumes of air travelling over greater distances, show greater effects of inertia and Coriolis force than do the slope winds, and consequently tend to have an elongated clockwise elliptical hodograph lagging a few hours behind the temperature-difference (mountain vs. free-air) cycle. This system is also described in Ref. 58. The maximum up-valley wind occurs in mid-afternoon, and the maximum down-valley wind shortly after sunrise.
- (d) Cross-valley components due to differential slope heating. The temperature difference between opposing slopes due to their orientation with respect to the sun has already been discussed. Cross-valley

winds of considerable magnitude and practical importance due to this horizontal density differential have been observed in the Columbia River Valley by Hewson (Ref. 61) and Cross (Ref. 62). A theory to account for them quantitatively has recently been developed by Gleeson (Ref. 63) utilizing particle dynamics with inertia and Coriolis force considered. The result is again an elongated clockwise-rotating hodograph (not elliptical because of the absence of a nocturnal reversal) which should reduce to a direct cross-valley oscillation for small valleys where lag and rotation can be neglected. In a NE-SW oriented valley, this current reaches its maximum development in mid-morning, and therefore leads the other cycles discussed so far.

Other diurnal cycles which could probably be detected in this area but are of lesser importance are the varying stability effect on lee-wave or lee-eddy currents described by Morgans (Ref. 64) in a summary of earlier work by many investigators and by Colson (Refs. 65-67) and Queney (Ref. 68) in more recent theoretical and observational studies, and the large scale quasi-monsoonal components found by Wagner (Ref. 69) and related to the mountain-plain and continent-ocean distributions. In a very general treatment of the diurnal variation of the wind E. Kleinschmidt, Sr. (Ref. 70) has shown how various local cycles in the horizontal pressure distributions (mountain-valley, land-sea) are combined with the "convective" cycle (modification of the large-scale pressure-gradient effect by the diurnal variation of eddy-mixing) and how among other things, two elongated clockwise elliptical components may combine, with proper phase and direction

angles, to produce a counter-clockwise resultant hodograph.

Fig. 142 contains diurnal resultant wind hodographs for the five seasons Fall, 1949 through Fall, 1950 for a selection of stations. The "type" stations 003 (west Bethel Valley), 005 (Chestnut Ridge Slope), 010 (Haw Ridge Slope) and 006 (Chestnut Ridge Top) represent, respectively, mid-valley, SE-facing slope, NW-facing slope and ridge-top exposures. The remaining stations represent problematical exposures to be typed by comparison with the foregoing. The seasons may be briefly characterized as follows:

Fall 1949: relatively strong NW gradient, large amplitude of the diurnal cycles.

Winter 1949-1950: moderate W gradient, small diurnal amplitude.

Spring 1950: very strong W gradient, large diurnal amplitude.

Summer 1950: moderate W gradient, moderate diurnal amplitude.

Fall 1950: weak NE gradient, moderate diurnal amplitude.

Obviously the characteristic local hodographs are not simply displaced from the origin by various amounts each season in accordance with the mean gradient wind for the period: the diurnal variation of the frictional component affects their shapes considerably. The patterns will be discussed station by station.

Station 003 (West Bethel Valley), the typical mid-valley station, generally has an elongated clockwise hodograph with the maximum up-valley (SW) component about 2-3 p.m., the maximum down-valley component 6-9 a.m., the

maximum NW cross-valley component 6 p.m. and the maximum SE cross-valley component 11 a.m. The cross-valley components have the correct phase to be accounted for by differential slope heating and have an amplitude of about $\frac{1}{2}$ mph, in comparison with an up-down valley amplitude of about 3 mph. However, in the fall of 1950 the NW gradient, producing a maximum NW component of the surface wind about noon and a minimum at night, apparently overbalanced the thermal cross-wind to produce a counter-clockwise hodograph. This is almost exactly the combination shown in Kleinschmidt's Fig. 4K (Ref. 70, part 3). In the spring of 1950, on the other hand, the frictional cycle with a strong W gradient reinforced the local up-down-valley regime, as in Kleinschmidt's Fig. 4C.

Station 005 (Chestnut Ridge Slope), facing SE, always has a more or less broad clockwise hodograph. The maximum speed occurs at the time of the maximum up-valley breeze and is intermediate in direction between upslope (SE) and up-valley (SW). The downslope component reaches a maximum 2-5 a.m. and the amplitude of the slope circulation is about 2 mph at the anemometer level (35 ft.). From the observations reported in the literature it appears likely that the down-slope current is stronger closer to the ground.

Station 010 (Haw Ridge Slope), although its SE down-slope wind is completely masked by calms, characteristically has a counter-clockwise hodograph resulting from the superposition of the up-down-valley and up-downslope cycles, a few hours out of phase, and with the latter component in the opposite sense to that at station 005 (again resembling Kleinschmidt's Fig. 4K). Both the opposition of the thermal cross-valley component to the

slope component and the obstructing effect of the surrounding forest combine to reduce the amplitude of this hodograph to about $1\frac{1}{2}$ mph in the up- and down-valley direction (about the same as at station 005) and about $\frac{1}{2}$ to 1 mph in the up- and downslope direction.

Station 006 (Chestnut Ridge Top) has a well-developed clockwise hodograph with less up- and down-valley amplitude but greater cross-valley amplitude than has station 003. It would appear, then, that this station is subject entirely to the large-valley circulation with its greater slope and cross-valley currents, since it would be expected to be independent of the small-valley circulation. In most seasons a marked nocturnal SE component, not as strong as the daytime one, appears between 9 p.m. and 3 a.m. Since this appears at all the stations in the Southern Appalachian Valley and increases in importance towards the Great Smoky Mountains, it is very likely a mountain wind crossing the entire valley and partially overcoming the weaker Cumberland Mountain drainage current.

Station 002 (Whiteoak Creek), the first of the "problem" stations, is located in the gently SE-sloping valley of Whiteoak Creek. We have already seen that the day wind is downslope (N) and the night wind upslope (SE) with respect to this valley. Now it is seen that the diurnal resultant hodograph forms a counter-clockwise loop in all seasons, suggestive of a NW-facing slope. It is, in fact, almost a mirror-image of the station 005 hodograph. If the diurnal wind regime at this station is determined entirely by its location with respect to the Haw Ridge axis, regardless of

the Whiteoak Creek Gap, then no significant diurnal through-flow can be expected.

Station 015 (South Whiteoak Gap) was installed for the purpose of testing whether through-flow occurred. Its hodograph is that of a SE-facing slope,, clockwise and with its long axis perpendicular to the ridge line. The diurnal components of the wind at stations 002 and 015 apparently converge during the day and diverge during the night, with no significant parallel flow (in the same sense at both stations) at any time of the day. Thus it can be concluded that the gap acts somewhat as a ravine in filtering out NE and SW winds, but not as a channel for density currents from the higher to the lower valley.

Station 012 (X-10 water tower) is the last of the local stations represented in Fig. 142. It is high enough to be above the layer of influence of the cross-valley wind induced by differential heating of the slopes of the small ridges. However, like station 006, it has a broader clockwise hodograph than does station 003, so that it can be concluded that it is under the influence of stronger cross-valley currents induced by heating and cooling of the larger mountains, and obstructed by the small ridges. Here, too, as at station 006, the northwesterly gradient of the fall of 1949 virtually cancelled out the cross-valley thermal circulation, but did not reverse it as at station 003.

The larger scale topographical features possess even less symmetry than do the local ridges, and the diurnal hodographs at the large-valley airport

stations reflect this. Fig. 143 shows diurnal resultant wind hodographs at Bristol, Knoxville, Chattanooga, Rome and Smithville for each season, averaged over periods of 3 to 10 years, and only those observations with 3/10 or less cloudiness being used in order to exaggerate diurnal influences.

Bristol has a long clockwise hodograph oriented E-W, and roughly elliptical except for an indentation from the south between about 8 p.m. and 3 a.m. reminiscent of a similar indentation in the station 006 and 012 hodographs, and presumably due to a Great Smoky Mountain drainage wind.

Knoxville shows this southerly or southeasterly component to a much more marked degree, consistent with its relative closeness to the highest portion of the mountain range. The fall and winter hodographs at Knoxville are actually counter-clockwise, as at a NW-facing slope station.

The spring hodograph is figure-8 shaped, the day wind rotating clockwise and the night and early morning wind counter-clockwise. The summer hodograph is a fairly normal clockwise mid-valley type with the exception that the day wind is slightly inclined from the valley axis (southwesterly) towards the mountains (northwesterly), and a slight nocturnal south wind is still evident.

At Chattanooga the seasonal hodographs resemble those at Knoxville, being counter-clockwise in fall and winter, 8-shaped in spring and summer.

The relative direction of the down-valley wind, most marked at 8-9 a.m. is here northerly as contrasted with a maximum relative NE component at Bristol 4-5 a.m. and at Knoxville 5-6 a.m. The relative day wind at Chattanooga is, surprisingly, westerly.

The Rome, Georgia hodographs repeat those of Chattanooga to a great extent, the maximum northerly component now occurring between 9 a.m. and noon, but with northerly-northwesterly resultants being the rule throughout the day.

Smithville, outside the valley on a very broad general slope facing the Mississippi-Ohio Valley on the west and northwest, shows a well-developed clockwise hodograph with the night-day axis oriented roughly NW-SE. The combination of S or SW average gradient and this slope circulation is approximately that shown by Kleinschmidt in Ref. 70, Part 3, Fig. 4d or 4e, and the result is a broad, clockwise ellipse.

To summarize the evidence from diurnal resultant hodographs with respect to the thermally induced wind components, it can be said that the up- and down-valley circulation has an amplitude of 3-5 mph, with the maximum up-valley component generally westerly occurring about 3 p.m. throughout the valley, and maximum down-valley component, varying from easterly at Bristol to northerly at Chattanooga and Rome, occurring progressively later down the valley, from 4-5 a.m. at Bristol to 9 a.m. at Rome, a distance of over 250 mi. (obviously this "crest" does not represent the same air at all the stations). The cross-valley components are quite variable, the mid-morning breeze, for instance, being directed toward the NW at Oak Ridge above the

local ridge-top level, and also at Bristol, but towards the SE at Knoxville, Chattanooga and Rome. While the main evening cross-valley components are generally opposite to these, a more or less pronounced SE drainage wind component can be seen at all large-valley stations during the early night hours. Within the smaller Oak Ridge valleys, the large cross-valley components are missing, an independent and roughly parallel circulation, of smaller amplitude, being set up. At mid-valley, the cross-valley amplitude is about $\frac{1}{2}$ to 1 mph compared with 1-2 mph above ridge-top level and at Bristol and Knoxville. On the local slopes themselves, the up- and downslope amplitude is 1-2 mph with the maximum upslope wind occurring near noon. No air drainage through small gaps in the ridges, such as Whiteoak Creek Gap in Haw Ridge, is evident, the local diurnal components being most readily explainable as slope or ravine winds with comparable diurnal amplitude of oscillation (1-2 mph). As a result the portion of the Whiteoak Creek drainage basin within Bethel Valley acts somewhat as a "frost pocket", the lowest daily minimum temperatures recorded in this area being those at station 002. The $\frac{1}{2}$ -1 mph converging flow of cold air during the night over an approximate area of 1 sq. mi. and depth of 50 ft. requires an average upward velocity of the order of 100-200 ft. per hr. which is too slow to be measured directly by the methods employed in this survey, but is of the same order as the observed rate of rise of the isothermal or isentropic surfaces in the mid-valley soundings during the early night. A less stable valley pool surmounted by a stronger inversion, resulting from this low-level convergence, is observable in the late night and early morning soundings.

29. Wind-Flow Patterns Determined by Large-Scale Aperiodic Variables.

It is evident from the preceding discussion, and particularly from Figs. 133 - 138, that diurnal variations account for only a part (more or less than half, depending upon exposure) of the wind variability at a given location. The remainder, aperiodic in nature, is related to the large-scale variables associated with inter-diurnal weather changes and with the systems appearing on synoptic weather maps. Clues to the nature of such relationships can be found in the literature. Heywood (Ref. 71) found that certain conditions of temperature difference between the high ground and the valley, vertical temperature gradient, and wind above the higher ground were favorable for the development of drainage winds in a small valley. Hewson (Ref. 61) correlated the wind directions in the Columbia River gorge with those several thousand feet higher. These examples illustrate the two different types of terrain effects: (a) diurnal thermal effects which may be reinforced or inhibited by aperiodic weather conditions and (b) mechanical effects which are entirely dependent on the aperiodic large-scale wind flow and the degree of turbulent exchange (partly diurnal).

Tests of a number of variables available on the punched cards have been carried out, some variables eliminated, combinations of the remaining variables chosen which would represent relatively homogeneous categories covering a range of values of each variable, and tabulations made of hourly wind

direction frequency and average speed at each station, as well as listings of the pibals, temperature soundings and gustiness data, under each category. A complete discussion of this study would be too voluminous to be included in the present report: however, some examples of the resulting local wind flow patterns will be given, showing their relation to the large-scale variables (Figs. 144 - 148).

The independent variables, and class intervals of each, which are used in categorizing the governing conditions, are as follows:

- (a) Season: winter (Nov.-Apr.), summer (May-Oct.)
- (b) Time of observation: morning (7-10 a.m.), day (11 a.m.-4 p.m.), evening (5-8 p.m.), night (9 p.m. - 6 a.m.)
- (c) 5000 ft. (MSL) wind direction: SW, W, NNW (NW and N), ENE (NE and E), SSE (SE and S)
- (d) 5000 ft. wind speed: light (5-14 mph), moderate (15-29 mph), strong (30-59 mph)
- (e) 5000 ft. stability ($T_{850mb} - T_{sfc}$): unstable ($\leq -15^{\circ}F$: includes neutral), average (-14 to $-5^{\circ}F$), stable ($\geq -4^{\circ}F$)
- (f) 200 ft. stability ($T_{183} - T_5$): unstable ($\leq -1^{\circ}F$: includes neutral), moderately stable (0 to $+5^{\circ}F$), very stable ($\geq +6^{\circ}F$).

All available observations for the period Jan., 1949-Oct., 1950 were used in determining the frequency of each of the resulting 1080 categories, on the basis of which 88 categories were selected, containing an average of 82 hours of observation per category (varying from 18 to 287), and

together covering 45% of the total observation period. The categories have been chosen in a pattern which would contain all classes of each variable and combinations of each with at least two classes of each of the others. On the whole, the winter half of the year provided a greater variety of wind speeds and stability combinations, and the summer a greater variety of upper wind directions.

In each of the following 20 examples of local wind flow maps associated with specific combinations of the independent variables, the prevailing wind direction is shown by a large arrow-tail at each station which had 10 or more hourly observations. The percent frequency of this and the two adjacent directions (16-point scale) combined is entered to the nearest whole percent as a number next to the wind arrow. The average speed of these three directions combined is represented by the feathers on the arrow: each half-feather represents 1 mph. The second most frequent direction, when it is at least 3 points removed from the primary, is represented in a similar way by a smaller arrow. The percentage of calms is entered next to the station dot, preceded by the letter c, whenever it is equal to or greater than that of the secondary prevailing direction. Maps of this type constitute a guide for forecasting or interpolating local winds for this area or any topographical analogue, given the gradient wind, approximate temperature distribution of the lowest 4000 ft., season and time of day, and they also provide a measure of the probability of such a forecast or estimate being correct.

(a) Seasonal Differences (Fig. 144f).

- (1) Winter day, SW moderate, unstable/unstable
- (2) Winter night, SW moderate, stable/moderately stable
- (3) Summer day, SW moderate, unstable/unstable
- (4) Summer night, SW moderate, stable/moderately stable.

This 5000 ft. wind direction (SW), like W, has a sufficiently high frequency of occurrence throughout the year to permit narrowing the class interval to a single sector (8-point scale). It is here used as the common direction in the comparison of seasons and time of day and will also be used in studying variations with speed and stability. The moderate speed category (15-29 mph at 5000 ft. MSL), similarly, will be used in examining the effects of direction, as well as of season, time of day and stability. The stability categories unstable/unstable (5000 ft. stability/200 ft. stability), typical of midday throughout the year, and stable/moderately stable, the most common nocturnal type, will both be used in comparing the various combinations of the other elements. The patterns appearing in these four maps are similar to the typical night and day patterns which have already been described in some detail, with the exception that the homogeneity of the upper wind and stability greatly reduces both the scatter of observed local winds and the seasonal variation. In both seasons, the day pattern is one of up-valley winds, 70-90% southwesterly or west-southwesterly, with average speeds 7-12 mph, and with slight up-slope components at the slope stations. While this gradient wind is associated with predominantly southeasterly flow through Whiteoak Creek Gap

(frictional flow from high to low pressure), a considerable frequency of converging flow is also indicated on map 3 between stations 015 and 002, the latter having the least dependable (lowest frequency) prevailing direction in both seasons. The night maps in both seasons show a more even split between up- and downvalley directions at most valley stations than in the average night distribution, and a greater frequency of calms, to be expected in view of the opposition of the gradient wind to the drainage wind. Local slope winds having a westerly component are favored (stations 001, 010) and only those stations having northeasterly local slope winds (004, 016) show any significant predominance of that direction. Station 003, the level valley point, has a virtual equipartition between northeasterlies, southwesterlies and calms in both seasons. The main deviations of the summer half-year from the winter can be attributed to foliage (more calms at station 010, more downslope wind at the 40 ft. anemometer level at stations 002 and 005), or to less depth of the drainage current due to shorter duration of cooling (smaller easterly-northeasterly frequencies at the higher stations 005, 008, 007 and 012).

(b) Changing Gradient Wind Direction, Day (Fig. 145)

- (5) Summer day, W moderate, unstable/unstable
- (6) Summer day, NNW moderate, unstable/unstable
- (7) Summer day, ENE moderate, unstable/unstable
- (8) Summer day, SSE moderate, unstable/unstable.

Together with map 3 of (Fig. 144), these show the effects of varying the gradient wind direction only, under typical daytime conditions. Little

change in the local flow pattern occurs with a shift from SW to W: a slight shift of direction at the highest stations, 006 and 007, an increase in the northwesterly frequency at the NW-facing slope and gap stations, 010 and 002, a corresponding decrease in the opposing slope winds at stations 005 and 015, and a 1 mph decrease in the average up-valley velocity at the valley stations 003, 004, 012 and 016. When the W wind aloft is replaced by NNW (map 6), the surface up-valley frequency decreases markedly from 79-87% to 44-52%, and the average speed decreases further by 1-2 mph, accompanied by the appearance of a significant frequency of northeasterlies. A turning to a more westerly or northwesterly prevailing direction is almost universal, downslope winds now predominating at station 005, and an appreciable frequency of northwesterly through-flow (about 29%) being indicated by stations 002 and 015. With an ENE gradient wind (map 7) of moderate speed, the up-valley winds virtually disappear, the frequency of surface northeasterlies rising to over 90%. Cross-isobar northwesterlies are favored at stations sheltered from the gradient flow (002, 015). A reversal to predominantly up-valley flow (39-61%) is brought about by a further shift of the gradient wind to SSE, with significant secondary SE maxima crossing the valley, reflecting a reinforcement of the thermal cross-wind. The upslope wind at station 005 has its maximum frequency and speed with this upper wind direction, and SE through-flow is again favored at the gap stations 002 and 015. The ridge-top winds (stations 006 and 007), as usual, follow the upper direction most closely.

(c) Changing Gradient Wind Direction, Night (Fig. 146)

(9) Summer night, W moderate, stable/moderately stable

- (10) Summer night, NNW moderate, stable/moderately stable
- (11) Summer night, ENE moderate, stable/moderately stable
- (12) Summer night, SSE moderate, stable/moderately stable.

These maps repeat the direction sequence of Fig. 145 but with typical nocturnal stability, as in map 4, Fig. 144. It is at first surprising to find that the frequencies of southwesterlies and calms generally increase at the expense of northeasterlies, at the valley stations, when the gradient wind shifts from SW to W. However, it has been mentioned previously that the frictional component of the surface wind, crossing the isobars from high towards low pressure, is greater at night than in the daytime relative to the gradient component. It appears that the angle of 30° or so clockwise between the valley axis and the W gradient wind is more favorable to the up-valley wind than the slight (15°) counterclockwise angle of the SW gradient. Since no corresponding relation was noted under daytime conditions (maps 3 and 5), it would appear that the frictional component is relatively small in proportion to the gradient component during the day. The great excess of valley northeasterlies with a SSE cross-valley gradient wind (map 12) over those with a NNW gradient (map 10) is further evidence of pronounced frictional flow not appearing in the daytime, when the prevailing up-valley winds have much the same frequency with either NNW or SSE cross-valley gradient winds. By and large, however, it is the gradient winds in the ENE quadrant which most favor the down-valley drainage current at the well exposed stations, particularly at right-top level, where the frequencies of northeasterly winds approach 100%. The tendency for the more sheltered local winds to

blow to the left of the gradient wind is quite pronounced at the slope and gap stations, the SE-facing stations (005 and 015) showing the best-developed downslope flow with an ENE gradient wind while the NW-facing stations (002 and 010) show complete inhibition of downslope flow under these conditions. The most favorable gradient wind for the SE night wind at station 002 is, surprisingly NNW, and at station 005, similarly, northerly winds are more frequent with a SSE than with a NNW gradient. To summarize, while surface wind directions nearly parallel to the gradient direction are the rule at ridge-top level, winds in sheltered locations blowing to the left of the gradient direction at an angle of 45 to 90° or more are favored at night. In the daytime, on the other hand, only the most sheltered stations show this frictional turning to any appreciable extent, the more open valley stations showing the channelled direction closest to that of the gradient wind, with nearly even splitting under cross-valley gradients.

(d) Variation of Gradient Wind Speed (Fig. 147)

- (13) Winter day, SW strong, unstable/unstable
- (14) Winter night, SW strong, stable/moderately stable
- (15) Winter day, SW light, unstable/unstable
- (16) Winter night, SW light, stable/moderately stable.

Changes in gradient wind speed alone have a pronounced effect upon prevailing surface wind directions and their steadiness as well as upon their speeds, especially under nocturnal inversion conditions. In the daytime

the variation is mainly quantitative. Comparing maps 13 and 15 of Fig. 147 with map 1 of Fig. 144, it is seen that as the speed of the SW wind at 5000 ft. MSL increases from light (5-14 mph) through moderate (15-29 mph) to strong (30-59 mph), the frequencies of mid-valley surface southwesterlies (stations 001, 003, 004) increase from 55-64% to 73-95% and then to 84-100%, and the average speeds at 18-40 ft. from 4-5 mph to 10-12 mph and then to 11-13 mph. At the ridge-top level the steadiness of the wind increases as the gradient wind increases from light to moderate, but appears to remain the same or decrease as the gradient wind increases beyond moderate. This high speed effect is not observed with cross-valley gradients (not shown here) and is presumably due to intense turbulence in the wind blowing along the ridges. The prevailing daytime direction at N. Whiteoak Gap (station 002), always SE with a SW gradient, increases in frequency from 58% with a light gradient to 84% with strong, and the upslope wind at station 005 (including the S and ESE winds) similarly increases from 83 to 96%. At night, on the other hand, a reversal takes place at most valley stations, from prevailing northeasterlies when the SW gradient is light to prevailing southwesterlies when it is strong. The Melton Hill wind shows this reversal quite dramatically, shifting from 57% NE with an average speed of 14 mph when the gradient wind is SW light to 40% SSW averaging 9 mph with a moderate SW gradient and 44% SW averaging 11 mph with a strong SW gradient. An apparent paradox associated with this reversal is the increase in the frequency of calms at many stations when the upper wind speed is raised from light to moderate. The relatively even split between NE, SW and calm at valley stations, already noted in the discussion

of map 2, is seen to be a transitional phase between prevailing NE with lighter gradients and prevailing SW with stronger ones.

(e) Varying Stability (Fig. 148)

- (17) Winter night, SW moderate, average/moderately stable
- (18) Winter night, SW moderate, stable/very stable
- (19) Winter night, SW moderate, stable/unstable
- (20) Winter morning, SW moderate, stable/unstable.

The effect of an increase in nocturnal stability with a southwesterly gradient is much like that of decreasing the gradient wind speed, in that the local winds are accentuated at the expense of the gradient wind. The conditions of maps 17 and 18 are the same as those of map 2 except for less stability in the deeper layers in map 17 and greater stability in the lowest few hundreds of feet in map 18. The valley stations show prevailing southwesterlies in the former and prevailing northeasterlies in the latter. At most valley stations the frequency of calms is less in the very stable case than in either of the others, an exception being station 001, where local southwesterly drainage is favored by less stable conditions. It is of interest that the S-SW prevailing direction at Melton Hill (007), and to a lesser extent at Chestnut Ridge (006) is favored by either a decrease in the stability of the upper layer or an increase in the stability of the lower layer. Just the reverse is found when the lower layer is neutral or unstable (map 19) while the upper layer remains stable. Cut off from the gradient flow, stations 006 and 007 then have predominantly easterly winds,

while the valley stations, still more dominated by drainage currents than in map 2 (more stable lower layer) or 17 (less stable upper layer), are less so than in map 13 (maximum stability throughout). The wind observations in maps 19 and 20 are selected under identical categories of all the variables except time of day. The stability type, stable/unstable, is characteristic of the morning transition period as well as being a nocturnal type accompanying fog or cloudiness. The wind flow in the morning case differs from the nocturnal one in the direction of closer resemblance to the typical daytime or unstable pattern. Still predominating in the face of a moderate SW gradient, the northeasterly winds have on the whole a lower frequency and greater speed. There is evidence of considerably more mixing in the morning case, the frequencies being relatively homogeneous over the area: 43-45% northeasterly at the valley stations (001, 003, 004) and 22-29% each way at the higher stations (005, 006, 007, 012). The percentage of downslope winds remains about the same as at night, and the station 002 wind blows out of the gap, the typical night flow. Thus this category seems to select morning cases in which the effects of solar radiation on the wind flow pattern have hardly appeared, but in which the nocturnal flow, at its strongest and deepest, is on the verge of being dissipated. However, this stability type, probably more than most of the others, is one which must be interpreted with caution since it can arise from several very different causes. Among these are post-cold-front situations in which the synoptic pressure patterns require northeasterly flow in the lowest thousand feet or so surmounted by southeasterly flow aloft, in which case the deviation of the local winds from the 5000 ft. winds

cannot be attributed to stability and local effects.

The results of the foregoing analysis, supported by an examination of many more combinations of variables, can now be summarized briefly. Local winds follow the gradient wind direction and speed most closely under stable conditions typical of daytime, and increasingly as the strength of the gradient wind increases. Up- and downvalley gradient winds under these daytime conditions are accompanied by quite reliable parallel flow in the valleys, the frequencies approaching 100%. Daytime cross-valley gradient winds, on the other hand, produce a nearly indeterminate local flow evenly split between up- and down-valley winds, with directions slightly to the left of the gradient wind (counter-clockwise, that is, towards lower pressure) being slightly favored at very high gradient speeds, while the normal daytime southwesterly flow is favored at lower gradient speeds. Night winds follow a local drainage pattern with greater or less fidelity as the gradient wind vector is more or less favorable and as the stability of the deeper layers is more or less developed. The most favorable gradient wind directions are some 45-90° to the right (clockwise) of the local drainage direction. Stable stratification generally reduces the dependability of the hourly wind directions at valley stations: any gradient wind other than that which reinforces the local drainage current simply introduces a large uncertainty in the flow pattern, as well as a large frequency of calms. Gradient winds which oppose local drainage winds reduce the frequency (probability, steadiness, or dependability) of the latter. This reduction is least at low gradient speeds, and increases as the gradient

increases, with the frequency of calms at first increasing and then, as the gradient completely overbalances the local drainage, again decreasing. There is some evidence that internal mechanisms exist which produce variations in the local flow pattern under essentially constant external conditions. Inertial oscillations, changes in the depth of the cold air pool, and fog formation are examples of such mechanisms. Thus, while admittedly the independent variables employed in this study are not necessarily the sole or even the most powerful ones, while the methods of determining them have been somewhat crude, and the class intervals perhaps not as narrow as might be desired, it appears that even with perfect control of the large-scale conditions, a certain indeterminacy would still be found in the local wind patterns.

30. The Three-Dimensional Wind Pattern

In the preceding sections, the wind flow patterns have first been discussed in terms of quasi-horizontal layers taken one at a time: the valley bottom, mid-slope level, ridge-top level, and various upper levels; these patterns have then been compared with one another under various conditions of stability, time of day or season. Now they will be briefly examined in relation to the space coordinates, and in particular the vertical coordinate.

Seasonal profiles of wind speed vs. height above ground up to 5300 ft. obtained from pibals both at Oak Ridge and at Knoxville during the two-year period Nov. 1948 - Nov. 1950 are shown in Fig. 149, Oak Ridge profiles for the lowest 850 ft. are shown in greater detail in Fig. 150: day, night and average curves are shown for each season. In Fig. 151, the corresponding

annual curves are shown, together with annual graphs of the diurnal variation of the wind speed at each level. No attempt will be made here to analyze these profiles in terms of logarithmic or power law parameters (Ref. 72). Suffice it to say that neither law fits within the error of the observations, but that the values of the parameters of either law which can be obtained by fitting narrow layers, and the vertical and diurnal variations of these parameters, have been found to be, on the whole, consistent with those reported by other investigators (Refs. 73, 74). Of course in the presence of local slope currents which make their maximum contribution to the velocity vector at various levels from a few feet to a few hundreds of feet above the ground, it is not to be expected that any simple mathematical formula will be applicable. Qualitatively, it can be observed that (a) more surface frictional reduction appears to occur at Oak Ridge than at Knoxville, compensated by increased velocity in the vicinity of 500-2000 ft. above ground, with equalization between the two stations above that layer; (b) the average increase with height is directly related to the stability in the lowest 1000 ft., being greatest at night and least in the daytime, and to the large-scale horizontal temperature gradient above 1000 ft., being greatest in the winter and least in the summer; (c) there is evidence of a two-layer distribution of shearing stress somewhat similar to that analyzed in idealized form by Poppendiek (Ref. 75), particularly at night, the lower layer being of the proper depth in the spring season (300 ft.) to be accounted for by the ridges, while in the other seasons the depth (50-100 ft.) is so much less that it may better be accounted for by low-level drainage currents. Both these factors

are undoubtedly in operation: we have already seen that the SW drainage flow at station 001 (at which these profiles were obtained) decreases in intensity from 18 ft. to 54 ft. above ground, and also that the relative diurnal speed variation at ridge top and mid-valley stations suggests that the ridges have a pronounced retarding effect at night on the valley air but much less on that above them, while in the daytime both hill and valley wind speeds are affected only by smaller-scale surface roughness elements (trees, etc.); (d) the Knoxville 2-year average speed profile is nearly identical to the average over the 23-year record, so that the Oak Ridge data for this 2-year period can also be considered to be approximately normal.

An average diurnal wind speed time cross-section of the lowest 5000 ft. for Sept.-Oct. 1950 (cf. Fig. 81 and Ref. 47) is presented in Fig. 152 as an aid in visualizing the continuous joint variation of wind speed with height and time. Better documented than the temperature time-section of Fig. 81, it is also somewhat more irregular. However, the main features stand out clearly: the nocturnal momentum stratification of the lowest layers, the rapid vertical equalization accompanying the inversion break-up after sunrise, the frictional loss of momentum to the ground through convection up to the top of the adiabatic layer (about 4000 ft.) in mid-day and the return to night-time conditions with the gradual increase of stability in the evening. A speed maximum in the vertical profile (perhaps a micro-jet of the type proposed by Rossby in Ref. 54) in the layer 1500-2500 ft. appears at all observation times between 6 p.m. and 9 a.m.

The patterns of the horizontal components of the wind which have been described in the preceding sections must also be accompanied by patterns of vertical motion. Up- and downslope winds have so far been studied solely in terms of their horizontal components. The existence of compensating vertical motions in mid-valley has been deduced without observational confirmation. The only direct observations of vertical velocities extending over a horizontal area were those obtained by means of zero-lift (neutral) balloons. These have been analyzed by F. Gifford (Ref. 76). and his results with respect to average patterns are quoted in the following paragraphs.

Neutral balloon data from 100 observation periods, comprising some 250 * balloon runs were plotted in the form of horizontal (x-y) and vertical (x-z) trajectories. The latter were then found to be readily classified into four qualitative types represented schematically in Fig. 153. Type A represents daytime instability with light winds: the balloons characteristically move up and down through several thousand feet without travelling very far. Type B also occurs during the daytime, but is associated with stronger winds and often with more cloudiness and less instability than is Type A. Type C occurs at night, with moderate to strong winds: the balloons go out in steady paths, two or more often being virtually superimposed. The classifications of 30 observation periods by this system were found to correspond almost exactly to their classifications according to the Brookhaven turbulence typing system based on the wind direction trace (Ref. 77). In the light of these observations, it is possible to infer from the wind-direction trace what sort of paths the air parcels are following. The types of the initial sample of 100 observation periods were

also found to correspond to certain ranges of the 5000 ft. MSL wind speed and the 180-ft. vertical temperature gradient (Fig. 154), the same variables used in classifying the microneet wind flow patterns. Already available on all the neutral balloon observation punched cards as part of the 10-digit classification code, these variables were then used to sort the entire body of neutral balloon observations into types A, B, C and D.

The distribution of average vertical velocity is shown in Fig. 155 as a function of distance and height along two narrow sectors, one down-valley (230° - 239°) and the other across Chestnut Ridge (320° - 329°), for the four types. Only balloons which travelled in these directions from the release point (station 001) were used in obtaining these averages. In the Type A panel, the extent and intensity of regions of upward and downward motions are about the same for cross-valley as for up- and down-valley flow, and there is no clear indication of a purely mechanical lifting effect of the ridge. It is interesting that even though these are averages over a large number of observations, the mean vertical velocity is not zero. It is not known whether the same patterns would have resulted if the balloons had been released at some other point, say near an area which now appears as a center of negative vertical velocity. At least near the release point it is evident why vertical velocities must appear to be positive, on the average: otherwise the balloons would be carried to the ground and would never leave the immediate area. It doesn't seem likely that this process of natural selection could influence the averages for any great distance unless some real organization of the motion existed, either with respect

to spacing of convective up- and downdrafts independent of location, or with respect to terrain features. The alternating positive and negative areas more than 1000 ft. above the valley axis suggest the former type of organization, with all balloons fed into convective updrafts. The positive and negative areas closer to the ground, on the other hand, such as the downdraft area at a distance of 5000 ft. down the valley, at the head of the Raccoon Creek drainage, the updraft area at 10,000 ft. distance as the selected valley azimuth intersects the slope of Chestnut Ridge, and the shallow positive layer along Chestnut Ridge Slope in the cross-valley sector, leading to a maximum updraft over the crest, suggest terrain effects. The negative area more than 1000 ft. above the mid-slope portion of the cross-ridge sector is not obviously in either category: If it is associated with the terrain, it shows that the downward currents compensating for the upslope winds are not necessarily confined to the middle of the valley.

The Type B panel still shows centers of positive and negative vertical velocity in the down-valley direction which cannot readily be associated with specific features of the topography. The horizontal spacing of the centers is roughly twice that of Type A. Again, the centers in the cross-ridge sector do appear to be associated with the topography: upward velocity components are found over the warmed slope (also the slope which would give mechanical lift to the northwestward-moving air current) with a maximum over the crest, and a low center of downward motion occurs on the relatively cool (also leeward) side of the ridge.

Type C shows much less average vertical velocity, virtually confined to

gentle upward motions, the balloons which reach the highest altitude being those with the greatest upward velocity (which looks suspiciously like a buoyancy effect). One point of possible meteorological significance is the updraft on the near portion of Chestnut Ridge slope. After this rise, apparently the balloons levelled off and crossed the ridge and next valley without, on the average, any further vertical displacement.

In Type D, the balloons ordinarily did not leave the local valley, but rose slightly from the release point, drifted slowly a short distance, and sank to the ground. Those which reached altitudes greater than a few hundred feet generally followed Type C trajectories. A shallow downslope current with vertical components less than 1 mph appears to be indicated in the cross-ridge section, but the upper positive centers are too strong to be accounted for by the nocturnal drainage circulation.

These results can be briefly summarized as follows. Type A conditions (light wind, unstable) produce mainly convective eddies of large vertical amplitude and relatively little influence of the terrain features. Type B conditions (strong wind, unstable) produce thermal eddies of a similar character, but much more elongated in the direction of the wind, and with some evidence of mechanical up- and downdrafts in the cross-ridge winds. Type C conditions (strong wind, stable) permit balloons to be carried up out of the valley layer but otherwise produce no appreciable vertical motions, the average ascent being very gradual when the direction is down-valley, but being concentrated at the first slope when in a cross-valley direction. Type D conditions (light wind, stable) result in the neutral balloons (and,

presumably, air parcels) being largely confined to the valley in which they were released, rising slightly in midvalley, and drifting slowly away, to sink again nearer the slope. Trajectories of Types C and D frequently occur on the same nights, the deciding factor apparently being the height of rise of the balloon.

Thus the conclusions to be drawn from Gifford's analysis of the neutral balloon observations fit in with those arrived at through a study of the micronet wind records: during the day, the ridges have little mechanical effect on the air motion, being low in relation to the vertical amplitude of the convection currents and far apart in relation to the horizontal travel of air parcels at any level. Thermal valley-ridge circulations exist in the mean, but contribute only a fraction of the total wind vector observable at any time, being overshadowed either by the internal convective eddies of the atmosphere or by moderate gradient winds. During the night the reverse is true: the gentle slope circulations are of major importance in the valley-bottom layer, except with strong gradient winds or abnormally weak inversion development, while the layer above the ridge-tops moves more or less independently in response to the larger-scale mountain-valley currents and synoptic-scale pressure fields, with relatively minor horizontal or vertical perturbation attributable to the small ridges, which act only as macroscopic roughness elements in creating an abnormally large drag on the lowest layers. Air parcels originating in the valley during typical daytime conditions are likely to be carried upward to heights of the order of 2000-3000 ft. within distances of a few thousands of feet in any direction,

and are just as likely to be brought down again (while being constantly mixed with air from other sources) after a comparable length of travel. During typical night conditions air parcels near the valley floor have a considerable likelihood of remaining within a few thousand feet of the initial point and within the valley layer for periods of many minutes or even hours. There is, however, a certain amount of exchange at the top of the valley layer between valley air, which enters the upper stream and is carried off by it, and the adjacent air layer, which is partially entrained in the descending currents along the slopes. This exchange increases with increasing gradient wind and decreasing stability, at first halting local currents which oppose the momentum brought downward from aloft, then changing the valley circulation to a primarily frictional one, deflected more or less to the left of the upper stream to the extent allowed by the restraining walls of the valleys, ravines and gaps.

31. Turbulence

Turbulent diffusion is the primary mechanism by which impurities are dispersed in the atmosphere, and also as has been seen at so many different points in the preceding sections, the primary mechanism by which heat and moisture are transferred to and from the earth's surface by the atmosphere, and by which momentum generated in the free atmosphere by horizontal pressure gradients is transferred to the surface layers and dissipated by friction. Two somewhat different kinds of turbulence can be recognized: thermal turbulence, or convection, associated with superadiabatic lapse rates, and mechanical turbulence, associated with the impingement of the

wind against surface obstacles, or with the internal shearing stresses between adjacent air layers. In view of the foregoing analysis (and numerous studies by others) it is obvious that the "independent variables", wind speed and stability, are themselves greatly dependent upon the degree of vertical turbulent exchange, so that all these interdependent variables may be considered to be ultimately dependent upon more fundamental variables such as the solar radiation, terrestrial radiative heat loss, and large-scale horizontal pressure gradient. However, since the wind velocity (and its vertical gradient) and stability are so much more readily measured locally, and since their climatological (diurnal, seasonal, vertical, topographical) variations are relatively well known, they are the most valuable parameters for classifying the state of turbulence of the lower atmosphere.

Thermal eddies attain relatively large size by comparison with mechanical eddies in the lowest thousand feet over level or moderately hilly country. The wind direction and speed traces of Figs. 11 and 17, which were used to illustrate instrumental characteristics, are daytime records, and contain apparently unorganized fluctuations (turbulent eddies) from the shortest periods which the instrument was capable of recording (a few seconds) up to periods of the order of 20-30 min. However, it has been noted by many investigators, notably Giblett (Ref. 78), Smith (Ref. 77) and Lowry (Ref. 79) that the larger-scale eddies virtually disappear under stable temperature stratifications, and that even those with periods of a few seconds are largely suppressed in moderate inversions.

Gifford (Ref. 76), in analyzing the Oak Ridge neutral balloon observations,

in which the reading interval (30 sec.) set a lower limit of the order of a minute on the period of fluctuations which could be observed, found well-developed eddies in the unstable cases (Types A and B, Fig. 153), but none in the stable cases (Type C and D). Frequency distributions of vertical velocity show the magnitude of these fluctuations. When each of the small areas defined by 10 degree azimuth sectors and 1000 ft. distance intervals within 10,000 ft. are classified as valley, upslope, crest, downslope or irregular with respect to trajectories originating at station 001, the resulting frequency distributions of vertical velocity over each terrain type and for each turbulence type are as shown in Fig. 156 (only azimuths 230°- 49° were used: a separate analysis for azimuths 50°- 229° gave essentially similar results). The arrows indicate the 12.5 and 50 percentile values of vertical velocity.

The Type A and B frequency distributions are considerably broader than those for Types C and D, and none of the turbulence types shows any pronounced variation with the terrain type. The excess frequency of large upward and downward velocity components in the Type A and B cases over those in Types C and D must be attributable almost entirely to large-scale thermal eddies, more or less randomly distributed with respect to terrain. Their magnitude is sufficiently greater than the vertical velocities, resulting from thermal slope winds, mechanical lifting or balloon buoyancy effects (the presumed causes of the recorded nocturnal vertical velocities, which contain the same $\frac{1}{2}$ - $1\frac{1}{2}$ mph positive bias appearing in daytime distributions), that it would appear permissible to consider the standard

deviations of the Type A and B distributions a characteristic measure of the intensity of thermal turbulence. These standard deviations obtained from Gifford's histograms are of the order of 2-3 mph.

From the continuous wind records which are available at many stations equipped with anemometers and wind vanes much more detailed information regarding the frequency distributions of the fluctuating velocity components, at least in the horizontal plane, could theoretically be obtained. However, such information has not been obtained to any great extent in the past, for the following reasons:

- (a) The laborious computations necessary to obtain the standard turbulence parameters most useful in theoretical work, such as functions of the mean square velocity components, or autocorrelation functions.
- (b) The subjectivity and difficulty of interpretation of results when the usual convenient approximations, such as turbulence types, estimated "width of trace", average amplitude or range of fluctuation, etc., are used.
- (c) The confusion as to what measure or parameter of turbulence would prove to be most useful.

In the Oak Ridge study, ranges of speed and direction over periods of 3 or 15 min. have been used in order to obtain average values based on numerous observations. These measures were selected because they are easily and objectively obtained by clerical personnel, they are statistically related

to root mean square fluctuations in a simple way, and the disadvantage of large scatter of the individual readings could be overcome by using large numbers of observations obtained under selected meteorological conditions. The more hours of observations processed, the narrower and more homogeneous the meteorological categories could be made, so that variations due to causes independent of those being studied could be largely eliminated by averaging over these homogeneous categories. The observations analyzed here consist of the ranges of direction and speed in the third quarter of each hour based on vane-selsyn and cup-generator data at 6, 18, 54 (station 001) and 154 (station 012) ft. in the valley, and 75 ft. above a 400 ft. ridge (station 019), and averages of four 3-min. heated-thermopile speed range readings per hour at 6, 18 and 54 ft. The periods of record are July 19-Oct. 3, 1950, at 6, 18 and 54 ft., the full year 1950 at 154 ft. and the months of February and March, 1951, at Pine Ridge top. Vertical temperature gradient observations over appropriate layers were available during each of these periods. Diurnal and seasonal variations of the wind speed and direction ranges and their variations with mean hourly speed and stability will be presented, followed by an analysis of their relation to the root mean square fluctuations and the behavior of the latter. This entire analysis has been presented at a meeting of the American Meteorological Society, May, 1952, in Washington, D. C. (Ref. 80).

The diurnal variations of the wind direction range in each season at 154 ft. above ground (station 012), sorted by 5 mph intervals of mean hourly speed and averaged by 4-hour periods, are shown in Fig. 157. There is clearly a midday maximum of directional gustiness in all seasons, with low steady

night values, the diurnal variation being particularly pronounced at low wind speeds and tending to disappear when the mean wind exceeds 15 mph. The pattern at lower mean speeds is strikingly similar both to the diurnal curve of low-level lapse rate (Figs. 77-79) and to that of low-level wind speed (Fig. 132). The absolute values and diurnal amplitudes are greater in the spring and smaller in the fall than in the other seasons particularly at the lower mean speeds. Average ranges are 50-120° throughout the day at wind speeds of 15 mph or more, increasing with lowering mean speed to 80-170° at night and 200-300° in midday.

Similar graphs of the wind speed range appear in Fig. 158. While there is again a tendency for daytime maxima at low mean speeds, decreasing in amplitude with increasing speed, this trend is almost masked by a steady increase of speed range with increasing speed at all hours. As in the case of the direction range, the highest values at all hours as well as the largest relative daytime maxima occur in the spring quarter.

When the speed range is divided by mean speed and the observations sorted by low-level stability ($T_{183} - T_5$, station 012) and plotted against mean hourly speed, the seasonal graphs of Fig. 159 result. It is quite interesting that in neutral temperature gradients (curve B), the ratio of speed range to mean speed is virtually independent of wind speed except in the lowest speed interval, where underestimation of the mean speed by the generator anemometer may introduce an appreciable error. In unstable gradients (curve A) the ratio is larger than in the neutral case, that is, the gustiness is larger in proportion to the mean speed. Likewise, in

stable gradients (curves C, D and E), the gustiness is less than in the neutral case. Furthermore, as the wind speed increases, the curves for different lapse rates approach a common value. There are thus indications in all the seasonal averages that, at least at wind speeds greater than 5 mph, the relative gustiness (ratio of gustiness to mean speed) is independent of wind speed under neutral stability and independent of stability at large wind speeds. The neutral value approached does vary seasonally, being greatest in the spring and least in the fall. This shows that eddies generated in the layers above 200 ft., in which the seasonal variation of instability follows this same pattern, are also of importance.

Confirmation of the relative speed-gustiness pattern is given by the graphs of direction range when plotted in the same manner (Fig. 160). However, there are still large decreases with increasing wind speed in the low speed ranges, under all temperature gradients, so that anemometer errors cannot be the complete explanation. Apparently some large relative fluctuations of the wind vector occur at low speeds, even under stable conditions. The analyses of the delicate balances involved in the local wind flow patterns presented in the earlier sections of this report give ample cause to expect unsteadiness in the wind at night.

Annual graphs are given in Fig. 161 of the four kinds shown in Figs. 157-160. These show the variations already discussed, somewhat smoothed. The similarity of the lower two graphs, one based on fluctuations of the wind speed and the other on oscillations of the direction vane, is striking.

In order to convert these raw observations of speed and direction range to turbulence parameters which can be used in calculating diffusion or in making climatological comparisons between various locations, some definitions and theoretical relations must be considered. These are given in concise form in Fig. 162. The wind speed, s , is the scalar magnitude of the horizontal wind vector. The component in the direction of the mean wind is designated by u . Frenkiel (Ref. 81) has shown that, in general, the mean value of u over a given period of time, designated \bar{u} , is smaller than the mean speed \bar{s} by an amount varying with the intensity of transverse turbulence σ_v . From his theoretical approximations it follows that the standard deviation of the scalar speed, σ_s , is a satisfactory first order approximation to the root mean square longitudinal component σ_u . It can similarly be shown* that the root mean square transverse component, σ_v , is approximately the product of the mean speed, \bar{s} , and the tangent of the standard deviation of direction, σ_d . The "intensity of turbulence," T_x and T_y , as defined in aerodynamics can also be obtained by means of these same approximation formulas. The assumptions are that the longitudinal (σ_u) and transverse (σ_v) components of the turbulence are nearly equal and that they are small by comparison with the mean wind vector. These assumptions are not always correct; nevertheless, it is felt that the results obtained by using these approximations are essentially correct. Thus both rectilinear horizontal components of the turbulence can be obtained from observations of the mean speed, standard deviation of speed and standard deviation of direction, obtained by conventional instruments. It is, of course, assumed that a time interval can be selected over which such means and

*See following page for footnote.

*The derivation proceeds as follows:

From Frenkiel:

$$(\bar{s})^2 \approx (\bar{u})^2 (1 + T_y^2) \equiv (\bar{u})^2 \sigma_v^2 \quad (\text{Ref. 81})$$

from which

$$(\bar{u})^2 \approx (\bar{s})^2 - \sigma_v^2 \equiv (\bar{s})^2 - k^2 \sigma_u^2. \quad (1)$$

These are the approximate relations between \bar{u} , \bar{s} and the gustiness, where

$$k = \sigma_v / \sigma_u$$

Also from Frenkiel:

$$\overline{s^2} \approx (\bar{u})^2 (1 + T_x^2 + T_y^2) \equiv (\bar{u})^2 + \sigma_u^2 + \sigma_v^2 \quad (\text{Ref. 81})$$

from which

$$\sigma_u^2 \approx \overline{s^2} - (\bar{u})^2 - \sigma_v^2. \quad (2)$$

But

$$\overline{s^2} \equiv \overline{(\bar{s} + s')^2} = \overline{(\bar{s})^2 + 2\bar{s}s' + (s')^2}$$

and since \bar{s} is constant and $\overline{s'} = 0$ over the averaging period,

$$\overline{s^2} \equiv (\bar{s})^2 + \overline{(s')^2} \equiv (\bar{s})^2 + \sigma_s^2 \quad (3)$$

Substituting from (1) and (3) into (2):

$$\sigma_u^2 \approx (\bar{s})^2 + \sigma_s^2 - (\bar{s})^2 - \sigma_v^2 - \sigma_v^2 = \sigma_s^2.$$

Thus σ_u is satisfactorily approximated by σ_s , assuming, as Frenkiel does, that

T_x and T_y are small. Now, under this assumption,

$$|\sigma_v^2 - \sigma_u^2| \ll (\bar{s})^2$$

so that, recalling that u as well as s satisfies (3):

$$\sigma_v^2 \approx \frac{(\bar{s})^2 \sigma_v^2}{(\bar{s})^2 - \sigma_v^2 + \sigma_u^2} \approx \frac{(\bar{s}) \sigma_v^2}{(\bar{u})^2 + \sigma_u^2} = (\bar{s})^2 \frac{\sigma_v^2}{\bar{u}^2}$$

But if $\sigma_u \ll \bar{u}$, then $v'/u \approx v'/\bar{u}$, so that

$$(\bar{s})^2 \frac{\sigma_v^2}{u^2} \approx (\bar{s})^2 \overline{[(v')^2/u^2]} = (\bar{s})^2 \overline{(v'/u)^2} \equiv (\bar{s})^2 \sigma_{\tan d'}^2$$

For small T_y ,

$$\sigma_{\tan d'} \approx \tan \sigma_{d'}$$

which has been satisfactorily verified by observations, so that

$$\sigma_v \approx \bar{s} \tan \sigma_{d'}$$

standard deviations are to be computed. This is, in fact, a question which is related to one of the central problems of atmospheric turbulence, namely, the spectrum. The intervals adopted here (3-15 min.) are such as can conveniently be studied by means of wind records designed as they are for general purposes, and also such as must be of the proper order of magnitude for the study of diffusion over distances of the order of a mile or so.

In order to obtain the necessary standard deviations of wind speed and direction from our range data, it has been necessary to assume that, on the average, the range, S or D , in a given size sample is a constant multiple of the standard deviation, σ_s or σ_d , and that the tangent of the standard deviation of direction, $\tan\sigma_d$, is approximately equal to the standard deviation of the tangent $\sigma_{\tan d}$. Fig. 163 shows the results of 14 fast runs, obtained by speeding up the anemograph chart drives, and evaluated in terms of all the statistical parameters necessary to test these last two assumptions. It is seen that the average ratio of range to standard deviation over a 15-min. interval is 4.2 ± 1.5 in the case of wind speed and 6.8 ± 1.5 in the case of wind direction. These mean ratios are used for deriving the standard deviations in the subsequent analysis. The ratio of range to standard deviation for the heated-thermopile wind speed data was also found to be about 4. The maximum error introduced by the approximation of $\sigma_{\tan d}$ by $\tan\sigma_d$ was found to be of the order of $\pm 20\%$. The resulting average behavior of the turbulence parameters in relation to the hourly average wind speed, stability and height above ground will now be discussed without further regard to the degree of scatter about the means,

the closeness of fit to the original observations, or the relative effectiveness of various possible choices of independent variables. Suffice it to say that the best data were obtained at the 54 ft. level, the highest level (consequently having the highest speeds and most reliable speed measurements) at which cup, heated-thermopile, vane and accurate thermopile temperature-gradient data were all available. Cup anemometer data have been used when the wind speed was 6 mph or over, and heated-thermopile data below 6 mph.

Fig. 164 shows the graphs of σ_u , σ_v , T_x and T_y for the 54 ft. level sorted into narrow class intervals of stability ($T_{54} - T_4$) and plotted against the hourly mean wind speed \bar{s} . The most surprising result is that the standard deviations of both the transverse (σ_s) and longitudinal (σ_u) components of the eddy velocities appear to fall on straight lines when plotted in this way. The line representing observations with neutral stability ($T_{54} - T_4 = -0.4$ to -0.1°) passes through the origin, indicating that under these conditions the turbulence in the surface layer is purely mechanical, disappearing in the absence of a mean wind. The lines for superadiabatic lapse rates ($T_{54} - T_4$ less than -0.4) are roughly parallel, indicating that the mechanical component (rate of variation with mean speed) is unaffected by instability. These lines are displaced upward rather regularly, indicating that there is a steadily increasing thermal component with increasing instability, independent of the wind speed. The thermal component of the turbulence is apparently considerably greater in the lateral (σ_v) than in the longitudinal (σ_u) direction. In inversion

conditions ($T_{54} - T_4 \geq 0$) straight lines can still be drawn, with decreasing slope while still passing through the origin, as in the neutral case, as if the turbulence, now purely mechanical, is increasingly damped out with increasing stability. The points representing the average σ_v for the lowest speed class, 0.5 to 2.0 mph are above the straight line, a non-linearity already observed in the station 012 direction range graphs (Fig. 160).

When the intensity components T_x and T_y (or σ_u/u and σ_v/u) are plotted in the same manner, the resulting curves are very similar in appearance to those of speed range/mean speed in Fig. 159 and direction range in Fig. 160: the intensity in neutral stability ($T_{54} - T_4$ between -0.4 and -0.1°) is independent of speed and the longitudinal and transverse components are equal (isotropic, or $K = 1$); in unstable conditions the intensity tends to increase without bound as the mean speed approaches zero and to approach the neutral value asymptotically with increasing mean speed, and in stable conditions generally lower values are observed except at the lowest speeds. The intensity curves are not as simple to interpret meteorologically or to use for extrapolation as are the σ curves.

Neutral stability observations obtained from the three independent sources at the 54 ft. level (σ_u from generator-cup anemometer records, σ_u from thermopile anemometer records and σ_v from vane-selsyn records) are combined in the left-hand graph of Fig. 165. The equality of the transverse and longitudinal components under these conditions, the agreement of cup and thermopile data in the 5-10 mph interval, and the displacement of cup

data at low speeds due to negative errors in the mean speed are clearly borne out. The variation of $\overline{\sigma}_v$ with height in neutral stability is shown in the right-hand graph of Fig. 165. While the 6 ft. and 18 ft. data show more scatter (at least partly due to sorting these observations on the 54 ft. mean speed rather than on the speed observed at each level), they, as well as the 154 ft. data, can be reasonably well approximated by straight lines passing through the origin, and with decreasing slope as the elevation increases. That is to say, the gustiness associated with a particular mean speed is greatest nearest the ground and decreases with distance from the ground, a behavior which might be expected in mechanical turbulence but perhaps not in thermal turbulence. The variation of the latter has not been examined, since different observations and class intervals of vertical temperature gradient were used for sorting the 154 ft. gustiness data from those used for the 6, 18 and 54 ft. data.

To complete the analysis of these turbulence observations, various parameters of the preceding graphs are shown in Fig. 166. The ratio of transverse to longitudinal, $\overline{\sigma}_v/\overline{\sigma}_u$ or K , is shown in relation to mean speed and stability for the 54 ft. level (upper left); it reflects the equality of these two components independent of mean speed for the neutral case, the excess of transverse over longitudinal turbulence in the unstable cases, decreasing with increasing speed, and the reverse in the stable cases. It is of interest that K ranges from about 0.7 to 2 in this graph, straining the limits within which Frenkiel's approximations can be considered applicable. The coefficient of mechanical turbulence at the 54 ft. level with

respect to wind speed, $\partial\sigma/\partial\bar{s}$ (upper right), is seen to be roughly constant in temperature lapse conditions for both components and to drop off with increasing inversion intensity, particularly in the transverse direction. This mechanical turbulence coefficient is seen (lower left) to decrease gradually with elevation above ground (roughly logarithmically), dropping by about one-third from 6 ft. to 154 ft., with the ridge-top observations fitting on the curve approximately at the correct height above ground. Finally, the thermal component (lower right), or vertical displacement of the zero-intercept $\sigma(0)$ in the σ vs. \bar{s} graphs, is seen to increase nearly linearly with increasing temperature lapse and to remain at zero with stability greater than neutral.

A brief summary of the findings with respect to turbulent eddy velocities in the Oak Ridge area can now be given. Daytime instability produces convective eddies with diameters of the order of several thousands of feet, periods of the order of 10-30 min., and both vertical and horizontal eddy velocities averaging about 2-3 mph at average wind speeds of 5-15 mph throughout the lowest 1000-3000 ft. Gust velocities of 5-10 mph lasting for fractions of a minute occur several times hourly under such conditions. The intensity of thermal turbulence varies directly with the lapse rate, dropping to zero in neutral or stable conditions. Mechanical turbulence generated by the wind in passing over rough ground is directly proportional to the wind speed and the root mean square eddy velocity decreases from about $1/3$ the mean speed at 6 ft. above the ground to about $1/5$ the mean speed at 150 ft. These eddies are smaller than the thermal eddies, with no periods greater than $\frac{1}{2}$ min. and with some at least as short as a few seconds. Mechanical eddies are damped out in inversions, dropping in the lowest 50 ft. from $1/4 - 1/3$ the mean speed under adiabatic conditions to about $1/6$ the mean speed with a 1°F inversion. At speeds under 3 mph, in inversion conditions, fluctuations of direction are ob-

weather patterns.

Throughout the year, the position and intensity of the great Bermuda-Azores anticyclonic belt have a determining effect on the climate of this region. Never far from its axis, the area has low average wind speeds and seasonally shifting directions. In the winter, the axis of high pressure is to the south, the winds aloft are from a westerly direction and relatively strong, and fronts and air masses follow one another in rapid succession. These weather systems bring frequent rain and dense cloudiness, restricting the daily temperature range and with it the development of low-level stability and instability. The deficit of incoming solar energy with respect to terrestrial radiative heat loss tends to maintain a relatively stable stratification throughout the troposphere. This stability, together with the strong latitudinal temperature gradient, permit the lowest layers to become at times very sluggish, with frequent fog and smoke accumulation. Spring brings an increased warming of the lower atmosphere and a gradual strengthening and northward migration of the oceanic high-pressure belt. Southwesterly winds blowing around its western side in the lowest thousands of feet carry heat and moisture: instability, showers, strong winds and turbulence typify this season, although alternating with more frequent clear skies, which produce large diurnal temperature ranges, well-developed nocturnal inversions and daytime lapse rates, and a minimum of fog, low ceilings or poor visibilities. The influx of tropical air continues in the summer, with much lower wind speeds up to high levels; fronts and air-mass contrasts are at a minimum and diurnal cycles well developed. A separate high-pressure cell in the eastern United States, accompanying continental

cooling and maximum northward displacement of the semi-permanent anticyclonic belt, produces light, predominantly northeasterly winds in the lower layers, stability, clear skies, large-amplitude diurnal cycles and a minimum of precipitation.

The effects of the Southern Appalachian Mountains are considerably different in the cold and warm halves of the year. The winter westerlies and large-scale cyclonic storms, encountering these highlands, produce large orographic variations of precipitation, with a maximum on the side of each mountain range facing the prevailing rain-bearing wind. Normally SW, this direction shifts somewhat from year to year, so that Oak Ridge, in a transition zone between the Cumberland Mountain maximum (>65 in. per year), and the mid-valley minimum (about 45 in. per year), has a highly variable annual total precipitation averaging about 50-53 in. per year. Winter cloudiness and fog are increased by the presence of the mountains, while the wind flow varies from up- and down-valley diurnal breezes in the relatively clear, calm periods to highly variable directions and speeds associated with the large-scale weather systems. A sheltering effect of the Cumberland Plateau can be seen in the low average wind speeds, relative infrequency of cross-valley wind directions at low altitudes, and a lack of snow or extreme cold throughout the large valley by comparison with the more open country to the west. In the summer half of the year, on the other hand, up- and down-valley winds generated by mountain-valley temperature gradients are more the rule and tend to moderate the temperature maxima, while precipitation is of a highly irregular shower type with much

less orographic variation. Up-valley (SW) winds are favored by the general circulation pattern of the spring season, while down-valley winds, common at night throughout the year, become the prevailing winds in the fall.

The influence of the small ridges on the climate is highly subject to the large-scale conditions, being limited in the presence of excessive cloudiness or strong winds to a channelling of the wind flow, enhancement of turbulence and reduction of average speed. No significant orographic effect on precipitation or cloudiness is attributable to them, but fog and smoke are more prevalent in the valleys, and particularly near rivers, than on the ridges. With lightening of the large-scale winds and clearing of the sky, however, characteristic local patterns of temperature and wind, associated with the diurnal heating and cooling cycle, emerge. The ridge-tops and sunlit slopes become warmer than the free air at the same level during the day, and upslope surface wind components amounting to about 2 mph are added to the large-valley breeze and gradient wind in the vicinity of the main ridges. At night the reverse occurs, both with respect to temperature and wind distribution, even the smaller rises and depressions of the valley floor being associated with downslope drainage flow, collection of cool air in the hollows, and development of local temperature differences of 5° F. or more between differently exposed valley stations and between valleys and ridges. Wind speeds are comparable at equal heights above ground during the day, as convective eddies thousands of feet in both horizontal and vertical dimensions add random components of about 3 mph to the mean wind vectors. At night, on the other hand, the weak

local circulations, with horizontal velocities of the order of 1 mph and much smaller vertical components, are insulated from the momentum of the upper air currents, which move across valleys and ridges with little horizontal variation in velocity above the ridge top level, with higher speeds than in the daytime, and with only short-period (few seconds) turbulent eddies of the order of $\frac{1}{4}$ or less of the mean speed, compared with $\frac{1}{2}$ or more in the daytime.

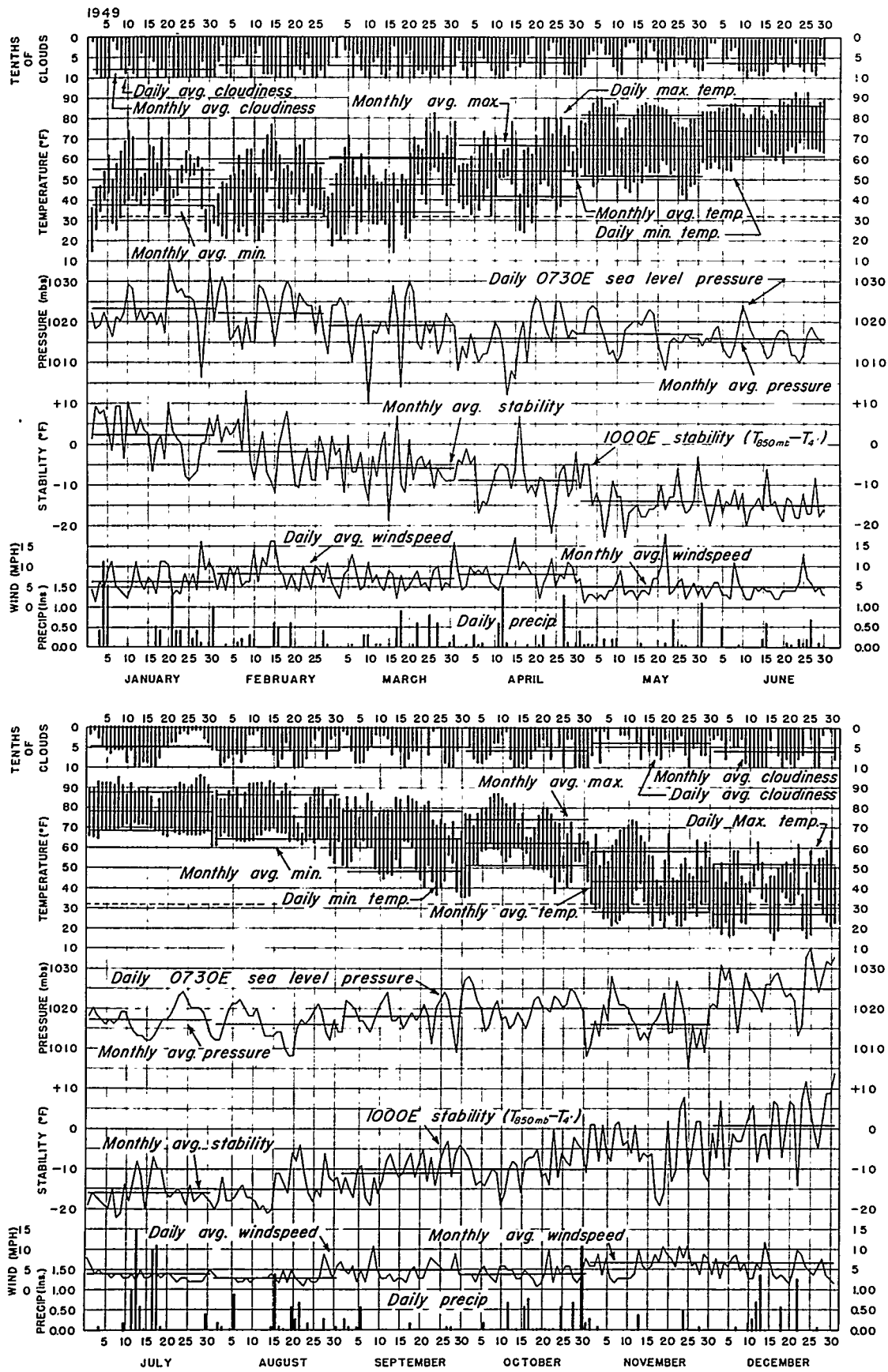


Fig. 34 Daily weather graph, 1949.

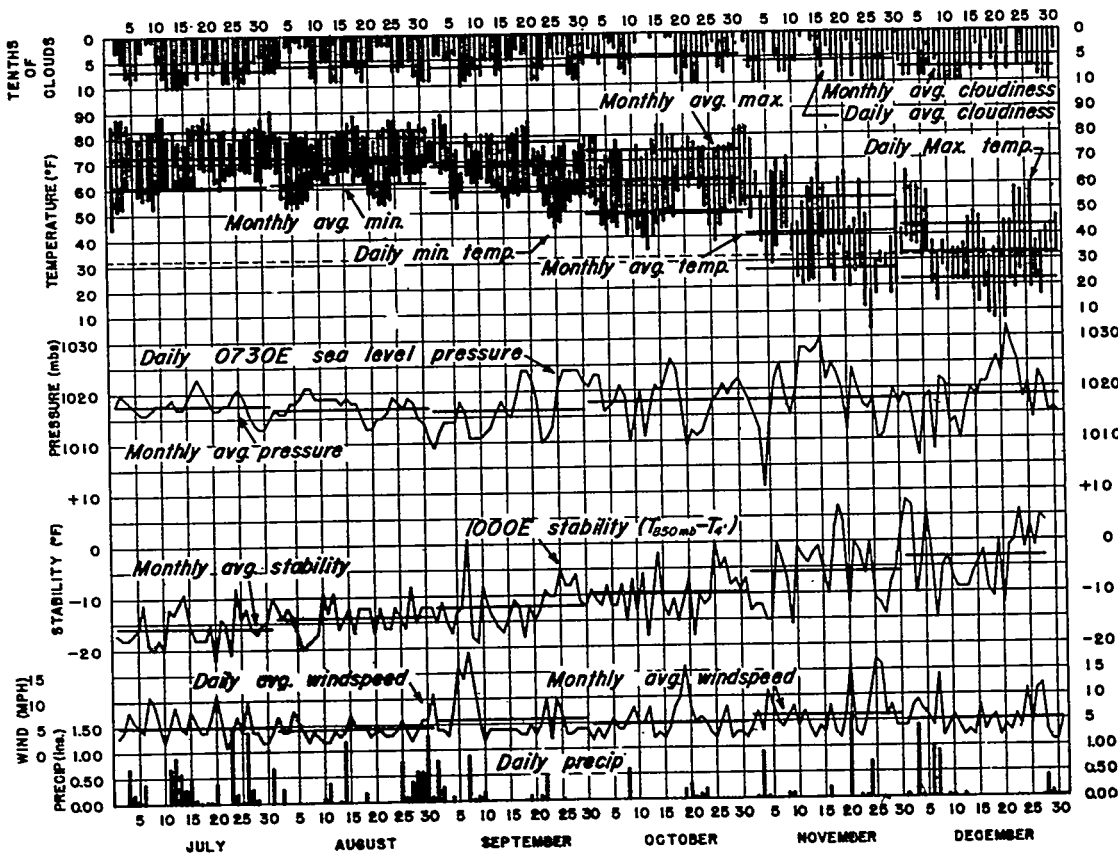
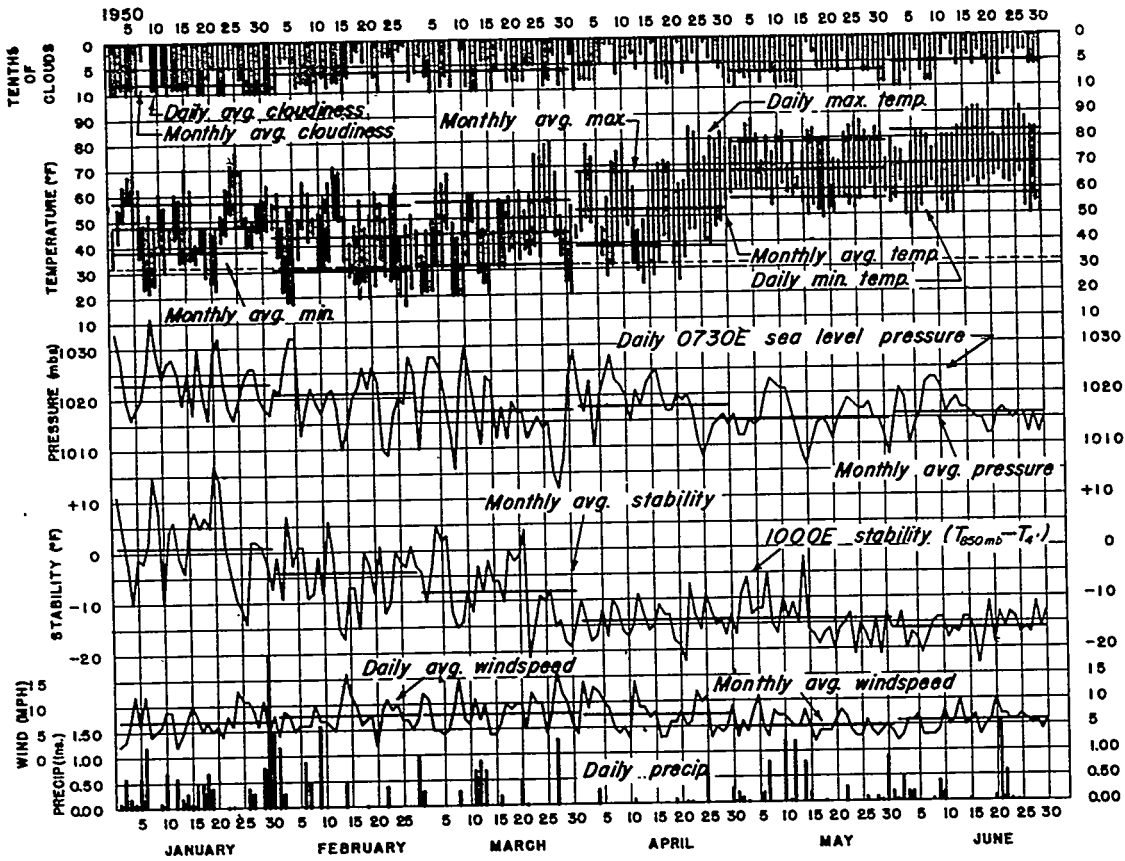


Fig. 35 Daily weather graph, 1950.

377

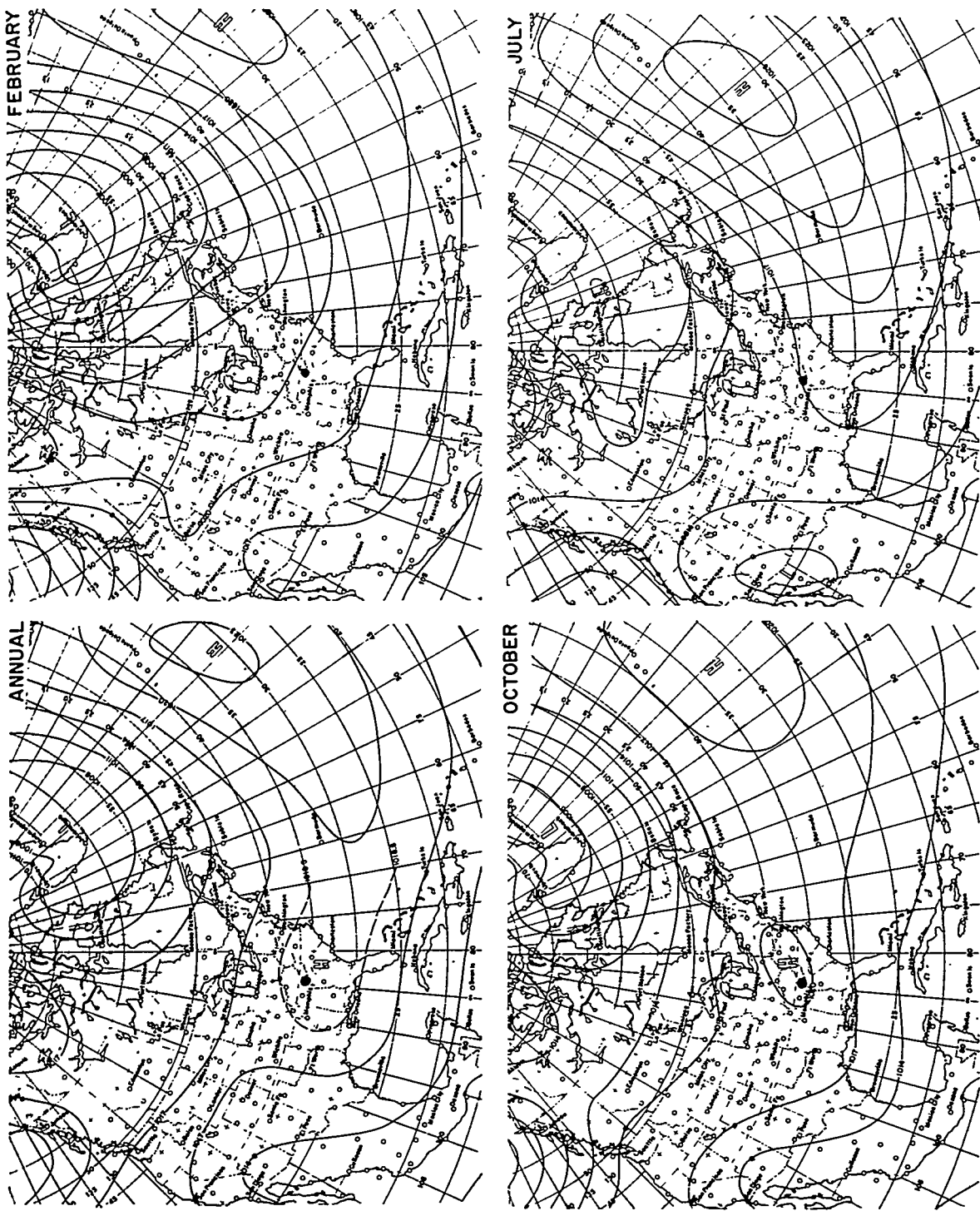


Fig. 36 Normal sea level pressure distribution over North America and the North Atlantic Ocean: annual, February, July, and October.

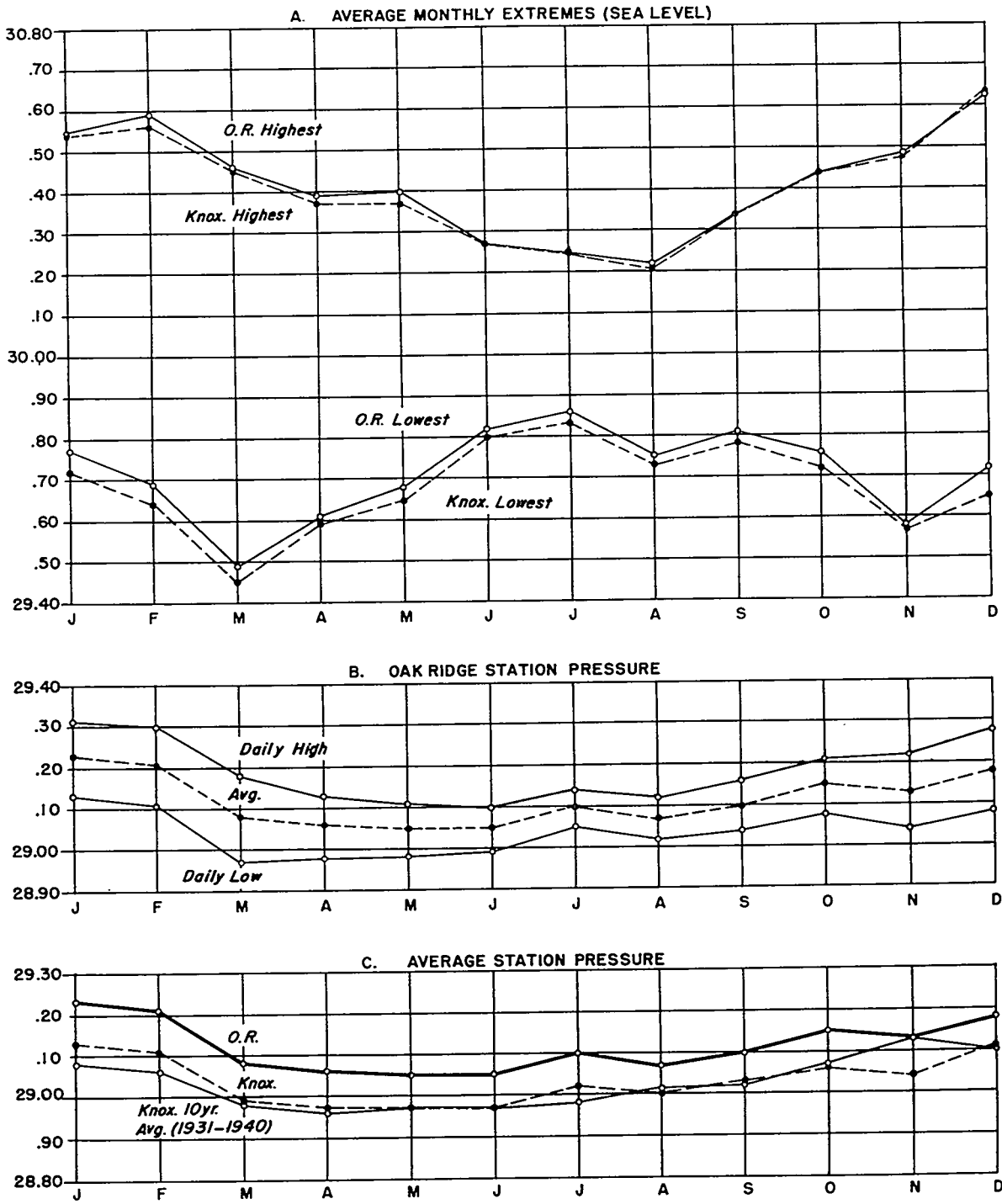


Fig. 37 Average Monthly Barometric Pressure, Oak Ridge and Knoxville. (1949 - 1951).

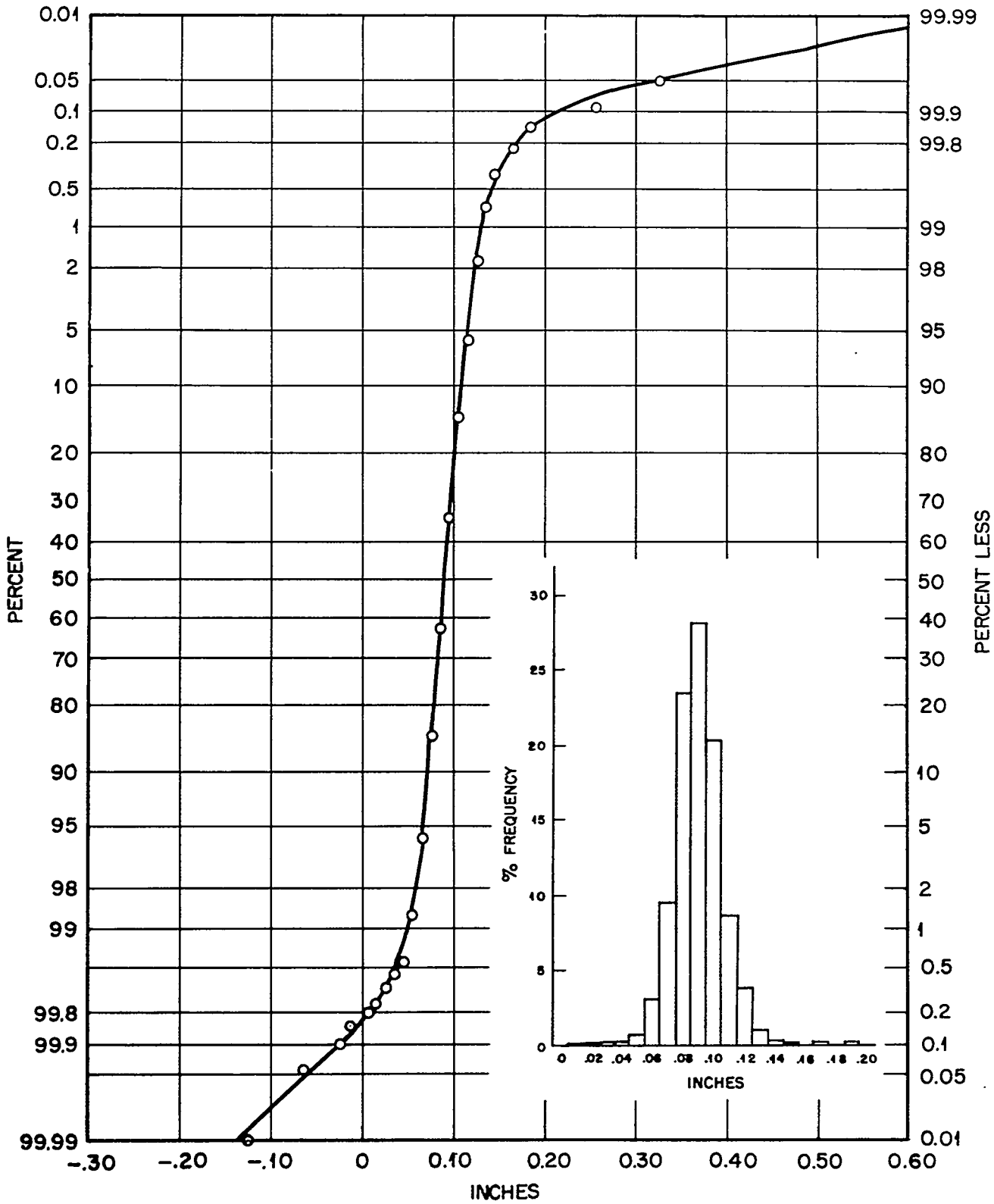


Fig. 38 Frequency of station pressure difference, Oak Ridge minus Knoxville.

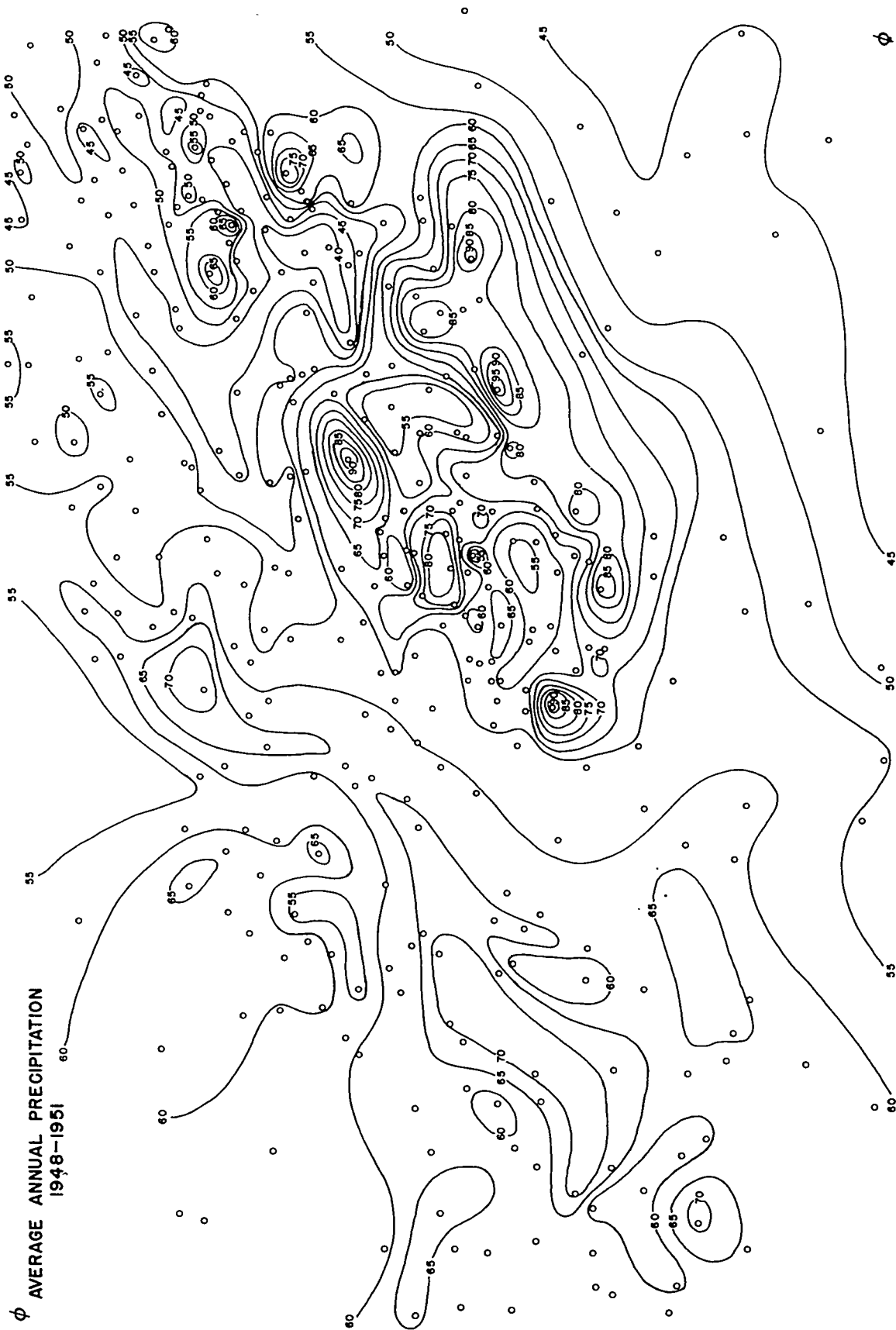
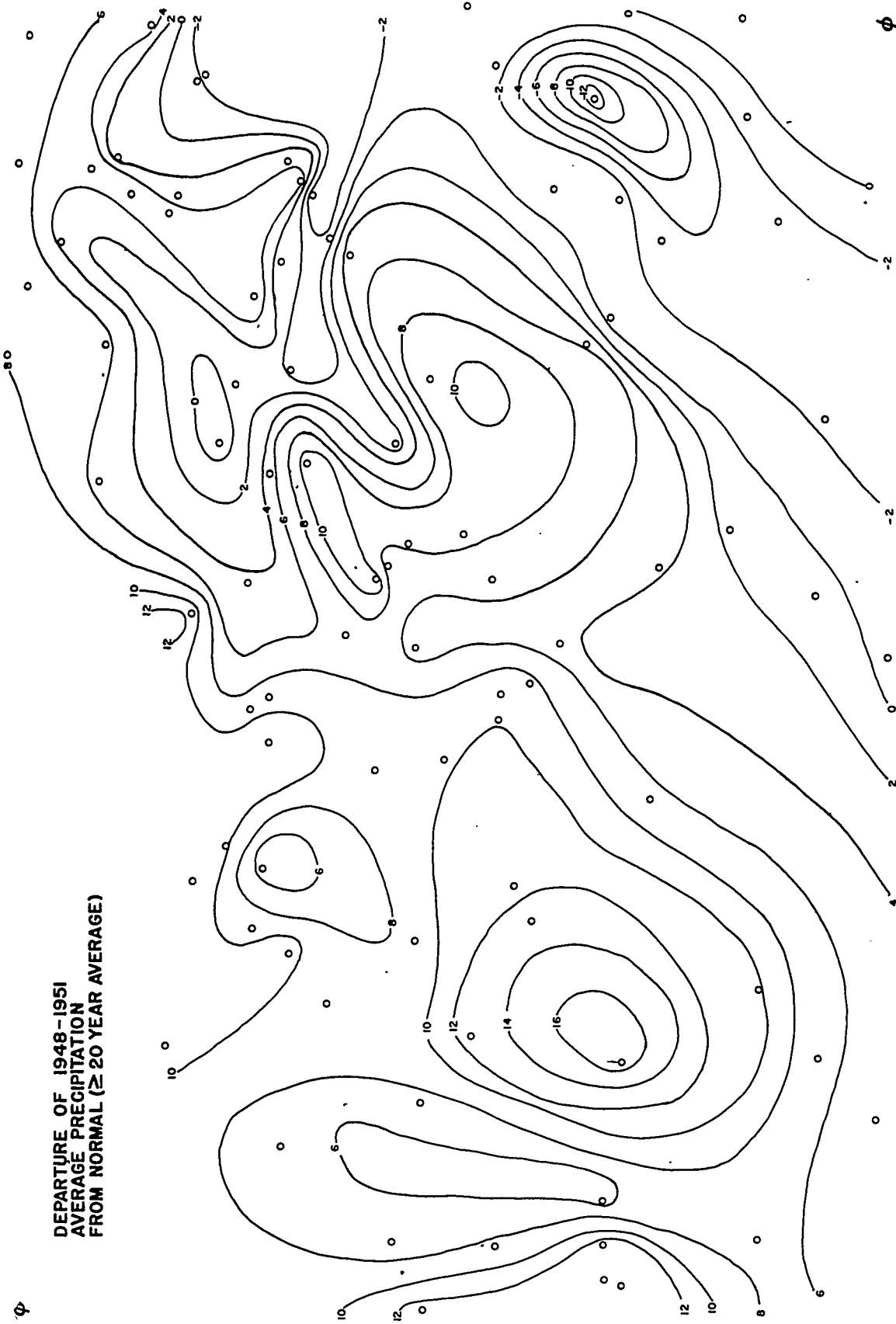


Fig. 39 Map of average annual precipitation, 1948-1951, Southern Appalachian area.

1
2
3
4
5
6
7
8
9
10
11
12
13
14
15
16
17
18
19
20
21
22
23
24
25
26
27
28
29
30
31
32
33
34
35
36
37
38
39
40
41
42
43
44
45
46
47
48
49
50
51
52
53
54
55
56
57
58
59
60
61
62
63
64
65
66
67
68
69
70
71
72
73
74
75
76
77
78
79
80
81
82
83
84
85
86
87
88
89
90
91
92
93
94
95
96
97
98
99
100



DEPARTURE OF 1948-1951
AVERAGE PRECIPITATION
FROM NORMAL (\geq 20 YEAR AVERAGE)

Fig. 40 Map of departure of 1948-1951 average precipitation from normal, based on stations in the Southern Appalachian area having 20 years record or more.

381

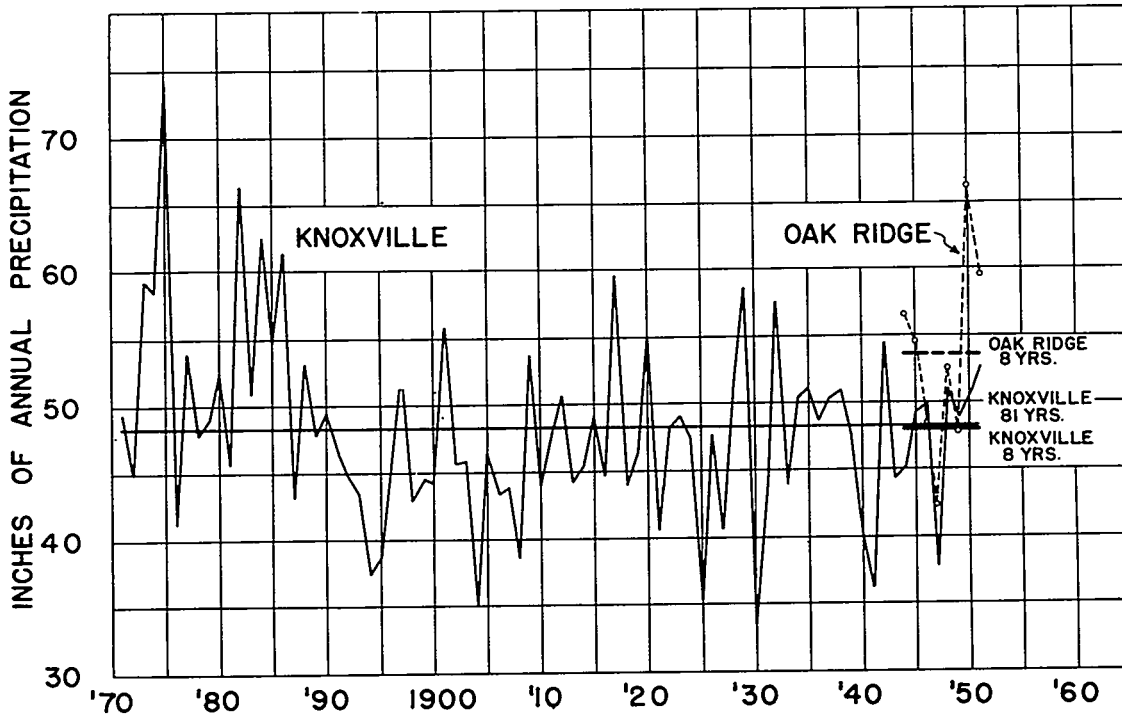
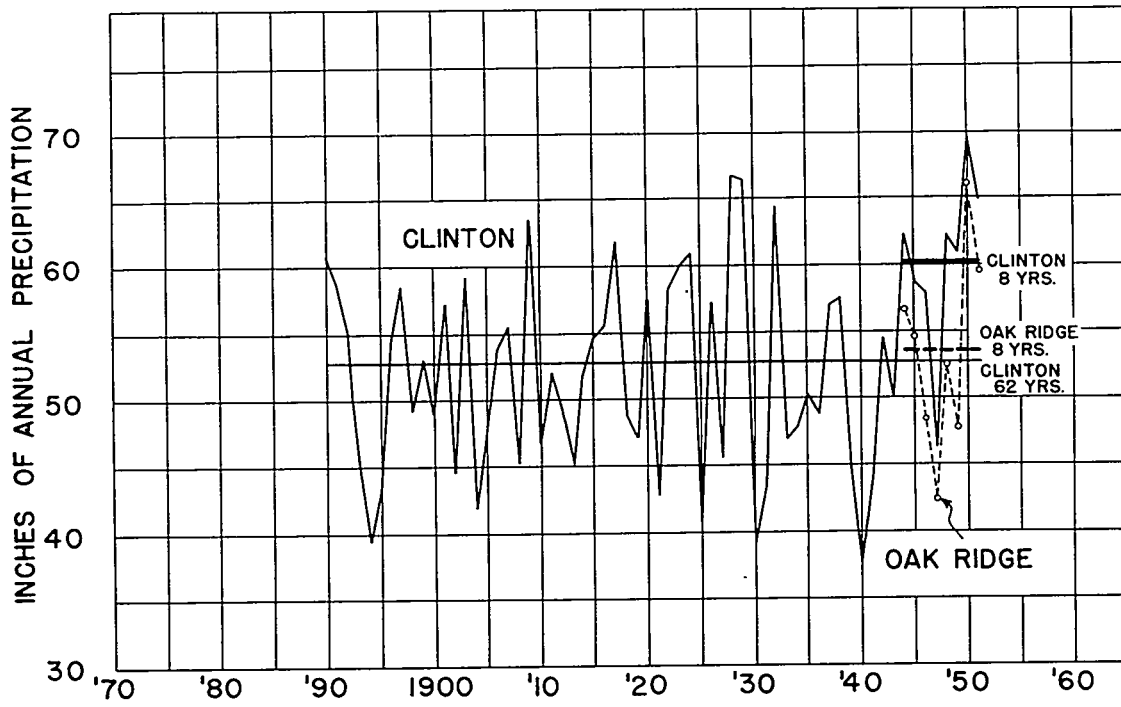


Fig. 41 Annual total precipitation for each year of record: Clinton and Knoxville compared with Oak Ridge (X-10).

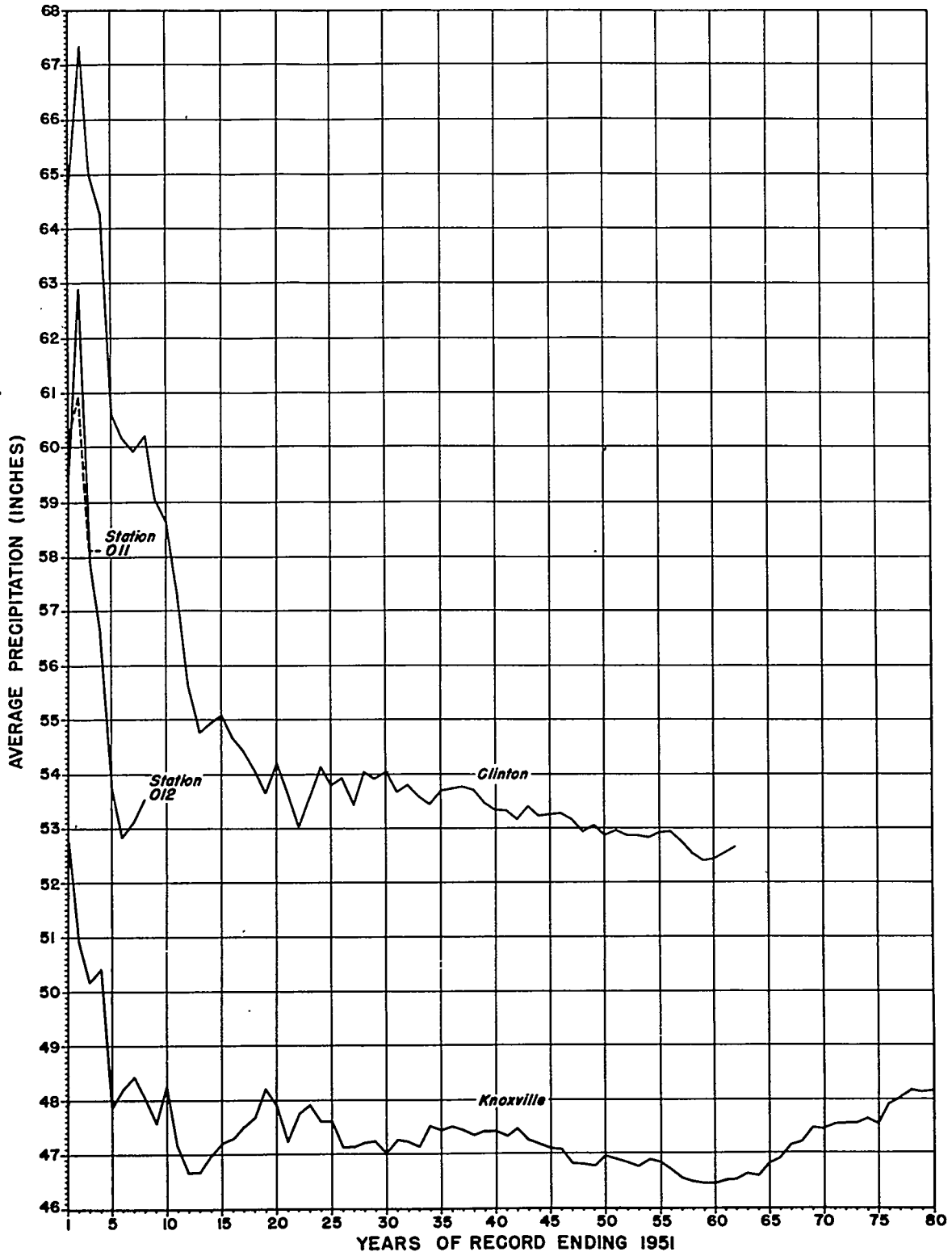


Fig. 42 Average annual precipitation for Clinton, Knoxville and Oak Ridge (X-10) as a function of length of record used.

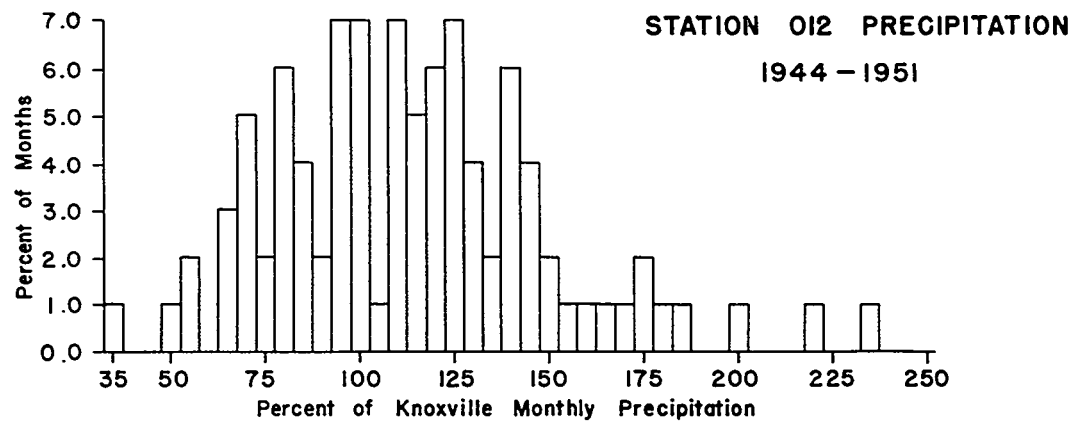
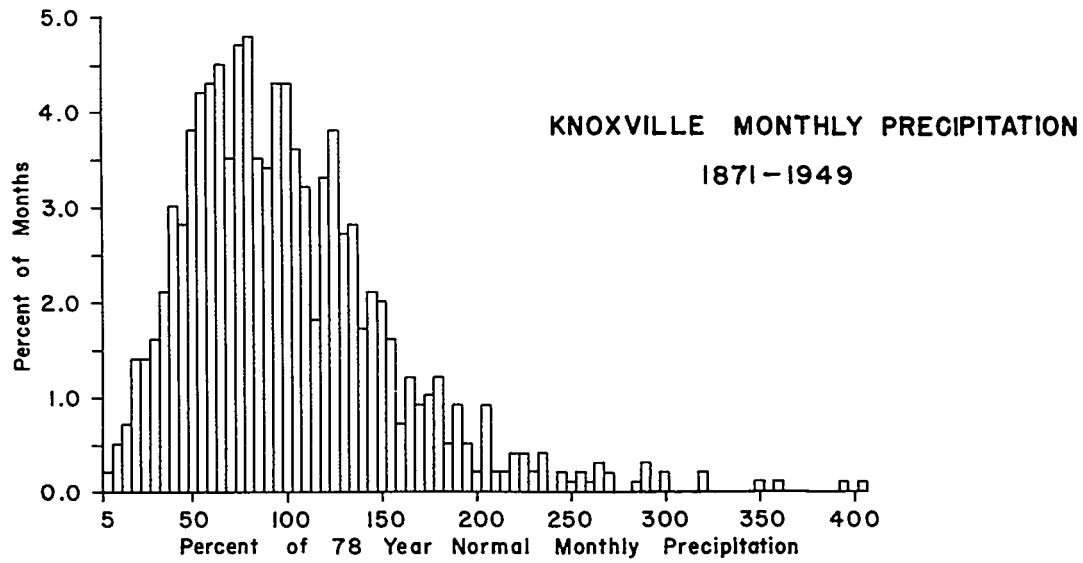
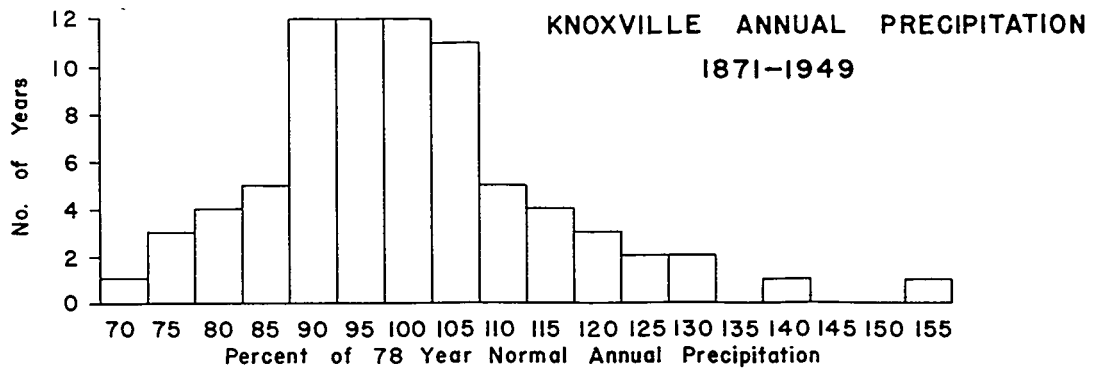


Fig. 43 Frequency distribution of (a) Knoxville annual precipitation, (b) Knoxville monthly precipitation and (c) the ratio of Oak Ridge (X-10) to Knoxville monthly precipitation.

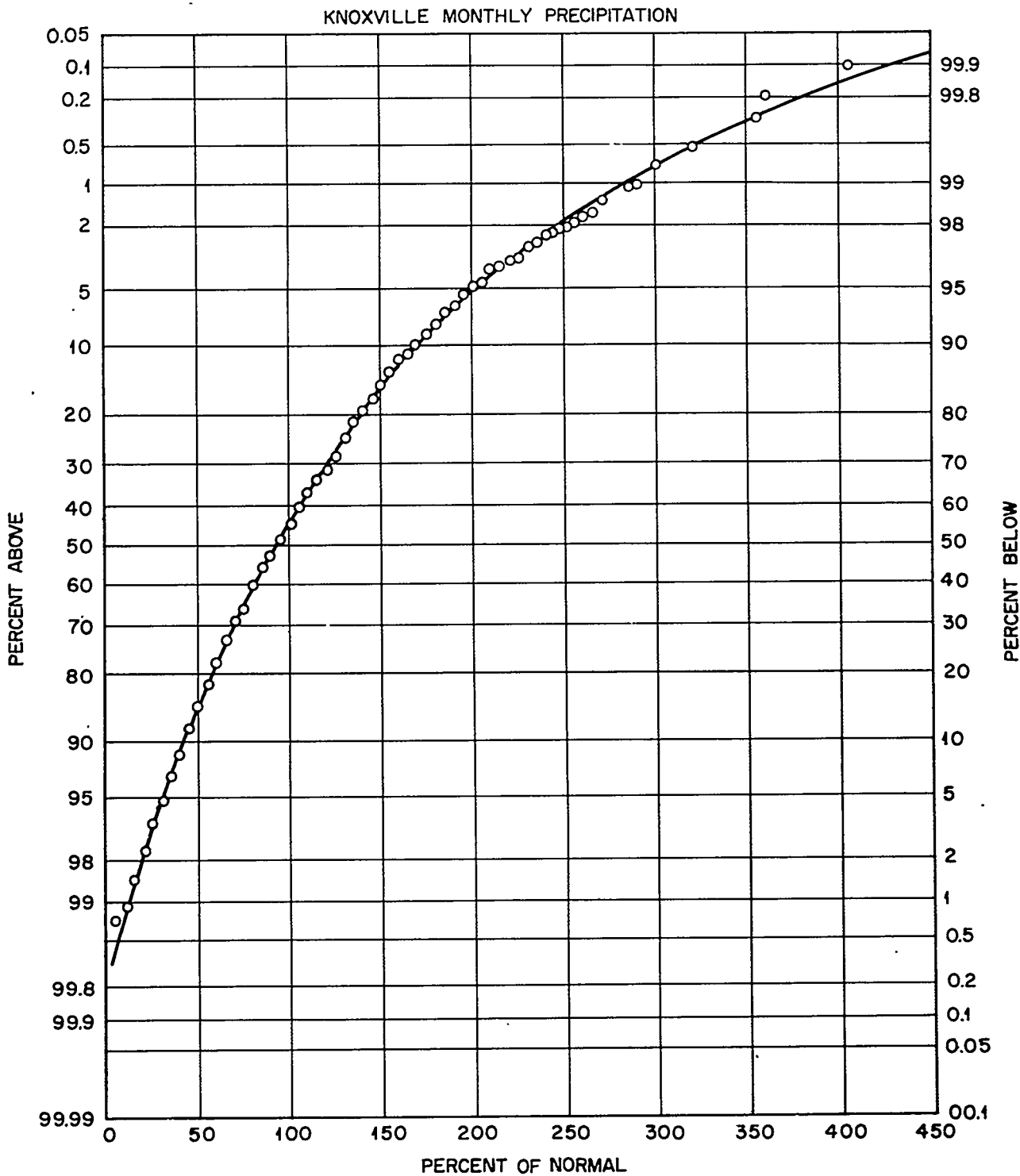


Fig. 44 Probability graph of Knoxville monthly precipitation (1871-1949) expressed as a percentage of the monthly average of record.

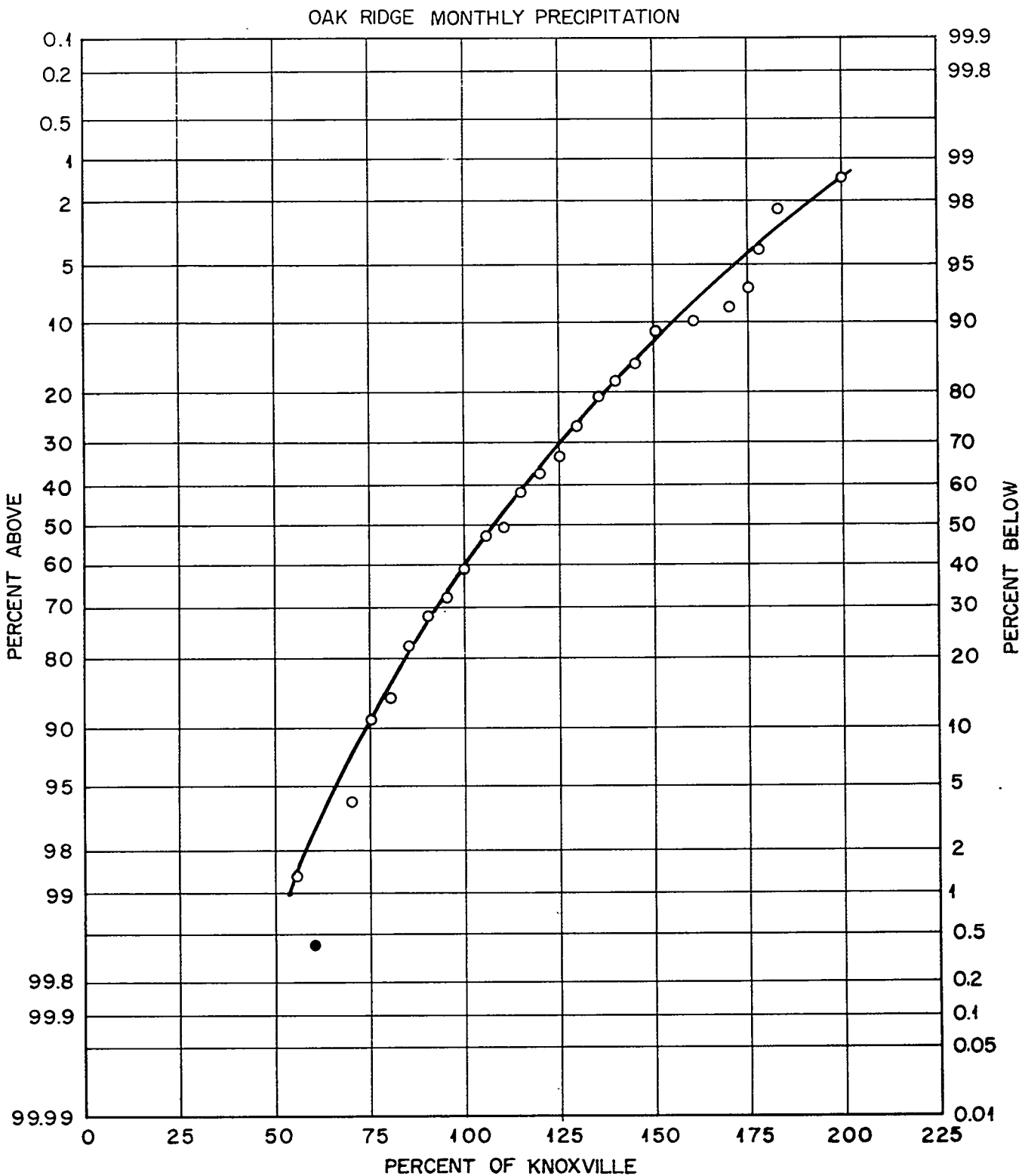


Fig. 45 Probability graph of the ratio of Oak Ridge (X-10) to Knoxville monthly precipitation.

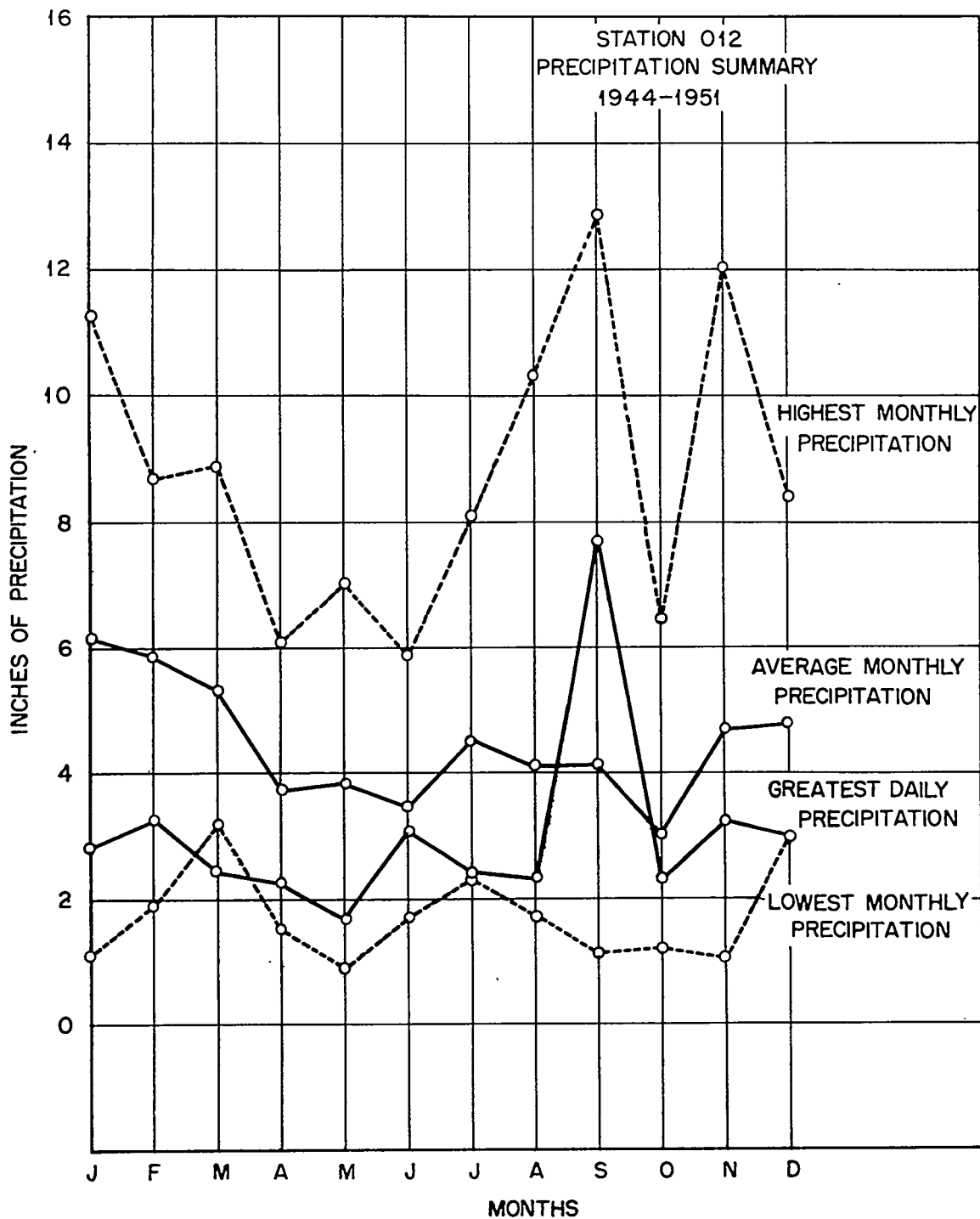


Fig. 46 Monthly average and extreme precipitation, Oak Ridge (X-10), 1944-1951.

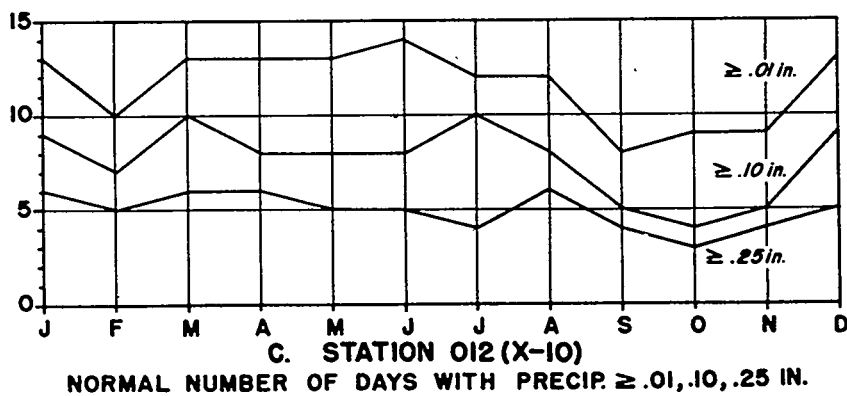
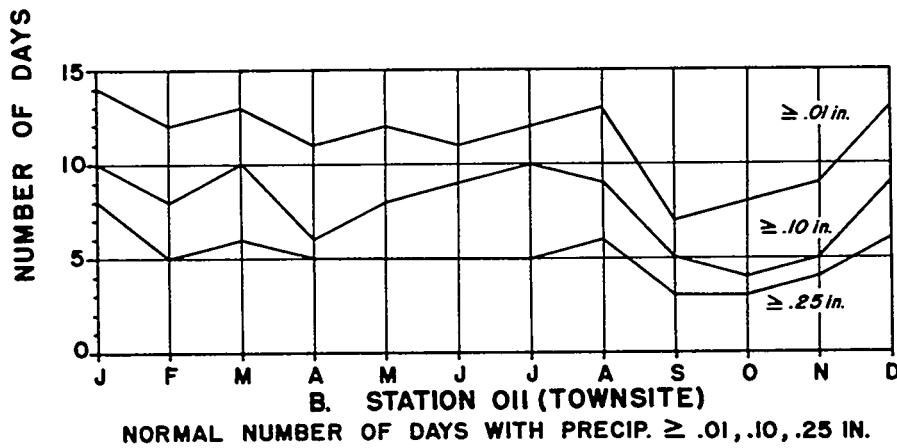
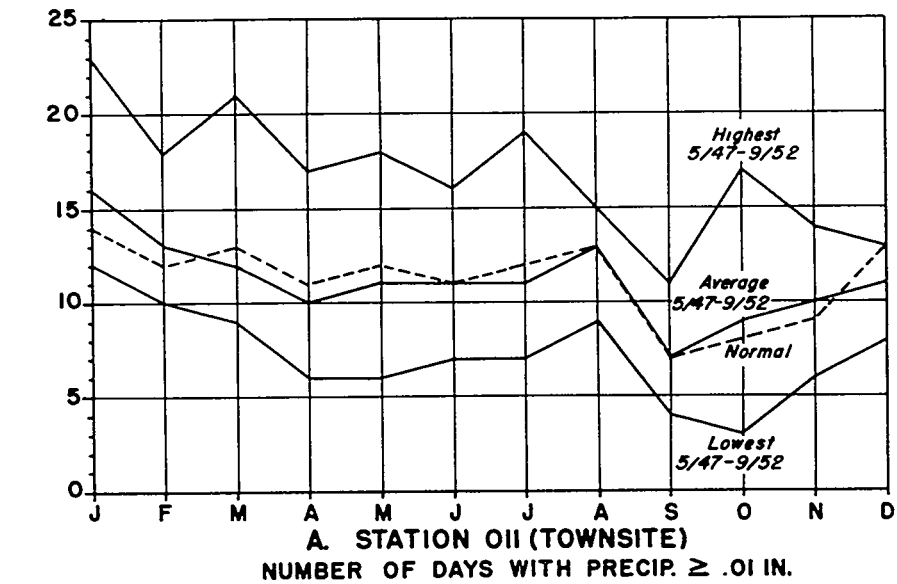


Fig. 47 Average monthly frequency of precipitation equal to or exceeding 0.01, 0.10 and 0.25 in., Townsite (O11) and X-10 (O12) stations.

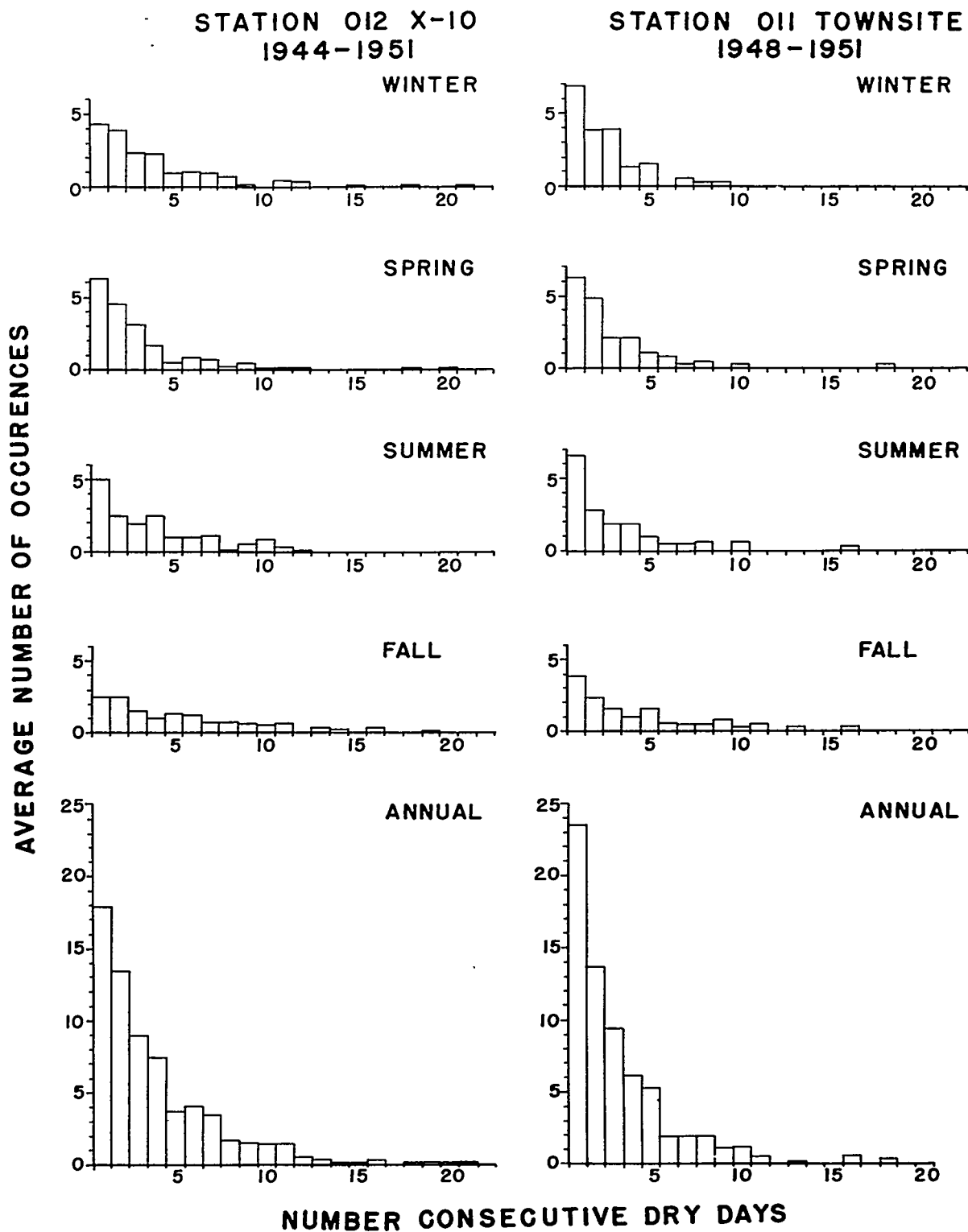


Fig. 48 Frequency distribution of number of consecutive days without measurable precipitation, seasonal and annual, Townsite (011) and X-10 (012) stations.

390

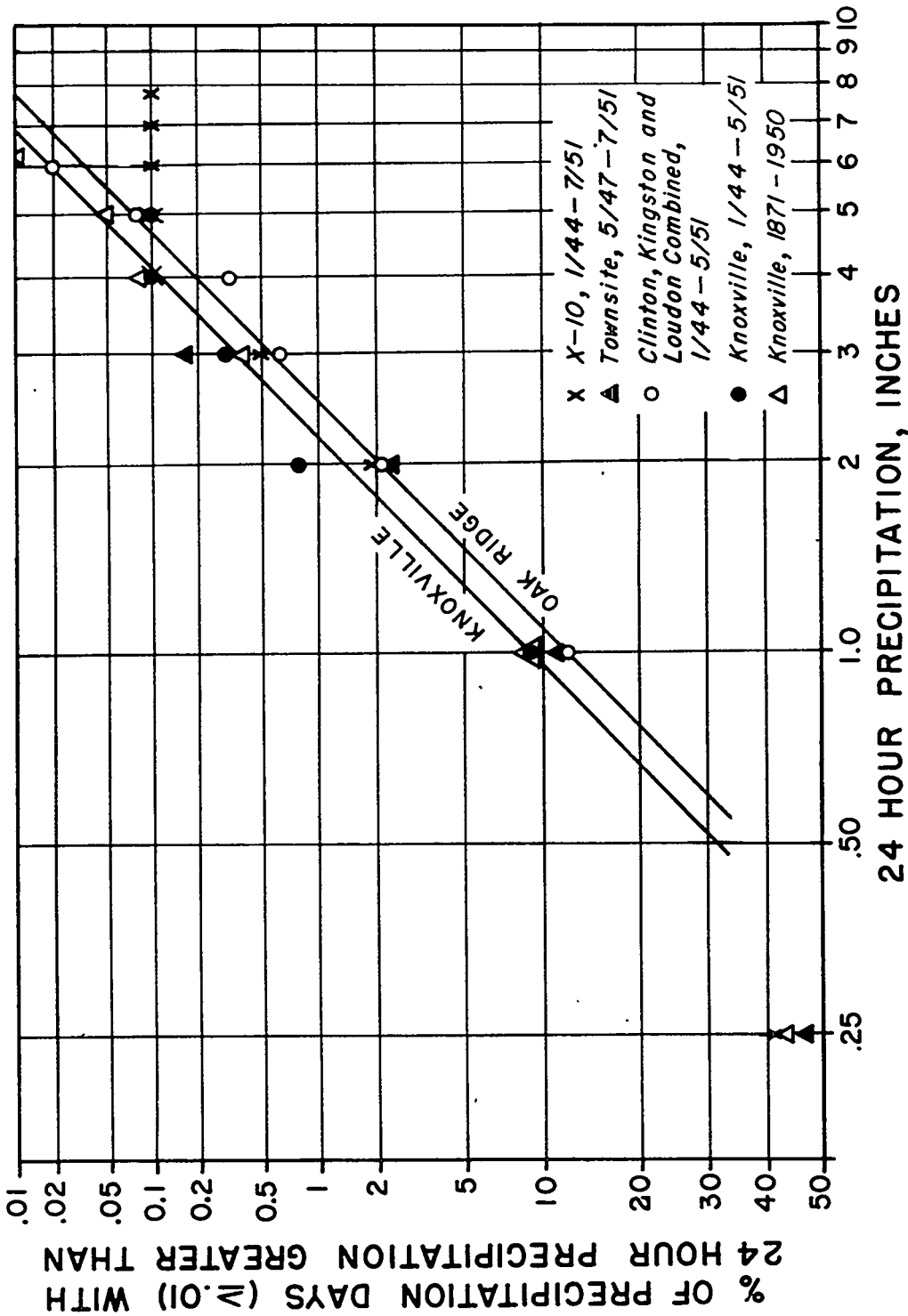


Fig. 49 Probability graph of logarithm of 24 hr. precipitation, with frequency expressed as a percentage of precipitation days (days with 0.01 in. or more), Oak Ridge and neighboring stations.

ANNUAL FREQUENCY OF OBSERVED WEATHER
SOUTHERN APPALACHIAN AREA

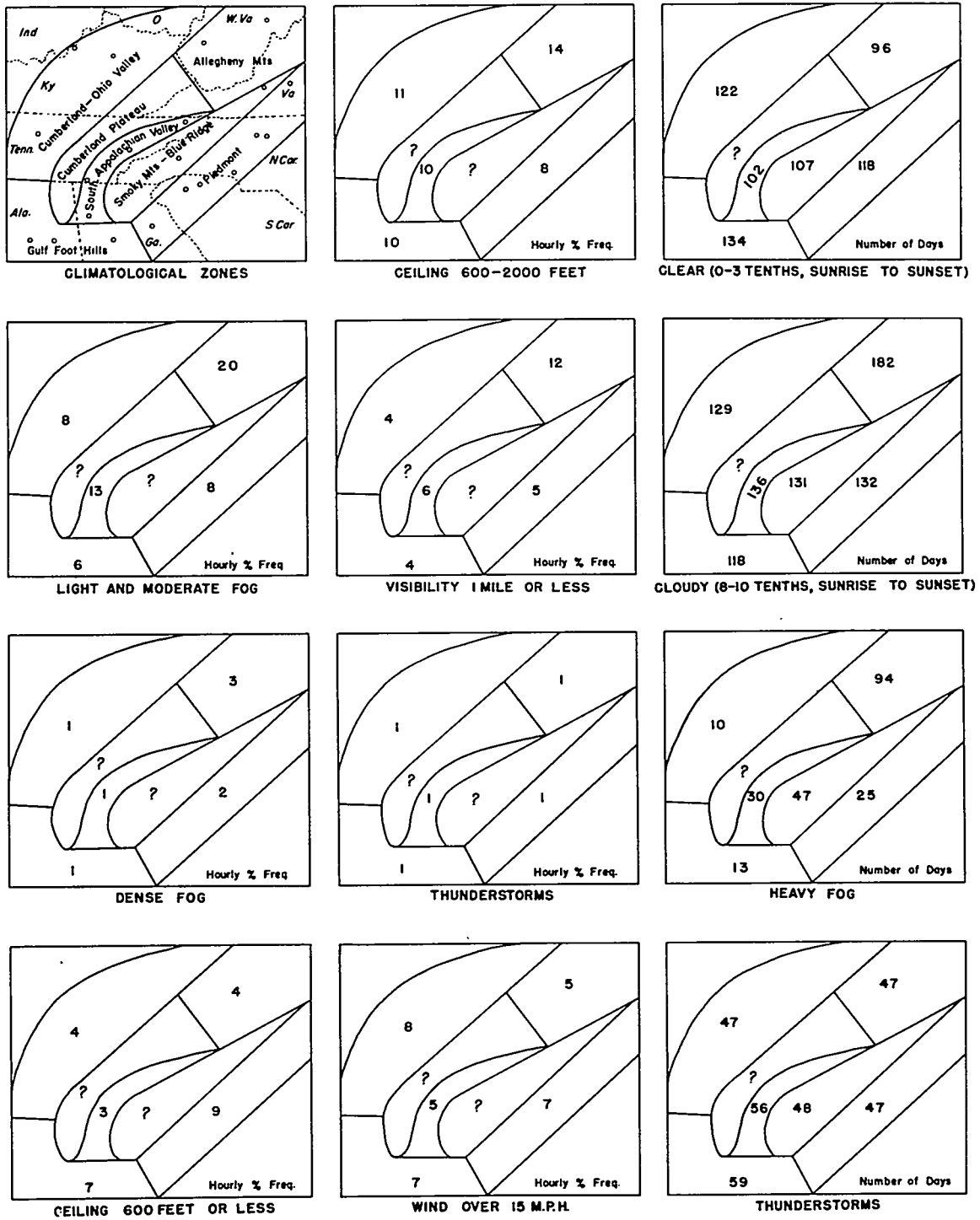


Fig. 50 Schematic maps of the Southern Appalachian area divided into broad zones, showing the annual frequencies of various weather phenomena in each zone.

373

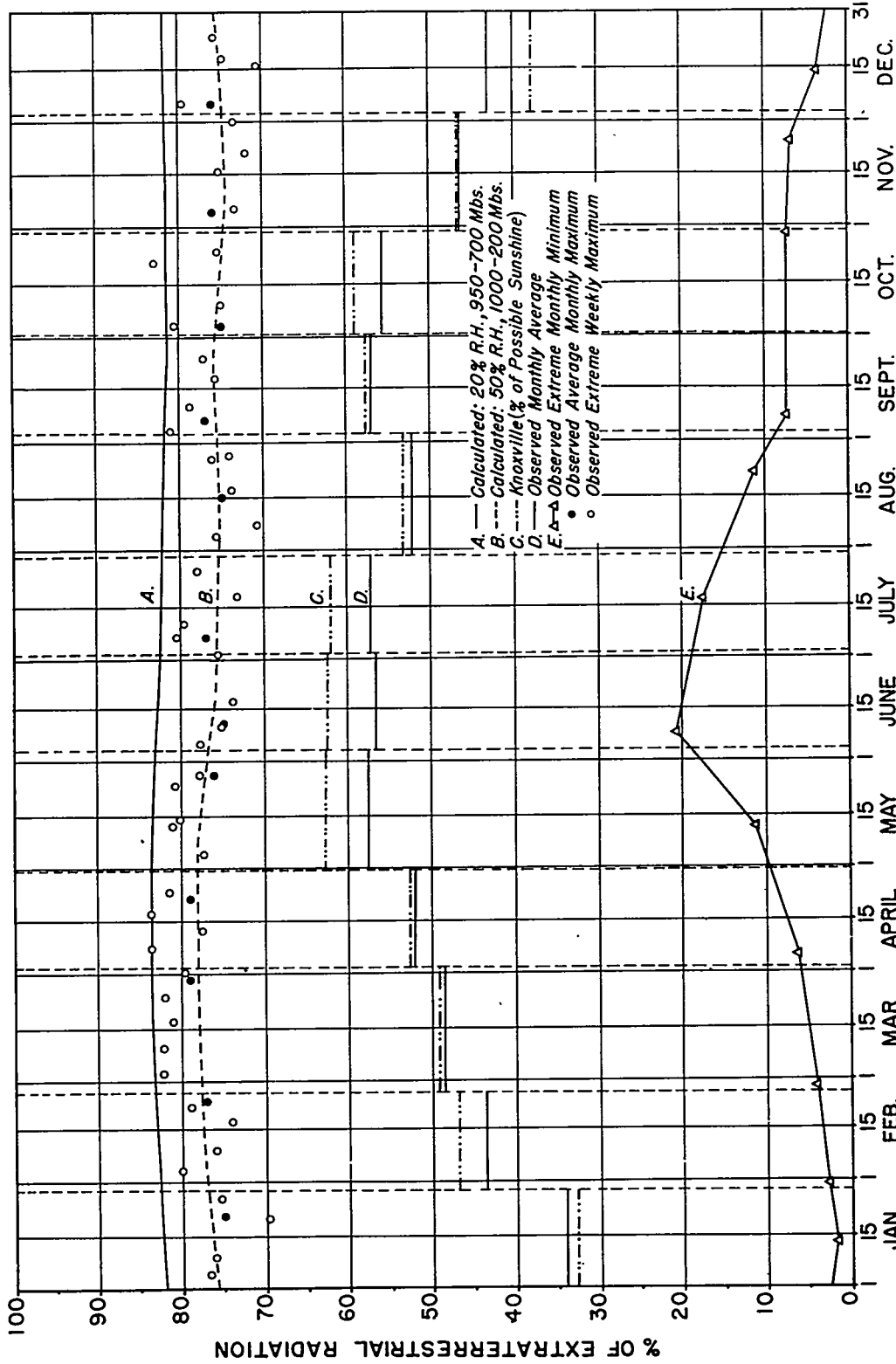


Fig. 51b Annual variation of average and extreme daily total solar radiation expressed as a percentage of theoretical extra-terrestrial solar radiation.

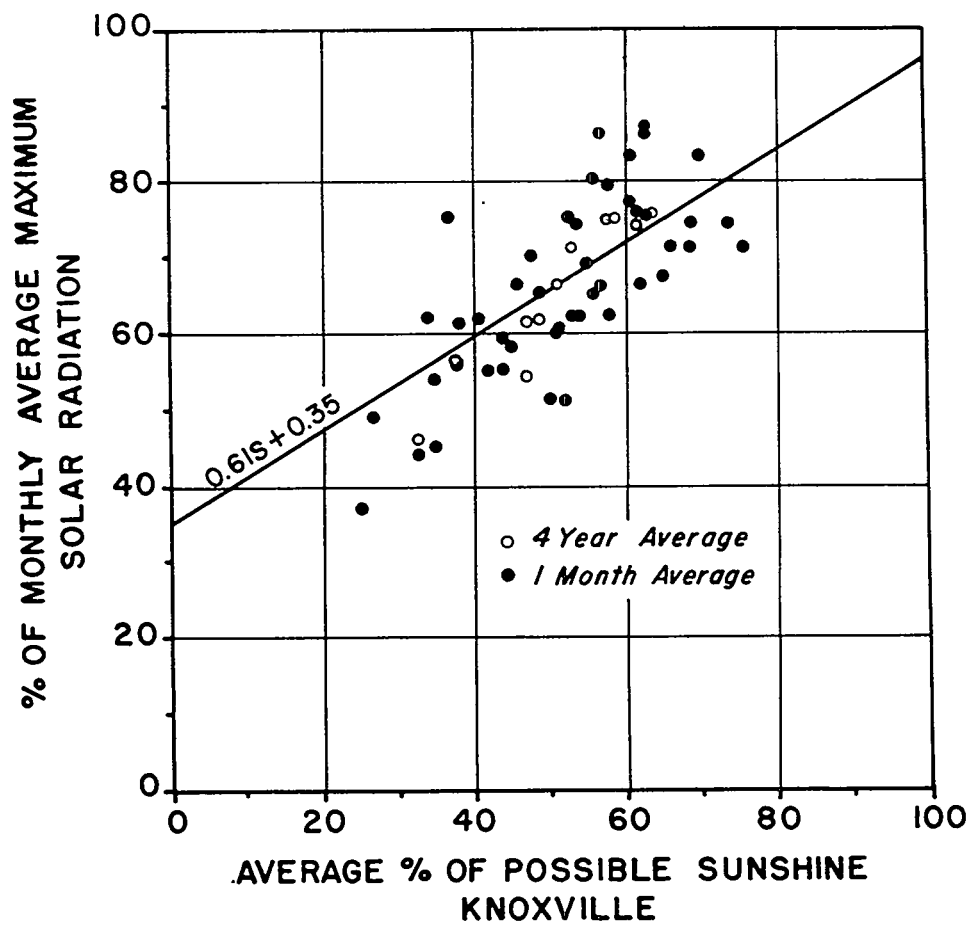


Fig. 52 Monthly average solar radiation (Oak Ridge) vs. sunshine duration (Knoxville).

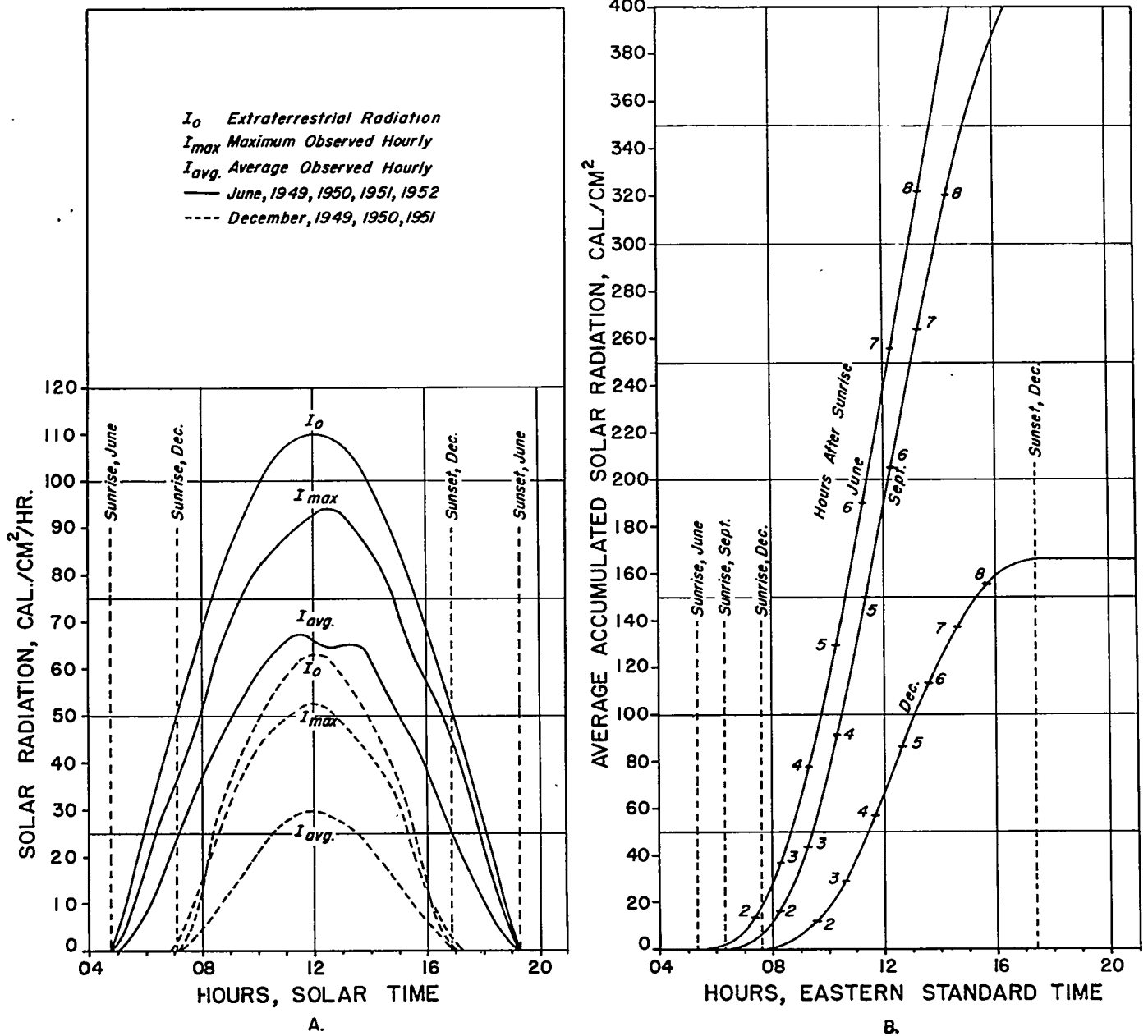
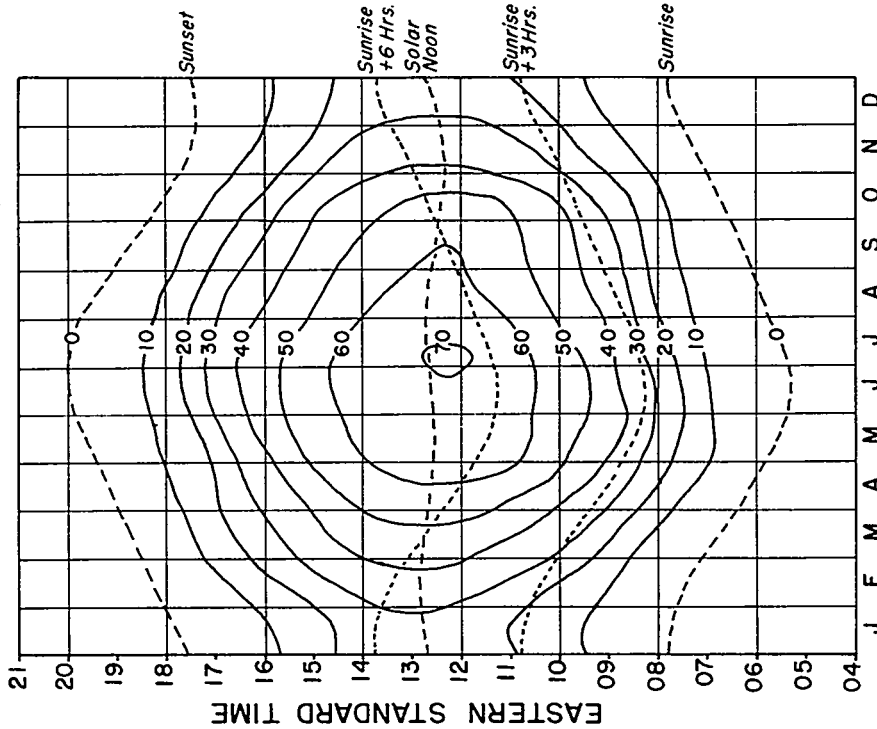


Fig. 53 Examples of diurnal variation of solar radiation: A. hourly total; B. accumulated total.

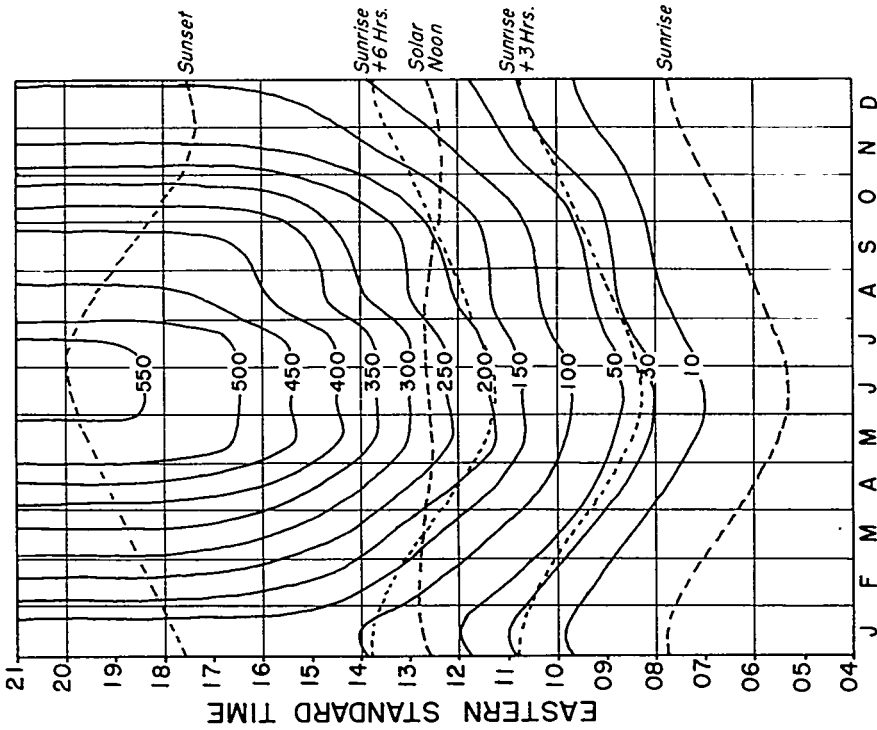
396

AVERAGE SOLAR RADIATION, CAL./CM²/HR.
DIURNAL AND ANNUAL VARIATION, 1949-1952



A.

ACCUMULATED HOURLY SOLAR RADIATION, CAL./CM²
DIURNAL AND ANNUAL VARIATION, 1949-1952



B.

Fig. 54 Combined annual and diurnal pattern of solar radiation: A. hourly average; B. average total accumulated since sunrise each day.

West

Southeast

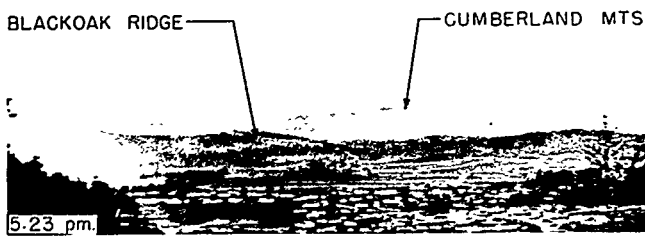
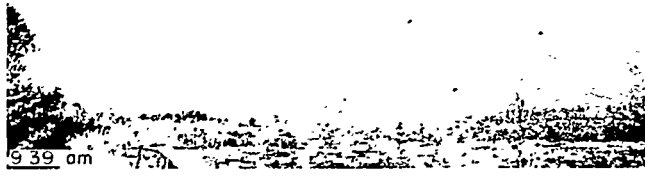
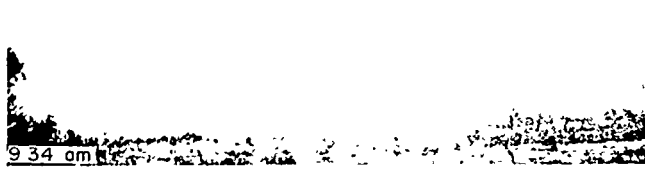
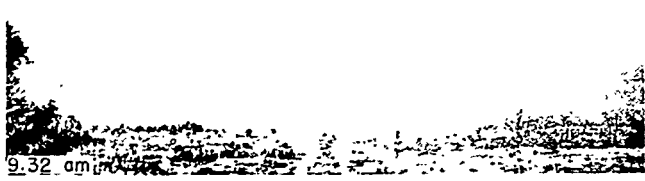
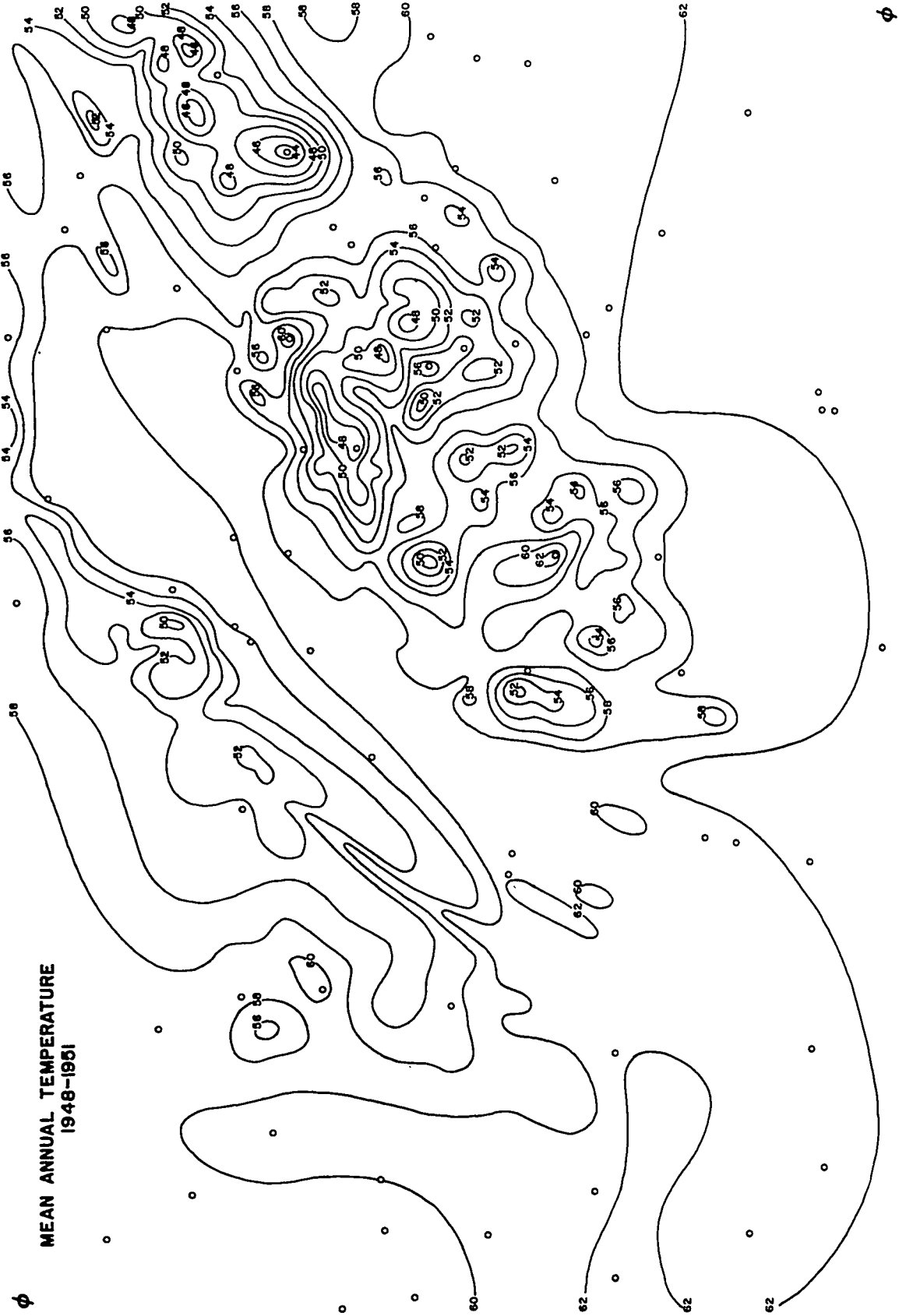


Fig. 55 Series of photographs showing dissipation of morning ground fog simultaneously in two valleys.

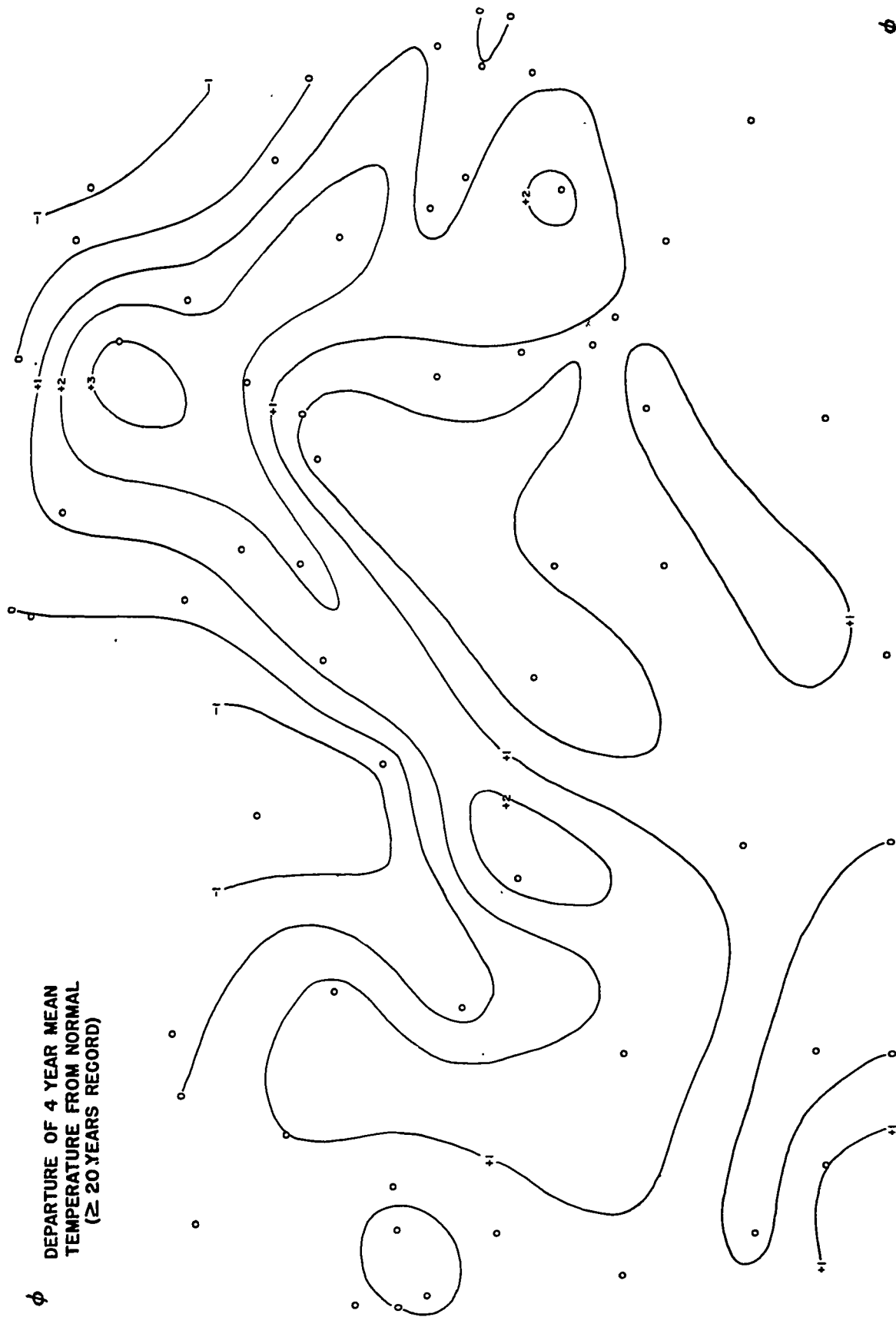
378



MEAN ANNUAL TEMPERATURE
1948-1951

Fig. 56 Map of mean annual temperature, 1948-1951, Southern Appalachian area.

399



DEPARTURE OF 4 YEAR MEAN
TEMPERATURE FROM NORMAL
(\geq 20 YEARS RECORD)

Fig. 57 Map of departure of 1948-1951 mean temperature from average of record based on stations in the Southern Appalachian area having 20 years record or more.

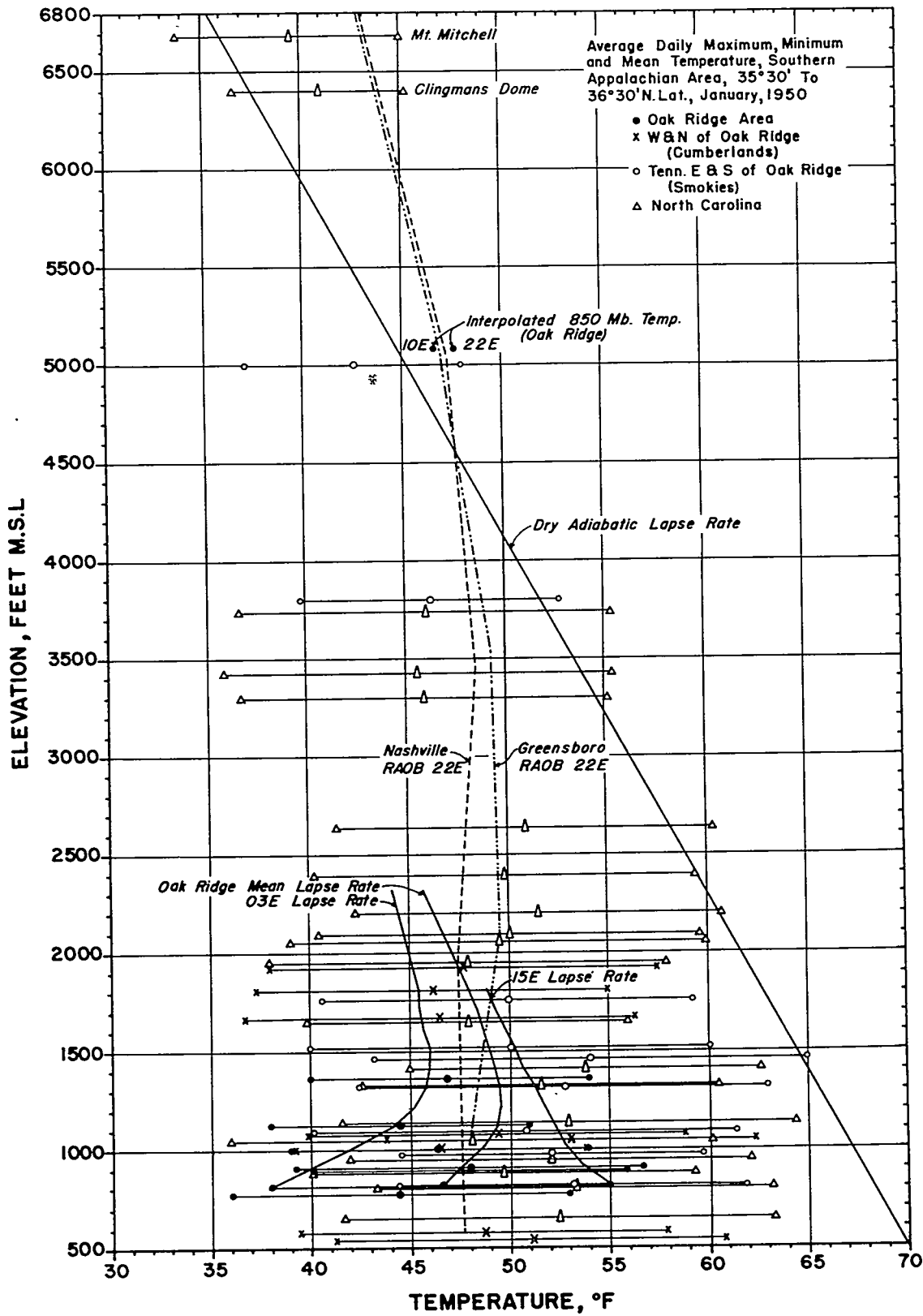


Fig. 58 Average daily maximum, minimum and mean temperature vs. altitude, Southern Appalachian area, Jan. 1950.

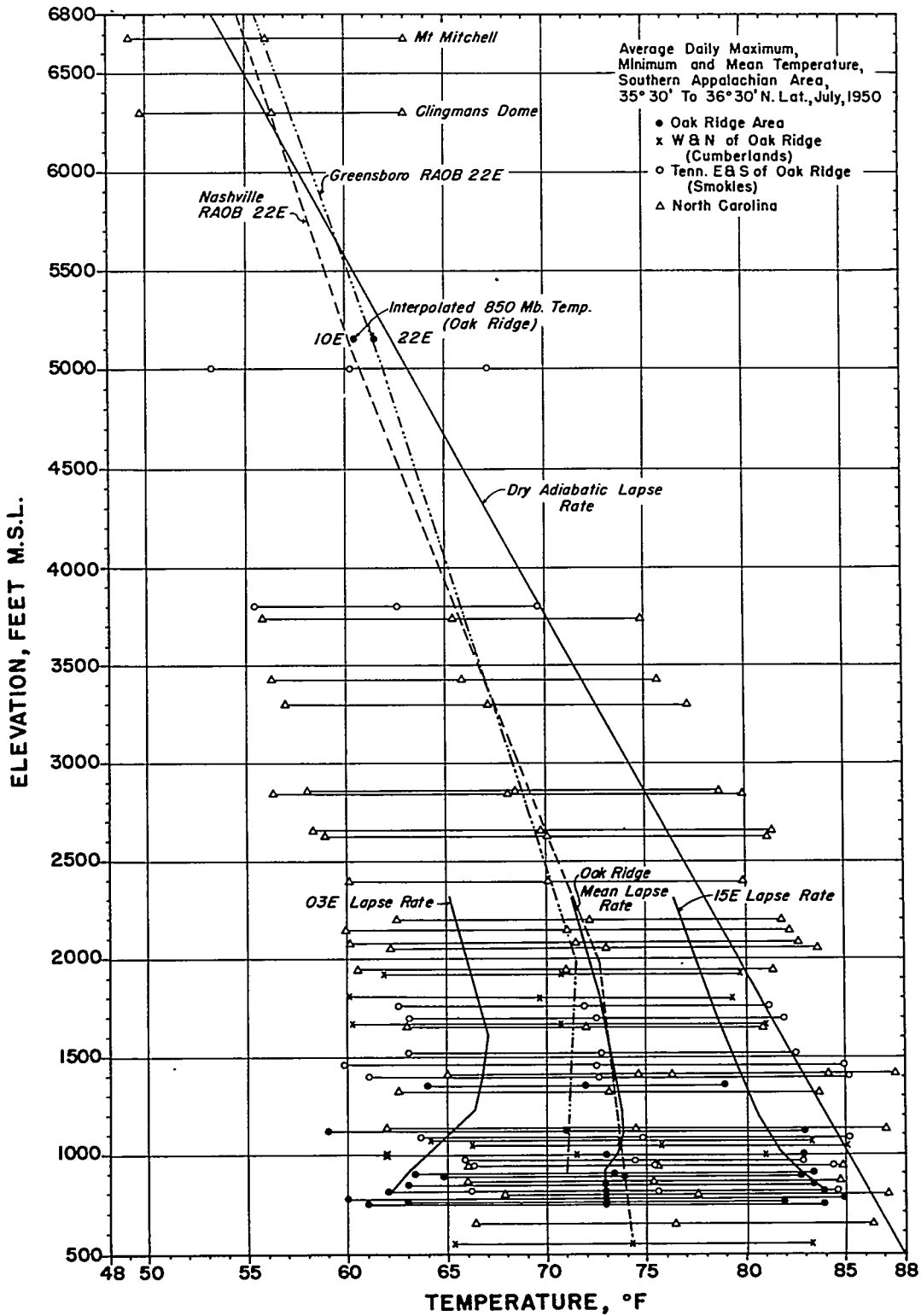


Fig. 59 Average daily maximum, minimum and mean temperature vs. altitude, Southern Appalachian area, July 1950.

MEAN MONTHLY TEMPERATURE
STATION 012, JAN. 1945-DEC.1952

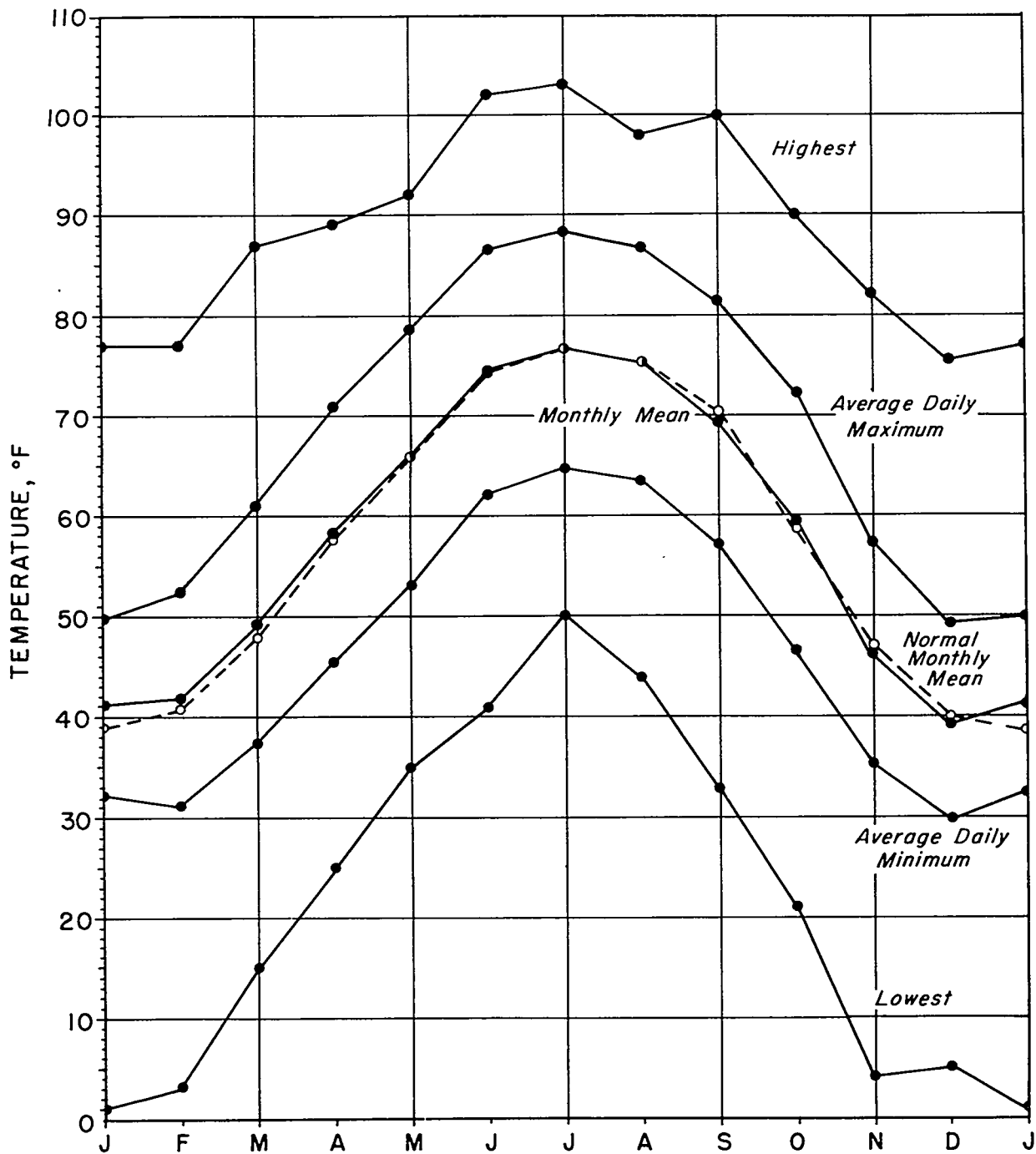


Fig. 60 Monthly average and extreme temperatures, Oak Ridge (X-10), 1945 - 1952.

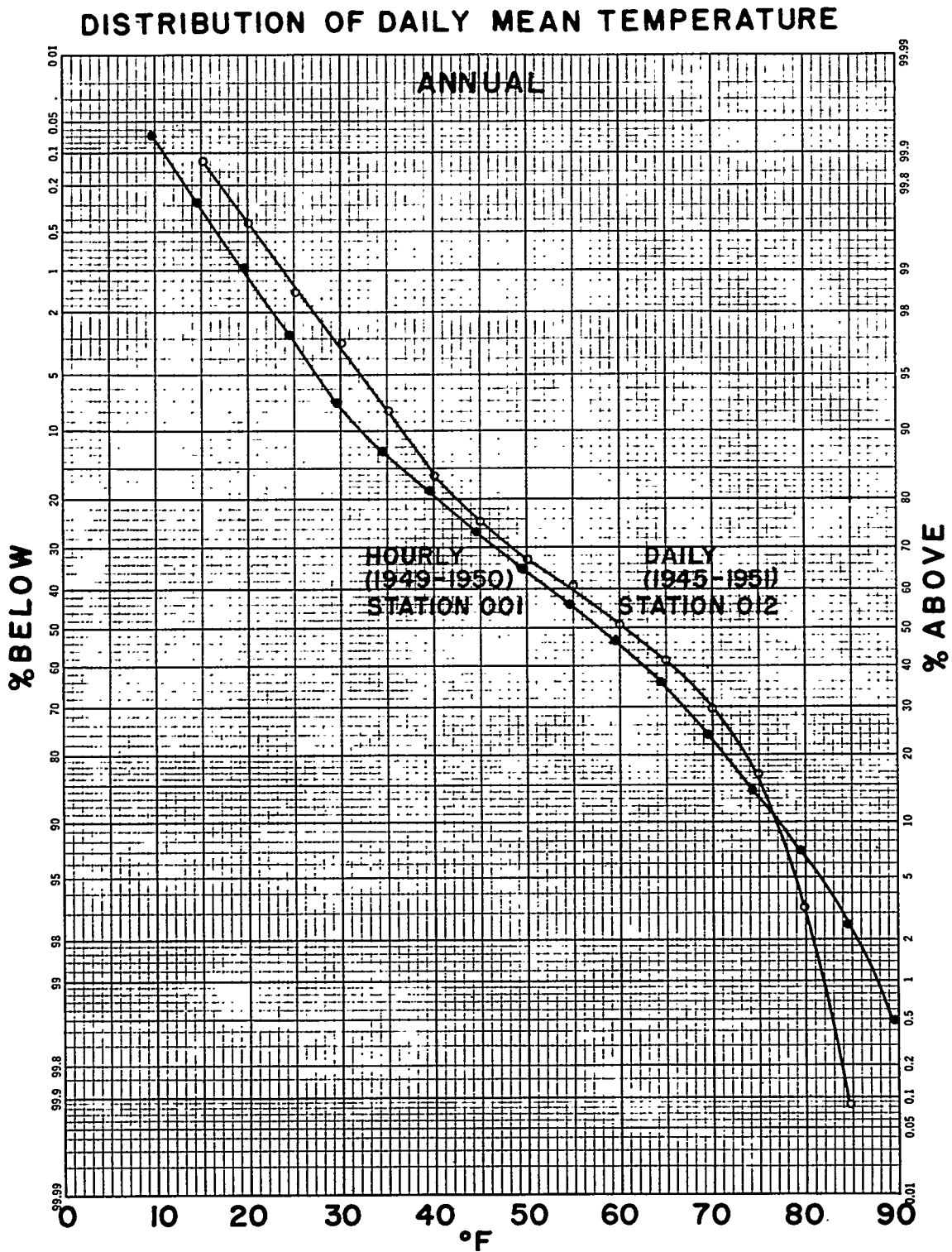


Fig. 61a Probability graph of daily mean temperature, Oak Ridge (X-10): Annual, stations 001 (1949-1950, based on hourly temperatures) and 012 (1945-1951, based on daily maximum and minimum temperatures).

DISTRIBUTION OF DAILY MEAN TEMPERATURE 1945-1951

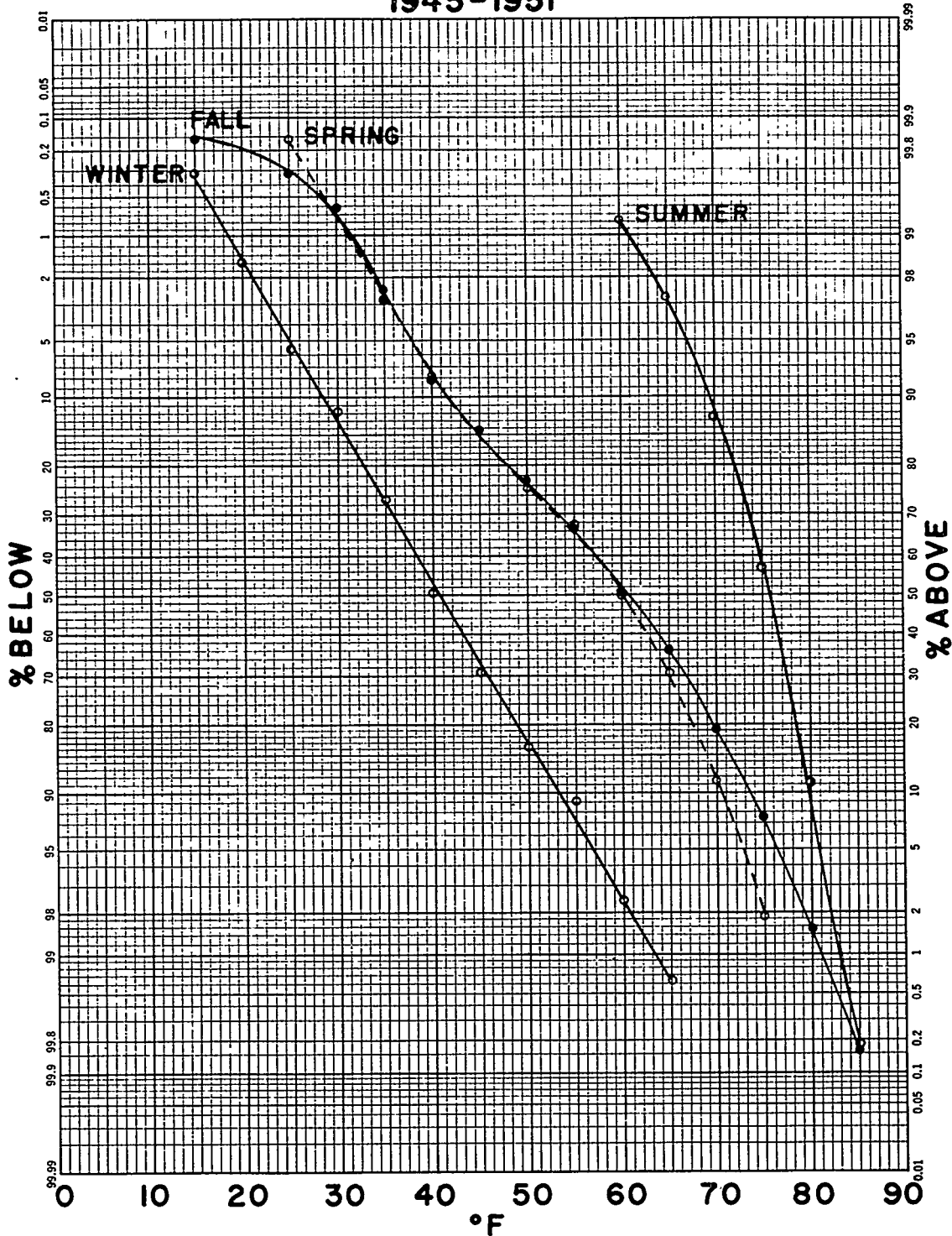


Fig. 61b Probability graph of daily mean temperature, Oak Ridge (X-10) seasonal, station 012, 1945-1951.

DISTRIBUTION OF DAILY MAXIMUM TEMPERATURES 1947-1951

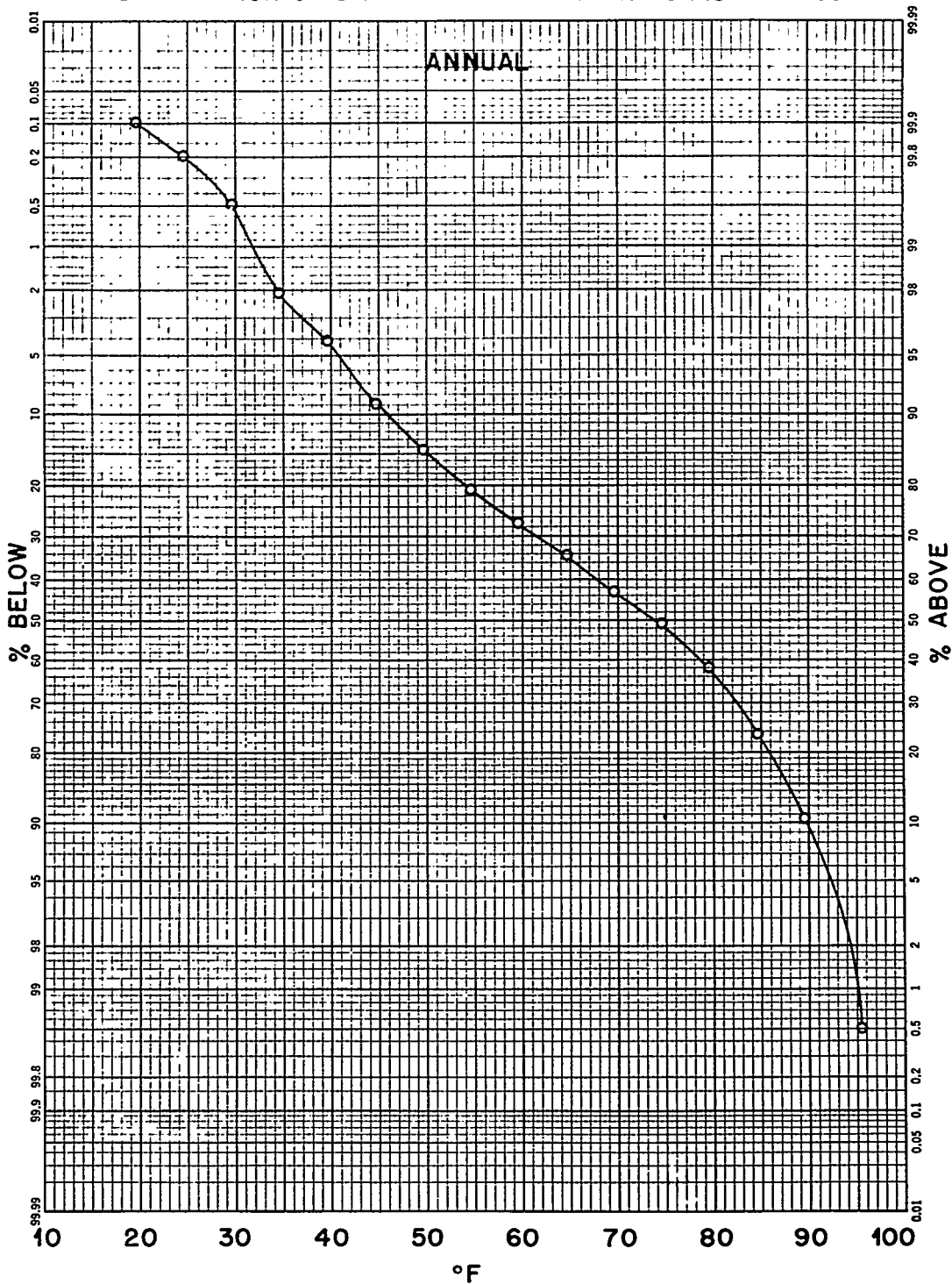


Fig. 62a Probability graphs of daily maximum temperature, Oak Ridge (X-10, station 012, 1947-1951): annual.

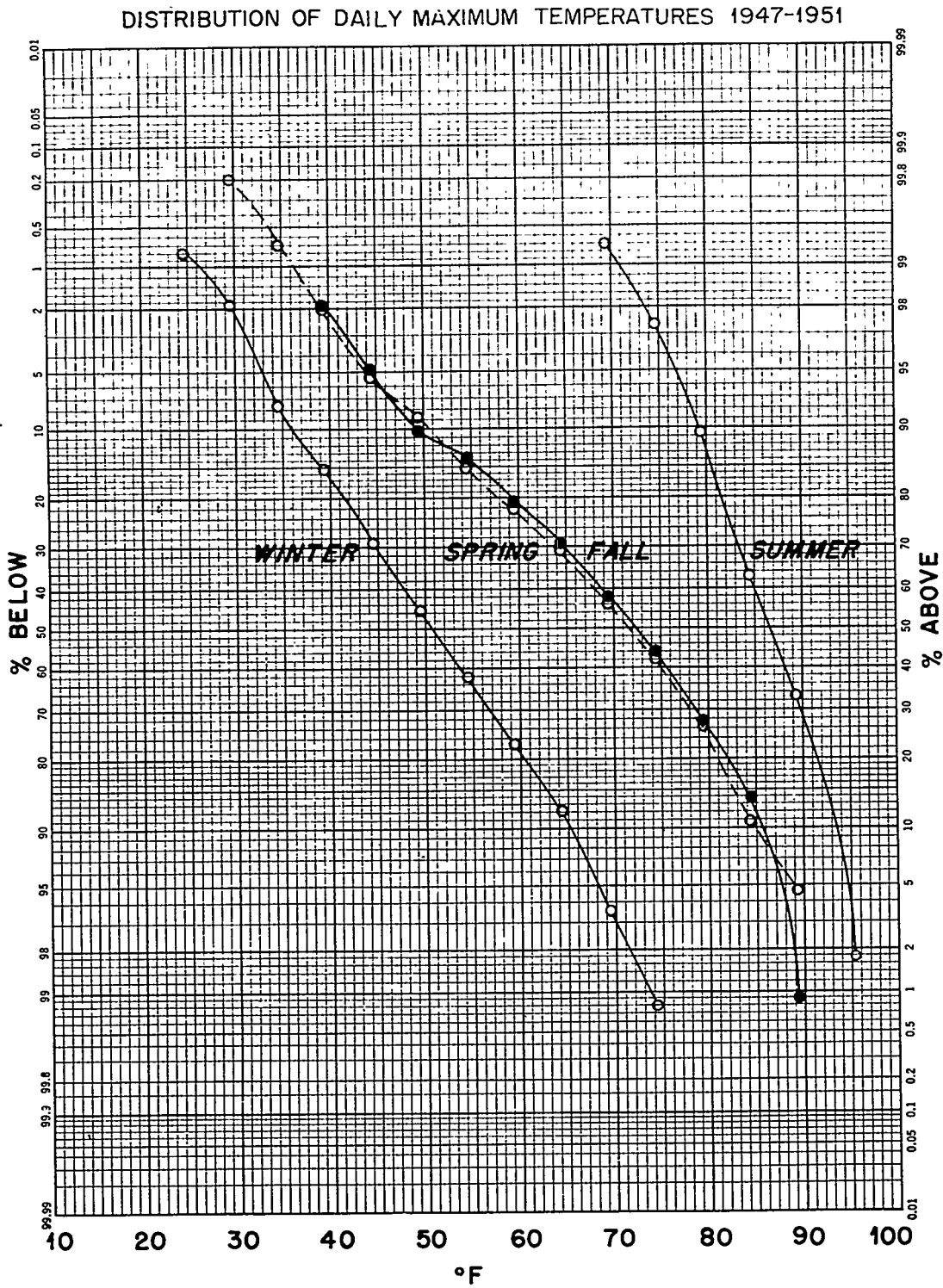


Fig. 62b Probability graphs of daily maximum temperature, Oak Ridge (X-10, station 012, 1947-1951): seasonal.

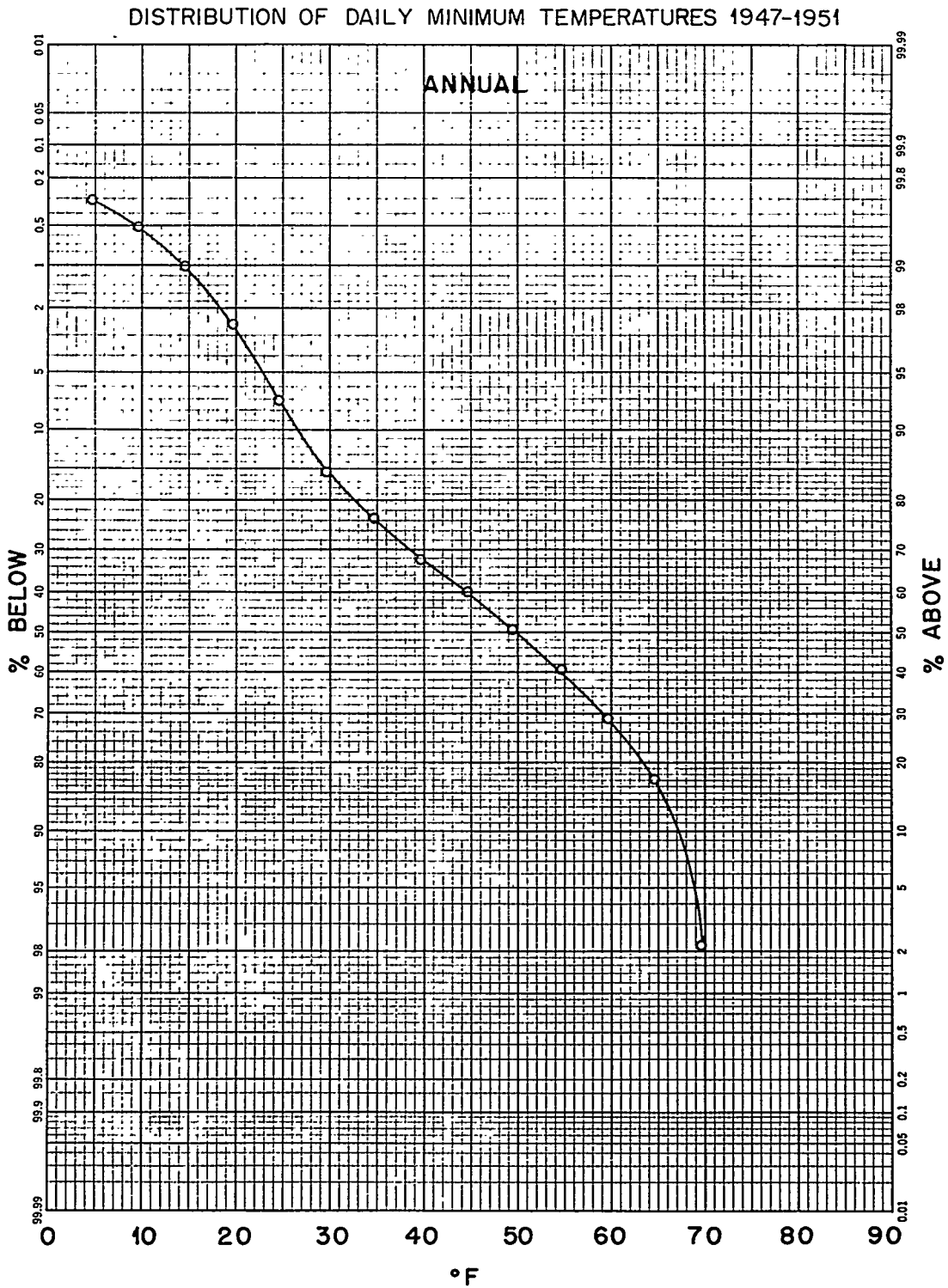


Fig. 63a Probability graphs of daily minimum temperature, Oak Ridge (X-10, station 012, 1947-1951): annual.

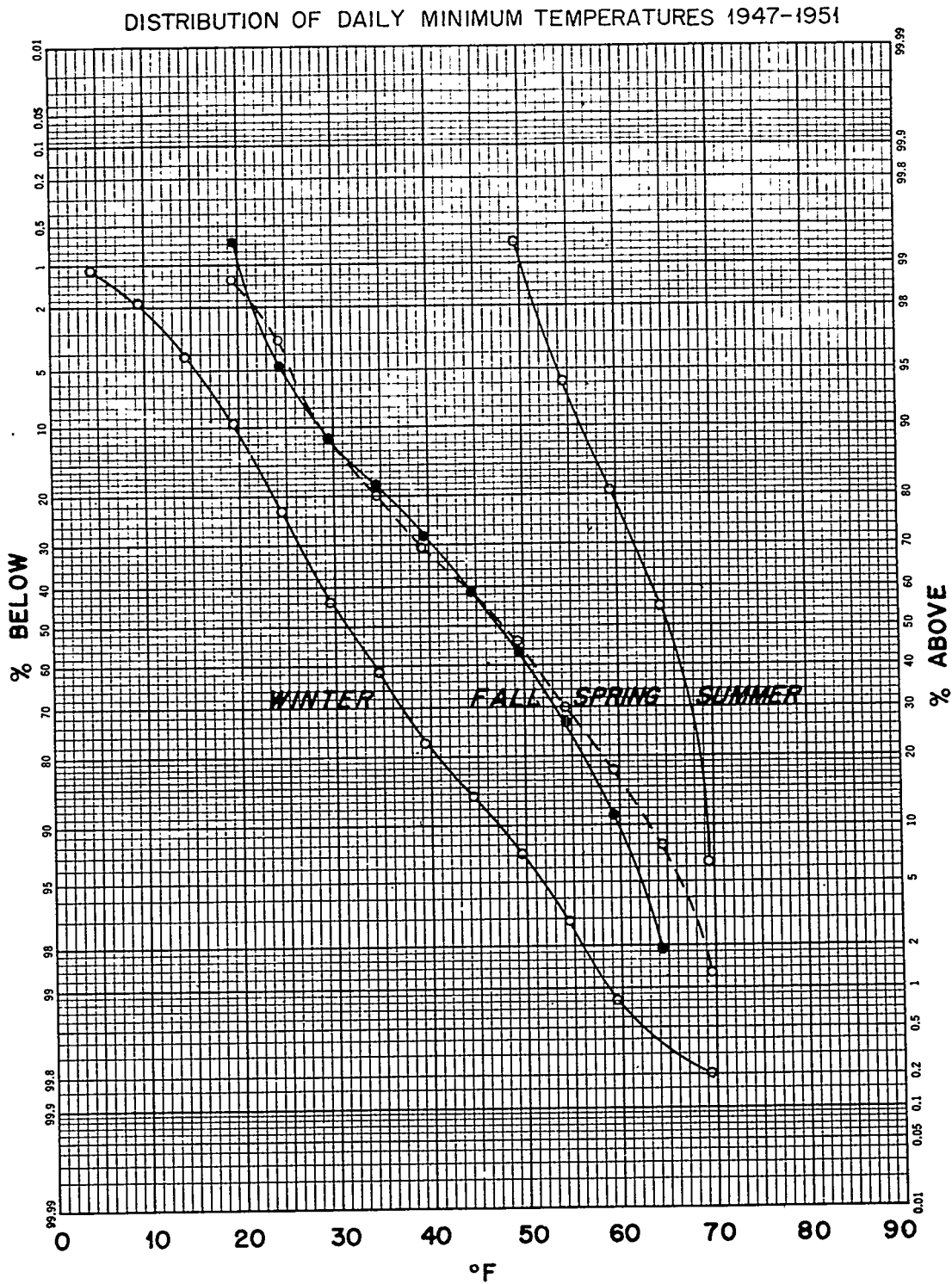


Fig. 63b Probability graphs of daily minimum temperature, Oak Ridge (X-10, station 012, 1947-1951): seasonal.

MONTHLY DEGREE DAYS (Adjusted To 30 Years 1921-1950)

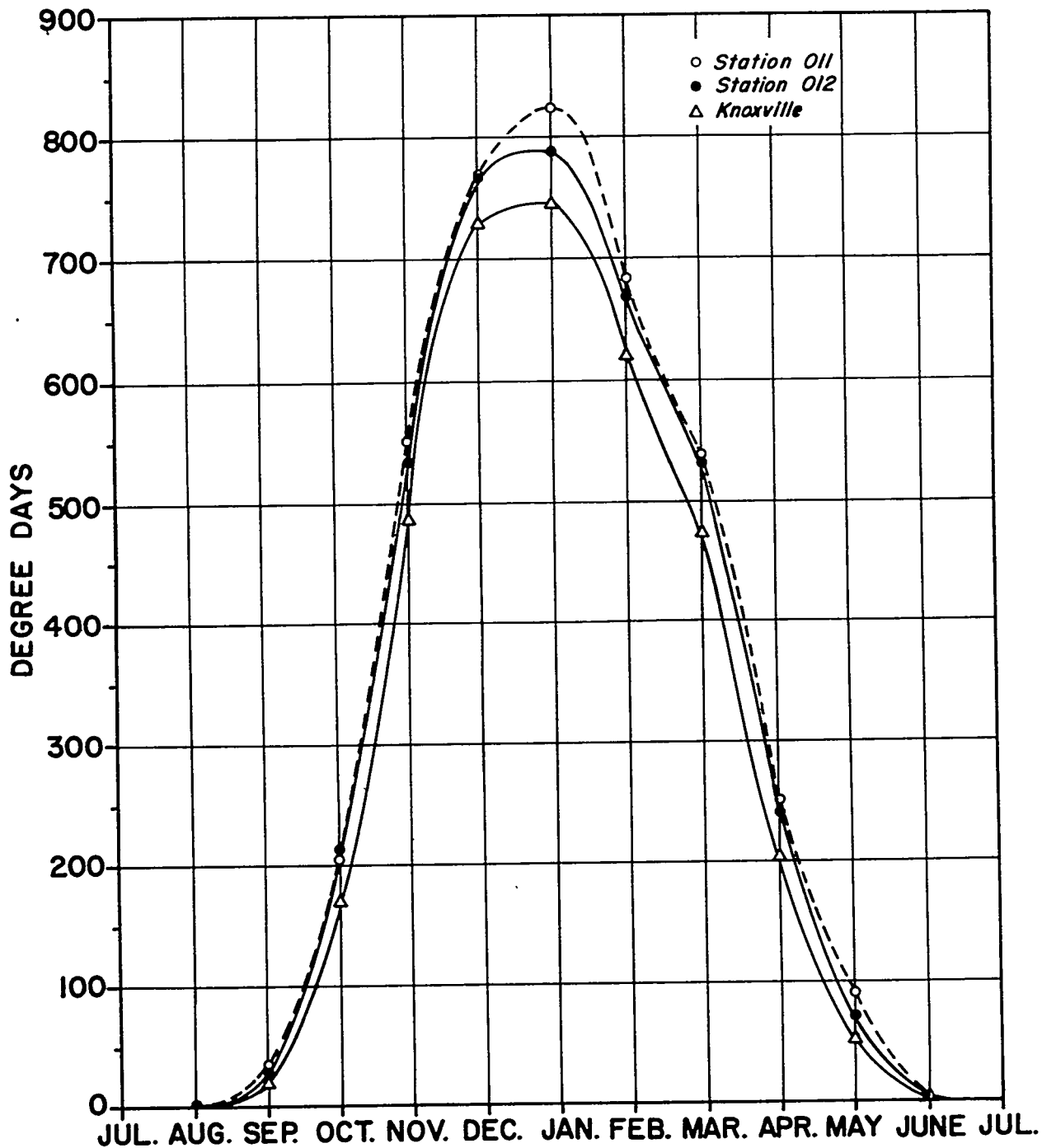


Fig. 64a Normal degree days, Knoxville, Oak Ridge Townsite (011) and X-10 (012), adjusted to the 30-year period 1921 - 1950, monthly total.

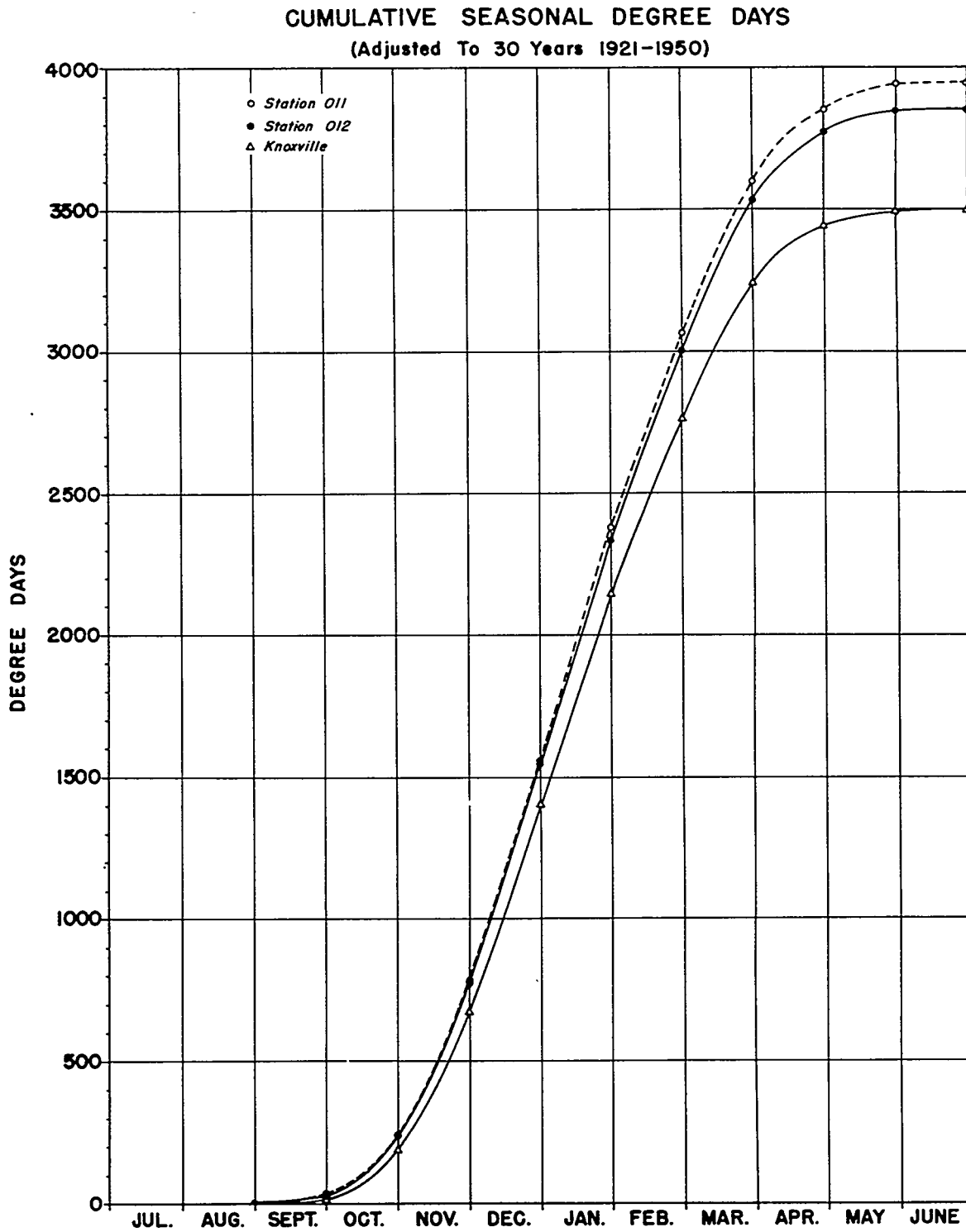


Fig. 64b Normal degree days, Knoxville, Oak Ridge Townsite (011) and X-10 (012), adjusted to the 30-year period 1921 - 1950, accumulated seasonal total.

ANNUAL FREQUENCY OF DAILY TEMPERATURE RANGE STATION 012, 1/49 - 10/50

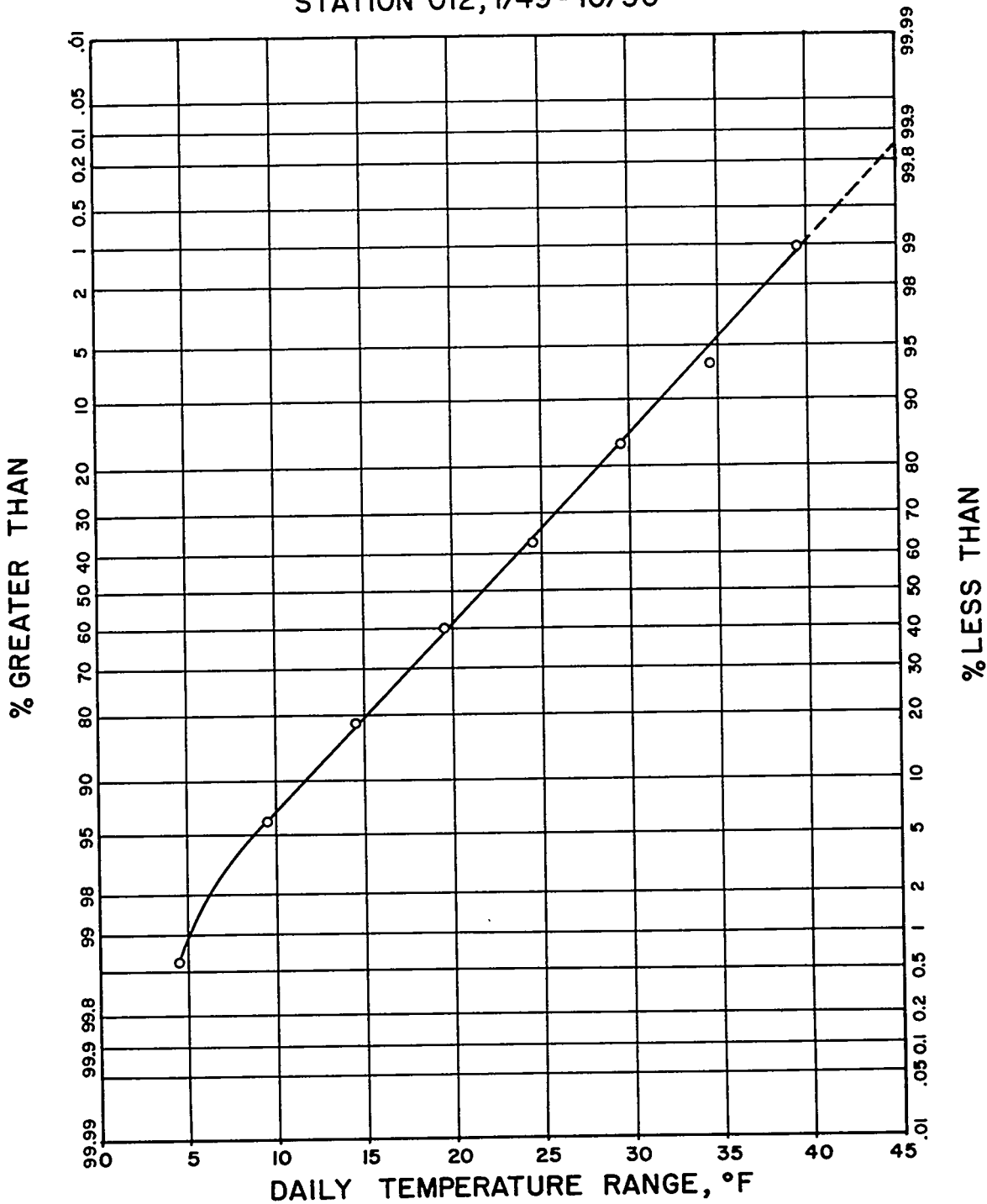


Fig. 65 Probability graph of daily temperature range, station 012, annual, 1949 - 1950.

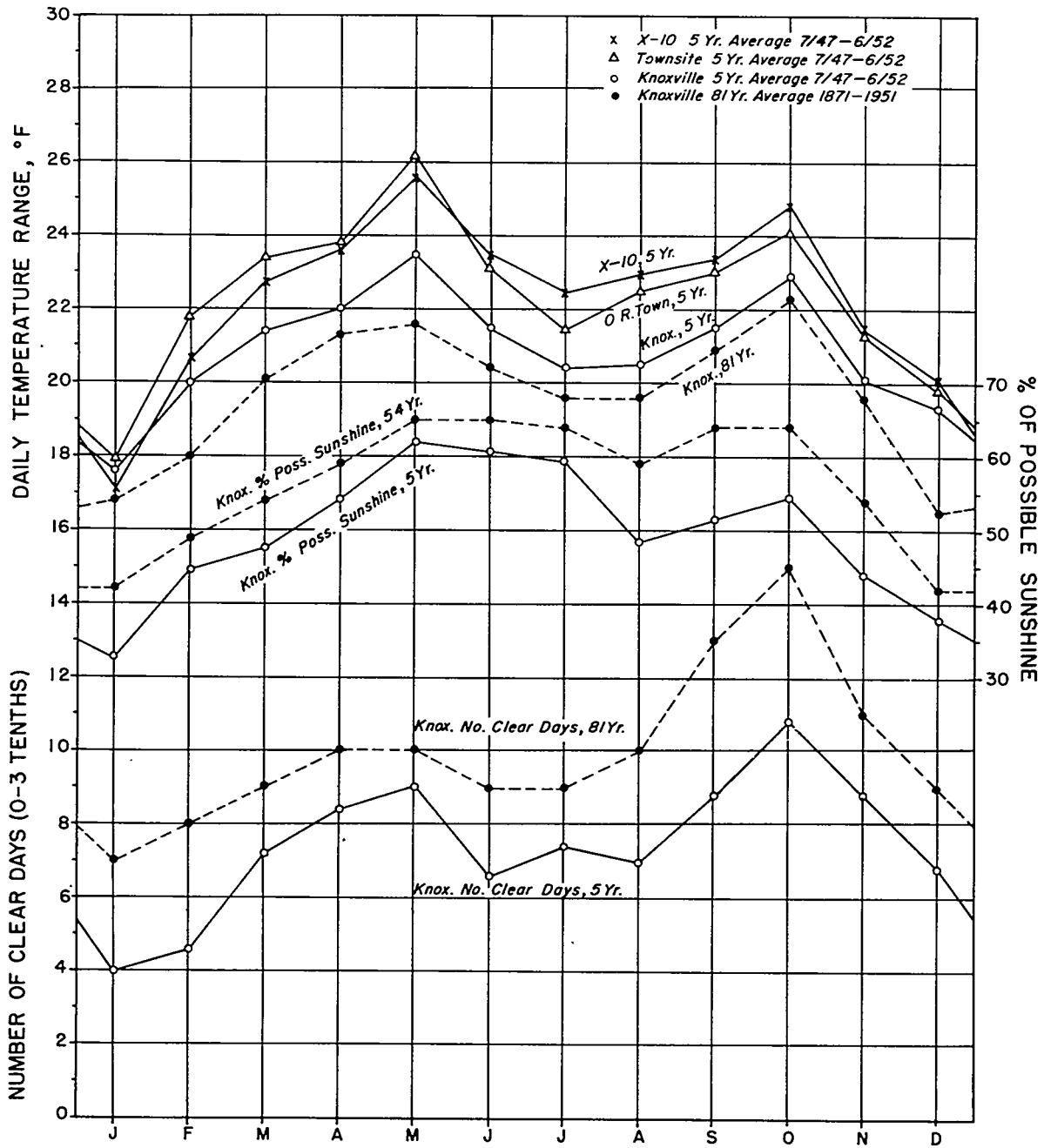


Fig. 66 Monthly averages of the daily temperature range at Knoxville and Oak Ridge, percent of possible sunshine and number of clear days at Knoxville.

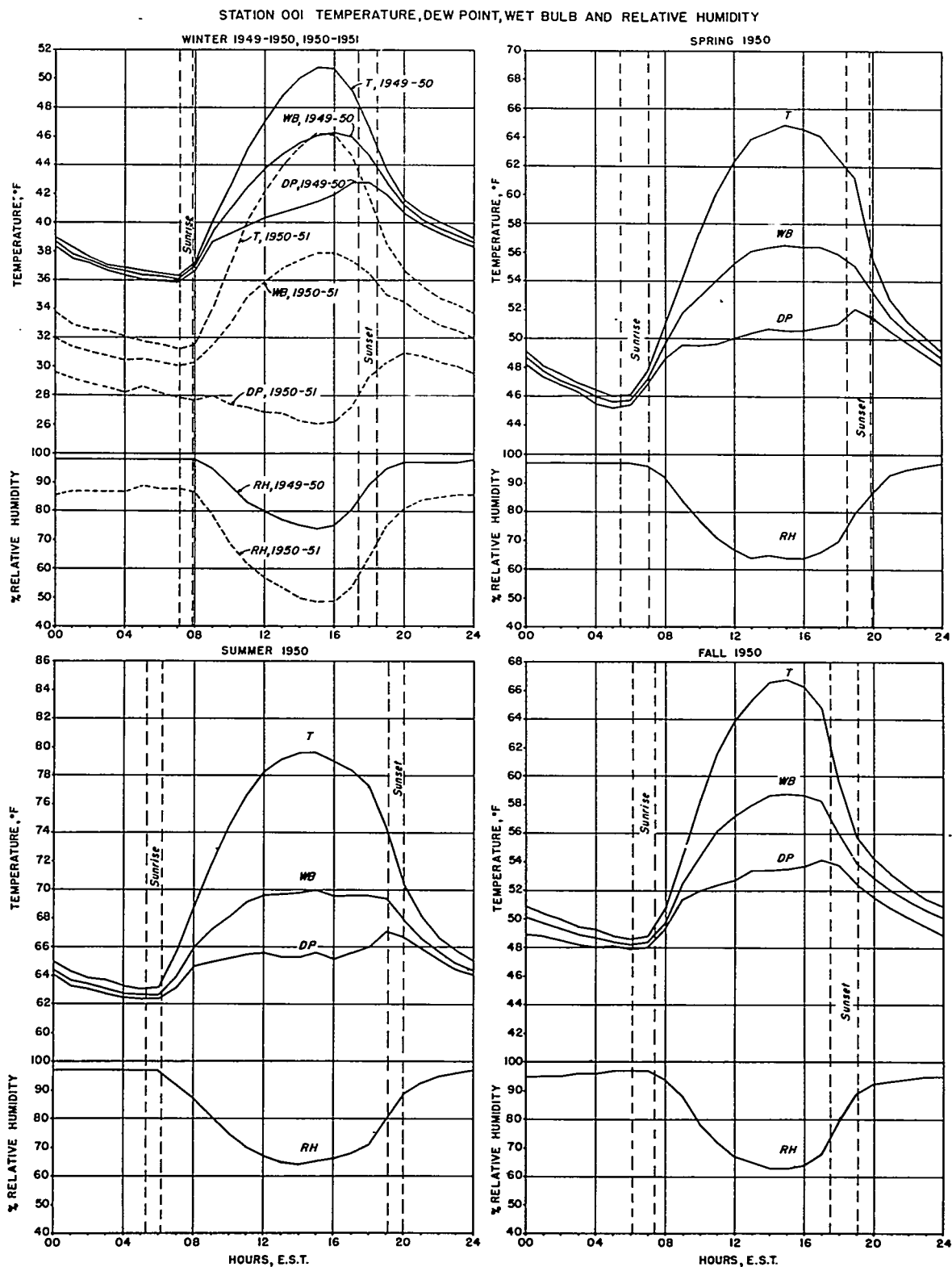


Fig. 67 Diurnal curves of temperature, wet bulb temperature, dew point and relative humidity for station 001 (X-10 hutment) by seasons, Dec. 1949 - Feb. 1951.

AVERAGE TEMPERATURE FALL 1949

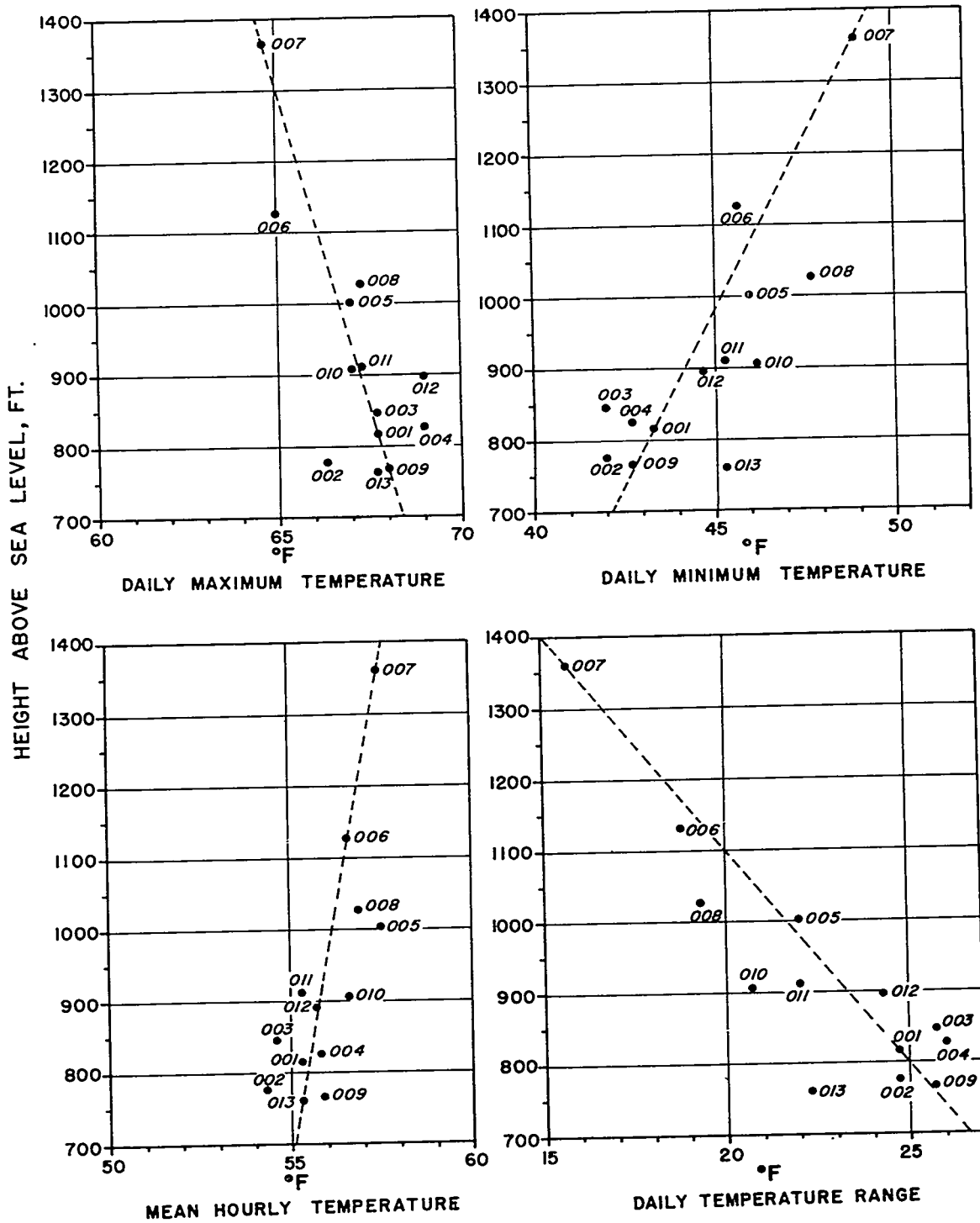


Fig. 68 Average daily maximum, minimum and mean temperature and average daily temperature range at microneet stations plotted against station elevation, Fall 1949.

MICRONET DIURNAL TEMPERATURE AND DEW POINT CYCLES, FALL 1949

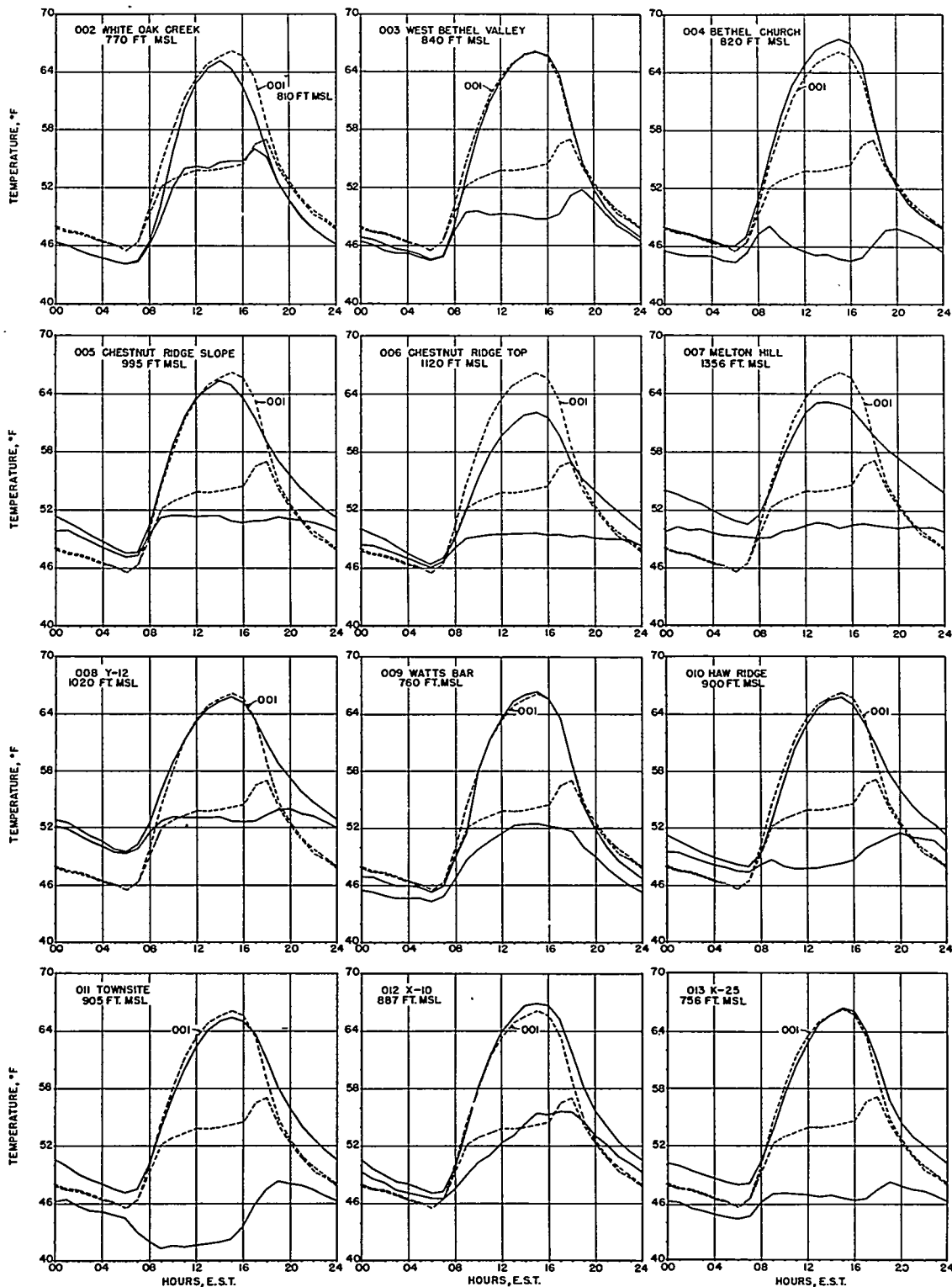


Fig. 69 Diurnal curves of temperature and dew point at micronet stations compared with station 001, Fall 1949.

FREQUENCY OF TEMPERATURE DIFFERENCE
OAK RIDGE MINUS KNOXVILLE

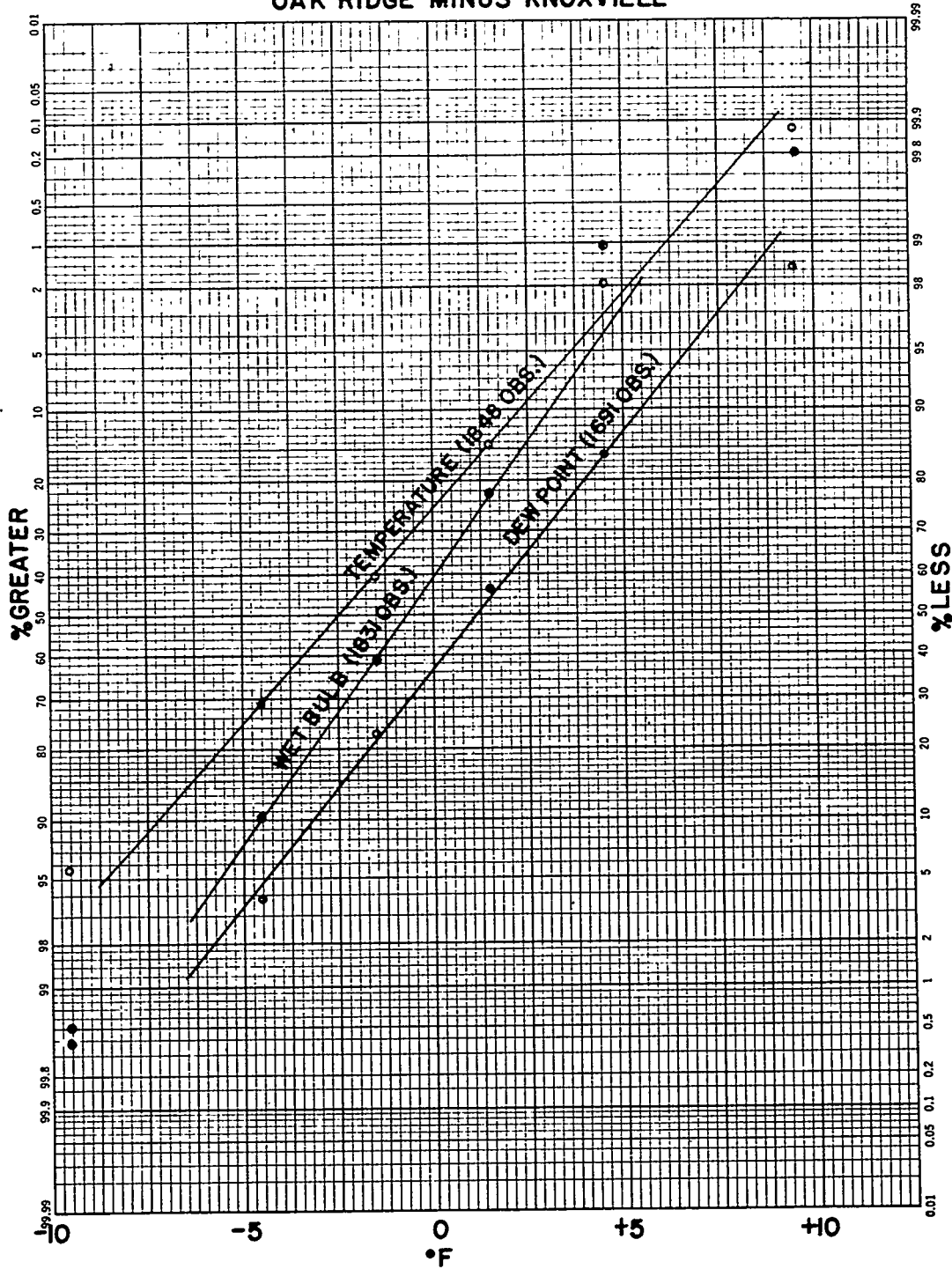


Fig. 70a Probability graphs of temperature difference, Oak Ridge minus Knoxville, June 1949-Oct. 1950: temperature, wet bulb temperature and dew point.

FREQUENCY OF TEMPERATURE DIFFERENCE
OAK RIDGE MINUS KNOXVILLE

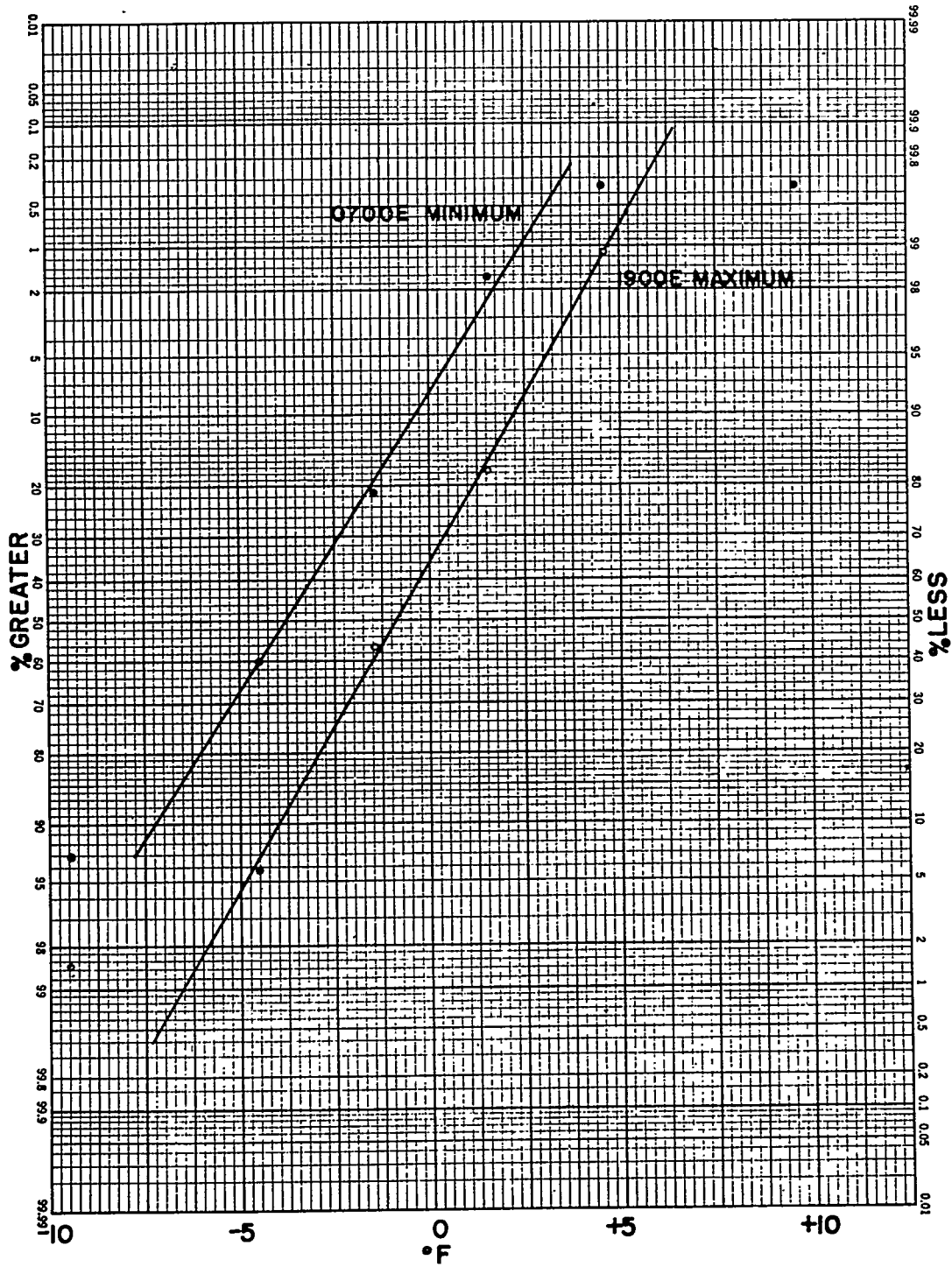


Fig. 70b Probability graphs of temperature difference, Oak Ridge minus Knoxville, June 1949-Oct. 1950: 7 a.m. 6-hrs. minimum and 7 p.m. 6-hr. maximum.

FREQUENCY OF TEMPERATURE DIFFERENCE
OAK RIDGE MINUS KNOXVILLE

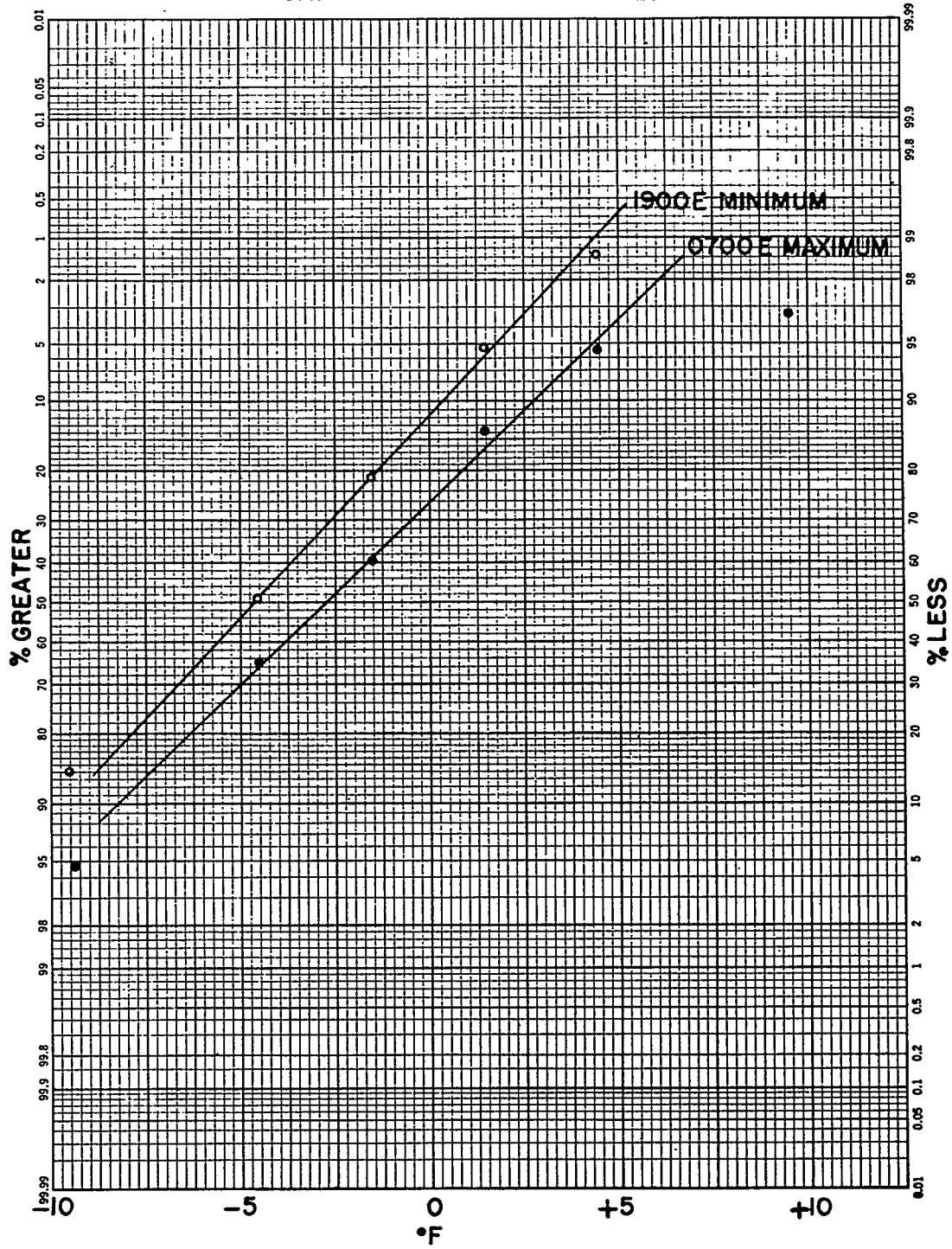


Fig. 70c Probability graphs of temperature difference, Oak Ridge minus Knoxville, June 1949-Oct. 1950: 7 a.m. 6-hr. maximum and 7 p.m. 6-hr. minimum.

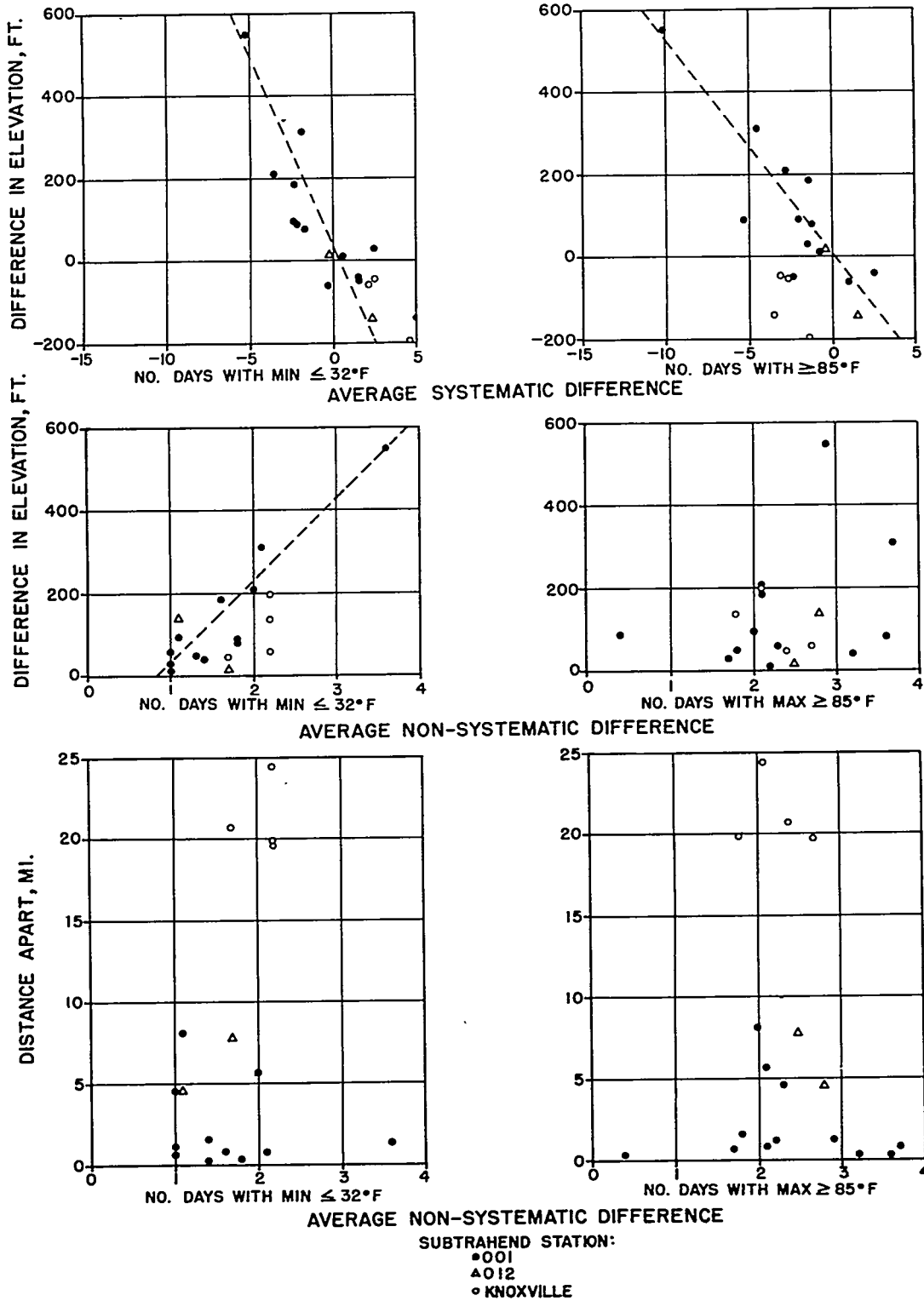


Fig. 71 Difference between stations in monthly frequency of daily temperature extremes.

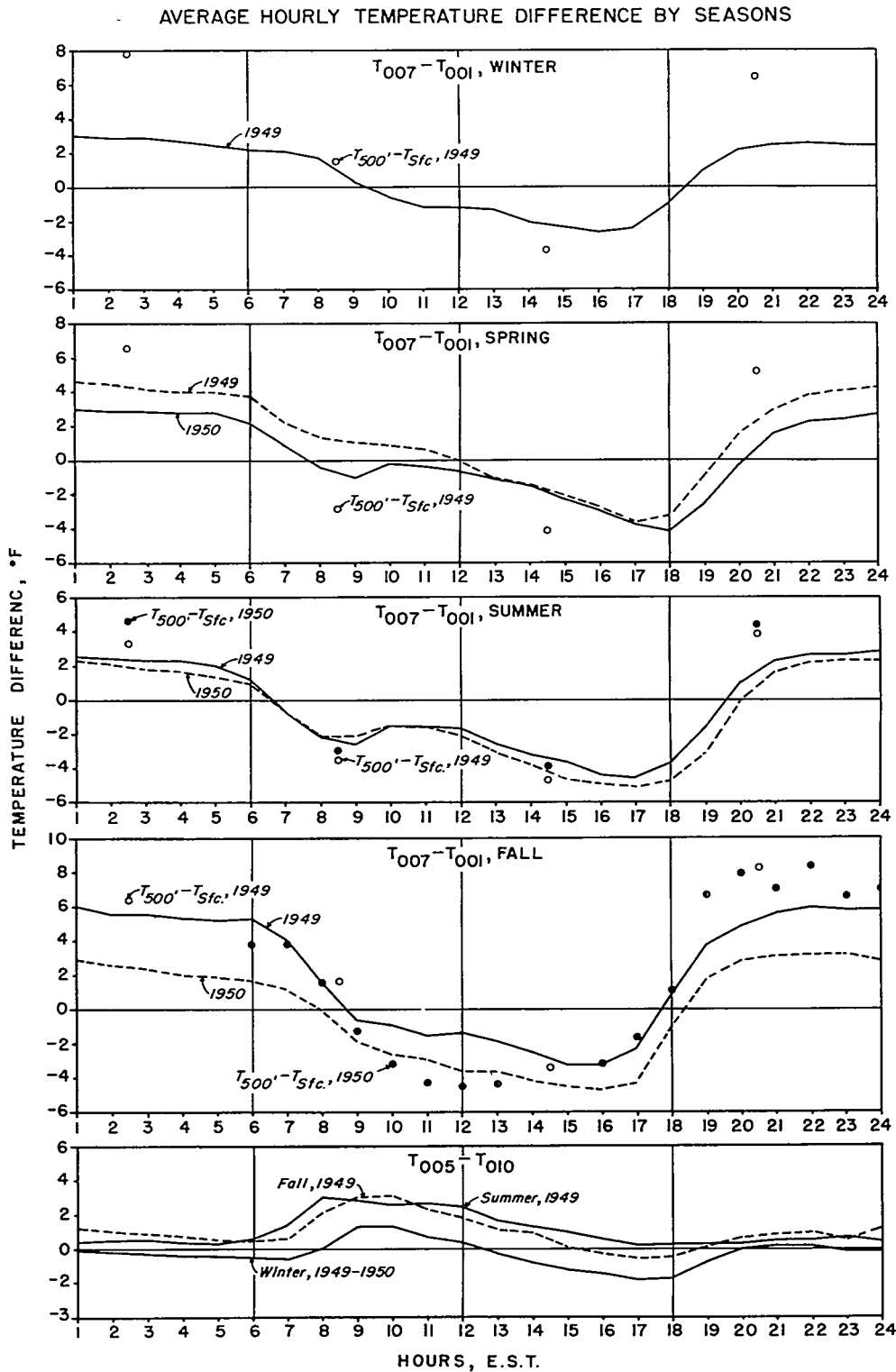
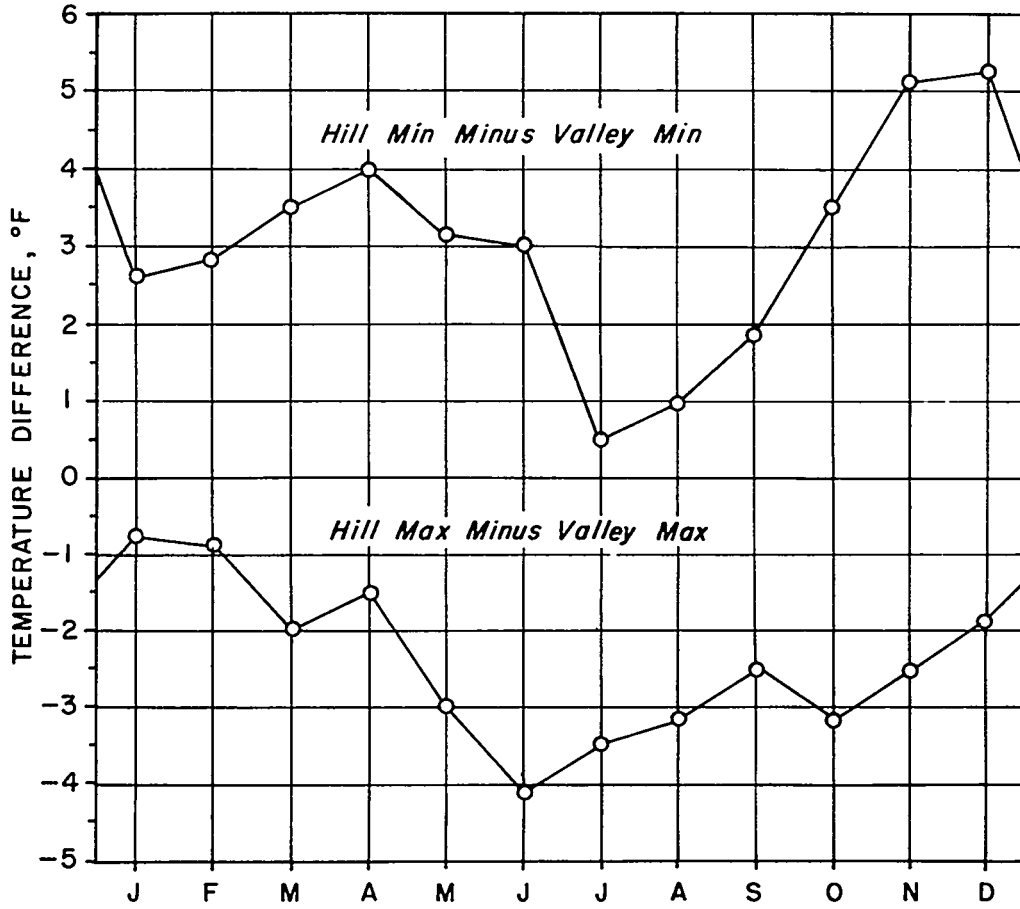


Fig. 72 Diurnal curves of average temperature difference, by seasons, between hill and valley stations (compared with corresponding free-air vertical temperature differential), and between opposing slope stations.



HILL STATIONS: 006, 007, 019
 VALLEY STATIONS: 001, 002

Fig. 73 Monthly average hill-valley differential of daily max and min temperature, 1949 - 1950.

422

NW-SE TERRAIN PROFILES ADJOINING OBSERVATION POINTS

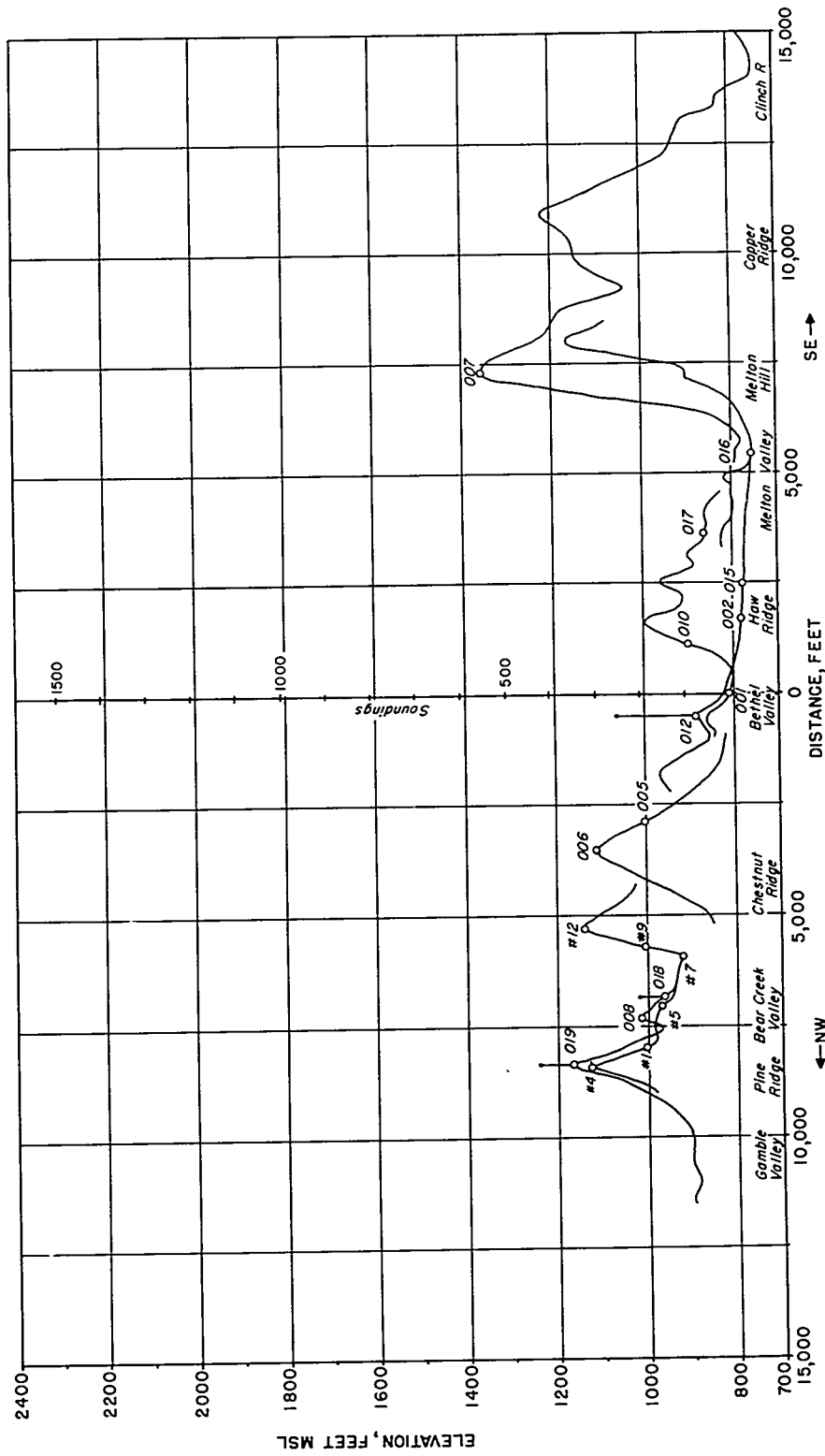


Fig. 74 NW-SE terrain profiles adjoining automobile, micromet and blimp temperature observation points.

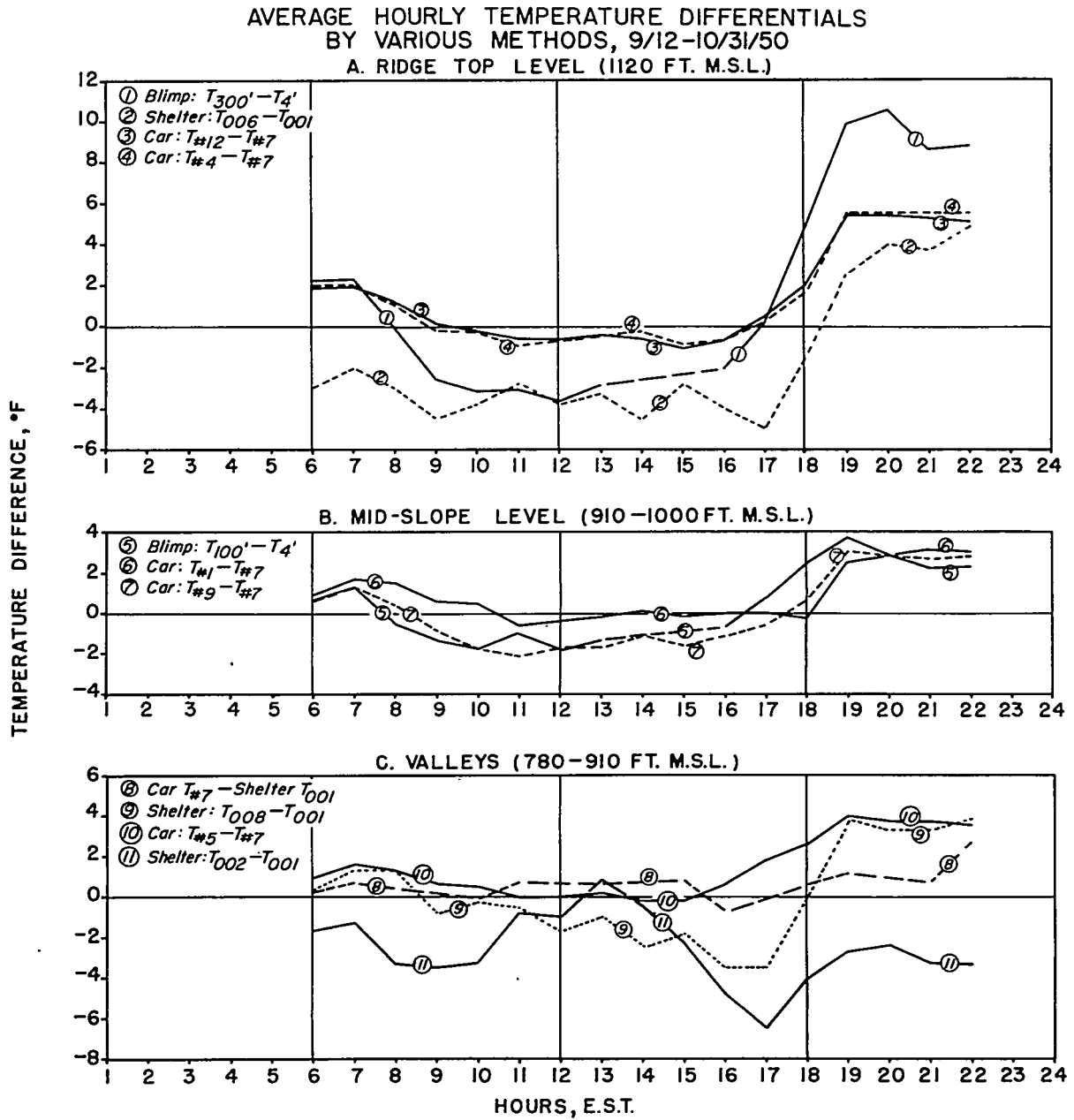
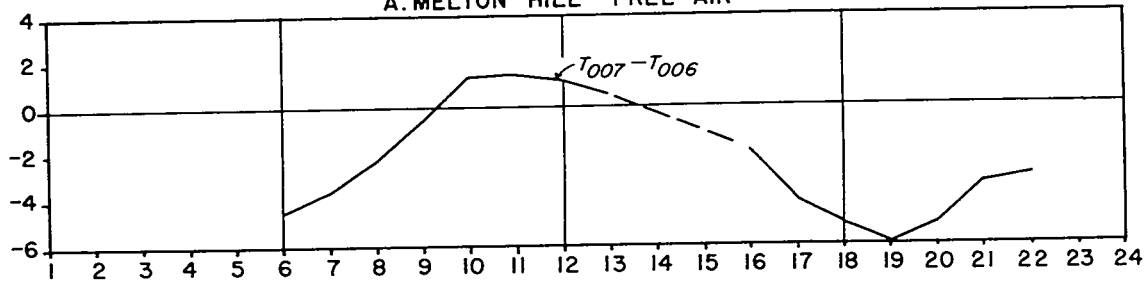
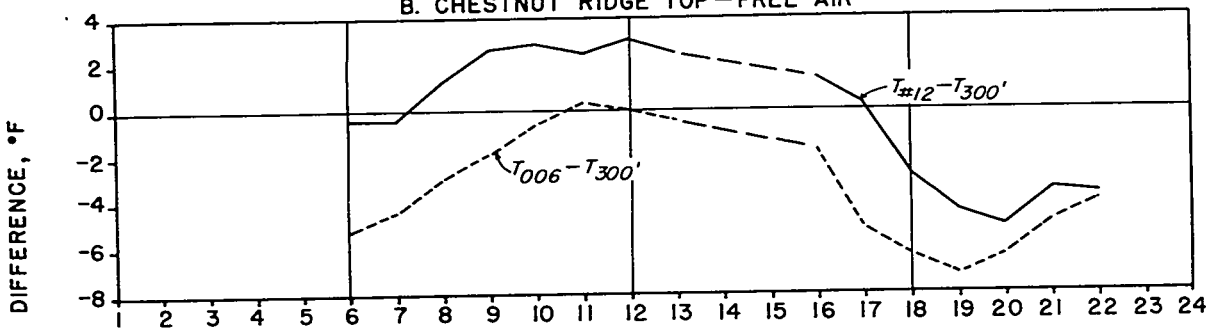


Fig. 75 Average hourly temperature differentials with respect to valley bottoms obtained by various methods during automobile temperature surveys, Sept. 12 - Oct. 31, 1950.

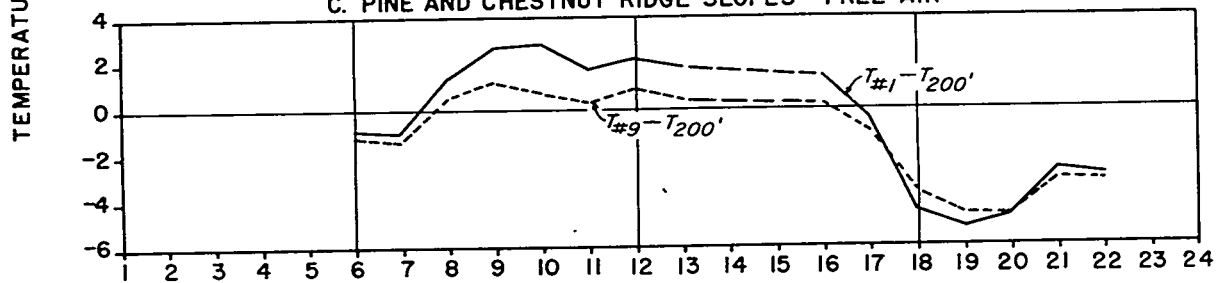
AVERAGE HORIZONTAL TEMPERATURE DIFFERENCE DURING
 AUTOMOBILE RUNS, 9/12-10/31/50
 A. MELTON HILL - FREE AIR



B. CHESTNUT RIDGE TOP - FREE AIR



C. PINE AND CHESTNUT RIDGE SLOPES - FREE AIR



D. SE-FACING SLOPE - NW-FACING SLOPE

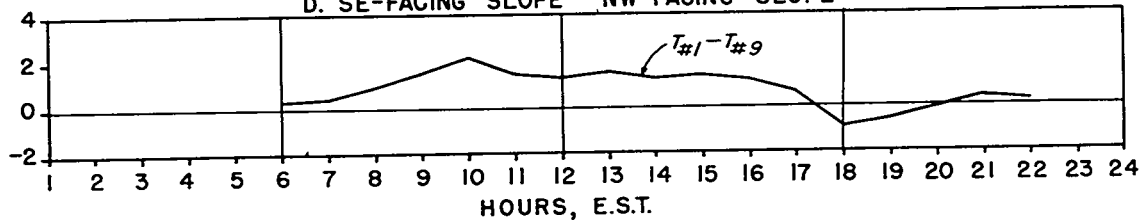


Fig. 76 Average hourly horizontal temperature differentials at hilltop and mid-slope levels obtained during automobile temperature surveys, Sept. 12 - Oct. 31, 1950.

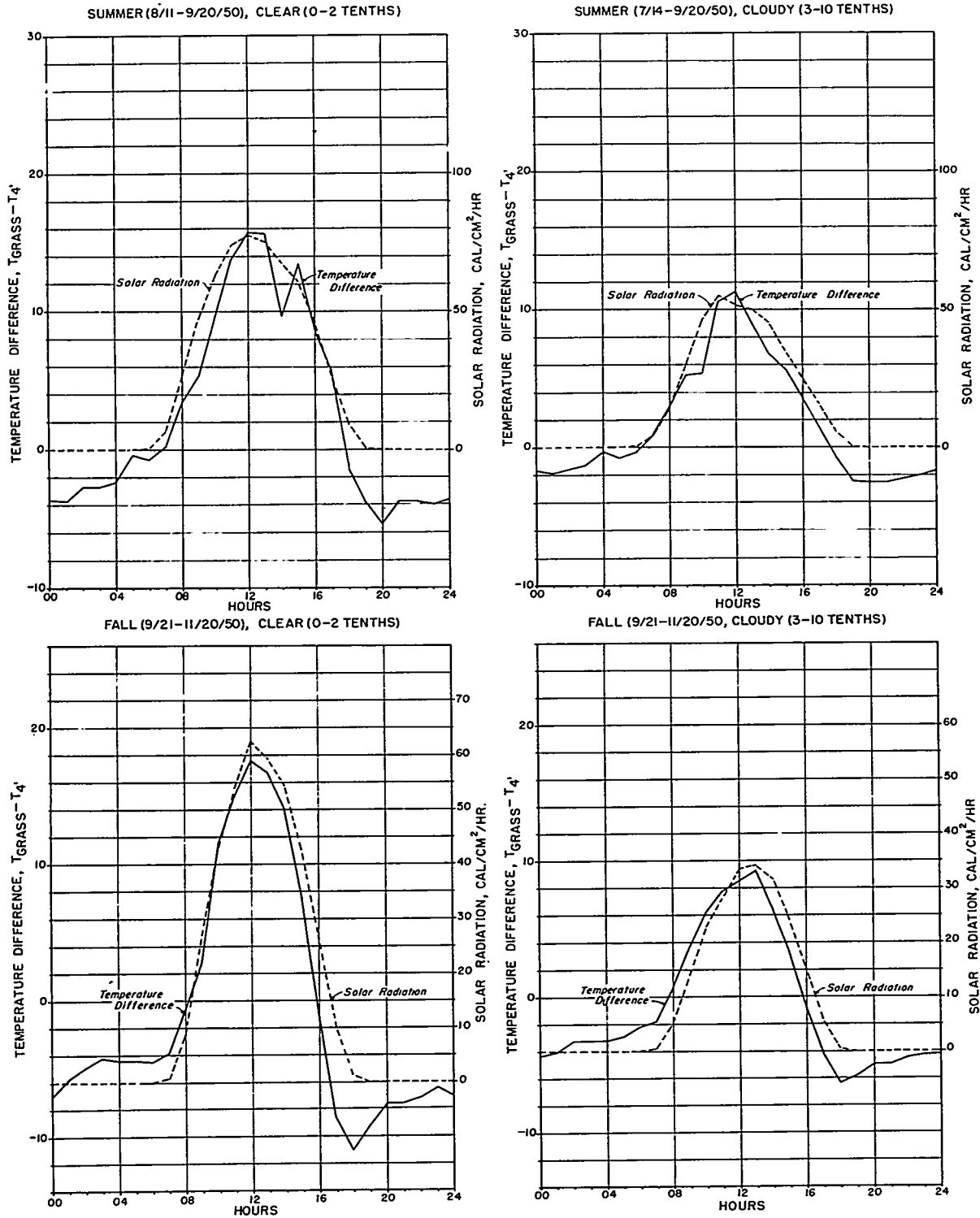
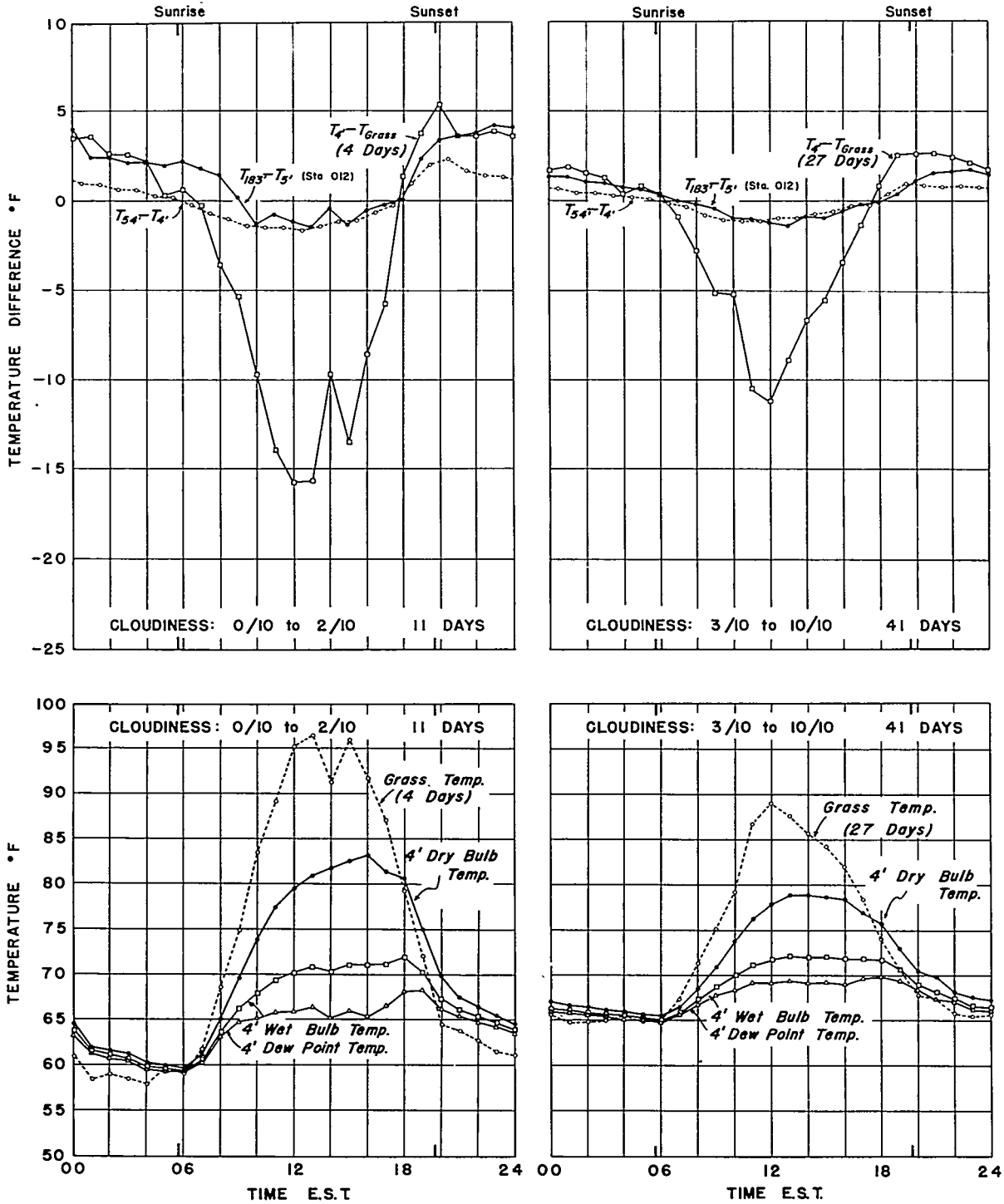
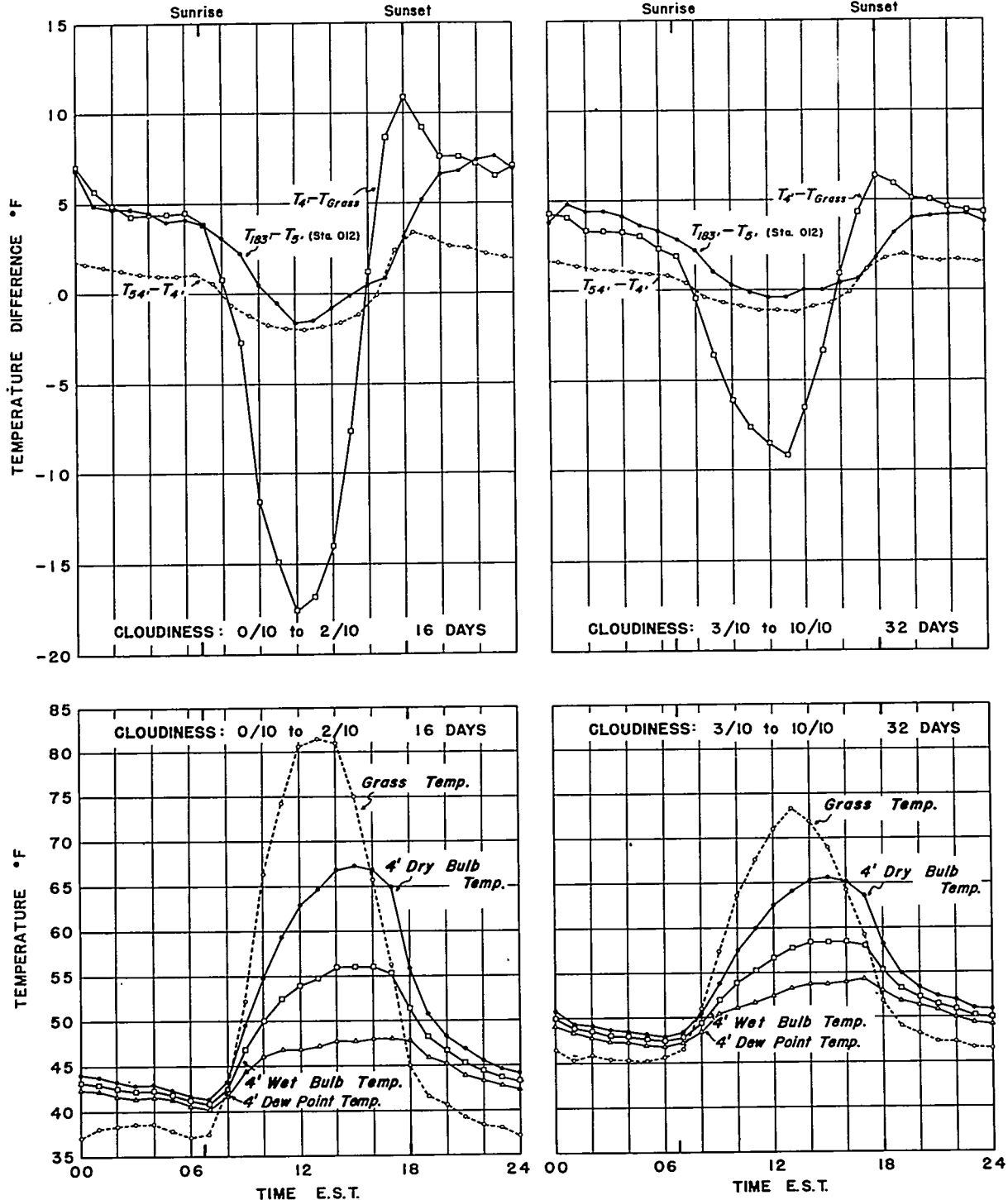


Fig. 77 Comparison of diurnal curves of $T_{grass} - T_4$, and solar radiation for a summer period and a fall period, separated into two classes of cloudiness.



July 14, - September 20, 1950
Only Days With Complete Data Used

Fig. 78 Comparison of average diurnal curves of $T_4 - T_{Grass}$, $T_{54} - T_4$, $T_{183} - T_5$, T_{Grass} , T_4 , 4' wet bulb temperature, and 4' dry bulb temperature for a summer period (July 14 - Sept. 20, 1950), separated into two classes of cloudiness.



September 21, - November 30, 1950
 Only Days With Complete Data Used

Fig. 79 Comparison of average diurnal curves of $T_4 - T_{grass}$, $T_{54} - T_4$, $T_{183} - T_5$, T_{grass} , T_4 , 4' wet bulb temperature and 4' dew point temperature for a fall period (Sept. 21 - Nov. 30, 1950), separated into two classes of cloudiness.

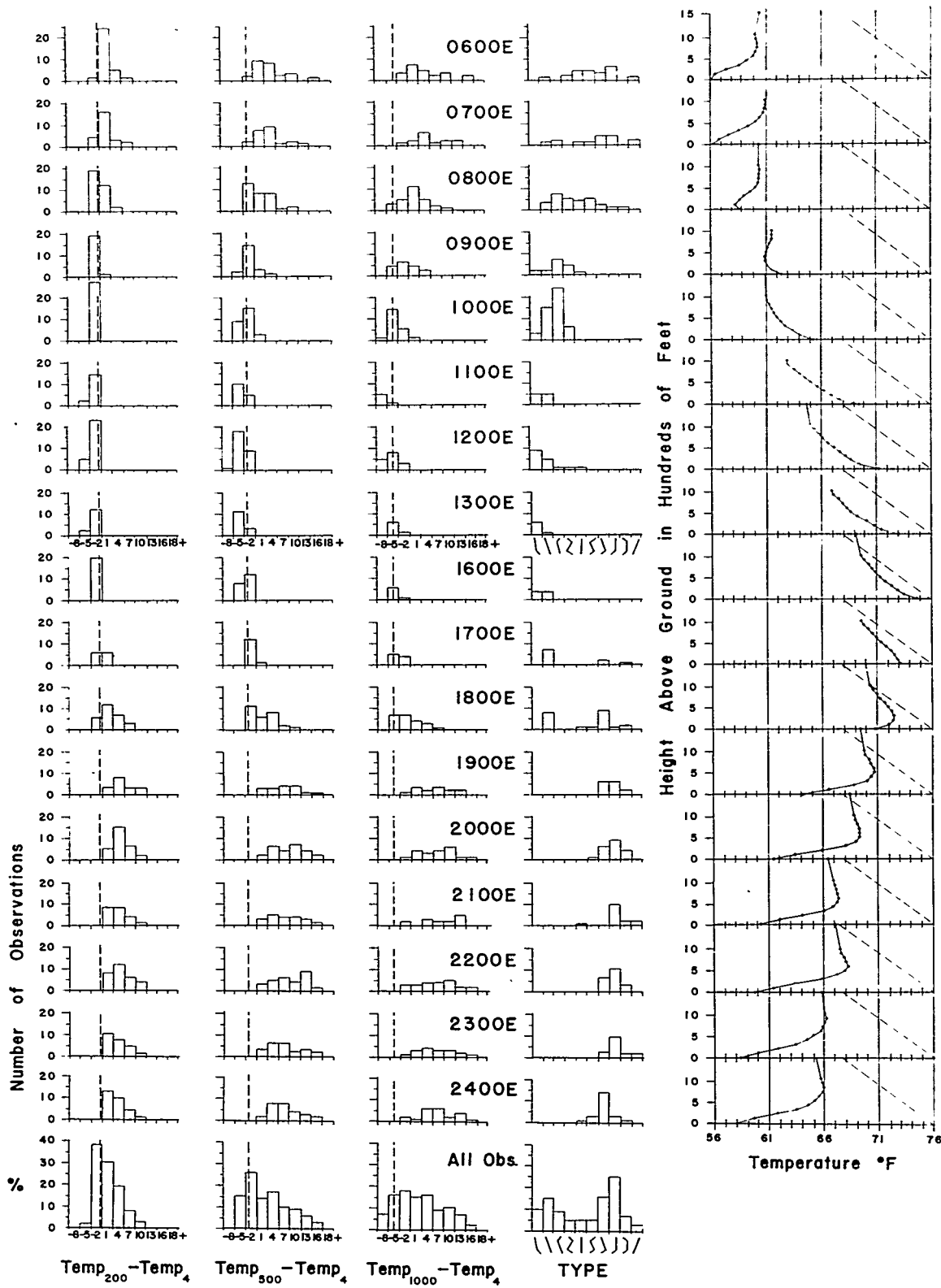


Fig. 80 Hourly and total frequency distributions of $T_{200} - T_4$, $T_{500} - T_4$, $T_{1000} - T_4$, and sounding type, and hourly curves of temperature vs. height based on average lapse rates, obtained from captive balloon temperature soundings, Aug. 23 - Nov. 3, 1950.

429

AVERAGE TEMPERATURE TIME CROSS-SECTION, °F, SEPT.-OCT. 1950

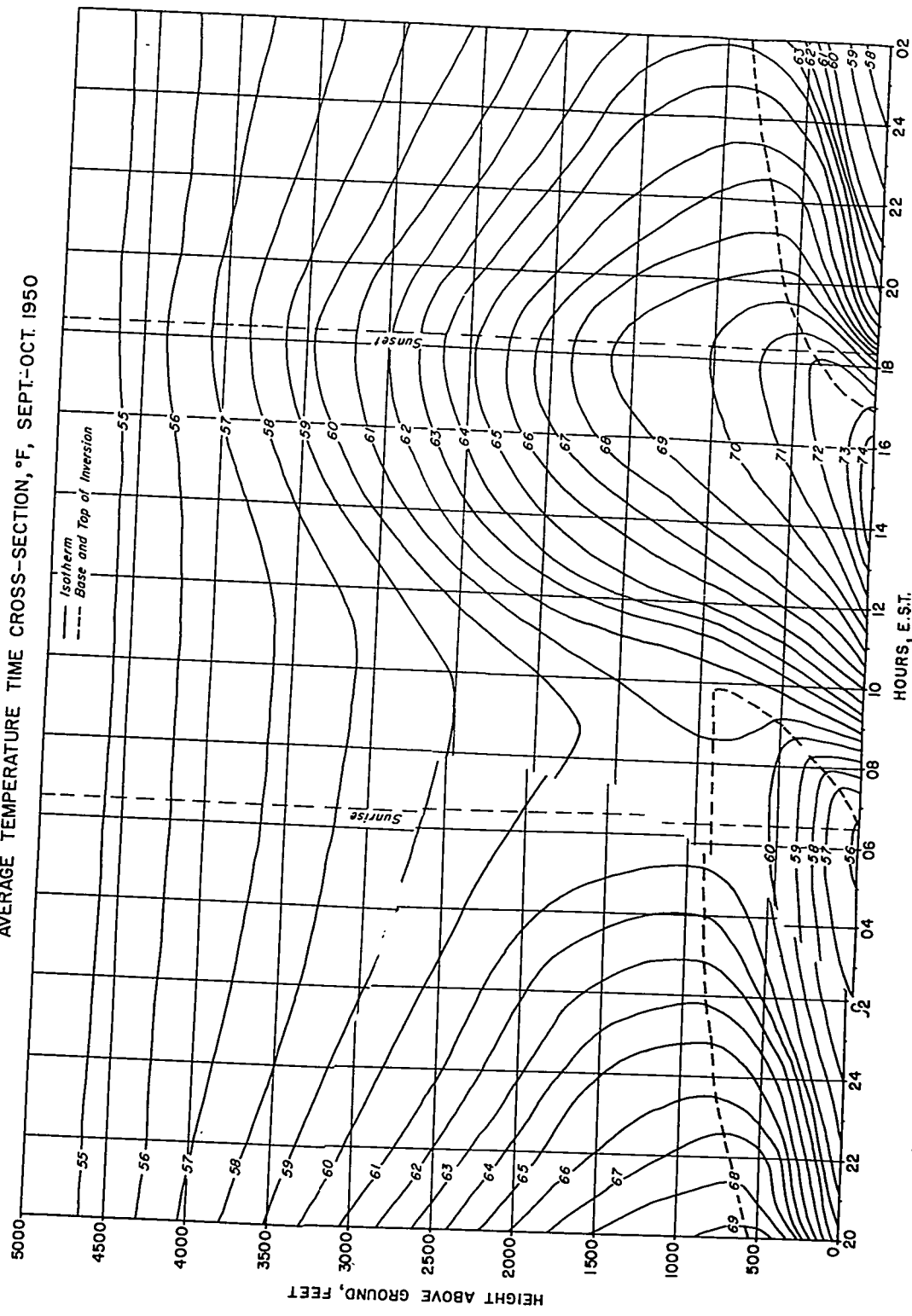


Fig. 81 Average temperature time cross-section (°F) of the lowest 5,000 ft., Sept. - Oct. 1950.

DISTRIBUTION OF TEMPERATURE GRADIENT 1949-1950

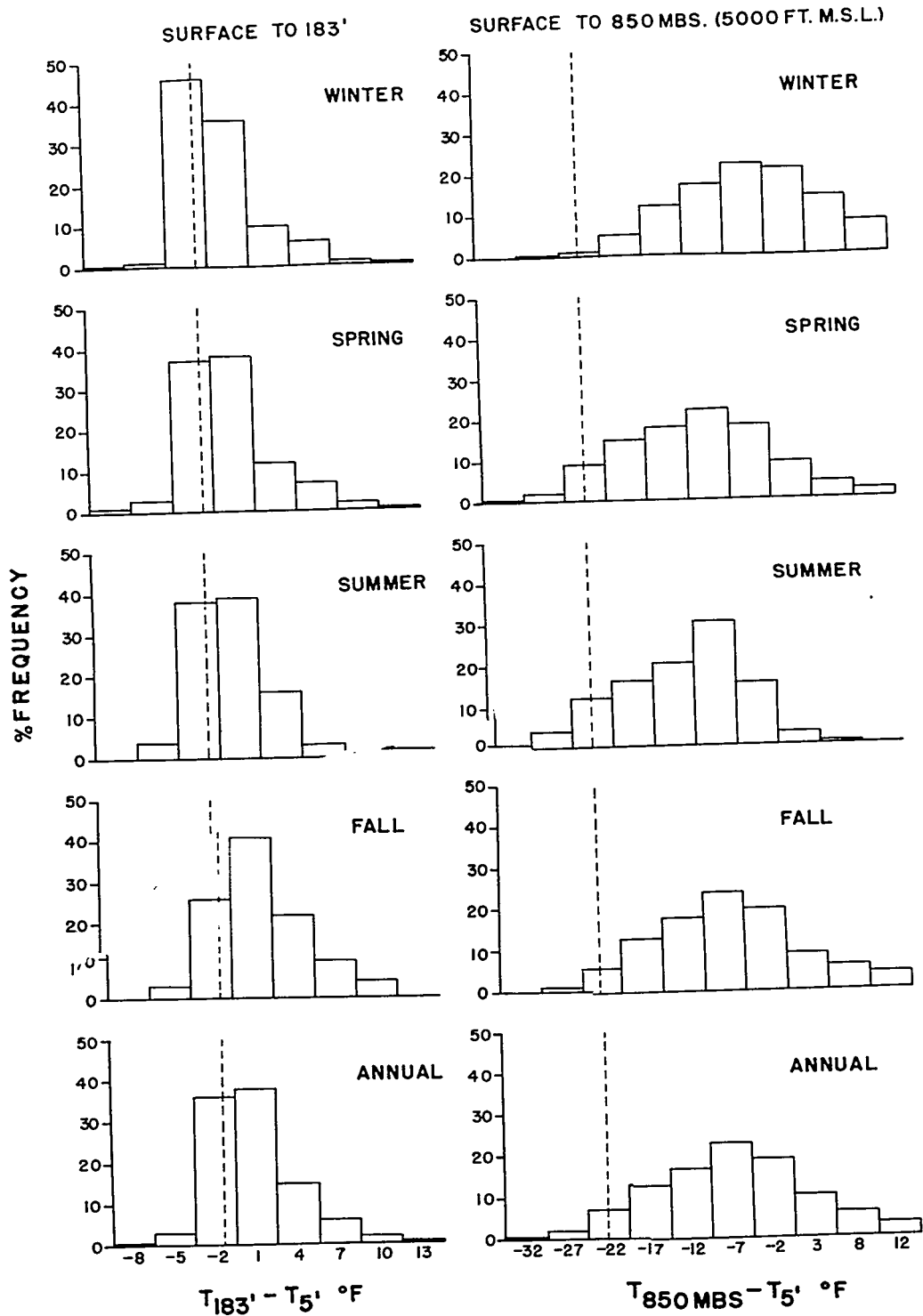


Fig. 82 Frequency distribution of $T_{183} - T_5$ and $T_{850 \text{ mb}} - T_5$ by seasons and annually, 1949 - 1950.

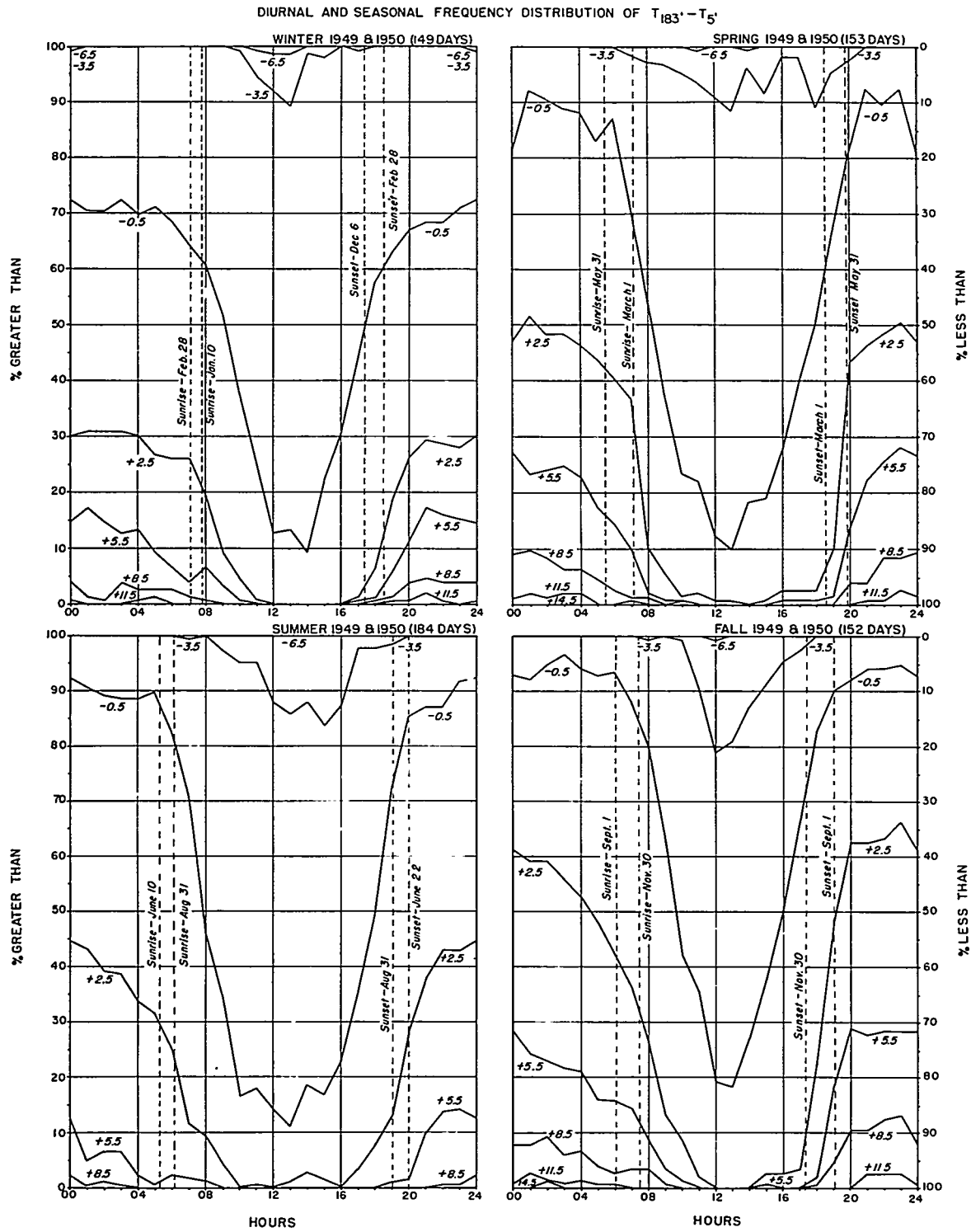


Fig. 83 Diurnal curves of cumulative frequency of $T_{183} - T_5$ by seasons, 1949 - 1950.

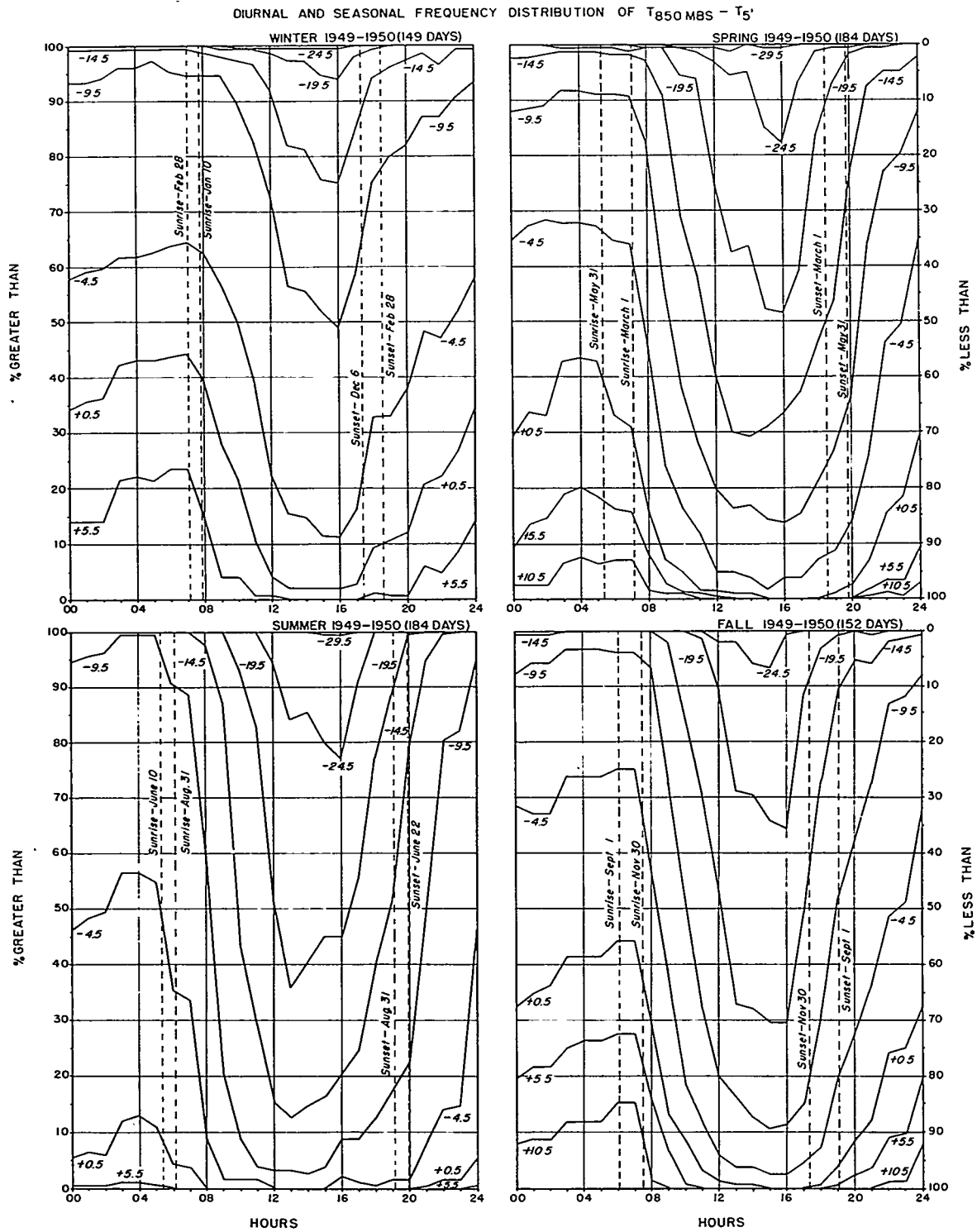


Fig. 84 Diurnal curves of cumulative frequency of $T_{850\text{ mb}} - T_5$ by seasons, 1949 - 1950.

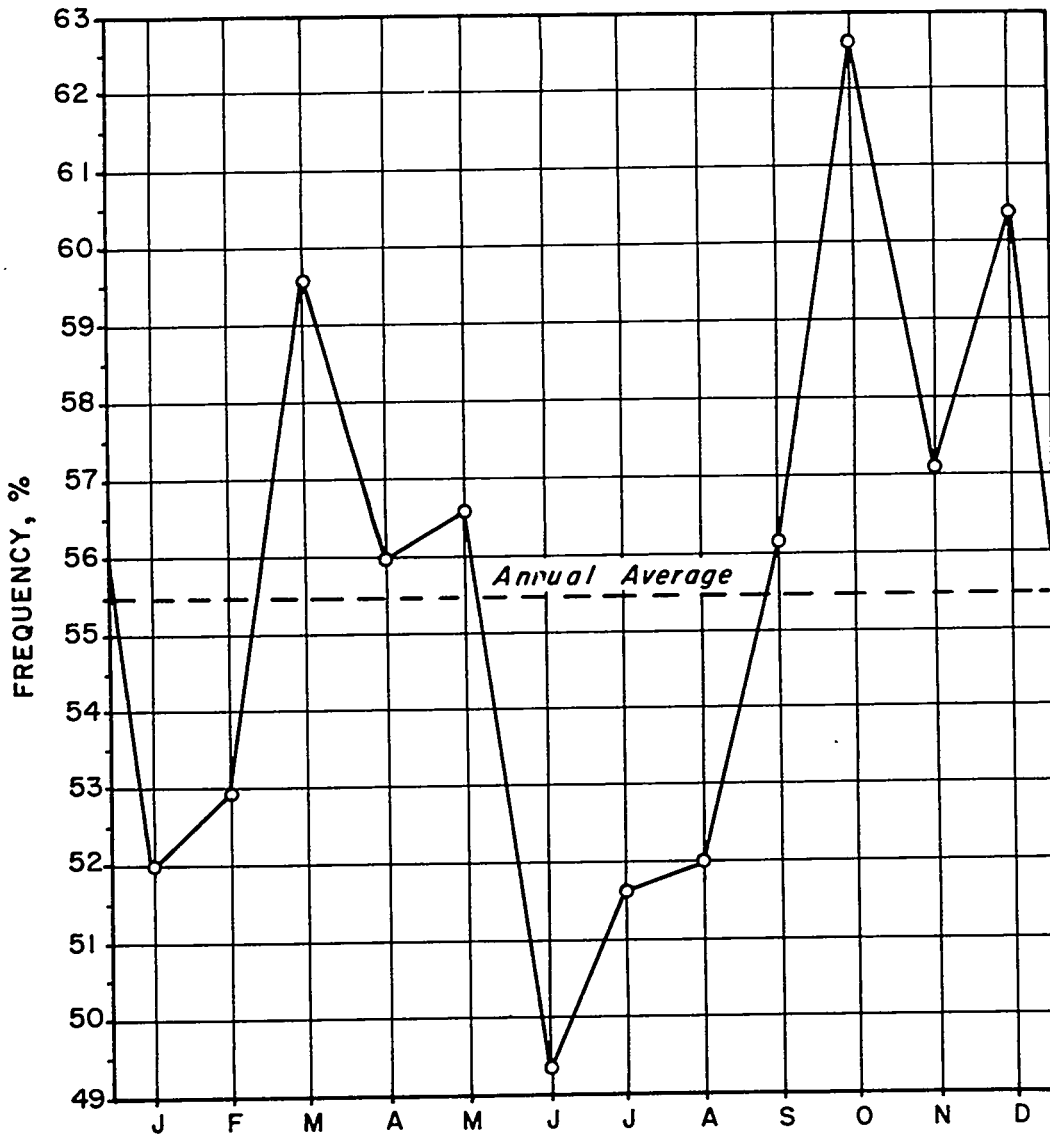


Fig. 85 Average monthly frequency of inversion
 ($T_{183'} - T_{5'} \geq 0$) station 012, 1944 - 1951.

4-34

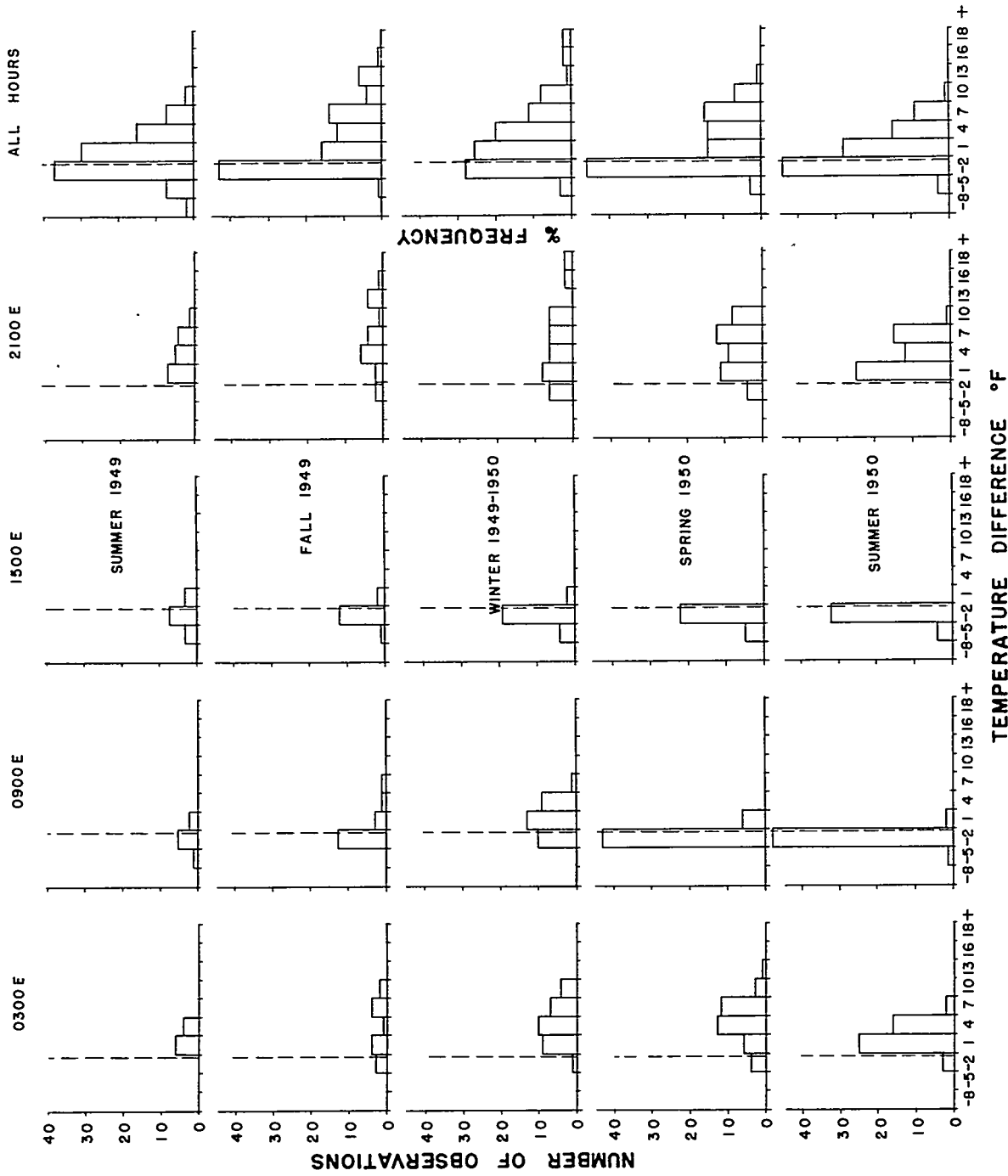


Fig. 86 Frequency distribution of $T_{200} - T_{14}$ by time of day and season.

435

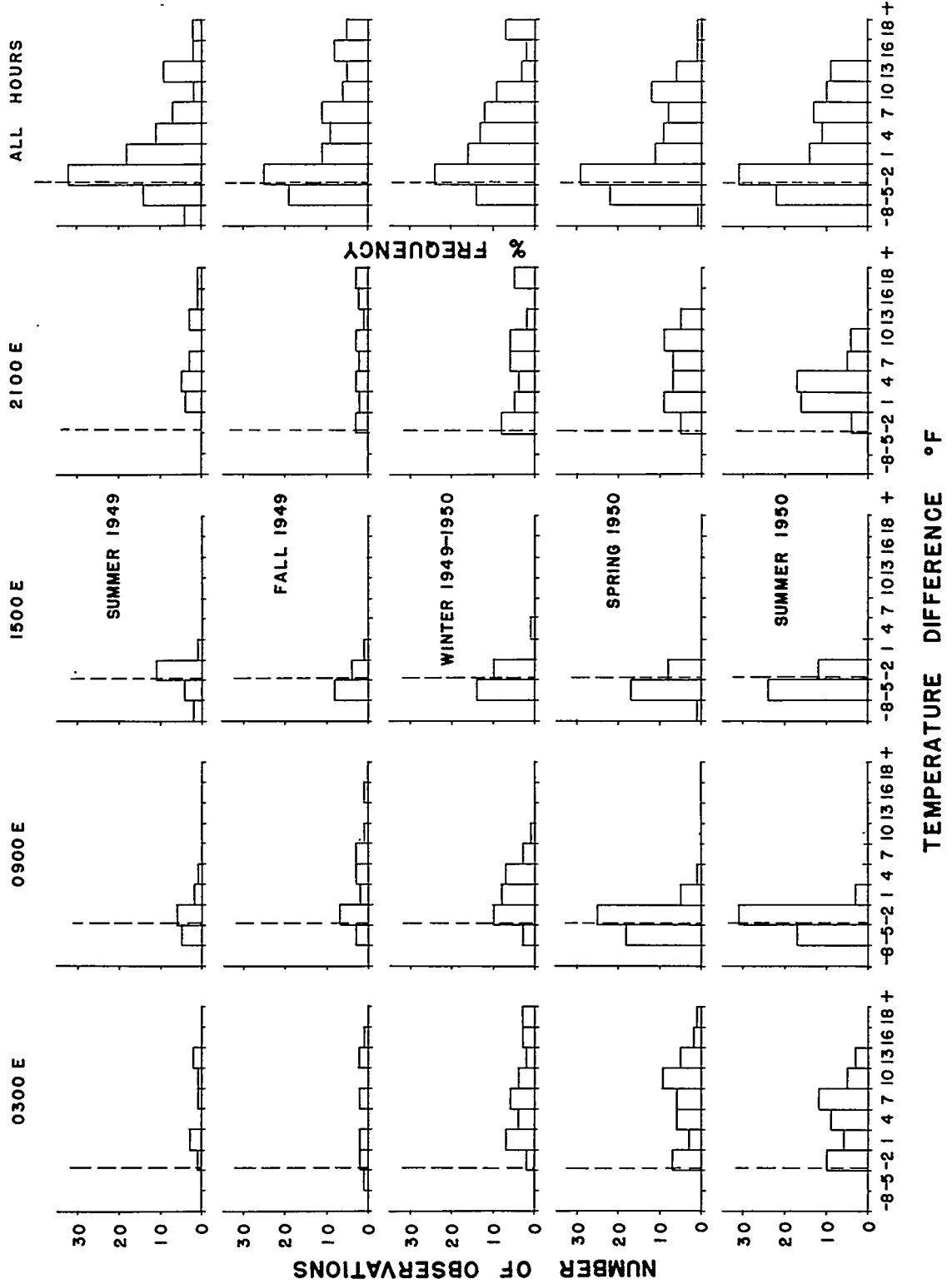


Fig. 87 Frequency distribution of T₅₀₀ - T₁₄ by time of day and season.

436

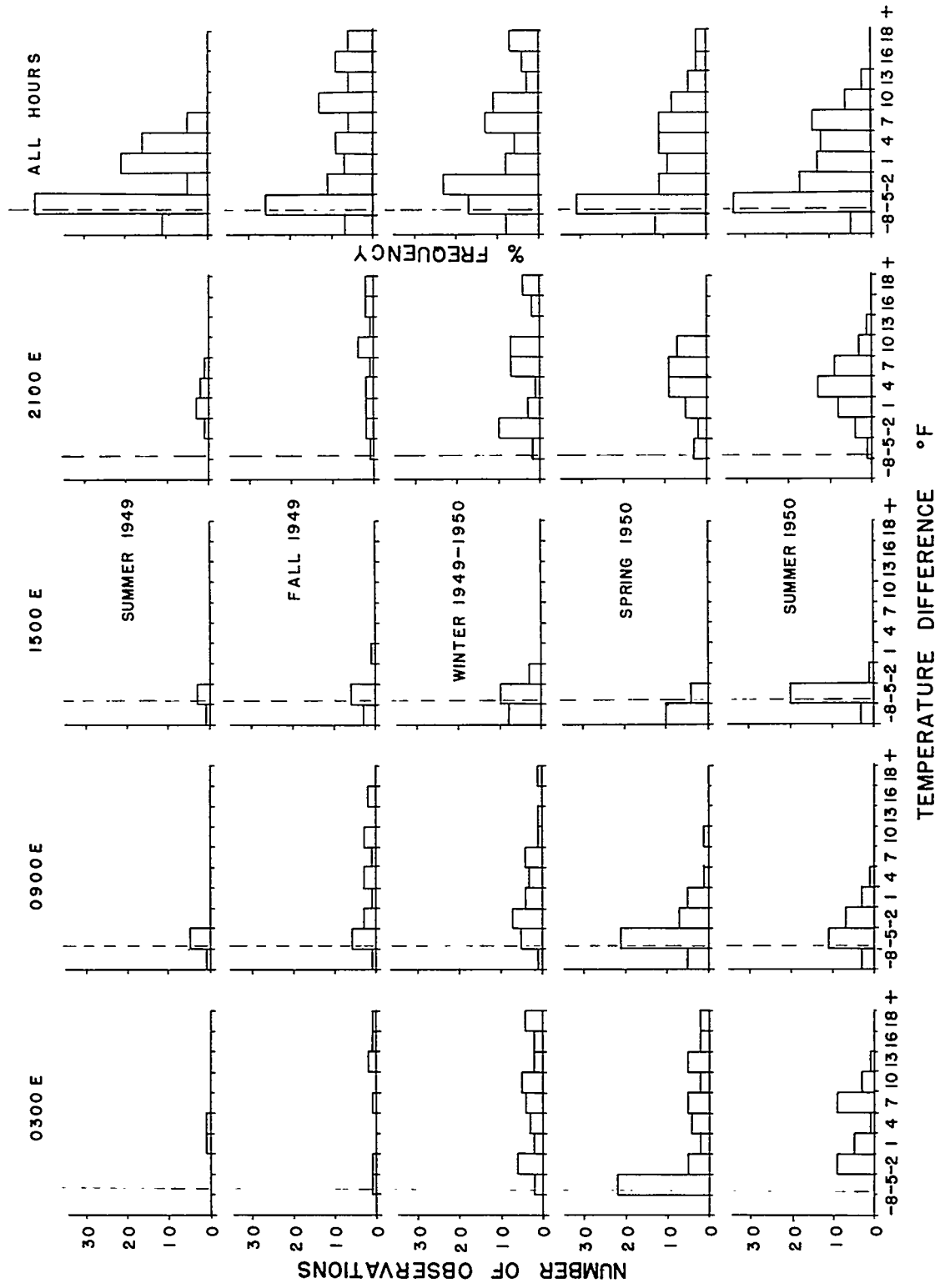


Fig. 88 Frequency distribution of T₁₀₀₀ - T₁₄ by time of day and season.

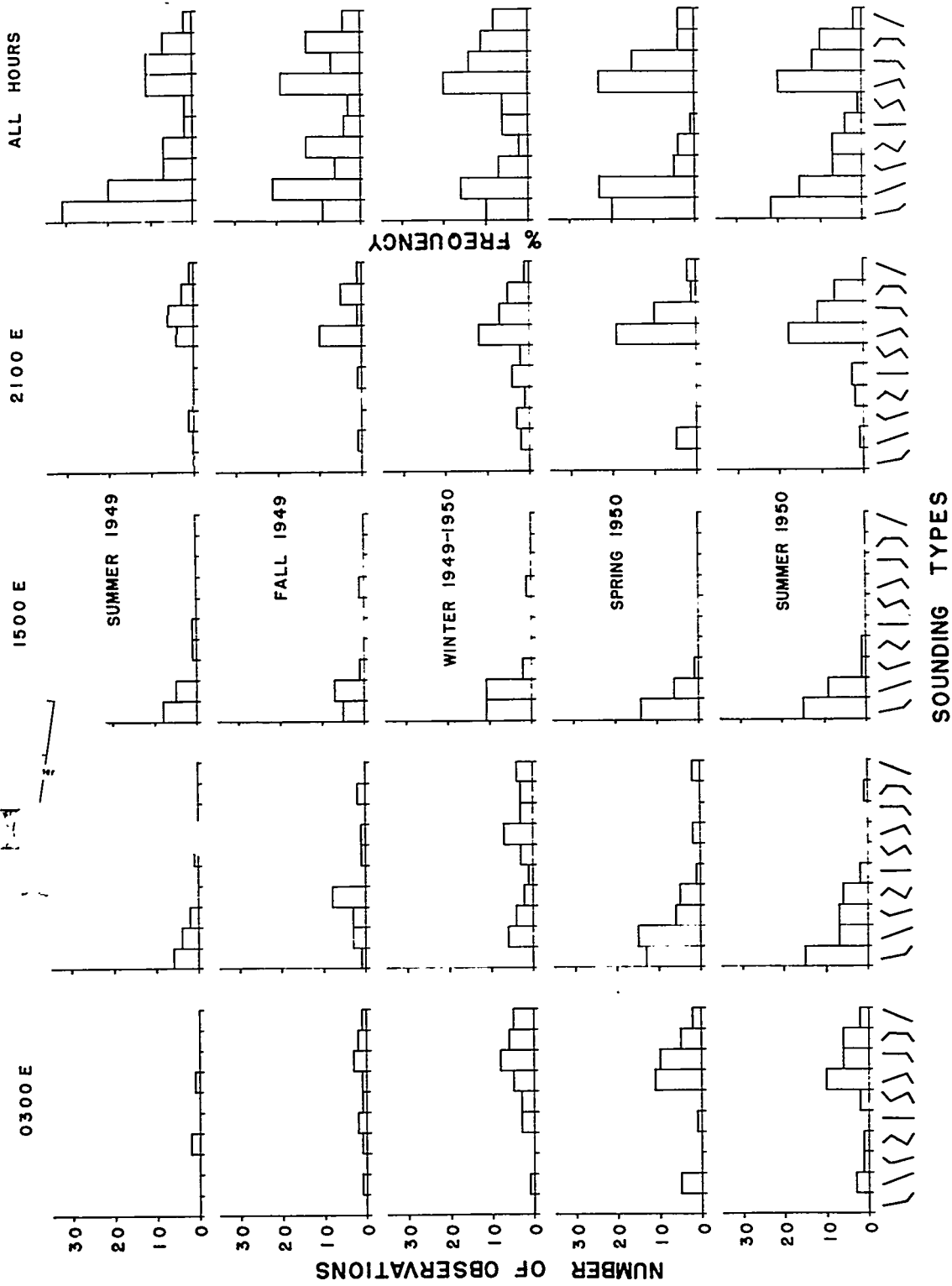


Fig. 89 Frequency distribution of sounding type by time of day and season.

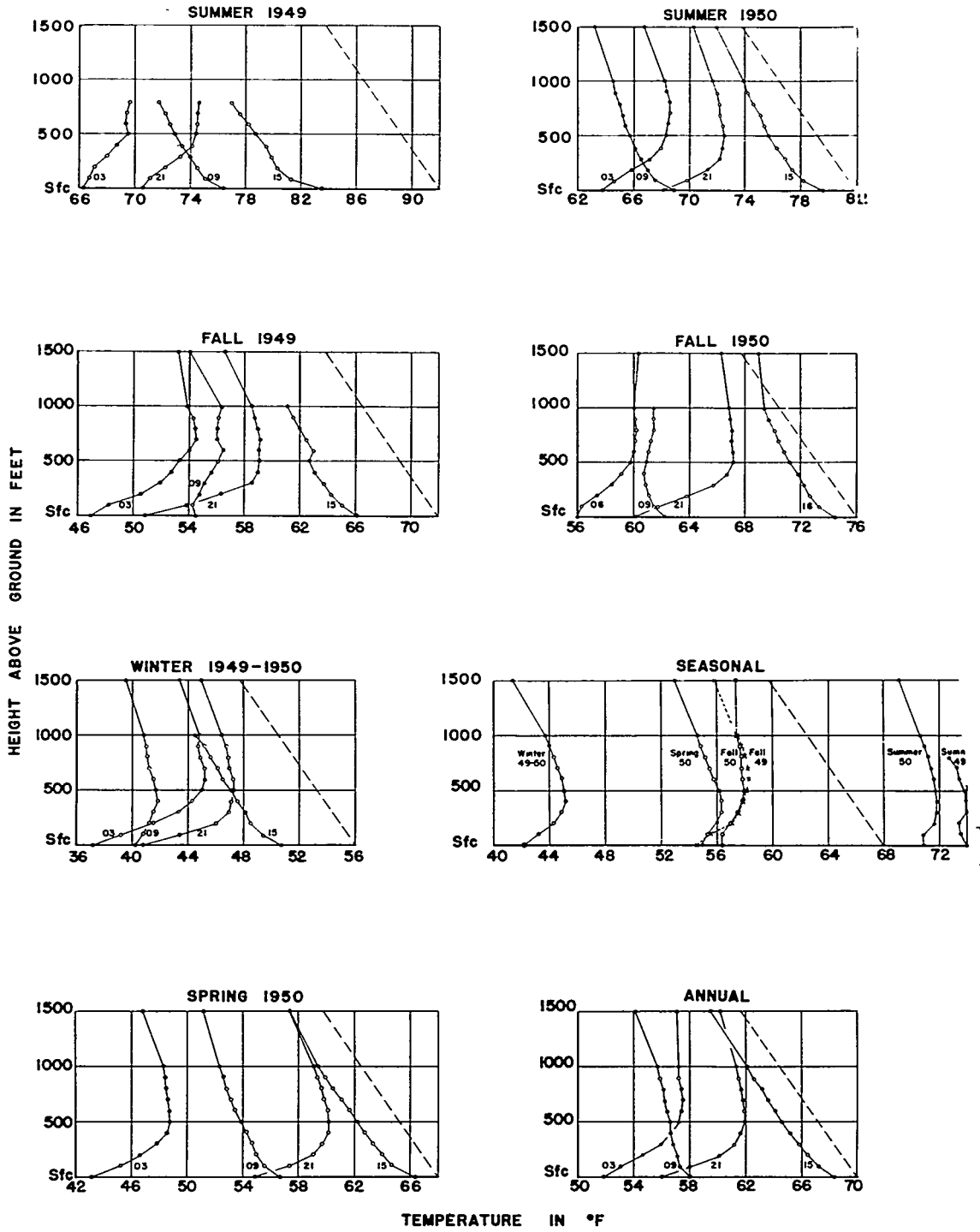


Fig. 90 Average temperature vs. height curves for the lowest 1500 ft. by time of day and season.

TEMPERATURE AND TEMPERATURE GRADIENT COMPARISON
PINE RIDGE TOP VS. SOUNDINGS, MARCH 5-9, 1951

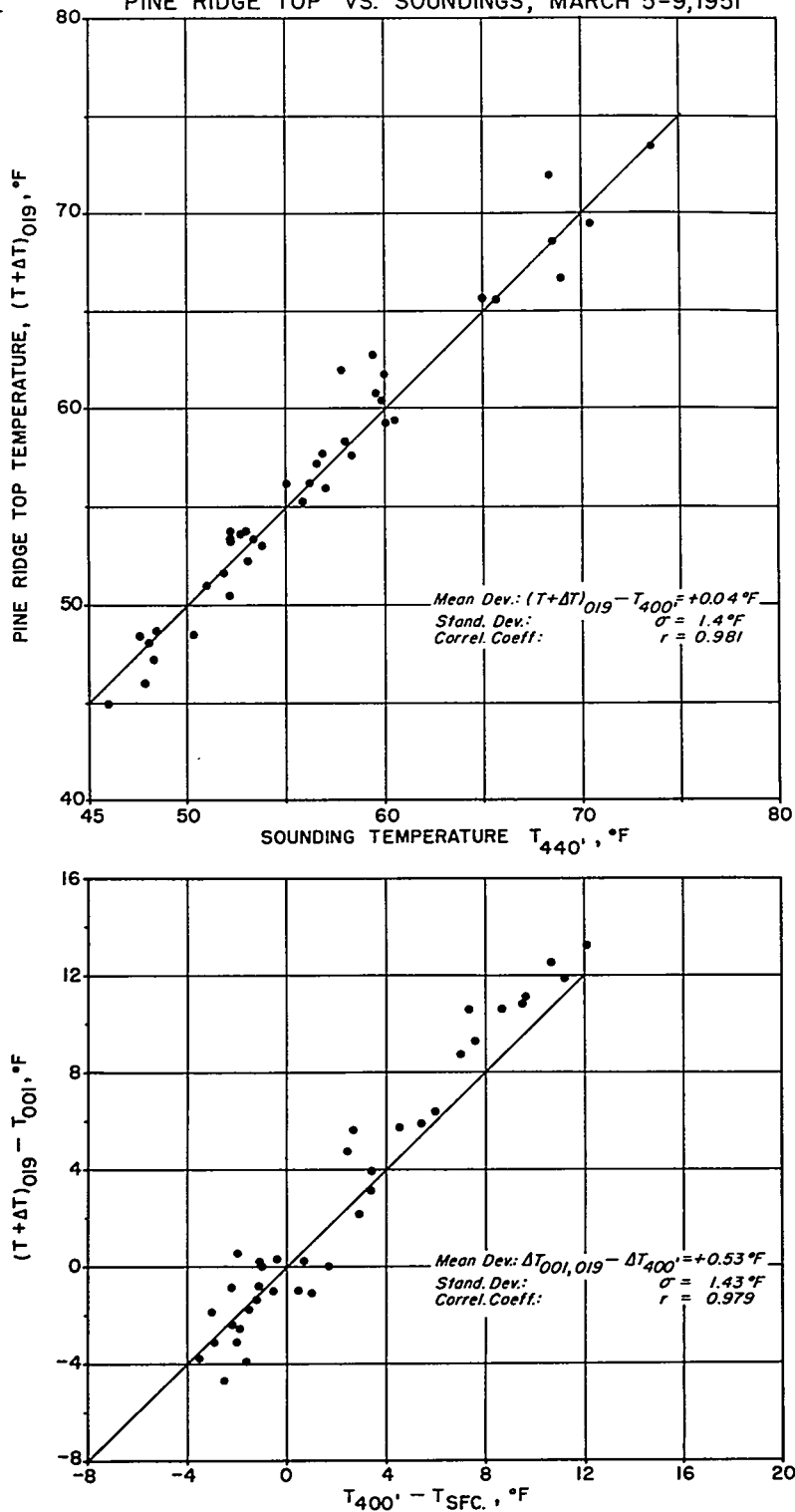


Fig. 91 Temperature 80 ft. above Pine Ridge top vs. free-air temperature, and comparison of temperature differentials between this level and valley bottom.

A40

ANNUAL
2000m

φ

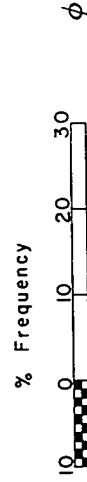
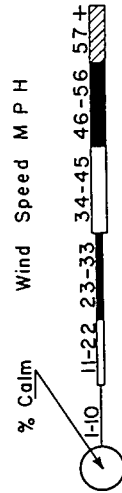
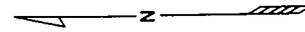
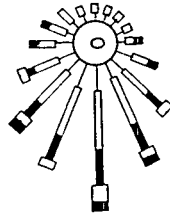
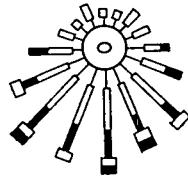
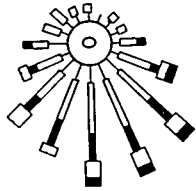
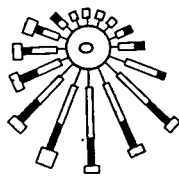


Fig. 92 Annual pilot balloon wind rose map for the 2000 m (6600 ft) MSL level, Southern Appalachian area.

441

ANNUAL
1500m

φ

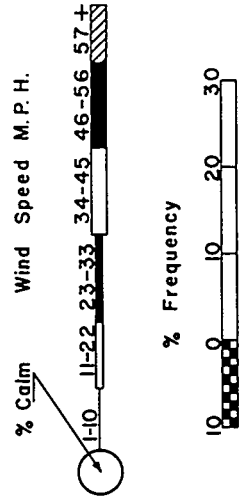
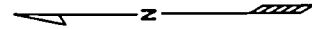
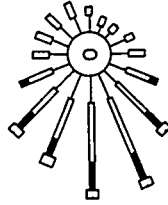
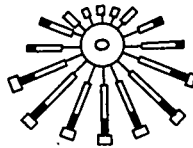
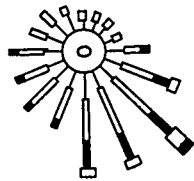
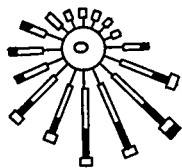
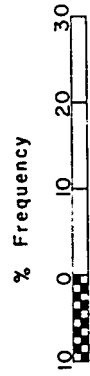
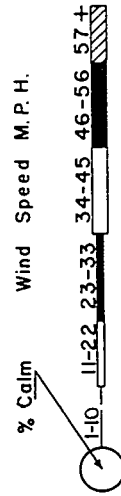
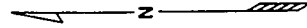
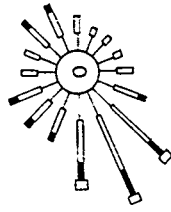
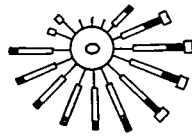
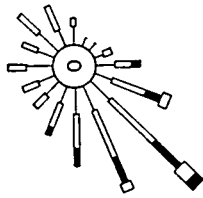
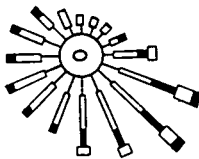


Fig. 93 Annual pilot balloon wind rose map for the 1500 m (5000 ft) MSL level, Southern Appalachian area.

442

ANNUAL
1000m

φ



φ

Fig. 94 Annual pilot balloon wind rose map for the 1000 m (3300 ft) MSL level, Southern Appalachian area.

443

ANNUAL
500m

φ

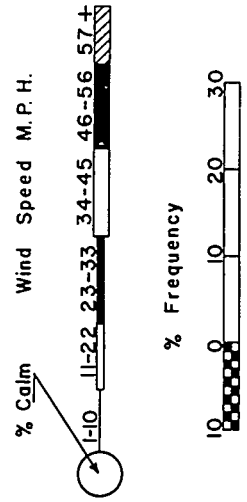
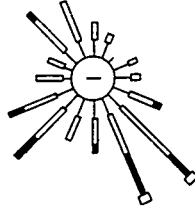
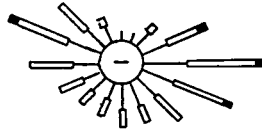
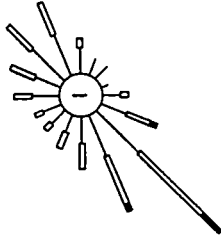
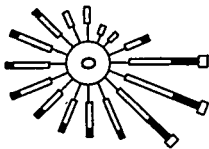


Fig. 95 Annual Pilot balloon wind rose map for the 500 m (1700 ft) MSL level, Southern Appalachian area.

4-14-4

ANNUAL
SURFACE
ALL OBS

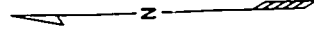
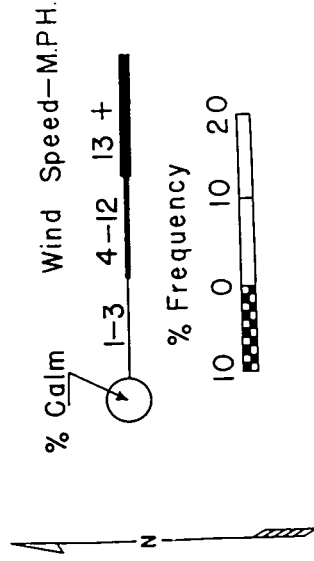
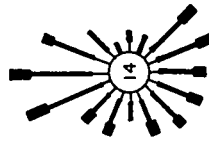
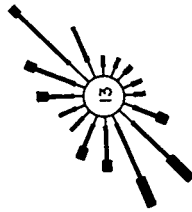
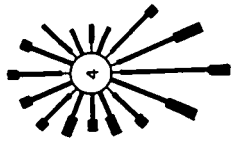
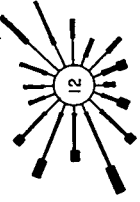
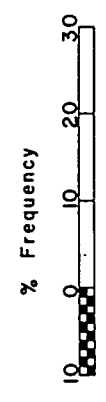
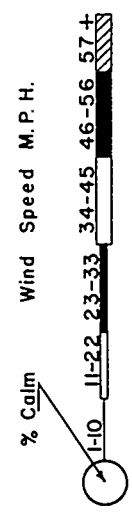
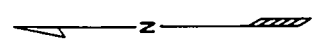
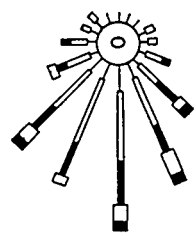
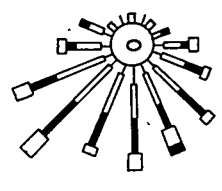
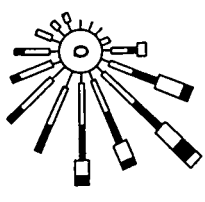
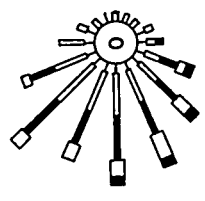


Fig. 96 Annual surface wind rose map, Southern Appalachian area.

445

WINTER
1500m

φ



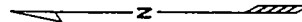
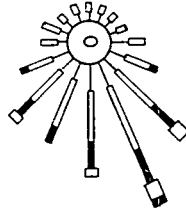
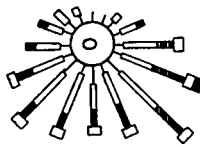
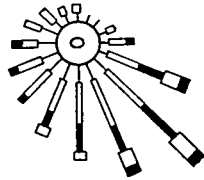
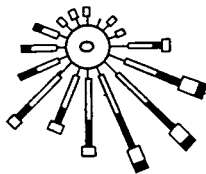
φ

Fig. 97 1500 m wind rose map, Winter, Southern Appalachian area.

446

SPRING
1500m

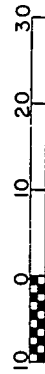
φ



% Calm



% Frequency

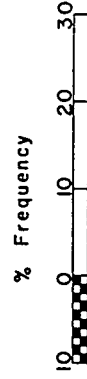
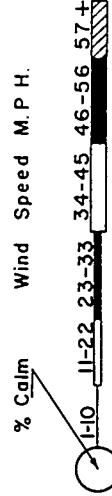
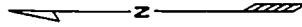
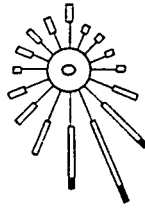
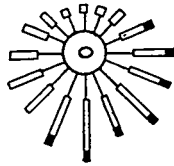
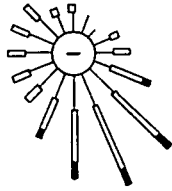
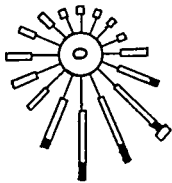


φ

Fig. 98 1500 m wind rose map, Spring, Southern Appalachian area.

SUMMER
1500m

φ



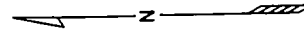
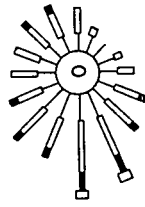
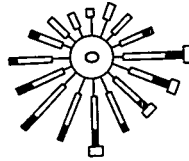
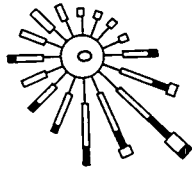
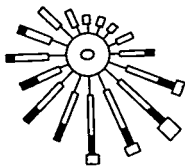
φ

Fig. 99 1500 m wind rose map, Summer, Southern Appalachian area.

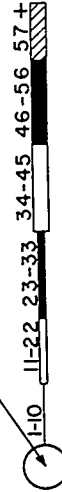
448

FALL
1500m

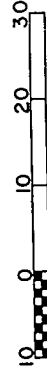
φ



% Calm



% Frequency



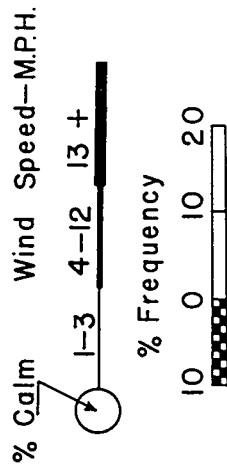
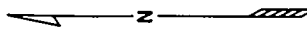
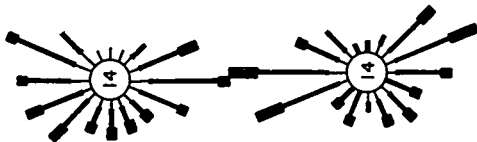
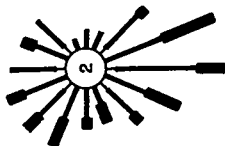
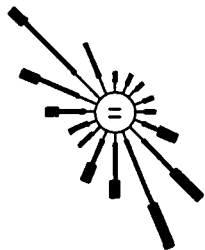
φ

Fig. 100 1500 m wind rose map, Fall, Southern Appalachian area.

4411

WINTER
SURFACE
ALL OBS

φ



φ

Fig. 101 Surface wind rose map, Winter, Southern Appalachian area.

14

14

14

14

14

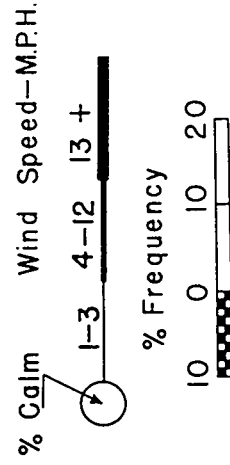
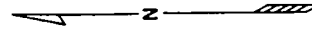
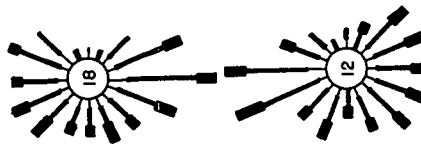
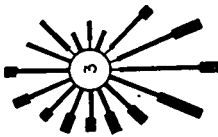
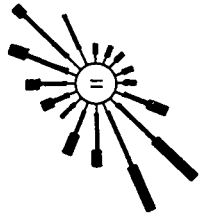
14

14

450

SPRING
SURFACE
ALL OBS

φ



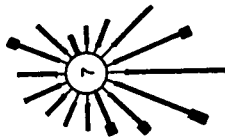
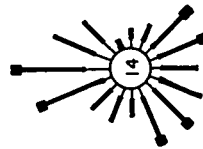
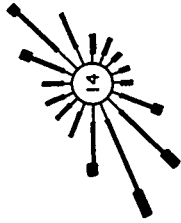
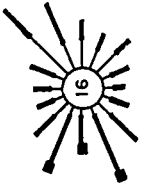
φ

Fig. 102 Surface wind rose map, Spring, Southern Appalachian area.

4

i

451



SUMMER
SURFACE
ALL OBS

φ

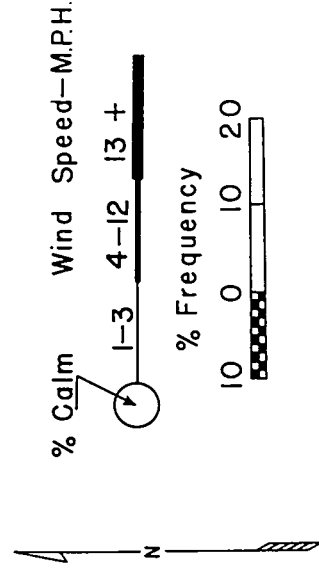


Fig. 103 Surface wind rose map, Summer, Southern Appalachian area.

452

FALL
SURFACE
ALL OBS

φ

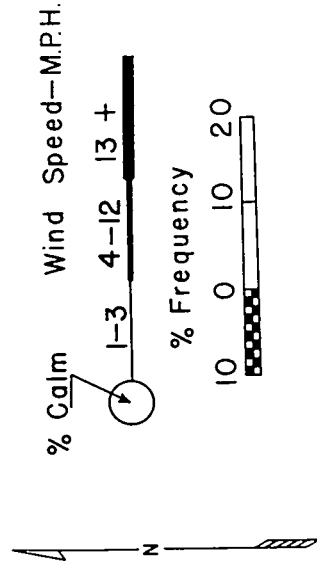
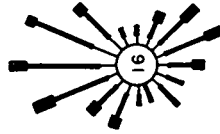
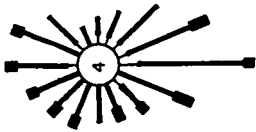
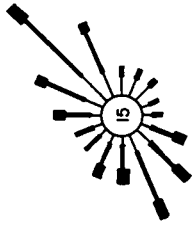
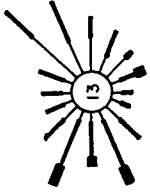
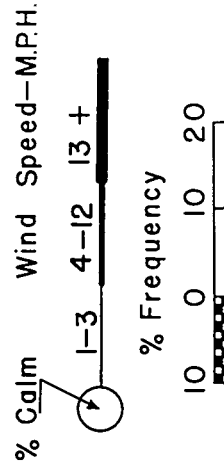
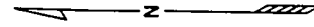
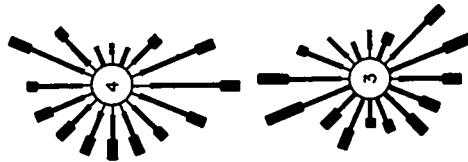
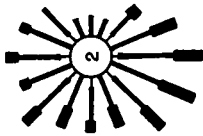
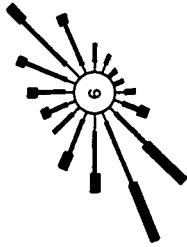
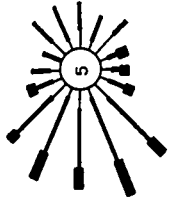


Fig. 104 Surface wind rose map, Fall, Southern Appalachian area.

45

ANNUAL
SURFACE
1000E-1700E

φ



φ

Fig. 105 Annual daytime wind rose map, Southern Appalachian area.

154

ANNUAL
SURFACE
2200E-0500E

φ

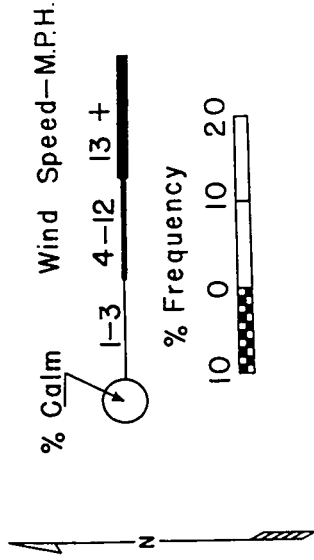
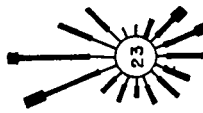
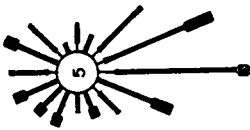
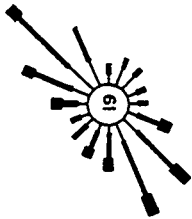
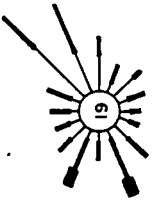
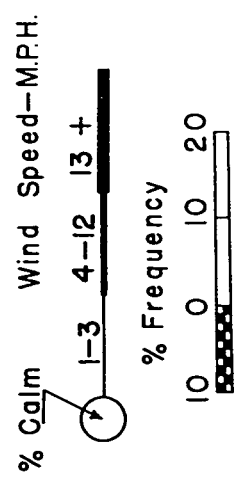
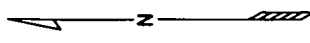
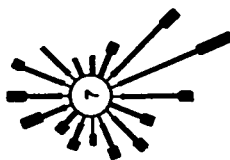
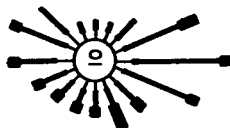
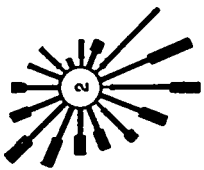
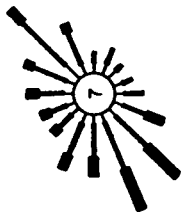
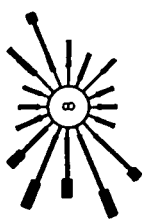


Fig. 106 Annual nighttime surface wind rose map, Southern Appalachian area.

4-55

φ
ANNUAL
SURFACE
PRECIPITATION



φ

Fig. 107 Annual surface wind rose map for observations with precipitation occurring, Southern Appalachian area.

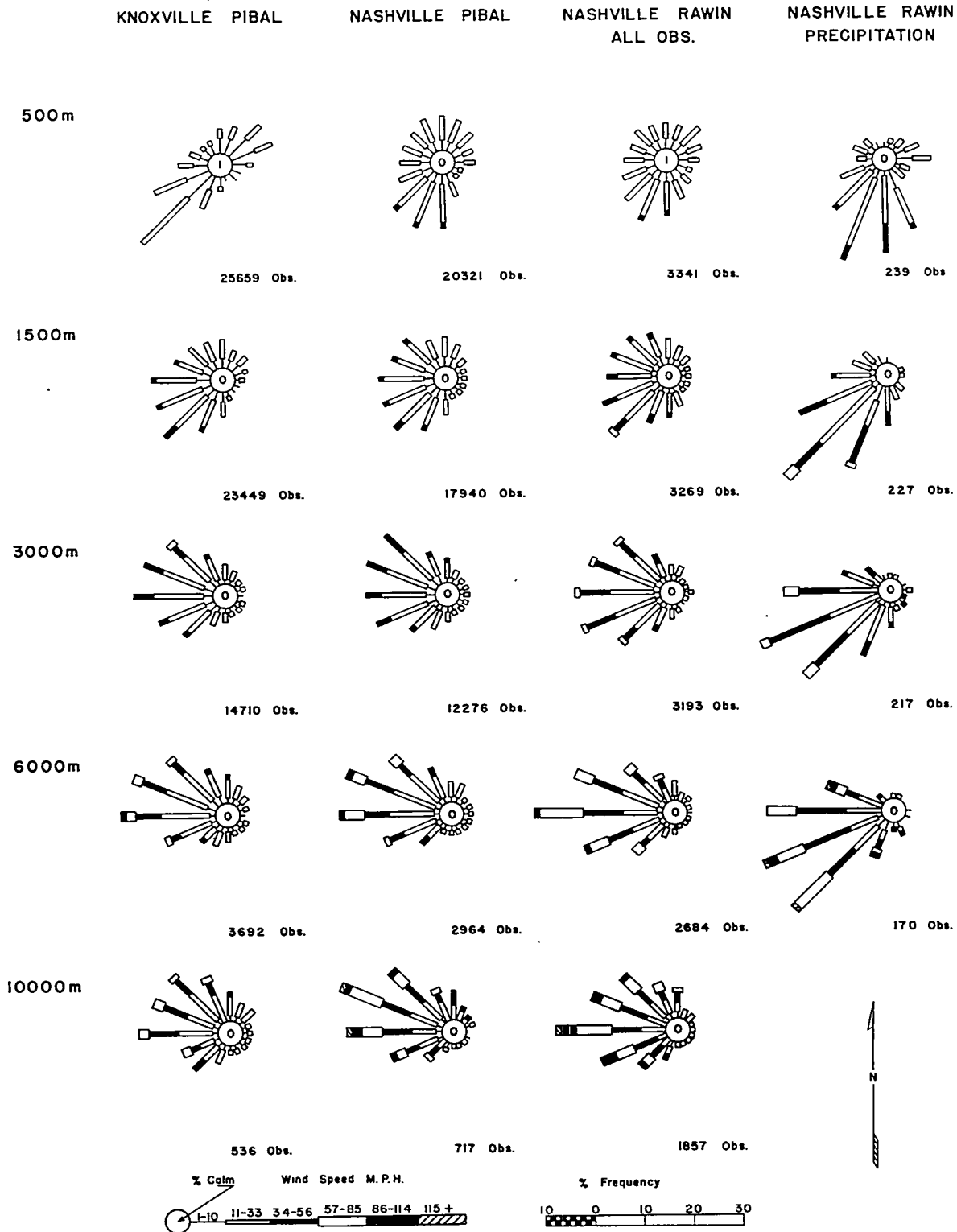


Fig. 103 Annual upper air wind roses comparing Knoxville pibals, Nashville pibals, all Nashville rawins, and Nashville rawins with precipitation occurring at time of observation.

Fig. 110 Spring upper air wind roses comparing Knoxville pibals, Nashville pibals, all Nashville rawins, and Nashville rawins with precipitation occurring at time of observation.

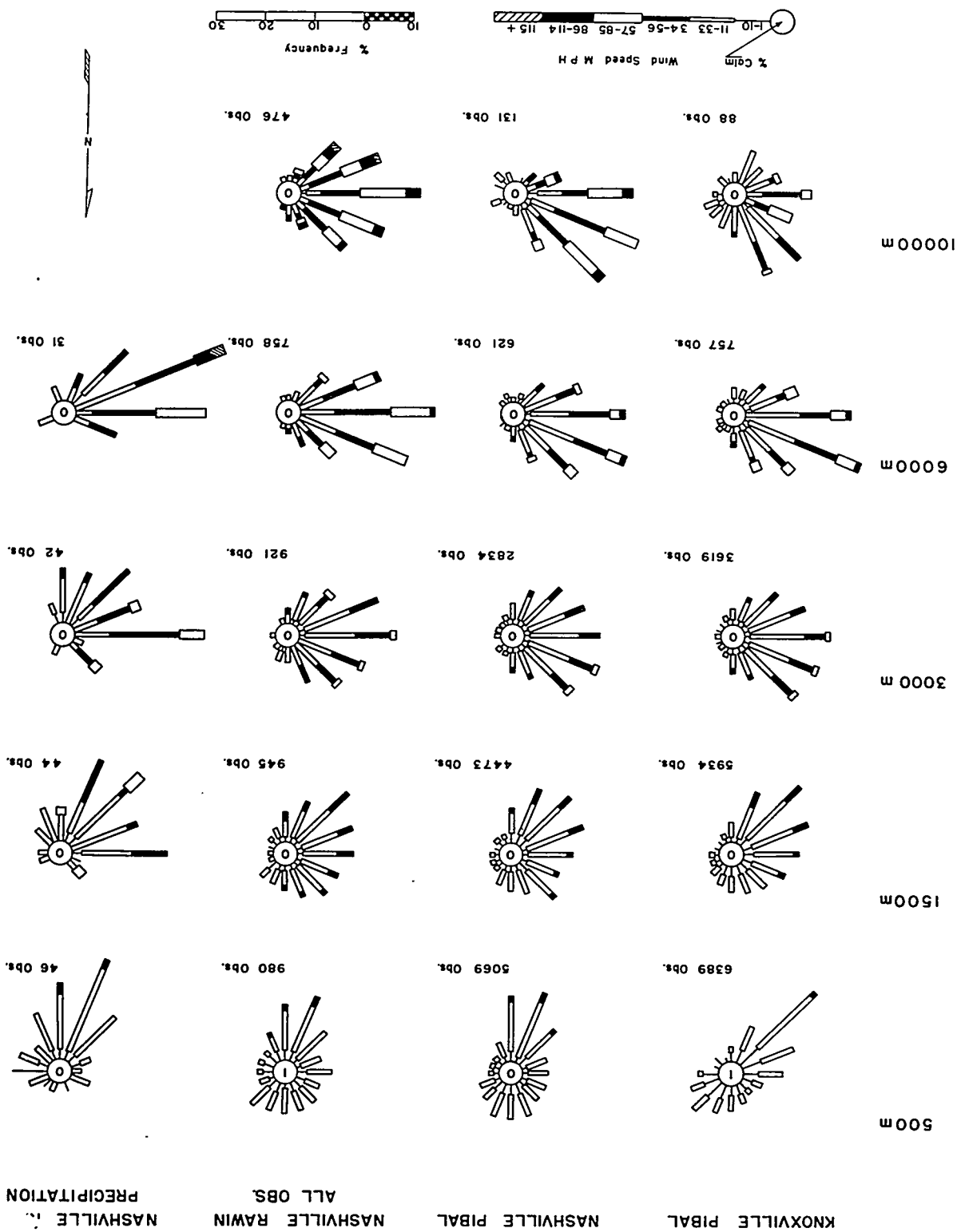
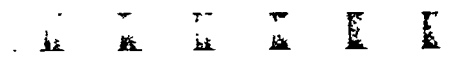
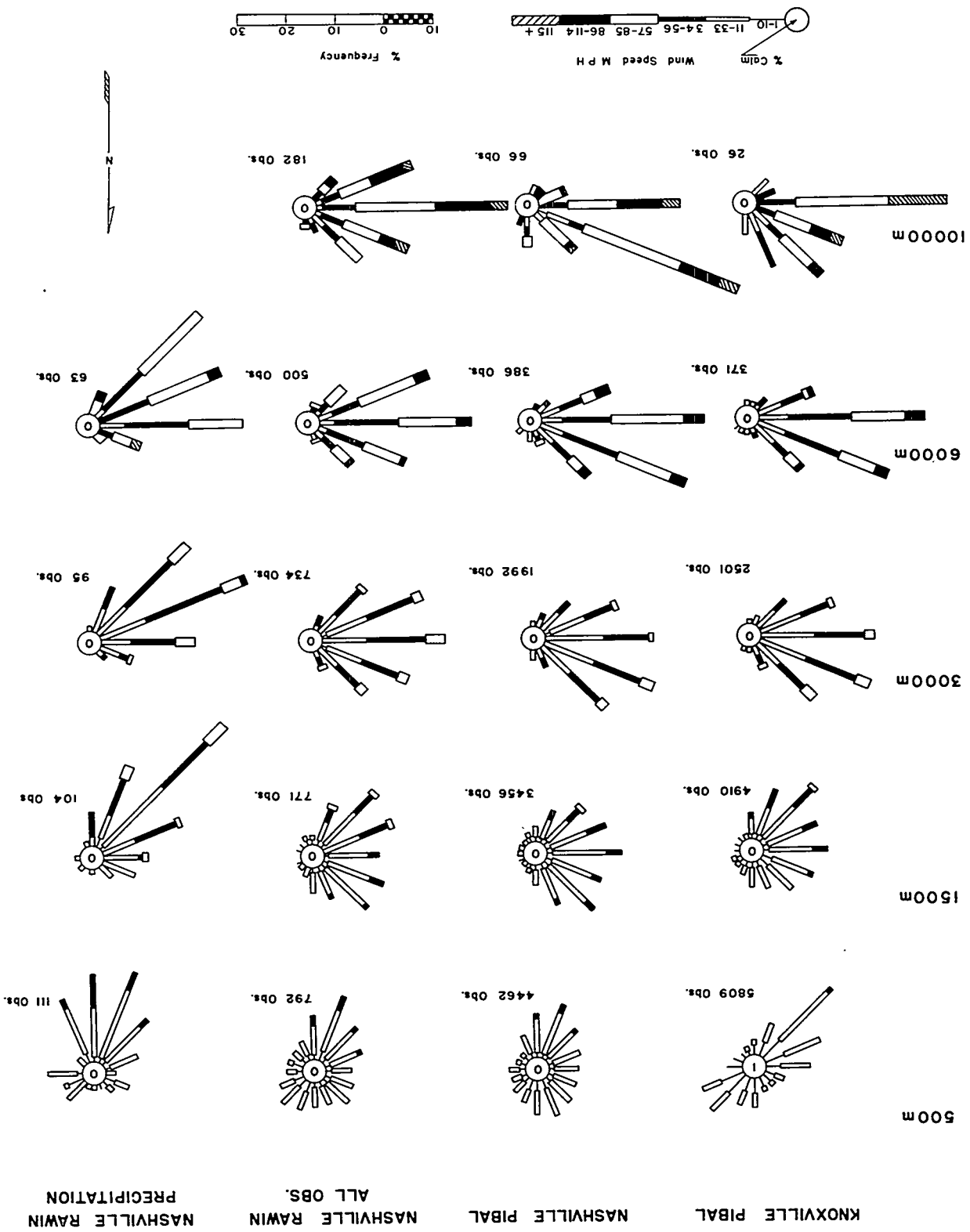


Fig. 109. Inter upper air wind roses comparing Knoxville PIBALs, Nashville PIBALs, all Nashville rawins, and Nashville rawins with precipitation occurring at time of observation.



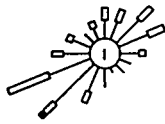
KNOXVILLE PIBAL

NASHVILLE PIBAL

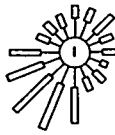
NASHVILLE RAWIN
ALL OBS.

NASHVILLE RAWIN
PRECIPITATION

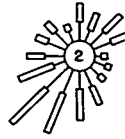
500m



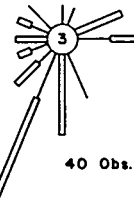
6763 Obs.



5460 Obs.

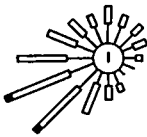


874 Obs.

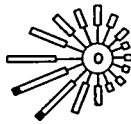


40 Obs.

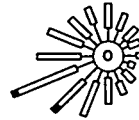
1500m



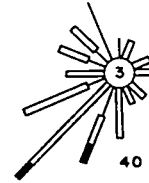
6418 Obs.



5162 Obs.

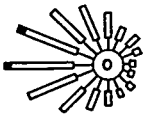


871 Obs.

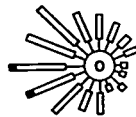


40 Obs.

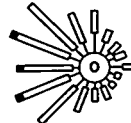
3000m



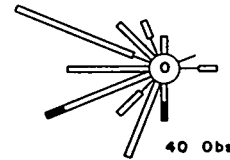
4455 Obs.



3898 Obs.

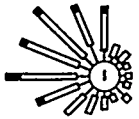


863 Obs.

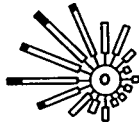


40 Obs.

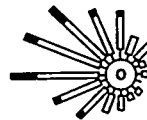
6000m



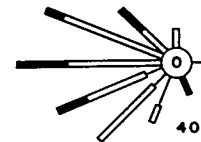
1308 Obs.



927 Obs.

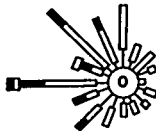


831 Obs.

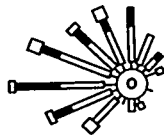


40 Obs.

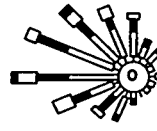
10000m



210 Obs.



194 Obs.



774 Obs.

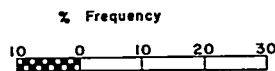
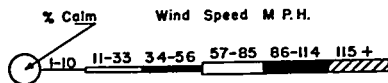


Fig. 111 Summer upper air wind roses comparing Knoxville pibals, Nashville pibals, all Nashville rawins, and Nashville rawins with precipitation occurring at time of observation.

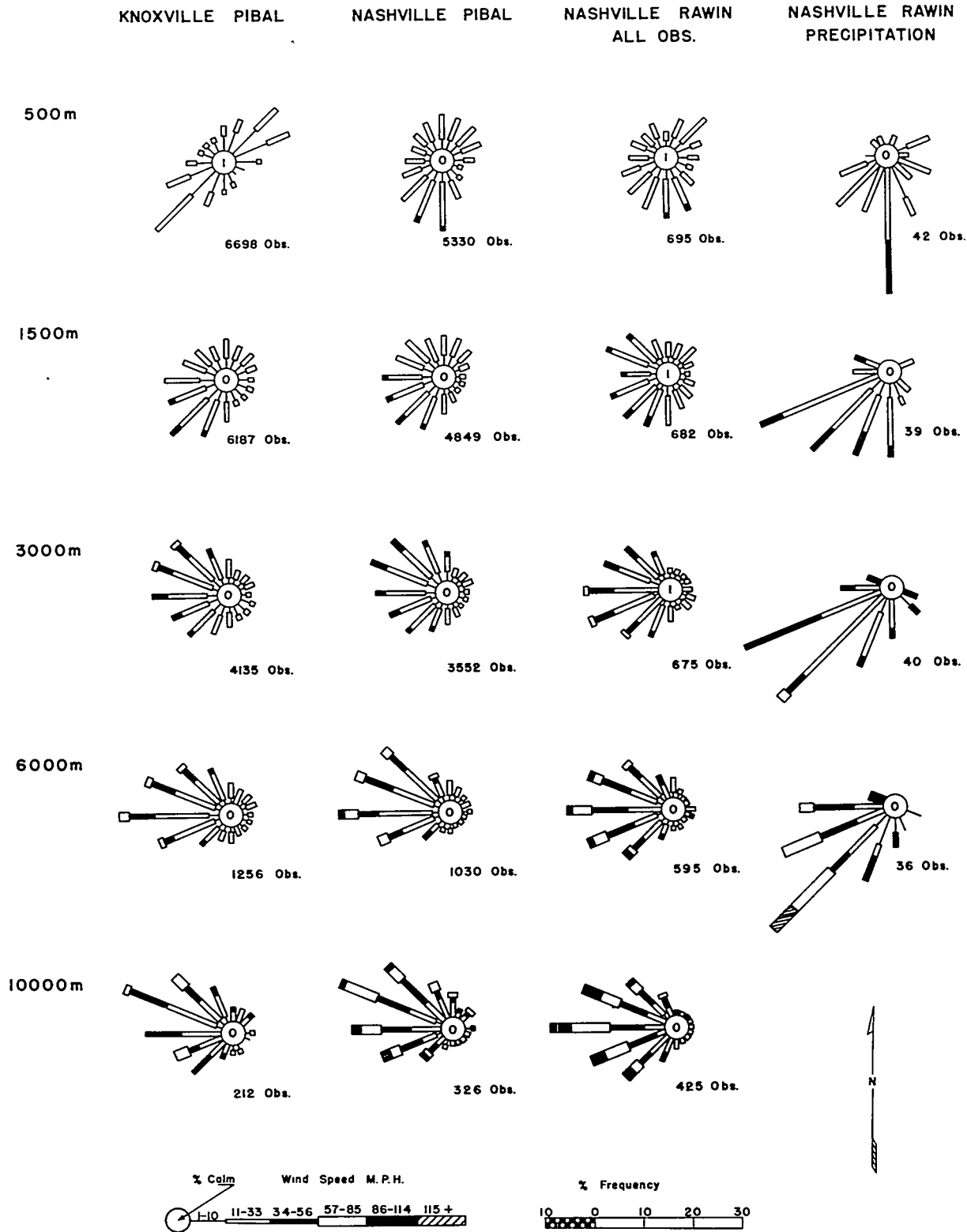


Fig. 112 Fall upper air wind roses comparing Knoxville pibals, Nashville pibals, all Nashville rawins, and Nashville rawins with precipitation occurring at time of observation.

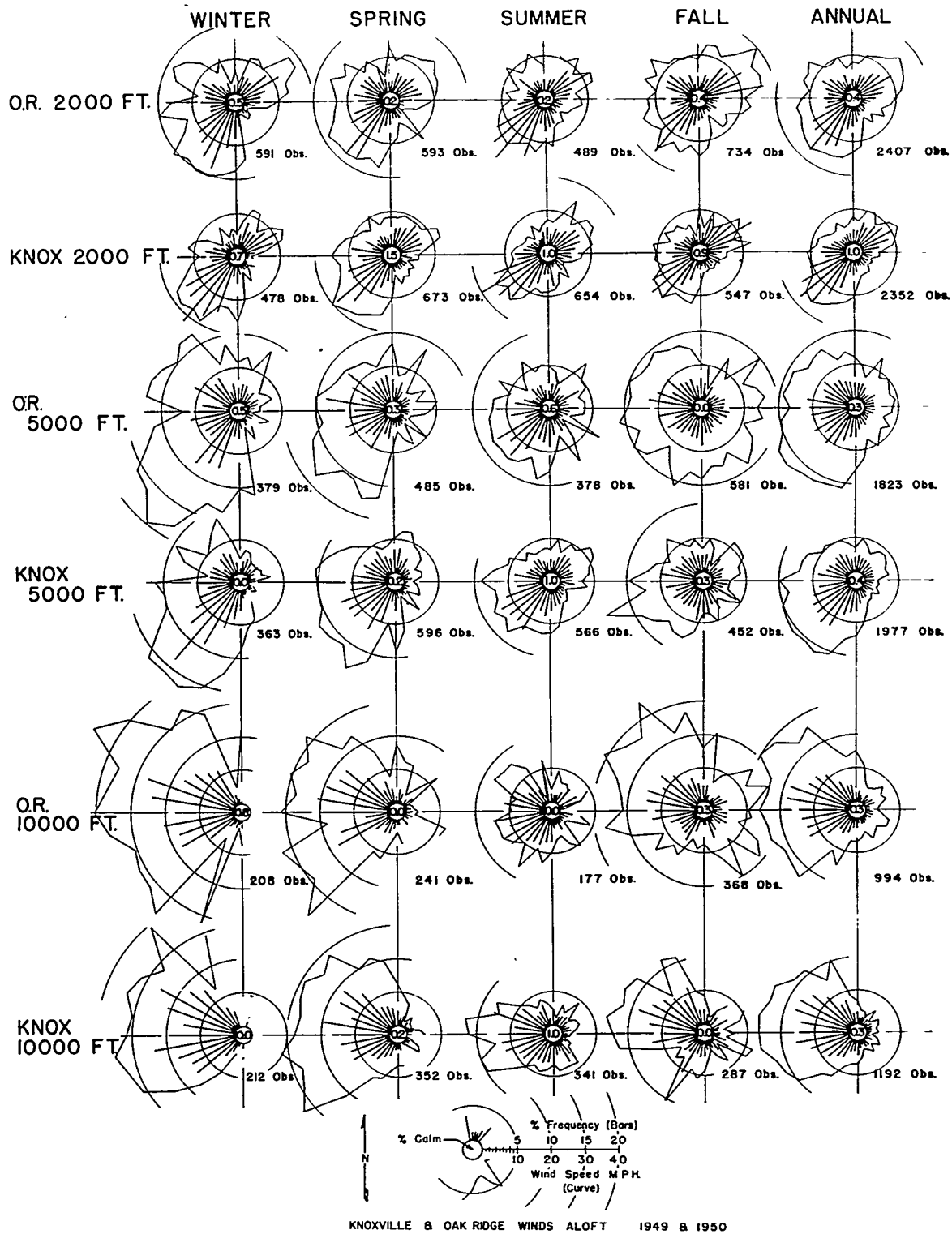


Fig. 113 36-point Oak Ridge and Knoxville upper air wind direction frequency and mean speed from each direction, by seasons and annual, 1949 - 1950.

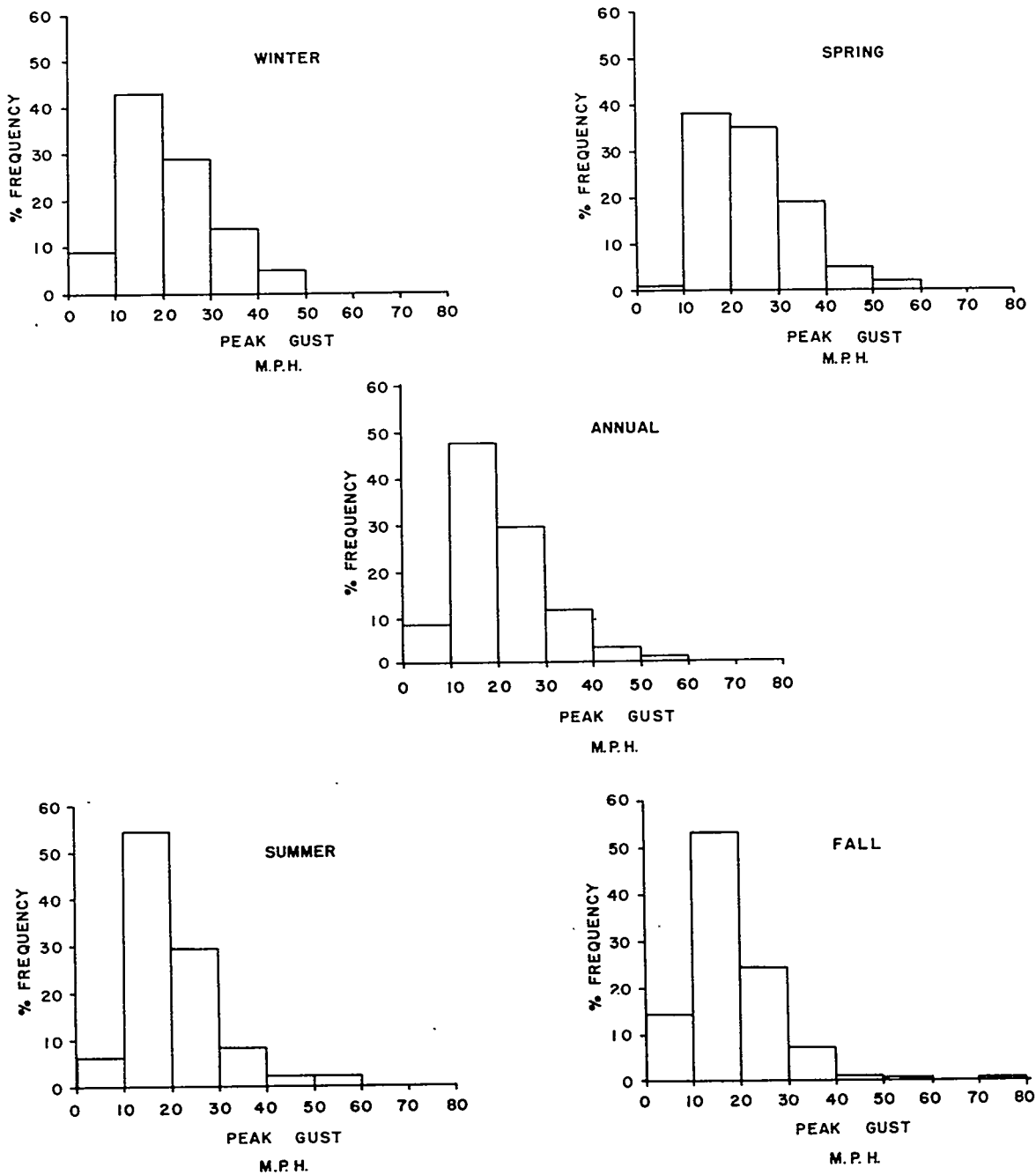
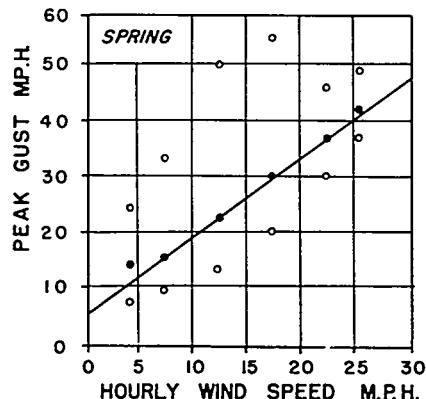
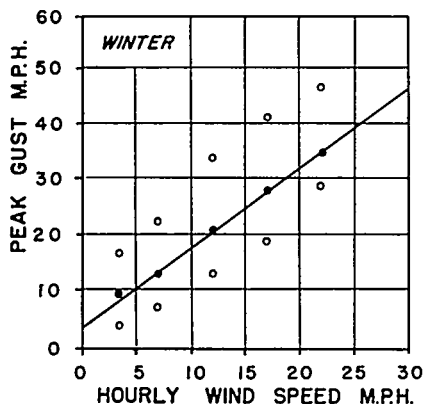
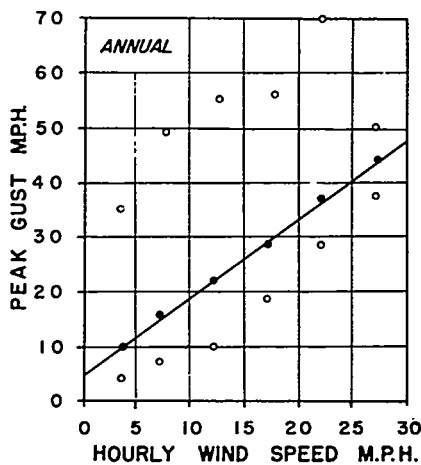


Fig. 114 Peak gust frequency distribution by seasons and annual, X-10 (012), Sept. 1949 - Nov. 1951.

STATION 012
140 FEET



• Mean Peak Gust



◦ Extreme Peak Gust

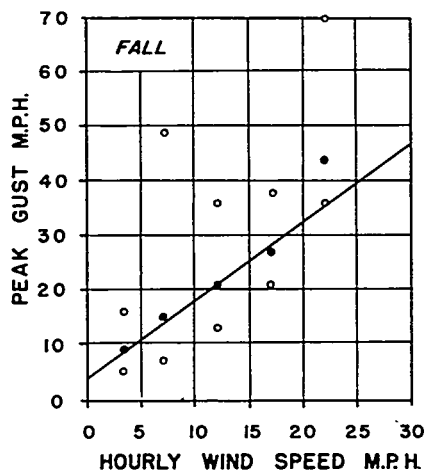
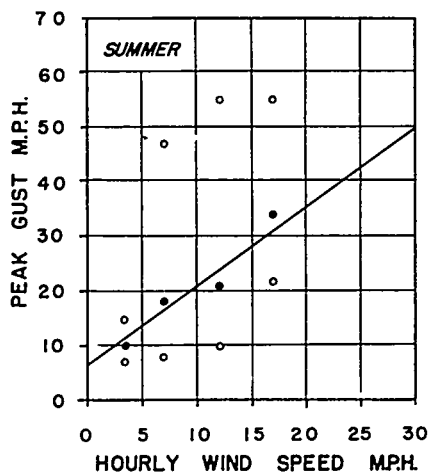


Fig. 115 Average daily peak gust as a function of average wind speed for hour containing peak gust, seasonal and annual, X-10 (012), Sept. 1949 - Nov. 1951.

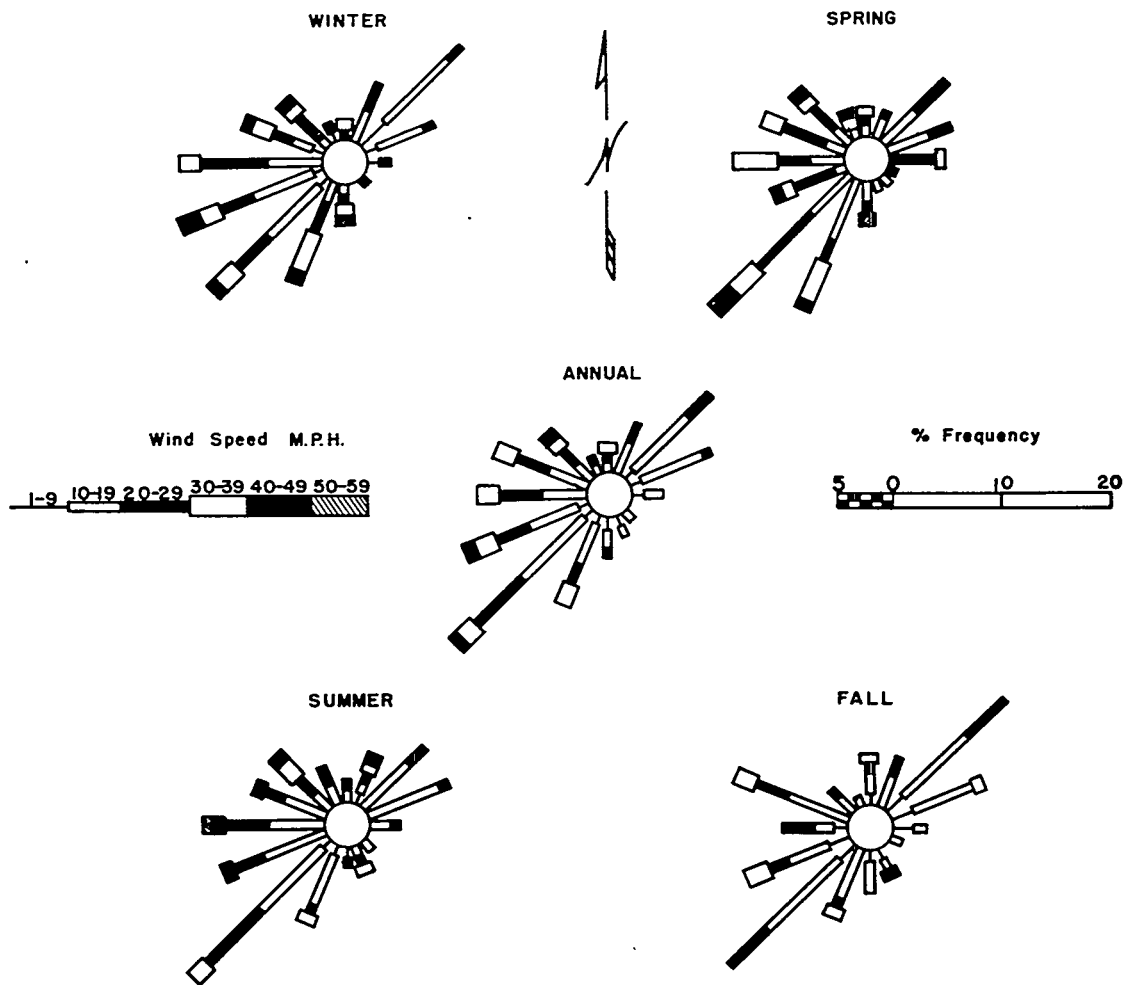


Fig. 116 Daily peak gust frequency by direction and speed, seasonal and annual, X-10 (012) Sept. 1949 - Nov. 1951.

φ



Fig. 117 Annual wind rose map, Bethel Valley-Melton Valley area.

φ

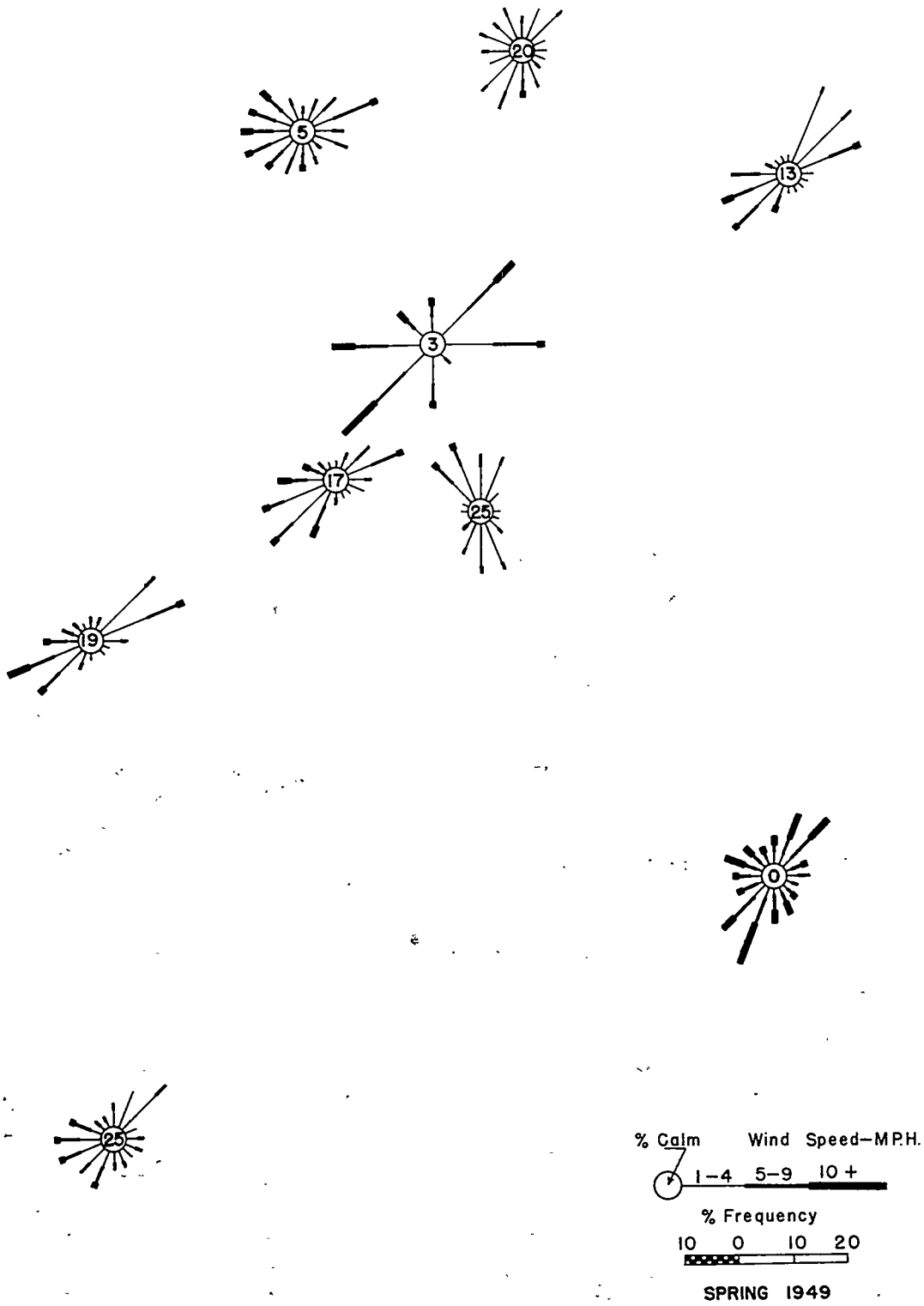


Fig. 118 Wind rose map, Bethel-Melton Valleys, Spring, 1949.

φ

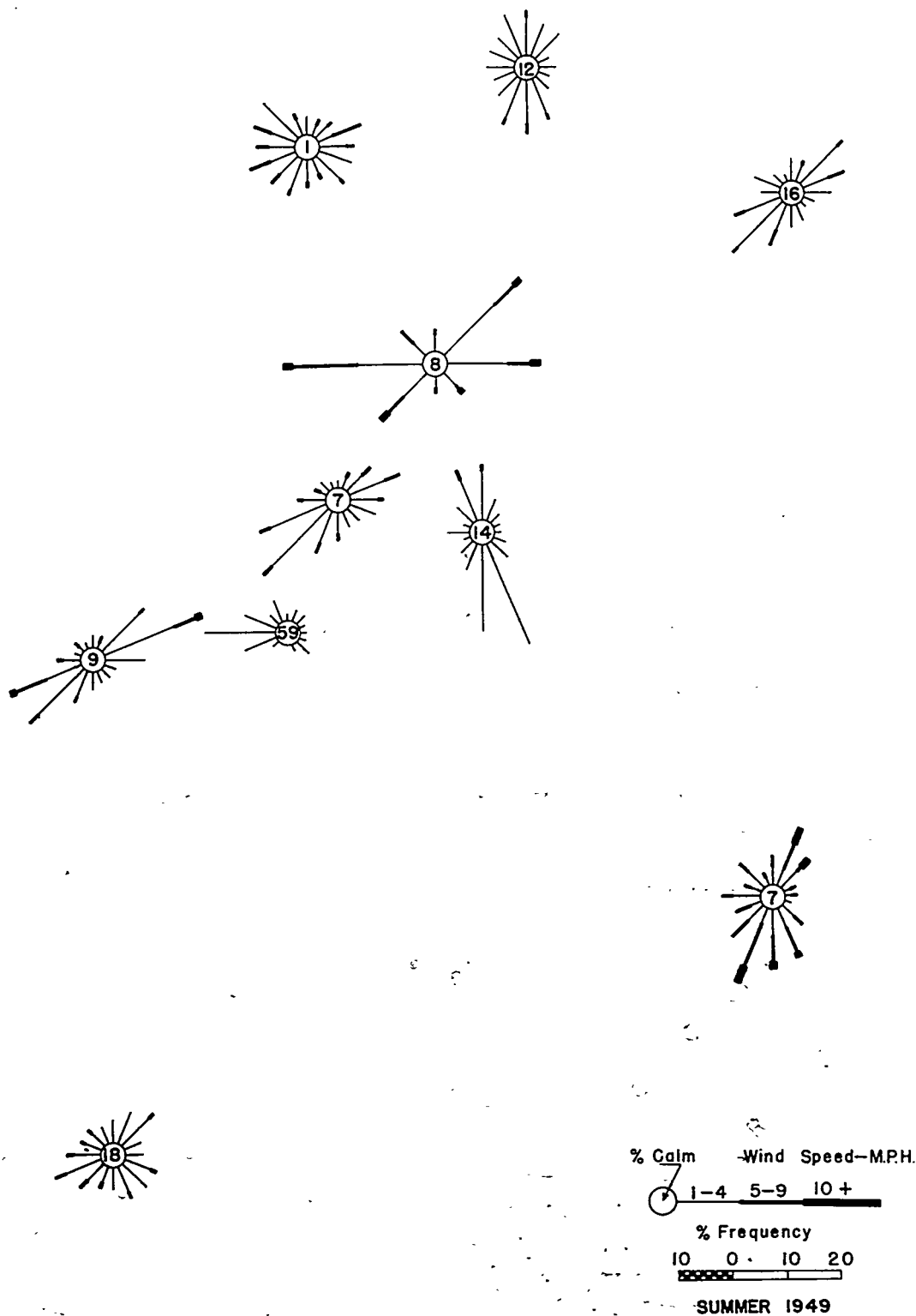
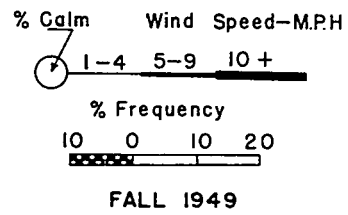
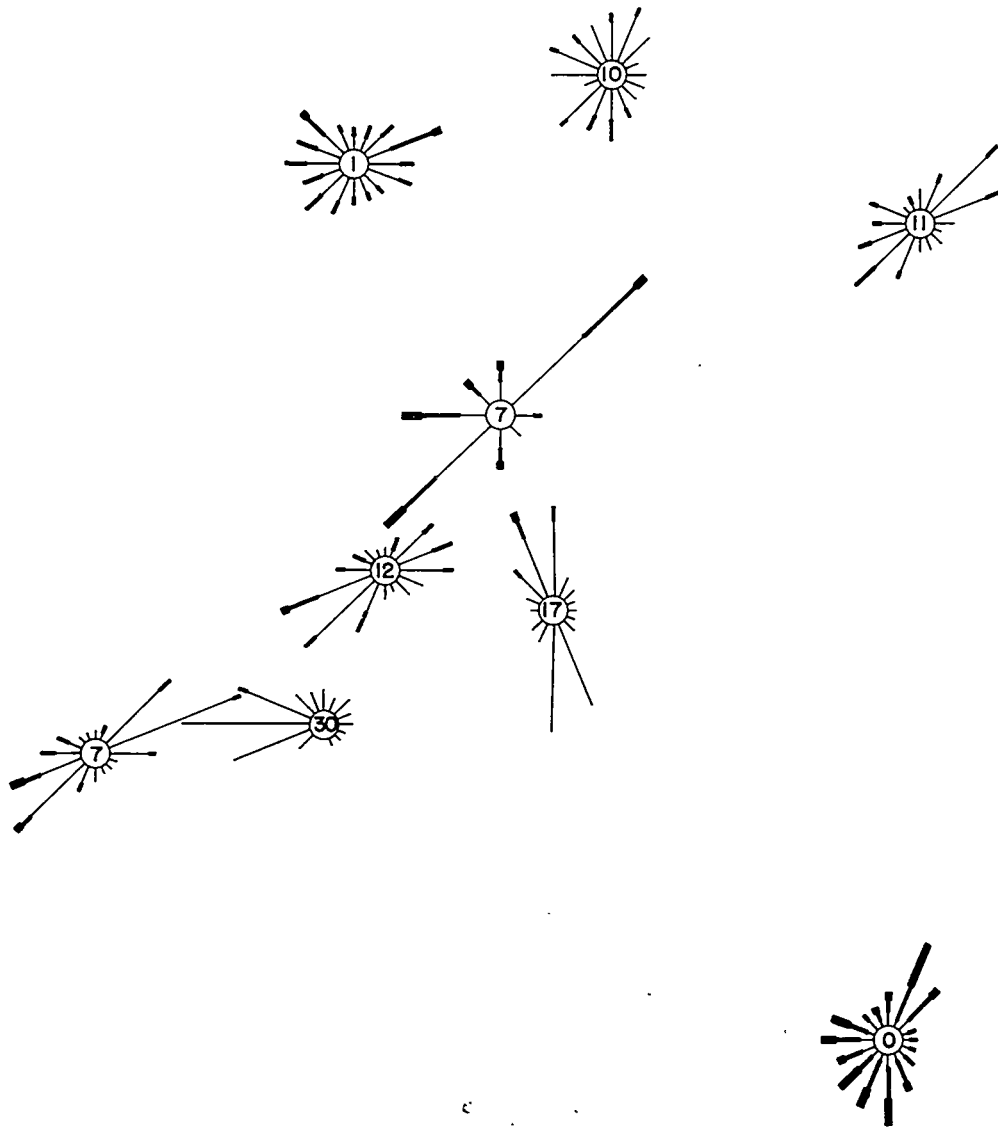


Fig. 119 Wind rose map, Bethel-Melton Valleys, Summer, 1949.

φ



φ

Fig. 120 Wind rose map, Bethel-Melton Valleys, Fall, 1949.

φ

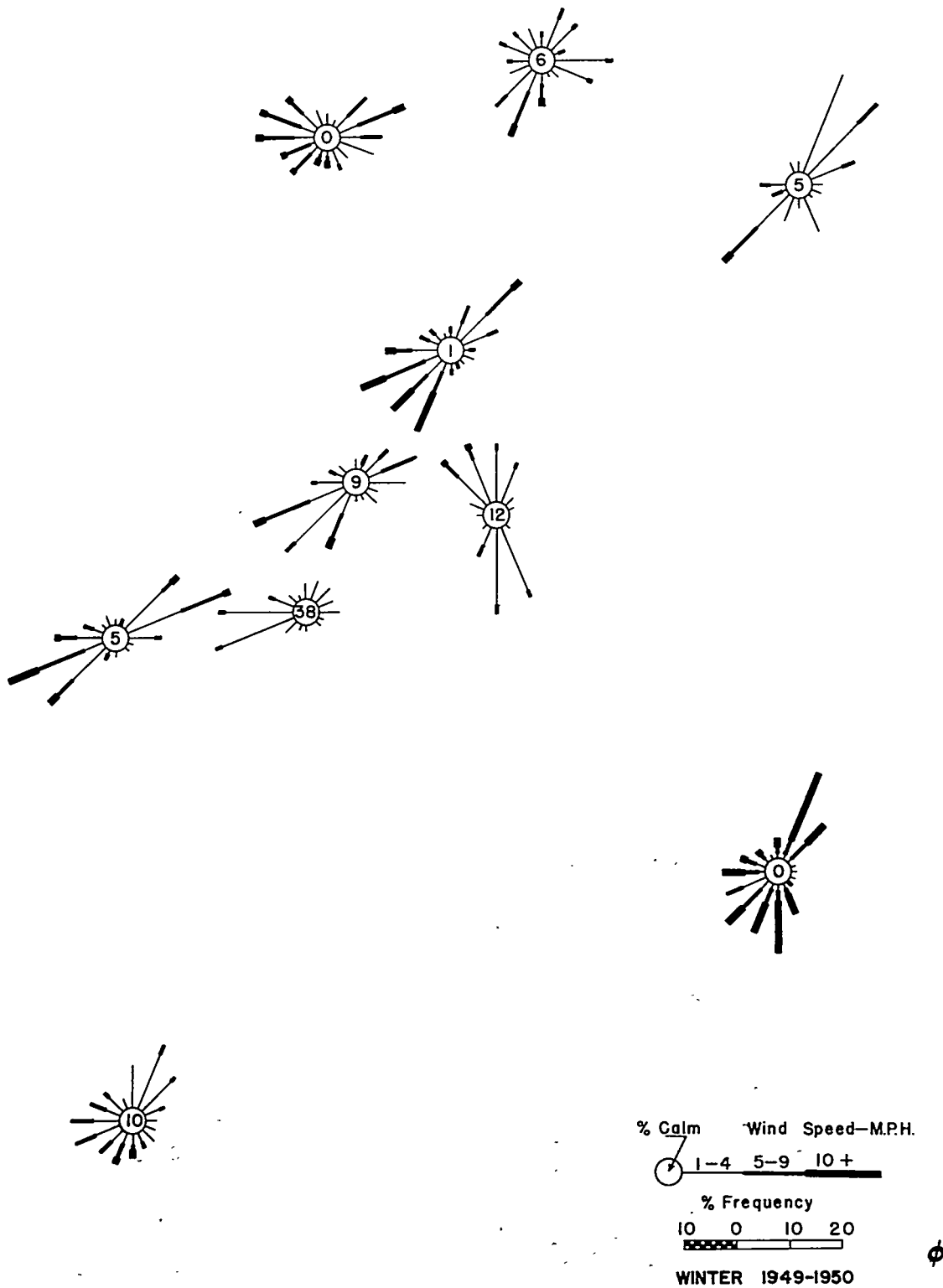


Fig. 121 Wind rose map, Bethel-Melton Valleys, Winter, 1949-1950.

φ



Fig. 122 Wind rose map, Bethel-Melton Valleys, Spring, 1950.

φ

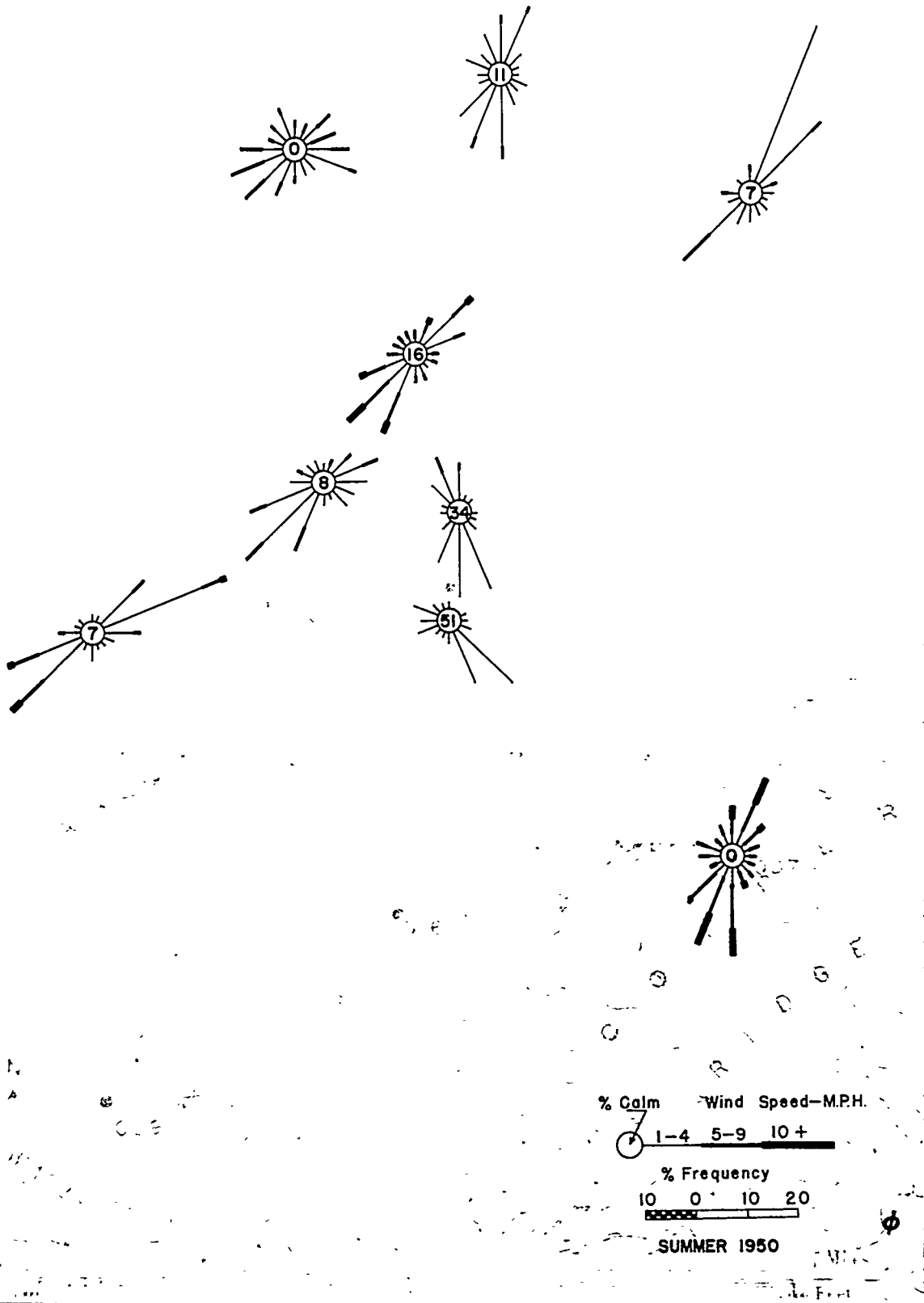


Fig. 123 Wind rose map, Bethel-Melton Valleys, Summer, 1950.

φ

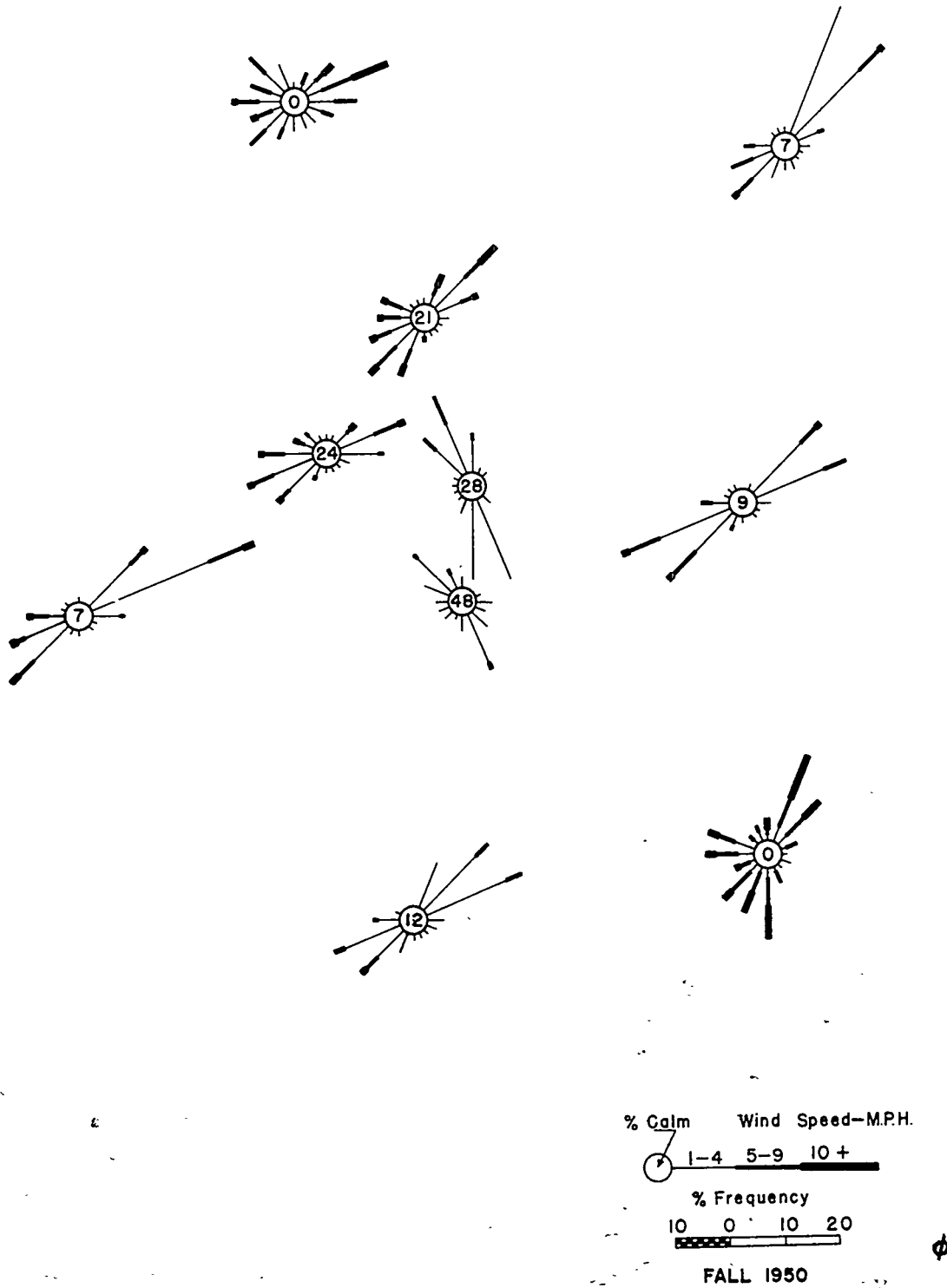


Fig. 124 Wind rose map, Bethel-Melton Valleys, Fall, 1950.

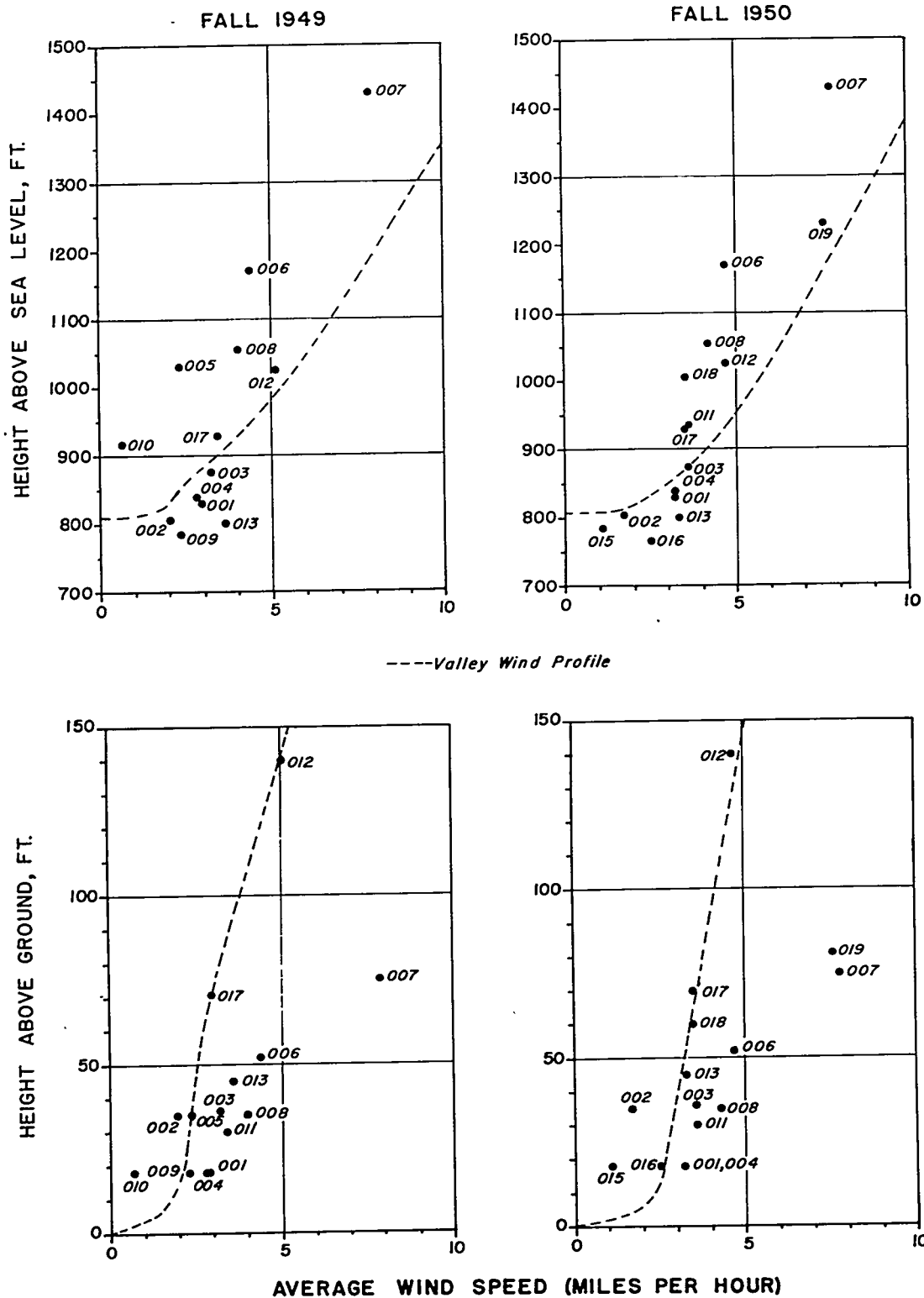


Fig. 125 Average wind speed at micronet stations plotted against anemometer height above sea level and above ground, Fall, 1949 and Fall, 1950.

ANNUAL WIND ROSES

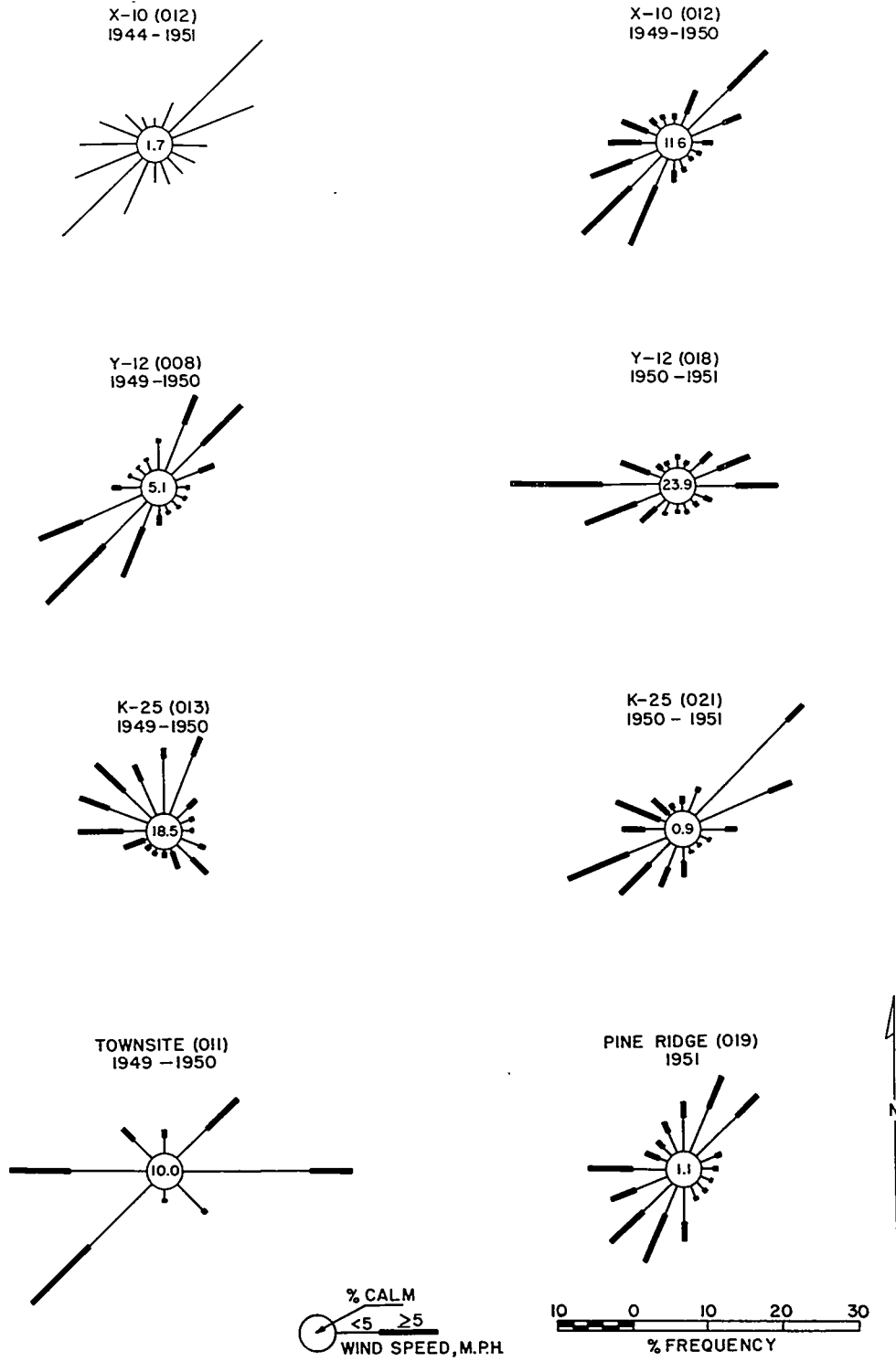


Fig. 126 Wind roses for Oak Ridge plant and town sites.

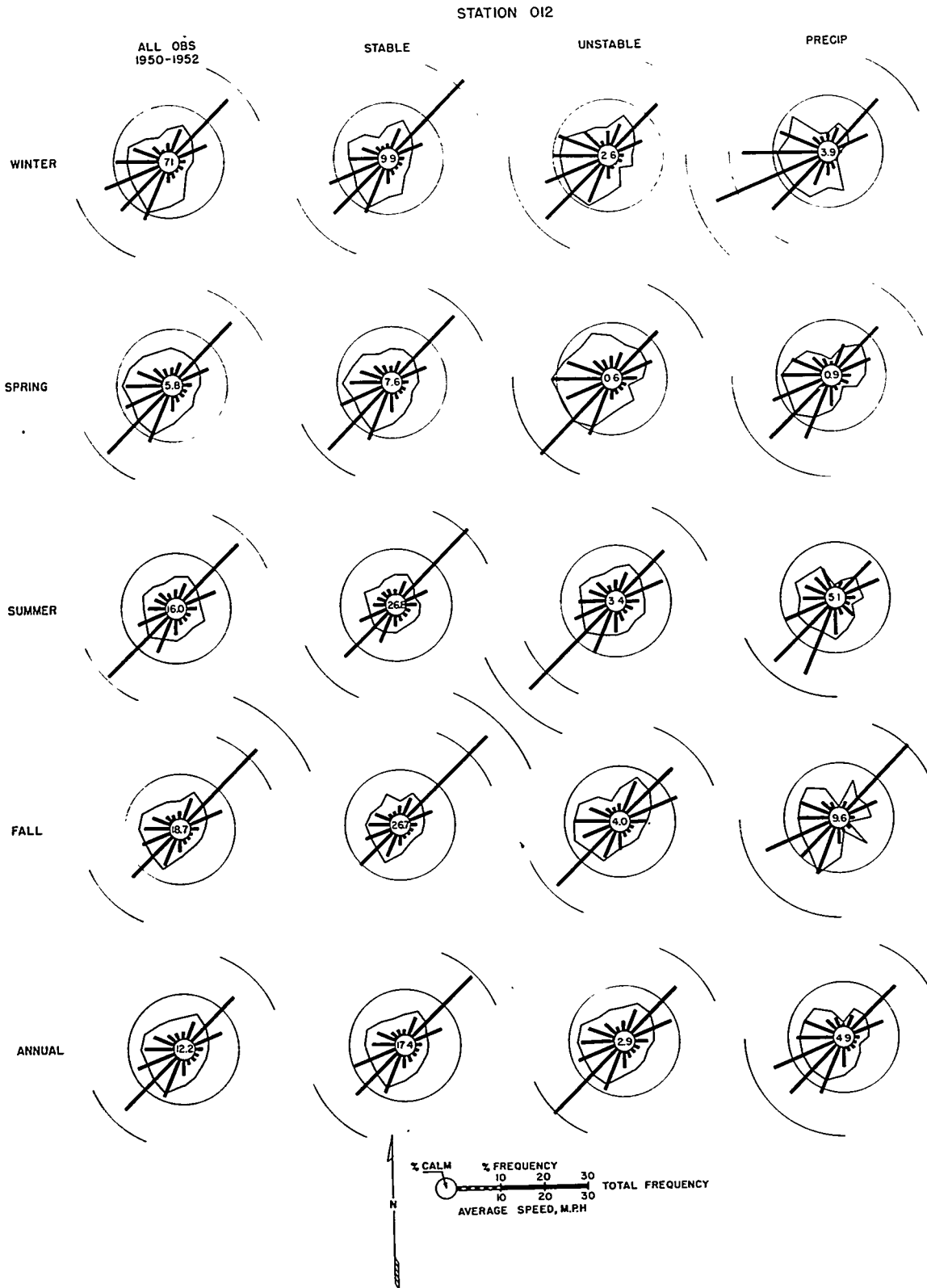


Fig. 127 X-10 (012) wind roses for stable ($T_{183} - T_5 \geq 0$) and unstable ($T_{183} - T_5 < 0$) conditions observations with precipitation, and total, by seasons and annual, 1950 - 1952.

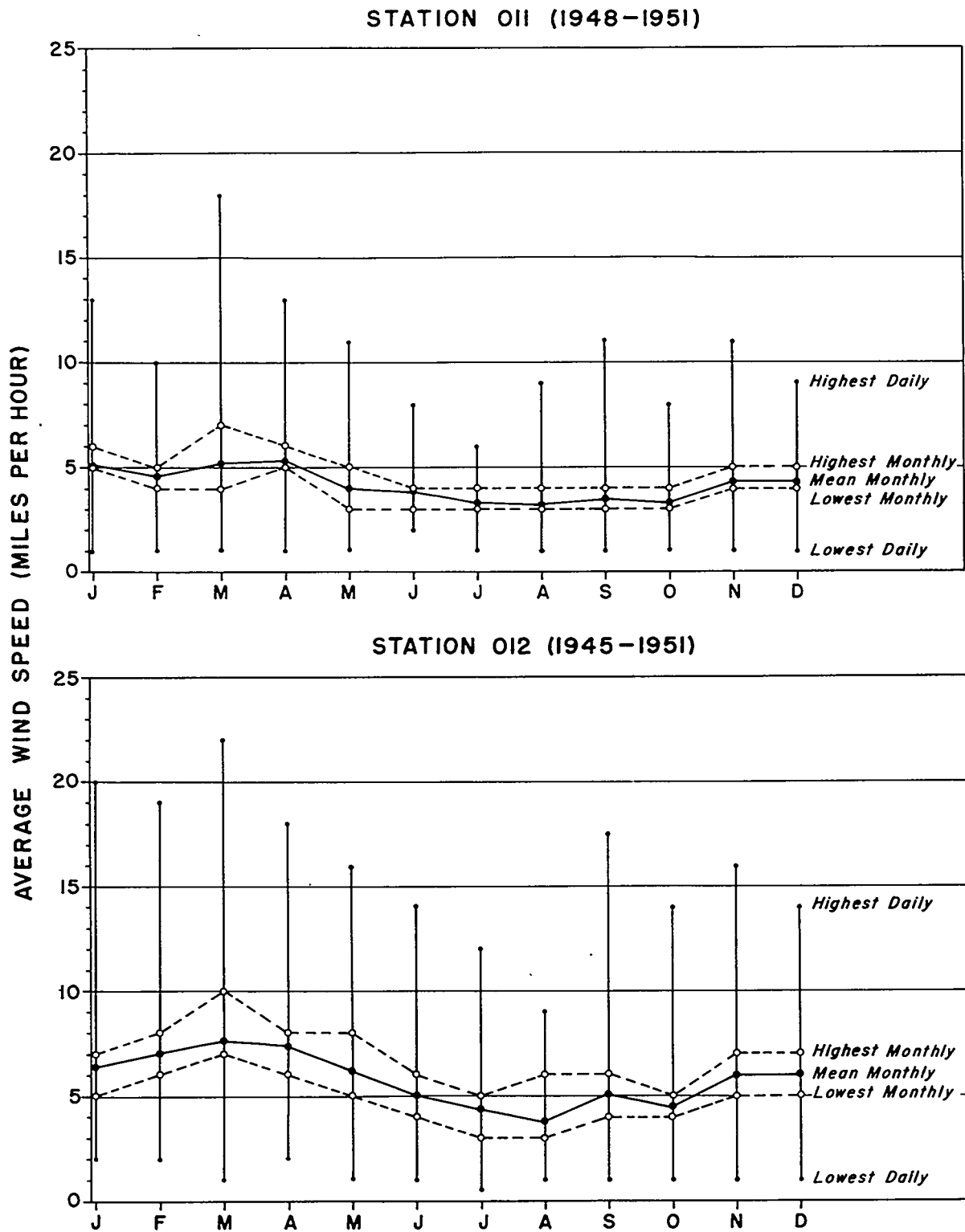


Fig. 128 Annual curves of monthly mean and extreme wind speed, Townsite (O11) and X-10 (O12).

WIND SPEED PROBABILITY GRAPHS
ALTITUDE AND SEASONS

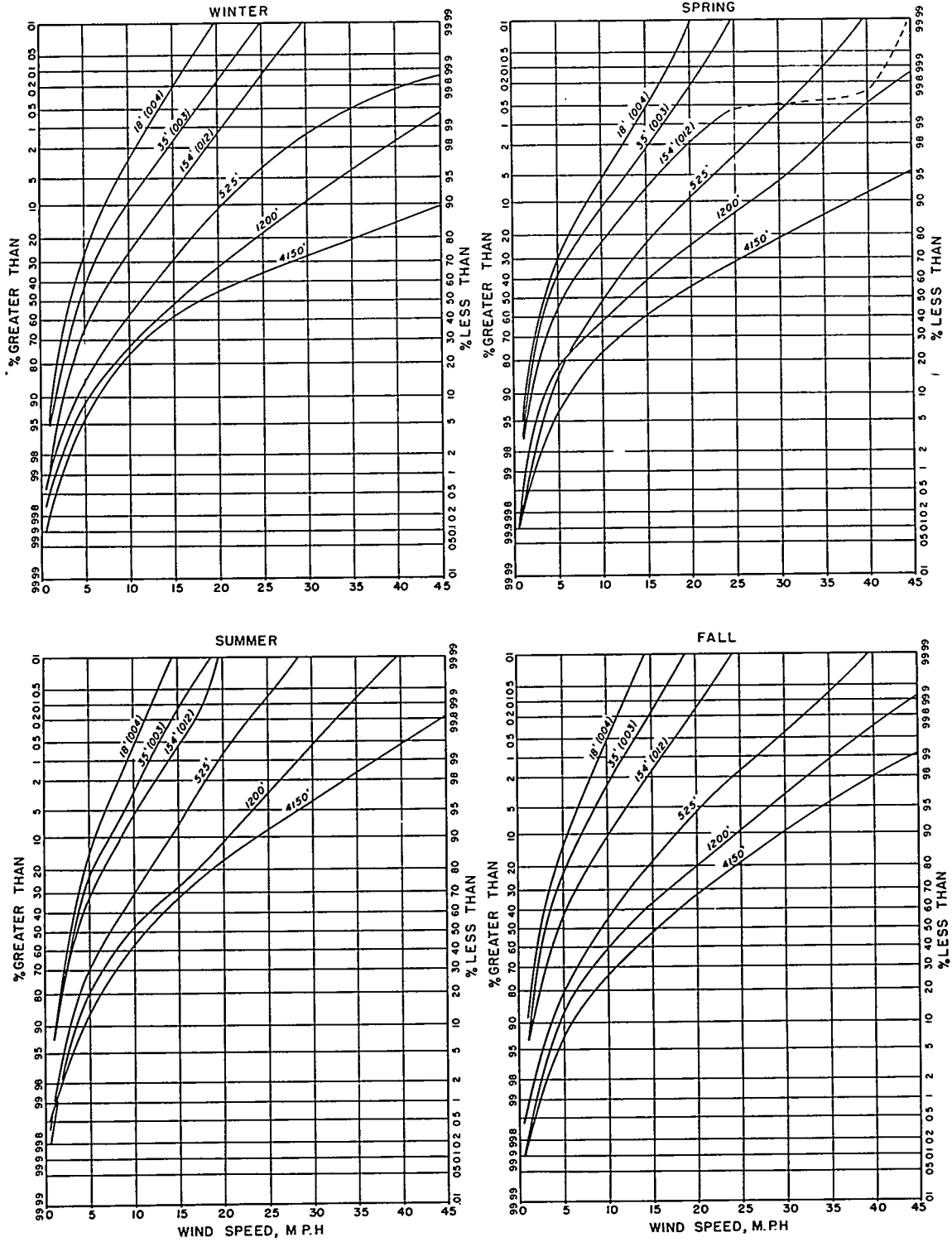


Fig. 129 Probability graphs of wind speed by altitude and season.

WIND SPEED PROBABILITY GRAPHS
EXPOSURE

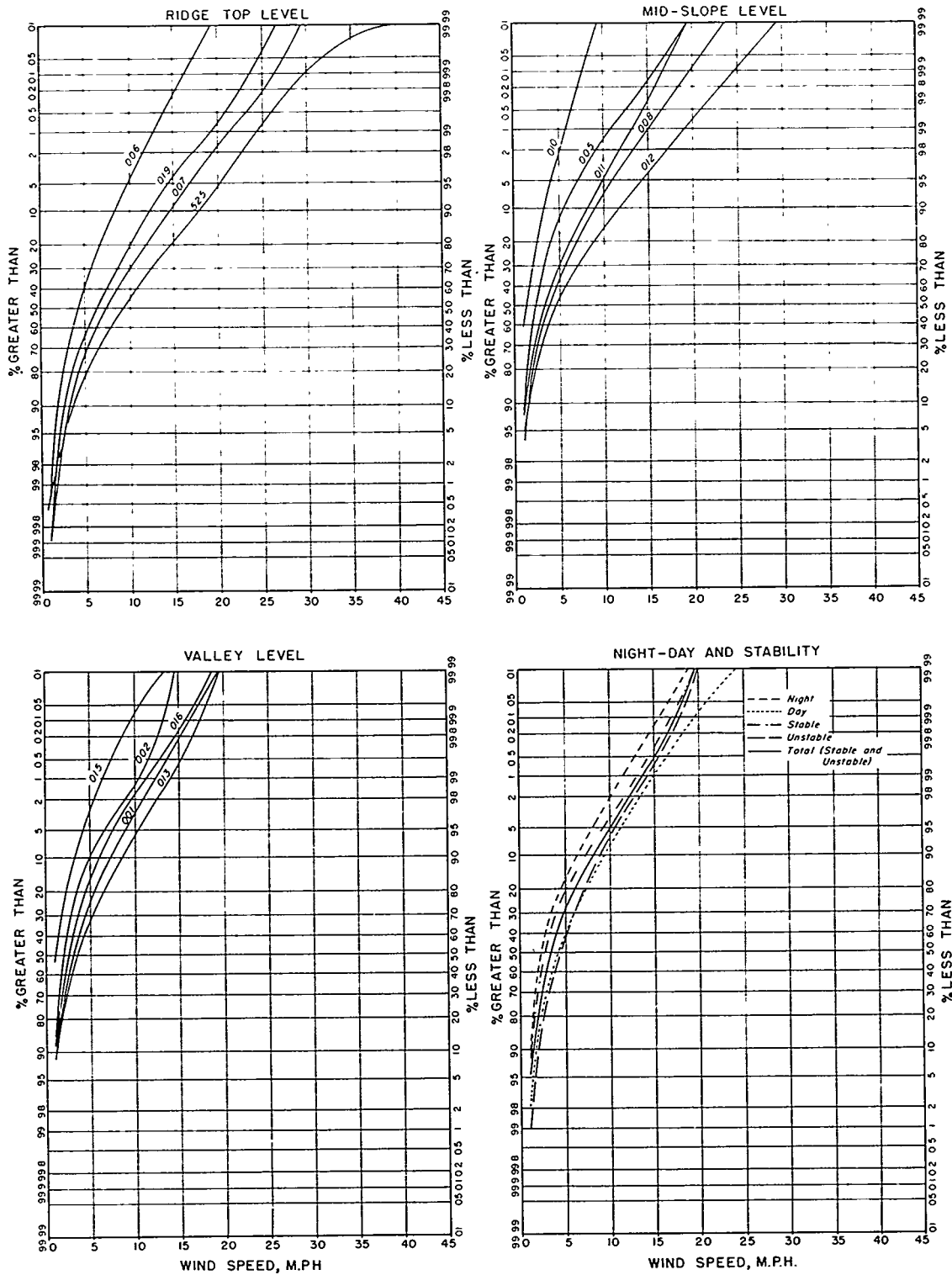


Fig. 130 Probability graphs of wind speed at variously exposed micronet stations, annual.

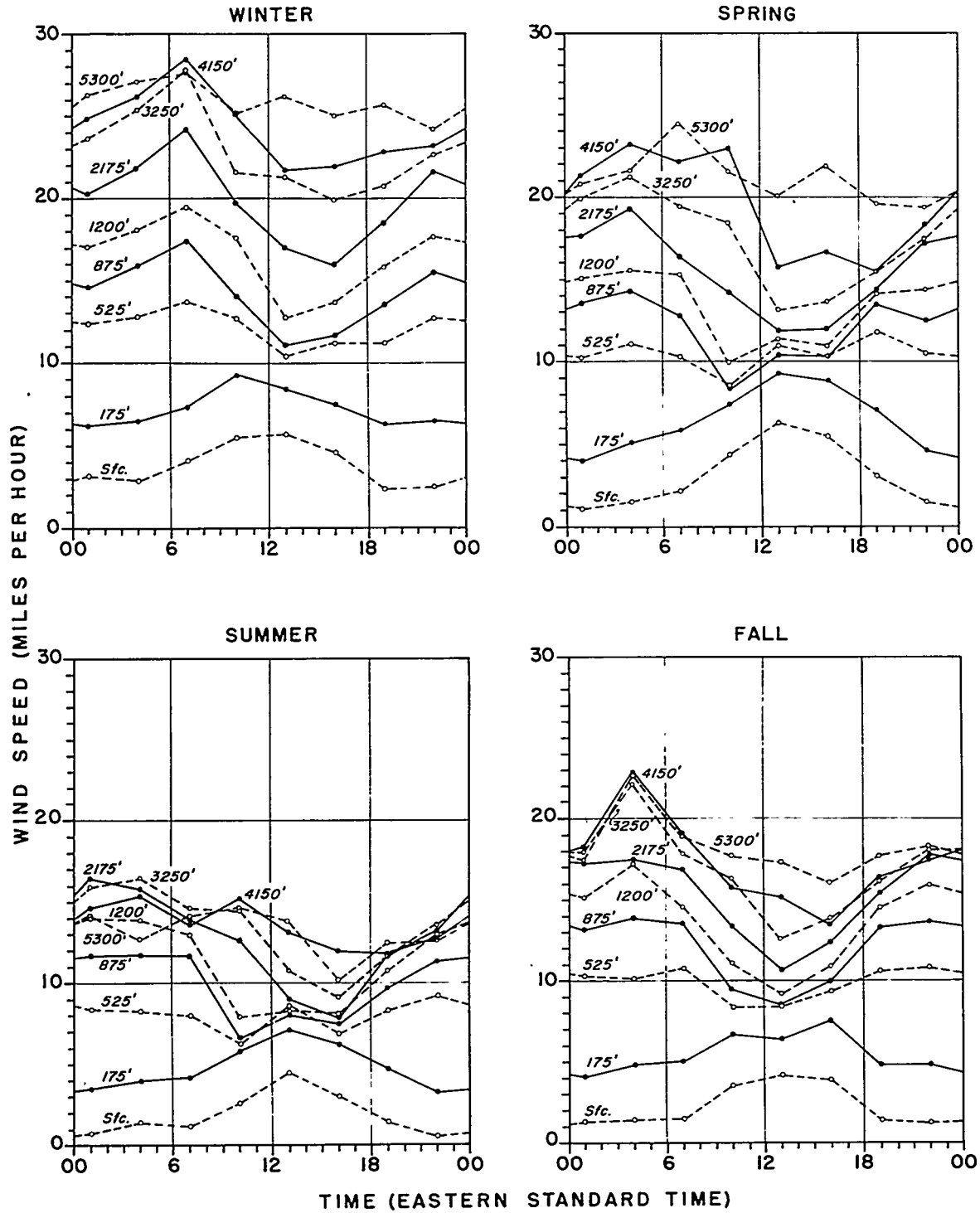


Fig. 131 Diurnal curves of average upper-air wind speed by altitude and season.

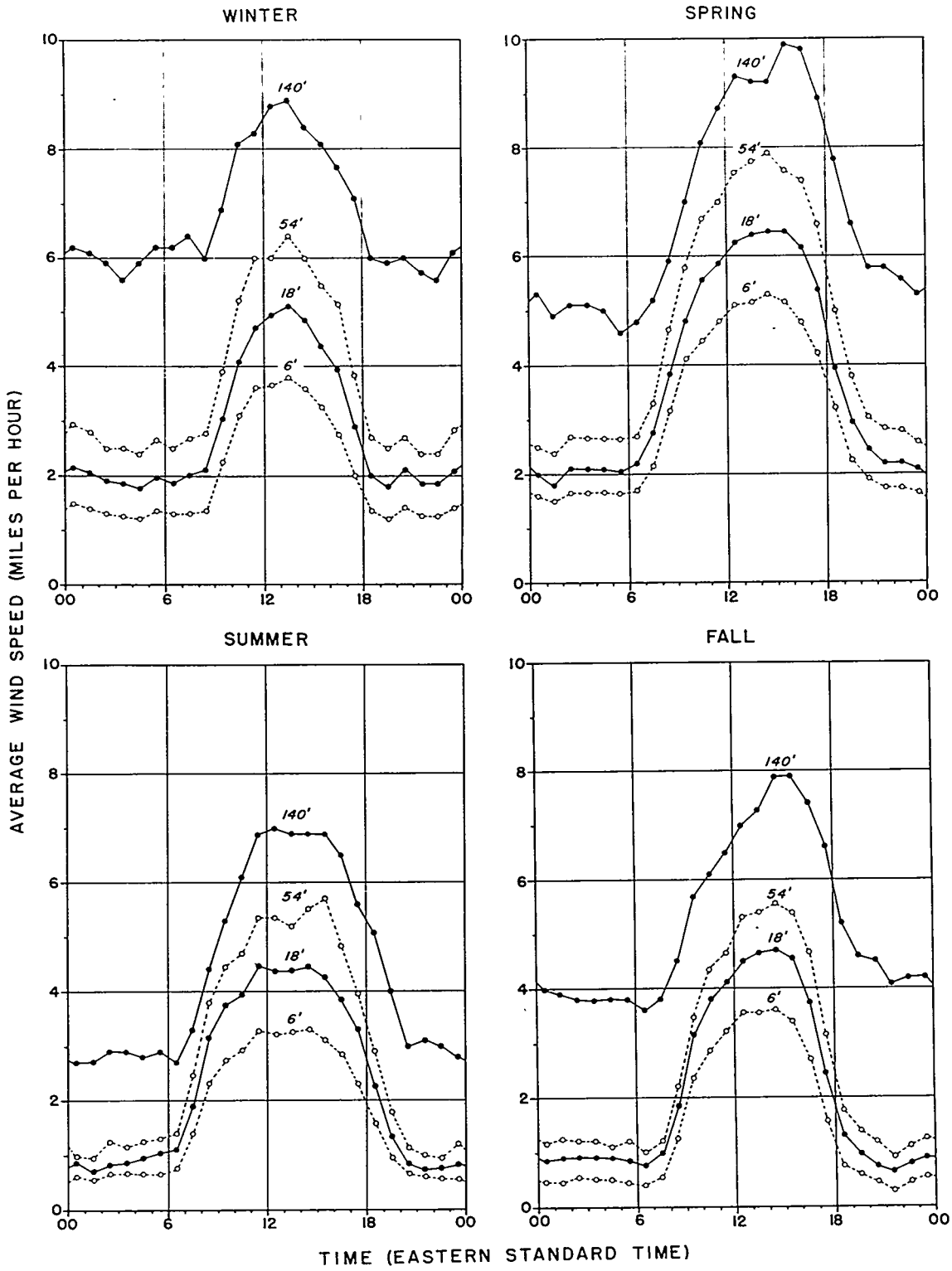


Fig. 132 Diurnal curves of average mid-valley anemometer wind speeds by altitude and season.

DIURNAL VARIATION OF WIND DIRECTION AND SPEED
 MELTON HILL (007), 1431 FT MSL —
 WEST BETHEL VALLEY (003), 876 FT MSL □

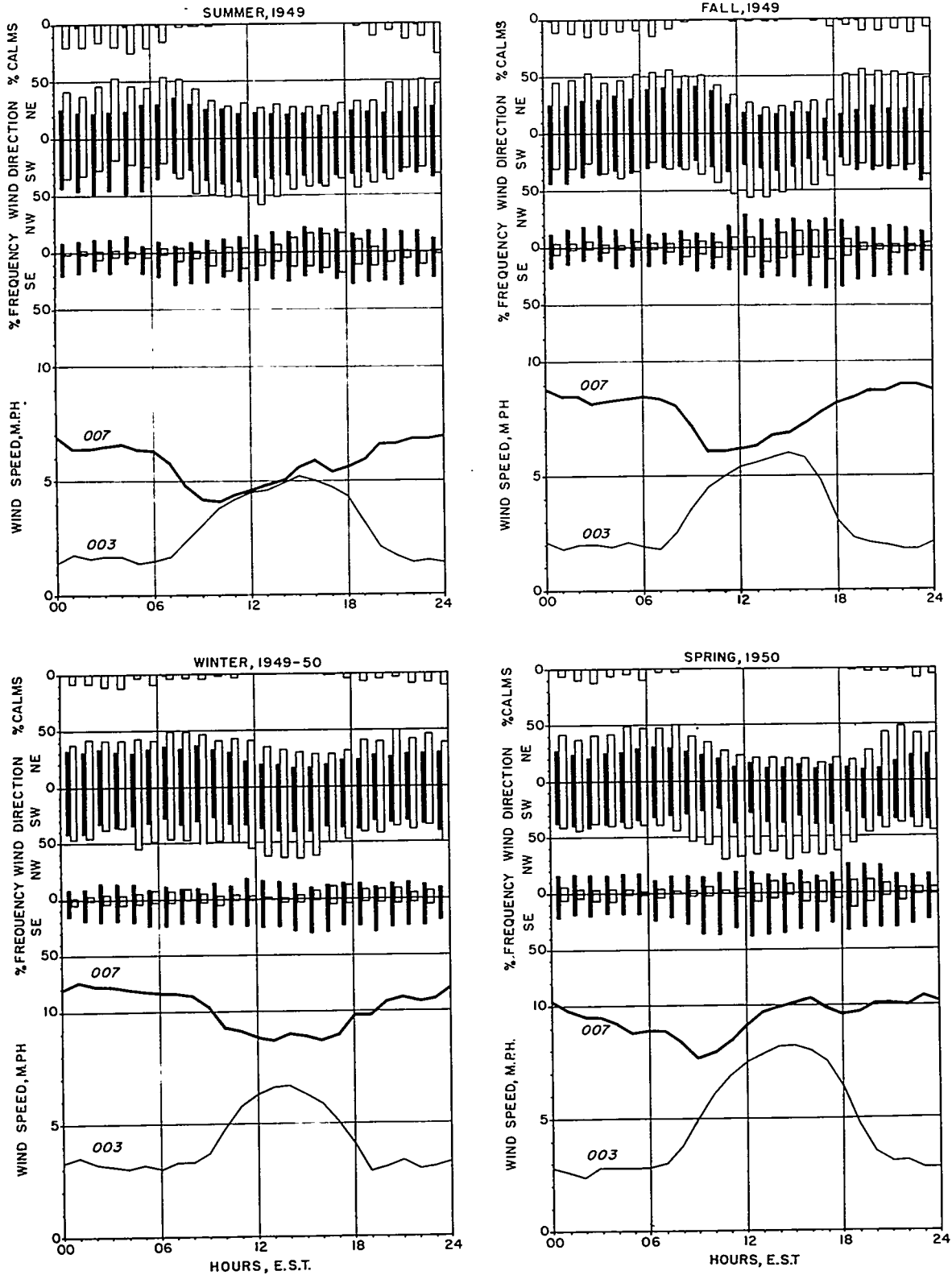


Fig. 133 Diurnal graphs of wind direction frequency and average speed by seasons, comparing hilltop (007) and valley (012) stations.

DIURNAL VARIATION OF WIND DIRECTION AND SPEED
 CHESTNUT RIDGE TOP (006), 1172 FT MSL —
 X-10 WATER TOWER (012), 1041 MSL □

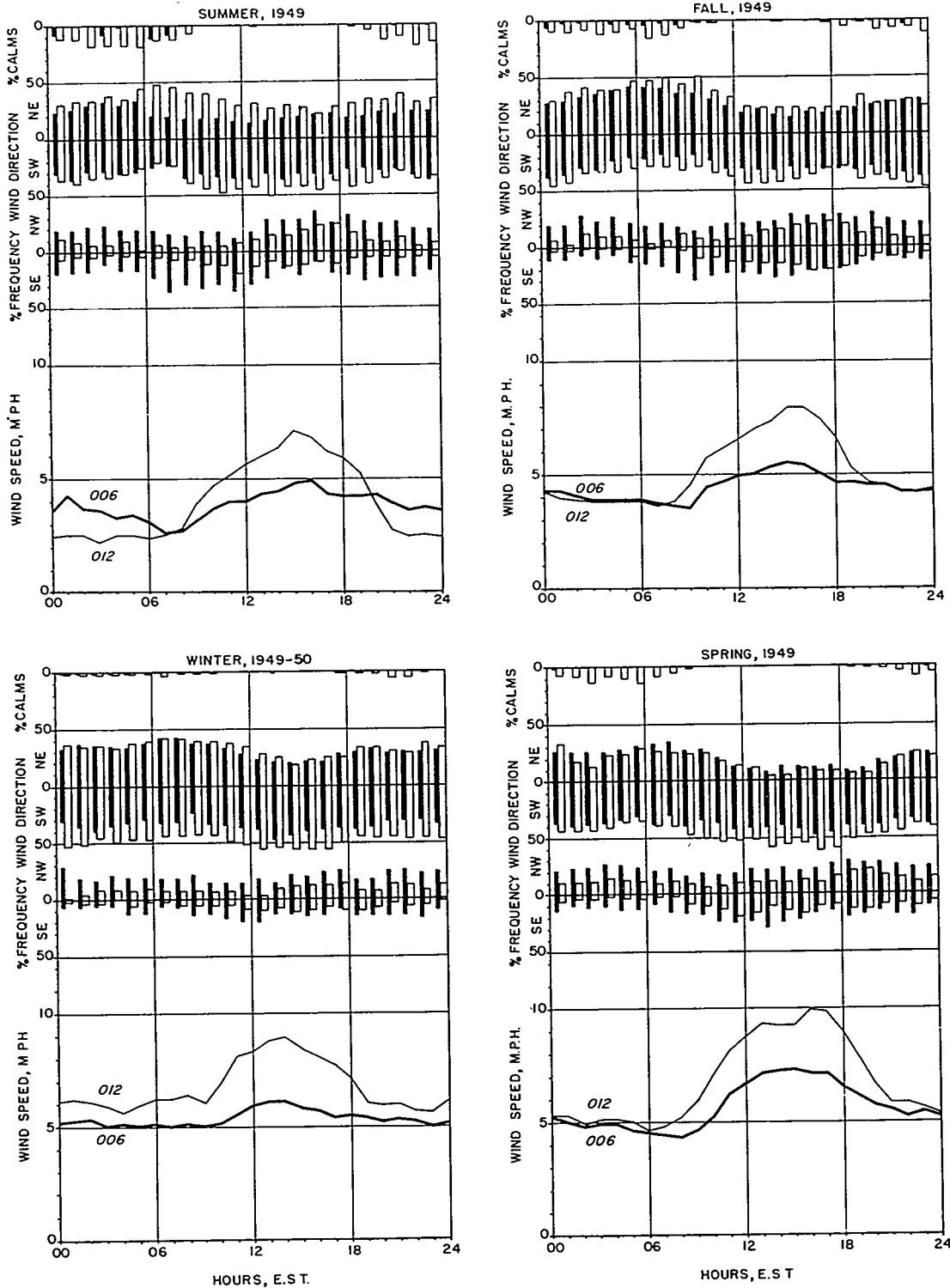


Fig. 134 Diurnal graphs of wind direction frequency and average speed by seasons, comparing a ridge top (006) and mid-valley near ridge top level (012).

DIURNAL VARIATION OF WIND DIRECTION AND SPEED
BETHEL CHURCH (004), 820 FT. MSL —
X-10 HUTMENT (001), 810 FT. MSL □

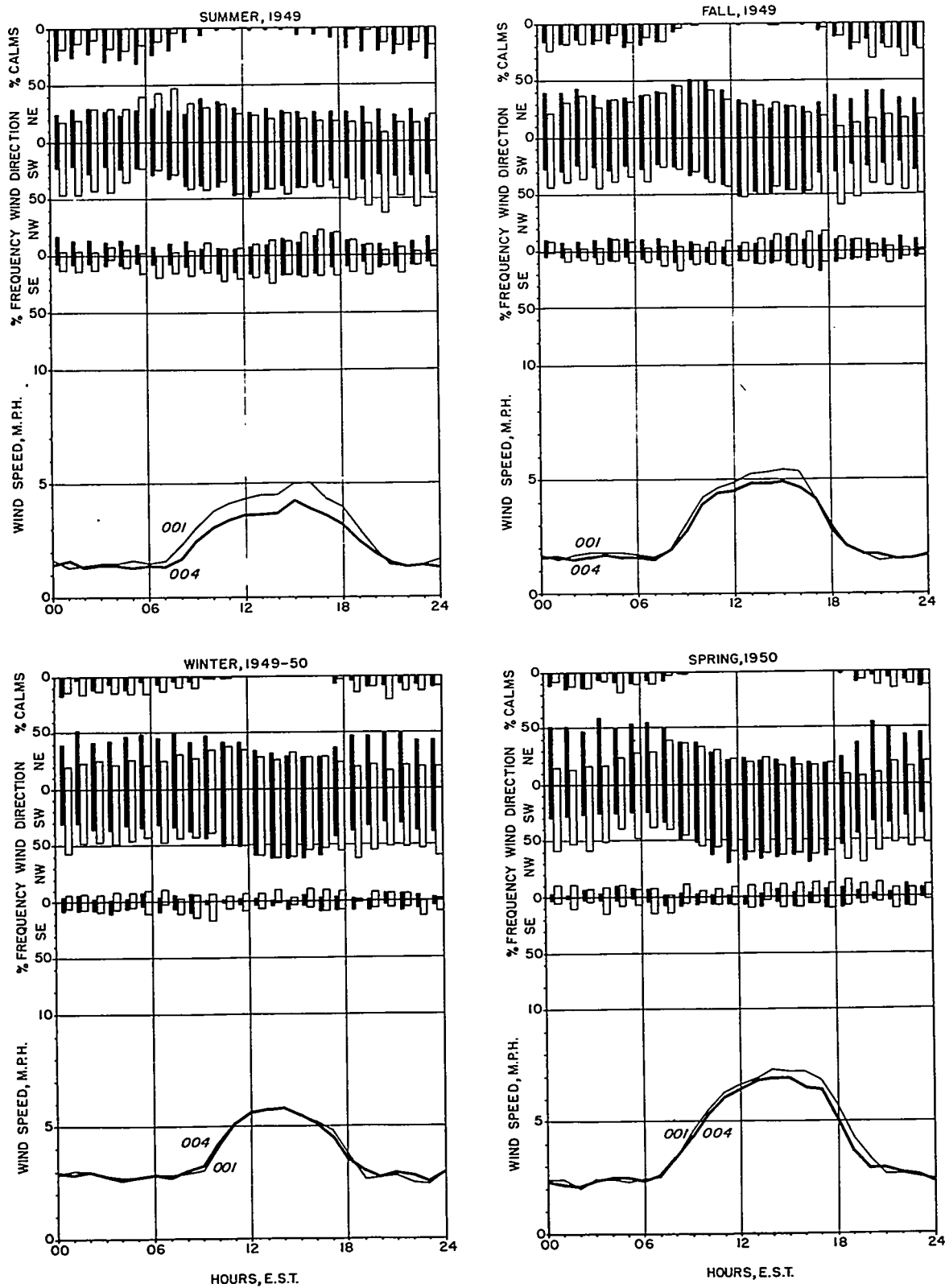


Fig. 135 Diurnal graphs of wind direction frequency and average speed by seasons, comparing southwestward-draining (004) and northeastward-draining (001) valley stations.

DIURNAL VARIATION OF WIND DIRECTION AND SPEED

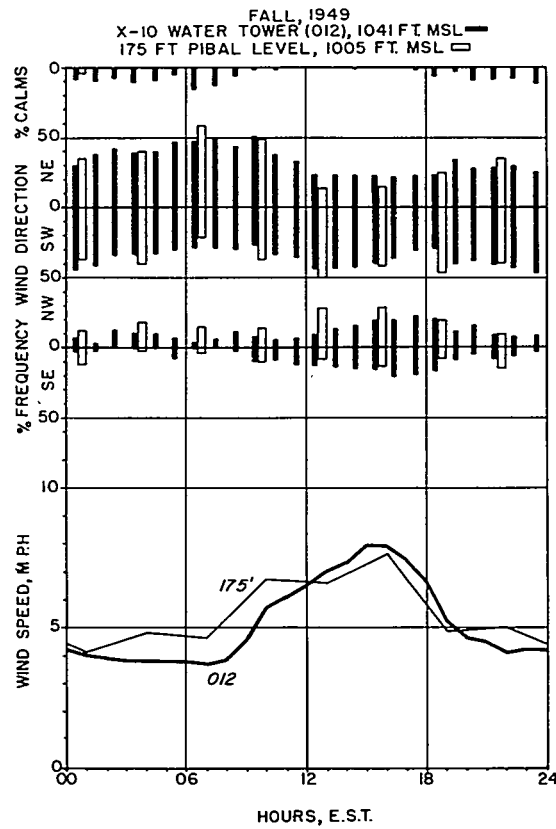
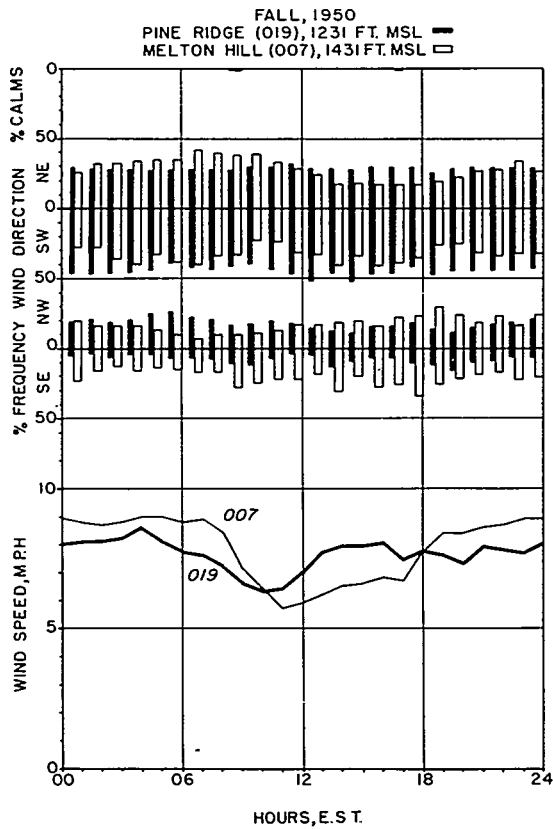
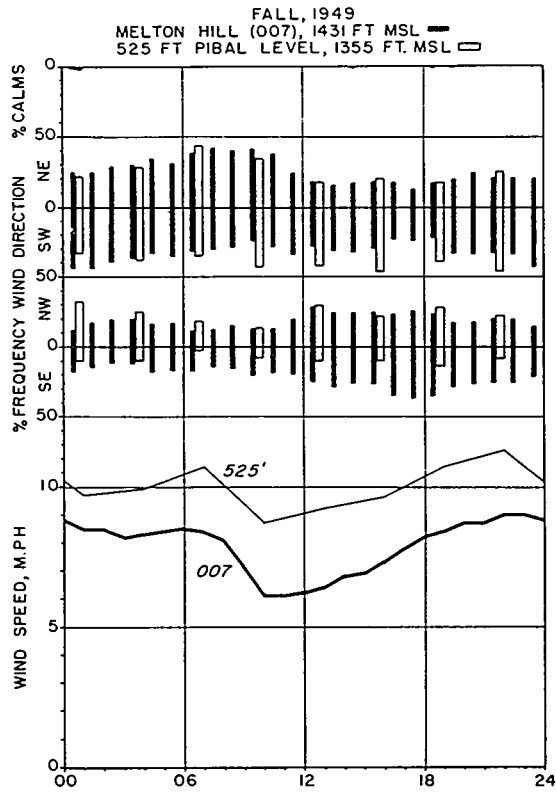
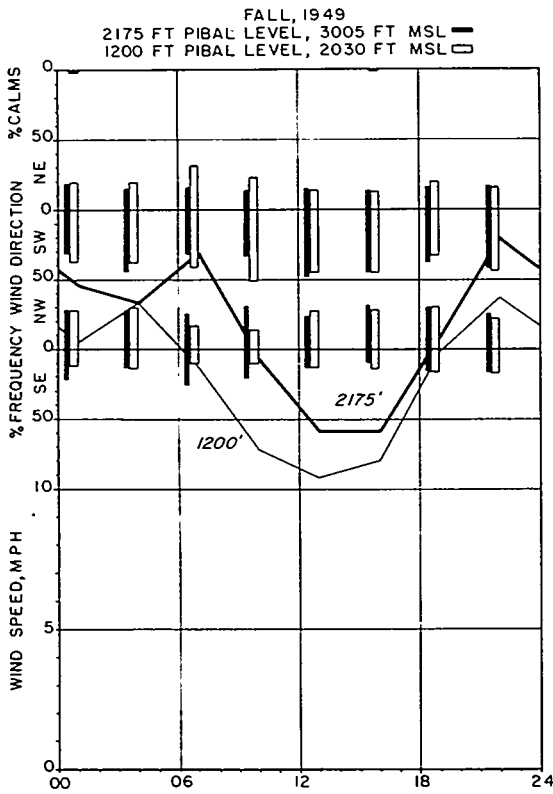


Fig. 136 Diurnal graphs of wind direction frequency and average speed, Fall, 1949, comparing different altitudes and exposures at and above ridge top level.

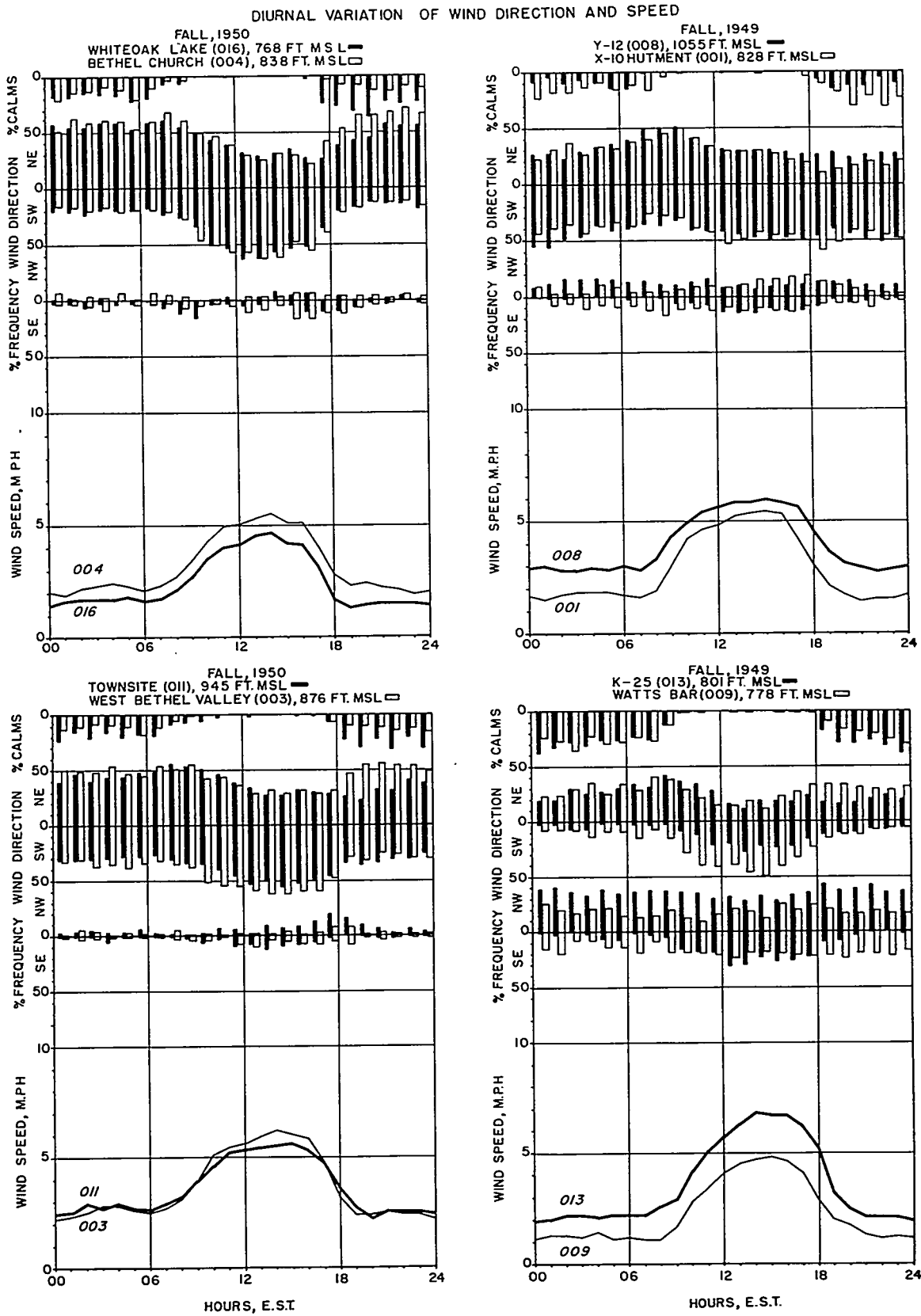


Fig. 137 Diurnal graphs of wind direction frequency and average speed, comparing parallel-draining stations in different valleys.

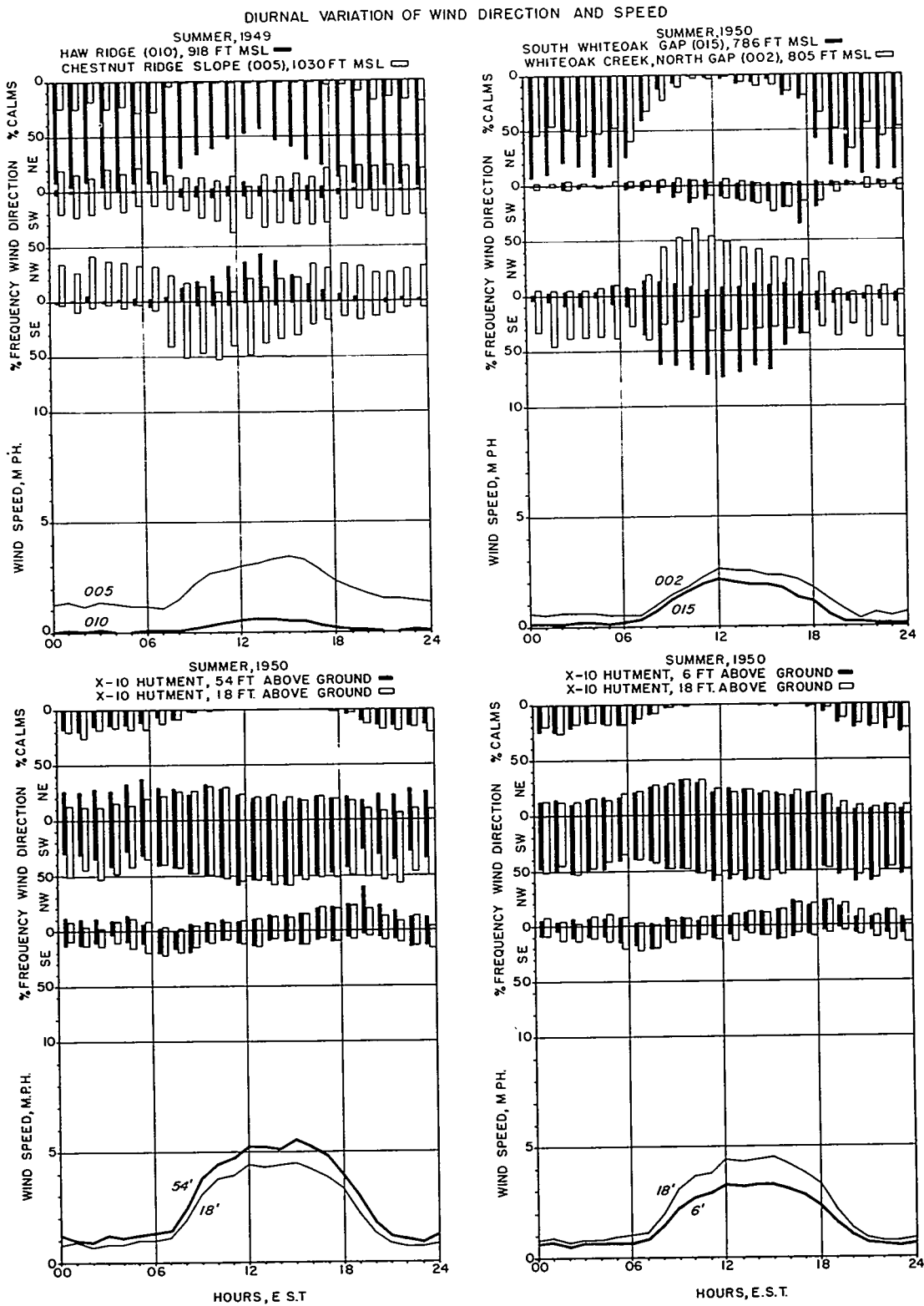
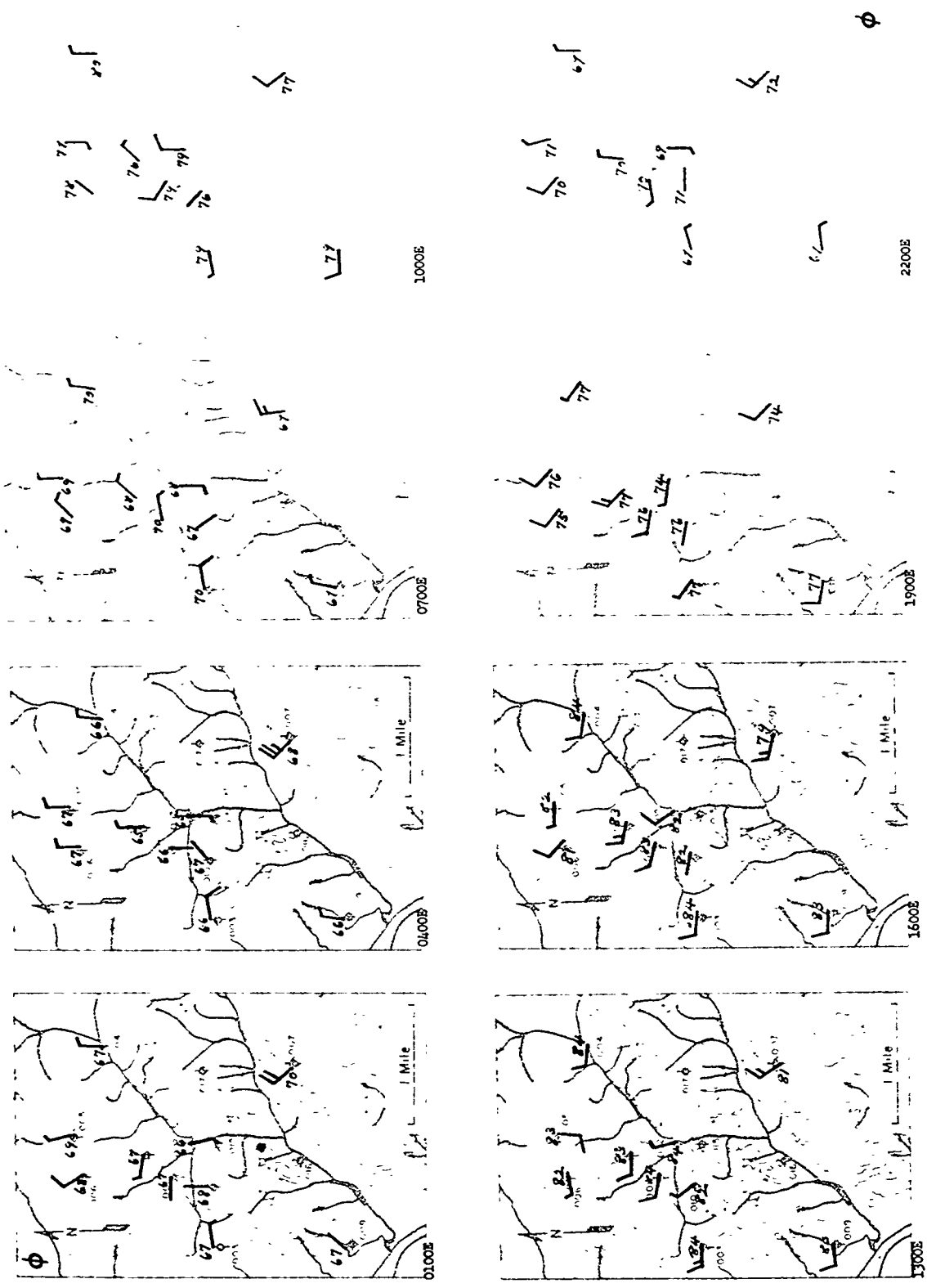


Fig. 138 Diurnal graphs of wind direction frequency and average speed, comparing opposite slope exposures and different altitudes near valley bottom.



Fig. 139 Photograph of smoke from
HC pot near station 001
June 2, 1949, 6:45 a.m.,
looking SE and showing SW
wind in lowest 50 ft.,
NE wind above.

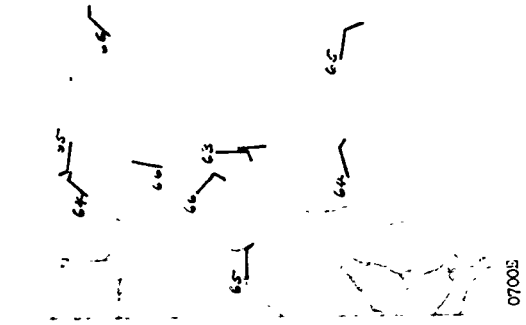
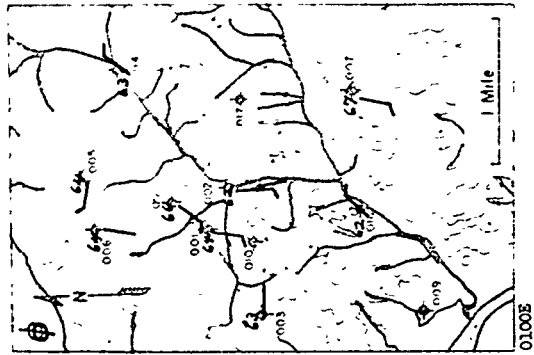
488



Jun, Jul, Aug, 1949

Fig. 140 Resultant surface wind maps for Bethel-Melton Valley area, by time of day, Summer 1949.

487



OAK RIDGE LOCAL DIURNAL RESULTANT WIND HODOGRAPHS

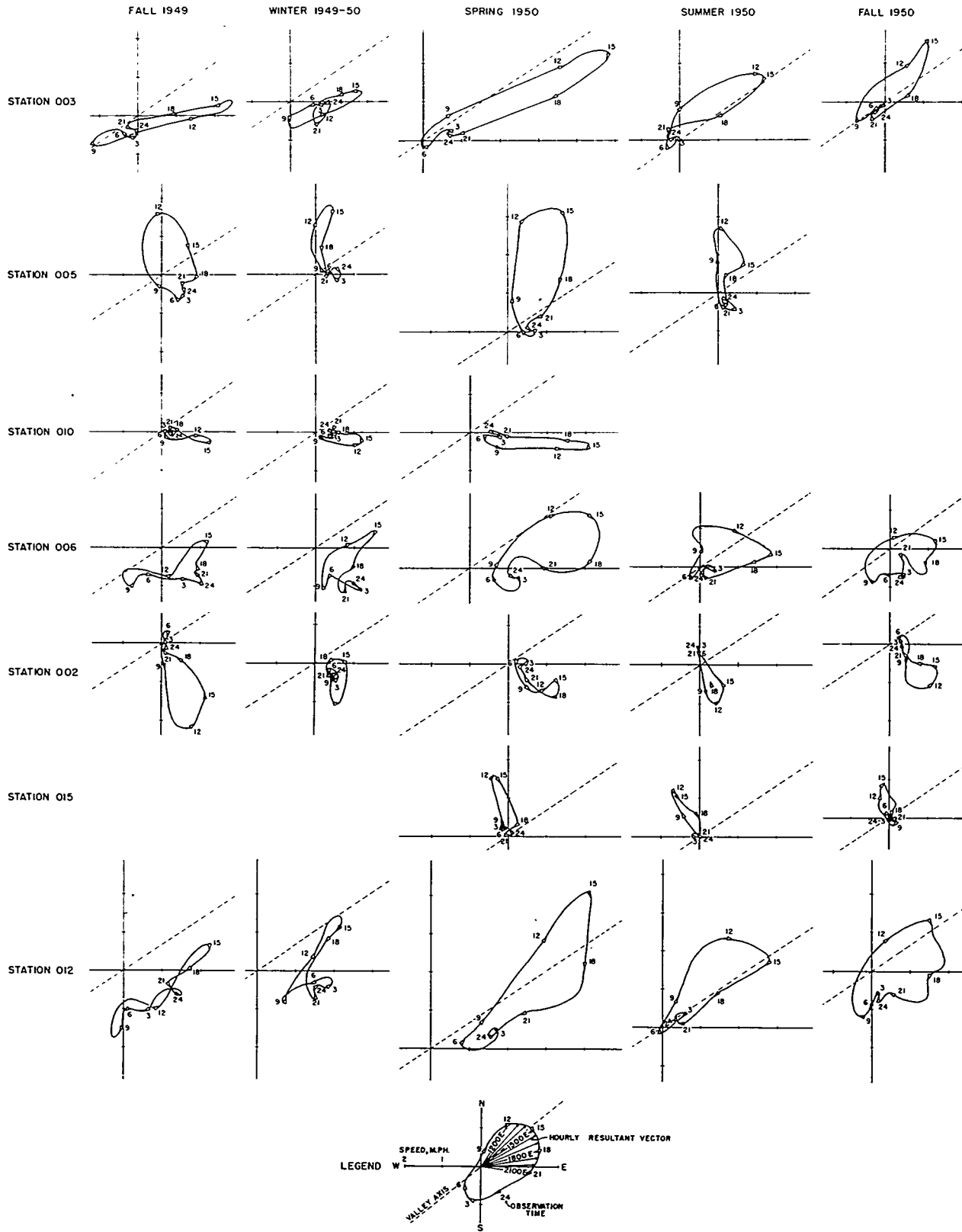
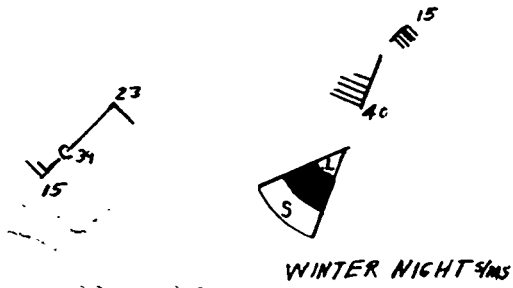
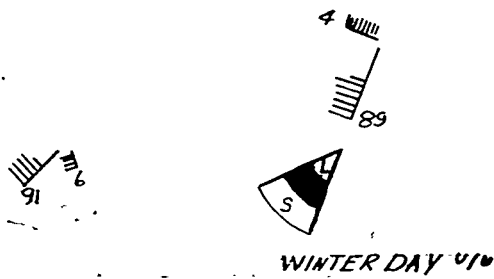
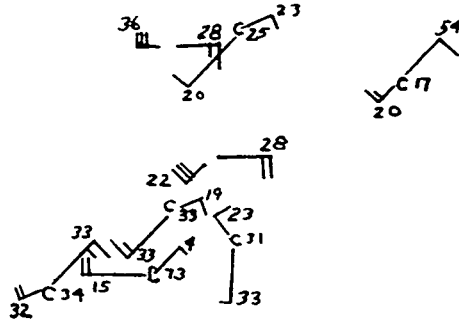
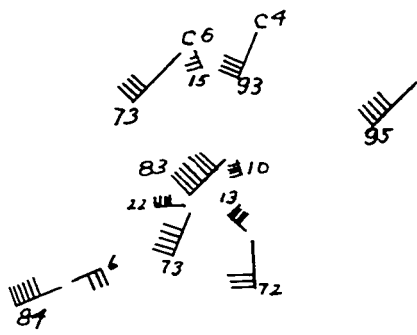


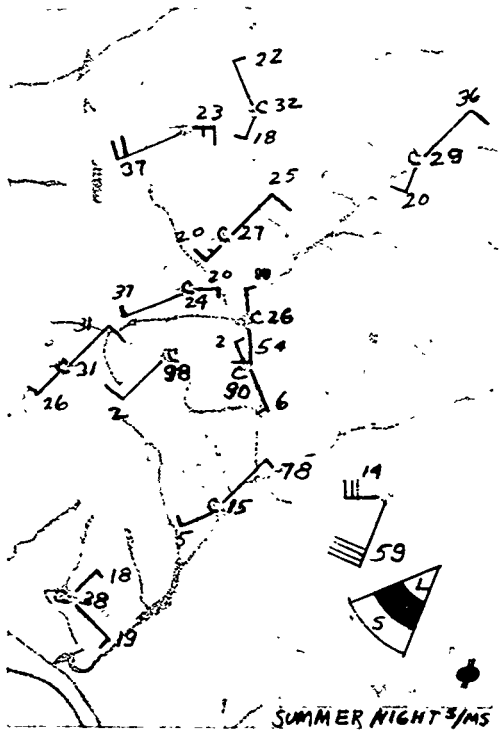
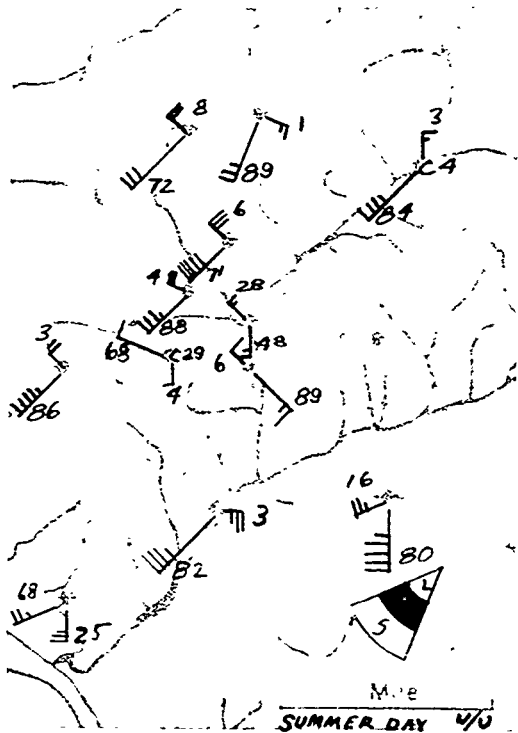
Fig. 142 Diurnal resultant wind hodographs for Oak Ridge micronet stations, by seasons.

φ



WINTER DAY 4/10

WINTER NIGHT 3/MS



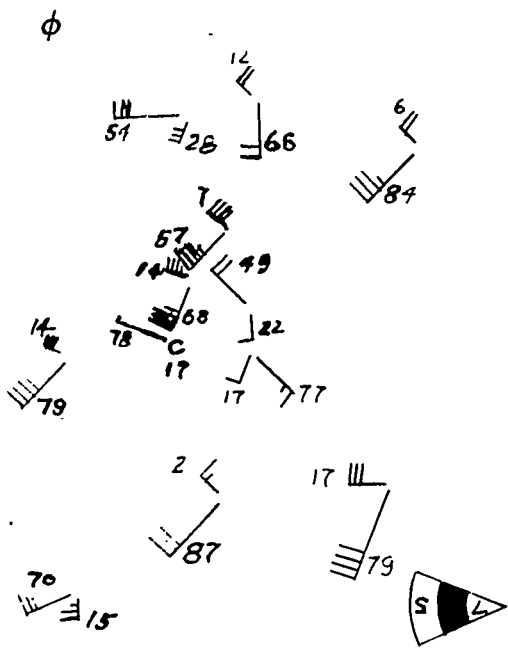
SUMMER DAY 4/0

SUMMER NIGHT 3/MS

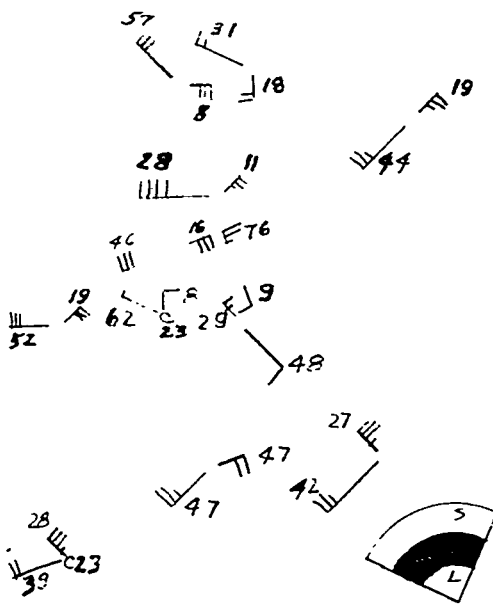
ERRATUM

Page 492

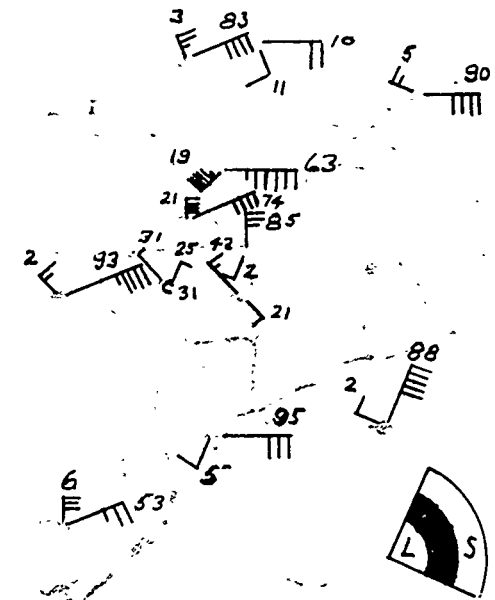
The figure legend has been omitted and should read; Fig. 144—Local wind flow pattern as a function of large-scale variables: Maps 1-4, showing effects of time of day and season.



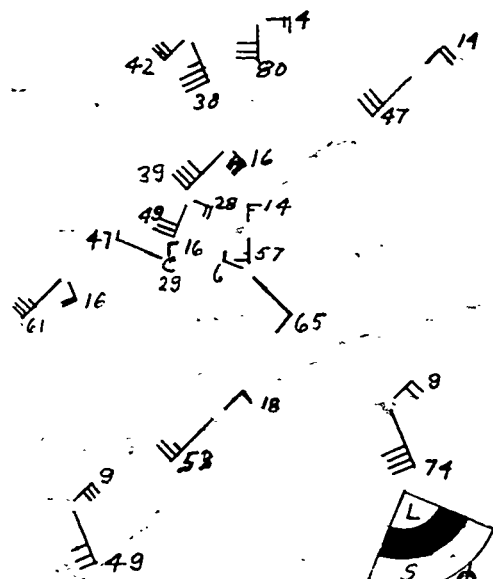
SUMMER DAY 4/0



SUMMER DAY 4/0



SUMMER DAY 4/0



SUMMER DAY 4/0

Fig. 145 Local wind flow pattern as a function of large-scale variables: Maps 5-8, showing effects of large-scale wind direction in midday conditions.

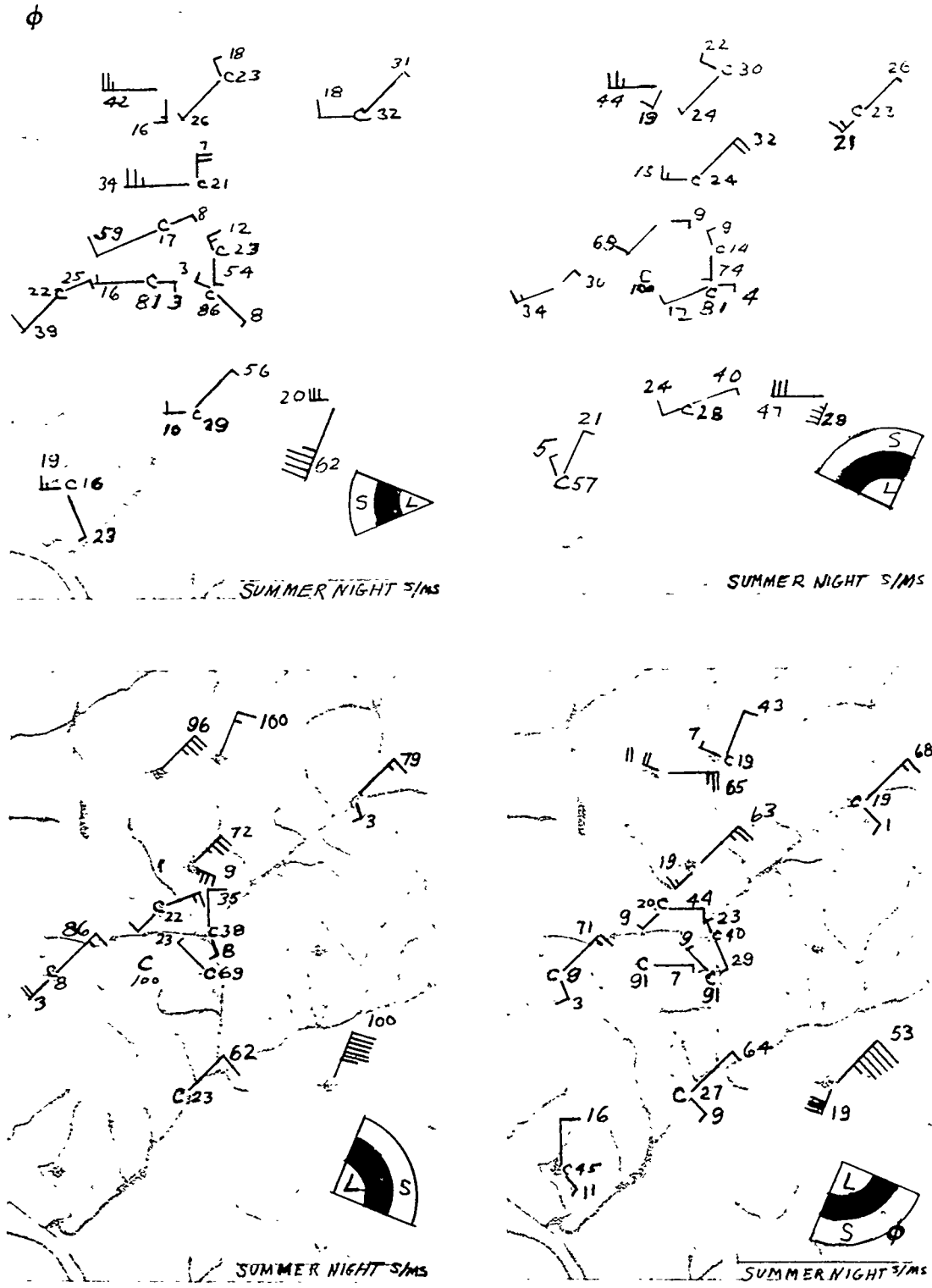


Fig. 146 Local wind pattern as a function of large-scale variables: Maps 9-12, showing effects of large-scale wind direction in nighttime conditions.

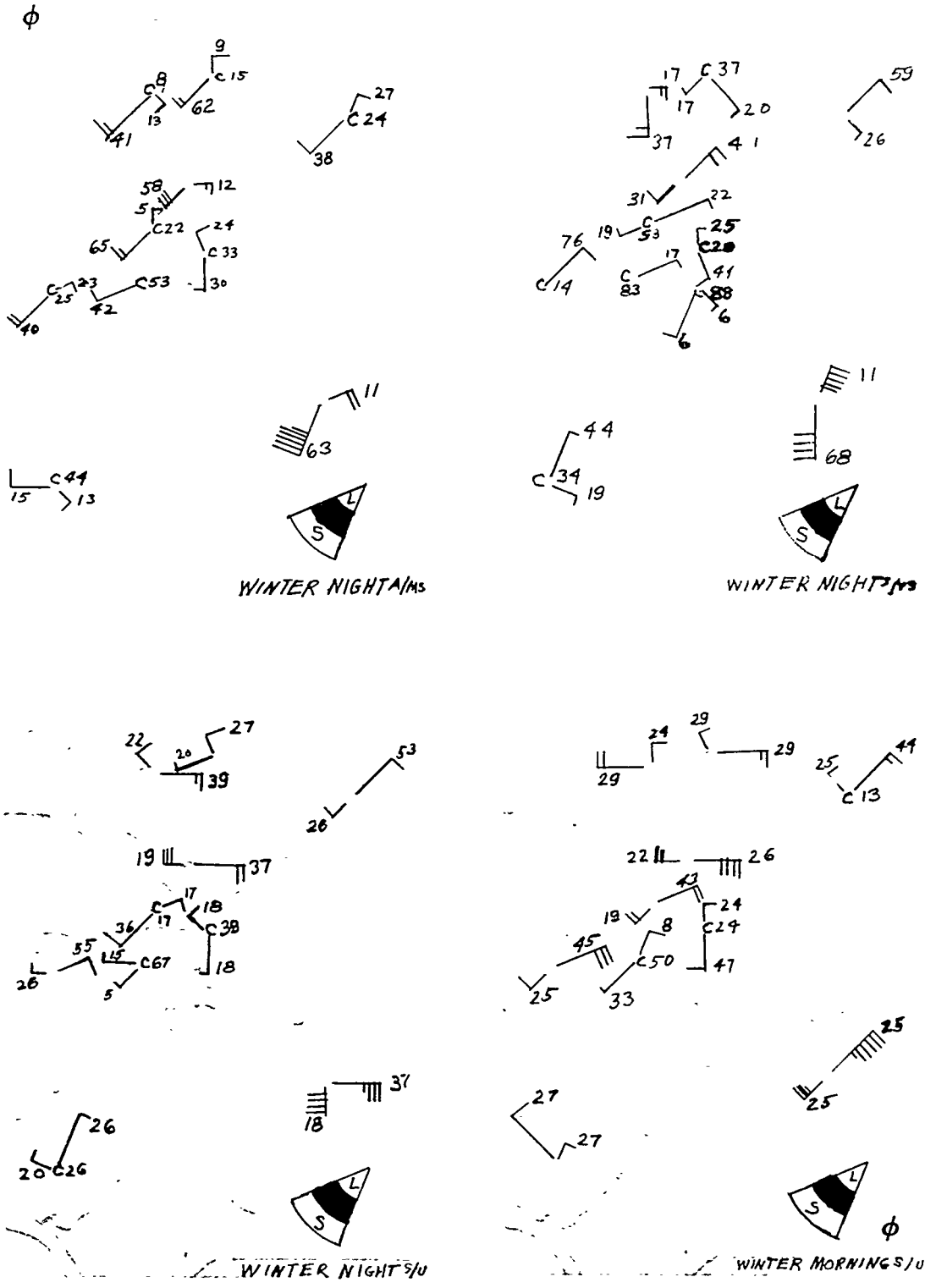


Fig. 148 Local wind flow pattern as a function of large-scale variables: Maps 17-20, showing effects of stability variations.

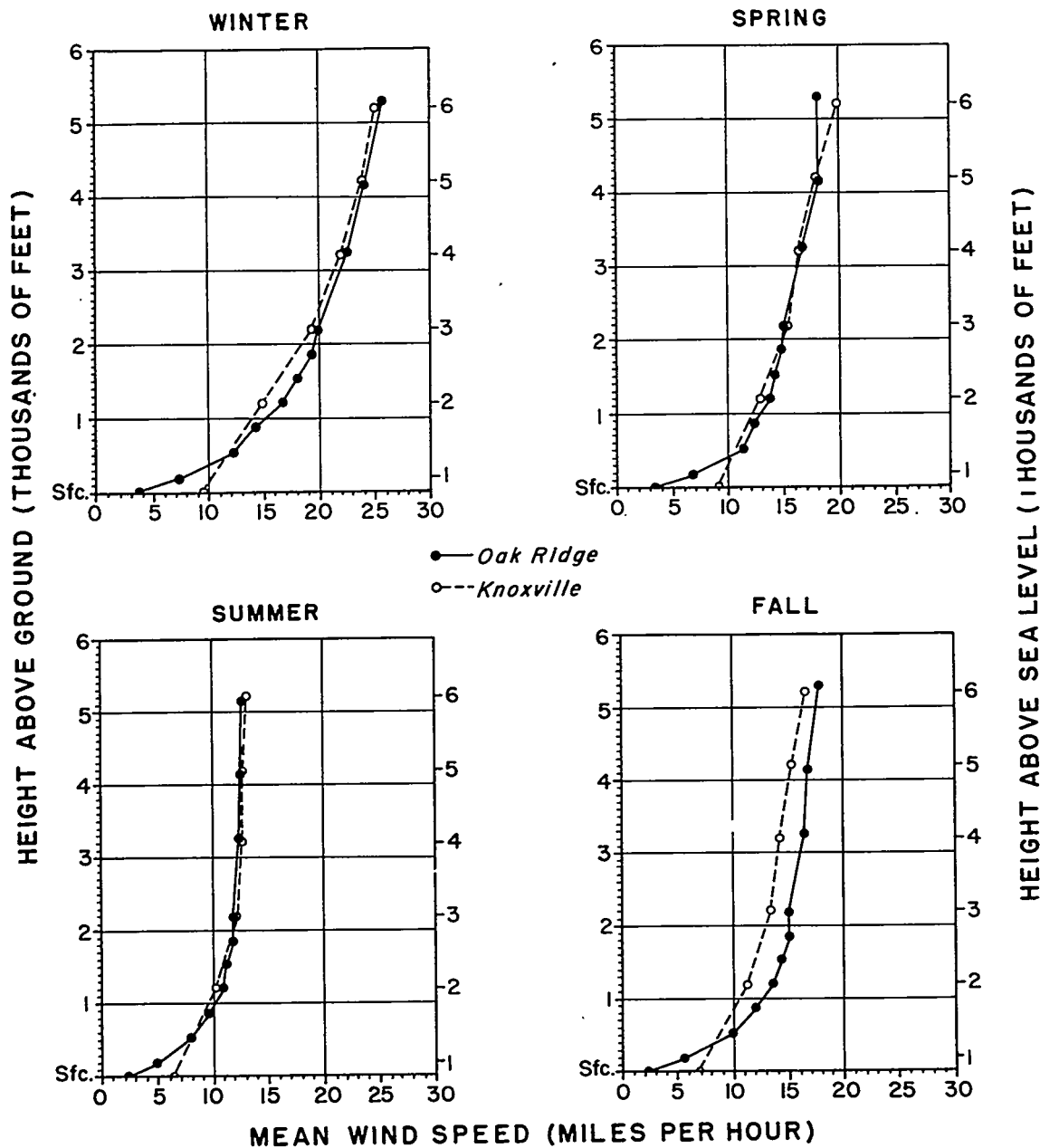


Fig. 149 Vertical profiles of mean wind speed in the lowest 5300 ft., Oak Ridge and Knoxville, by seasons.

WIND SPEED PROFILE

• Anemometer
 ○ Pibal

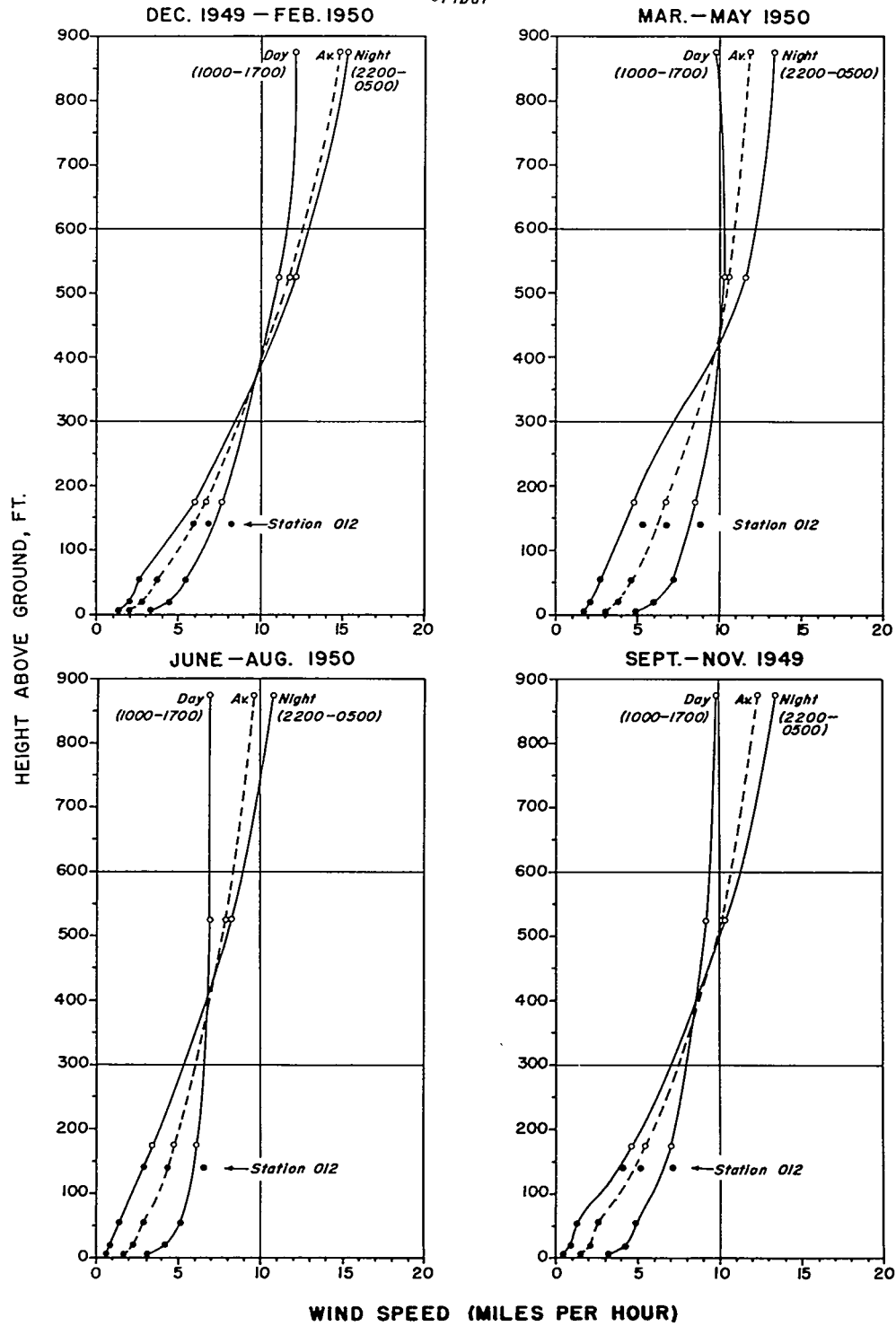


Fig. 150 Vertical profiles of mean wind speed in the lowest 850 ft. at Oak Ridge, day, night, and average by seasons.

ANNUAL

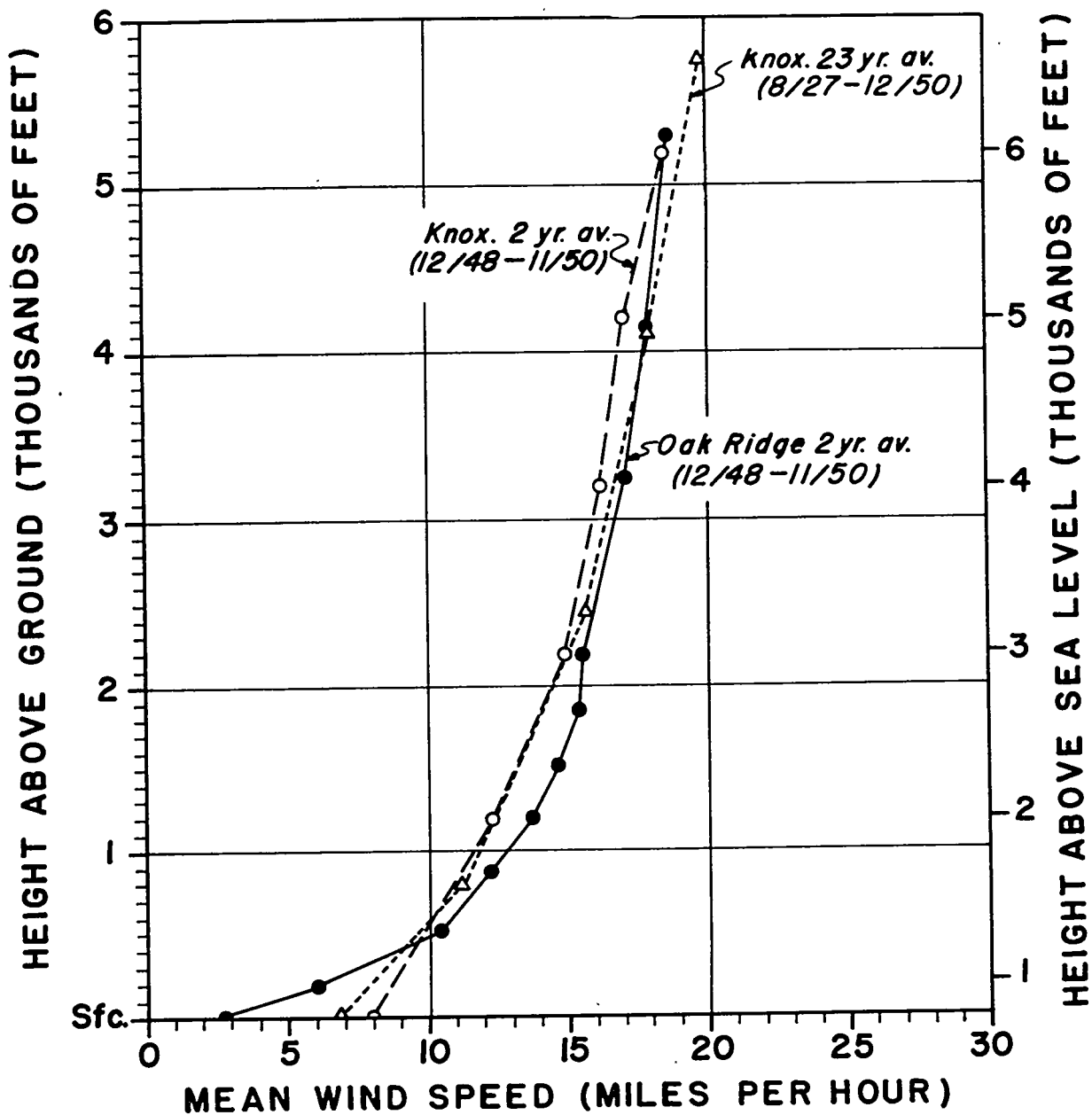


Fig. 151a Vertical profiles and diurnal curves of annual mean wind speed, profiles up to 5300 ft.

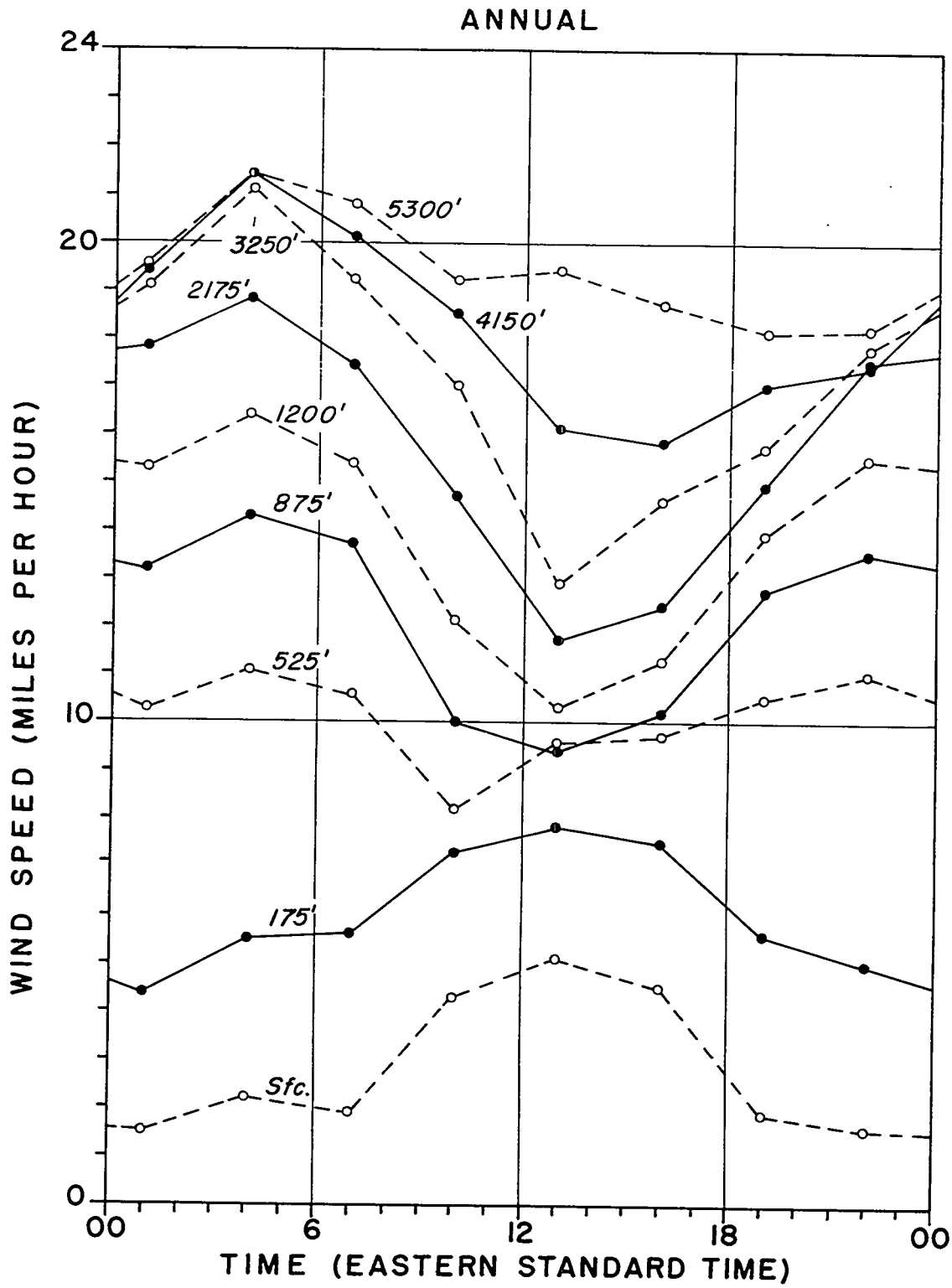


Fig. 151b Vertical profiles and diurnal curves of annual mean wind speed, diurnal curves up to 5300 ft. (pibal'd).

WIND SPEED PROFILE ANNUAL (9/49-8/50)

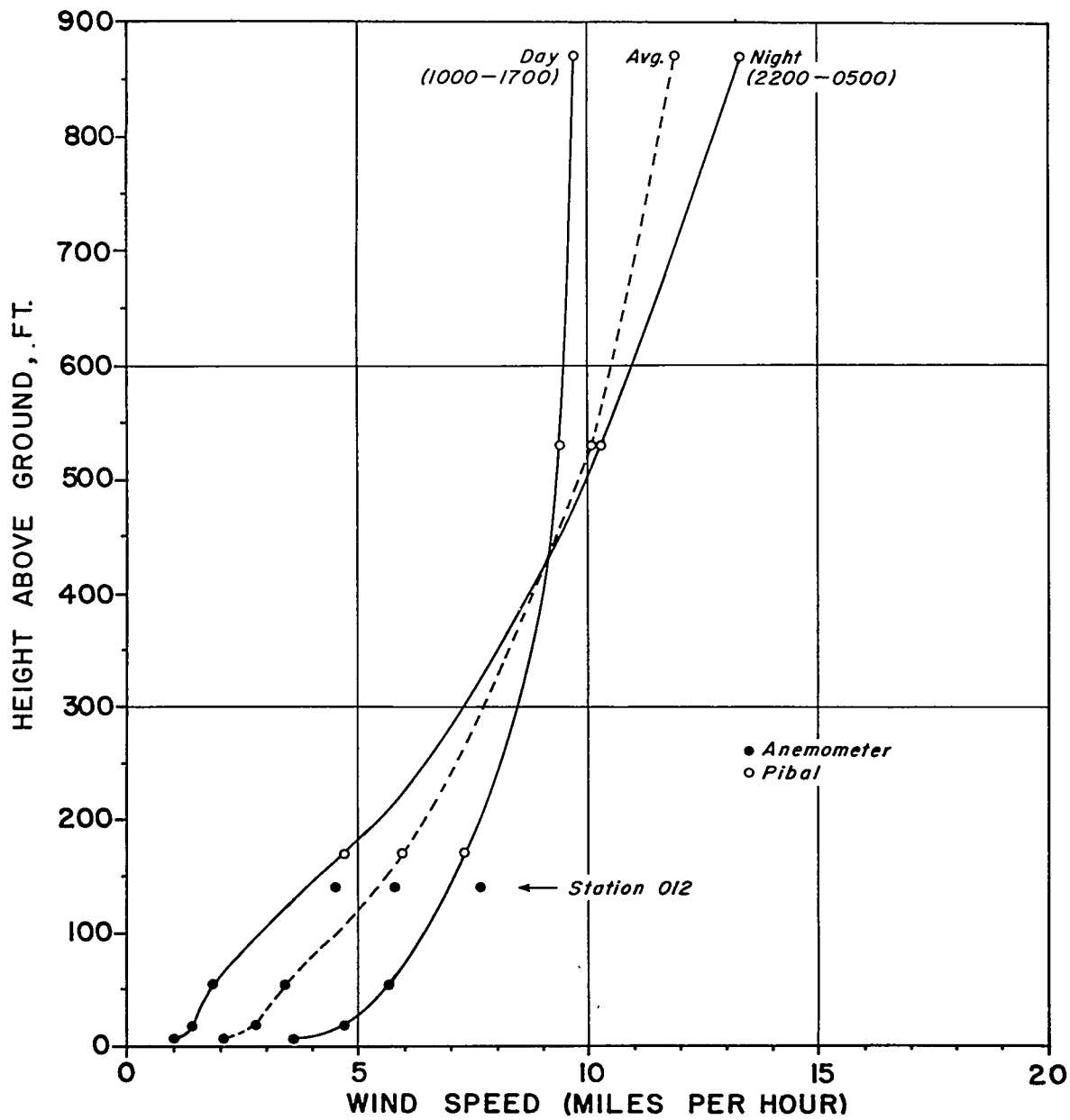


Fig. 151c Vertical profiles and diurnal curves of annual mean wind speed, more detailed profiles up to 850 ft.

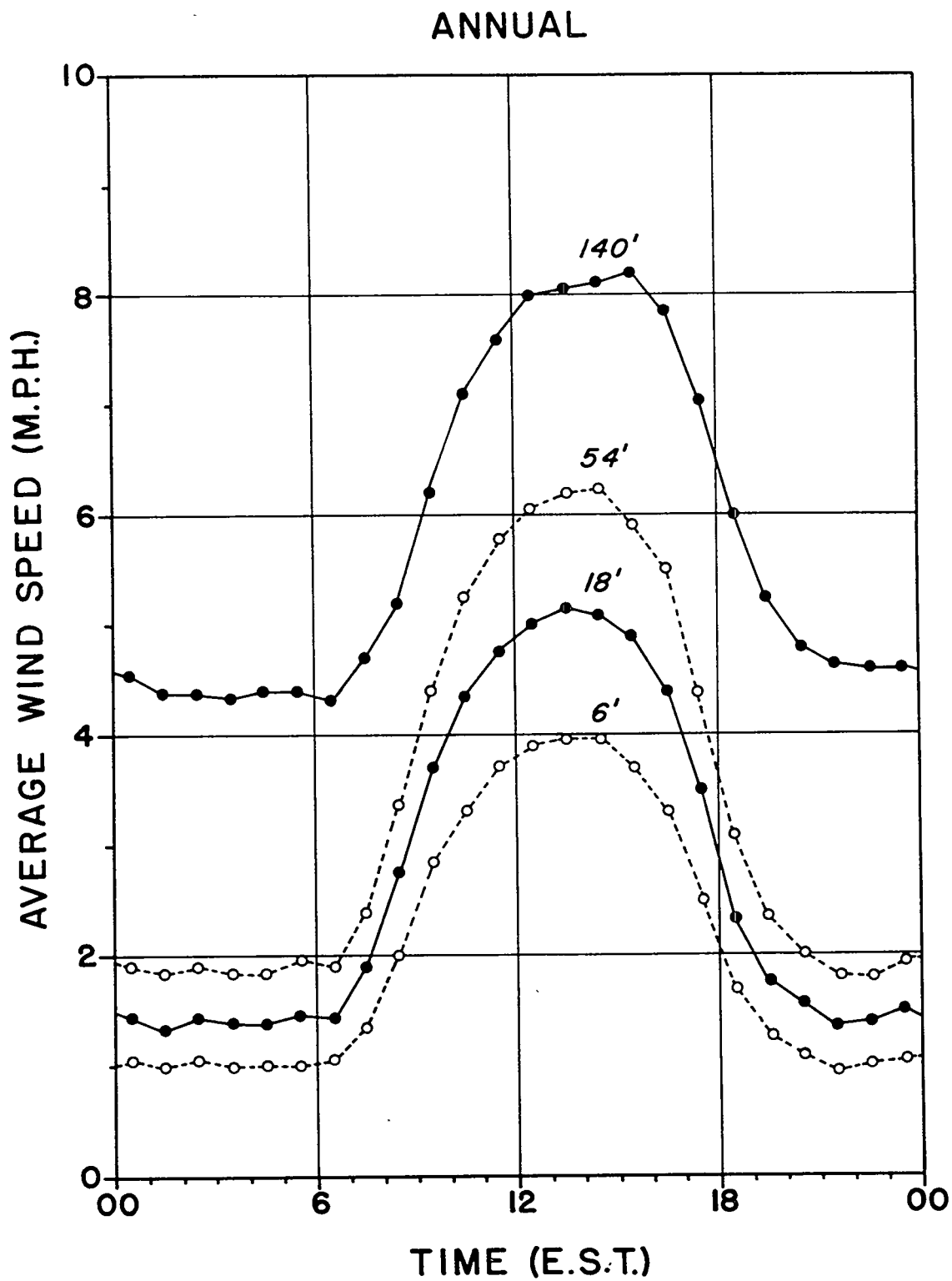


Fig. 151c Vertical profiles and diurnal curves of annual mean wind speed, diurnal curves up to 140 ft. (anemometer).

503

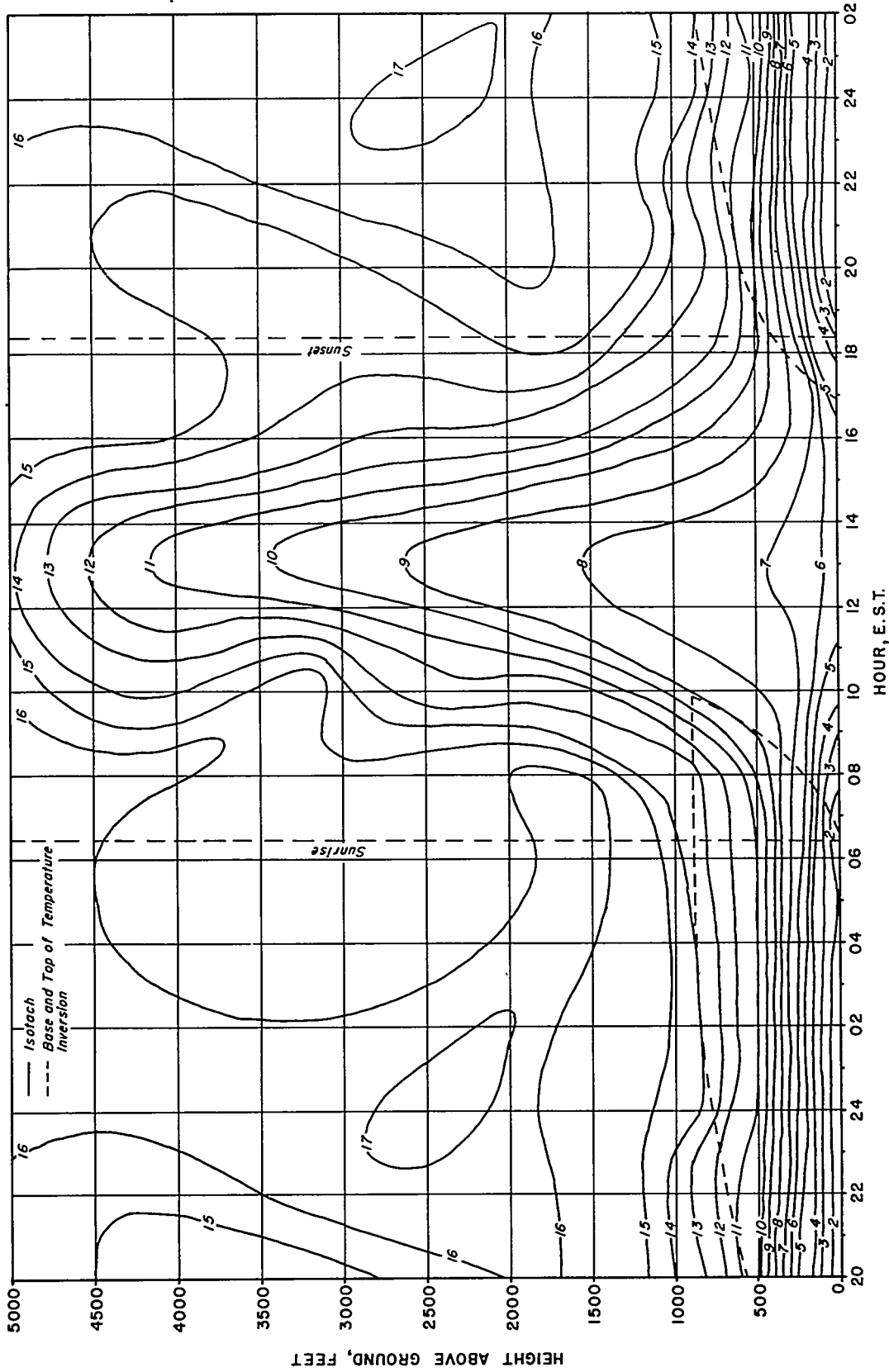


Fig. 152 Average wind speed time cross-section, M.P.H. Sept. - Oct., 1950

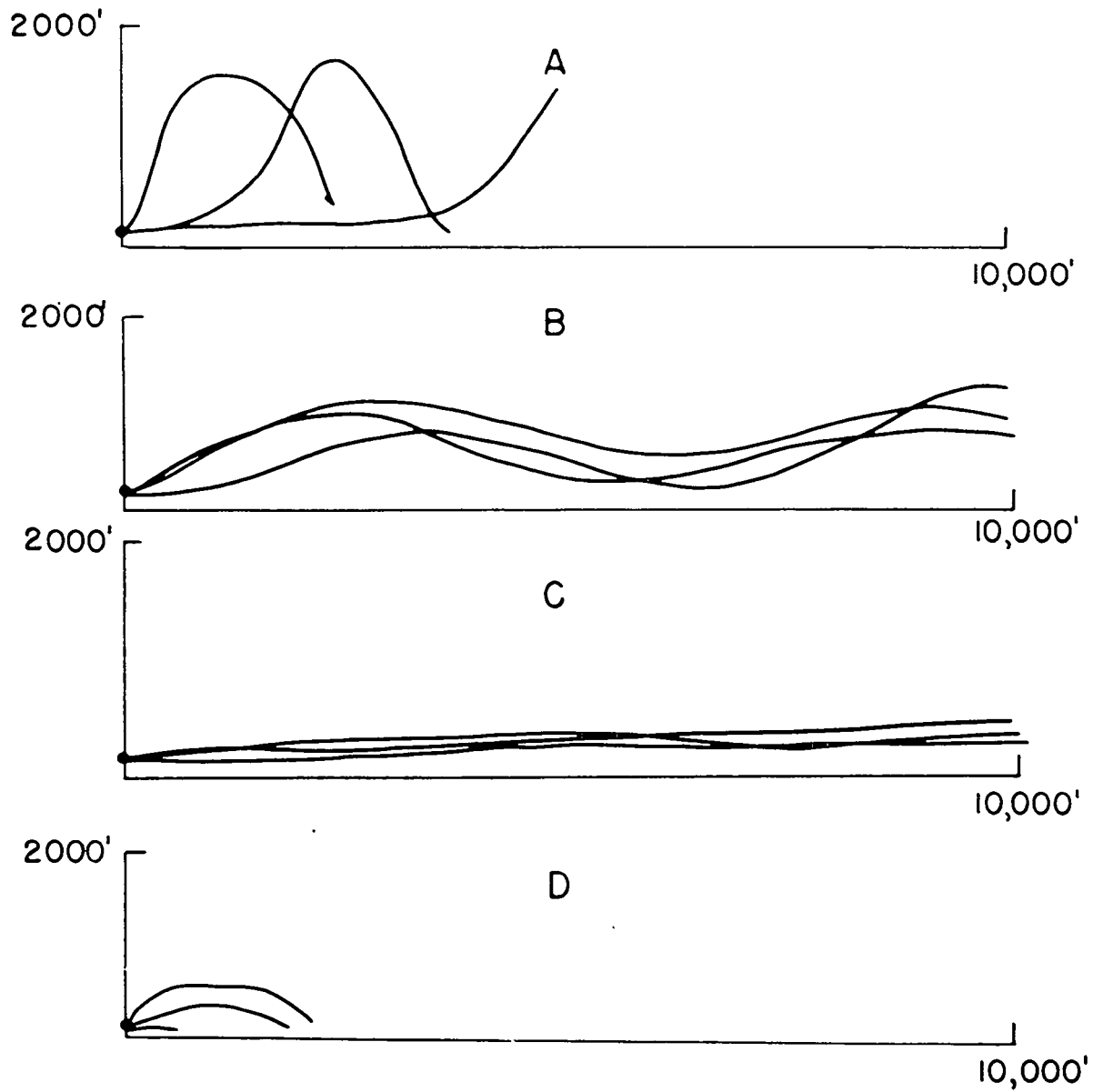


Fig. 153 Schematic X-Z plots of the four types of neutral balloon trajectories.

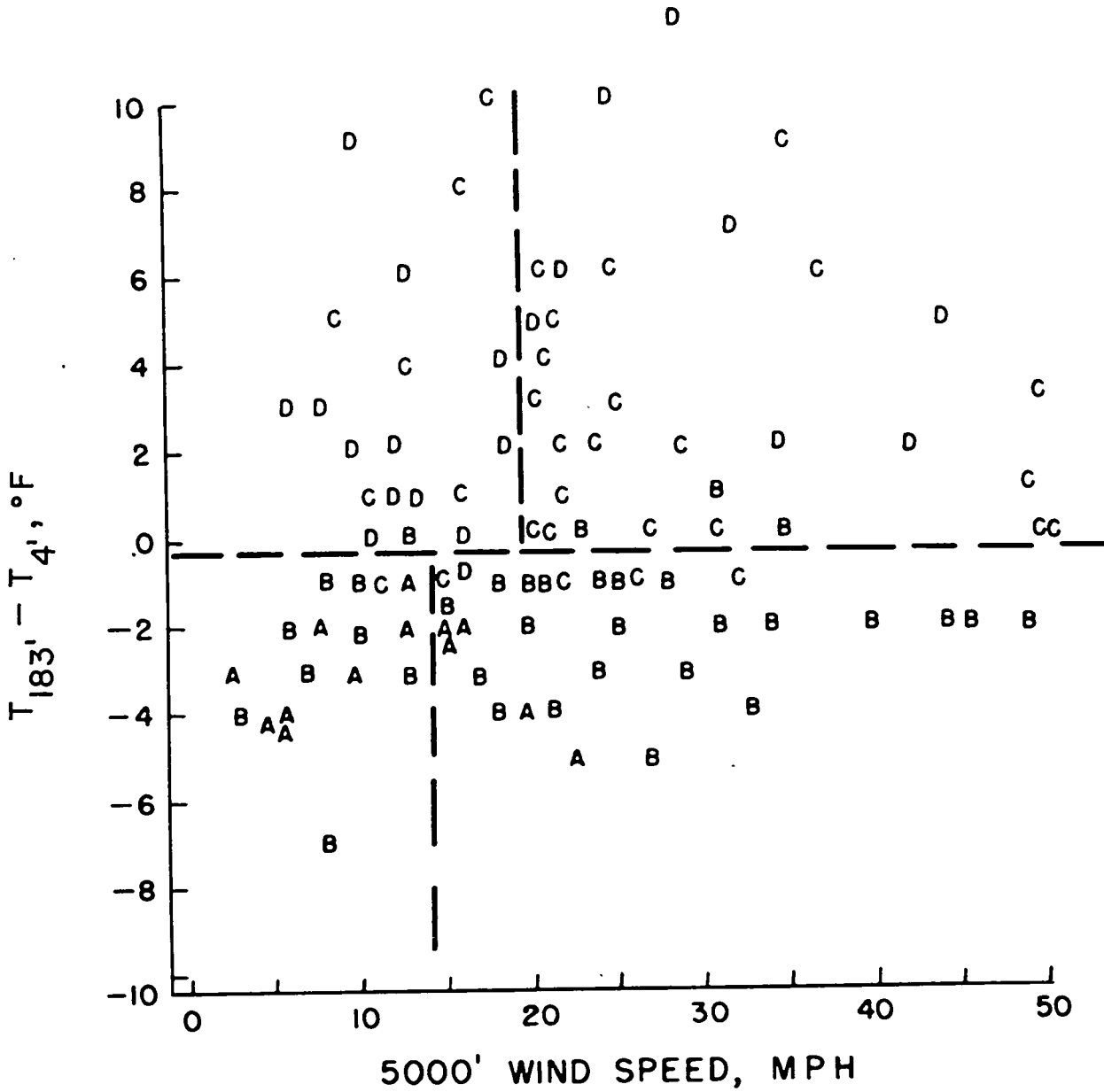


Fig. 154 Scatter-diagram of neutral balloon trajectory type as a function of 5000 ft. wind speed and 180 ft. stability.

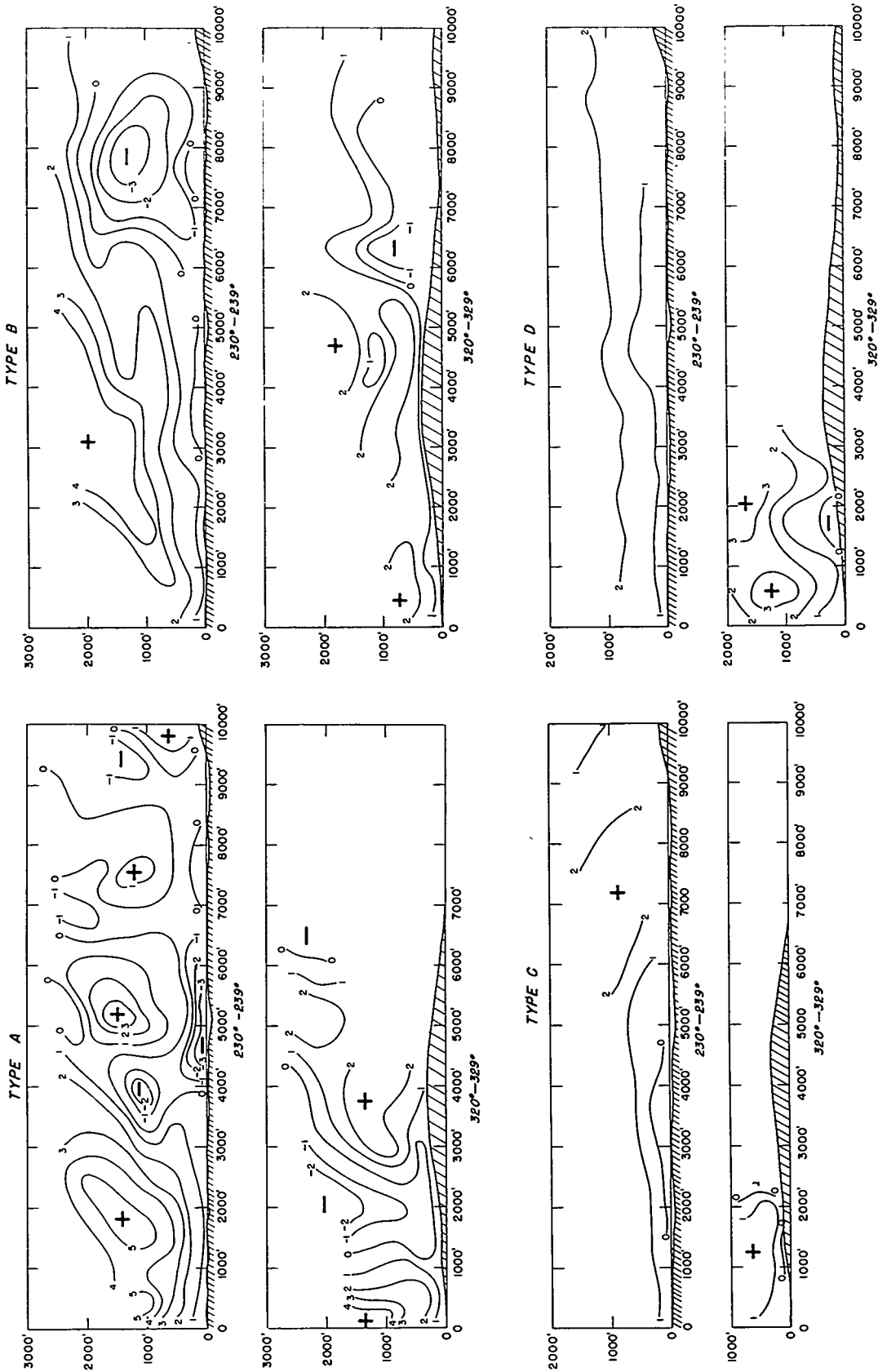


Fig. 155 Average vertical velocity of neutral balloons in two narrow azimuth sectors, as a function of distance and height, by turbulence type.

506

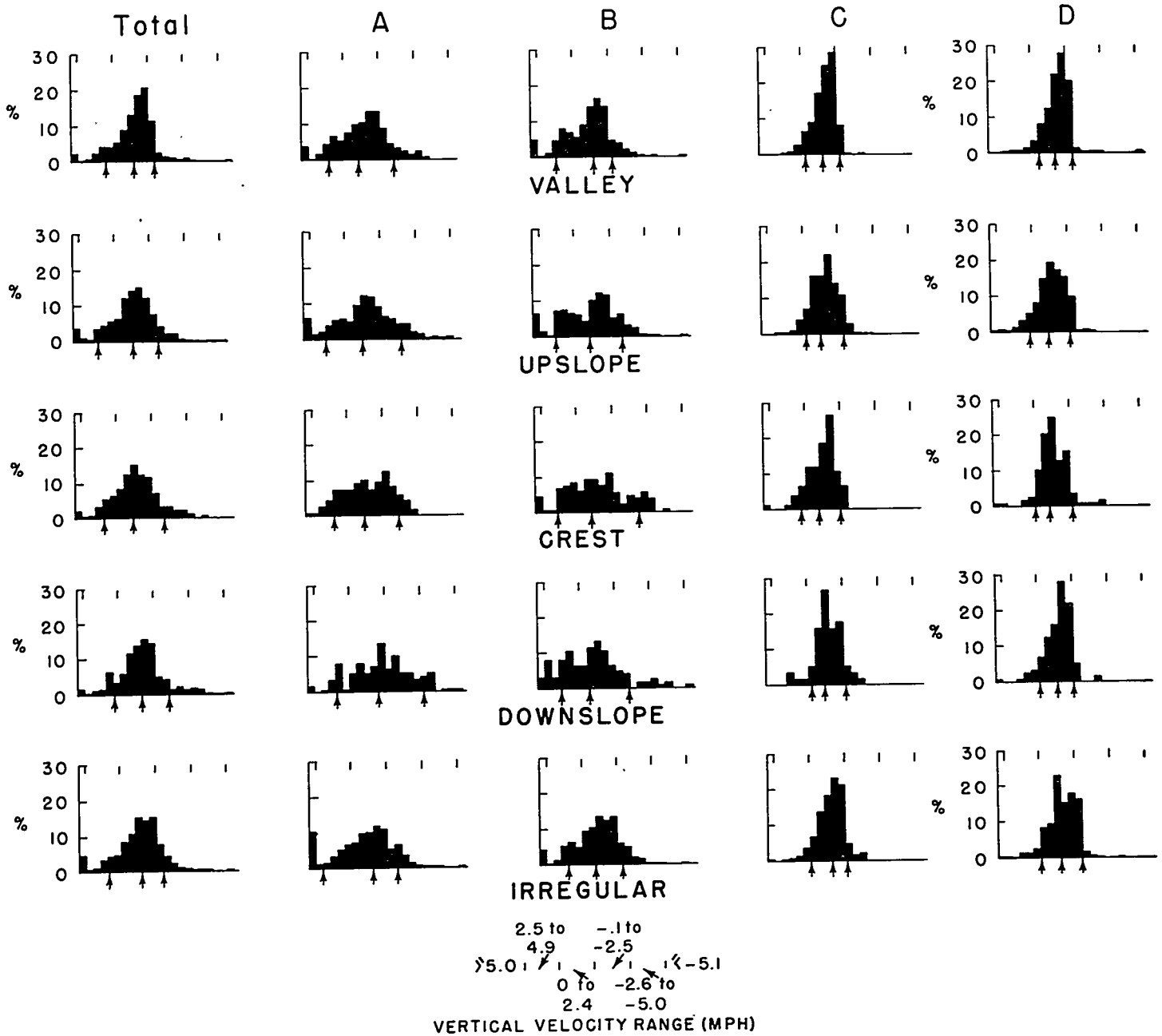


Fig. 156 Frequency distributions of vertical velocity of neutral balloons, azimuth 230 - 249°, by turbulence type and aspect of underlying terrain.

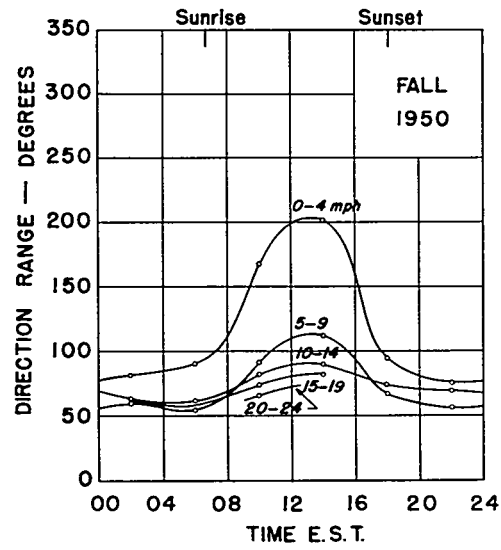
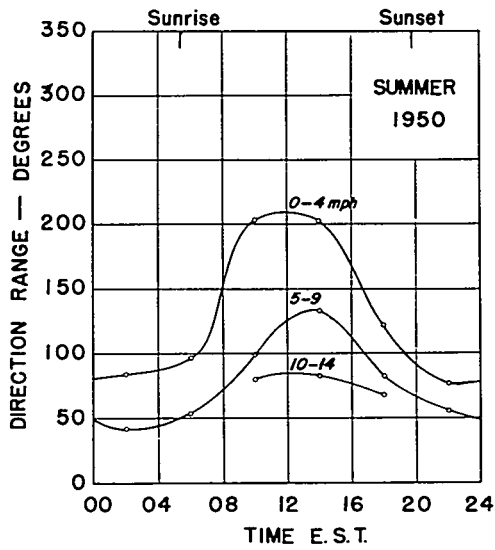
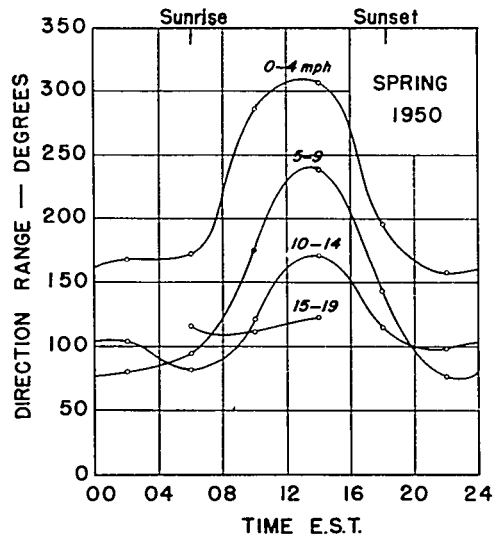
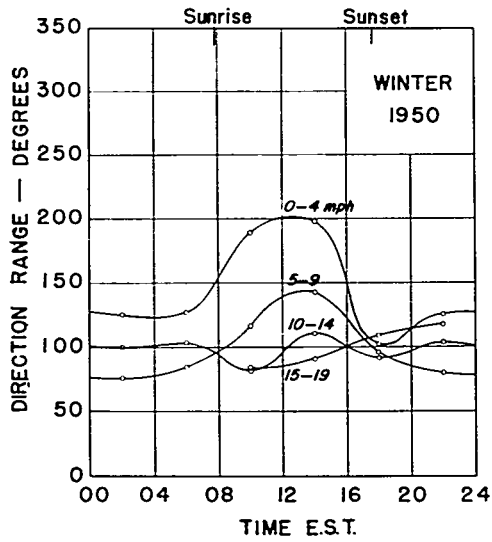


Fig. 157 Diurnal curves of average 15-min. wind direction range, 154 ft. (station O12), by wind speed and season.

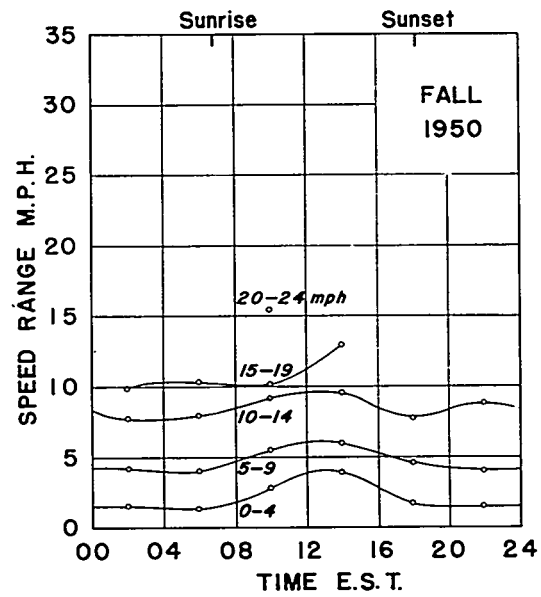
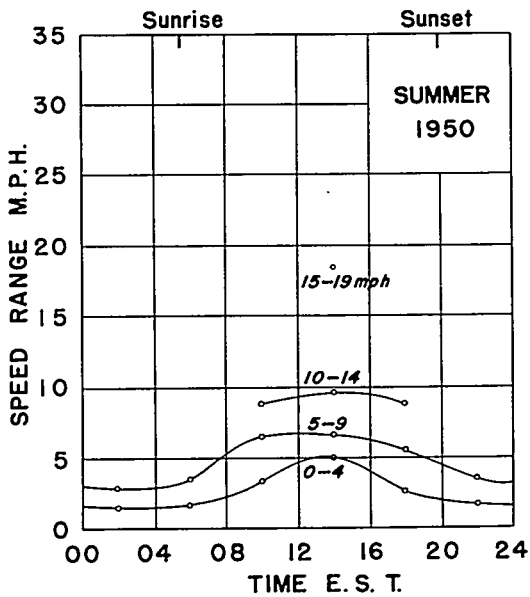
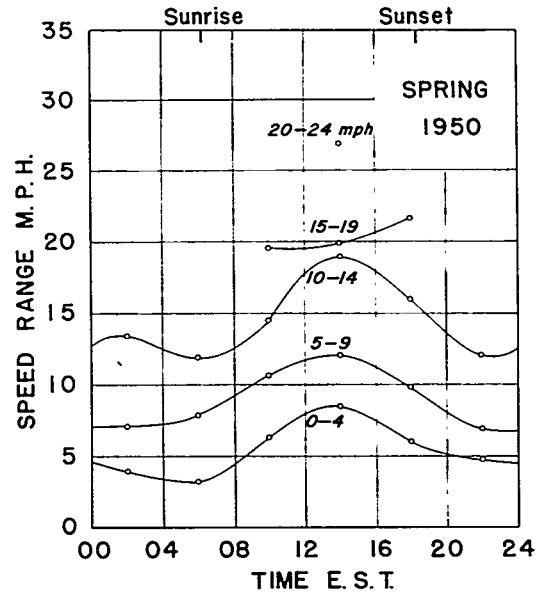
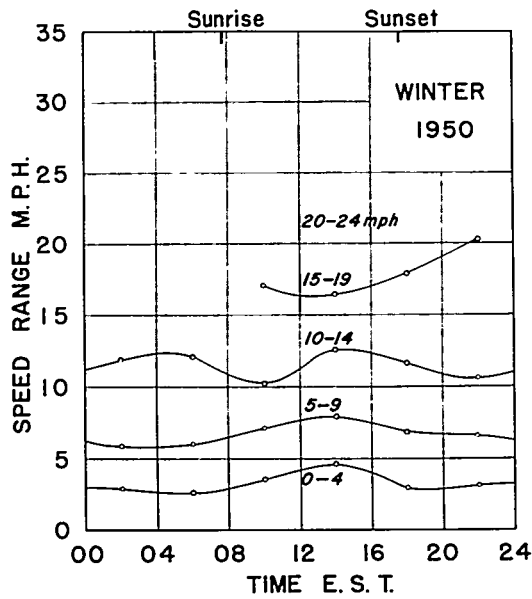


Fig. 158 Diurnal curves of average 15-min. wind speed range, 154 ft. (station 012), by wind speed and season.

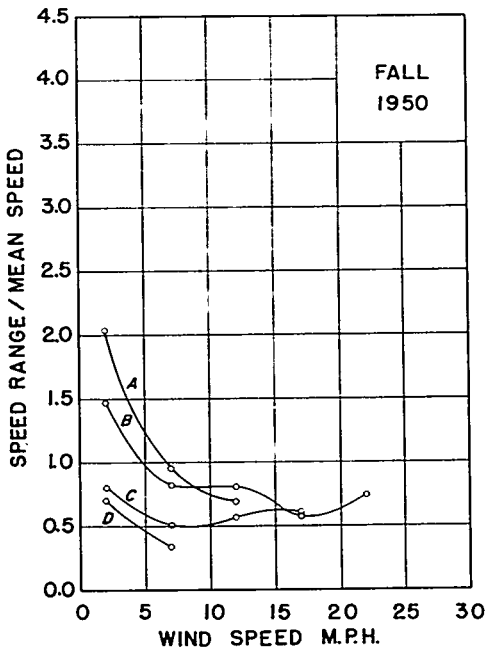
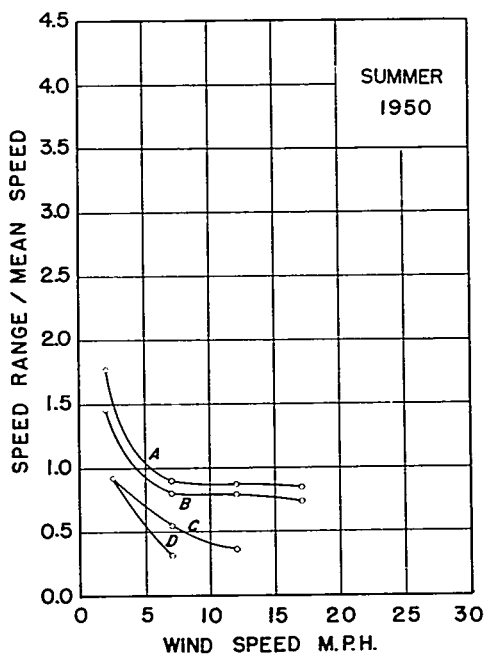
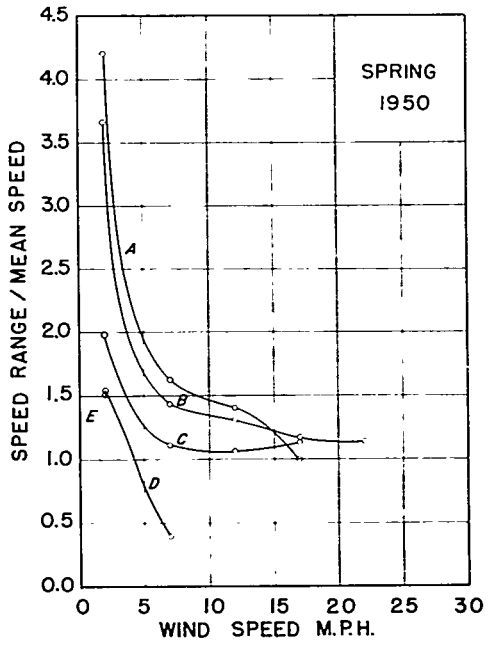
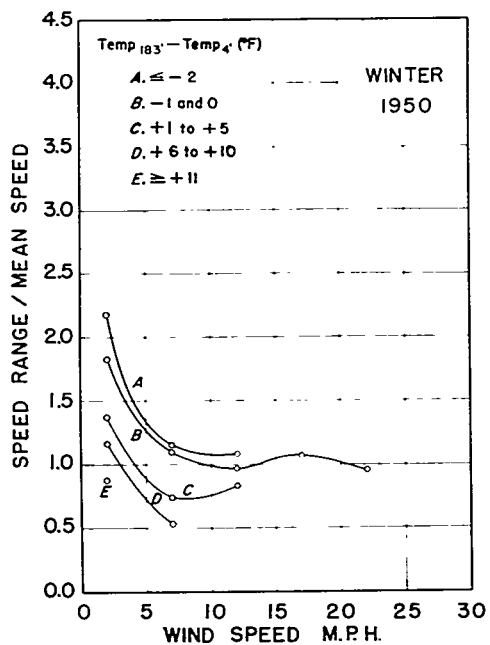


Fig. 159 Ratio of 15-min. speed range to hourly mean speed as a function of hourly mean speed, 15 1/4 ft. (station 012), by stability and season.

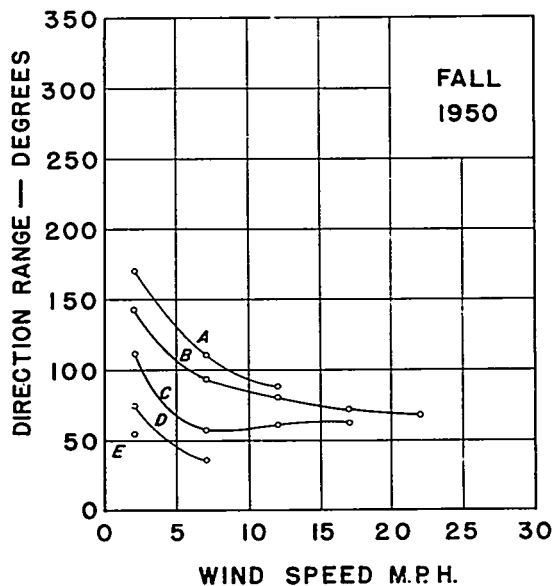
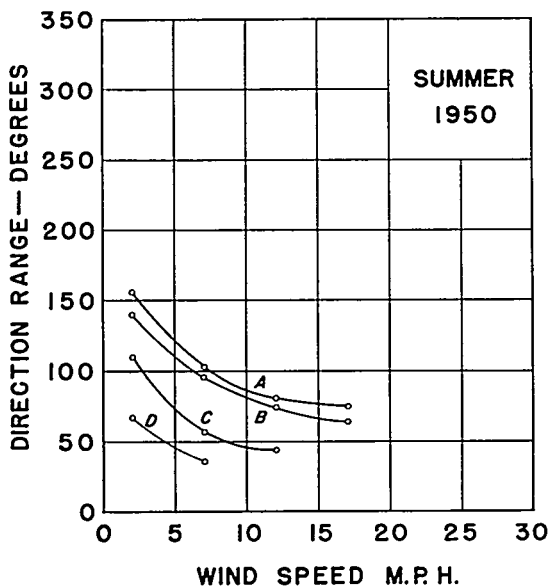
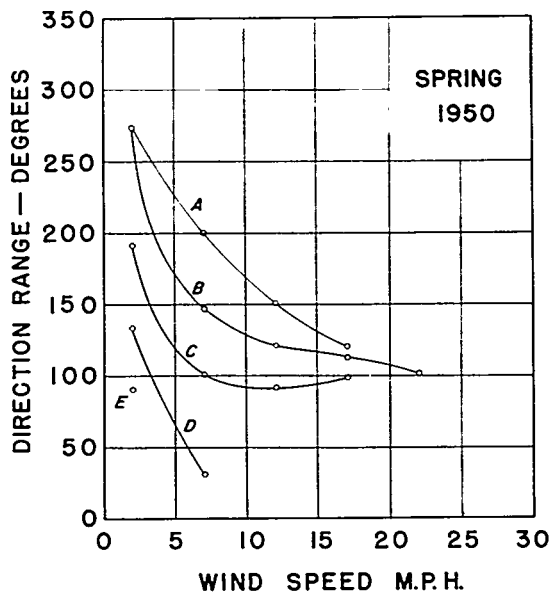
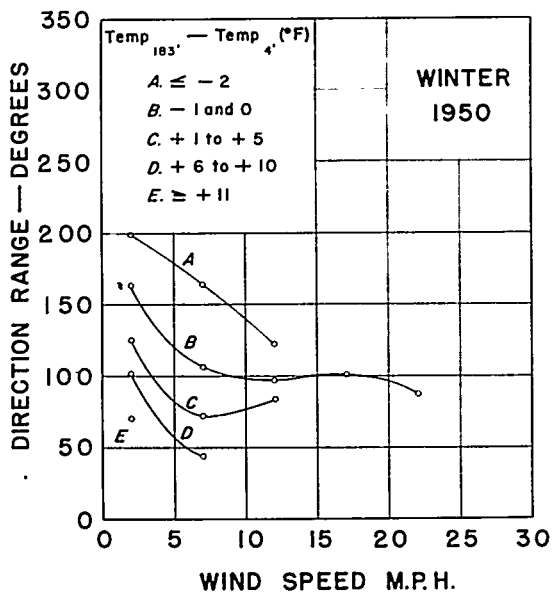


Fig. 160 15-min. wind direction range as a function of hourly mean wind speed, 154 ft. (station 012), by stability and season.

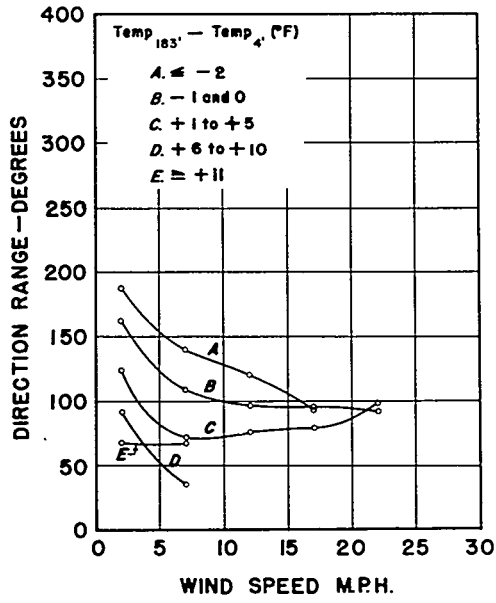
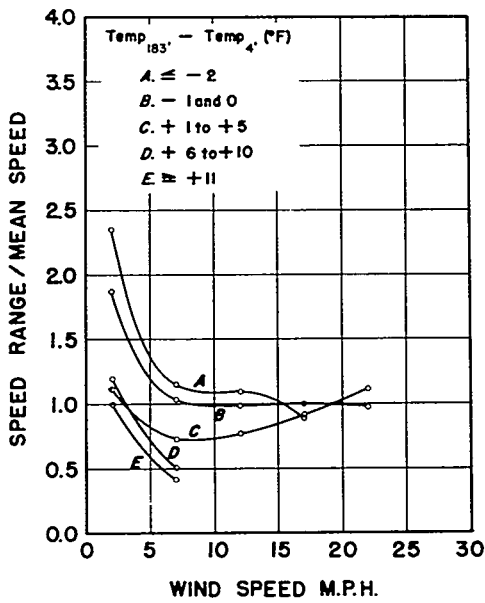
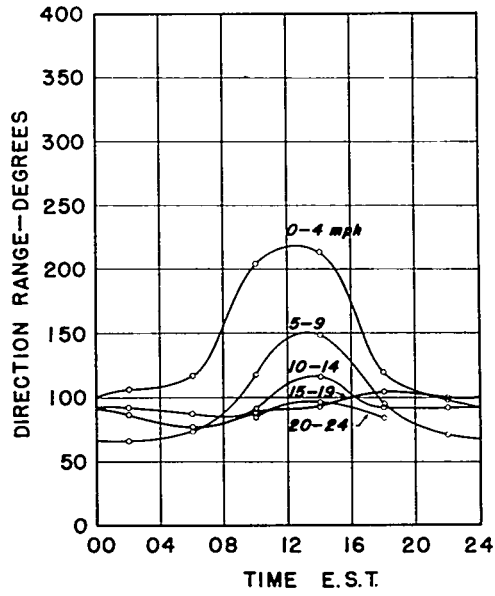
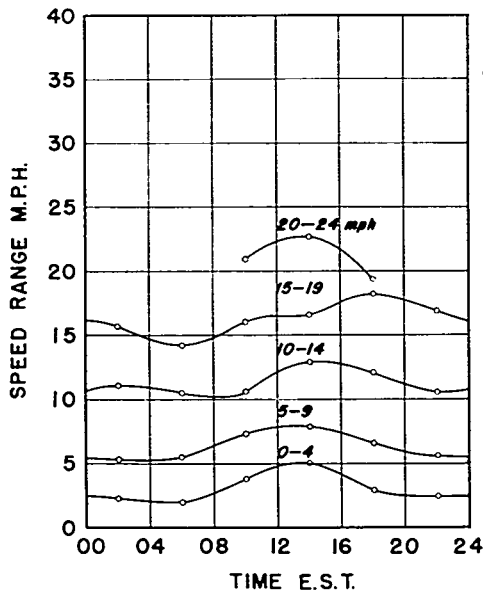
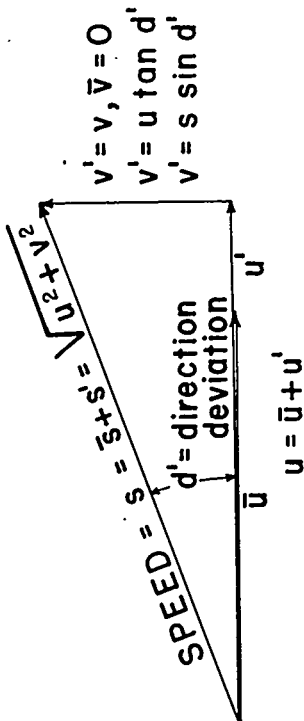


Fig. 161 Annual graphs of 15-min. wind direction and speed ranges as functions of time of day, wind speed and stability, 154 ft. (station 012), 1950.

DEFINITIONS



$S = s_{\max} - s_{\min} = \text{Speed Range}$ $D = \text{Direction Range}$ $\kappa = \frac{\sigma_V}{\sigma_U}$
 $\sigma_S = \sqrt{\bar{s}^2}$ $\sigma_U = \sqrt{\bar{u}^2}$ $\sigma_D = \sqrt{\bar{d}'^2}$ $\sigma_V = \sqrt{\bar{v}^2}$

THEORETICAL APPROXIMATIONS

$(\bar{s})^2 \approx (\bar{u})^2 + \sigma_V^2$
 $\bar{s}^2 \approx (\bar{u})^2 + \sigma_U^2 + \sigma_V^2$

(F.N. Frenkiel

J. Meteor. Oct. 1951)

CONSEQUENCES

$\bar{u} \approx \bar{s} \sqrt{1 - \sigma_V^2}$

$\sigma_U \approx \sigma_S$

$\sigma_V \approx \bar{s} \sigma_{\tan d'}$

$T_x = \frac{\sigma_U}{\bar{u}} \approx \frac{\sigma_S}{\bar{s} \sqrt{1 - \sigma_V^2}}$ $= \frac{\sigma_S}{\bar{s} \sqrt{1 - \kappa^2 \sigma_S^2 / \bar{s}^2}}$

$T_y = \frac{\sigma_V}{\bar{u}} \approx \frac{\sigma_{\tan d'}}{\sqrt{1 - \sigma_V^2}}$

EMPIRICAL APPROXIMATIONS

$\frac{\sigma_S}{\bar{s}} \approx \text{constant} = 4.2$

$\sigma_{\tan d'} \approx \tan \sigma_D$

$\frac{D}{\sigma_D} \approx \text{constant} = 6.8$

Fig. 162 Definitions and approximations used in turbulence analysis.

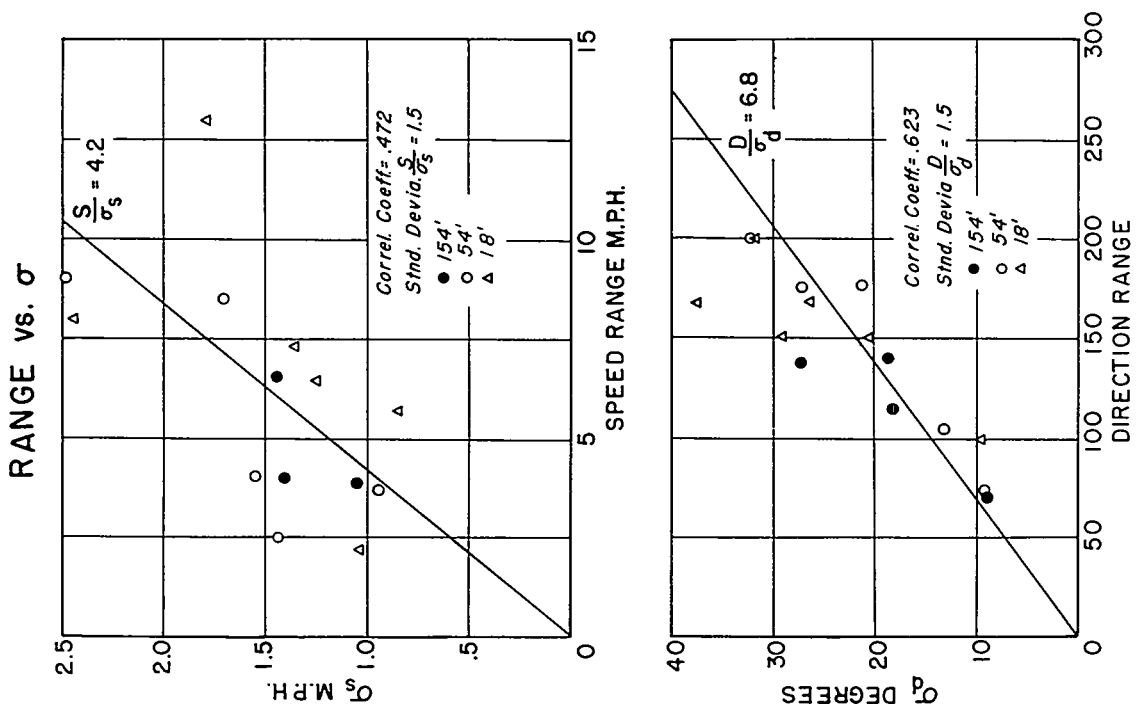


Fig. 163 Tests of turbulence approximations and determination of the ratio of 15 min. range to standard deviation, based on fast runs.

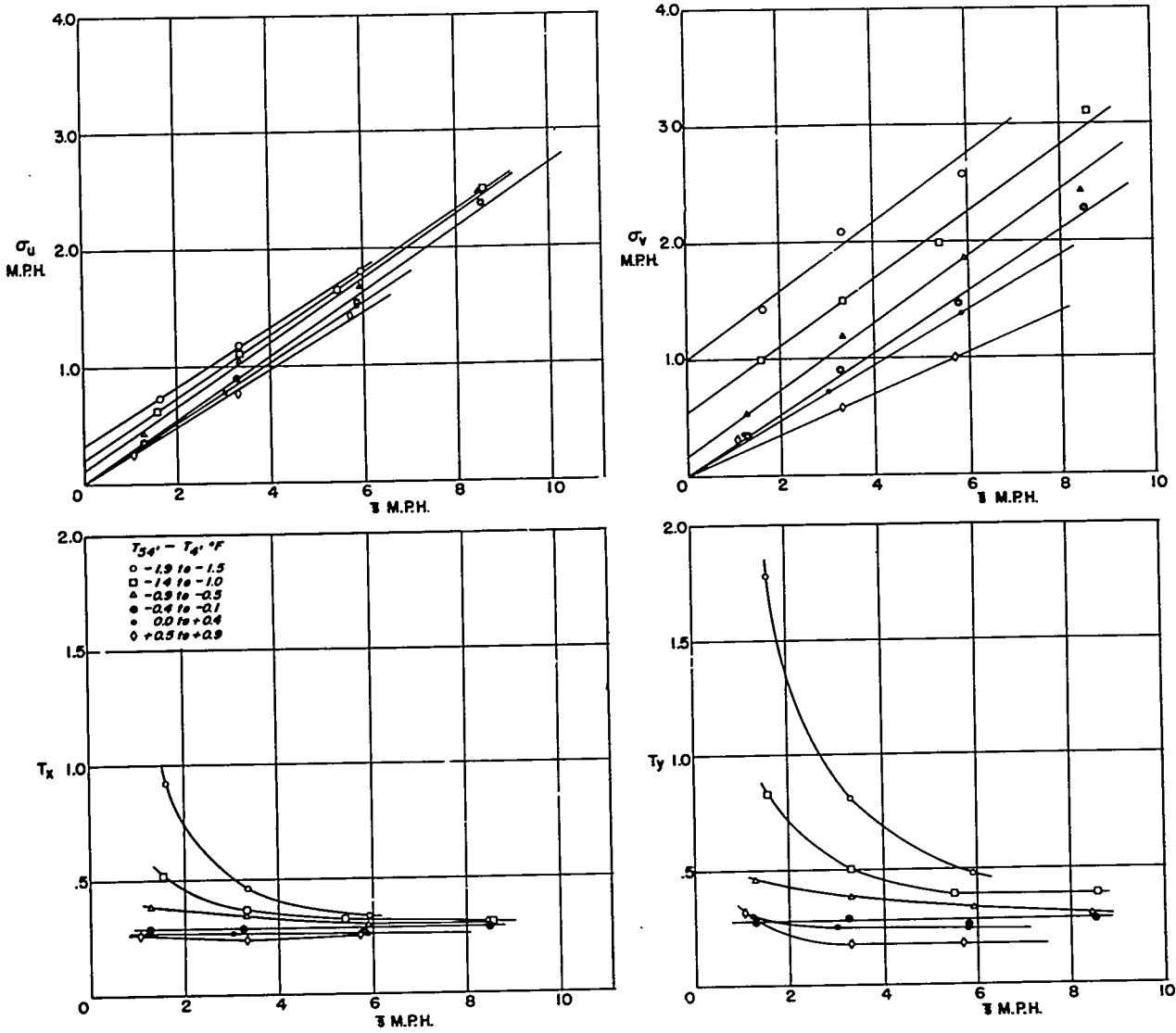
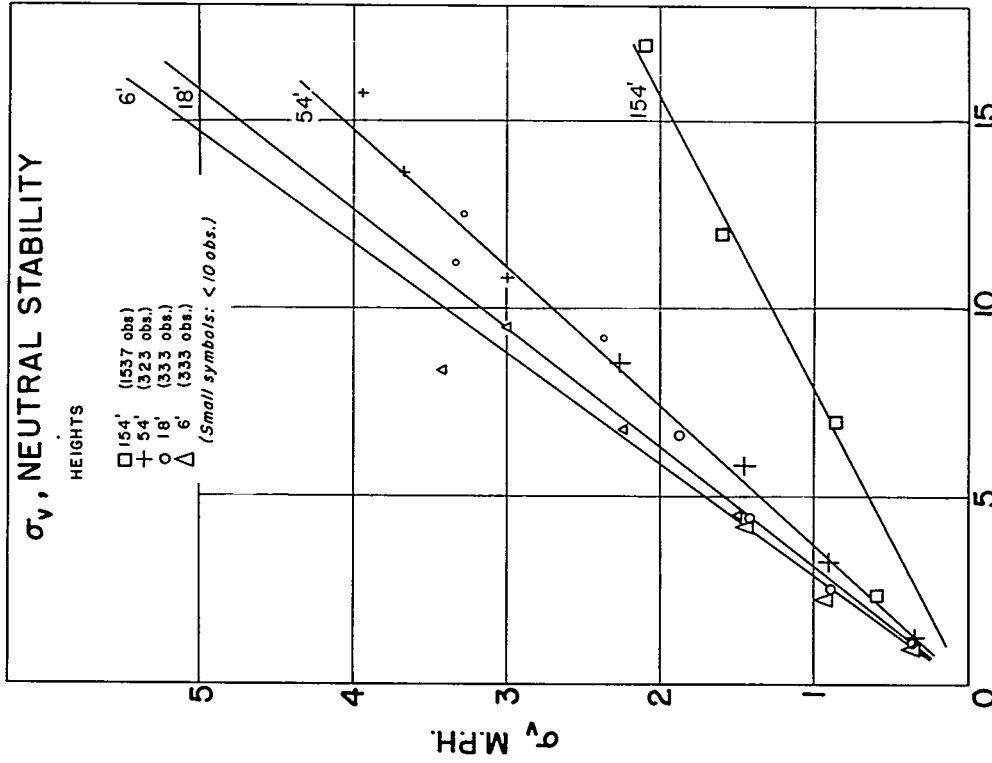
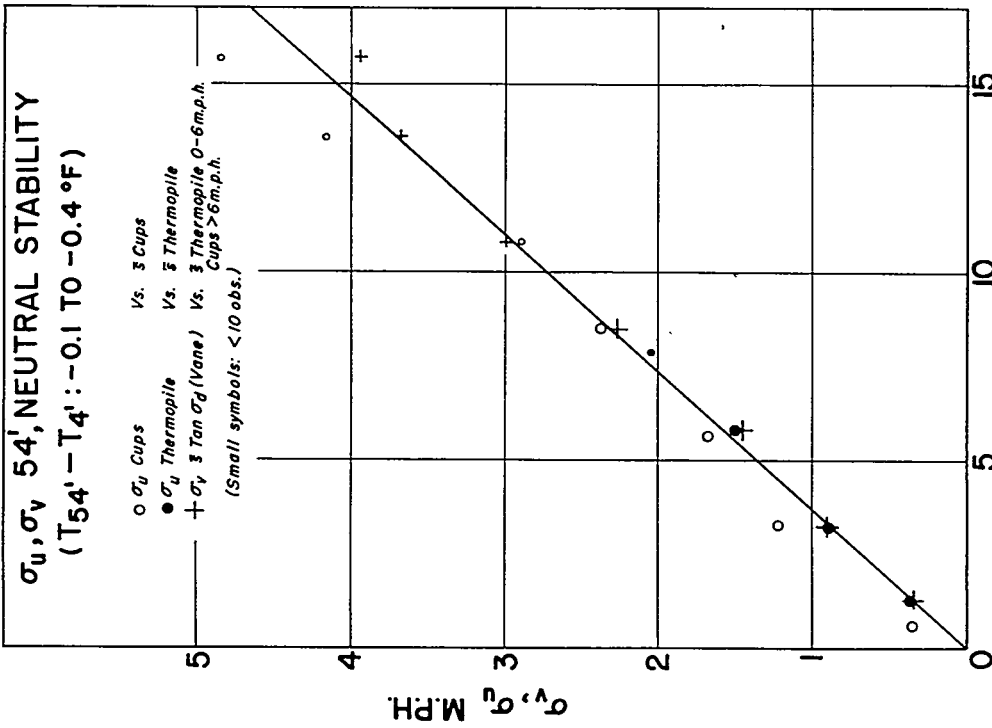


Fig. 164 Longitudinal and transverse components of absolute (σ_u , σ_v) and relative (T_x , T_y) intensity of turbulence as functions of hourly mean wind speed, sorted by stability, 54 ft. (station 001), July 19 - Oct. 3, 1950.

516



$\bar{\sigma}$ MEAN WIND SPEED M.P.H.

$\bar{\sigma}$ MEAN WIND SPEED M.P.H.

Fig. 165 Absolute intensity of turbulence as a function of hourly mean wind speed in neutral stability, comparing different methods of measurement at the same height (54 ft.), and the same method of measurement at different heights.

517

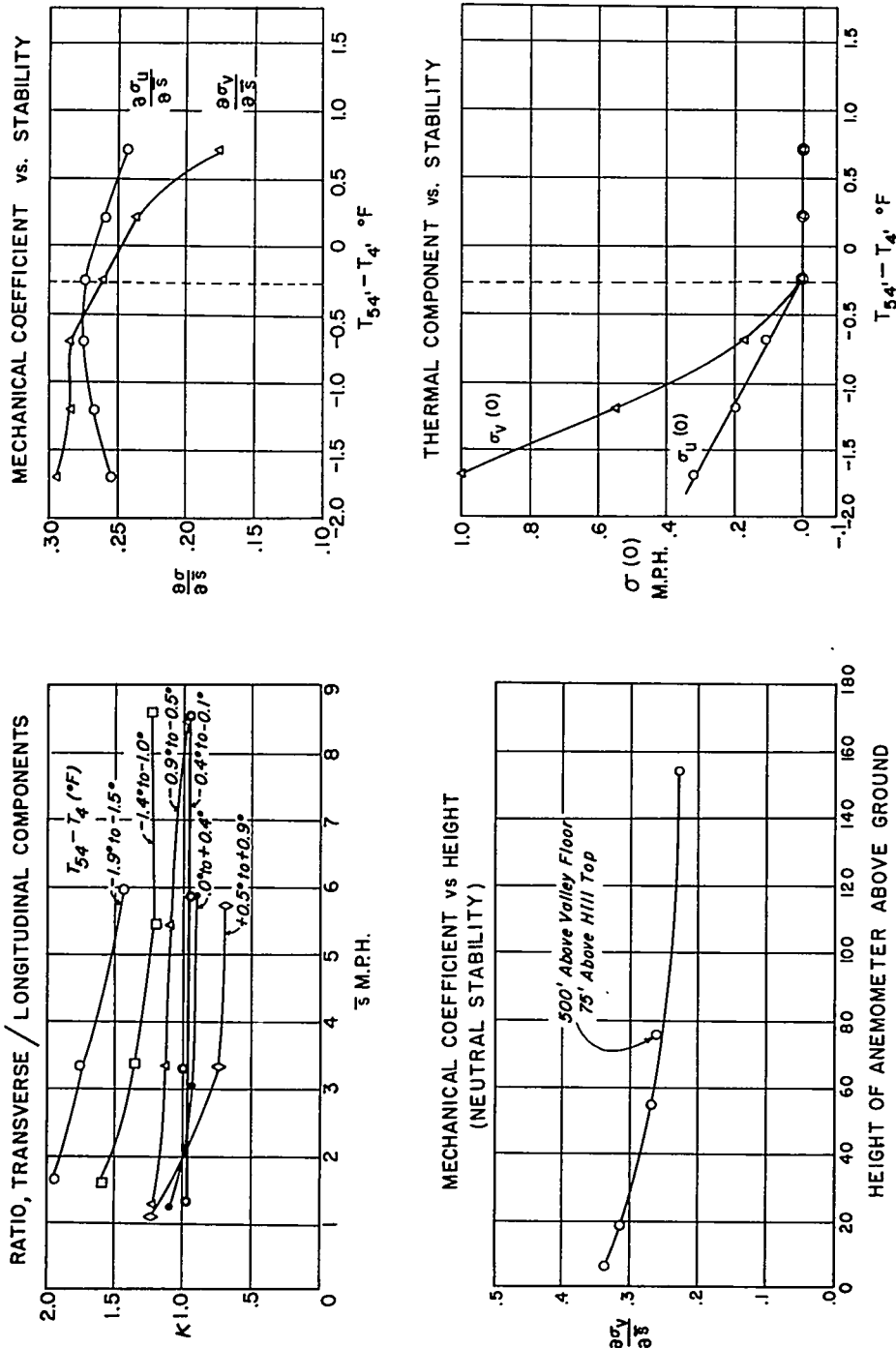


Fig. 166 At constant stability: $\sigma \approx \sigma(0) + \bar{u} \frac{\partial \sigma}{\partial \bar{u}}$
 $\sigma(0) \equiv$ Thermal component
 $\frac{\partial \sigma}{\partial \bar{u}} \equiv$ Mechanical coefficient

A METEOROLOGICAL SURVEY OF THE OAK RIDGE AREA

U. S. Weather Bureau

Oak Ridge, Tennessee

PART IV. ATMOSPHERIC DIFFUSION

Descriptive Observations of Diffusion

1. Smoke Trails

Processes of eddy diffusion and exchange have been encountered in many earlier sections of this report, notably those on visibility, local and vertical temperature variations, local and vertical wind variations, coupling between local and general wind streams, and turbulence. The interdependence of all these phenomena as well as the wide range of eddy sizes involved render both theoretical and empirical quantitative formulation of the laws of atmospheric diffusion very difficult. Qualitatively, on the other hand, fairly clear associations can be found between the rate and character of spreading of smoke trails (used as a visual tracer) on the one hand and the wind speed, vertical temperature gradient and gustiness on the other (References 11, 82, and 83). It will be recognized immediately that these are not completely independent variables, being in turn dependent upon the diffusion of momentum and heat. More fundamental variables are the horizontal pressure and temperature gradients, large scale vertical motion, net radiative heat flux, previous history (temperature, stability, momentum and turbulence) of the air and roughness and configuration of the underlying surface, but these are less readily measured.

The behavior of smoke trails originating next to the ground, as a function

of wind speed (18 ft., station 001) and vertical temperature gradient ($T_{183} - T_5$ station 012), is illustrated by the photographs in Fig. 167, all taken from "A₂" theodolite position facing SE, and with the wind direction at station 001 either NE or ENE. Each picture is a composite of several photographs taken within a period of a few minutes. At the lowest speeds it is clear that the effect of stability is to produce horizontal flow with a minimum of eddying, while the effect of instability is to produce large vertical and transverse eddies tending to mask the mean wind. The smoke spreads away from the ground, thinning most rapidly in the unstable case, while in the stable case it remains concentrated at the ground to greater distances. With increasing wind speed the resemblance of the three stability types to one another increases, the angles of vertical spreading in the inversion and lapse types approaching that of the neutral type. The thinning of the smoke with distance increases with increasing wind speed, remaining somewhat greater in lapse than in inversion conditions up to 10 mph. The area of Haw Ridge visible above the smoke can be taken as an inverse measure of the rate of vertical diffusion with respect to horizontal travel. This area decreases from stable towards unstable, decreases with increasing wind speed in the stable case, increases with increasing wind speed in the unstable case. When the increased longitudinal dilution due to wind speed is taken into account, it is seen why the visibility improves so rapidly at the higher wind speeds. In addition, there is some indication of a larger horizontal spacing of the eddies with increasing wind speed and with increasing instability.

These same patterns of vertical diffusion have also been observed in the photographs of smoke from the X-10 pile and steam plant stacks. In order to compare these patterns with those found in the gustiness data, measurements of the ratio of half-width z (ground to edge in the case of surface smoke, center to edge in the case of stack smoke) of the visible smoke plume to its length x at a distance of about 400 ft. along the plume have been made on both surface and stack smoke photographs. An average ratio has been obtained for the group of photographs taken at each observation time and these have in turn been averaged by wind speed and stability categories. Only observations with NE or ENE wind at 18 ft. have been used for surface smoke measurements, and only those with NE, ENE, SW or WSW for stack smoke measurements. In the more numerous categories, the range of observed values is often very nearly equal to that of the entire body of data, yet the averages fall into a pattern quite similar to those of the longitudinal, transverse and vertical eddy velocities obtained by means of wind vanes and anemometers. The results of the smoke measurements are shown in Fig. 168 together with the corresponding lateral gustiness graph for the 154 ft. level (annual average, 1950, station 012) for comparison with the stack plume widths, and both lateral and vertical gustiness graphs for the 18 ft. level (July 19 - Oct. 3, 1950, station 001) for comparison with the surface plume widths.

The plume width curves, while more irregular than those of gustiness (probably due to paucity of observations), resemble them in showing an increase from inversion (stable) to lapse (unstable) conditions, a

decrease at first with increasing wind speed and an approach to a steady value, independent of wind speed and stability, at high wind speeds. Numerically, the average visible plume widths, relative to length, are slightly smaller than the corresponding root mean square eddy velocities, relative to mean wind speed. The major anomaly, a tendency towards small plume widths under conditions of large lapse, particularly when accompanied by high wind speed, may be accounted for by the extremely rapid thinning of the smoke under these conditions. A more quantitative interpretation of these relationships will be presented later.

In addition to the variation of rate of diffusion with wind speed and stability, a variation of the character of the smoke plume can also be seen in Fig. 167. Under conditions of light winds and temperature inversion (illustrated also by Fig. 139) the edges of the smoke are smooth and soft, indicating an absence of medium and large scale eddies already noted in the analysis of the turbulence observations. Large temperature lapses, on the other hand, are accompanied by highly irregular trails, with alternating upward puffs and prolonged downdrafts which are closely related to the oscillations (thermal convective eddies) seen in wind vane and anemometer records and in neutral balloon trajectories obtained under similar conditions. With increasing wind speed, the medium-scale, relatively unorganized mechanical eddies become more and more predominant, regardless of the thermal stratification. Of course, it should be remembered that the intense mechanical turbulence accompanying high wind speeds tends to produce a uniform distribution of potential temperature, i.e.,

to destroy large lapses and inversions and convert them to more nearly adiabatic (neutral) gradients. For this reason both large lapses and large inversions in the surface layers become rare at wind speeds exceeding 8 mph.

2. Radioactivity Traces

In an area such as that surrounding the Oak Ridge National Laboratory with its multifarious low-grade sources of radioactivity and its complex microclimate, the interpretation of outdoor radioactivity measurements is far from simple. Natural radioactive gases emanate from the earth at a variable rate depending upon the state of the ground, decay through complex chains of daughter activities, and are dispersed into the atmosphere to varying degrees depending upon the turbulent exchange. Man-made radioactivities issue from the pile, laboratories and chemical pilot plants in a bewildering diversity of alpha, beta and gamma emitters of varying energies, half-lives and physical states.

With the help of specialized instrumentation supplied by Dr. F. J. Davis of ORNL, Health Physics Division, some resolution of the more important radioactive components of the Oak Ridge atmosphere has been possible. Fig. 169 illustrates typical diurnal and aperiodic variations of natural atmospheric radon (alpha) concentration, atmospheric gamma radiation resulting mainly from pile operation, and beta-gamma particulate activity resulting from miscellaneous Laboratory operations as well as from natural sources. Radon, which emanates from the soil in a manner somewhat analogous to the evaporation of soil moisture has a characteristic diurnal

variation at 3 ft. above ground roughly parallel to that of the relative humidity. Its concentration is high at night (about 10^{-9} curies/m³) when vertical mixing is at a minimum, drops rapidly in the morning as soon as the low-level inversion is destroyed by solar heating of the surface, remains low during the afternoon (below the instrument threshold: of the order of 10^{-11} curie/m³), and again rises gradually during the evening. This 100-fold diurnal variation of concentration, which would probably be approximated over any extensive, steady area source of contamination, is independent of the wind direction and has been found to be essentially the same at several observation points at different directions and distances from the Laboratory.

When the incident gamma radiation dosage-rate is corrected for natural background (earth, atmospheric and cosmic) by subtracting the lowest half-hour average in each 24-hour period (longer if necessary to exclude wind directions from known sources), the remainder (Fig. 169) reflects primarily the wind direction. Exposure rates averaging a few μ r/hr. (micro-roentgens per hour) occurred in the example shown whenever the wind blew towards the detector from the pile stack (and occasionally when the wind instrument registered calm). The peaks are greatly reduced at 3 miles from the stack. These excursions were evidently due to A^{41} activated in the pile cooling air and discharged through the stack, but it is impossible to determine from the gamma observations alone whether radio-argon was present in the air immediately surrounding the detector or only at some distance (up to several hundred feet) away. If uniformly distributed throughout the atmosphere within several thousands of feet of the

detector only about 3×10^{-9} curies/m³ would have been required to produce the observed peaks (5 μ r/hr.). However, the clouds of radioactivity were undoubtedly much smaller and more concentrated: using a typical z_0/x (from the smoke plumes) of 0.2, a total instantaneous diameter of some 1200 ft. would be expected at a distance of one mile, with most of the material concentrated in smaller puffs and eddies within this. Fluctuations of wind direction away from the detecting instrument during the half-hour averaging period would also have reduced the observed averages considerably below what would have been obtained in the middle of the stream. Thus the concentrations within the plume must be considered to be of the order of 10^{-8} to 10^{-7} curie/m³ at 1 mile under average meteorological conditions and subject to considerable meteorological variation. The quantitative analysis will be presented in a later section, following a discussion of the diffusion formulae and parameters. It is interesting to note that while the concentration determination is quite ambiguous, the exposure is measured quite precisely, and the half-hourly averages 1 mi. downwind of the stack are found to be of the same order of magnitude as the natural gamma background: some 3 to 10 μ r/hr.

Very little particulate beta-gamma contamination is found in the atmosphere by means of the constant air monitors employed by the ORNL Health Physics Division. Measurable concentrations are virtually only found under inversion conditions, and then are a small fraction of the natural radon concentration (1 to 3×10^{-10} curie/m³) and independent of wind direction so that a natural origin is indicated for at least a part of

this activity. Occasional rises can be traced to particular operations in the Laboratory, with favorable winds.

Superimposed upon the broader patterns of stack-gas radiation shown by the half-hourly averages, the original beta and gamma records reveal a much finer structure, with fluctuations down to the limiting resolution period of the instrument (of the order of 1-3 min.). Fig. 170 shows instrument charts illustrating the typical diurnal changes in character of these traces and their variation with distance from the stack. On the finer time-scale as on the broader, the rises and falls at 1 mi. mainly reflect shifts of the wind towards and away from the direction of the detecting stations with respect to the stack. This is true of both the beta and gamma charts, since the "beta" detector is also quite sensitive to gamma radiation and should properly be called a beta-gamma counter. However, while the gamma and beta-gamma exposures are roughly equal at night (before 8:15 a.m., time of first breaking of the inversion) there is a noticeable difference between them during the daytime due to a definite contribution from beta radiation. The radioactive argon from the pile cooling air emits both beta and gamma rays. Since gamma rays can be detected for hundreds of feet in the air while the beta particles have a maximum range of only a yard or two, the relative proportions of these components received at a given point vary with the distance and size of the radioactive cloud. If the proportion of gamma to beta radiation in an infinite, uniform cloud is taken as a yardstick, the proportion of gamma radiation will be much less than this inside a

small cloud, while the beta radiation will be virtually nil if the cloud is some distance (more than a few yards) from the detector. Thus the radiation received at the ground from the nocturnal stack gas trail is almost entirely gamma radiation, since the radioactivity is almost entirely contained in a narrow layer some hundreds of feet above the ground. In the daytime, on the other hand, many puffs of stack gas reach the ground at one mile, so that considerable beta radiation is received.

Calibration formulas have been developed by F. J. Davis (Ref. 84) which permit a rough estimate to be made of the concentration and size of the radioactive cloud. For example, two 15 min. periods have been chosen from the records at 1 mi. shown in Fig. 170, during which the stack gases were being carried towards the detector: 3:27 - 3:42 a.m., when there was a 4° inversion, and 9:35 - 9:50 a.m., when the $T_{183} - T_5$ registered 0. The total incident radiation, concentration, and estimated radius of a uniform cloud necessary to give the observed gamma radiation are shown in Table 46 for the two cases.

The examples given in Table 46 illustrate a fundamental difference between inversion conditions on the one hand and neutral or lapse conditions on the other, in observations of radioactive stack gases at the ground within a few miles of the source. Gamma detectors downwind of an elevated source receive exposures of comparable magnitude from both the concentrated trails several hundred feet above the ground characteristic of inversion conditions and the relatively dilute puffs some hundreds of feet in radius which surround them during lapse conditions. Beta radiation, on the other

TABLE 46

RADIOACTIVE EXPOSURE, CONCENTRATION AND CLOUD RADIUS, APRIL 29, 1951

<u>Time</u>	<u>3:27-3:42 a.m.</u>	<u>9:35-9:50 a.m.</u>
T ₁₈₃ - T ₅ , °F.	74	0
Gamma, roentgens/hr.	9 x 10 ⁻⁶	14 x 10 ⁻⁶
Gamma plus beta, roentgens/hr.	9 x 10 ⁻⁶	20 x 10 ⁻⁶
Beta only, roentgens/hr.	0	6 x 10 ⁻⁶
Beta concentration, curie/m ³	0	24.4 x 10 ⁻⁹
Gamma from infinite, uniform cloud of this concentration, roentgens/hr.	0	43 x 10 ⁻⁶
Gamma infinite/gamma observed	0	3.1
Radius of uniform cloud giving this ratio	Remote	400 ft.

hand, is of importance only under lapse conditions, unless the source is close to the ground. The smoother character of the trails at night and the more irregular, broken-up character in the daytime are also clearly shown by Fig. 170.

In the records obtained at 3 mi. and $5\frac{1}{2}$ mi. from the stack, some additional characteristics of the radioactivity are illustrated. First the compensating effects of dilution and radioactive decay, in the case of the isotope under consideration, are of interest. The wind speeds increased from 1-5 mph before 8:00 a.m. to 6-12 mph after that time, but the 2 to 4 fold increase in dilution resulting from this increased wind speed was overshadowed by a corresponding decrease in travel time from the source to the detector. Radioargon, having a half-life of 110 min.,

would have decayed to a fraction of its original concentration at the distant station when the wind speed was light, as shown by Table 47

TABLE 47

RADIOACTIVE DECAY OF A⁴¹: FRACTION REMAINING
AT EACH STATION AS A FUNCTION OF WIND SPEED

Wind speed, mph	1	2	3	4	5	10	20
Station 1, 1.0 mi.:	0.68	0.83	0.88	0.91	0.93	0.96	0.98
Station 2, 3.1 mi.:	0.30	0.55	0.67	0.74	0.79	0.89	0.94
Station 3, 5.4 mi.:	0.14	0.36	0.50	0.60	0.66	0.82	0.90

As a result of this compensating effect the observed concentrations drop off rapidly with distance under all conditions, so that at $5\frac{1}{2}$ mi. they are hardly detectable above the statistical fluctuations characteristic of the radioactive background. However, since the peaks appear to broaden out with increasing distance, slight rises can be measured somewhat more accurately than closer to the stack where the fluctuations are shorter and more abrupt, particularly in neutral or lapse conditions.

The relatively prolonged rise of both beta and gamma radiation, but particularly of the former, at 1 and 3 mi. after 8:00 a.m. illustrates an important phenomenon which was first completely described by Hewson (Ref. 85) and which has come to be known as the "morning fumigation". This is a simultaneous rise in ground concentration at many points, various distances downwind, due to the abrupt downward mixing of stack gases which had been carried out in a concentrated stream aloft during the night. Its persistence is due to the continued presence of the upper part of the

nocturnal inversion above the original gas trail level for some time after lapse or neutral conditions have been established below. Were it not for the low wind speeds and resulting decay of the radioactivity with distance, similar peaks could be expected at $5\frac{1}{2}$ mi.

Conditions favorable for the appearance of definite peaks due to radio-argon at $5\frac{1}{2}$ mi. downwind of the stack are illustrated in Fig. 171. It is seen that the wind at Station 012 (154 ft. above the valley) shifted from a more westerly direction towards the valley axis about 4:40 a.m., and at Station 019 (80 ft. above a 400 ft. ridge) about 4:50 a.m. The wind speed at Station 012 during the half-hour following this shift was near 6 mph and that at Pine Ridge (019) about 14 mph. In spite of these relatively high speeds an inversion of 2° F. was recorded at Station 012. The gamma activity at 1 mi. began to show small peaks at about 4:20 a.m., reflecting occasional brief puffs of wind in the proper direction preceding that time. Increasingly large rises began at 4:40, 5:10, and 5:45. A single large peak was recorded at $5\frac{1}{2}$ mi. between 5:25 and 5:40 a.m. From these data it appears that the travel time from the source to the detector at $5\frac{1}{2}$ mi. was only about 35-45 min., (corresponding to a wind speed of 8-9 mph) so that only some 20% of the original activity would have decayed. The moderate stability and small gustiness combined to prevent rapid lateral or vertical spreading of the trail. Thus a combination of large wind speed (preventing decay enroute) and stability (preventing rapid diffusion) are required to enable A^{41} from the pile cooling air to be detected above natural background at distances greater than

about 3 mi. Another probable contributing factor in this case is the lowering of the plume height with increasing wind speed, an effect which will be considered in more detail later.

The morning transition from stable to unstable flow including a typical "fumigation" are illustrated in some detail in Fig. 172. A shallow inversion ($T_{154} - T_4$ and $T_{183} - T_3$ both about 1° F.) persisted until 6:30 a.m., followed by a change in the lowest 54 ft. to neutral by 7:00 a.m. and unstable thereafter. The lowest 183 ft. became superadiabatic by about 7:40. The 154 ft. wind direction showed only short period fluctuations of small amplitude before 6:50, followed by almost complete damping out of turbulence until 7:45, when gustiness characteristic of daytime lapse gradually began. The wind speed was rather steady at about 5 mph throughout the morning. During the period before 7:45, only smooth, long rises appeared in the gamma traces at 1 mi., and at 7:15, following a period of particularly steady, direct upvalley flow one such peak appeared also at 3 mi. The stack gas stream may be presumed to have been high, narrow, concentrated and slightly meandering during this period. Beginning about 7:50 the 3 mi. recorder showed a series of high, irregular peaks, preceding a similar but larger and more irregular series at 1 mi. starting about 8:20. The earlier occurrence at 3 mi. is evidence of the erratic nature of downward mixing. After 9:00 a.m. the typical daytime lapse pattern became established, with irregular short, occasionally intense puffs at 1 mi. corresponding to periods of wind direction $235-240^\circ$; becoming broader and so weak as to be almost undetectable at 3 mi.

An interesting example of the evening transition to stable flow with reversal of the valley breeze is shown in Fig. 173. Four sharp peaks of gamma radiation roughly equal to the background radiation occurred between 3:10 and 3:50 p.m. on this occasion, following swings of the wind vane towards 235-240°. More diffuse rises occurred shortly after 4:00, 4:30 and 5:15 p.m., followed by $1\frac{1}{2}$ hours of wind directions 20-30° off the valley axis. Until 4:30 p.m., a superadiabatic temperature lapse was registered in both the 54 ft. and 183 ft. layers, followed at first by gradual stabilization, then by rapid formation of a 2°F. inversion in 54 ft. by 6:05 and 183 ft. by 7:15. A 5 minute period of smooth, direct SW wind flow from the stack towards the 1 mi. detector at 6:50 - 6:55 was followed by a full-scale gamma peak (3 times background). However, by this time the surface wind (18 ft. Station 004) at the detector had been light NE-ESE, that is, opposite to the direction of movement of the gas trail, for about 1 hour. At 7:50 the stack-level wind in turn suddenly reversed, remaining northeasterly for the night. During the calm preceding the reversal of the wind vane, and for half an hour following the reversal, the gamma activity rose to the order of twice background, exhibiting a typical long, smooth nocturnal peak. Evidently the radioactivity carried up the valley by the last puff of the afternoon up-valley breeze was brought back over the detector when the nocturnal down-valley movement deepened to the level of the stack-gas stream.

3. Effects of Buildings, Forest, Ridges and Gaps

The foregoing discussion of the diffusion of smoke and gases in the vicinity of the Oak Ridge National Laboratory has been limited to the case of

direct up- or down-valley flow. Surface smoke trails were further limited to those travelling southwestward from Station 001, that is, away from the built-up Laboratory area and over relatively unobstructed terrain. Additional complications are introduced by flow at low altitude over buildings or trees, or by cross-ridge wind directions.

Isolated buildings and other abrupt obstructions produce systematic distortions of the mean flow, up-drafts and horizontal spreading generally occurring on the windward side, down-drafts and enhanced turbulence on the leeward side. These effects have been found in smoke photographs taken in the Y-12 and K-25 Areas. In inversion conditions, the vertical effects are decreased, and horizontal spreading around obstacles increased. In built-up areas containing many buildings, the main effects are increased turbulent mixing and horizontal spreading, persistent local air currents greatly differing from the mean wind, and stagnation of clear or contaminated air in sheltered spaces, particularly in light winds. Again the effect of a temperature inversion is to produce exaggerated horizontal spreading within the spaces between buildings, and local stagnation. It should be remembered, however, that surface inversions are not as intense in built-up areas as in open country, so that the layer containing buildings will have a more uniform vertical distribution of contamination at night than will the corresponding layer over open ground.

Forests affect the mean flow and character of diffusion somewhat the same as buildings but in a more generalized manner; slowing down or even stagnation of air accompanied by enhanced lateral (or even up-wind) spreading

within the forest, and increased turbulence above the forest canopy.

Flow across ridges under daytime light wind conditions would not differ much from that along the valley axis. With stronger winds, systematic up-drafts develop on the windward slopes (see Fig. 155, Type B). No systematic lee down-drafts are detectable in the smoke or neutral balloon observations with the source in a valley bottom, with the exception of shallow downslope drainage at night. Gaps through the ridges affect only those smoke trails emitted directly upwind of them, a striking effect being the horizontal spreading of the smoke, as it issues from the gap, along the leeward side of the ridge. Some eddying of the up- and down-valley winds into and out of gaps and ravines has been observed, and contaminants once entering in such an eddy may persist after the more exposed portion of the trail has blown by. Some arching of smoke trails over ridges has been observed; no definite evidence has been obtained as to whether smoke or gas plumes emitted near ridge top level under inversion conditions actually come in contact with the elevated portions of the ground. From considerations of ridge and free-air nocturnal temperature distributions, it would seem that the mid-valley source would have to be well below ridge-top level for such contact normally to occur.

Diffusion Formulas and Parameters

4. General Point Source Formulas

The atmospheric diffusion theory of O. G. Sutton, first published in 1932 (Ref. 86) has been refined and adapted, by its author, to a host of specific applications, covering almost the entire range of diffusion problems experienced at Oak Ridge and many others (summarized in Ref. 87,

Chapter 8). As a result of its widespread application in the fields of chemical warfare, (Ref. 74, and 88) industrial air pollution abatement, (Ref. 89, 90, 91 and 92) hydrologic evaporation studies (Ref. 93, 94), and radioactive waste disposal (Ref. 83, 95), a background of familiarity with the properties, short-comings and range of applicability of this theory has been built up in recent years. While in each field of application Sutton's formulas represent only one of several equally satisfactory approaches, they seem to incorporate the essential variables in a uniquely flexible manner, allowing direct application in all these fields. Because of this background of experience with them, and their flexibility, Sutton's formulas have generally been taken as the starting point for solving practical problems of diffusion during the Oak Ridge meteorological survey program. However, it should be emphasized that the verification of this theory is still far from complete, particularly in conditions of large lapse or inversion, and at distances of more than a few miles from the source.

Sutton's basic "first approximation" concentration formulas are as follows:

(1) Instantaneous point source:

$$X(x, y, z, t) = \frac{Q}{\pi^{3/2} C_x C_y C_z (\bar{u}t)^{3(2-n)/2}} \exp \left[-(\bar{u}t)^{n-2} \left(\frac{x^2}{C_x^2} + \frac{y^2}{C_y^2} + \frac{z^2}{C_z^2} \right) \right]$$

DIFFUSION FORMULAE AND PARAMETERS

(For ready reference)

For convenience the formulae for the diffusion of matter discussed on pages 534-542 (formulae 1 to 23) are listed. Some have been rearranged for clarity and (7) has been corrected:

1.
$$\chi_{(x,y,z,t)} = \frac{Q}{\pi^{3/2} C_x C_y C_z (\bar{u}t)^{3(2-n)/2}} \exp \left[-(\bar{u}t)^{n-2} \left(\frac{x^2}{C_x^2} + \frac{y^2}{C_y^2} + \frac{z}{C_z^2} \right) \right]$$
2.
$$\chi_{(x,y,z,t)} = \frac{Q \exp[-y^2/C_y^2 x^{2-n}]}{\pi C_y C_z u x^{2-n}} \left\{ \exp \left[\frac{(z-h)^2}{C_z^2 x^{2-n}} \right] + \exp \left[\frac{(z+h)^2}{C_z^2 x^{2-n}} \right] \right\}$$
3.
$$\frac{\bar{u}_2}{u_1} = \left(\frac{z_2}{z_1} \right)^{n/(2-n)}$$
4.
$$C_x^2 = \frac{4\nu T_x^{2-2n}}{(1-n)(2-n)u^n} \quad C_y^2 = \frac{4\nu T_y^{2-2n}}{(1-n)(2-n)u^n} \quad C_z^2 = \frac{4\nu T_z^{2-2n}}{(1-n)(2-n)u^n}$$
5.
$$u = \frac{u^*}{k} \ln \left(\frac{z}{z_0} \right)$$
6.
$$\chi_{(\bar{u}t)} = \frac{2Q}{C^3 \pi^{3/2} (\bar{u}t)^{3(2-n)/2}} \exp \left[-\frac{h^2 (\bar{u}t)^{n-2}}{C^2} \right]$$
7.
$$TID = \frac{2Q}{\pi \bar{u} C^2 (\bar{u}t)^{2-n}} \exp \left[-\frac{h^2}{C^2 (\bar{u}t)^{2-n}} \right]$$
8.
$$\chi_{\max} = \frac{2Q}{h^3 \left(\frac{2}{3} \pi e \right)^{3/2}} \quad \bar{u}t = \left(\frac{2h^2}{3C^2} \right)^{1/(2-n)}$$
9.
$$TID_{\max} = \frac{2Q}{\pi e u h^2} \quad \bar{u}t = \left(\frac{h^2}{C^2} \right)^{1/(2-n)}$$
10.
$$\chi_{(x)} = \frac{2Q}{\pi C_y C_z \bar{u} x^{2-n}} \exp \left(-\frac{h^2}{C_z^2 x^{2-n}} \right)$$

11. $\chi_{\max} = \frac{2Q}{\pi e \bar{u} h^2} \left(\frac{C_z}{C_y} \right)$ $x = \left(\frac{h^2}{C_z^2} \right)^{1/(2-n)}$
12. $(ut)_0 = \left(\frac{Q/\chi_0}{C^3 \pi^{3/2}} \right)^{2/3(2-n)}$ $x_0 = \left(\frac{Q/\chi_0}{\pi C_y C_z \bar{u}} \right)^{1/(2-n)}$
13. $\chi(x) = \frac{2Q}{\pi C_y C_z \bar{u} x^{2-n}}$
14. $x = h \bar{u} / \bar{w}$ $x' = \sqrt{x^2 + h^2}$
15. $\chi(x) = \frac{Q}{\sqrt{2\pi} C_y \bar{u} h x^{(2-n)/2}}$
16. $\bar{\chi} = \frac{2Qf}{\alpha \sqrt{\pi} C_z \bar{u} x^{(2-n)/2}} \exp\left(-\frac{h^2}{C_z^2 x^{2-n}}\right)$
17. Deposition = $\frac{Q}{\sqrt{2\pi} C_y \bar{u} x^{(2-n)/2}}$
18. Deposition = $\frac{Q}{\pi C^2 (\bar{u} t)^{2-n}}$
19. $h + \Delta h = \text{effective height}$
20. $\Delta\theta = \frac{Q}{2\pi^{3/2} \rho c_p C^3 Z^{3(2-n)/2}}$
21. $Z_{\max} = \left(\frac{Q}{2\pi^{3/2} \rho c_p C^3 \partial\theta/\partial Z} \right)^{0.276}$
22. $z = C_z x^{(2-n)/2} \sqrt{\ln \frac{Q/M}{\sqrt{\pi} C_z \bar{u} x^{(2-n)/2}}}$
23. $x = \left(\frac{Q/M}{\sqrt{\pi} u C_z} \right)^{2/(2-n)}$

(2) Continuous point source at height h (m) above ground:

$$\chi(x,y,z) = \frac{Q \exp(-y^2/C_y^2 x^{2-n})}{\pi C_y C_z u x^{2-n}} \left\{ \exp \left[\frac{(z-h)^2}{C_z^2 x^{2-n}} \right] + \exp \left[\frac{(z+h)^2}{C_z^2 x^{2-n}} \right] \right\}$$

- where χ = concentration (gm./m.³).
- Q = source strength (gm. for instantaneous source, gm./sec. for continuous source, or, in the case of radioactive contaminants, curies and curie/sec. respectively).
- x, y, z = downwind, cross-wind and vertical coordinates measured from the center of the moving cloud in the instantaneous case, and from a point on the ground directly beneath the source in the continuous case (m).
- t = time after instantaneous release (sec.).
- u = mean wind speed (m./sec.).
- n = a non-dimensional parameter associated with the stability and identified with the exponent in the power-law wind velocity profile through the formula:

$$(3) \quad \frac{\bar{u}_2}{u_1} = \left(\frac{z_2}{z_1} \right)^{n/(2-n)}$$

The range of n is from 0 to 1, the value 1/4 being widely used for the case of neutral (adiabatic) equilibrium (the "1/7 power profile").

C_x, C_y, C_z = generalized non-isotropic diffusion coefficients

$[(m)^{n/2}]$ defined as follows:

$$(4) \quad \begin{cases} C_x^2 = \frac{4 \sqrt{n} T_x^{2-2n}}{(1-n)(2-n)u^n} \\ C_y^2 = \frac{4 \sqrt{n} T_y^{2-2n}}{(1-n)(2-n)u^n} \\ C_z^2 = \frac{4 \sqrt{n} T_z^{2-2n}}{(1-n)(2-n)u^n} \end{cases}$$

As n approaches 0, C_x , C_y and C_z reduce to $\sqrt{2}T_x$, $\sqrt{2}T_y$ and $\sqrt{2}T_z$.

ν = kinematic viscosity of air, which varies, in the vicinity of Oak Ridge, from 1.4×10^{-5} gm. m.⁻¹ sec.⁻¹ at low temperature and high pressure to 1.8×10^{-5} gm. m.⁻¹ sec.⁻¹ at high temperature and low pressure. T_x , T_y , T_z = components of the non-dimensional (relative) intensity of turbulence.

Sutton has suggested that for "fully rough" flow the molecular kinematic viscosity, ν , should be replaced by a "macroviscosity", M , of the order of 10^{-2} m.² sec.⁻¹. This quantity can be evaluated under conditions of neutral stability, in which case the wind profile follows the logarithmic law:

$$(5) \quad u = \frac{u_*}{k} \ln \frac{z}{z_0}$$

where z_0 = a roughness length characteristic of the underlying surface.

k = von Karman's constant = 0.4 (non-dimensional).

u_* = the "friction velocity", i.e. the velocity whose square, multiplied by the density, is numerically equal to the shearing stress at the air-earth interface.

Then $N = u \cdot z_0$.

Typical values of C_y and C_z for large lapse, neutral, moderate inversion and large inversion, and the resulting concentrations as a function of stack height and distance for unit emission rate ($Q = 1$ gm./sec.) have been tabulated by Sutton (Ref. 89) using the molecular viscosity and by M. L. Barad and G. R. Hilst (Ref. 96) using the macroviscosity.

5. Formulas for Special Cases

The following special cases are encountered sufficiently frequently in practical applications to justify listing their formulas:

- (6) Central ground concentration at a point downwind of an instantaneous elevated source, assuming $C_x = C_y = C_z = C$. Let $x = 0$, $y = 0$, $z = h$, double x to allow for reflection by ground.

$$x(\bar{u}t) = \frac{2Q}{\pi^{3/2} c^3 (\bar{u}t)^{3(2-n)/2}} \exp \left[-(\bar{u}t)^{n-2} h^2/c^2 \right]$$

- (7) Total integrated dosage (TID) at a point on the ground downwind of an instantaneous elevated source. Integrate (1) with respect to x/\bar{u} from $-\infty$ to $+\infty$, holding $\bar{u}t$ constant; $y = 0$, $z = h$. Units: gm./sec./m.³ or curie sec./m.³

$$TID = \frac{2Q}{\pi c^2 \bar{u} (\bar{u}t)^{2-n}} \left[\frac{-h^2}{c^2 (\bar{u}t)^{2-n}} \right]$$

- (8) Maximum ground concentration and distance of maximum downwind of an instantaneous elevated source. Set $\frac{\partial x}{\partial t} = 0$.

$$x_{\max} = \frac{2Q}{\left(\frac{2}{3}\pi e\right)^{3/2} h^3}$$

$$\bar{u}t = \left\{ \frac{2h^2}{3C^2} \right\} \frac{1}{2-n}$$

- (9) Maximum integrated dosage at the ground and distance of maximum downwind of an instantaneous elevated source. Set $\frac{\partial}{\partial t} (\text{TID}) = 0$

$$\text{TID}_{\max} = \frac{2Q}{\pi e \bar{u} h^2}$$

$$\bar{u}t = \left(\frac{h^2}{C^2} \right) \frac{1}{2-n}$$

- (10) Ground concentration downwind of a continuous elevated source.

$$y = z = 0.$$

$$x(x) = \frac{2Q}{\pi C_y C_z \bar{u} x^{2-n}} \exp\left(\frac{-h^2}{C_z^2 x^{2-n}}\right)$$

- (11) Maximum ground concentration and distance of maximum downwind of a continuous elevated source. $\partial x / \partial x = 0$.

$$x_{\max} = \frac{2Q}{\pi e \bar{u} h^2} \left(\frac{C_z}{C_y} \right)$$

$$x = \left(\frac{h^2}{C_z^2} \right) \frac{1}{2-n}$$

- (12) Correction for finite initial central concentration X_0 with Gaussian distribution. Substitute $\bar{u}t \neq (\bar{u}t)_0$ for $\bar{u}t$ in instantaneous source formulas and $x \neq x_0$ for x in continuous source formulas such that

$$(\bar{u}t)_0 = \left(\frac{Q/X_0}{\pi^{3/2} C_z^3} \right)^{2/3}$$

$$x_0 = \left(\frac{Q/X_0}{\pi C_y C_z u} \right)^{1/2}$$

If X_0 is a ground concentration, substitute $2Q$ for Q . $(\bar{u}t)_0$ and x_0 are distances of virtual sources, upwind of the real source, which would produce the given initial concentration X_0 at $\bar{u}t = x = 0$. All concentrations for $\bar{u}t < 0$ or $x < 0$ are fictitious.

- (13) Ground concentration downwind of a continuous ground source.

$$y = z = h = 0.$$

$$X(x) = \frac{2Q}{\pi C_y C_z \bar{u} x^{2-n}}$$

- (14) Axial concentration from a continuous elevated source, to be used in estimating maximum ground concentration resulting from downward deformation of the plume axis: substitute x' for x in formula (13), where x' is the minimum distance along the plume axis from the source to the point of measurement. For simple, large downdrafts of velocity \bar{w} , $x = h\bar{u}/\bar{w}$, and $x' = \sqrt{x^2 + h^2}$. For downdrafts in the lee of large buildings, $x' = x + h$. Such deformations would be expected

to be accompanied by extraordinarily large values of C_y and C_z . Situations of this type have probably produced the majority of the "least dilutions" reported by Church (Ref. 82), "eddy peak concentrations" reported by Gosline (Ref. 92) and "downwash" or "blowdown" concentrations reported by steam power plant investigators (Refs. 97 and 98).

- (15) "Fumigation" or trapping of material from a continuous elevated source in a shallow lapse or neutral layer surmounted by an inversion. Integrate (2) with respect to z from 0 to ∞ and distribute uniformly through depth h .

$$\bar{x}(x) = \frac{Q}{\sqrt{2\pi} C_y \bar{u} h x^{(2-n)/2}}$$

If the material being mixed downward has accumulated aloft during a period of stability, the values of C_y , \bar{u} and n should be those appropriate to the stable period.

- (16) Average concentration over a long period of time, from a continuous elevated source.

$$\bar{x} = \frac{2Qf}{\sqrt{2\pi} C_z \bar{u} x^{2-n/2}} \exp\left(-\frac{h^2}{C_z^2 x^{2-n}}\right)$$

where ϕ is the angular width of the sector over which the average concentration is measured. f is the wind direction frequency towards the sector ϕ during the sampling period.

- (17) Complete deposition ("fallout" or "rainout") of the trail downwind of a continuous elevated source.

$$\text{Deposition (gm./m.}^2) = \frac{Q}{\sqrt{2\pi} C_y \bar{u}_x^{(2-n)/2}}$$

The more complex case of partial deposition has been treated by Baron, Gerhard and Johnstone (Ref. 99).

- (18) Complete deposition ("fallout" or "rainout") at the center of the cloud downwind of an instantaneous source.

$$\text{Deposition (gm./m.}^2) = \frac{Q}{\pi C^2 (\bar{u}t)^{2-n}}$$

- (19) Correction for rise of cloud axis due to buoyancy and momentum at the source: substitute $h + \Delta h$ for h , where Δh is the increase in effective source height. Formulas for estimating these effects will be discussed in a later section.

- (20) Rise of a hot puff in a neutral atmosphere. Sutton gives:

$$\Delta\theta = \frac{Q}{2c_p \rho \bar{u}^2/2 C^3 Z^{3(2-n)/2}} \quad (\text{Ref. 95})$$

where $\Delta\theta$ = average temperature excess of cloud over environment.

Q = total heat released (cal).

c_p = specific heat of air at constant pressure.

ρ = density of air.

C = generalized diffusion coefficient, including effects of enhanced turbulence due to relative motion of the cloud and air; values of 0.3 to 0.6 $m^{1/8}$ were found by Sutton to give reasonable diffusion rates in the case of shell bursts and an atomic bomb test.

n = a stability index, taken by Sutton to be $\frac{1}{4}$ in all problems of this type.

This formula does not give any limit to the height of rise.

- (21) Rise of a hot puff in a stable atmosphere. As a first approximation, assume the potential temperature of the puff follows formula (20), while that of the atmosphere increases at a constant rate $\partial\theta/\partial z$. Equilibrium is reached when $\Delta\theta = z \partial\theta/\partial z$. Then,

$$z_{\max} = \left(\frac{Q}{2\sigma_p P T^{3/2} C^3 \partial\theta/\partial z} \right)^{0.276}$$

- (22) Vertical width of the visible plume from a continuous smoke source.

(a) Elevated source:

$$z = C_z x^{(2-n)/2} \left(\frac{\ln \frac{Q/M}{\sqrt{\pi} C_z u x^{(2-n)/2}}}{\sqrt{\pi} C_z u x^{(2-n)/2}} \right)^{\frac{1}{2}} \quad (\text{Ref. 88})$$

where z = vertical distance from plume axis to visible edge,

M = minimum visible smoke density per unit cross-section area in the line of sight ($gm./m.^2$), other symbols are defined as in formula (2).

(b) Surface source: double Q .

(23) Length of the visible plume from a continuous smoke source (viewed from one side).

(a) Elevated source:

$$x = \left(\frac{Q/M}{\sqrt{\pi} C_z \bar{u}} \right)^{\frac{2}{2-n}}$$

(b) Surface source: double Q.

6. Special Formulas for Radioactive Contaminants

(24) Decay correction. Multiply Q by $\exp(-0.693 t/T)$ for instantaneous sources and by $\exp(-0.693 x/\bar{u}T)$ for continuous sources, where T is the half-life in sec.

(25) Gamma exposure at the ground from a narrow trail of infinite length at a perpendicular distance r (m).

$$I \approx 180 (1 + b \mu r) e^{-\mu r E Q / \bar{u} r} \quad (\text{Ref. 84})$$

where I = gamma exposure rate in roentgens/hr.

μ = total absorption coefficient of air for gamma radiation
 $\approx 6 \times 10^{-3} \text{ m}^{-1}$ for energies between 0.05 and 4 Mev.

b = buildup factor due to back-scattering $\approx 4/7$ although experimental results have varied with the scale of the experiments.

E = Gamma energy in Mev.

Q = source emission rate (curie/sec.)

\bar{u} = wind speed (m./sec.)

r = h directly downwind.

Lowry (Ref. 100) has developed more involved gamma dosage formulas for a wide range of meteorological conditions.

7. Determination of Sutton's Concentration-Distance Index n

Sutton's original suggestion (Ref. 89) that suitable values of the parameter n could be determined from wind profiles by means of formula (3) has been modified considerably in his more recent writings and those of his co-workers (Ref. 74, 87). His tentatively recommended typical values, $1/5$, for large lapse, $1/4$ for neutral, $1/3$ for moderate inversion and $1/2$ for large inversion are representative of observations obtained under suitable conditions (similar to those at Porton), but even under very good observational conditions the reported values contain a wide scatter (e.g. Ref. 101). Over rougher surfaces these values of n are not even representative of the wind profiles, which, in general, do not closely follow a power law. But the most serious difficulty is that, except for the Porton test conditions, the values of n obtained from the wind profiles do not correspond properly to those representing the variation of concentration with distance from a source. Barad has shown (Ref. 102) that the behavior of a smoke plume from an elevated source during a strong inversion appears not to fit Sutton's generalized theory, and Sutton himself has recognized that the wind profile is more sensitive to surface irregularities than is the diffusion.

Both the general nature of the variation of the wind profile index with stability and the modifications mentioned by Calder (Ref. 74) and Sutton (Ref. 87) have been borne out, by and large, by the ~~Oak~~ Ridge observations despite the complex wind structure described in earlier sections of this

report. Many hundreds of determinations of n have been made, using data from all types of anemometers as well as from pilot balloons, with the following results.

a. At any value of the stability, as represented by the vertical temperature gradient, and in any layer within the lowest 500 ft., a scatter of values of n is obtained, ranging from 0 to 1.00.

b. Averages of large numbers of individual n values, grouped on the basis of stability or time of day, are generally higher than n values determined from ratios of average wind speeds, which, in turn, are generally higher than the values published by Sutton (Ref. 89). When the observations are grouped in narrow intervals of wind speed, of course, the results of the two methods approach each other.

c. Daytime observations, or observations obtained under neutral or lapse conditions, show more uniformity of n with height, i.e., closer conformity to a power law, than do night-time or inversion observations, in which n ordinarily increases with height. For example Table 48 gives values obtained from the wind speed profiles shown in Figs. 150 and 151. The nocturnal variation with height is not surprising in view of the shielding effect of the ridges, stagnation of air in the valley layer with enhanced shear above, and formation of shallow local slope breezes.

TABLE 48

n FROM AVERAGE WIND SPEED PROFILES

	<u>Day</u>	<u>Night</u>	<u>Average</u>
10 ft. to 40 ft.	0.3 - 0.4	0.3 - 0.7	0.3 - 0.5
25 ft. to 100 ft.	0.3 - 0.4	0.5 - 0.9	0.4 - 0.6
100 ft. to 400 ft.	0.2 - 0.5	0.8 - 0.9	0.5 - 0.7

d. No significant variation of n with wind speed is apparent. For example, Fig. 174-A and -B represent curves of n vs. temperature gradient in the layers 18 to 54 ft. and 18 ft. (station 001) to 140 ft. (station 012: 210 ft. above station 001 ground level) respectively. In each case average values of the wind speed at both levels have been obtained for narrow intervals of wind speed at one of the levels and of temperature gradient; the resulting values of n have then been averaged in somewhat larger intervals. Both graphs are based on contacting anemometer data. There is a slight tendency for the slope of the curves to decrease with increasing wind speed but this is masked by the irregularities and may not be significant. Again it can be noted that the difference between the shallower and deeper layer (showing deviation from a power law) is greatest in inversion conditions.

e. Values most nearly corresponding to those published by Sutton are obtained by means of contacting cup anemometers, in the lowest tens of feet above the surface. Fig. 174c, comparing the contacting cup anemometer with the cup-generator and heated-thermopile types in a restricted interval of 54 ft. wind speed, shows that, although closest agreement is found between

the latter two types, they give higher values than Sutton's. Fig. 174D, comparing smoothed average curves for the lower layer (roughly 50 ft.), the upper layer (roughly 200 ft.) and Sutton's values, shows that it is the lower layer which fits Sutton's profile parameter most closely. The Oak Ridge data most nearly resembling the Porton data, then, are those obtained under most nearly comparable conditions of observation.

f. Values of n have been determined from ratios of observed radioactivity at 1, 3 and $5\frac{1}{2}$ mi. northeast of the pile stack. Since the beta observations were unreliable with respect to stability of background and calibration, only gamma data were used. Nomograms were constructed from formulas (6) and (23) from which n could be read, given the wind speed, the gustiness (σ_v has been used to determine both C_y and C_z) and the concentration ratios. Observations for the period April 27-29, 1951, during which the instruments were functioning properly at all three distances, were used. Fifteen-minute average and peak radiation were obtained and grouped by wind speed and stability. Ratios of the average 15-min. exposure, average peak and extreme peak in each category, for only those observations which followed periods of wind direction $235-245^\circ$ by a suitable time lag depending upon the wind speed, were used to obtain values of n . The average range of values and number of observations in each category are shown in Table 49.

The tendency for n to increase with stability is very slight, but this is not surprising since the gamma radiation represents not the local concentration at the detector but an integrated concentration through some large

TABLE 49

n FROM DECREASE OF ATMOSPHERIC GAMMA RADIATION BETWEEN 1 AND 5 1/2 MI.
DOWNWIND OF THE PILE STACK, APRIL 27-29, 1951

<u>T₁₈₃ - T₅</u>	<u>2 mph</u>	<u>5 mph</u>	<u>10 mph</u>
0	---	---	0.32 ± 0.04 (2)
<0, /1	---	0.29 ± 0.05 (5)	---
/2 to /5	0.33 ± 0.09 (13)	0.28 ± 0.11 (5)	---
>/5	0.34 ± 0.09 (4)	---	---

volume (radius several hundred ft.). Thus, while the distant concentrations may be represented relatively well, those nearer the stack are overestimated in inversions and underestimated in lapse conditions. That is to say, the difference between inversion conditions, when the concentrated trail is aloft and the ground concentration near zero, on the one hand, and lapse conditions, when radioactivity is present at the ground but the cloud is broken up into small puffs, on the other hand, is smoothed out by the gamma observations. Nevertheless, it is gratifying to note that, when radioactive decay has been allowed for, the downwind concentration integrated through some volume near the ground falls off approximately as the inverse 1.66 to 1.72 power of the distance on the average. Since most of the cases represented in Table 48 fall in the "moderate inversion" category, this is in satisfactory agreement with Sutton's value of -1.67 for the exponent of x under these conditions, but differs significantly from the values of -1.3 to -1.6 which would be deduced from wind profiles in the appropriate layer. It is concluded that the use of Sutton's values or the

lower curve of Fig. 174D, relating n directly to the vertical temperature gradient, would be preferable to the use of wind profiles.

8. Appropriate Values of Sutton's Diffusion Coefficients C_x , C_y and C_z .

Using observed values of the gustiness and wind speed, and values of n derived from Fig. 174D, the generalized diffusion coefficients C_x , C_y and C_z can be calculated by means of formulas (4). The results of applying this method to the available Oak Ridge observations are summarized in Fig. 175. In extreme lapse conditions with light winds, higher values are observed than any shown in this figure, reaching 2.5 at 18 ft., 1.3 at 54 ft. and 0.5 at Pine Ridge (400 ft. above the valley). The three coefficients vary with wind speed and stability in the same general manner at the 18 ft. level, at which all three were observed, and the coefficient of transverse (crosswind) diffusion, C_y , shows a similar pattern at all levels at which wind vane observations were obtained. This pattern consists of a decrease of the coefficient with increasing thermal stability and with increasing wind speed, the latter variation being greatest under conditions of large lapse and light wind. At large wind speeds the coefficients tend to approach a common steady value, decreasing slightly with stability and altitude. Values of the coefficients corresponding to typical day, night and average conditions are given in Table 50, and the variation of C with height above the valley floor is illustrated by Fig. 176.

Sutton's published values (Ref. 89) are included in Fig. 176 for comparison. The two sets of data follow a common qualitative pattern: an approximately

TABLE 50

OBSERVED VALUES OF C_x , C_y AND C_z FOR TYPICAL CONDITIONS

Height above valley	18 ft.	54 ft.	230 ft.	420 ft.
Height above ground	18 ft.	54 ft.	154 ft.	80 ft.
Station number	001	001	012	019

a. Daytime (superadiabatic lapse: $n = 0.15$ to 0.20)

Wind speed, mph	5	6	8	9
C_x , $(m)^{n/2}$	0.27	0.25	0.15	-
C_y , $(m)^{n/2}$	0.34	0.28	0.22	0.21
C_z , $(m)^{n/2}$	0.23	-	-	-

b. Night-time (moderate inversion: $n = 0.30$ to 0.40)

Wind speed, mph	1	2	5	9
C_x , $(m)^{n/2}$	0.12	0.11	0.07	-
C_y , $(m)^{n/2}$	0.14	0.11	0.08	0.08
C_z , $(m)^{n/2}$	0.14	-	-	-

c. Average (neutral stability: $n = 0.25$)

Wind speed, mph	3	4	6	9
C_x , $(m)^{n/2}$	0.19	0.17	0.12	-
C_y , $(m)^{n/2}$	0.20	0.17	0.15	0.13
C_z , $(m)^{n/2}$	0.21	-	-	-

logarithmic decrease of C_y with height, with lapse values about $7/4$ times the average, and moderate inversion values $2/3$ times the average. The fact that the Oak Ridge values are somewhat larger than Sutton's, and increasingly so with height, is not at all surprising, since the three major

differences between the two sources of data would all favor such a departure: (a) the Oak Ridge observations represent 15-min. gustiness while Sutton's are based on 3-min. observations; (b) the Oak Ridge wind speeds are much less than those used by Sutton; and (c) the increased roughness at Oak Ridge, and particularly the effects of the ridges at the upper levels, would be expected to increase the gustiness and, with it C_y . Thus these two sets of data can be considered to be reasonably consistent with one another.

An attempt has been made to obtain an empirical check on the magnitude of C_z by calculating smoke plume widths by means of formula (21) and comparing with the observations previously discussed. Sherwood (Ref. 88) in presenting this special integration of Sutton's diffusion equation as an application to the theory of smoke screens, gives the minimum mass of oil smoke per unit area in the line of sight for screening as 0.33 gm./m.^2 . As a first approximation let us arbitrarily assume that 1/10 this concentration would define the visible edge of the cloud. (Only the order of magnitude is of importance in this calculation.) The average source strength of an 8-pound smoke pot entirely consumed in 12 min. would be 5 gm./sec. so that Q/M is approximately $150 \text{ m.}^2/\text{sec.}$ and $C_z(C_y$ is used as an approximation for C_z at stack level) can be obtained from Figs. 174 and 175 for the appropriate meteorological conditions. Table 51 and Fig. 177 summarize the results of such calculations.

Two main sources of difficulty could be anticipated in attempting such an

TABLE 51

CALCULATED AND OBSERVED SMOKE PLUME WIDTHS AT 400 FT.

T183 -T5	u	Surface			Stack		
		Z Calc.	Z Obs.	Z Obs. - Z Calc.	Z Calc.	Z Obs.	Z Obs. - Z Calc.
OF.	mph	ft.	ft.	ft.	ft.	ft.	ft.
-2	2-4	90	144	54	-	-	-
	5-7	56	128	72	-	-	-
	8-10	48	76	28	-	-	-
-1	0-1	140	136	-4	-	-	-
	2-4	64	116	52	45	100	55
	5-7	39	100	61	32	80	48
	8-10	34	92	58	25	120	95
	11-13	-	-	-	21	70	49
	14-16	-	-	-	16	60	44
0 to /3	0-1	73	116	43	55	50	-5
	2-4	33	84	51	28	80	52
	5-7	25	84	59	18	60	42
	8-10	-	-	-	16	70	54
	11-13	20	76	56	-	-	-
	17-19	-	-	-	12	60	48
A4	0-1	32	108	76	26	70	44
	2-4	16	72	56	11	70	59
	5-7	-	-	-	6	50	44

analysis: first, Q/M is not known, particularly for HC smoke, which probably adsorbs relatively large quantities of moisture and second, thermal and aerodynamic turbulence generated by the smoke source have not been taken into account. An error in Q/M would have to be very large in order to have a noticeable effect, since only the square root of the logarithm of this quantity enters into the formula. In order to account for the ratios of 2 to 5 between calculated and observed values, Q/M would have to be increased by a factor of roughly 10^2 to 10^6 , varying with wind speed in a manner contrary to that of the relative humidity, a necessary factor in hygroscopic adsorption. For an increase of only 1000 in Q/M , over 900 gal. of water would have to be added to the smoke in its first 400 ft. of travel during the 12-min. burning time, so that this source of uncertainty does not appear to be adequate to account for the observed discrepancies. However, since the differences between observed and calculated widths are nearly all about 40-60 ft. without any appreciable trend with wind speed or stability, the second factor, namely, enhancement of the meteorological diffusion due to the aerodynamic disturbance created by the source, may be the main cause of error. In fact, if 52 ft. are added to all the calculated widths to allow for this initial disturbance, the observed and calculated widths agree rather well on the whole.

This, of course, does not constitute an experimental verification of C_z , which could actually be much too small, with an error which increases with increasing wind speed and increasing stability (errors in n could easily produce this effect). On the other hand, there is a possibility

that C_z is of the proper magnitude, but that at this short distance the effect of the source disturbance is of a comparable magnitude. Unfortunately, the smoke trails were not reliably visible at greater distances. This question is an important one, since downwind concentrations are essentially proportional to the inverse square of the diffusion coefficient, so that a 40% error in C_z will result in a 2-fold error in the calculated concentration, whereas an error of a factor of 5 in C_z will result in a 25-fold error in the concentration.

9. Studies of Plume Rise

The height of rise of a stack gas plume depends upon the combined effects of "aerodynamic" turbulence induced in the wind stream by both the stack and the jet itself, and "meteorological" turbulence in dissipating the vertical momentum and buoyancy of the stack gases, and also upon the temperature stratification of the atmosphere. Many incomplete, oversimplified or empirical solutions to this complex problem have been published in recent years. Two formulas, containing both momentum and buoyancy terms, which have recently come into wide use, that of Bosanquet, Carey and Halton (Ref. 103) and that of Davidson (Ref. 104) based on Bryant's wind tunnel data, give results differing from one another by an order of magnitude when applied to specific problems. An empirical formula obtained by Rupp, Beall, Bornwasser and Johnson (Ref. 24) on the basis of wind tunnel experiments aimed at predicting the behavior of the X-10 Pile Cooling-air exhaust stream, recommends itself on the grounds of extreme simplicity, but takes into account only the momentum effect. In all the formulations,

the primary meteorological effect is a decrease of plume height with increasing wind speed.

Measurements of the apparent height of rise of the centerline of the smoke plumes emitted by both the X-10 Pile stack and the X-10 steam plant stack were made by means of the smoke photographs, with the sample restricted to up-and down valley directions (perpendicular to the line of sight). More careful observations of the same sort have been obtained by F. W. Thomas of the Tennessee Valley Authority, Division of Health and Safety, at the Watts Bar Steam Plant, about 40 mi. SW of the Oak Ridge area. (Ref. 105). The pertinent characteristics of the three stacks and their effluents are summarized in Table 52. The observed plume heights, plotted against wind speed, are shown in Fig. 178, together with curves representing the three formulas mentioned above.

TABLE 52

STACK AND EFFLUENT PARAMETERS

	<u>X-10 Pile</u>	<u>X-10 Steam Plant</u>	<u>Watts Bar Steam Plant</u>
Stack height	200'	180'	160'
Orifice diameter	5'9"	9"	14"
Exit velocity	45 mph	5 mph	34 mph
Exit temperature	180° F	400° F	350° F
Volume emission rate	110,000 cfm	27,200 cfm	300,000 cfm
Heat emission rate	8.3x10 ⁵ cal/sec	7.1x10 ⁵ cal/sec	66x10 ⁵ cal/sec

In each case, the curves of Bosanquet et. al. (curves 1, 2 and 3) lie above nearly all the observations forming an upper envelope, while those of Davidson-Bryant and Rupp et. al. fit only the lowest points,

the latter forming a rough lower envelope. While both the great disparities between the various theoretical predictions and the wide scatter of the observed points are discouraging, there is a definite downward trend of plume height with increasing wind speed. To test the applicability of a simple inverse relationship, the product $u\Delta h$ was computed for all the observations and averages obtained under various groupings. These averages are given in Table 53. The Rupp et. al. formula is a simple inverse relation in which the product $u\Delta h$ is a constant for each stack:

$$u\Delta h = 1.5 vd$$

where Δh is the height, measured above the orifice, at which the plume levels off.

v is the stack gas exit velocity

d is the diameter of the stack orifice.

This constant is also given in Table 53. It is clear that this formula gives only a part of the actual rise, which is not surprising since it does not take into account any buoyancy. The observed values of $u\Delta h$ do not show a marked systematic variation with wind speed, in comparison with the scatter, so that the mean value may be considered a constant of each stack, as a first approximation. The difference $u\Delta h - 1.5 vd$ has been plotted against the heat emission rate, Q_H , in Fig. 179.

Except for an error in the case of the X-10 Steam Plant observations which is greater than the standard error of this mean, the buoyancy component seems to be approximately $3 \times 10^{-4} Q_H$. The heat emission and stack gas velocity are much more accurately known for the X-10 Pile and the Watts Bar Steam Plant than for the X-10 Steam Plant, an error of a factor of

TABLE 53

PRODUCT OF PLUME HEIGHT (FT.) AND WIND SPEED (MPH)

	<u>X-10 Pile</u>	<u>X-10 Steam Plant</u>	<u>Watts Bar Steam Plant</u>
1-6 mph	610 (4 obs.)	483 (19 obs.)	2250 (69 obs.)
7-15 mph	780 (4)	441 (14)	3732 (24)
16-21 mph	417 (3)		
Lapse	574 (10)	480 (18)	3186 (42)
Inversion		421 (16)	2176 (51)
Mean	620 (11)	452 (34)	2632 (93)
Median	650	433	2000
10 percentile	120	22	0
Standard deviation	410	324	2950
Standard error of the mean	124	56	306
1.5 vd	390	68	720
$3 \times 10^{-4} Q_H$	249	213	1980

2 in the latter being not improbable.

It is seen from Table 53 that $u\Delta h$ is larger in lapse than in inversion conditions, some 10% at the X-10 steam plant and 50% at the Watts Bar Steam Plant. Thus the stability can be taken into account within the accuracy of the data by adding 10-20% to the mean in lapse conditions and subtracting a like amount in inversions. The first approximation formula for average conditions is, then:

$$(26) \quad \Delta h = \frac{1.5 \text{ vd} + 3 \times 10^{-4} Q_H}{u}$$

where Δh and d are in feet, u and v in mph, and Q_H in cal./sec.

The existence of such a simple inverse relationship between plume rise and wind speed would have interesting consequences with respect to the maximum concentration of stack effluent attainable at the ground. If the stack parameters are lumped in the constant $A = 1.5 \text{ vd} / 3 \times 10^{-4} Q_H$ (ft. x mph) $= 1.5 \text{ vd} / 4 \times 10^{-5} Q_H$ (m.²/sec.), the effective plume height above ground is

$$h / \Delta h = h / \frac{A}{u}$$

When this expression is substituted for h in Sutton's formula (11) for the maximum ground concentration from a continuous source (care must be taken to convert to the proper units), and the turbulence is assumed to be isotropic (approximately true for stacks more than 100 ft. high) so that $C_z/C_y = 1$, this formula becomes

$$\chi_{\max} = \frac{2Q}{\pi e} \frac{1}{u(h / \frac{A}{u})^2} = \frac{2Q}{\pi e} \frac{u}{(uh / A)^2}$$

This expression has a maximum at $u = \frac{A}{h}$, in contrast to the original formula, which gives concentrations increasing without bound as the wind speed approaches 0. This same result is obtained with the earlier formulas of O.F.T. Roberts (Ref. 106) and W. Schmidt (Ref. 107). The maximum possible ground concentration, in the absence of vertical deformation of the mean wind, is then:

$$(27) \quad \chi_{\max \text{ poss}} = \frac{Q}{2\pi e A h}$$

The critical wind speed, A/h , at which this concentration occurs is higher, the greater the jet velocity and buoyancy of the effluent, but the maximum

ground concentration is, of course, lower.

Sutton's maximum ground concentration formula can, of course, be maximized under other assumptions with regard to Δh . The Davidson-Bryant formula, for instance, is

$$\Delta h = \frac{(v)}{(u)}^{1.4} d(1 + \Delta T/T) = B/u^{1.4}$$

where ΔT is the excess of the stack gas temperature over ambient,

T is the stack gas temperature,

$$B = v^{1.4} d (1 + \Delta T/T).$$

The critical velocity in this case is:

$$u_{\text{crit}} = \left(\frac{1.8B}{h} \right)^{1/1.4}$$

and the maximum concentration attainable at the ground:

$$(28) \quad X_{\text{max}} \text{ pos } \frac{0.064 Q}{h^{1.3} B^{0.7}}$$

Such formulas permit the estimation of the minimum stack height necessary to dispose of a pollutant at a given rate while keeping the ground concentration always below some established tolerance level (X_{max}). From the inverse first-power formula, for instance:

$$(29) \quad h_{\text{min}} = \frac{Q}{277eAX_{\text{max}}}$$

Similarly, the stack draft and diameter can be found in terms of the other variables, but this would seem to be carrying the mathematical reasoning somewhat farther than the accuracy of the empirical formula justifies.

Quantitative Diffusion Observations10. Radioargon Concentrations

Since the emission rates of the many other radioisotopes discharged into the atmosphere are relatively small, variable and for the most part not accurately known, the quantitative analysis will be limited to that of the radioargon (A^{41}) from the X-10 Pile. It is hoped that the results will be capable of some generalization.

Two difficult problems must be solved before the observations can be compared with the theory. First, the radioactivity indications resulting from Pile argon must be separated from those due to other sources, and, second, the radiation dosage-rates recorded by the instruments must be interpreted in terms of the concentrations, sizes and locations of the clouds of radioargon producing them. Both problems are complicated by the fact that the beta counters were either excessively unstable or completely inoperative during most of the observation program.

In the qualitative discussion of the radioactivity traces, given in an earlier section, it was found that the indications of the radon monitoring instrument and of the standard Health-Physics constant-air-monitor showed no particular correlation with wind direction and therefore did not reflect the presence of Laboratory effluents to any appreciable degree. The gamma and beta-gamma count-rate-meter traces, on the other hand, contained essentially two parts: a relatively steady background radiation, and, added to it, numerous deflections, of various magnitudes, highly correlated with wind directions from the Laboratory towards the detectors. Only the gamma and beta-gamma records have therefore been

used in the study of the Pile argon.

Both beta and gamma records suitable for analysis were continuously available at all three distances for a three-day period, April 27-29, 1951, during which the wind was blowing from the stack towards the three measuring stations a considerable portion of the time, both day and night. Although deficient in strong lapse conditions, this period has supplied the best records for comparison of beta and gamma radiation. During the major part of the period September 1 - November 3, 1950, although the beta records were unreliable, fairly complete gamma records were available at two distances to the NE and one to the SW of the stack: this period has been used for a more critical study of the gamma records alone.

The beta and gamma records of April 27-29, 1951 will be discussed first since they furnish necessary links in interpreting the gamma observations and in verifying the theoretical predictions. The procedure has been as follows:

- (1) Gamma background levels were chosen, normally the lowest 15-min. average during each 24-hr. period. This value was ordinarily quite stable, that is, the recorded radiation returned to within a few chart divisions of this value whenever the wind was from a direction other than 220-260°. The gamma background was about 0.012 mr./hr. at station #1, 1.0 mi. NE of the stack, 0.011 mr./hr. at station #2, 3.1 mi. NE, and 0.026 mr./hr. at station #3, 5.4 mi. NE.

- (2) The average gamma minus background was recorded for each 15-min. period with wind direction 228° to 247° , following a suitable time lag $t = x/u$.
- (3) Fifteen-minute beta-gamma readings were obtained by a similar process except that beta background values were chosen on a shorter time-basis, since they fluctuated enough in a matter of hours to mask all the Pile-argon readings. This procedure was somewhat arbitrary, and two background values have been used, one high enough to eliminate nearly all non-Pile indications, the other low enough to eliminate nearly all negative readings.
- (4) The observed gamma radiation minus background was subtracted from the beta reading for each 15-min. period, and the remainder, presumably due to beta radiation alone, was converted to concentration of A^{41} in curie/m.³, assuming a uniform distribution within a few yards of the detector.

The concentrations obtained by this method, averaged by classes of wind speed and stability, are shown in Fig. 180, together with theoretical curves of "downwind" (centerline) concentration \bar{X} from formula (10) and average (20° sector) concentration $\bar{\bar{X}}$ from formula (16), with appropriate corrections for plume height and radioactive decay. All parameters have been determined on the basis of local observations as discussed in the preceding paragraphs, and are given in Table 54. Generally speaking, the average values tend to follow the $\bar{\bar{X}}$ curve as to order of magnitude, while the highest observations lie between the $\bar{\bar{X}}$ and \bar{X} curves. It is

TABLE 54

PARAMETERS FOR CONCENTRATION AND EXPOSURE CALCULATIONS

$T_{183} - T_5$ OF.	n	\bar{u}_{154} mph	Δh m	\bar{u}_{plume} m./sec.	σ_v deg	C_y (m) ⁿ /2
-1 and 0	0.25	1	189	0.6	11	0.14
	0.25	2-4	63	1.5	13	0.14
	0.25	5-7	31	2.9	10	0.11
	0.25	8-10	21	4.3	10	0.10
	0.25	11-15	15	6.2	10	0.095
.1 to .5	0.33	1	170	0.6	5	0.068
	0.33	2-4	57	1.6	8	0.077
	0.33	5-7	28	3.0	7	0.065
	0.33	8-10	19	4.4	7	0.057
	0.33	11-15	13	6.3	7	0.055
	0.33	16-20	9	8.6	7	0.052
≥ .6	0.50	1	151	0.7	10	0.074
	0.50	2-4	50	1.7	7	0.047
	0.50	5-7	25	3.2	7	0.039
	0.50	8-10	17	4.7	7	0.035
	0.50	11-15	12	6.6	7	0.032
	0.50	16-20	8	9.0	7	0.029

$$Q = 5.6 \times 10^{-3} \text{ curie/sec.}$$

$$h = 61 \text{ m.}$$

$$\theta = 30^\circ$$

$$f = 1.00$$

$$E = 1.3 \text{ mev}$$

$$T = 110 \text{ min.}$$

$$\mu = 6 \times 10^{-3} \text{ m}^{-1}$$

interesting to note that at 1 mi. the observed concentrations fall off sharply with increasing stability, while at 3.1 mi. the highest concentrations occur with moderate stability, as predicted by theory. At 5.4 mi. the observed values are too low to be taken very seriously, in view of the uncertain background, but are apparently of the same order of magnitude as the theoretical average concentration. A tendency for the

observed concentrations to increase with wind speed somewhat more than predicted could well be due to errors in Δh . From these scattered observations it can only be said that the theoretical downwind concentration X is apparently a rough upper limit to the 15-min. average, and the average concentration over the 20° wind direction sector within which all observations were accepted approximates the observed averages within the error of measurement. A possible exception occurs in the stable cases at 1 mi., where significantly higher concentrations were observed than predicted; however, since general Laboratory wastes were not eliminated in this analysis, it is not surprising to find some low-level contamination near the source in stable conditions. It should be noted that the kinematic (molecular) viscosity has been employed in calculating C_y . From this it appears that the use of observed gustiness values instead of those published by Sutton provides the increased dilution necessary to account for the observed concentrations in rough terrain without the use of the macroviscosity. This would be a desirable feature since the macroviscosity can, at present, only be computed in the neutral case. The gamma readings were likewise converted to concentrations on the assumption of uniform distribution throughout the space above the level of the detector. The ratio of the relatively realistic concentration indicated by beta radiation to this fictitious gamma concentration can be interpreted in terms of the size and location of the radioactive argon cloud, as has been shown in an earlier paragraph. The average ratios, by stability and distance, together with the cloud radius which they imply, are given in Table 55.

TABLE 55

BETA/GAMMA RATIOS AND CLOUD RADIUS

<u>T₁₈₃ -T₅</u> <u>°F.</u>	<u>1.0 mi. NE</u>			<u>3.1 mi. NE</u>			<u>5.4 mi. NE</u>		
	<u>Beta/</u> <u>Gamma</u>	<u>Radius</u> <u>Ft.</u>	<u>No. of</u> <u>Obs.</u>	<u>Beta/</u> <u>Gamma</u>	<u>Radius</u> <u>Ft.</u>	<u>No. of</u> <u>Obs.</u>	<u>Beta/</u> <u>Gamma</u>	<u>Radius</u> <u>Ft.</u>	<u>No. of</u> <u>Obs.</u>
≤ -2	20.6	67	1	-	-	0	-	-	0
-1 and 0	4.4	96	13	2.6	440	10	2.0	570	3
+1 to +5	0.3	remote	25	1.1	1000	28	0.2	remote	15
≥ +6	0.3	remote	10	0.0	remote	9	0.1	remote	6

Confirming the evidence presented previously in the discussions of qualitative diffusion behavior and of the parameter n , the gamma-deduced concentration is seen to be too low in lapse and neutral conditions and too high in inversion conditions. This behavior is readily accounted for as follows: the trail is highly irregular in lapse and neutral conditions, relatively narrow portions passing across the detector giving large beta and small gamma readings, and these puffs become broader with increasing distance; in inversion conditions, on the other hand, the trail is mainly aloft at all distances, giving very little beta radiation in proportion to the gamma. The gamma observations of the period September 1 - November 3, 1950, then, should not be interpreted in terms of concentration, unless multiplied by the ratios in Table 55, which are not considered sufficiently reliable for such an analysis to have much validity.

11. Radioargon Gamma Dose-Rate

By means of formula (25), the gamma observations can be compared with the theoretical gamma radiation from a line of A^{41} at the height of the plume

axis. Before making this comparison, an attempt was made to eliminate diurnal and other general background fluctuations as well as general Laboratory air contamination other than from the Graphite Pile. This was done by the following procedure:

- (1) The background radiation was defined for each 24-hour period at each station as the lowest 15-min. average for that period at that station. This background varied in the range 0.01 to 0.02 mr./hr.
- (2) Fifteen-minute averages of gamma minus background were read off the charts for all periods following by suitable time lags ($t = x/u$) periods of wind direction towards the detector from the stack, plus or minus 15° . Since stations were located both NE and SW of the stack, upwind readings were also obtained for each period.
- (3) Observations were grouped and averaged according to station, wind direction, Pile emission rate, stability ($T_{183} - T_5$) and wind speed (154 ft. station 012).
- (4) Average upwind readings in each category were subtracted from the corresponding downwind averages.
- (5) Pile-off readings were subtracted from Pile-on readings by meteorological categories.

The number of 15-min. observations at one or more stations by categories are shown in Table 56.

The results, for Pile emission rates 5-6 mc./sec., are plotted in Fig. 181, in units of 10^{-6} roentgen (microroentgen, μr) per hour. Curves of theoretical dose rate with the gas trail directly overhead ($r = h / \Delta h$), halfway

TABLE 56

NUMBER OF GAMMA OBSERVATIONS, SEPT. 1 - NOV. 3, 1950

Wind Speed (mph)	Lapse (≤ -2)	Neutral (-1 and 0)	Inversion ($\neq 1$ to $\neq 5$)	Lapse (≤ -2)	Neutral (-1 and 0)	Inversion ($\neq 1$ to $\neq 5$)
1	0	0	11	0	35	90
2-4	2	17	13	10	80	80
5-7	10	25	5	20	50	38
8-10	4	9	0	18	25	8
11-15	4	1	0	17	33	0
16-20	4	2	0	7	12	0

between the center and edge of the wind direction sector used

($r^2 = [h \neq \Delta h]^2 \neq x^2 \tan^2 7\frac{1}{2}^\circ$), and at the edge of the sector

($r^2 = [h \neq \Delta h]^2 \neq x^2 \tan^2 15^\circ$) are shown for comparison. It should be men-

tioned that average negatives values as large as 2 ur/hr. occurred in some categories after the subtractions were made, indicating excesses of upwind over downwind or Pile-off over Pile-on concentration. This value can be considered the probable error due to fluctuations of calibration and background or errors in timing. The April 27-29 gamma data, obtained without this filtering system, are also plotted for comparison.

Average 15-min. dose-rates never approach the theoretical values derived on the assumption that the line source is directly overhead. However, the highest 15-min. averages tend to agree with or exceed slightly those

calculated on the assumption of a $7\frac{1}{2}^\circ$ deviation of the wind direction from the detector axis while the averages of many such observations within a 30° wind sector centered on the station appear to fall between the $7\frac{1}{2}^\circ$ and 15° deviations. Stability seems to have only a slight systematic effect, lapse conditions giving somewhat higher exposures than inversions at the 1.0 and 1.4 mi. stations. The predicted decrease of gamma dose-rate as the wind speed decreases below about 5 mph, reflecting the effect of increased plume height is borne out by these observations. Little difference is noted between the carefully filtered observations of the fall period and the raw gamma minus background of the spring period: the upwind and pile-off readings, which commonly reached 5 ur/hr. and occasionally 7-8 ur/hr. were still a minor part of the observed excess of gamma radiation above the 24-hour background, the major contribution being that of the Pile radioargon. Still, this major contribution when averaged over 15-min. intervals, is only equal to the natural background radiation (10-20 ur/hr.). Peaks of short duration (the resolving time of the recorder is of the order of 1-2 min.) have reached 26 ur/hr. at 1.0 mi., 21 ur/hr. at 1.4 mi., 13 ur/hr. at 3.1 mi., and 5 ur/hr. at 5.4 mi. all but the last approaching within about 40% of the theoretical value directly beneath the plume.

In summary, considering the uncertainties in both the choice of parameters in the theoretical equations and the interpretation of the observations, the concentrations of A^{41} averaged over a moderate number of observations of average 15-min. beta radiation agree as well as could be expected with the values obtained by averaging Sutton's equation over the appropriate

wind direction sector, while the highest of these 15-min. averages approach the theoretical "downwind" or "centerline" concentrations. The concentration close to the stack (1 mi.) decreases with increasing stability while that farther away (3 mi.) increases at moderate inversion intensities, then decreases; the average 15-min. gamma exposure, on the other hand, shows only a slight effect of stability, being fairly well approximated under all conditions by assuming a line source of radiation at plume height, which makes an average angle at the stack of $7\frac{1}{2}$ to 15° with the direction of the detector. Under moderately stable conditions with wind speeds of 5-10 mph, the ground concentration at 3 mi. exceeds that at 1 mi. in spite of radioactive decay; the gamma radiation, on the other hand, decreases with increasing distance under all conditions. The heat and momentum of the stack jet appear to be effective in preventing the occurrence of prolonged high concentrations or exposures in light winds, in much the same manner as can be deduced by substituting the effective plume height, determined from smoke observations, for the physical stack height in the formulas.

570

INVERSION (STABLE)

($T_{183} - T_5 > 0$)



0-1 mph.



2-4 mph.



5-7 mph.

no observations

8-10 mph.

NEUTRAL

($T_{183} - T_5 = 0$ or $-1^{\circ}F$)



LAPSE (UNSTABLE)

($T_{183} - T_5 < -1^{\circ}F$)



Fig. 167 Selected photographs of surface smoke trails, station 001, looking SE from "A2" theodolite position, with ENE or NE winds, arranged by stability ($T_{183} - T_5$, station 012) and wind speed (18 ft. contacting anemometer, station 001).

571

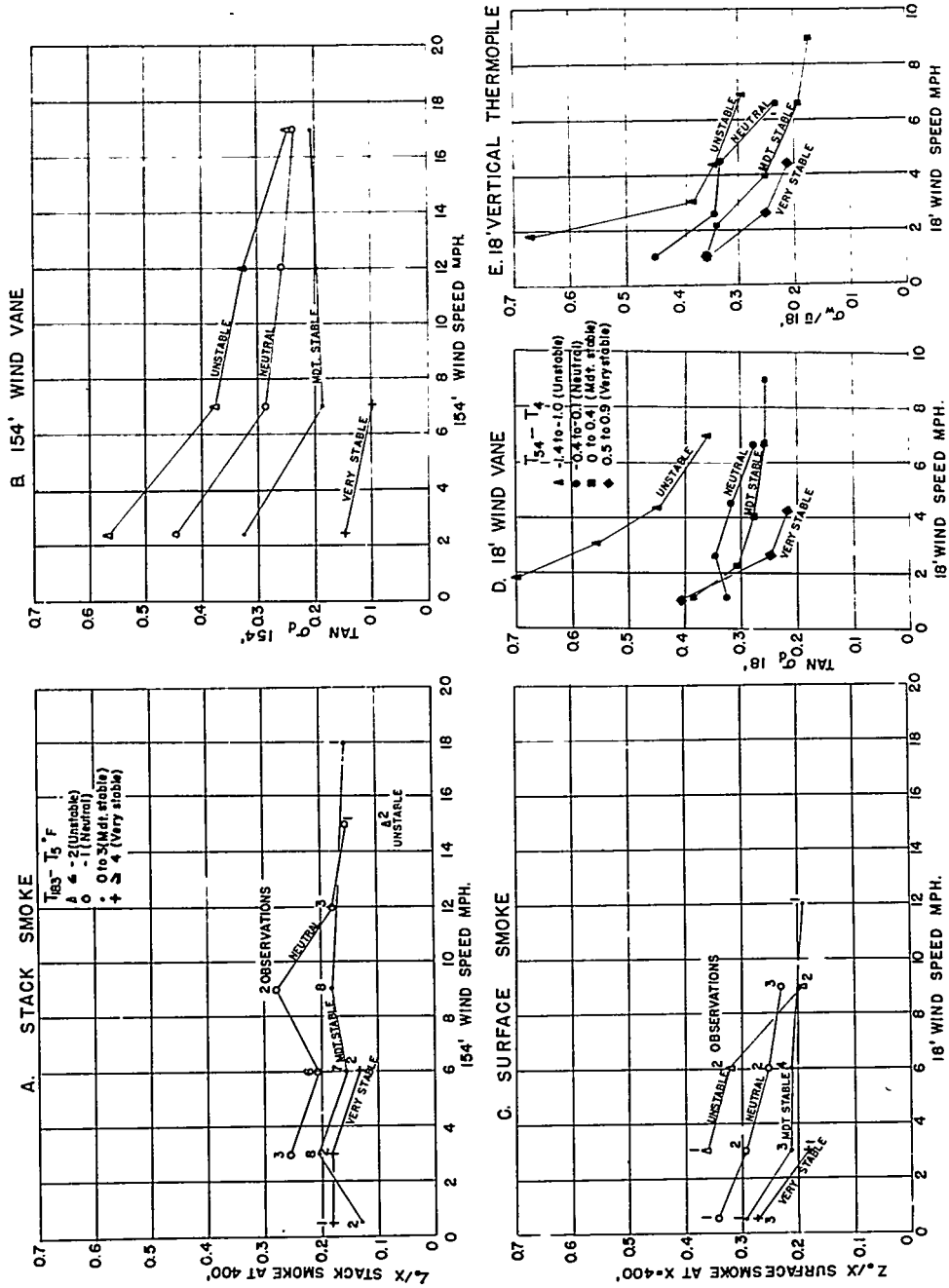


Fig. 168 Ratio of vertical half-width (Z_0) of surface and stack smoke plumes to length (x) at approximately 400 ft. along the plume, obtained from photographs and averaged by wind speed and stability groups, compared with similarly averaged observations of vertical gustiness (σ_w/u from vertical and horizontal airmeter probes) and lateral gustiness ($\tan \sigma$ from wind vane).

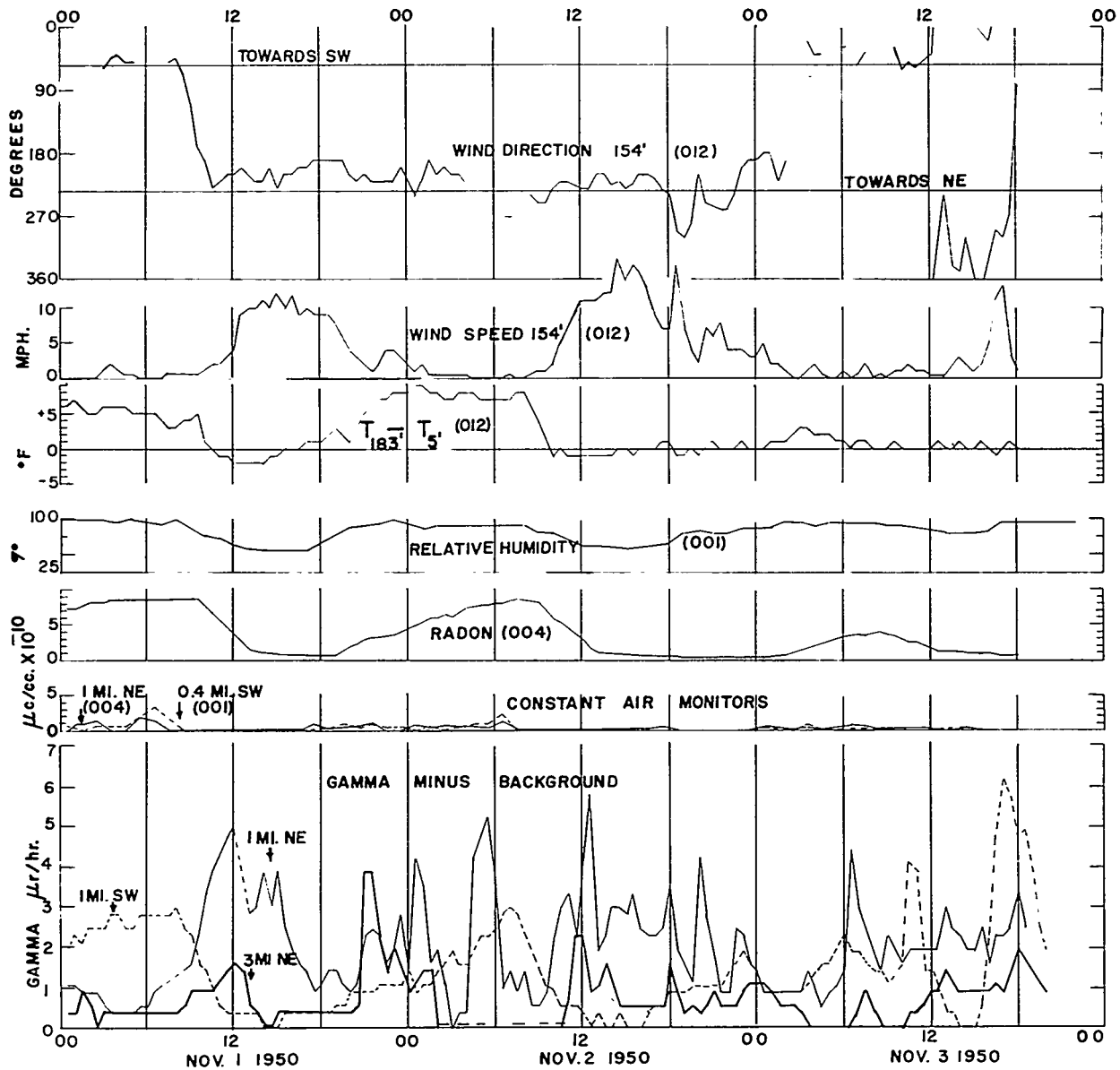


Fig. 169 Typical 3-day sequence of half-hourly radioactivity and meteorological observations. Top to bottom: 154 ft. wind direction, 154 ft. wind speed, $T_{183} - T_5$, 4 ft. relative humidity, radon (alpha) concentration (units of 10^{-10} curie/ m^3), beta-gamma particulate concentration at 0.4 mi. SW and 1 mi. NE of pile stacks (units of 10^{-10} curie/ m^3) and incident gamma radiation above daily minimum ("background") at 1 mi. and 3 mi. NE and 1 mi. SW of pile stack (units of 10^{-6} roentgen/hr).

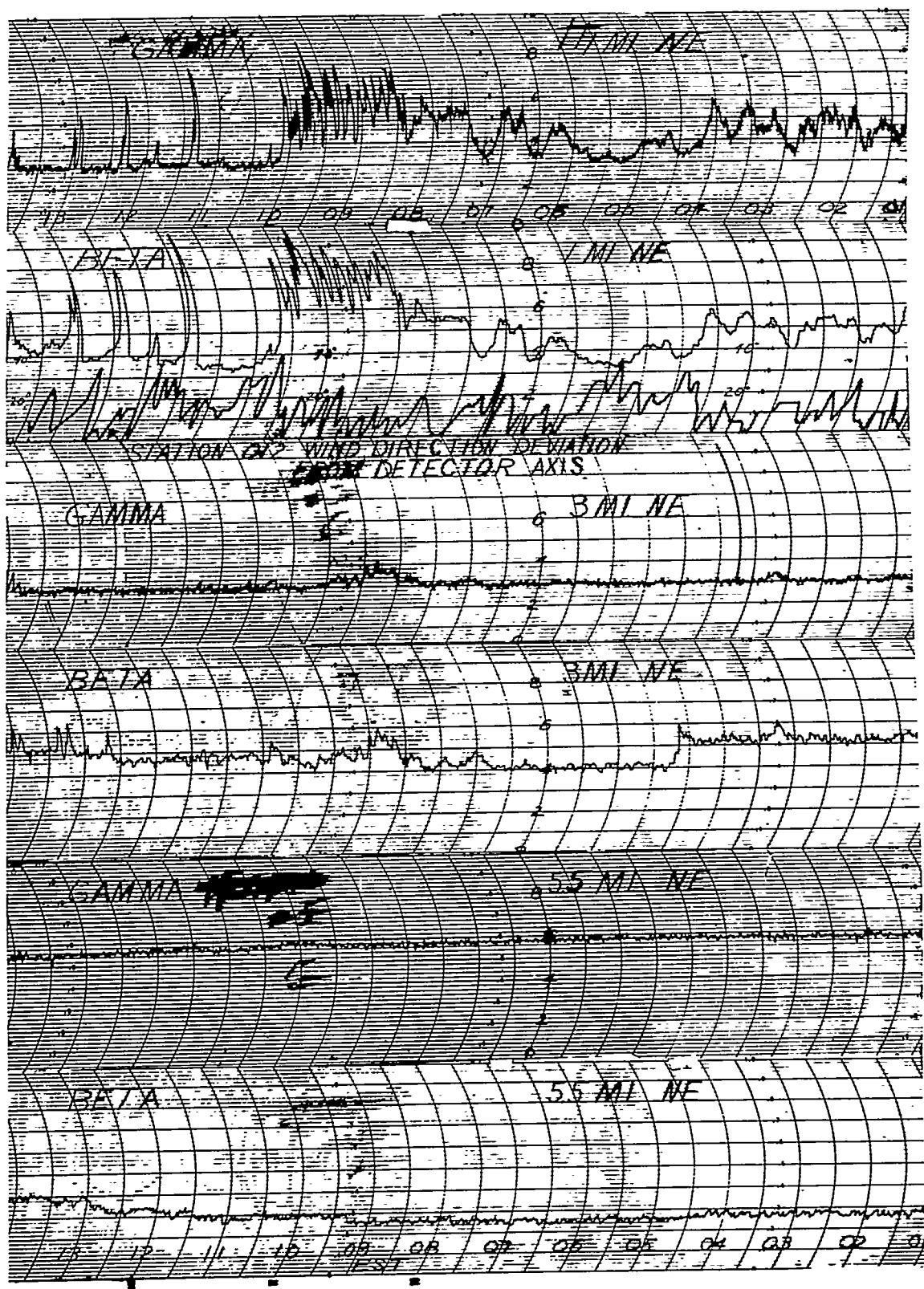


Fig. 170 Beta and gamma count-rate-meter traces at 1, 3, and 5 1/2 mi. NE of the Pile stack (arbitrary prints, not uniform), April 29, 1951, 1 a.m. to 1 p.m., with prevailing SW winds. Graph of 4-min. average departure of wind direction from detectors added for comparison.

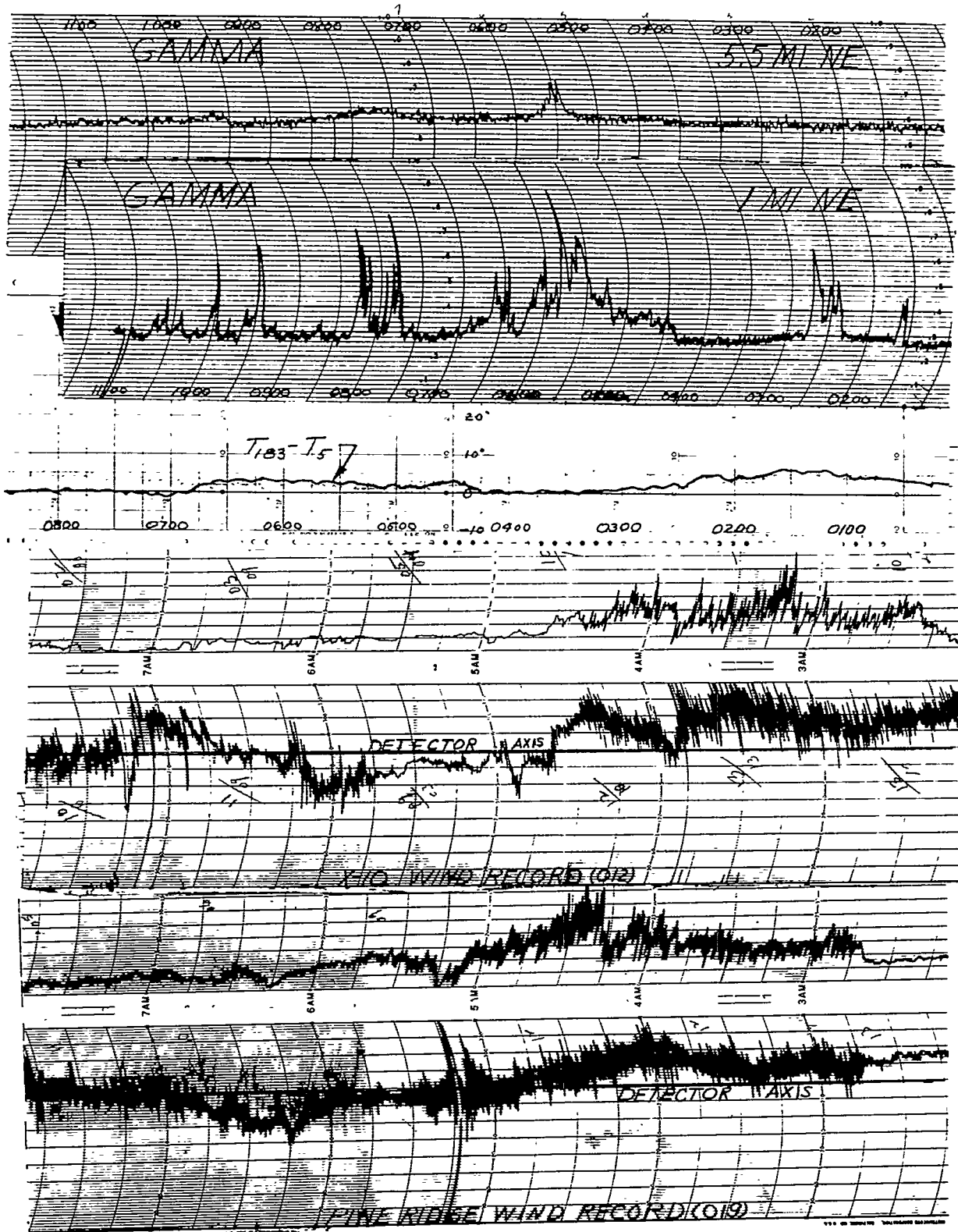


Fig. 171 Gamma traces at 1 mi and 5 1/2 mi and wind direction and speed at stations 012 and 019, May 4, 1951, 2-8 a.m.

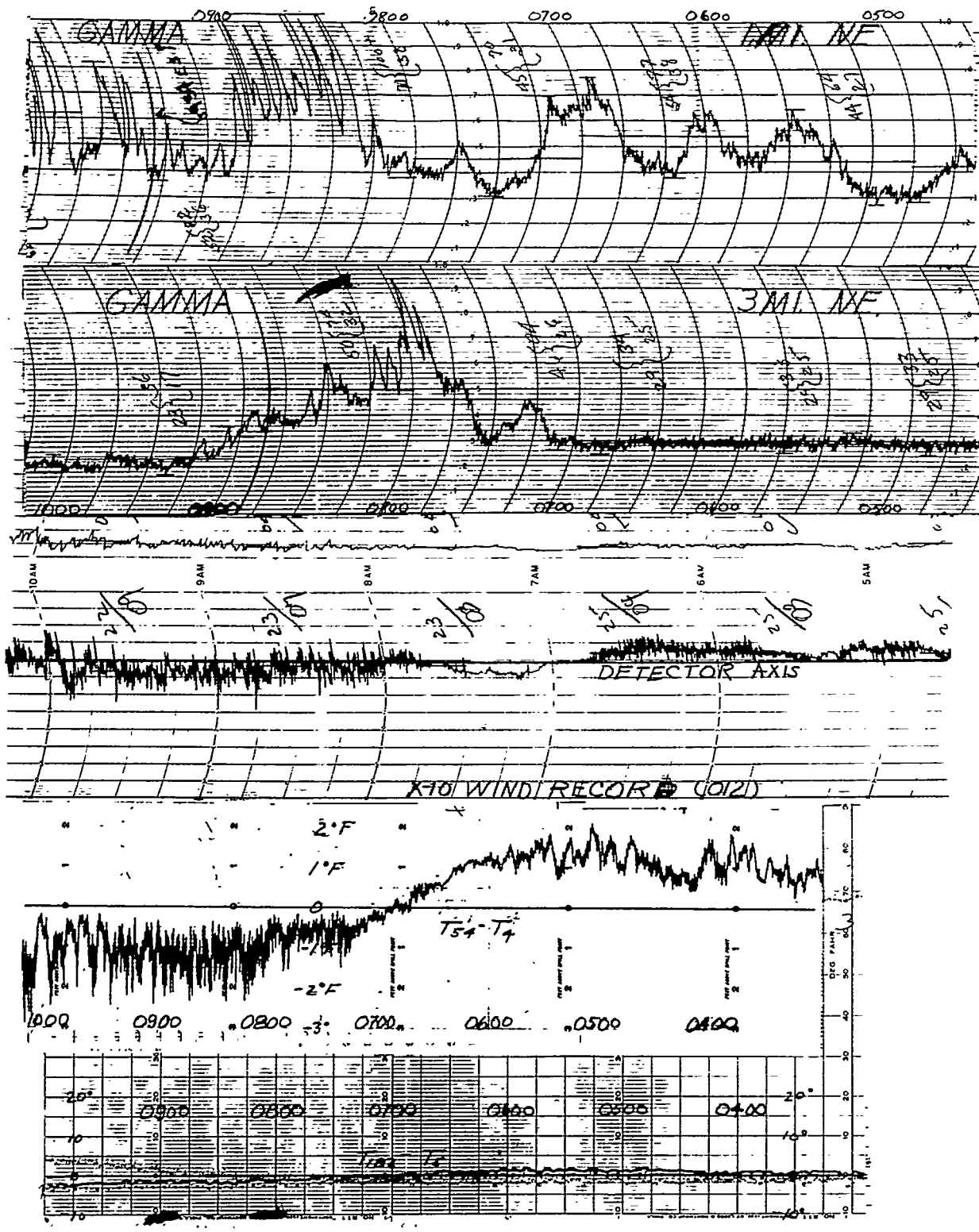


Fig. 172 Gamma traces at 1 and 3 mi, wind speed, and wind direction at station 012, $T_{54} - T_4$ (station 001) and $T_{183} - T_5$ (station 012), Aug. 2, 1950, 5-10 a.m.

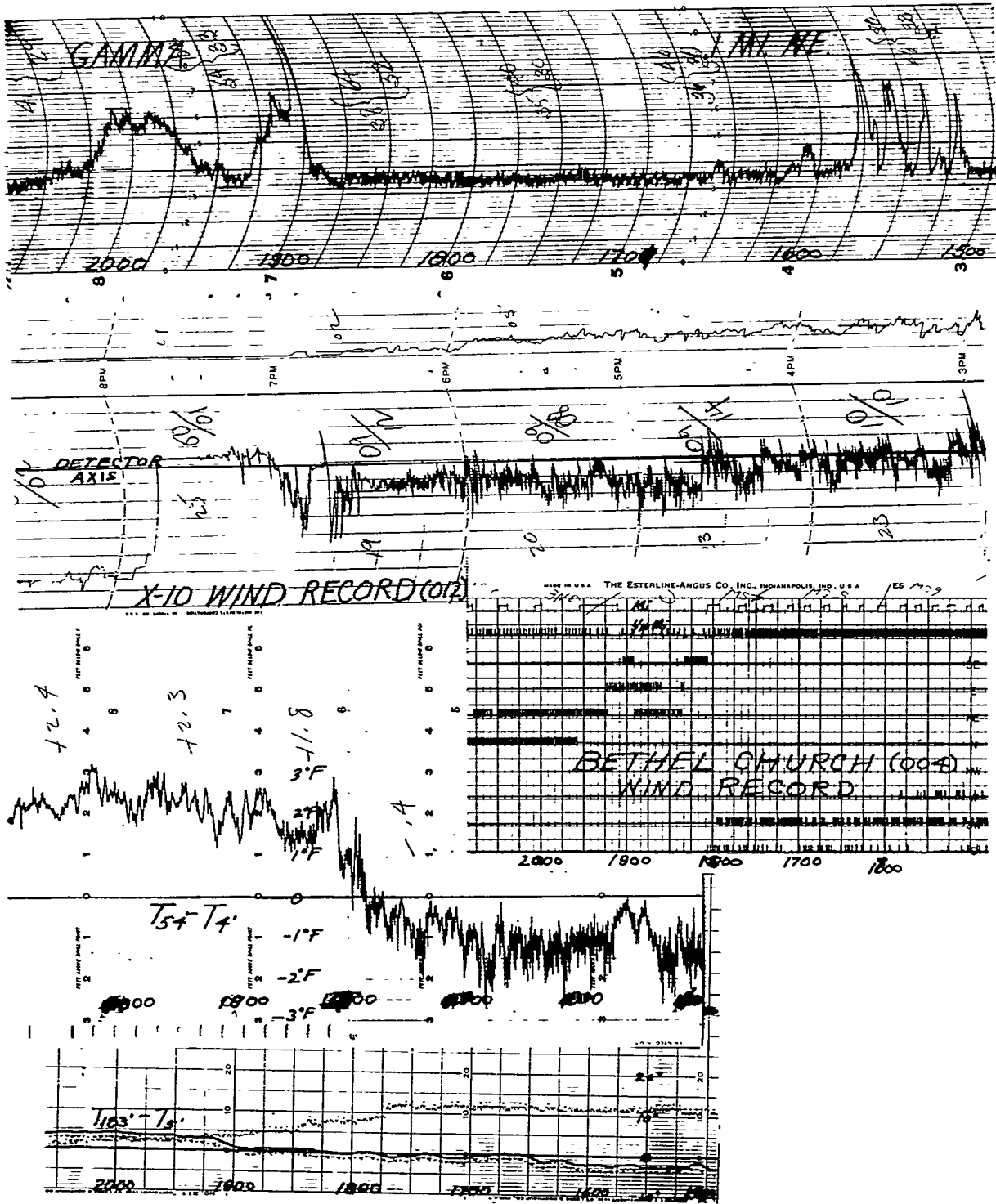


Fig. 173 Gamma trace at 1 mi, wind direction and speed at stations 012 (151 ft) and 004 (18 ft contacting, 1 mi NE of stack), T54-T4 (station 001) and T183-T5 (station 012), Aug. 8, 1950, 3-8:30 p.m.

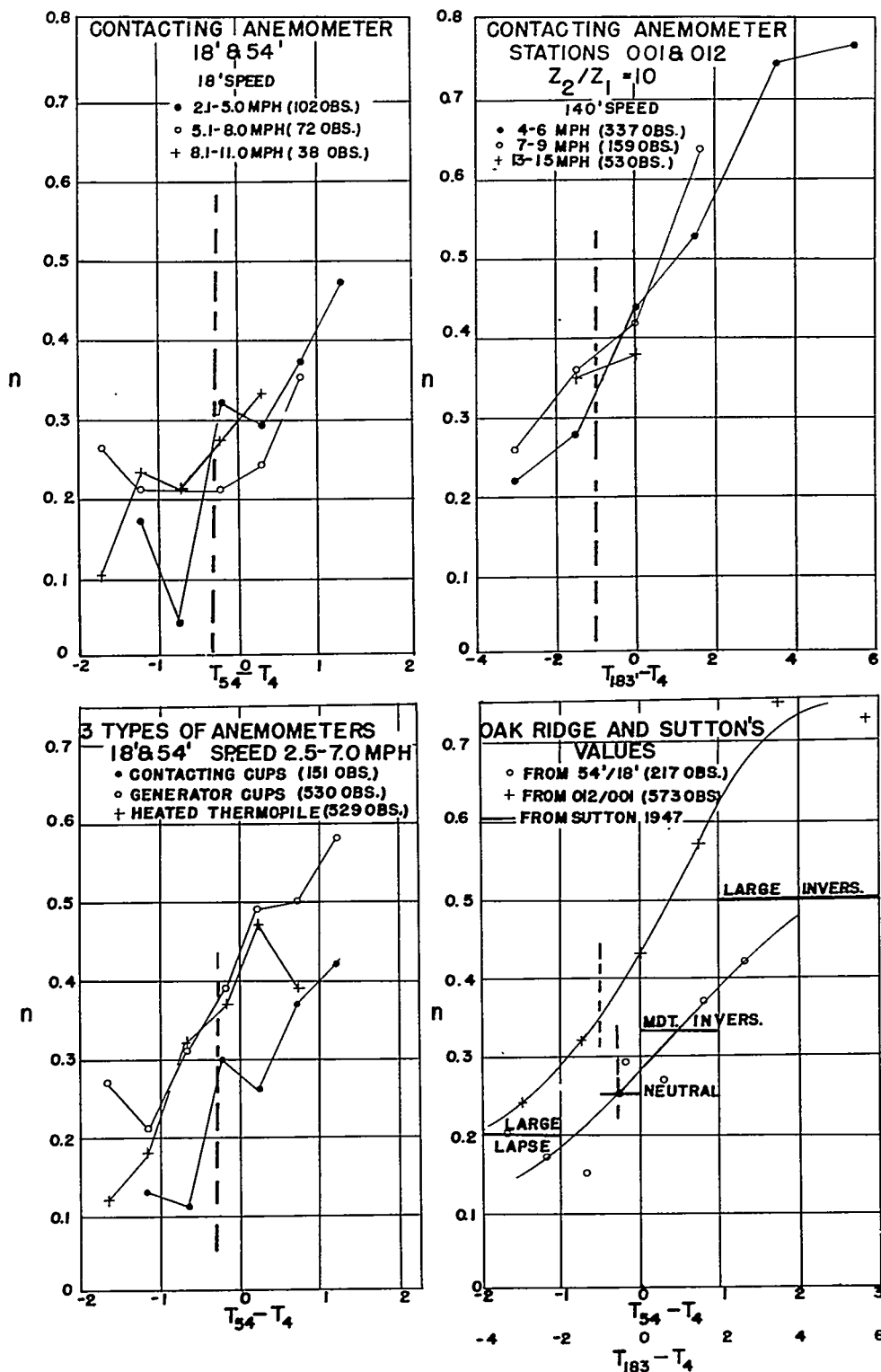


Fig. 174 Sutton's parameter n vs. stability, by wind speed, altitude and instrument type.

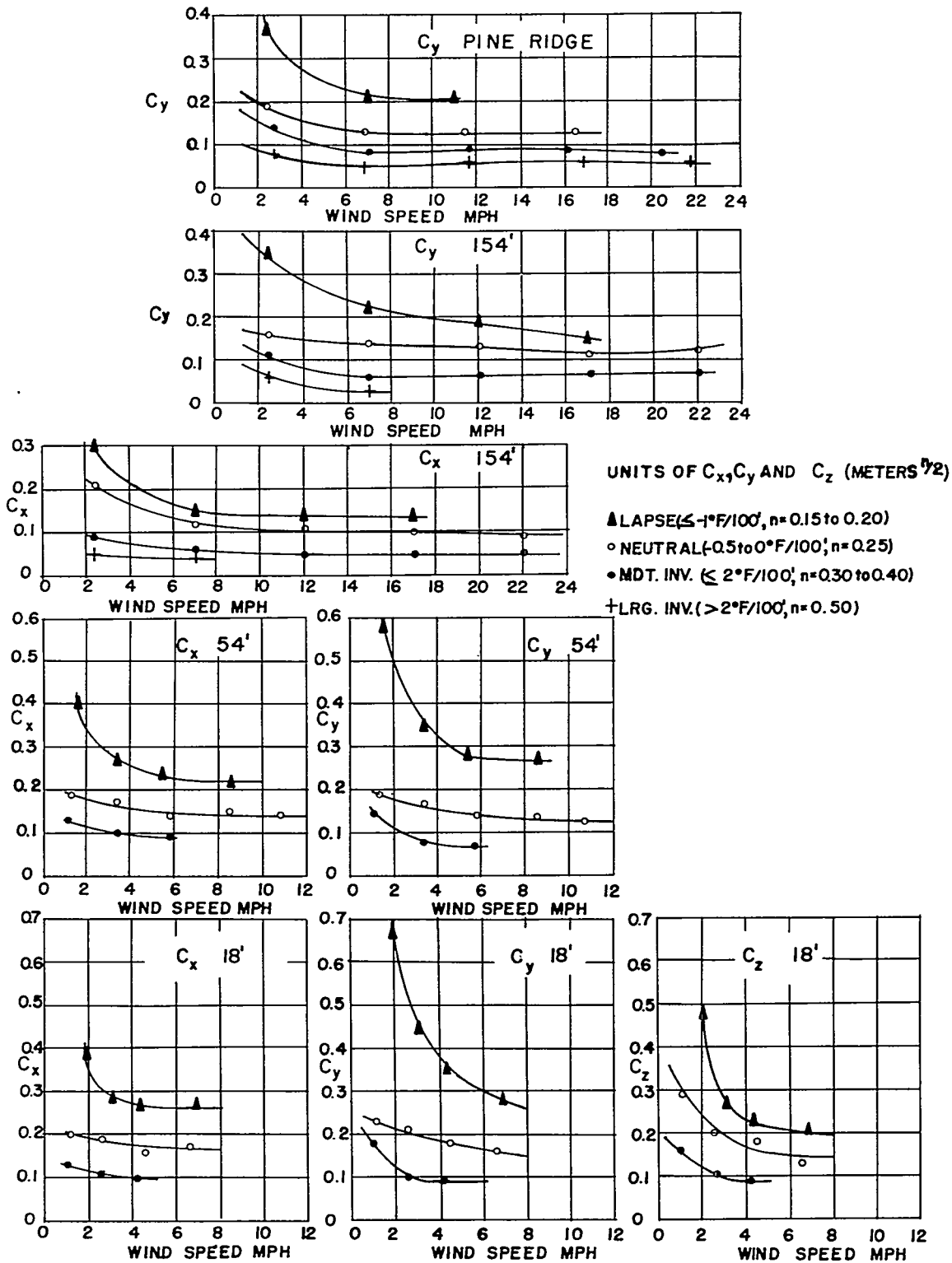


Fig. 175 Observed C_x , C_y , and C_z vs. wind speed and stability.

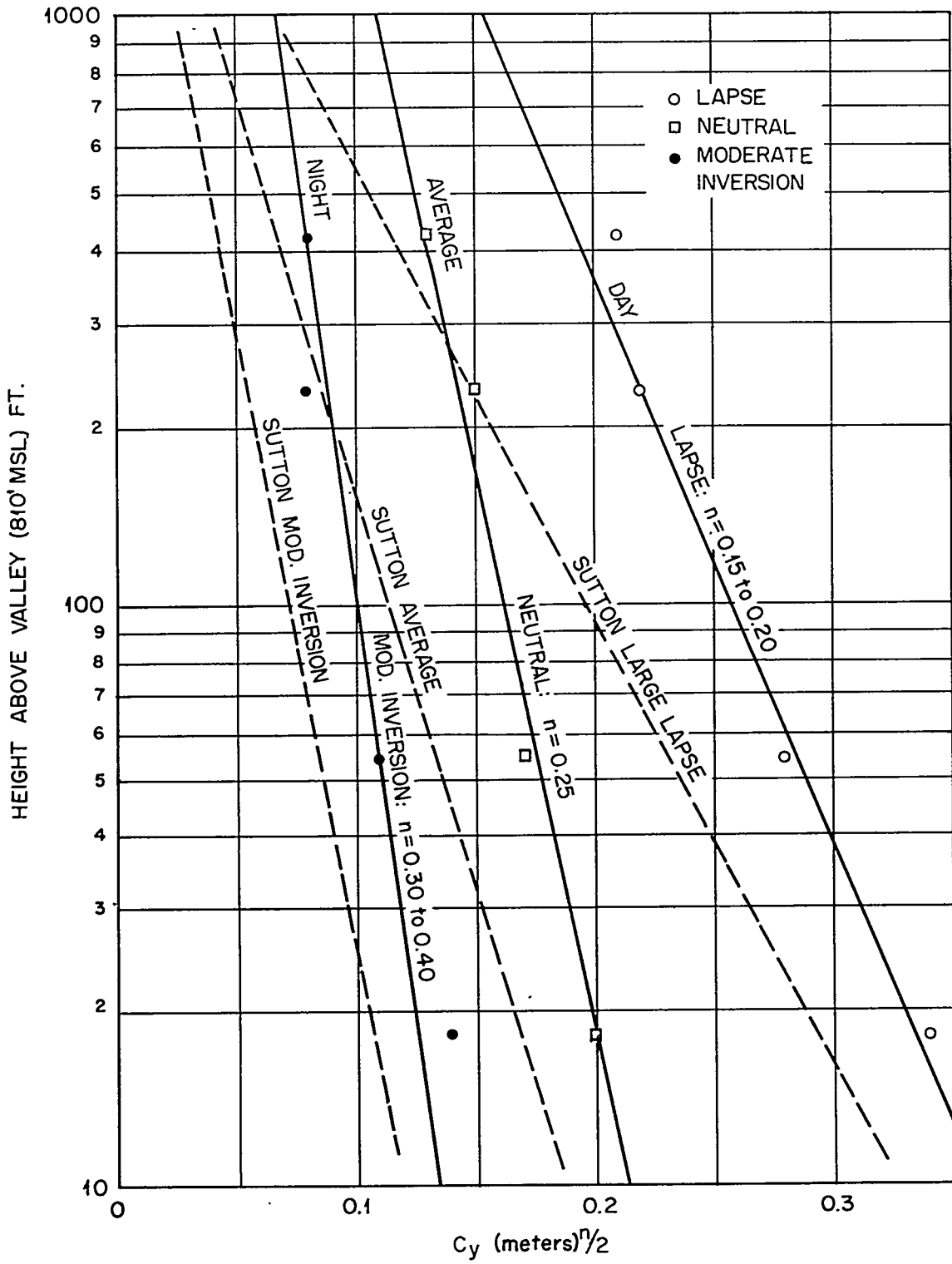


Fig. 176 Variation of C_y with height.

580

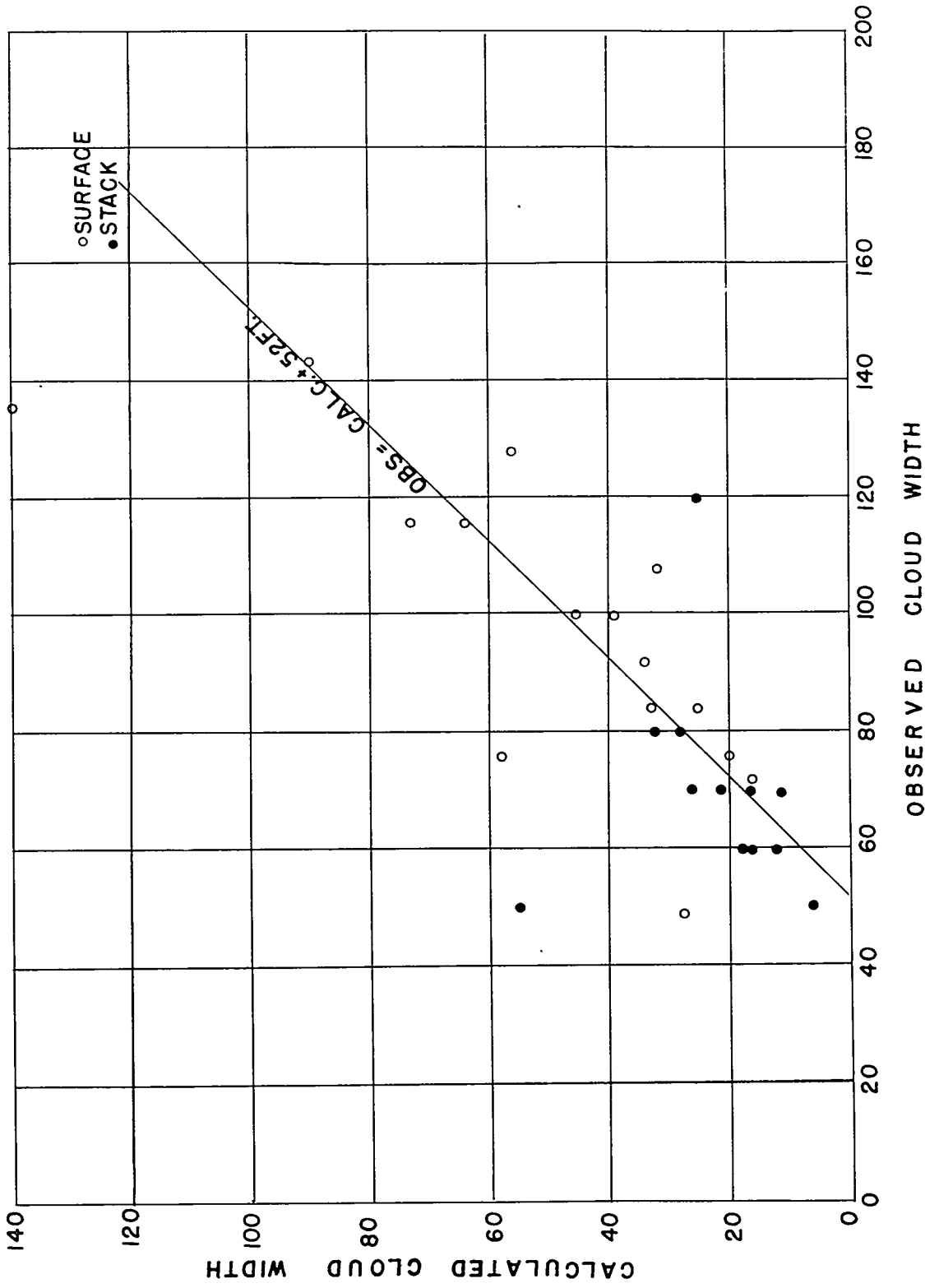


Fig. 177 Observed vs. calculated smoke plume widths at 400 ft.

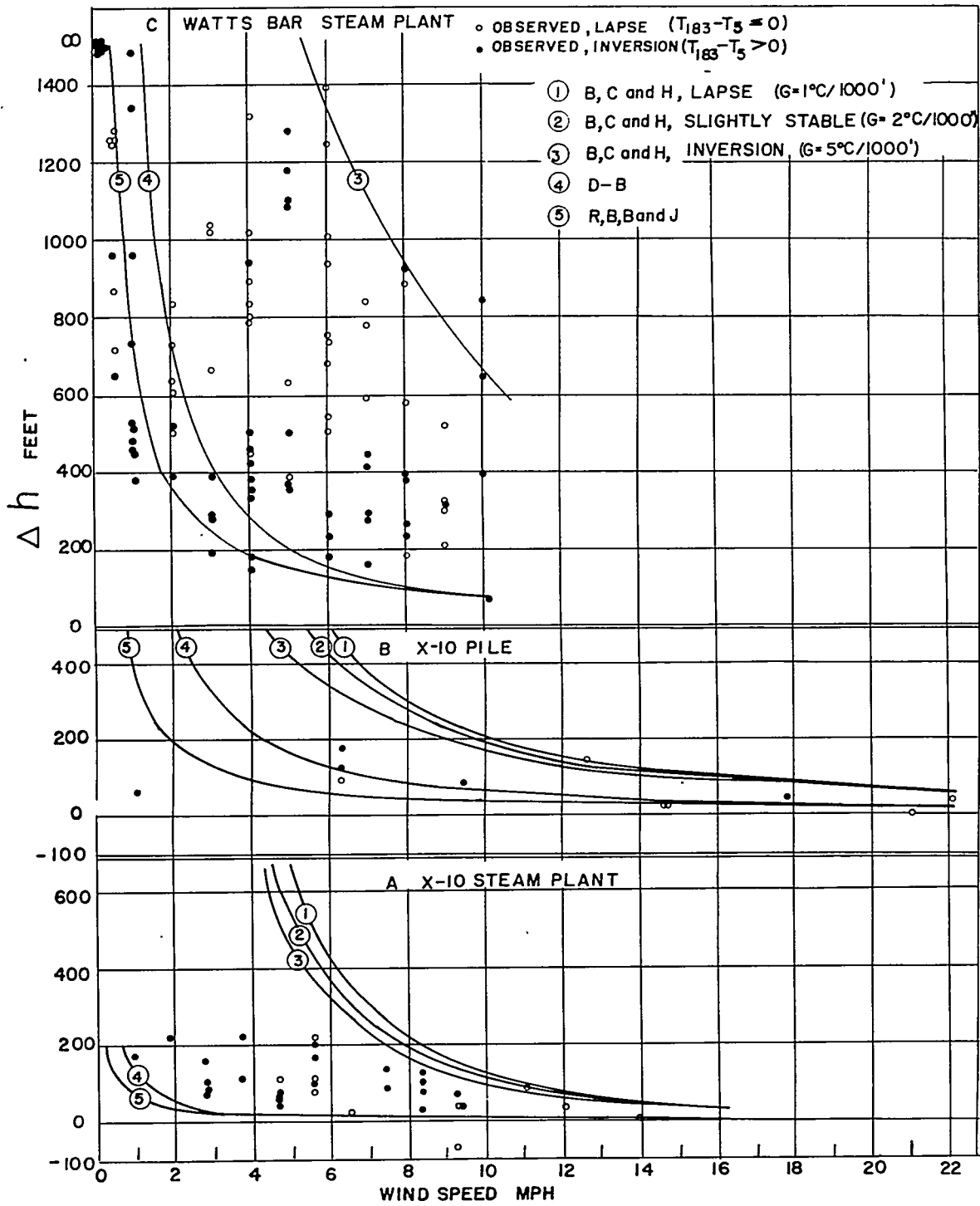


Fig. 178 Observed and calculated plume heights.

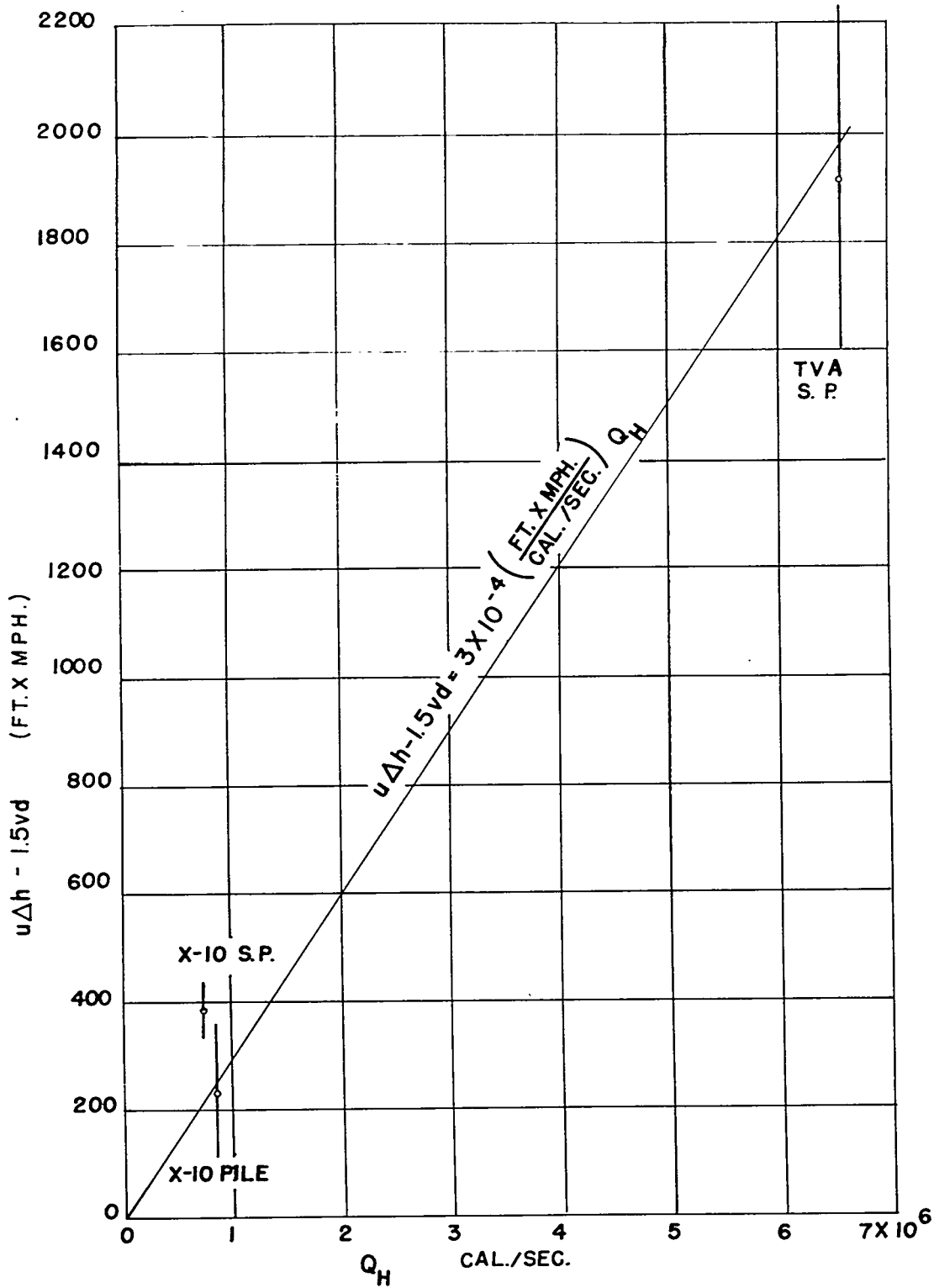


Fig. 179 Thermal component of plume rise.

583

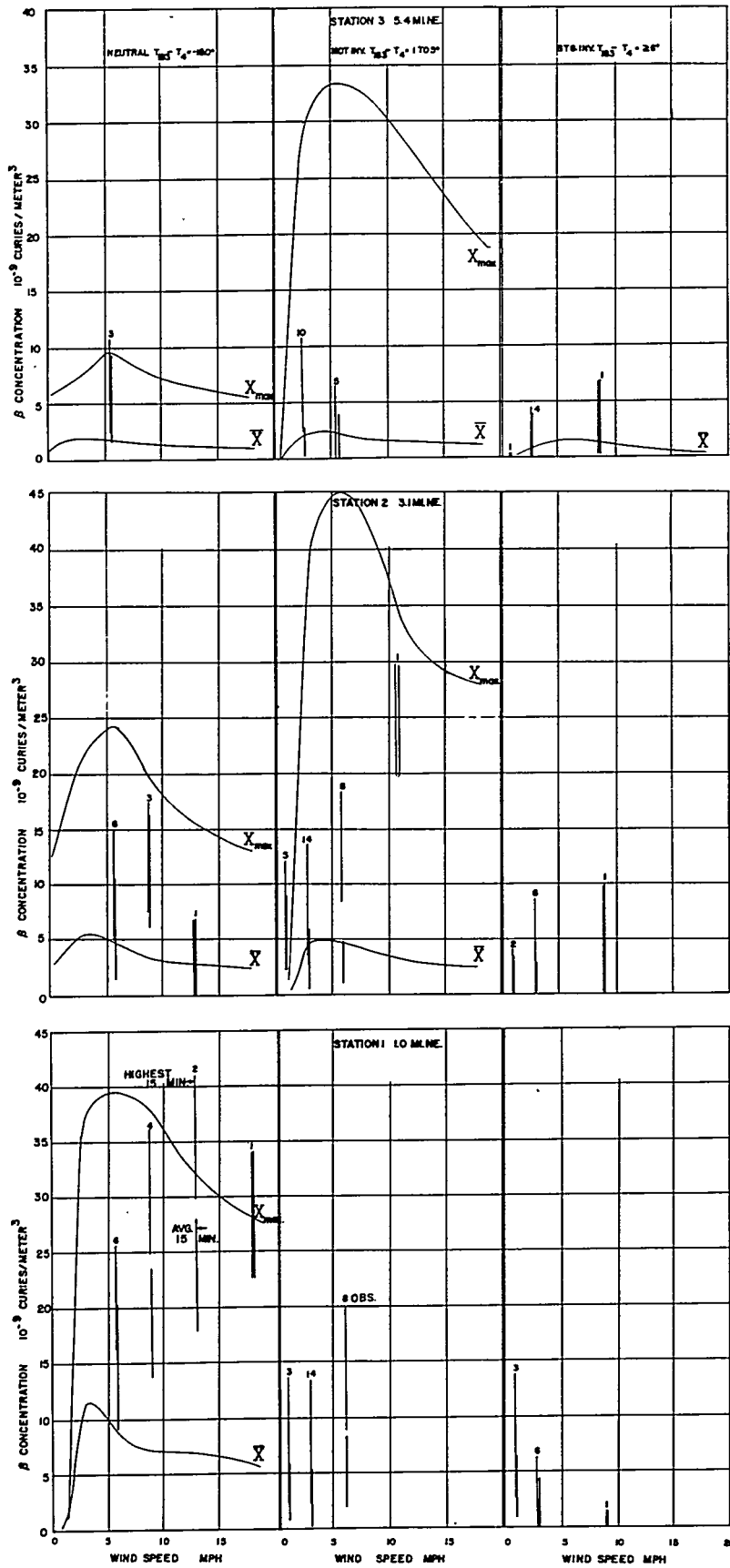
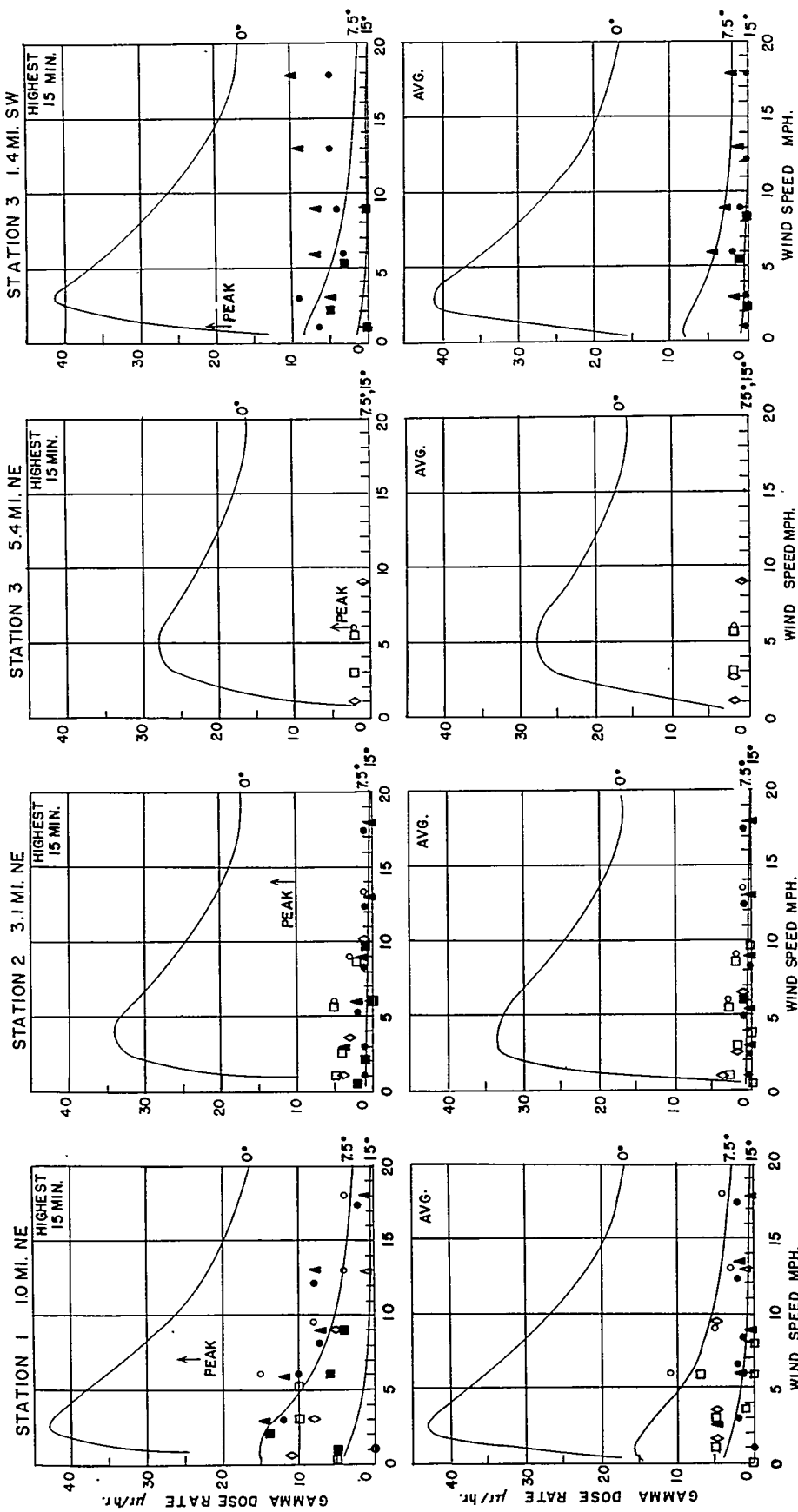


Fig. 180 Concentration of A^{41} in units of 10^{-9} curie/m.³ at 1.0, 3.1 and 5.4 mi. NE of X-10 Pile, under neutral ($T_{183} - T_{15} = 0$ or $-10^\circ F.$), moderately stable ($T_{183} - T_{15} = +1$ to $+5^\circ F.$) and very stable ($T_{183} - T_{15} = +6^\circ F.$ or more) conditions, plotted vs. station 012 wind speed and compared with theoretical downwind concentration \bar{X} and average concentration \bar{X} . Average and highest 15-min. observed concentration are shown; the vertical segments from the "high-background" value to the "low-background" value and indicate the degree of uncertainty due to choice of beta background level. The number of 15-min. observations is shown above each symbol.

59-1



T₁₈₅-T₁₄
 ▲ ± 2°F
 ● -1 to 0°F
 ■ 1 to 5°F
 ◇ ≥ 6°F
 ↑ HIGHEST PEAK (APPROX. 1 MIN.)
 9/1/50-11/3/50 4/27/51-4/29/51

Fig. 181